Retrofitting of Mechanically Degraded Concrete Structures Using Fibre Reinforced Polymer Composites

David Bohua Tann
BSc(Eng) MSc CEng MIMM

This thesis is submitted in partial fulfilment of the requirements of the University of Glamorgan/Prifysgol Morgannwg for the degree of

DOCTOR OF PHILOSOPHY

School of Technology

University of Glamorgan

March 2001

CERTIFICATE OF RESEARCH

This is to certify that, apart from where specific reference to other publications is made, the work presented in this thesis is the result of the investigations undertaken by the candidate.

D. B. Tann
(Candidate)

05/06/2001
(Date)

Professor R. Delpak
(Director of Studies)

5 June 2001
(Date)

Professor M. M. K. Lee
(Supervisor)

7 June 2001
(Date)

Professor P. C. Robery
(Supervisor)

7th June 2001
(Date)

DECLARATION

I declare that neither this thesis, nor any part of it, has been presented, or is currently submitted in candidature for any degree at any other academic institution.

D. B. Tann
(Candidate)

30 March 2001

(Date)

DEDICATION

To Lannie, Michael and Jonathan,
and to my parents and sisters

ACKNOWLEDGEMENT

I am indebted to many people who have helped me during the course of this study. First of all, I wish to record my gratitude to Professor Ramiz Delpak, my Director of Studies, for his guidance and supervision. His wisdom, experience and professionalism have been truly inspirational.

I wish to sincerely thank my second supervisor Professor Peter C. Robery, of Maunsell Ltd, for his help, advice and encouragement. Professor Marcus M. K. Lee, of Southampton University, is also acknowledged for his encouragement.

Dr Paul Ewings, of Exchem Mining & Construction Ltd, is to be thanked specially for his continuing support in the generous and unconditional provision of FRP composite materials and adhesive systems used in this study, as well as his constructive criticisms and comments during this work.

I am also grateful to the following people and organisations:

- The University of Glamorgan and in particular Professor Richard Neale, Dean of Research and Consultancy, for the award of a grant which enabled me to take a partial sabbatical from my lecturing duties.
- The Royal Academy of Engineering, for the award of an International Travel Grant that enabled me to present part of the work at the first ASEM Seoul conference.
- Dr Vahig Peshkam, formerly R & D Director at Mouchel Consulting Ltd., for encouraging us to take up the research work in structural repair and composite strengthening back in 1995.
- Fibreforce Composites Ltd., for providing part of technical information and the permission to use their copyright diagrams.
- All my colleagues at the Division of Civil Engineering, in particular Ken Pugh, for their help in undertaking some of the scheme administrative duties which would have otherwise been my "fair share".
- The staff at the Structural Laboratories, especially Paul Marshman and Anthorny Salmon for their assistance in the experimental work. Also David Gould and Terrance Powell, for their help in preparing graphics of the work for use in various conference presentations.
- My former students who worked with utter enthusiasm, and contributed to the building of a substantial experimental database on repair and strengthening of RC beams over the years. They include: Vasoulla Vassou, David Gray, Alun James, Costas Papaleontiou, Ka-ping Due, Tiong Woon, Antonis Marnerakis, Spiridon Kassis, Emyr Issac, Andrea Kokias, Mohamad Al-Hajeri, Maria Flouda, So-lee Sun, Kevin O'Meara, Bill O'Regain, Alex Tasioulas and Hamood Al-Meri.

Finally, I cannot end without thanking my wife Lan for her support and well-stretched patience, and young Michael and Jonathan, for the endless hours and weekends that they happily spent without the deserving company of their Dad.

ABSTRACT

This research involves the study of the short term loaded behaviour of mechanically degraded reinforced concrete (RC) flexural elements, which are strengthened with fibre reinforced polymer (FRP) composites. The two main objectives have been: (a) to conduct a series of realistic tests, the results of which would be used to establish the design criteria, and (b) to carry out analytical modelling and hence develop a set of suitable design equations. It is expected that this work will contribute towards the establishment of definitive design guidelines for the strengthening of reinforced concrete structures using advanced fibre composites.

The experimental study concentrated on the laboratory testing of 30 simply supported, and 4 two-span continuous full size RC beams, which were strengthened by either FRP plates or fabric sheets. The failure modes of these beams, at ultimate limit state, were examined and the influencing factors were identified. A premature and extremely brittle collapse mechanism was found to be the predominant type of failure for beams strengthened with a large area of FRP composites. A modified semi-empirical approach was presented for predicting the failure load of such over strengthened beams. Despite the lack of ductility in fibre composites, it was found that the FRP strengthened members would exhibit acceptable ductile characteristics, if they were designed to be under strengthened. A new design-based methodology for quantifying the deformability of FRP strengthened elements was proposed, and its difference to the conventional concept of ductility was discussed. The available techniques for ductility evaluation of FRP strengthened concrete members were reviewed and a suitable method was recommended for determining ductility level of FRP strengthened members.

A non-linear material based analytical model was developed to simulate the flexural behaviour of the strengthened and control beams, the results were seen to match very well. The parametric study provided an insight into the effects of various factors including the mechanical properties and cross sectional area of FRP composites, on the failure modes and ductility characteristics of the strengthened beams. Based on the findings of the experimental and analytical studies, design equations in the BS 8110 format were developed, and design case studies have been carried out. It was concluded that fibre composites could effectively and safely strengthen mechanically degraded reinforced concrete structures if appropriately designed. The modes of failure and the degree of performance enhancement of FRP strengthened beams depend largely on the composite material properties as well as the original strength and stiffness of the RC structure. If the FRP strengthened elements were designed to be under-strengthened, then the premature and brittle failure mode could be prevented and ductile failure mode could be achieved. It was also found that existing steel reinforcement would always yield before the FRP composite reached the ultimate strength.

Furthermore, a critical reinforcement ratio, above which FRP strengthening should not be carried out, was defined. It was concluded that FRP strengthening is most suitable for reinforced concrete floor slabs, bridge decks, flanged beams and other relatively lightly reinforced elements. The study also revealed that to avoid a brittle concrete failure, existing doubly reinforced members should not be strengthened by FRP composites.

Keywords: Fibre Reinforced Polymer, Carbon, Glass, Aramid, Composite, Reinforced Concrete, Repair, Strengthening, Retrofitting, Structural Ductility, Analytical Modelling, Deformability, Under Strengthening, Over Strengthening, Design Guidelines.

CONTENTS

CHAPTER 5 ANALYTICAL MODELLING OF FRP STRENGTHENED RC ELEMENTS

CHAPTER 6 PREMATURE TEARING-OFF BEHAVIOUR OF FRP STRENGTHENED RC BEAMS

CHAPTER 7 DUCTILITY AND MOMENT REDISTRIBUTION OF FRP STRENGTHENED BEAMS

LIST OF FIGURES

LIST OF TABLES

NOTATIONS

κ	curvature
Δ	general deformation
β	reinforcement position factor, = $d/(h + t_a + t_p/2)$
Ω	shape factor for concrete stress block
$\Delta_{0.95Pu}$	generic deformation at 95% of peak ultimate load
ξ_1	constant defining depth of equivalent rectangular stress block
$\varepsilon_{1,2...6}$	surface strains of concrete from top to bottom of test beams
τ_{ave}	average FRP concrete interface shear strength
σ_c, f_c	concrete compressive stress
ε_{ct}	average tensile strain of concrete
ε_{cu}	ultimate concrete strain (=0.0035)
φ_{df}	deformability index
φ_{du}	ductility index
ε_m	average reinforcement strain in crack width calculation
γ_{mc}	material factor of safety - concrete
γ_{mE}	factor of safety of FRP modulus of elasticity
γ_{mF}	material factor of safety – FRP
γ_{ms}	material factor of safety - steel
κ_o	initial curvature under dead load before strengthening
ε_o	concrete strain at peak stress, or initial strain under dead load
ρ_p	external FRP composite ratio
ε_p	strain in FRP plate
σ_p	stress in FRP composites
ε_{pu}	ultimate strain of FRP composite (failure strain)
ε_{pu}	ultimate strain in FRP plate
δ_s	deflection at service load
δ_s	reference deflection for ductility calculation
ρ_s	steel reinforcement ratio
Δ_s	deformation under service load

σ_s	stress in steel reinforcement
δ_{sc}	deflection at serviceability limit state of cracking
ρ_{scr}	critical steel reinforcement ratio for under strengthening
δ_{sd}	deflection at serviceability limit state of deflection
ε_{su}	ultimate strain of steel reinforcement
σ_t	concrete tensile stress
ε_t	tensile strain of concrete
κ_u	curvature at ultimate limit state
a_{cr}	distance from point of crack width to nearest bar
A_{pmax}	maximum cross section area of FRP for ductile strengthening
A_{pp}	area of FRP plate provided
A_{pr}	area of FRP plate required
A_s	cross section area of tension steel
A_s'	cross section area of compression steel
A_{sv}	cross section area of shear links
b	section width
c	moment curvature constant for a given beam configuration
c_{min}	nominal cover to reinforcement
ε	concrete strain
d	effective depth
d'	distance to the compression reinforcement
E_c, E_o	modulus of elasticity of concrete
E_{el}	elastic stored energy
E_p	modulus of elasticity of FRP plate
E_{tot}	total energy
η	factor = $\varepsilon/\varepsilon_o$
f_c	compressive stress in concrete
F_c	compression in concrete
f_{ck}	concrete cylinder strength
f_{ct}	tensile strength of concrete
f_{cu}	characteristic strength (cube) of concrete
f_p	stress in FRP plate
F_p	tension in FRP composite

f_{pd}	design strength of FRP composites
f_{pf}	design strength of composite for shear strengthening
f_{pu}	characteristic strength of FRP plate
f_s	stress in steel reinforcement
F_s	tension in steel reinforcement
F_t	tension in concrete
f_y	yield strength of bare steel reinforcement
f_y^*	yield strength of embedded steel reinforcement
f_{yd}	design strength of steel reinforcement
h	overall beam depth; depth of FRP composites in shear strengthening
I	second moment of area
K, K'	factors in flexural design of RC members
l	effective span of RC elements
l_p	total bonded lenftg of composite
M	Applied bending moment
M_o	initial moment before strengthening
M_u	ultimate moment of resistance
P	applied load
P_u	ultimate collapse load
R	radius of curvature
t_a	thickness of adhesive layer
t_p	thickness of FRP plate
V	shear resistance
v	shear stress (subscripts c-concrete; p-composites)
W_{cr}	surface crack width
x	neutral axis depth for non-strengthened reinforced section
x_{sb}	neutral axis for FRP strengthened fully balanced section
x_{so}	neutral axis depth for over-strengthened section
x_{su}	neutral axis for under strengthened section
y	depth of centroid of the concrete stress bock

CHAPTER 1

GENERAL INTRODUCTION

1.1 FOREWORD

Of those members of the general public, who are accustomed to the highest expectations in building and safety standards, perhaps not many realise that there is a certain physical analogy between a load resisting structure and a human body. A human being, whose body may be subjected to various forms of virus attacks from time to time during his or her life span, needs to seek clinical help and advice. Also where necessary, expert medical treatment may be required to cure the diagnosed illness. Similarly, a structure is likely to suffer from a variety of environmental and mechanical degradation causes during its expected service life. In order to maintain a "healthy" structure, or more desirably, to prolong its service life, it is often important for the owners of the structure to consult another type of specialist, - the structural engineers who specialise in repair and rehabilitation. To this end, this thesis is dedicated to a new "treatment technique" for the special doctors to treat their "patients" - namely the degraded structures.

But what really is a structure? Why would it suffer from degradation and need to be repaired and strengthened? From the view point of a design engineer, a structure can be essentially defined as an entity of a group of solid bodies, assembled together in such a way as to safely resist any external forces that may act upon it. Such an assembly is therefore naturally subjected to gradual material deterioration as its age approaches the

design limit. In the process, the strength and stiffness of the structure will be reduced, and its ability to safely resist the original design level of allowable forces will be seriously affected. Furthermore, during the normal service life of the structure, any excessive in-service loading caused by storms, earthquakes, alterations to the structure, accidental overloading or change of use may result in the structure being weakened or damaged, and lead to its malfunction or even eventual failure.

1.2 DEFINITION OF REPAIR AND STRENGTHENING

There are four repair-related terms that have often been used interchangeably in the construction maintenance industry. These are, Repair, Strengthening, Retrofitting, and Rehabilitation. The candidate and his director of studies have in a number of technical presentations suggested that these terms should be clearly distinguished as follows.

- **Repair** – This refers to the technical process in which degraded structural elements are treated by means of partially replacing material or adding additional components such as external reinforcement, so as to restore or enhance the combined characteristics and hence the expected structural performance, to or near the originally specified levels.
- **Strengthening** - This is the process to enhance the structural performance over and above the originally specified levels, usually by means of adding extra structural components such as steel or advanced composite plate bonding or fabric wrapping.
- **Retrofitting** – This term is more often used in North America. It originally refers to equipping a vehicle with new parts, and is now extended to mean any activities of restoring and enhancing the structural properties and performance.
- **Rehabilitation** – This is a generic term indicating any aspects of repair and strengthening. Moreover, the rehabilitation work is not necessarily limited to the structural sense, any non-structural or decorative alterations to the appearance of a structure, for example, can also be termed as rehabilitation.

It is important to point out that strengthening work can be carried out on perfect structures as well as degraded ones. In the latter case, it is usually necessary to repair the structures and regain the original strength and stiffness before strengthening work takes place. To this end, the strengthening process may also be regarded as an extension of repair. Repair work can be structural or non-structural. The purpose of localised material repair such as patching up a small area of degraded concrete in RC structures, is often to prevent the localised areas of damage from spreading out, thus limiting or avoiding any possible consequential structural degradation.

1.3 THE NEED FOR STRUCTURAL REPAIR AND STRENGTHENING

Maintenance managers and structural engineers in the developed countries are now faced with an increasingly large number of impaired structures. There may exist many buildings, bridges and other infrastructures across the world that are regarded as structurally deficient and are in need of repair and upgrading. It is difficult, however, to carry out a well co-ordinated nationwide "health monitoring" for all structures, especially related to private building structures, since most of their respective owners or users have vastly different requirements and expectations of the properties. A good thermometer indicator of structural integrity, would be the current conditions of public buildings, bridges, airports, power plants and other general installations and infrastructures in a nation. The following sections present a brief summary of the infrastructures in the United States and the United Kingdom. In the developing world, the situation is generally much more serious.

1.3.1 The USA

In the United States, the American Society of Civil Engineers (ASCE) has given the national infrastructure an average grade of "D", which represents a poor state of the backbone that is vital to the growth of to the US economy (see Appendix E). Even though a grade of "C-" was given to America's 581,862 bridges, a total of 182,762 bridges (31.4%) are rated as structurally deficient or functionally obsolete by the Federal Highway Administration (FHwA). It was estimated that $80 billion (£50

billion) would be required to eliminate the backlog of bridge deficiencies and maintain appropriate repair level (FHwA, 1997). The schools received the worst grade of "F", nearly 60% of all school have at least one major building problem and need extensive repair work to be carried out. It is claimed that a total capital investment of $1.3 trillion ($1.3 x 10^{12} or approximately £813 billion) will be required to repair and renew America's infrastructure to meet its growing needs. In addition, a national public-private partnership will need to be established to coordinate the work. Table 1.1 shows the summary of the above report (ASCE, 1998). The total value of the US infrastructure is estimated to be $20 trillion (NSF, 1993), thus the rehabilitation costs will be 6.5% of the total capital value. Although $1.3 trillion is a large sum, such a percentage should be regarded as an acceptable level of investment.

Table 1.1 Extract of the ASCE Report Card for America's Infrastructures

Subject	Grade	Comments	Repair Costs ($ billion)
Roads	**D⁻**	59% of roads are in poor, mediocre or fair condition.	**357**
Bridges	**C⁻**	31.4% of bridges are rated structurally deficient or functionally obsolete.	**80**
Schools	**F**	One third of all schools need extensive repair or replacement, nearly 60% of schools have at least one major building problem	**112**
Dams	**D**	More than 200 documented dam failures across the country in recent years, 2100 are now considered unsafe.	**1**
The total investment needs for the five-year period is estimated to be $1.3 trillion. This figure also includes financial requirement for other infrastructures such as Mass Transit, Aviation, Drinking Water, Wastewater, Solid Waste and Hazardous Waste.			**A** = Exceptional **B** = Good **C** = Mediocre **D** = Poor **F** = Inadequate

1.3.2 The UK

In the United Kingdom, the situation is only slightly better. Since the late 1980's, the annual spending in the structural repair and refurbishment market is estimated to be typically just under 50% of the total turnover in the UK construction industry. In 1988,

the UK repair and rehabilitation works had a gross value of approximately £15 billion (Thomas, 1989), while by the end of 1996, this figure had increased to around £26 billion, still just half of the total spending in the construction industry. Considering bridges for example, many have now weight restrictions placed on them due to structural deficiencies. There are approximately 80,000 reinforced or prestressed concrete bridges across the nation that carry traffic today, mostly owned by the Highways Agency (HwA) and local authorities. The others are owned by private organisations such as Railtrack Plc (around 10% of its 40,000 bridges are of concrete structures), British Waterways and Rail Property Ltd (Lynn, 1999).

The annual road traffic volume in Great Britain (excluding Northern Ireland) has increased dramatically over the past half century as shown in Figure 1.1 (DETR, 1999). The traffic volume was 53.1 billion vehicle kilometers in 1950, and by the end of 1999, this figure reached 467.08 billion vehicle kilometers, a net increase of 779% within a 50 year span. This sharp increase in traffic volume has undoubtedly resulted in the accelerated mechanical degradation of road bridge structures, especially those designed and built over 30 - 50 years ago.

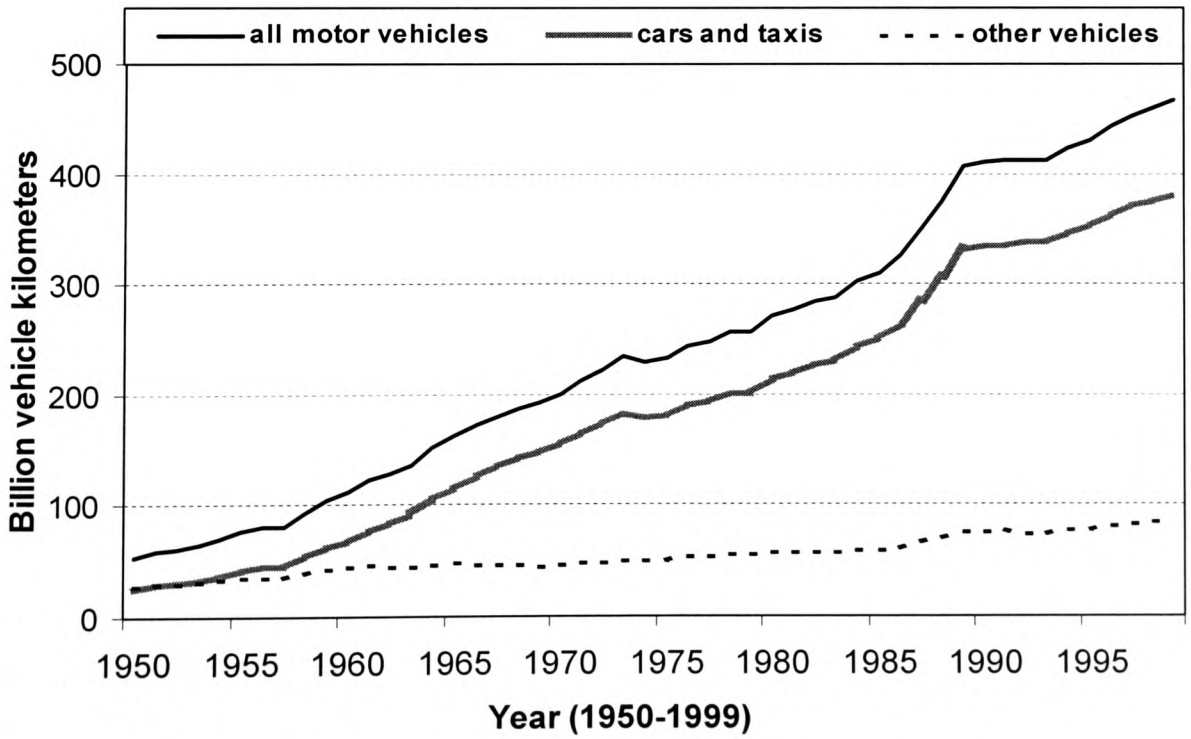

Figure 1.1 Road Traffic Increase in Great Britain Since 1950

It is acknowledged that vehicles today are becoming heavier. Until 1999, the official UK gross limit for articulated vehicles and drawbar-trailer combinations with 5 or more axles has been 38 tonnes. Nearly all other EU countries except Ireland have higher gross vehicle weight and axle load limits than that of the UK, as shown in Table 1.2 (DOT, 1997).

Table 1.2 Lorry Weight Limit in EU Countries

Lorry Weight Limits (tonnes) for Articulated Vehicles and Drawbar-trailers Combinations in EU Member States				
Country	**Number of axles**			**Axle Weight Limit**
	4	**5**	**6**	
Austria	38§	38§	38§	11.5
Belgium	39	44	44	12.0
Denmark	38	44	48	11.5
Finland	36	44	53	11.5
France	38	40*	40*	13.0
Germany	36	40	40*	11.5
Greece	38	40	40	11.5
Ireland	35	40	44	10.5
Italy	40	44	44	12.0
Luxembourg	38	44	44	12.0
Netherlands	41	50	50	11.5
Portugal	38	40	40	12.0
Spain	38	40	40	11.5
Sweden	38	40#	40#	11.5
United Kingdom	**35**	**38****	**38****	**10.5**
EC Directive Limits (International Movements)	38	40*	40*	11.5

** 44 tonnes for combined transport.*
*****Pre-1999 limits,** 44 tonnes for combined road/rail transport.*
§ Austria permits a 5% tolerance on this limit allowing, in effect, 40 tonnes. Austria also allows 42 tonnes for container transport.
 # Higher weights allowed for certain long vehicle combinations.

After the implementation of the EU Directive 96/53/EEC, UK roads presently have to accept 5-axle vehicles from any member state. This could be up to 2 tonnes heavier and with 1 tonne more loads on the drive axle. Furthermore, almost all of the existing 38 tonne lorries in the UK can be redesignated as 40 tonne vehicles since their maximum design weight is usually above 40 tonnes. The consequences of such a seemingly small

increase should cause much greater alarm than perhaps officials have realised. Although the 2 tonne of gross weight increase amounts to just over 5% of the original allowable weight, and the drive axle load increases by just 9.5%, the road wear such load increases will cause is expected to be much greater. It is important to point out that it is the maximum axle weight, not the gross vehicle weight, which controls the road wear. Road wear is approximately the maximum axle weight raised to its 4^{th} power. For a one tonne increase of drive axle load from 10.5 tonne to 11.5 tonne, it will be equivalent to a 44% increase in road wear.

In 1987, the then Department of Transport published a report on the assessment of highway bridges (DOT et al., 1987), which called for a nationwide Bridge Assessment and Strengthening Programme. In late 1989, the Local Highway Authorities began assessing and strengthening bridges in their area of responsibility. The assessment work included checking the physical conditions of the bridges and using numerical methods to evaluate the load carrying capacities. This programme was originally intended to be completed by 1 January 1999, when under an EU Directive 96/53/EEC (formerly 85/3/EEC), 40 tonne lorries were allowed on UK roads. However, by the end of 1999, only 35,000 of the 41,600 local authority owned bridges in England, which were identified to be in need of structural assessment, were actually assessed. In Wales and Scotland only 41% and 75% of the bridges in this category have been assessed respectively (Lynn, 1999). To date, no specific and official data or results of UK bridges assessment and strengthening programme have been published. However, a brief report on the nation's infrastructure has been published recently by the Institution of Civil Engineers and the New Civil Engineer magazine (see Appendix E). It was conservatively estimated that around one-sixth (13,000) of all concrete bridges in Great Britain need some form of repair and strengthening (Tann & Delpak, 1999). This estimation is made after extensive discussions with bridge engineers and local authority officials, and in consultation with some limited publications (NAO, 1996).

1.3.3 Europe

Although no authoritative statistical data on the state of Europe's infrastructure is available, it is generally accepted in the engineering community that within the

European continent, there is a large scale problem of material deterioration in reinforced and prestressed concrete structures that were built over 30 years ago. The rapid economic development across the continent has inevitably resulted in increased burden on national infrastructures, with the goods carrying vehicles becoming much heavier and traffic volume considerably greater than the values for which roads and bridges were originally designed. It is estimated that the steel reinforcement corrosion within Europe costs the construction industries £1.0 billion per year (Clarke 1993).

1.4 CLASSIFICATION AND CAUSES OF DAMAGES IN STRUCTURES

1.4.1 Categories of Damage in Structures

All types of damage in structures are not necessarily structural. Natural degradation usually starts with gradual material deterioration due to ageing or aggressive environmental influence. Localised mild material damage, if diagnosed correctly, can usually be repaired without causing serious structural damage. Damages in concrete structures may be defined and classified into the following types:

Material Damage – When natural or accelerated deterioration results in significant alteration of material properties, material damage has taken place. Such degradations are usually irreversible, where they will continue developing into the neighbouring area of the damaged zone. If not physically arrested and controlled, they will eventually cause complete material failure. Typical examples of material damage in reinforced concrete structures include carbonation of concrete and chloride ingress into the depth of the elements.

Mechanical Damage – If the material damage occurs in part of a solid body, which is undergoing mechanical action, then the mechanical properties of that solid continuum will be adversely affected. A typical case is that the compressive strength of degraded concrete will be lower than its originally designated value.

Structural Damage – This category is relative to the overall performance of a structure. Any change to a structure which adversely affects its stability or its ability to resist load safely, may be regarded as structural damage. Structural damage can be broadly grouped into two further categories:

a) *Serviceability Damages* – those which can maintain structural stability under normal service load, but unacceptable for normal structural functioning; and

b) *Ultimate Damages* - those that result in ultimate failure of a structure or its elements.

Serviceability damages in reinforced concrete structures include excessive crack distribution, excessive crack width, unacceptably large deformations (deflection and/or rotations), and excessive load induced vibration. Such damages are usually repairable if diagnosed at the early stage and causes of damages clearly identified and controlled.

Unlike serviceability damages, ultimate structural damages such as flexure, shear or axial modes of failure, usually result in complete ending of service life for the structure or its elements. These damages are more difficult or even impossible to repair, unless they are contained in a relatively localised area, in which case thorough structural and feasibility assessment should be carried out prior to commencing any remedial work.

1.4.2 Causes of Damage in Reinforced Concrete Structures

1.4.2.1 Material damage

Material deterioration of reinforced concrete structures can take many forms, but the corrosion of steel reinforcement is the most serious problem that causes more damage to concrete than many other forms of environmental attack. However, the corrosion of steel is often caused indirectly by the weakness of concrete. Carbonation of and chloride ingress into concrete are the two typical corrosion mechanisms in reinforced concrete structures. The steel reinforcement or prestressing tendons usually remain in a passive state since they are protected by the surrounding concrete cover that forms an alkaline layer around the steel. However, this passivity can be destroyed either by carbonation,

the steady diffusion of carbon dioxide from the atmosphere into the concrete, or by the action of chlorides, primarily from the marine environment or caused by the de-icing salts used on highway structures during the cold seasons (Clarke, 1993). The cracks in concrete, under service load, speed up the process of these chemical attacks. Once the steel becomes "depassivated", a complex electro-chemical corrosion process can then take place in which current flow is generated. Clarke gave a concise and vivid description of the steel corrosion process:

> "*...the flow of current from the cathodic region through the steel to the anodic region, and back through the concrete. A supply of oxygen and water, passing through the concrete, is required to fuel the cathodic reaction. At the anode, the iron is dissolved away in the form of ferrous hydroxide. With sufficient supply of both water and oxygen, the ferrous oxide will form rust*".

Rust, by its very nature, occupies a volume several times that of the parent metal, an expansive force is thus formed in the corroded area, which causes the concrete to crack initially, and results in full spalling eventually with the steel bars being fully exposed. Mild material degradation usually develops into severe material deterioration with time, and if not eradicated, will result in mechanical damage and ultimately lead to structural failure.

Other causes of concrete material damage include acid attack, frost action and alkali aggregate reaction. More recently, the foundations of a number of 30-year old bridges in Gloucestershire were fund to be affected by a form of sulphuric acid attack that involves the formation of the mineral thaumasite ($CaSiO_3.CaCO_3.CaSO_4.15H_2O$). An expert group was set up by the Department of Environment, transport and Regions (DETR) to study this phenomenon (Clark, 1999). In recent years, a few types of repair materials, mostly polymer modified and cementitious based, have been developed for the repair of damaged concrete (Robery *et al*, 1997).

1.4.2.2 Mechanical damage

Specifically, mechanical damage can occur in RC structures and repair or strengthening work is thus required due to the following:

- Untreated material deterioration in natural or aggressive environment.
- Change of use or regulations, which may result in loading increase.
- Inadequate initial design.
- Insufficient or incorrectly located reinforcement, or incorrectly/poorly executed construction details.
- Alteration of structural arrangement.
- Accidental over loading, impact, earthquake and terrorist attack.

The focus of the present study is on the rehabilitation of mechanically degraded reinforced concrete elements. Although material deterioration leads to eventual mechanical and structural damage, the principle aspect of investigation in the current work is the structural behaviour of RC members that require strengthening or upgrading due to normal service loading or overloading.

1.5 TRADITIONAL METHODS OF STRUCTURAL STRENGTHENING

1.5.1 Adding Extra Reinforced Concrete

Traditionally the method of adding additional reinforced concrete to the existing members has been deployed in many concrete strengthening projects. It is usually reliable and effective in enhancing the member load carrying capacity, but the construction process is often long and labour intensive. The size of the existing members have to be increased which may also result in practical site difficulties. The principle of this strengthening method is simple, i.e., to provide additional load resistance by combining the existing member with a new component of similar material configuration. If the shear resistance of an existing RC beam is insufficient, additional shear links may be provided external to the existing beam, new concrete is then cast to form a protective cover around the whole section as shown in Figure 1.2(a). Flexural capacity can be enhanced by adding additional tension reinforcement and increasing the existing beam effective depth as shown in Figure 1.2(b). This assumes that the component has ample residual compressive strength to balance the newly mobilised tension reinforcement.

The minimum extra depth to the existing beam in flexural strengthening is usually between 80 to 100 mm. As a result, a considerable increase in self-weight and reduction in headroom in buildings such as multi-storey car parks, and highway bridge girders, will accompany such a strengthening technique.

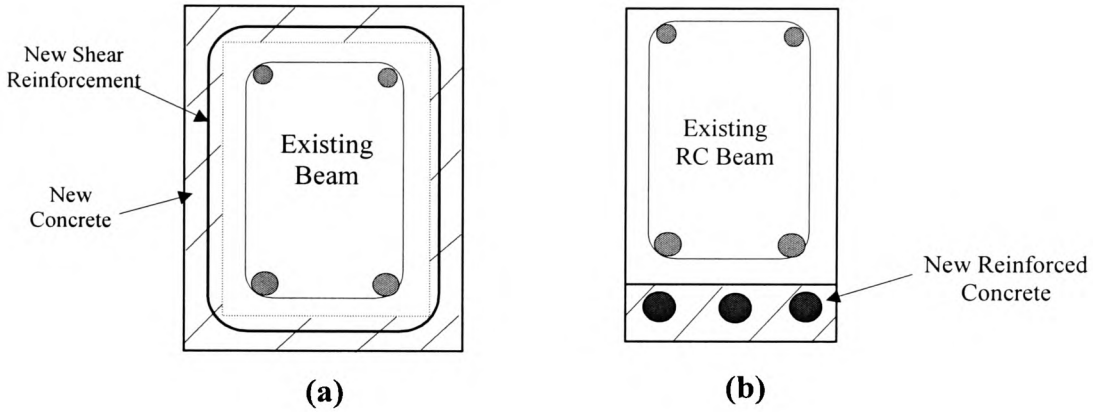

Figure 1.2 Traditional Strengthening Method by Adding Extra Reinforced Concrete **(a)** Shear Strengthening, **(b)** Flexural Strengthening.

1.5.2 External Steel Plate Bonding

1.5.2.1 Background of application

The method of upgrading existing reinforced or prestressed concrete structures by external steel plate bonding using suitable structural adhesive system is a major strengthening technique. So far there has been extensive research and wide application. This section gives a brief introduction on the application of this method in the repair and strengthening of structurally damaged RC elements.

The principle of steel plate bonding is to use the tensile strength of steel plate to supplement the internal tension steel reinforcement, hence increase the flexural capacity of the original beam. Steel plate is glued to the tension face of the RC beam using epoxy based adhesive systems to transfer stresses from concrete beam to the steel plate as shown schematically in Figure 1.3. The adhesive layer plays a critical role in ensuring full composite action between the concrete and the steel plate.

One of the first known cases of steel plate bonding took place in Durban, South Africa in 1964. It was found after construction that reinforcing steel bars had been omitted in several beams, and as a remedial measure, external steel plates were bonded to the soffit of these beams to act as tension reinforcement (Fleming & King, 1967). Since then the quality of structural adhesives has been improved considerably, and steel plate bonding technique has been steadily applied in many countries including Switzerland, France, Japan, Australia, Belgium, Poland, the United States and the United Kingdom.

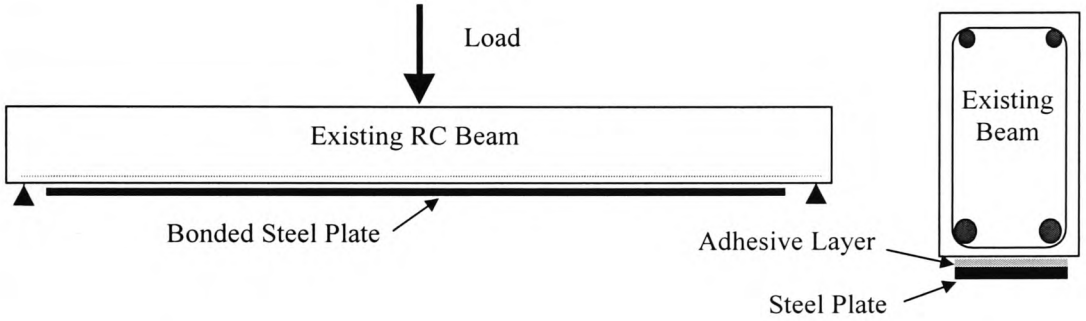

Figure 1.3 External Steel Plate Bonding for Flexural Strengthening

In the UK, the first case of steel plate bonding can be traced back to 1974, when the Deham Bridge was strengthened. This was followed by the Quinton Bridges over the M5 motorway in 1975. The then Transport and Road Research Laboratory (TRRL) together with the adhesive manufacturers and the Department of Transport, carried out considerable research and development. The first report was published shortly afterwards (Irwin, 1975). Macdonald (1978) and Macdonald and Calder (1982) subsequently reported a series of tests on steel plated RC beam of 4.90 m length. They found that the loading required to cause a crack width of 0.1 mm was increased by 95%, while the post cracking stiffness of these beams increased by an average of between 35 to 105%. The technique gained wide acceptance and was used for bridges and buildings to strengthen concrete elements in both the tension and compression zones (Swamy *et al*, 1987). The New Civil Engineer (NCE) and other professional news bulletins over the years have reported a series of bridges strengthened by such methods. An illustrative but not exhaustive list of bridges with external steel plate bonding is compiled as shown in Table 1.3.

Table 1.3 List of Bridges Strengthened by External Steel Plate Bonding in the UK*

Year	Bridge	Local Authority
1974	Deham Bridge	Suffolk
1975	M5 Quinton Interchange Bridges	Hereford & Worcester
1977	M25 Swanley Interchange	Kent
1977	A4120 Pen-y-Bont Bridge	Dyfed
1977	Pen-y-Llyn Isaf	Gwynedd
1982	M1 Brinsworth Road Bridge	Yorkshire
1986	A10 Brandon Reek Bridge	Norfolk
1987	M2 Farthing Corner Footbridge	Kent
1987	M1 Stainbury-Teversal Bridge	Derbyshire
1988	Olive Road Railway Bridge	Hove, East Susses
1989	A56 Cedars Overbridge	Cheshire
1989	Manor Road railway Bridge	East Sussex
1990	Finavon Bridge	Forfar, Scotland
1990	Asten Fen Bridge	Lincolnshire
1991	Ducks Marsh Bridge	Devon
1991	Stakeford Bridge	Northumberland
1991	Bures Bridge	Suffolk
1991	Bridgewater Road Bridge, Brent	London
1992	Quidhampton Bridge	Hampshire
1992	A23 Bolney Flyover	East Sussex
1992	Mythe Bridge Tewkesbury	Gloucestershire
1993	Great Bridge, Romsey	Hampshire
1993	Duttons Road Bridge, Romsey	Hampshire
1993	Plas Bridge	Gwynedd
1993	Kirkstead Bridge	Lincolnshire
1994	Pakrhill Road Bridge, Bexley	London
1994	Market Harborough Bridge	Leicestershire
1994	Pont Geinas Bridge	Clwyd
1994	Wisbech Town Bridge	Cambridgeshire

* **Source:** - Mays and Hutchinson (1988), Richards (1996), BA 30/94 (1994), and complied from trade magazines including Construction Repair, New Civil Engineer, and from company trading brochures.

1.5.2.2 Disadvantage of steel plate bonding

Although steel plate bonding technique had been proven as an effective and economic means of increasing the bending as well as shear capacities of RC elements, it was recognised that there were also a number of distinctive disadvantages as outlined below. There is an urgent need to seek alternative and more sustainable strengthening materials for use in the new century.

- *Plate Peeling-off* - In most steel bonded beams, sudden plate separation at one end of the steel plate was observed to be a major failure mode, and end anchorage at the end of the steel plate thus became a necessity. This involves drilling holes through the steel plate into the concrete and bolting the plate to the strengthened structure. When the structure to be strengthened has small cross section, such drilling may damage the main internal reinforcement.
- *Heavy Weight, Difficult Handling, Joints* – Due to the heavy self-weight of steel plates, elaborate temporary support systems are usually needed during the installation process, and in some cases, even permanent propping may be required under the service load conditions. In order to avoid stresses being induced normal to the adhesive layer during curing, steel plates are required to be delivered to site completely flat, and the feasible transportation length is thus limited to between 6 and 8 metres. This leads to more complications for design and installation work as the plates need to be lap jointed, since structures often have greater span than this length. Butt welding is considered unpractical since it may damage the adherent. The steel plate bonding process is therefore regarded as time consuming and labour intensive.
- *Difficult to cut to shape* – It has been noted that during strengthening work of irregularly shaped structures, it becomes more difficult to cut and install the steel plates on site.
- *Susceptibility to Corrosion* - The greatest concern in steel plate bonding, however, is the problem of corrosion of the steel plates. Since the plates are bonded externally, they are even more susceptible than the internal steel reinforcement in RC structures to potential and prolonged environmental attack even though protective coating or other form of encasement may be applied.

1.6 STATE OF THE ART STRENGTHENING USING FRP COMPOSITES

1.6.1 Background

The advanced composite materials used in the construction industry can be summarised into three main categories, they are Carbon Fibre Reinforced Polymer (CFRP) composites, Glass Fibre Reinforced Polymer (GFRP) composites and Aramid Reinforced Polymer (AFRP) composites. Aramid is probably better known by its trade name Kevlar®. The mechanical properties of the advanced composites will be discussed in Chapter 3, but essentially these materials are composites that combine various fibres with a thermoplastic or thermosetting matrix. The fibre contents are usually between 60 – 75%, it is therefore somewhat misleading, that these composite materials should be called "fibre reinforced plastics", as is often the case. The word plastic, as a noun, often carries with it indications of flimsiness and even poor quality, and in reality the properties of FRP composite materials cannot be more different from that of plastics.

The research work in applying advanced fibre reinforced polymer composite materials to civil engineering structures started in the 1980's in North America, Japan, China and Switzerland. The world's first major composite bridge was built in 1982 in Miyuan County near Beijing, China (NCE, 1983). The bridge, which consisted of five 21 metres long spans of glass fibre reinforced polymer (GFRP) box girders, took only five months to build. It has a span of 20 metres and a width of 9.6 metres, and only weighs 30 tonnes, 80% lighter than a comparable concrete bridge. This highly decorated bridge has functioned well up to the present day. It has been carrying a large volume of daily traffic including pedestrians, cyclists, horse drawn carts, buses and heavy good vehicles. This bridge was largely experimental, although the details were not released, the Chinese officials confirmed that it was much more expensive to build this bridge than a conventional one of the same size. In the UK, the world's longest composite footbridge was completed in 1993 over River Tay at Aberfeldy (Slavid, 1993). The bridge, which links two halves of a golf course, was entirely built from composite materials. The main centre span of 63 m consisted of GFRP deck with GFRP towers, while the stay cables were made of Kevlar fibre ropes. The construction took only 10 weeks in bad weather, and no crane was used. More recently, various FRP rods were used as reinforcing bars as replacement of internal steel reinforcement in tackling the steel corrosion problems

(ACI, 1996; Clarke *et al* 1996). The actual use of advanced composites as plate bonding strengthening materials, however, did not start until the early 1990s (Ballinger 1997). The first reported application was in Switzerland where the composite research work was pioneered and developed at the Swiss Federal Laboratories for Materials Testing and Research (EMPA). The Ibach Bridge over Rivers Emme and Reuss and Highway N2, near the city of Lucerne, had several of its prestressing tendons severely damaged during drilling works to install new traffic signals. It was repaired shortly after in July 1991, with externally bonded CFRP plates of 5000 mm long by 150 mm wide and of 2.0 mm thickness (Meier, 1992). The total weight of CFRP material used was only 6.2 kg, compared to 175 kg of steel which would have otherwise been needed for the repair. The work was completed in one day and only a light mobile platform was used, eliminating the need of the more conventional but expensive scaffolding.

Steiner (1996) reported CFRP strips being successfully used to strengthen balconies in Germany to reduce excessive deflection. A shopping centre in Winterthur, Switzerland was extensively strengthened using a total of 3000 metres CFRP strips of between 10 and 16 metres long, 100 mm wide by 1.2 mm thick.

The very first application of FRP strengthening in the United Kingdom was the roof slab strengthening project in the Kings College Hospital Joint Education Centre, in 1996 (NCE, 1996). An extra office floor was added to a flat concrete roof in the congested south London site. The new floor was required to be strengthened to take up 3.0 kN/m^2 live load. The narrow width (80 mm) of the roof supporting beams prevented the conventional steel plate bonding being applied, since the required width to thickness ratio would have led to a design of a relative thick (>10 mm) steel plate. Drilling holes through the beams for steel plate anchorage would have inevitably led to damaging the main steel reinforcement. A total of 1.3 km length of CFRP plates were used, and the project was completed in just 4 weeks with half the workforce that would otherwise have been required for steel plate bonding.

A few other selected, representative FRP composites application examples are compiled in Table 1.4. It is clear that the general trend of applying FRP for strengthening RC structures is steadily developing.

Table 1.4 List of Buildings/Bridges Strengthened by FRP Composites in the UK*

Year	Structure	Strengthening Problem	Composite Solution
1996	Kings College Hospital Education Centre, London.	Converting an existing roof slab into an office floor, increasing live load to 3.0 kN/m^2.	1.3 km of CFRP plates bonded to soffit of 11 m long, 80 mm wide beams.
1997	Devonshire Place Bridge, Skipton.	Tendons in the prestressed edge beam were damaged, weakening flexural capacity.	Single CFRP Sheet bonded to beam soffit.
1997	Nestle Chocolate Factory, Tutbury.	Floor loading increased by 30% due to installation of new plant machinery.	CFRP Plate bonded to 11 beams supporting the floor.
1997	Yarborough School, Lincoln.	The precast concrete staircase was installed upside down. Minimum disruption to school essential.	80 m long of CFRP plates were bonded to the bottom of the staircase.
1998	BSI Car Park, London.	64 under-strength columns needed strengthening.	CFRP fabric strip loops bonded to columns.
1998	Alders Department Stores, Croydon and Portsmouth.	Holes were cut for installation of new lifts.	250 m of CFRP plates were bonded alone the edges of the floor area to be cut.
1998	St Columb Major Road Bridge, Cornwall.	Chloride ingress led to the repair of the bridge, and strengthening was needed to resist 40 tonne vehicles.	CFRP plates were bonded to the bridge deck after it was repaired.
1998	A30 Bible Christian Bridge, Bodmin.	Bridge columns weak in impact load resistance.	Multiple layers of C/G/AFRPs wrapped on 3 columns respectively.
1999	A413 Farm Underpass, Great Missenden, Bucks.	The bridge needed strengthening to meet the 40 tonne load requirement.	180 m length of CFRP plates were bonded to the soffit of bridge deck.
1999	Oaklands 8-storey carp park, Manchester	Main supporting columns structurally damaged, temporary propping was in place.	CFRP fabric sheets wrapped around columns,
2000	Barnes Bridge, A34/M56 link over M60, Manchester.	Deficiency in flexural capacity for the new 40 tonne HGV loading.	Bridge deck bonded with 5,500 m length of high modulus CFRP plates.

* Source: Extracted and compiled from professional magazines including the New Civil Engineer, Construction Repair, Concrete, and trading newsletters and brochures of construction related companies including: Balvac, SBD, Sika, Makers Industrial, DML, Du Pont, Feb MBT, Mouchel, Maunsell, Concrete Repaired Ltd etc. The trading names of the FRP products used in these strengthening projects have been removed.

1.6.2 Reasons for Using FRP Composites

There are many reasons, as well as advantages, in using advanced composites in the construction industry.

(1) **Sustainable Infrastructure** - A large part of the infrastructures in most developed countries, which were built some decades ago, are now facing large scale material degradation as highlighted in section 1.3. According to some of the leading experts in the field (Head, 1996, Scalzi *et al* 1999), the remedial work needed, which may require substantial repair and wholesale replacement in some cases, will be very expensive and cause massive traffic disruption to the already overcrowded infrastructure. These problems are serious enough to cause great concerns among the government authorities, as the predictions for the growth of national economies, which depend heavily on a sound national infrastructure, are being modified to take account of the possible effects. It becomes a top priority for governments to encourage the engineering community to find solutions for rapid and sustainable infrastructure repair and enhancement. FRP composite materials and adhesive systems are considered to be pertinent to play such a role, since they offer high strength, with potentially good durability and excellent corrosion resistance. Unlike steel, FRP composites are unaffected by electrochemical deterioration and can resist the corrosive effects of acids, alkalis, salts and similar aggressive chemical attacks under various temperatures (Hollaway, 1993).

(2) **Innovation in Construction** - The construction industry today, is still a relatively labour intensive and produces poorer quality products in comparison with the aerospace or car manufacturing industries. Many of the material corrosion problems outlined in section 1.3, may be attributed to poor workmanship (Head, 1996). The UK government agencies have recognised the need for new and innovative approaches to construction. The largest government funding body – the Engineering and Physical Sciences Research Council has issued calls for more research in "CMP - Construction as a Manufacturing Process (EPSRC, 1999)", which encourages the use of high quality system, with

reduced labour cost, improved safety and high construction speed. The availability of advanced fibre reinforced lightweight composites have great potential in addressing these issues. As Head (1996) remarked, the FRP materials "can be used on their own or with other materials; can be shaped into high quality modular systems in the factory; can be delivered to site faster at lower cost and can be unloaded and assembled more safely into large structures using robotics".

(3) **Costing** – The average price for carbon fibres dropped from US$20/lb in 1990 to US$6.50/lb in 1998 (Buyukozturk, 1999). Although the FRP materials are still more expensive than their conventional steel counterpart at the completion of a project, the whole life cost of FRP strengthened structures is believed to be lower. This is because FRP strengthened structures will have much less in-service maintenance need. The reduction of construction time also indirectly reduces the cost. Consider the Bible-Christian Bridge pier strengthening project, for example, even though the column wrapping strengthening work was the first of its kind in the UK, it took on average only just over one day for the strengthening part of the work on each of the three columns to be completed. At all times during the strengthening work, one lane of the A30 dual carriageway remained open to traffic. Had the conventional method of column enlargement with added reinforced concrete been used, the time it would have taken to complete the project, according to the local council official in charge of the work, would be at least 6 weeks. Peshkam and Leeming (1994) presented a cost comparison of bridge replacement against strengthening it with FRP composites. They estimated that a 40% of savings could be achieved. More recently, Robery and Innes (1997) presented a comparison of relative overall project cost for strengthening by steel, RC and FRP (e.g., Replark), it was shown that the average overall costs of strengthening structures by composites was just 60-70% of the steel strengthening costs.

(4) **Environmental Merits** – Another advantage of using FRP composites in construction is that they offer low energy consumption during the manufacturing process. The use of sustainable raw materials and advantageous properties such

as low thermal conductivity for reduced energy consumption, when used in buildings, will be of great benefit to preserving our natural environment.

(5) **Material Availability** – Since the ending of the cold war in the early 1990's, the market for advanced FRP composites, which were primarily developed for the defence and aerospace industries, has been drastically reduced. The material manufacturers have thus begun focusing their attention on the potentially very large construction market. However, as Head (1996) pointed out, the-large-volume-low-margin construction market is significantly different from the low-volume-high-profit-margin of the defence or aerospace industries, and manufacturers are studying the ways of mass production with minimum costs. The FRP materials for the defence and aerospace industries are not necessarily the best for application to structures, as there exist fundamental differences in material requirements. It is unlikely, for example, that the very high strength (up to 5,500 N/mm^2) of FRP composites will be of greater benefit to a civil engineering structure than a more common composite material with much lower ultimate strength (say 1750 N/mm^2). This will be demonstrated in Chapters 4 and 5. Consultations with a number of leading FRP composite materials manufacturers and suppliers in the UK confirm the candidate's suggestion that more research on FRP materials suitability for civil engineering needs to be carried out. It will require well co-ordinated and considerable investment and effort in research and development work from the material manufacturers as well as the civil engineering consultants, researchers, contractors and the clients. It is necessary to clearly specify, with the least modification to the existing material production process, what the most suitable FRP materials for civil engineering application are. Generally speaking, it is anticipated that the availability of FRP composites will continue with increasing supplies and better suitability for application in the construction industry.

(6) **Technical Advantages** – In comparison with mild steel, commonly used in the construction industry, FRP composites have higher strength to weight and stiffness to weight ratios. They also offer much better corrosion resistance, excellent fatigue and creep properties, low thermal conductivity and can be used

in combination with steel and concrete to achieve many desired characteristics. During the strengthening work of the A23 Bolney Bridge in East Sussex (Table 1.3) in 1992, some 38 tonnes of steel plates were added to the concrete deck, which involved numerous lap joints and anchor bolts, and increased the contract and labour costs significantly. Had FRP composite materials been used, only about 7.5 tonnes of CFRP plates would have been needed, and the installation process would have been much quicker (Peshkam, 1995). With regards to the behaviour of FRP strengthened elements in fire, limited studies carried out by Deuring in 1994 at EMPA, showed that the FRP strengthened beams had a much superior fire behaviour than their steel plated counterparts (see section 2.4.4.4). Due to their low thermal conductivity, the CFRP laminates gradually burnt at the plate surface causing the gradual loss of cross sectional area, and hence a phased overall reduction of beam strength and stiffness. The FRP plates did not become detached from the concrete beam until after over an hour in fire, whilst the steel plates became separated after only a matter of minutes of exposure. Karbhari (1997) presented a generic guidance on the material selection for bridge strengthening, comparing steel with FRP composites on a number of factors as shown in Table 1.5. It should be pointed out that these comparisons were made on the basis of material performance alone without considering the cost implications, which could change the overall suitability of the system for a given case.

Table 1.5 Comparison of Material Suitability (Karbhari, 1997)

Characteristic	Steel	CFRP	GFRP	AFRP
Relaxation & Creep	+	+	=	-
Moisture Resistance	=	+	-	=
Alkali Resistance	+	+	-	=
Thermal Stability	=	+	-	=
Resistance to Salt Water	-	+	=	=
Fatigue Behaviour	=	+	-	=
Performance Indicators: + Best; = Fair; - Poor.				

1.6.3 Disadvantages of FRP as Strengthening Materials

The significant disadvantage of FRP composite materials is that they lack the desirable ductility. All FRP composites have a linear stress-strain relationship until failure with no plasticity. This characteristic has caused great concern among the structural engineers, since it may cause a brittle failure mode, which should be avoided in civil and structural engineering. In Chapter 7 of this thesis, the ductility issue will be discussed and a new method of quantifying structural ductility will be presented.

Other concerns on the use of FRP composite as strengthening materials include its fire resistance, although previous researches have concluded that FRP materials have good fire resisting properties. More research still needs to be carried out on this topic. The proper functioning of FRP materials also greatly depends on the quality of the bonding adhesive system. In the extremely hot weather conditions when temperatures can reach high 40's or low 50's ^{o}C, the composite action between the FRP material and the concrete could be adversely influenced (See Chapter 3). In such cases, the suitability of the adhesives to be used should be carefully checked, and the properties should be correctly specified.

1.6.4 Significance of Current Research

Despite the fact that much research work on the flexural and shear strengthening of RC structures has been carried out, the FRP strengthening technique is still far from being accepted as a routine design option. There remain a number of issues to be resolved. The most pressing one is that currently there are no definitive official design codes or guidelines on strengthening design, engineers have to exercise their judgement and discretion on individual design cases. The UK Concrete Society has published design guidance (December 2000). This is expected to be the first phase of consultation documents and are likely to be subject to updating. The results of the current research would make a detailed contribution towards establishing a set of definitive design guides in the near future. Since FRP materials do not normally have any plasticity, the question, and even the definition of ductility of FRP strengthened structures, remains a major aspect of debate among researchers. This research intends to review all the

existing methods and find or suggest a suitable methodology for this extremely important issue in structural strengthening design.

There has been a tendency to use high factors of safety for the FRP materials, some proposals are using factors as high as 7.7 (Concrete Society, 2000). Whether this approach is "safe" as it is intended, is questionable, the current research intends to address the issue and make conclusive suggestions. In general, more research and development contribution, as is the purpose of the current study, is therefore vital for the civil engineering community to achieve a thorough understanding of the in-service and ultimate behaviour of FRP strengthened structures. The new materials and techniques will lead to an exciting new era, and permanently change the way structures have been strengthened for the past few decades.

1.7 AIMS, SCOPE AND STRUCTURE OF THE THESIS

1.7.1 Aims and Objectives of Research

From a comprehensive review of the FRP strengthening research activities, it can be seen that there is still a distinctive lack of design guidelines as stated in Section 1.6.4. The main objective of the current research, therefore, is to make a contribution towards the overall understanding and appreciation of the mechanical behaviour of FRP strengthened reinforced concrete beams and other flexural members. A set of design equations and guidelines based on the format of the current codes of practice used in the UK such as BS 8110, BS5400 and EC2, will be established. The specific aims of the research are:

a) To carry out a comprehensive and critical literature review of previous research work related to the flexural and shear strengthening using FRP composite materials.
b) To carry out an experimental investigation on the failure modes of FRP strengthened reinforced concrete elements at the Ultimate Limit State, and hence identify an acceptable mode(s) of failure.
c) To establish a new methodology of quantifying structural ductility for concrete members strengthened by FRP composites.

d) To develop a non-linear analytical model for predicting the structural behaviour of FRP strengthened RC flexural elements.

e) To propose a set of design equations for CFRP strengthened RC members including design procedures for flexure and shear, based on the laboratory study results.

f) To make other practical design recommendations for CFRP strengthening.

1.7.2 Research Methodology

In view of the large quantity of research work already carried out by other researchers, (to be presented in Chapter 2), the strategy for the current research project is to extract the most salient results from existing literature, and then concentrate more on the design aspects of FRP strengthening. The final design equations will be in similar format as the current UK codes of practice BS 8110, and the material properties used will be of a generic nature rather than individual manufacturer specifications. Since the research work is closely related to the practical application of FRP as strengthening materials, the candidate has made consultations in the past few years with leading experts in the industry. One of the supervisors, as a Director in charge of structural maintenance and repair in a major international civil engineering consulting firm, is an authority in concrete materials and structural repair himself. He has given valuable advice to the candidate on the latest development of repair materials, standards and FRP material application.

The main thread of the research is the result of combining extensive literature review, experts advice, experimental evidence together with analytical modelling and desk top study, and the candidate's own previous experiences as a structural designer.

1.7.3 Scope and Structure of the Thesis

The thesis is divided into nine interrelated chapters, each covering a specific subtopic. Chapter 1, as seen already, presents a general background of the history, the needs, application examples and current practices on structural repair and strengthening, and outlines the aims and objectives of the current research.

In Chapter 2, a comprehensive literature review on the technical aspects of FRP strengthening in flexure and shear is presented. Significant focus has been given to the latest research results published after the mid 1990's, while a summary and clear reference have been given to the earlier research work.

Chapter 3 includes discussions on the FRP material properties, and a brief introduction of the manufacturing techniques and processes. The structural requirements of the bonding adhesives are discussed, and methods of evaluating the mechanical properties of adhesives are also presented. The importance of surface preparation together with surface treatment techniques has been included.

Chapter 4 presents the main experimental investigation. The test results on four groups of FRP strengthened/reinforced beams are reported. The laboratory test set up, casting, testing, plate bonding processes are included, and the experimental data presented includes desk top analysis of the mechanical behaviour.

In Chapter 5, a non-linear analytical model based on the material constitutive laws has been developed to simulate the flexural response of FRP strengthened RC elements. The modelling results are then compared with the experimental data. A parametric study has been carried out to determine the influence of various factors on the flexural behaviour, and conclusions are drawn.

There exists an extremely sudden and brittle failure mechanism for some FRP strengthened RC beams, namely the premature tearing-off of the concrete cover at the internal reinforcement level, with FRP composites still well bonded to the torn-off cover. This failure mode is discussed in Chapter 6, and existing theories in estimating the plate-end normal and shear stresses or the failure load are presented, together with recommendations on measures to prevent such a dangerous failure mode.

The review of ductility measurement methods is included in Chapter 7, together with the study on moment redistribution in continuous RC beams strengthened by FRP composites. The differences between structural deformability and ductility are discussed, and a new method of quantifying the deformability index is proposed.

Recommendations for determining ductility are made, together with suggestions on how to improve structural deformability and ductility for FRP strengthened flexural members.

Chapter 8 presents the development of design guidance in accordance with the existing British Standards used in the industry. Design equations in flexure and shear are derived to include a number of design case studies. Conclusions are drawn on over and under strengthened sections.

Finally, Chapter 9 is a project summary, and major conclusions from the study are concisely presented. The limitations of the present work are highlighted and suggestions for further work are also included in this chapter.

CHAPTER 2

Strengthening of RC Elements Using FRP Composites – A Literature Review

2.1 INTRODUCTION

> *"The challenge in any research area is to harness the findings of different research groups to identify a coherent mass of data which enables research and practice to be better focused"* – **Professor Michael C. Forde** (1997).

It was indeed a great challenge for the candidate to do just that in the present study. This Chapter presents the most up to date research results on the bending and shear strengthening methods incorporating FRP composite materials. Much of the earlier work from mid 1970s to late 1980s on steel plate bonding had a profound influence on the subsequent research on FRP strengthening techniques. Comprehensive reviews of research work on steel plate bonding, have been presented by Jones and Swamy *et al* (1980, 1982, 1985, 1986, 1988, 1989), Ladner (1983), Charif (1983), Swamy *et al* (1987, 1995), Eberline (1988), Rahimi (1996), and Hollaway and Leeming (1999). The current review will consider only FRP strengthening works, it aims to be comprehensive but not exhaustive, special emphases will be given to the latest developments during the past four years.

2.2 A BRIEF REVIEW OF PAST RESEARCH

2.2.1 Flexural Strengthening - Major Pre 1996 Works

The early research work on FRP plate strengthening concentrated on the viability of the method. Most of the study was experimental. Reinforced concrete beams were strengthened with bonded FRP plates, usually Glass FRP (GFRP) plates, using various adhesives that had been used in steel plate bonding. The GFRP composite plates used in the early 1990s were generally of low strength (typically with failure strength less than that of the steel reinforcement yield strength) and of considerable thickness of up to 10 mm. The idea of using FRP composite plates in lieu of steel was first developed in Switzerland by Meier (1987) and Kaiser (1989). This was in the light of the problems associated with steel plate bonding as highlighted in Section 1.5.2.2. Unfortunately, the candidate has not been able to benefit from these reports as they were written in German. This section will present the main research work in the chronological order.

Saadatmanesh *et al* **:-**

The earliest work published in English can be traced back to the University of Arizona in the USA. Saadatmanesh and Ehsani (1989) presented a paper in a special ASCE congress, where they reported their pilot study of the behaviour of GFRP plated RC beams and the suitability of epoxy adhesives as bonding agents. In total five RC beams of 1.675 m in length were tested, with one as a control beam and the other four being bonded with 6.0 mm thick GFRP prelaminated plates, each using a different type of adhesive. The adhesives, which were tested on aluminium substrates, had typical shear strengths of around 14 N/mm^2. It was found that the ultimate strength of the beam plated with the flexible epoxies did not show any increase over that of the unplated control beam, an indication that none or only minimum shear stress transfer had taken place between the concrete beam and the GFRP plate. On the other hand, the beam plated with the most rigid epoxy resin did not facilitate any ultimate strength increase either, the plate "peeled off" in a sudden and brittle manner shortly after tensile cracks in the concrete emerged. The other beam strengthened using a more viscous, polymer modified adhesive showed much increase in strength as well as stiffness, when it was

loaded to failure. The cracks in the concrete tension zone were more evenly distributed, and with reduced widths when compared to the control beam.

This study confirms the suggestion that a suitable adhesive system with approriate level of strength and flexibility is crucial to an effective FRP strengthening, which in essence, is also true for steel plate bonding, albeit the latter usually incorporates bolts anchorage as well. The structural requirements of adhesives for FRP strengthening will be discussed in more details in Chapter 3.

Following this initial study, Saadatmanesh and Ehsani (1990b, 1991) and An et al (1991), continued testing another five doubly reinforced rectangular beams and a T-beam. All of the beams were again strengthened with 6.0 mm thick GFRP plates, and using the epoxy identified as most suitable in their earlier study discussed above. This was a two-part, rubber-toughened epoxy with a consistency similar to that of a cement paste. It is worth pointing out at this stage that the GFRP plates had an average ultimate tensile strength of only 400 N/mm^2, even lower than the 456 N/mm^2 yield stress of the steel bar used in the study. The rectangular beams were 455 mm deep by 205 mm wide, while the T-beam had a flange width of 610 mm, flange thickness of 75 mm, and its overall depth was 455 mm. The beams were reinforced with typical tension reinforcement ratios (Beam A –1.8%, Beam C – 0.32%, all others including the T-beam - 1.2%). All beams had two compression reinforcing bars of 13 mm diameter, and were heavily reinforced in shear (Typically T13@ 150 mm c/c, A_{sv} = 265 mm^2) to ensure flexural only failure. The beams were all simply supported, the effective span was 4.575 m, and were tested under a 4-point loading configuration with the pure bending region of 0.61 m in the mid span of the beam.

Test results showed increase in final failure load, and decrease in deflection against the calculated values. No control beams were used to provide comparison on the experimental results. It was noted that all of the beams failed in almost the same way, the peeling-off of the GFRP plates in 4 beams and "debonding" of the concrete cover at the reinforcement level. The study concluded that GFRP plated RC beams achieved significant increase in the beams flexural strength, and the increase in ultimate flexural strength was greater in beams with lower steel reinforcement ratios.

This was one of the pioneering works on FRP plate strengthening, there were, however some shortcomings in the study.

a) The study did not include tests of any control beam, the comparison was made with predicted values only.
b) There was no convincing evidence that the GFRP plates had any significant contribution to the beams ultimate strength.
c) For the tension reinforcement ratios that were used, it was unnecessary to provide compression reinforcement in the pure bending zone.
d) The length of the pure bending zone of 0.61m, was much smaller than the shear span of 1.983 m.
e) It seemed that the final failure of the beams did not occur in the bending zone, thus it would be difficult to judge the flexural behaviour and hence the increase in ultimate flexural strength.

Similar flexural tests of CFRP strengthened RC beams are intended to be carried out in the current study, where the above issues will be addressed and reported in Chapter 4.

Meier *et al* :-

In Switzerland, Meier and Kaiser (1991) and, Meier (1992) reported their work progress at EMPA on the replacement of steel plates in the strengthening of RC beams by the lightweight CFRP laminates. For the first time, CFRP plates of ultimate tensile strength of 1482 N/mm^2 and elastic modulus of 115 kN/mm^2 were reported to have been used in the repair of the Ibach Bridge (See Section 1.6.1). Meier summarised that most highway bridges in the developed world were built during the boom in highway bridge construction after 1945, and were now facing material deterioration. Modern materials such as FRP composites would, therefore, play an important role in repair and rehabilitation. However, he warned that "even in the future they (FRP composites) will not replace classical materials such as steel, concrete and wood but rather supplement them" (Meier, 1993). In the same year, Meier *et al* (1993) presented a more detailed study on CFRP strengthening. Loading tests were performed on twenty-five 2 m span beams and one beam of 7 m span. The experimental study drew the following conclusions.

(a) The strain-compatibility method is valid in the section analysis of CFRP strengthened beams.

(b) Shear cracks may lead to peeling-off of the strengthening sheets, and hence the shear crack development should be considered at the design stage.

(c) Flexural cracks are spanned by the CFRP sheet and do not influence the loading capacity.

(d) CFRP strengthened beams should result in a much finer crack distribution compared to the unstrengthened control beam (Meier and Kaiser, 1991).

(e) The difference in the coefficients of thermal expansion between the CFRP composites and concrete does not affect the loading capacity.

The study also found the following failure modes of the CFRP strengthened beams.

- Tensile failure of the CFRP sheet.
- Concrete failure in compression.
- Peeling-off of CFRP sheet.
- Shearing of concrete in the tension zone.
- CFRP interlaminar shear.
- Failure of tension steel bars in fatigue tests.

It was stated that the CFRP peeling-off failure was due to an uneven concrete surface. For thin sheets of less than 1 mm, an extremely even bonding surface would be required, otherwise the CFRP sheets would slowly peel off during loading. The study also recommended that for design purposes, the CFRP sheets should fail during yielding of steel reinforcement and before the compressive failure of the concrete. Furthermore it stated that failure of the steel bar should not occur before reaching the permitted loads.

Ritchie *et al* :-

Additional studies were carried out at the Lehigh University in the USA. Ritchie *et al* (1991) tested 16 RC beams of 2.4 m simple span, and of cross section 300 by 150 mm. Fourteen of the beams were externally strengthened with either Glass, Carbon or

Aramid FRP plates, while the other two were used as control beams with the internal tension reinforcement ratio of 0.65% for all beams. All beams were over designed in shear to avoid brittle shear failure.

Tests results of these beams showed an increase in stiffness of between 17% to 99% over the unplated beams, and similar strength increase of between 19% to 99%. The study concluded that despite the reduced ductility of the FRP strengthened beams, the new performance would probably be still acceptable through proper design.

It was concluded that since the maximum recorded deflections in these beams represented a span-deflection ratio of less than 100 which is easily detectable.

This conclusion is, however, misleading. It confuses the span deflection with the structural ductility. It is possible that even though high magnitude of span deflection is present, the ductility of the FRP strengthened section is not necessarily acceptable, and the final failure mode could still be in a brittle manner.

Triantafillou *et al* :-

Triantafillou and his associates carried out much research work on FRP strengthening at the Massachusetts Institute of Technology (Deskovic *et al* 1995a and 1995b). Triantafillou and Plevris (1992) tested eight small concrete beams, all reinforced with two 4.6 mm diameter bars ($\rho_s = 0.39\%$). One beam was used as a control while the other seven were strengthened by high strength (1450 N/mm^2) CFRP sheets 1070 mm long, and between 0.20 and 1.90 mm thick. The percentages of CFRP reinforcement (ρ_{fc}) for the seven beams were 0.1, 0.13, 0.43, 0.43, 0.59, 0.59 and 1.26 respectively. The beams were all of 1350 mm in length with an effective simple span of 1220 mm, the cross section was 127 by 76 mm, and the effective depth 111 mm. The adhesives were applied in two steps, firstly a low viscosity epoxy was applied to the concrete and cured for six hours, before a high viscosity epoxy was applied to both the concrete and the CFRP sheets, and cured for three days.

The failure loads of the CFRP strengthened beams increased from 53% to 335% over the unplated control beam, while the mid span deflections at failure were shown to be

typically halved compared to the conventionally reinforced control beam. Of the eight beams tested to ultimate failure, the control beam failed by tension reinforcement yielding, the two beams with the two lowest CFRP reinforcement ratios (0.1% and 0.13%) failed by steel yielding first followed by CFRP rupture. All other beams failed either by debonding (tearing-off of the concrete cover, as is suggested and preferred in the current study), or FRP peeling-off. The study concluded that strengthening RC beams by CFRP sheets appeared to be a feasible way of increasing the load carrying capacity and stiffness characteristics of existing structures. It confirmed that concrete cracking had an important role in the peeling-off mode of failure. It concluded that the FRP peeling-off mechanism was related to the thickness of the CFRP composites, there appeared to be a critical thickness, beyond which brittle failure occurs without CFRP materials flexural strength being fully utilised, and as a result the ductility of the beam was adversely affected.

Analytical models were also developed in the above study to predict the ultimate loads under various failure mechanisms. These equations were believed to be the first in attempting to find an analytical means of correlating the experimental results. The design approach used was based on the strain compatibility theory, the ultimate strain of concrete was taken as 0.003.

For the case of steel yield-FRP rupture, the equilibrium of forces that defines the relationship between the ultimate moment capacity, the neutral axis depth, the material strength and reinforcement ratio, is shown in Equation (2.1). All notations are defined in the Notations section on page xx.

$$\frac{M_u}{bd^2 f_{cu}} = \frac{f_y}{f_{cu}} \rho_s \left(1 - \frac{y}{d}\right) + \frac{E_{fc} \varepsilon'_{fc}}{f_{cu}} \rho_{fc} \left(\frac{h}{d} - \frac{y}{d}\right) \tag{2.1}$$

For steel yielding followed by concrete crushing,

$$\frac{M_u}{bd^2 f_{cu}} = 0.85\xi \frac{x}{d}\left(\frac{h}{d} - \frac{\xi x}{2d}\right) - \frac{f_y}{f_{cu}} \rho_s \left(\frac{h}{d} - 1\right) \tag{2.2}$$

and for concrete compression failure,

$$\frac{M_u}{bd^2 f_{cu}} = 0.85\xi\frac{x}{d}\left(\frac{h}{d} - \frac{\xi x}{2d}\right) - \frac{0.003\left(1-\frac{x}{d}\right)}{\frac{x}{d}} E_s \rho_s \left(\frac{h}{d} - 1\right) \qquad (2.3)$$

Using the BS 8110 simplified rectangular stress block, ξ equals to 0.9, and for the Eurocode EC2 this value is 0.8.

Hutchinson *et al* :-

Meanwhile, similar research work started at Oxford Brookes University in the early 1990s. Hutchinson and Rahimi (1993) reported an experimental study in which twelve 2.3 m long RC beams with steel reinforcement ratio of 0.65% were strengthened with CFRP plates and tested. It was reported that the ultimate load carrying capacity of most of these beams increased by up to 230% over the unplated beams. They concluded that the concrete beams which were strengthened after being preloaded, showed no difference in behaviour to those which were strengthened without preloading.

Sharif *et al* :–

In Saudi Arabia, Sharif *et al* (1994) tested ten RC beams of 1250 mm by 150 mm by 150 mm, with steel reinforcement ratio of 0.98%, while two 6 mm compression bars were provided. All beams were preloaded to 85% of the ultimate load, and permanent central deflections of 4.5 mm to 5.4 mm were recorded. These damaged beams were then repaired by FRP materials, which consisted of three layers of woven roving fibreglass bonded in a plastic matrix, and with a ultimate strength of 170 N/mm^2. The study concluded that the shear and normal stresses at the plate curtailment increase with the increasing of FRP plate thickness, leading to premature failure by plate separation and tearing-off of concrete cover. Steel anchoring bolts were used at the plate ends on some beams, which eliminated the plate separation problem but the beams failed due to diagonal tension cracks. Furthermore it was concluded that the repaired beams developed sufficient ductility in the process of increasing their flexural capacities despite the brittleness of the FRP plates.

Chajes *et al* :–

Chajes *et al* (1994) reported more four-point loading tests on fourteen beams of similar sizes to those tested by Triantafillou and Plevris (1992). The beams were strengthened

by Glass, Carbon and Aramid FRP fabric sheets. A 36-57% increase in flexural strength, and a 45-53% increase in flexural stiffness over the control beam were reported. The beams strengthened with CFRP and GFRP sheets failed by rupture of the composite sheets, and the Aramid strengthened beams failed by crushing of concrete in the compression zone.

A collection of other works and the latest development by 1995 were edited by Taerwe (1995), by this time the advantages of FRP over steel plate strengthening were well recognised. Carbon FRP composites started to emerge as the strong candidate in material selection for strengthening works.

2.2.2 Flexural Strengthening - More Recent Works (1996-2000)

2.2.2.1 Introduction

The worldwide research interests in FRP strengthening have grown rapidly since the middle 1990's. Field applications were reported for the first time in 1996 in the UK (NCE, 1996) and Canada (Alexander *et al*, 1996). Clarke (1996) outlined the following key areas that needed further development for the FRP application in the design of durable structures to move forward.

- Establish standards for the production of FRP materials.
- Establish test methods, particularly accelerated durability tests.
- Establish design standard for both new build and repair.
- Establish liaison between suppliers and users of FRP.

Although, at the time, the above aspects were specifically related to the FRP materials being used as embedded reinforcement, they were also pertinent guides for developing new methodologies for the strengthening of RC structures using externally bonded FRP composites.

2.2.2.2 Database analysis

In what follows, many research results with regard to the design aspects have since been published (El-Badry, 1996). Bonacci (1996) reviewed a database of 64 FRP strengthened RC beams from 10 separate experimental studies most of which are

reviewed in the proceeding section. He also analysed the trend in failure modes together with strength and deformability. One third of the FRP strengthened beams showed an increase in strength of 50% or more over the control beams. He summarised that of all the reported beam tests, the failure modes were as follows:

- Debonding of FRP: 41 beams (64%)
- Tensile fracture of FRP: 14 beams (22%)
- Shear failure in beam: 5 beams (8%)
- Concrete crushing: 4 beams (6 %)

This highlighted the fact that debonding, or tearing-off of concrete cover as suggested in the current study, is the most prevalent mode of failure. It is also interesting to note that beams that failed in this manner had actual ultimate strength increase of over 100% against the conventionally reinforced control beams. Chapter 6 of the thesis is therefore dedicated to discussing this important aspect of behaviour. Bonacci also concluded that with proper design, externally strengthened beams could develop considerable deformation before failure.

2.2.2.3 Major studies

The ROBUST Project-:

Through the project ROBUST (st**R**engthening **O**f **B**ridges **U**sing polymeric compo**S**ite ma**T**erials), a UK government DTI-LINK supported Structural Composites Programme which started in 1994, Oxford Brookes University has been active in research work in FRP strengthening. Hutchinson and Rahimi (1996) summarised their research progress. A maximum tensile stress of 1500 N/mm^2 was reported to have been reached in the thinnest CFRP laminate in the strengthened beams, achieving a strength increases of up to 180%.

Quantrill ***et al*****:-**

Another ROBUST partner, the University of Surrey, conducted further research in this field. Quantrill *et al* (1996a) reported testing of 5 CFRP plate strengthened RC beams. The size of the beams was 1000 mm x 100 mm x 100 mm, with 3R6 and 2R6 steel bars as tension and compression reinforcement respectively. Test results confirmed the

effectiveness of FRP strengthening which showed an increase of 140% to 274% in ultimate load of the plated beams against the control beam. It is interesting to note that the plate end anchorage system had a profound influence in the failure mechanisms. All beams with plate end anchorage systems had recorded better performance than those without. One of the beams (B7) had its full length bonded with CFRP plate, it failed by concrete crushing after achieving the highest strength enhancement of 274%. Beam B6 which had an 860 mm length CFRP plate bonded to its soffit with no end anchorage, failed by the premature mode of concrete cover tearing-off, increased only 140% in its ultimate strength. This again confirms that the tearing-off mode of failure is likely to be the most important consideration in strengthening design. The study concluded that reducing the plate area results in the reduction of strengthening and stiffening and causes the ductility and the longitudinal FRP plate strain for a given load to increase.

Prediction of Plate End Stresses:-

When the values of the combined shear and normal stresses at the plate end(s) of FRP strengthened beams exceed the shear strength of the concrete, then tearing-off of concrete cover type of failure will occur. A rigorous analysis of the plate end stresses in steel plate bonding was developed by Roberts and Haji-Kazemi (1989). Although originally intended for steel plate bonding, the model was thought to be suitable for any materials since it involved an elastic and analytical solution. The original model was considered too complex for normal design purposes, and a simplified and approximate method was then published in the same year (Roberts, 1989).

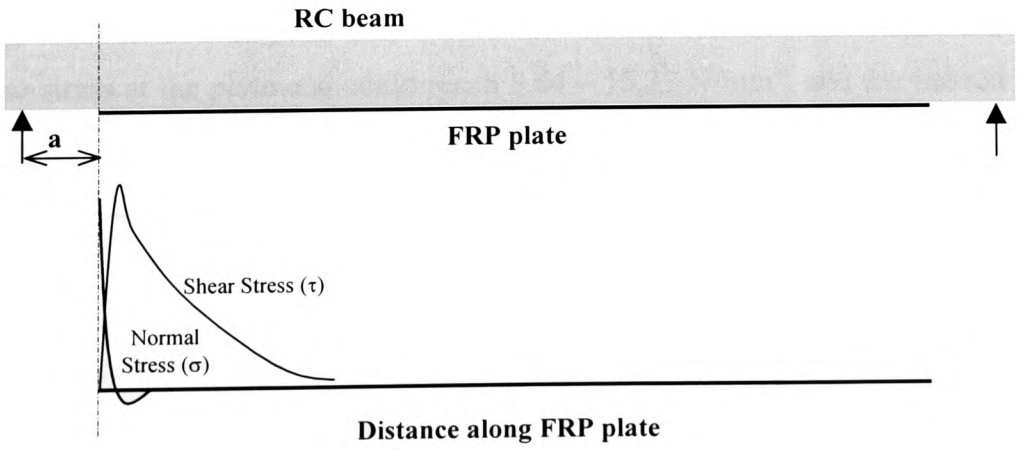

Figure 2.1 Stress Concentration at FRP Plate Ends (symmetrical)

It was found that the shear stress at the plate end would increase from zero to peak value, over a very short length of the adhesive layer, of the order of the adhesive thickness. The normal stresses or peeling stresses, which was influenced by the stiffness of the adhesive layer, were also confined to a short length at the plate end. It was concluded that the maximum shear and normal stresses, as indicated in Figure 2.1, can be realistically estimated as:

$$\tau_{max} = (V_o + M_o\{\frac{G_a b_a}{t_a E_p b_p t_p}\}^{0.5})\frac{b_p t_p}{I b_a}(h + \frac{t_p}{2} - x) \tag{2.4}$$

$$\sigma_{max} = \tau_{max} t_p (\frac{E_a b_a}{4 t_a E_p I_p})^{0.25} \tag{2.5}$$

where V_o and M_o are the applied shear force and bending moment at the plate cut off position. However, It was suggested that M_o be replaced by M*, which is the moment at a further distance of $(h+h_p)/2$ away and towards the middle span of the beam from the plate cut off point. If τ_{max} is known, then the above equations can be rearranged to predict the applied load, P_o, which causes the premature failure of concrete cover tearing-off, as follows:

$$P_0 = \frac{2\tau_{max}}{[1 + (\frac{t_p + t_c}{2})(\frac{G_a b_a}{t_a E_p b_p t_p})^{0.5}]\frac{t_p b_p}{I b_a}(h + \frac{t_p}{2} - x)} \tag{2.6}$$

In an accompanying paper published in the Magazine of Concrete Research, Quantrill *et al* (1996b) used the above simplified analytical procedure to predict the shear and peeling stress at the FRP plate end. It was reported that the maximum theoretical values of shear stress at the plate end could reach 8.84 – 15.32 N/mm^2, and the normal peeling stress 6.29 – 12.97 N/mm^2 for the prematurely failed GFRP strengthened beams with some form of end anchorage. For those unanchored GFRP plated beams, these plate end shear and normal stresses were estimated to be 6.97 – 9.62 N/mm^2 and 4.96 – 7.36 N/mm^2 respectively. These stresses seem to be almost unbelievably overestimated, since the horizontal shear stress of the concrete -mainly the contribution from the concrete tensile strength -is much lower than that presented in the paper. The study concluded that:

- The maximum values of plate end shear and normal stresses for CFRP strengthened beams appeared to be higher than those of GFRP strengthened beams.
- Beams with thicker adhesive bondlines appeared to sustain higher levels of shear and normal plate end stresses.
- The addition of side plates around the soffit plate ends appeared to only slightly increase the shear and normal stresses before failure occurred.
- FRP plates seemed to be able to sustain higher shear and normal stress than would steel plates before plate separation failure occurred.

In the current study, equations 2.4 - 2.6 were found to be inappropriate for estimating shear and normal stress values when tearing off failure occurs, which suggests that there may be fundamental differences in the tearing-off failure mechanisms between the steel and FRP plates bonded beams. (see Chapter 6)

Garden *et al*:-

Garden *et al* (1997) tested a series of RC beams. The beam sizes and reinforcement details were the same as that of Quantrill discussed above. The main parameters studied included the length and thickness of CFRP plates, the shear span variation and the end anchorage system. In total 16 CFRP strengthened beams were tested, 6 of which had end anchorage in the form of a reaction force normal to the plate or GFRP angles. A further two beams were used as unplated controls. Out of the 16 plated beams, all the ones without end anchorage failed by cover separation (tearing off), however, 4 out of the 6 anchored beams also failed by cover separation under the supports. The results showed that the ultimate capacity of the beam with GFRP end anchorage angles was only 1 kN higher than its counterpart without end anchorage. The researchers concluded that:

(a) CFRP materials are well suited for the upgrading of civil engineering structures. All the disadvantages associated with steel plate bonding can be overcome by using FRP composites instead.

(b) CFRP plates bonded to the tension face of concrete can reduce concrete tensile strains, and hence form narrower cracks.

(c) Ultimate failure of CFRP strengthened beams, typically tearing-off of concrete cover, is due to the longitudinal shear stresses in the adhesive layer. These stresses lead to the fracture of the weakest component of the plate-concrete bond, namely the concrete.

(d) More extended anchorage length results in greater ultimate moment. Anchorage mechanism can also act as a barrier to contain concrete fragments even after failure.

(e) Bonded CFRP plates increase the stiffness of the RC beams when the original stiffness of the member has degraded significantly, e.g., internal reinforcement yielding.

The above work had clearly demonstrated the potential of CFRP strengthening technique. It was evident however, that further experimental and analytical works were still needed to validate and expand these preliminary conclusions.

Nanni *et al*:-

In June 1997, Nanni (1997) published an overview under the title of "New technology becomes mainstream – CFRP strengthening", the article reported the latest CFRP strengthening application projects in Italy. These included the structural restoration of an industrial and a residential building, an exhibition pavilion, viaduct columns and bridge girders. All five projects were completed within a six months period in late 1996, it became evident that this new technology of structural rehabilitation would be one of the exciting developments that take the construction industry into the new century. Meanwhile, Arduini and Nanni (1997) conducted an experimental study on the strengthening of pre-damaged RC beams. Ten precracked beams were subsequently strengthened with CFRP sheets and loaded to ultimate failure. The study found that the performance of the strengthened precracked beam without sealing the cracks "were not significantly different from that of the strengthened virgin specimens". It also pointed out that the effectiveness of FRP strengthening was affected by the RC cross section shape and the amount of original reinforcement present. Furthermore, the carbon fibre stiffness, fibre direction and number of plies were said to have significant influence on the performance of the strengthened beams.

Garden *et al*:-

A continuation of experimental study on the anchorage length of CFRP strengthened beams was conducted by researchers at the University of Surrey (Garden *et al*, 1998). In a four-point bending load configuration, the anchorage length is defined to be the distance between the FRP plate end near the support and the loading point near mid span of the beam. In a previous study (Garden *et al*, 1997), it was found that if the full length of the beam had been bonded by the continuous CFRP plate (the full end anchorage length), with the support reaction normal to the plate, it would act as a barrier and help contain the fragmented concrete at ultimate failure. In the later study where the CFRP plate was cut at a distance from the support, cover separation was observed as shown in Figure 2.2. This was a typical "tearing-off" of concrete cover type of failure, where the concrete cover up to the internal steel reinforcement is separated from the steel bars but still well bonded to the composite plate.

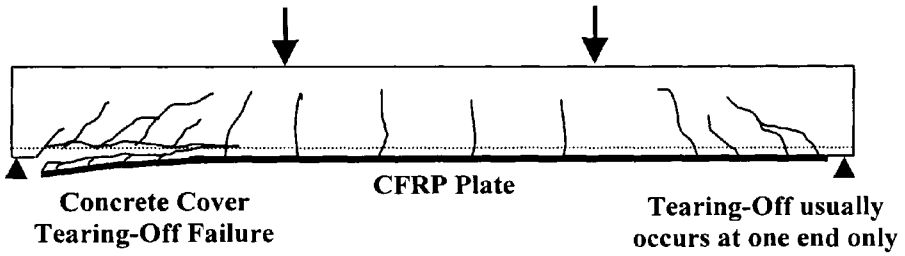

Figure 2.2 Typical Tearing-Off of Concrete Cover Reported in Literature

The study reported that such "cover separation" type of failure occurred in the shear span only. It also noted that the thickness of the separated cover and the length of the plate over which it remained bonded, were influenced by the shear/span depth ratios. Similar failure mechanisms were observed in the presented study. In addition, tearing-off in the zero shear regions, where the bonded plate length was less than the length of the pure bending zone, had also been evident in the current set of laboratory tests. Furthermore, the authors reported the maximum tearing-off length seemed to stop at the load point. In the current study, it was found that such a tearing-off failure mode, although only occurring at one end, could extend to as far as the middle span of the beam. The influencing factors are presented in Chapter 6. In the same study, Garden *et al* also load tested one 4.5 metres long four-point loaded beam and five 1.0 metre long cantilevers, a "partial cover separation" type of failure was reported. The term "partial

cover separation" was used to indicate failure in which "the internal reinforcement was exposed over only a part of the shear span", and a thinner layer of the concrete cover remained bonded to the rest of the plate length. The research concluded that the failure mode and the ultimate load were affected by the value of shear span to effective depth ratio. Under a low value of shear span/depth ratio, failure would be associated with longitudinal shear stresses in the adhesive at the ends of the plate. These stresses "lead to the fracture of the weakest component of the plate/concrete bond, - the concrete." This suggestion was also made in the team's earlier study reviewed above (Garden *et al*, 1997). This study certainly confirmed again that tearing-off failure was a common phenomenon in FRP plated beams. To a certain extent, this fact contradicts the conventional claim that only steel plate bonding needs end anchorage such as bolting which is not suitable for FRP plates.

In a separate study at the University of Sheffield (Swamy and Mukhopadhyaya, 1999) also concluded that plate debonding was a major problem associated with CFRP plate-bonding technology. However, whether the shear span to beam depth ratio is the only or most important factor that influences the tearing-off failure mode still remains questionable. The candidate will attempt to address this important topic in more detail in Chapter 6.

Other main FRP composites related research centres include the Intelligent Sensing for Innovative Structures (ISIS) group in Canada (www.isiscanada.com) and the Sheffield University based "ConFibreCrete" (www.shef.ac.uk/uni/projects/tmrnet/home.html) where the FRP in construction and design issues are currently being investigated.

2.3 MAJOR RESEARCH WORK IN SHEAR

Reinforced concrete beams or slabs are usually designed such that the flexural failure will occur before the members fail in shear, this is to avoid the brittle nature of the latter. In many existing structures it is often found that main elements such as bridge girders have insufficient shear capacities. Strengthening in shear is therefore of the same relative importance as flexural strengthening.

Shear Model by Al-Sulaimani *et al*:-

Among the early research works on FRP shear strengthening was that carried out by Professor Sharif's team at the King Fahd University of Petroleum and Minerals in Saudi Arabia (Al-Sulaimani, G. J. *et al*, 1994). Sixteen RC beams with low internal shear reinforcement were preloaded until the first shear crack appeared before they were repaired, using externally bonded GFRP plates to enhance the shear capacity. The 3 mm thick GFRP plates, which had a ultimate tensile strength of 200 N/mm^2, were made of three layers of woven roving fibre glass embedded in a plastic matrix. Three different repair configurations were used for external shear strengthening as shown in Figure 2.3. Test results indicated that using external bonded GFRP plates for shear strengthening was potentially a viable technique. The use of GFRP shear strips and shear wings resulted in similar increase in beams shear capacity. The failure of shear strips and wings was caused by GFRP plate peeling-off when the maximum shear stress at the bottom of the strips or wings reaches the interface shear strength, this behaviour was noted to be similar to that associated with flexural strengthening.

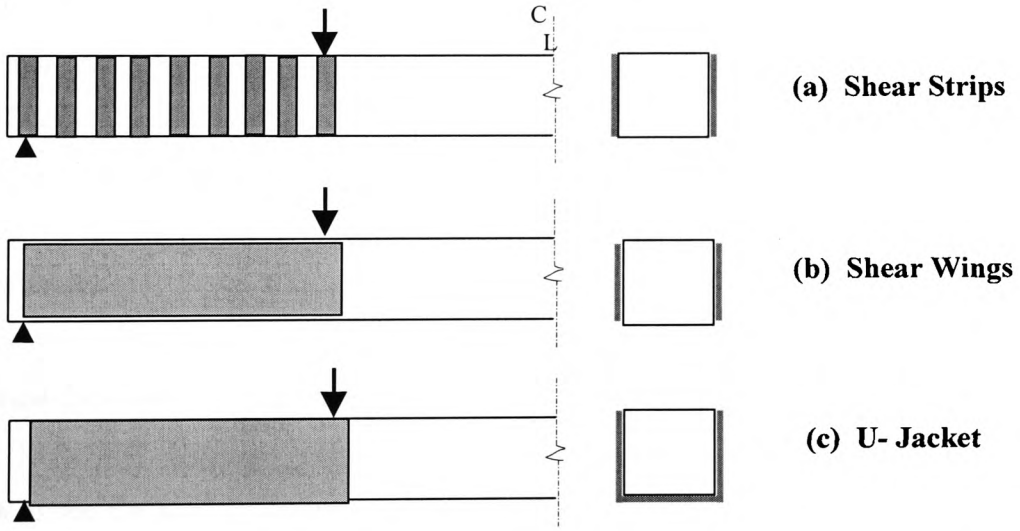

Figure 2.3 Three GFRP Shear Strengthening Schemes Used by Al-Sulaimani *et al*

The authors proposed three equations for evaluating the contribution from the FRP fabrics to the beams shear capacity. These were expressed by V_{ps}, V_{pw} and V_{pj} for the three repair schemes respectively as follows. They were based on the assumption that the average shear strength of the FRP concrete interface was 0.8 N/mm^2.

$$V_{ps} = \frac{2F_p d}{S_p} = \frac{2[\tau_{ave}(\frac{b_s h_s}{2})]d}{S_p} \quad (2.7)$$

$$V_{pw} = 2F_p = 2[\tau_{ave}(\frac{dh_w}{2})] \quad (2.8)$$

$$V_{pw} = 2F_p = 2[\tau_{ult}\frac{dh_j}{2})] \quad (2.9)$$

The study concluded that all three shear repair schemes restored the stiffness of the beam, which was degraded during the preloading stage. It was found that shear repair by the U-jacket method was the most effective one. No plate peeling-off was observed in these beams and the increase in shear capacities were significant which resulted in flexure failure of the beams. Furthermore the authors also noted that flexural repair had no significant effect on the beam stiffness at the reloading stage.

Although the work did show that shear strengthening was viable, the equations (2.4) – (2.6) are considered unrealistic and unrepresentative. These are all based on a constant FRP concrete interfacial shear stress of 0.8 N/mm^2, which is obviously an over simplification. The actual bond strength is likely to be affected by the type of composite and the concrete properties, as well as the adhesive mechanisms.

Chajes *et al*:-

Shortly after the work reported above, researchers at the University of Delaware published their work on the strengthening of RC beams using FRP fabrics (Chajes, *et al*, 1995). Eight RC T-beams were externally bonded with Carbon, Glass or Kevlar FRP fabrics in the form of a continuous U-Jacket to the soffit and web of the beam. For the wrapped beams, initial cracking occurred at higher load than that of the control beams. All beams failed in shear as no internal shear links were provided. The failure mode was brittle as expected of any shear failure. Inclined cracks were observed to occur at the same region as the control beams. No fabric debonding from the concrete surface had been noted. Just prior to failure, the strain measurement of the fabrics indicated that the fabrics had not reached their tensile capacity, however, all CFRP and GFRP fabrics immediately failed by being torn along the diagonal shear crack where the failure beam

failure was initiated. The eight FRP strengthened beams had ultimate strength increase of between 59.6% and 151.2% over the unstrengthened control beams. These excellent results clearly demonstrated the viability and effectiveness of using FRP composites for external shear strengthening.

Sato *et al*:-

Researchers in Japan also reported similar shear strengthening schemes. Sato *et al* (1996) tested five CFRP strengthened beams, and ultimate strength increases of between 69.7% and 129.3% were recorded. They concluded that CFRP sheets could significantly increase the shear capacity. CFRP attached to three faces (side-bottom-side) of the beams had performed better than CFRP sheets attached only to the two sides of the beams. The study also suggested that shear forces carried by the CFRP sheets was greater than that carried by the internal steel links since bond characteristics of CFRP sheets was better than the links. However, it was noted that four out of the five CFRP strengthened beams had CFRP sheets peeling-off from the concrete surfaces, which could lead to the assumption that the tensile stress in the CFRP sheets was high, or the bond strength at the CFRP concrete interface could have been exceeded.

Triantaffilou:-

In Greece, Professor Triantaffilou continued his research on FRP flexural and shear strengthening (Triantaffilou, 1998). He summarised the available experimental evidence in the literature and stated that failure of FRP reinforcement may be peeling-off or by tensile fracture at a stress which may be lower than the tensile strength of the FRP. The latter was because of the stress concentrations at locations such as the rounded corners or the debonded areas. In practice the shear failure mode of FRP strengthened beams may be a combination of peeling and FRP fracture, this makes the quantifying of the contribution from FRP composites to the total beam shear capacity a rather difficult process. Using the truss analogy and a simplified stress distribution pattern, the FRP contribution to shear capacity was defined by the following model:

$$V_p = \frac{0.9}{\gamma_f} \rho_f E_f \varepsilon_{f,e} b_w d(1+\cos\alpha)\sin\alpha \qquad (2.10)$$

In the above equation, the core issue is the determination of the effective FRP strain, $\varepsilon_{f,e}$, which depends on the area of FRP-concrete debonded interface. In previous studies, this strain was usually assumed to be constant. Triantafillou suggested that $\varepsilon_{f,e}$ could be approximately expressed as inversely proportional to the axial rigidity $\rho_f E_f$. In what follows, Khalifa *et al* (1998) experimentally determined the effective FRP strain for several rigidities of FRP sheets, and suggested using the following empirical equations:

$$\varepsilon_{f,e} = 0.0119 - 0.0205(\rho_f E_f) + 0.0104\,(\rho_f E_f)^2 \quad (\text{for } \rho_f E_f < 1) \tag{2.11}$$

$$\varepsilon_{f,e} = 0.00245 - 0.00065(\rho_f E_f) \quad (\text{for } \rho_f E_f > 1) \tag{2.12}$$

These equations seem to be heavily case dependent, and may not be applicable to a generic strengthening situation. For example, an axial rigidity of 2.9 N/mm^2, as a typical CFRP strengthening strip used in the current experiments, leads to a strain of only 0.000560 at failure, which is unrealistically low.

In the present study, experimental work confirmed that failure of FRP may be a combination of debonding and tensile fracture, attempt will be made to validate the existing theoretical models and identify the appropriate method for evaluating the FRP shear contribution.

Swamy *et al*:-

At the University of Sheffield, the research team led by Professor Swamy conducted more investigation on shear strengthening by external plate bonding (Swamy *et al*, 1999). In an experimental programme, ten full size RC beams were strengthened in flexure and shear by externally bonded steel or GFRP plates and U-shaped strips. Confinement plates were also used at the loading positions and compression zone to prevent early destruction of compression concrete. Two unplated beams were used as controls, one (SBB2) without any internal shear links and the other (SBB1) was provided with about 50% of internal shear reinforcement required for a flexure failure. Tests of the control beams indicated that the presence of internal shear reinforcement, even though inadequate, had significantly over performed the one without internal shear

reinforcement, with an 88.6% increase in the failure load. Other FRP strengthened beams had ultimate strength increase over the control beam (SSB2) of between 6.5% and 49%. It was noted, however, that only one beam failed in shear (NS1) which had a shear strength increase of just 12.2% against the control beam with inadequate internal shear links. Other beams failed mostly in flexure with diagonal shear cracks as would be expected of any typical under-reinforced RC beam. This confirmed that external shear reinforcement had been effective in transferring the brittle shear failure to a more ductile flexural failure, but the fact that the external shear reinforcement did not fail made it more difficult to quantify their shear capacity contribution. The authors suggested that the failure criterion of the external shear reinforcement was governed by the "anchorage efficiency" rather than by the tensile strength of the strengthening material. They concluded that the exact mechanism of failure of RC beams strengthened in shear was not clear, and it was not possible yet to quantify precisely the shear contribution of the various bonded plate components. Nevertheless, a model for predicting the average interfacial shear resistance between the U-shaped strips and the concrete was suggested by the authors as follows:

$$f_{av} = \frac{(v - v_c) b_v d s_p}{2 b_s L_b d} \tag{2.13}$$

This expression is fundamentally different from that of Triantafillou (1998), as discused in the preceding section. The present study will attempt to make contributions to the argument by analysing and comparing all the aforementioned shear models, presenting and justifying evidence based on the current experimental results.

2.4 FATIGUE, CREEP, DURABILITY, FIRE AND IMPACT LOAD

Although not covered in the current study, the fatigue, creep and other time dependent behaviour of FRP strengthened structures also need to be considered in the design stage. This section therefore presents a brief overview of researches in these areas.

2.4.1 Fatigue Behaviour

For a typical reinforced concrete deck of a highway bridge, the number of stress cycles during its service life is estimated to be 700,000,000 (Hollaway and Leeming, 1999). Fatigue is therefore an important loading consideration in the design of FRP strengthening works. Generally FRP composite materials have excellent fatigue resisting characteristics. Recent researchers have investigated the fatigue behaviour of FRP strengthened beams, all have reported encouraging results. Shahawy and Beitelman (1999) fatigue tested seven CFRP strengthened T-beams, the unplated beam went through 295,000 stress cycles before it was fatigued to failure. It was then repaired using two layers of CFRP sheets bonded to the full length of the beam, the repaired beam sustained 2,000,000 cycles before failure. A prolonged fatigue life was also achieved for all other partly and fully CFRP sheet wrapped virgin beams, which experienced between 1,800,000 and 3,215,000 of fatigue cycles. The result indicated that full wrapping was an effective method to strengthen fatigue critical structures. Barnes and Mays (1999) and Demers and Abdelgadir (1999) also reported similar findings. It seems that the fatigue fracture of the internal steel reinforcement would be a more critical design consideration rather then the strengthening CFRP composites, on the other hand, the application of CFRP composites seems an excellent way to reduce the possibility of fatigue failure of the conventionally reinforced concrete structures.

2.4.2 Creep

Long term creep is not perceived as a great concern in FRP strengthened structures. Ligday *et al* (1996) conducted an experimental investigation on the effect of sustained load acting on CFRP sheets strengthened RC beams. External wrapping was found to significantly decrease the rate of creep strain when compared with the conventionally reinforced concrete beams. They found the creep reduction factor for the beam in the study to be 0.3. However, long term records are presently not available, and the candidate has an open mind regarding the possible adverse creep effects, especially at the FRP-adhesive-concrete interface.

2.4.3 Durability

It is generally believed that FRP composites are much more durable materials than normal concrete (Clarke 1993). They have been successfully used for over 30 years in the highly stressed areas in the aerospace industry and to strengthen racing cars without any durability problems having been reported (Kim, 1995).

However, the successful application of FRP plate bonding, to a large degree, depends on the effectiveness of the bond line. The adhesive layer bonds the concrete and the FRP to form a composite action, so that the tensile stresses can be transferred from the concrete and the internal reinforcement to the external FRP plate. There are incompatibilities among the three component materials, for example, the coefficient of thermal expansion of the epoxy based adhesives is in the range of 44 – 120 x 10^{-6}/°C (Hancox, 1994); this value for concrete is expected to be from 6 to 13 x 10^{-6}/°C; while for Carbon FRP in the direction of fibre it is between -0.2 and -1.3 x 10^{-6}/°C (Hollaway, 1990). It is therefore important to assess the structural performance of CFRP strengthened structures which may be subject to large temperature variations. Researchers in Florida (Sen *et al*, 1999) reported a two year exposure study in which the long-term durability of the CFRP/epoxy bond system in a marine environment was investigated. They subjected CFRP bonded slab specimens to various wet/dry and hot (60C°)/cool cycles in salted water and natural outdoor exposure. Destructive tension and torsion tests of 100 specimens indicated that bond degradation was least for outdoor exposure (about 13%) and greatest for wet/dry cycles (about 27%). It was also found that bond deterioration occurred at locations where initial blemishes existed. These results are rather encouraging since the exposure conditions investigated were much more sever than the normally expected service environment. Other researchers also investigated CFRP strengthened beams under freezing temperatures (-25C°) (Nollet *et al*, 1999), and reported increases in both the flexural capacity and ductility, while the rigidity remained unchanged.

2.4.4 Fire Resistance

Hollaway (1993) listed all relevant fire testing methods for buildings and structures. However, research on the behaviour of FRP strengthened elements in fire is somewhat limited. In principle, all reinforced concrete structures and buildings are designed to have a certain time of resistance in the event of fire. The residual strength in a unstrengthened structure is therefore usually adequate should a fire occur. Nevertheless, it is desirable for designers to gain a good understanding of the likely behaviour of FRP strengthened elements in fire. In 1994, a series of fire tests were carried out at the EMPA, in Switzerland (Sika, 1998). Four CFRP plated beams were heated at a large furnace, to a temperature of 925C^{o} together with one unplated control beam and a beam strengthened with bonded steel plate. The tests were carried out in accordance with the ISO 834. After 8 minutes, the steel plated beam debonded and the plate fell to the floor, while the CFRP plates suffered only surface damage and finally debonded after one hour.

This superior behaviour of CFRP plate was because of its lower thermal conductivity, which reduced the heat transfer. In cases where more stringent fire protection requirements have to be met, additional protection can be provided by installing fire resisting boards around the FRP composites.

2.4.5 Impact Resistance

Accidental collisions of large goods vehicles with bridge girders or columns result in large quantity of strain energy dissipated into the impacted element sections. Erki and Meier (1999) conducted impact loading tests on two simply supported CFRP strengthened beams together with two steel bonded beams. The impact loading was induced by lifting and dropping one end of the beam at three given heights, which generated strain rates from an average of 0.057/s to a maximum of 0.8/s. The failure mode was reported to be either debonding or tensile fracture of the CFRP laminates. The CFRP strengthened beams performed well under impact loading, although there were reduced energy absorbing characteristics compared with the steel bonded

counterparts. The authors recommended that additional anchoring of CFRP laminates would always improve the impact resistance of CFRP strengthened beams.

2.5 SUMMARY OF FINDINGS FROM PREVIOUS RESEARCH WORK

The preceding section has presented a comprehensive literature review, although the candidate is prepared to accept that routine library and exhaustive internet web pages searches may still have missed a small amount of published material. Much of the work done has been based on experimental investigations of simply supported RC beams. These beams were externally bonded by carbon, glass or aramid FRP composites using various adhesives, and loaded to failure to evaluate the effectiveness of such a strengthening method. The main parameters studied in the major research works reviewed are listed in Table 2.1.

The growing worldwide interest in utilizing the advantages of FRP composite materials for infrastructure strengthening has been clearly demonstrated. The past ten years have seen the rapid development in both research and the actual site application of the FRP materials and the associated strengthening techniques.

It is now beyond any doubt that FRP composite strengthening technology "is here to stay" and grow in scope of applications. This is expected to play a significant role in maintaining and revitalising national infrastructures across the world. However, the candidate would wish to liken the current state of FRP strengthening technique with the previously mentioned "doctor-patients" analogy. A new medicine and/or a new treatment method has emerged, its effectiveness is widely expected, but it will take a few more years of clinical trial and research before it can be certified and routinely prescribed by doctors.

Likewise there are still many research and development needs related to the FRP materials and strengthening technique, which must be addressed by the research community. Only then can this still relatively new methodology be truly and routinely used wherever it is needed, and with confidence, by the design engineers.

Table 2.1 Summary of Study Parameters in Main FRP Composite Research

Researchers	Year	Country	1	2	3	4	5	6	7	8	9	10	11	12	13	14	15	16	17	18	19	20	21	22	23	24	25	26	27	28
Saadatmanesh and Ehsani	1989	Tucson, USA		✔		✔			✔	✔								✔												
Oehlers and Moran	1990	Adelaide, Australia				✔	✔	✔		✔		✔	✔	✔				✔										✔	✔	✔
Saadatmanesh and Ehsani	1991	Tucson, USA		✔		✔			✔									✔												✔
Meier and Kaiser	1991	EMPA, Switzerland					✔		✔		✔		✔				✔	✔						✔	✔	✔				
Ritchie *et al*	1991	Lehigh, USA	✔	✔	✔	✔			✔									✔			✔									✔
Triantaffilou and Plevris	1992	MIT, USA	✔	✔		✔		✔								✔		✔		✔									✔	✔
Triantafillou *et al*	1992	MIT, USA	✔	✔		✔			✔				✔		✔	✔		✔												
Meier, Deuring *et at*	1993	EMPA, Switzerland	✔				✔		✔		✔				✔			✔												
Hutchinson and Rahimi	1993	Oxford, UK	✔	✔		✔	✔		✔			✔		✔				✔					✔				✔			
Sharif *et al*	1994	Saudi Arabia		✔		✔		✔					✔	✔				✔			✔									✔
Chajes *et al*	1994	USA	✔	✔	✔		✔		✔					✔				✔									✔			
Al-Sulaimani *et al*	1994	Saudi Arabia					✔		✔									✔												✔
Deskovic *et al*	1995	MIT, USA	✔	✔		✔			✔										✔										✔	✔
Zhang and Raoof	1995	Loughborough, UK				✔												✔												✔
Varastehpour *et al*	1996	France		✔		✔			✔				✔		✔			✔												
Swamy *et al*	1996	Sheffield, UK	✔	✔		✔	✔							✔				✔												
Sata, Ueda *et al*	1996	Japan	✔			✔					✔				✔			✔												
Razaqpur and Ali	1996	Canada				✔	✔		✔									✔				✔								
Rahimi	1996	Oxford, UK	✔	✔		✔			✔	✔		✔		✔	✔			✔												✔
Arduini and Nanni	1997	USA	✔	✔					✔									✔												
Garden *et al*	1997	Surrey, UK	✔	✔	✔	✔	✔							✔	✔			✔												
Garden *et al*	1998	Surrey, UK	✔	✔	✔	✔	✔		✔					✔	✔															
Triantafillou	1998	Patras, Greece	✔				✔		✔						✔															✔
Malek *et al*	1998	Tucson, USA				✔	✔		✔									✔												
Ross *et al*	1999	USA	✔			✔					✔																		✔	
Concrete Society	2000	UK	✔	✔	✔	✔	✔																			✔		✔	✔	
Researchers	**Year**	**Country**	**1**	**2**	**3**	**4**	**5**	**6**	**7**	**8**	**9**	**10**	**11**	**12**	**13**	**14**	**15**	**16**	**17**	**18**	**19**	**20**	**21**	**22**	**23**	**24**	**25**	**26**	**27**	**28**

1-CFRP; **2**-GFRP; **3**-AFRP; **4**–Bending; **5**-Shear; **6**-Precracked Section; **7**-Virgin Strengthening; **8**-Concrete Strength; **9**-FRP Properties; **10**-Adhesive Properties; **11**-FRP Size, **12**-FRP Plates; **13**-FRP Fabrics; **14**-Adhesive Size, **15**-Beam Size; **16**-Four-Point Loading; **17**-Three Point Loading, **18**-Prestressed FRP; **19**-Anchorage Study; **20**-Dynamic Loading; **21**-Fatigue Tests; **22**-Temperature; **23**-Fire Tests; **24**-Field Application; **25**-Bond Strength; **26**-Surface Preparation; **27**-Design Recommendation; **28**-Failure Mode Study.

Based on the findings from the literature review, these research and development needs, in terms of strengthening design for flexural and shear and in relation to the current study, can be summarised as follows:

(a) There are many modes of failure reported for FRP strengthened beams, a preferred or acceptable failure mechanism must be clearly identified, and the factors that ensure or influence such failure should be understood. This is the basis of development for any design equations and guidelines.

(b) In many studies reviewed, doubly reinforced sections had been strengthened by FRP composites and tested to evaluate the structural behaviour of FRP strengthened elements. There is a fundamental concept here that needs to be addressed: Given that the design safety margin should be maintained, what RC elements can be strengthened and which ones cannot and should not be strengthened? What are the criteria for successful strengthening?

(c) The concrete cover tearing-off at the internal steel reinforcement level, with FRP composites still well bonded to the concrete surface, seems to be a very common type of failure. This failure mechanism is described as "premature" since it happens before the concrete or FRP composites reaches their ultimate strength. Although much work has been done on this topic as reviewed in Section 2.2.3, the estimation of the plate end stresses that cause such failure remains a topic of debate. Measures for preventing such failures should be studied.

(d) Structural ductility is a vitally important issue. From the literature review it is clear that FRP strengthened beams, although mostly intended to enhance the strength as well as stiffness, still exhibit acceptable ductility level if designed properly. However, a "proper" design needs to have its design parameters properly defined. It is the candidate's belief that FRP strengthened beams, which appear to have "good ductility index" values, may still fail in a very brittle manner at the Ultimate Limit State. It is

therefore important that the requirements for ductility should be considered in conjunction with the expected failure mode.

(e) Shear strengthening by FRP composites seems to be as effective as flexural strengthening. The determination of the shear capacity contribution from the FRP strengthening media, either shear strips, wings or U-jackets, is a complex process and needs to be more extensively studied.

(f) The influence of surface preparation and the physical configuration of the adhesive layer on the bond strength need to be investigated and quantified.

(g) The limitation, disadvantages and risks to clients, if any, of the FRP strengthening technique, need to be discussed and made known to the designers as well as the end-users.

CHAPTER 3

Properties of FRP Composites and Structural Adhesives

3.1 BASIC CONCEPT OF COMPOSITES

Any element made of two or more distinct materials is a composite. A composite element used for structural purposes can normally have an improved function in comparison to the performance of the constituent substances, if they were deployed in isolation. The first known case of construction related composites is perhaps the clay blocks and chopped straws, and horse hair in plasters, used by many to build houses since ancient times. Reinforced concrete, which has served mankind for over a century, is another example. In general, composites consist of reinforcements, which are of high strength and high stiffness, and the parent material that hosts and binds them. The host material, such as thermosetting or thermoplastic polymers, normally has low strength and low modulus of elasticity; it is continuous and is often referred to as a matrix. For the current study, only Fibre Reinforced Polymer (FRP) composites are considered. A selection of FRP related terminology is included in Appendix C.

The boundary between the reinforcement and the matrix is called interface. It can be controlled to produce the desired properties from the two material components for specific application. For structural engineering applications, this interface is generally made strong by maximising the chemical link between the reinforcement and the matrix

so that stresses distributed through the matrix can be effectively transferred to the stronger fibre components. The family of fibre reinforced polymeric composites used in the construction industry fall into three categories. These are Carbon Fibre Reinforced Polymer (CFRP), Glass Fibre Reinforced Polymer (GFRP) and Aramid Fibre Reinforced Polymer (AFRP). These composites are available in several different forms such as tow sheets and prelaminated plates. According to the fibre orientation, they can be further classified into three groups (Kim, 1995) as follows:

- *Unidirectional* - where all fibres are arranged in the same direction. The maximum strength and stiffness can be obtained in the fibre direction, and a maximum of 85% of fibre content by weight can be achieved.
- *Bidirectional* – where continuous fibres are at right angles, the strength and stiffness are high in both directions. Up to 65% woven fibre content by weight is possible.
- *Multidirectional (Random)* – discontinuous fibres such as chopped fibre strands are placed randomly, fibre content of up to 65% by weight can be achieved. The single ply sheet with randomly orientated fibres may be considered isotropic in the plane of the lamina.

In civil and structural engineering strengthening works, mostly unidirectional FRP composites are used, with some wrapping around applications adopting bidirectional fabrics. Overlapping two unidirectional FRP plies at right angles to each another has a similar effect to performance of bidirectional fabric sheets. The current study only deals with unidirectional FRP composites.

3.2 POLYMERIC MATRIX

3.2.1 Polymers

A polymer is an organic material of long chain molecules with high molecular weight, made by connecting many smaller molecules. These large numbers of smaller molecular units are called monomers. There are mainly two elements in the organic polymers –

carbon and hydrogen. Vast numbers of carbon compounds exist in nature and can also be synthesised. Carbon has four valencies and is able to satisfy any of these valencies by combining with other carbon groups or atoms having unsatisfied valency.

3.2.2 Function of Matrices

Apart from just binding the reinforcements, matrices play an important role in forming the overall composite characteristics. The reinforcing fibres are usually strong and brittle with high strength and stiffness. It is the matrix that protects the reinforcement from abrasion or environmental corrosion to prevent fracture. In order to transfer the load from the matrix to the reinforcement and reduce the chance of matrix failure, the adhesion between the matrix and reinforcement must be coupled with sufficient matrix shear, which is in general proportional to its tensile strength (Kim, 1995). In the design of a reinforced concrete (RC) beam, the transverse shear force, which exceeds the concrete shear strength, is carried by additional shear links, but in composite laminates, the transverse forces are carried by the matrix. There is therefore a tendency to provide a matrix with high strength. However, such a matrix is likely to be brittle and unsuitable for structural use. For civil and structural engineering applications, ductility is important, a balance or compromise between strength and flexibility therefore, needs to be made in selecting the most suitable matrix. Polymeric matrices have reasonable strength, good durability characteristics and are able to deform. As a result, they are considered suitable for use in the construction industry.

3.2.3 Polymer Matrices

Due to the very nature of organic compounds, there are many different polymer matrices that can be used to form composites. For the advanced composite materials that have the potential to be used in the construction industry, there are only two major families of binding polymer matrices, namely a thermosetting and a thermoplastic polymer. Table 3.1 lists the main matrices in thermoplastic and thermosetting. Although only a number of these listed are currently used in the composites for the construction industry, the rapid development in material technology warrants close attention of

structural engineers for any possible improvement or new development for composites materials for potential use in civil and structural engineering.

Table 3.1 Thermosetting and Thermoplastic Matrices – After Kim (1995)

Thermosetting	Thermoplastic
Acrylamate polymers	Acrylics (MMA monomer)
Alkyd & diallyl phthalate (DAP)	Nylons (NY)
Bismaleimides (BMI)	Polyamide-imide (PAI)
Epoxies (EP)	Polyetheretherketone (PEEK)
Malemines	Polyetherketone (PEK)
Phenolics	Polyetherimides (PEI)
Polyester	Polyether sulfone (PES)
Polyamides (PI)	Polypropylenes (PP)
Polyurethanes (PUR)	Polyethylenes terephthalate (PET)
Silicone (SI)	Styrenic copolymers (ABS, ACS)
Vinyl esters (or Vinylesters)	Thermoplastic polyimide (TPI)

Note: Bold type denotes currently used in FRP composites in construction industry.

3.2.3.1 Thermoplastic polymer

A thermoplastic polymer is a series of long chains of molecules lying next to each other. The chemical valency bond in the longitudinal direction is extremely strong, but the electrostatic attraction between the neighbouring chains is weak. This structure can be illustrated as shown in Figure 3.1(a). At the melt temperature, the thermoplastics can be softened and remoulded into a different shape. Upon cooling the polymer retains the new form. This heating, remoulding and cooling cycle can be repeated many times, but the resulting material becomes more and more brittle. PEEK and PES are examples of high performance, high technology polymers developed in recent years, which have vastly superior inservice properties to the normal thermoplastics.

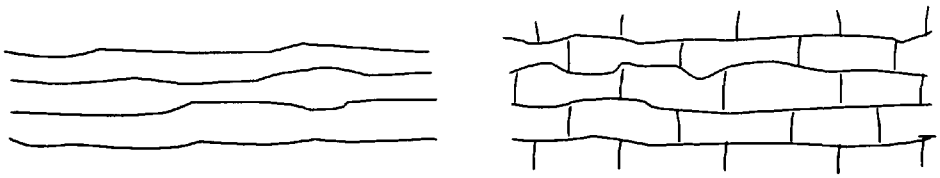

Figure 3.1 Schematic Representation of Polymeric Matrices – After Kim (1995)

3.2.3.2 Thermosetting polymer

A thermosetting polymer is made from liquid or semi-solid precursors. It can be regarded as a tightly bonded three-dimensional large molecule, which is formed through two stages. Firstly a substance with long chains similar to those of thermoplastic is formed, then the chains are crosslinked in the manufacturing process either at room temperature, or by heating and pressure. The curing process is called polycondensation or polymerization, it provides the crosslinking bonds between the long molecular chains. It can take anywhere between 10 minutes to a few hours, and the thermoset changes from liquid into crosslinked solid. The resultant material is called a thermosetting polymer. Once they are made, the thermosetting polymers cannot be reformed, re-liquefied or re-cured. A schematic representation of the thermosetting structure is shown in Figure 3.1(b).

3.2.3.3 Thermosetting resins used in the construction industry

Three thermosetting resins are currently used for producing composites used in the construction industry. They are, as listed in Table 3.1, polyester resin, epoxy resin and vinylester resin.

Polyesters – Polyesters are very commonly used in structural composites because of their relatively low costs and ease of processing, as well as their suitable properties for making good quality composites (Kim, 1995). Cure shrinkage and moisture intolerance are the major disadvantages (Robery, 2001). There are three types of polyester resins used in lamination. These are:

(a) *Orthophthalic* – is a general purpose resin.

(b) *Isophthalic* – is superior in weathering and chemical resistance.

(c) *Het-acid* – is used for fire retardance purposes.

Fire retardant resins are often more difficult and expensive to cure than non-fire-retardant categories. However, for structural application, it is important for the composites to have some degree of fire-resistance. A suitable amount of flame-retardant additives such as bromine is therefore normally added to the resins in the manufacturing process (Crowder *et al*, 1990) to achieve a good balance between good durability and fire properties, and the materials costs. Furthermore, appropriate amount of fillers such as aluminium trihydrate are often added to resins to improve mechanical properties, and pigments may also be added as appearance or protective agents, while added hydroxybenzophenones can absorb ultraviolet radiation and release it later.

Epoxies – Generally speaking, the strength and toughness of epoxy resins are superior to that of polyesters. These resins are thus able to operate in a higher temperature environment of up to 177°C, and sometimes as high as 316°C (Kim, 1995). They have good adhesion to many substrates, low shrinkage during polymerization, and are especially resistant to solvents and alkali attack. Epoxies resins however, are weak in resisting acid, weathering and ultraviolet radiation.

Vinylesters – Vinylesters have been used more recently to produce FRP composites. These are unsaturated esters of epoxy resin. They have similar properties as epoxies, but are often classified as a class of unsaturated polyester thermosetting resins because of similar processing and curing mechanisms.

3.3 REINFORCING FIBRES

Fibres are long and fine materials, which have an aspect ratio of, according to one of the experts in composite engineering Professor Hollaway (1990 and 1993), at least 10:1. Its maximum cross sectional area of 1.975×10^{-3} mm^2, which corresponds to an equivalent

diameter of approximately 0.05 mm for a circular section♦. The aspect ratio is defined as the length of the fibre to its diameter. For reinforcing fibres used in FRP composites, the minimum aspect ratio is likely to be around 1000 while the maximum could virtually be infinite for continuous fibres (Kim, 1995). There are three types of reinforcing fibres for FRP composites commonly used in the construction industry, these are discussed in the following sections.

3.3.1 Carbon Fibres

Carbon fibres have probably overtaken glass fibres in recent years and become the most important fibres commonly used today in strengthening degraded concrete structures. They are made by carbonizing organic precursor materials such as polyacrylonitrile (PAN) and mesophase pitch (MPP). Pan precursors are synthetic fibres, which form the bases for most commercial carbon fibre production. The fibre conversion yield is 50 – 55%, and PAN based carbon fibres have higher strength than any other precursor. The MMP pitch precursors are produced from petroleum asphalt or coal tar. Although pitch precursors are relatively low cost and high yield (about 75%), the manufacturing quality is somewhat more difficult to control since the properties of the raw materials may vary from batch to batch. Carbon fibres are made under high temperature, the conversion process includes stabilization, carbonization, graphitization, surface treatment and spooling, as illustrated in Figure 3.2.

The typical strength of carbon fibre ranges from 2000 to 5500 N/mm^2, while typical elasticity modulus is 160-400 kN/mm^2 but can reach up to 827 kN/mm^2 (Kim, 1995). Density of carbon fibres is of the order of 1900 kg/m^3, and the strain at failure can reach up to 2%, although most pitch based fibres will break at around an elongation of 0.3-0.9%.

♦ In both Professor Hollaway's books (1990 & 1993), this value is printed, or perhaps misprinted, as 0.25 mm.

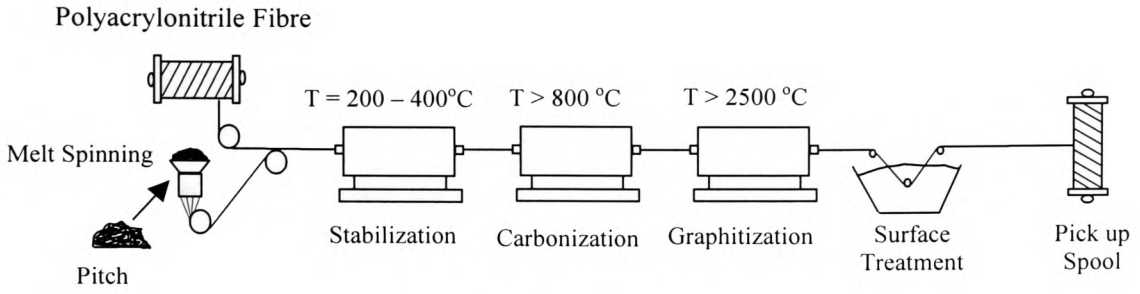

Figure 3.2 Manufacturing Process of Carbon Fibres –After Hollaway (1993, p32)

3.3.2 Glass Fibres

Glass fibre is the generic name for a series of inorganic fibres made of glass filaments. They are manufactured by continuous rapid drawing of molten glass. **E-glass** fibres (or electrical grade) are the most commonly used for general purpose structural applications, especially with polyester or epoxy matrices. **R-glass** has a magnesium-lime-aluminosilicate composition, it has higher tensile strength and modulus than E-glass, and is highly resistant to fatigue, ageing, temperature and corrosion. Other glass fibres which can be used as reinforcing fibres for GFRP composites include S-glass, A-glass, ECR-glass, AR-glass, C-glass and T-glass. Typical strength of glass fibres is between 1000 and 3000 N/mm^2, with modulus of around 85 kN/mm^2 and density of 2500 kg/m^3 (Hollaway and Leeming, 1999). The major drawback with glass fibres is that it is susceptible to alkali attack by leaching from concrete (Robery, 2001)

3.3.3 Aramid Fibres

The term "aramid" in aramid fibres comes from aromatic polyamide. It was introduced by Du Pont in 1972 under the trade name Kevlar, but is now also available in different versions and trade names such as Twaron and Technora, manufactured in the Netherlands and Japan. The molecular structure of aramid fibres is a combination of rigid benzene rings para-linked with hydrogen bonds in the transverse direction. Aramid fibres have much lower density (around 1400 kg/m^3) than carbon or glass fibres, and the strength and modulus are typically in between the carbon and glass fibres. Aramid

fibres are good in resisting fatigue and impact loads, and aramid fibre reinforced polymer composites are being increasingly used in structural engineering applications.

3.4 FIBRE REINFORCED POLYMER COMPOSITES

3.4.1 Manufacturing Process

Once suitable matrix and reinforcement are selected, they are ready to be made into composites. Many processing methods and techniques are available. They range from hand lay-up to pultrusion. The properties of the finished composites are closely related to the manufacturing method chosen. A detailed description of composite manufacturing processes is provided by Hollaway (1993). For construction industry related composites, four processing methods are of particular interest, they are Pultrusion, Vacuum bag, Filament winding and Wet lay-up.

Pultrusion – Pultrusion is perhaps the most important processing method relating to composites for construction. It is a continuous moulding process for producing composites with constant shape and cross sections. Firstly the reinforcing woven rovings and strand mat or other reinforcement are pulled through tanks of resin, and then through a heated steel die for shape forming. The die is heated to about 150°C which causes the resin to react, gel and cure (Hutchinson and Quinn, 1999). The pultruded composite is pulled either by reciprocating pullers or a caterpillar haul-off and then cut to the required length, as shown in Figure 3.3.

Fibre placement, resin formulation, die temperature, other additives and pulling speed are the major influencing factors to the final mechanical properties of the composites. Typical fibre content of around 65% is achievable for unidirectional fibre composites. Carbon and glass fibres are the most common reinforcements for pultruded shapes, although Kevlar fibres and others are now also increasingly processed by the pultrusion technique.

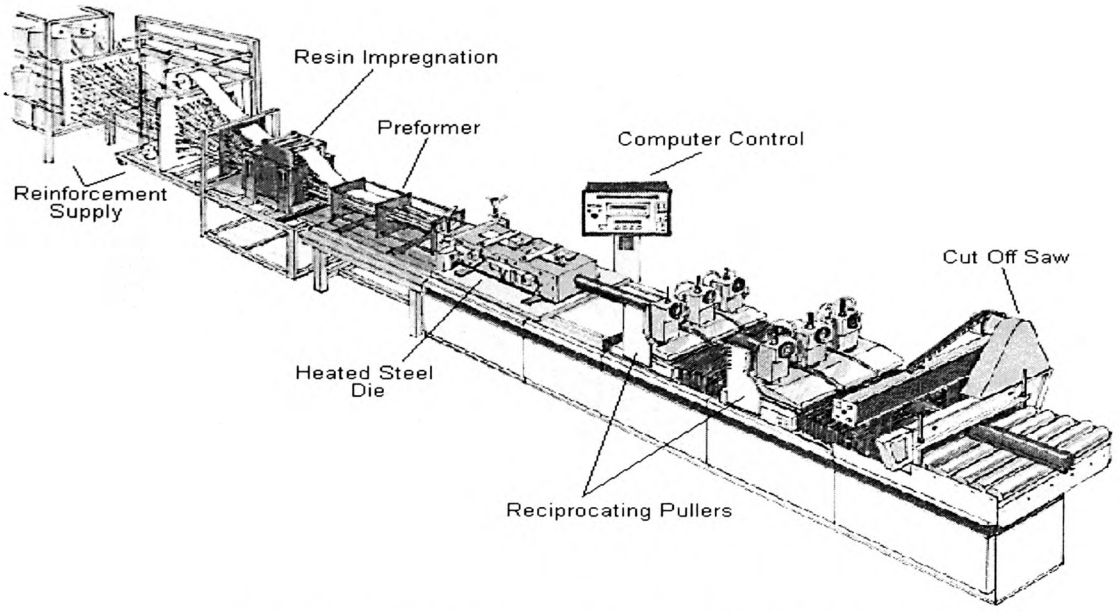

Figure 3.3 Pultrusion Process of FRP Composites
(Reproduced with permission from Fibreforce Composites Ltd)

Vacuum bag – Impregnated fibres are applied to a mould and rolled. A rubber or nylon sheet is placed over the lay-up and the air and excessive polymer is vacuumed out, before the mould is placed in an oven and heated up to 200°C. It may also be put in an autoclave where both heat and pressure are applied (Hutchinson and Quinn, 1999).

Filament winding – This is the oldest mechanical processing technique. Continuous rovings or single strands from a creel are passed through a bath of activated resin, and then via a comb with a swivelling head which is also called a "pay-out-eye", before they are wound to a rotating mandrel. The mandrel rotates at a constant speed, which determines the angle of the fibre orientation. The diagrammatic representation of the filament winding process is shown in Figure 3.4.

Wet lay-up – This is actually a site application technique. The FRP fabric sheets are bonded to the concrete surface layer by layer, using a suitable laminating resin. The main advantage of this approach is that the FRP shape and thickness can be well controlled. In case of wrapping around an existing column, this is the only viable means for FRP strengthening.

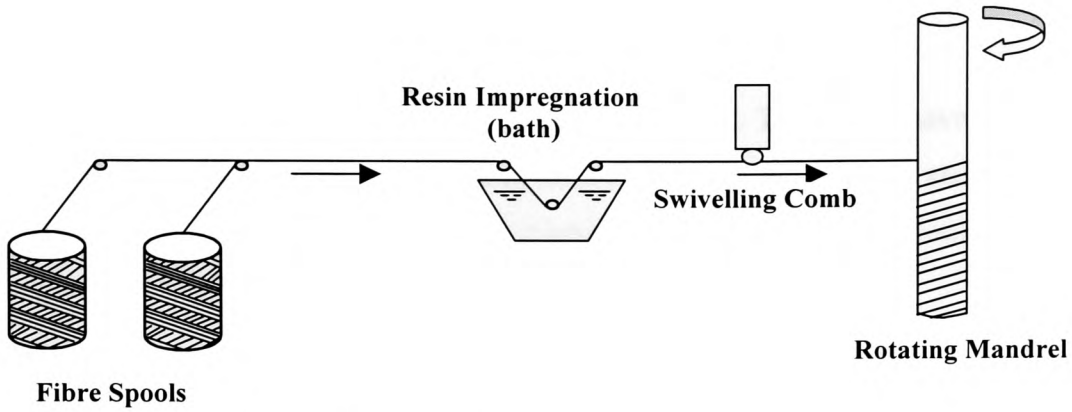

Figure 3.4 Schematic of Filament Winding Process

3.4.2 Carbon Fibre Reinforced Polymer (CFRP)

The typical carbon fibres currently used for construction related composites such as the PAN based Hyso Grafil Apollo HS or Torayca T700, have a tensile strength of around 5000 N/mm^2, a tensile modulus of around 230-260 kN/mm^2, and a failure strain of up to 2%. The unidirectional CFRP composites produced from these fibres in either epoxy or vinylester matrix, exhibit the following typical mechanical properties in the direction of the fibres (Kim, 1995, Hutchinson and Quinn, 1999):

- Tensile modulus: 155 – 165 kN/mm^2
- Tensile strength: 2500 – 3000 N/mm^2
- Elongation at break: 1.2-2.0%

Apart from their high specific strength and stiffness, which are defined as the strength and stiffness divided by the unit weight respectively, CFRP composites generally can be formulated to have many other desired properties such as in relaxation and creep, moisture resistance, alkali, salt water and other chemical corrosion resistance. They also have excellent thermal stability and fatigue behaviour. As a result, CFRP composites are now increasingly used as the preferred plate bonding materials in structural strengthening projects.

3.4.3 Glass Fibre Reinforced Polymer (GFRP)

The most common GFRP composites are E-glass fibre based. The fibres have a typical tensile strength of 1700-3500 N/mm^2, tensile modulus of 69-72 kN/mm^2 and strain at failure ranges from 3% to 4.8%. The unidirectional pultruded GFRP composites, made with a maximum of 65% fibre content, have typical properties as follows:

- Tensile modulus: 45 kN/mm^2
- Tensile strength: 1300 N/mm^2
- Elongation at break: 3.0%

3.4.4 Aramid Fibre Reinforced Polymer (AFRP)

The aramid fibres used as reinforcing agents in composites have higher modulus in comparison with other Kevlar fibres in the family. Kevlar 49 for example, has typical tensile modulus of 131 kN/mm^2, with tensile strength of 3600 N/mm^2 and a failure strain of 2.9%. The finished products of unidirectional composites have the following typical properties. Some AFRP composites have low compressive strength.

- Tensile modulus: 75 kN/mm^2
- Tensile strength: 1200-1400 N/mm^2
- Elongation at break: 1.5-2.9%.

The Concrete Society (2000) compiled a list of FRP strengthening systems that are currently available in the UK. The list includes details of all major suppliers, composites and adhesive materials properties. This information is reproduced and included in Appendix D.

3.5 ADHESIVE SYSTEMS

3.5.1 Type of Adhesives

In FRP plate strengthening works, correct choice of adhesives is frequently as important as the selection of the FRP material. The role of a suitable adhesive system, in plate bonding, is that it should transfer the stresses (mainly tensile and shear) from the highly stressed concrete to the strengthening plates, and maintain a full composite action between concrete surface and the strengthening plates. This principle has proven to be realistic with steel plate bonding systems which have been used widely for over twenty years. A good adhesive system would therefore result in full composite action at the interface of plate and concrete, and prevent any plate "peeling off" type of failure.

There are many types of industrial adhesives as listed in Table 3.2 (Kim, 1995, and Ciba-Geigy, 1993). The most common type of adhesive systems for plate bonding is the epoxy based variety, since they have many advantages over others for civil engineering construction applications, as described in details by Mays and Hutchinson (1992).

Table 3.2 Main Chemical-Reaction Based Industrial Adhesives

Adhesives	Description and Main Function
Anaerobics	Based on acrylics and often known as locking compounds or sealants, they harden with metal when air is excluded. Used to seal or retain threaded bolts.
Cyanoacrylates	Another acrylic based adhesive, cured through reaction with moisture on the surface to be bonded. Suited for plastic parts and rubber.
Toughened acrylics	Fast curing, high strength and toughness. Resin and catalyst are usually applied on either bond surfaces separately. Suitable for a wide rage of materials.
Epoxies	Based on epoxy resin and polyamine-based hardener, versatile adhesives with extremely strong and durable bonds. Suitable for most materials.
Polyurethanes	These fast curing adhesives provide strong impact resilient joints, useful for GFRP bonding by machines. Often used as primers.
Modified phenolics	These adhesives need heat and pressure for curing, suitable for high strength metal joints.

These epoxy based adhesives consist of two basic components, an epoxy resin and a polyamine based hardener. Due to the large variety of resins and hardeners available, many types of epoxy adhesive can be made with a wide range of desired properties, very strong and durable bonds can be made between concrete and FRP plates as well as many other materials. Researchers in South Africa (Tu and Kruger, 1996) studied the engineering properties of epoxy based adhesives, and concluded that they are well suited for bonding concrete to concrete or concrete to steel. Their higher mechanical strengths and lower elastic and shear moduli relative to concrete are able to accommodate strains under load and reduce the interfacial stress concentration in the joint assembly.

3.5.2 Resins

There are numerous types of base resins that can be formulated into epoxy adhesives, as described by Mays and Hutchinson (1992). The resins used for making epoxy based adhesives for application to plate bonding, according to the BA 30/94 requirements, should be based on the Diglycidyl ether of bisphenol A (DGEBA) or Diglycidyl ether of bisphenol F (DGEBF) or a blend of the two. The epoxy resins usually contain more than one epoxy group per module and the adhesive properties of epoxy are achieved by polymerisation using a cross-linking agent, or hardener, to form a 3-D polymer network.

3.5.3 Hardeners

The most commonly used cross-linking curing agent for room temperature curing epoxy adhesive is the aliphatic polyamine, though under high ambient temperature the rate of reaction could be rather fast. The polyamine-based hardener enables the adhesive to achieve good resistance to chemicals, solvents and moisture penetration through the bondline. Inert fillers and other additives may be added to improve the application or performance characteristics of the epoxy adhesives.

3.5.4 Adhesive Additives

In addition to the various formulations of resins and hardener components, other additives may be used for improving the mechanical properties of structural adhesives.

The principal epoxy additives and their function are summarised in Table 3.3. It can be seen that suitable additives may influence the product properties in many aspects. This is convenient to the designers when it becomes necessary, for example, to alter the flexibility and brittleness of the adhesives for a given load situation. Currently, the adhesive bonding systems are made with insufficient or no input from the design consultant. As a result, designers can only choose what there is available on the market rather than specifying an adhesive system that is particularly suitable for the strengthening work. This is partly due to the lack of in depth knowledge of the extended role the adhesives can play in FRP strengthening. This topic will be further explored in Chapter 6.

Table 3.3 Epoxy Additives – Compiled from Mays and Hutchinson (1992)

Additives	Function
Fillers	They are inert materials of organic or inorganic, should be electrically non-conductive, and highly moisture resistant, be able to withstand temperature of up to 120°C without degradation and with a maximum particle size of 0.1mm. They are used for cost reduction, and assisting gap filling, creep and exothermic reduction, corrosion inhibition and fire retardation.
Dilutents	Generally used for reducing viscosity for improved handling, or changing pot life, flexibility and glass transition temperature, T_g (defined in Section 3.6.2, p72). Reactive dilutents containing epoxy compounds can combine chemically with resin/hardeners, but non-reactive dilutents may adversely affect the adhesive property.
Flexibilisers	They are long chain molecules for mechanical plasticising, can increase ductility by neutralising the attraction between adjacent chains, and are used to increase impact resistance or peel strength.
Tougheners	Flexibilising actually reduce the adhesive strength, tougheners are thus added to improve the fracture energy by creating physically separating but chemically linked zones, which prevents crack propagation.
Adhesion Promoters	They are used to increase resin to surface adhesion, are also called coupling agents. The most popular ones are silanes which can either be mixed with the adhesive itself or applied to the substrate as a primer.

3.5.5 Primers

Adhesive-compatible primer coatings are essential for treating steel plate surfaces in steel plate bonding. It is believed that priming surface may improve the chemical bonding and reduce the variability of interfacial bond performance. For FRP plate bonding, priming is not usually required. However, priming the substrata surface of the

concrete may reduce the need for extensive mechanical surface treatment before applying adhesives. Colleagues of the candidate (Andreou and Delpak, 2000) have also reported a stiffness increase in Kevlar® strengthened beams where primer was used. In Chapter 6, a possible use of primer as a deliberately weaker layer in the bondline is discussed.

3.6 MECHANICAL PROPERTIES OF ADHESIVES

3.6.1 General Consideration

Currently the typical adhesive materials for plate bonding available in the UK market are epoxy based two-part systems, such as the Exchem Resifix 31 series, MBT Resin and Saturant systems, Sikadur-30 and Ciba-Geigy plate bonding adhesive systems etc. These are mostly specified in accordance with the BA 30/94(1994) guideline document, which was published in February 1994 by the then Department of Transport, and was originally intended for use in steel plate bonding systems. Before the mechanical characteristics of the adhesive layer are fully developed in FRP plate bonding, general adhesive properties need to be taken into consideration prior to and during the bonding application. These are summarised as follows:

Storage Life – This is the time during which the unmixed components of the adhesive can be stored without material deterioration. Most adhesives have a recommended shelf-life of less than a year, but it may be extended by storing them in a cool place such as in a refrigerator. BA 30/94 specifies a minimum of 6 months storage life.

Pot Life – Also called useable life, this is the time when a mixed adhesive can be applied to the adherends with sufficient thixotropy, which can aid wetting of the substrate during spreading. Most adhesives currently used have a pot life of 30-60 minutes, after which solidification takes place due to the hardener's cross-linking with the epoxy resin. The pot life can be extended at low temperature and decreased at high temperature as it quickens the curing process. BA 30/94 requires a minimum pot life of 40 minutes, the test method is specified in BS5350, Part B4.

Open Time – This is the maximum delay allowed after the adhesive has been applied to the concrete or the FRP, and before they are bonded together. This time is usually shorter than the pot life since opened joints may chemically react with the atmosphere. In BA 30/94, the joint open time is specified to be at least 20 minutes at temperature of up to 20°C.

Curing Time – This is the time after which the mechanical properties of the adhesive are sufficiently developed to or near its design values under normal ambient temperature of 10 – 30°C and in relative humidity of up to 95%. Most cold curing epoxy formulations take between 6 and 12 hours before they may be handled but it usually takes more than 24 hours for the full cure to be completed at 20°C. BA 30/94 allows a maximum of 72 hours for full cure and requires to have undergone negligible shrinkage at cure.

3.6.2 Structural Requirements of Adhesives for FRP Plate Bonding

Mays and Hutchinson (1992) investigated the structural requirements for adhesives in steel plate bonding. The results of this investigation were the basis for the then Department of Transport guidelines on steel plate bonding published by the Highways Agency in 1994. In the absence of a specific guide for the case of bonding FRP composite plates to the concrete, the BA 30/94 document has been used for such purpose in recent years. The principal structural requirements of the adhesives are summarised in Table 3.4 (BA 30/94, 1994). One of the most important properties is the Glass Transition Temperature (T_g), defined as the temperature above which the adhesives change from a structural material to a rubbery material. The present specification of 40°C is regarded too low for FRP bonding, and should be raised to at least 80°C (Robery, 2001). Apart from these structural properties, the plate-bonding adhesive should also have good moisture and creep resistance properties. They should be sufficiently flexible for gap-filling, but should be thixotropic and suitable for application to vertical or overhead surfaces, with sufficient bond developed between the overhead surfaces and the FRP plates on installation and during curing, so as to eliminate the need for temporary support. Furthermore, they should have good alkaline and other chemical corrosion resistance properties to ensure strong and durable joints.

Table 3.4 Summary of Structural Requirements of Adhesives for Plate Bonding

Property	Requirement
Glass Transition Temperature T_g	>40°C
Flexural modulus at 20°C*	4-10 kN/mm^2
Tensile Strength at 20°C	12 N/mm^2
Lap Shear Strength (Average at 20°C)	8 N/mm^2
Bulk Shear and Tensile Strength at 20°C	≥12 N/mm^2
Minimum Shear Strength** at 20°C	18 N/mm^2
Equilibrium Water Content by Weight	<3%
Mode I Fracture Toughness K_{1c}	≥ 0.5MNm$^{-3/2}$
Coefficient of Permeability	< 5 x 10^{-14} m^2/s

* Hutchinson and Quinn (1999) suggested that the lower boundary might be reduced to 1.0 GPa.
** Measured by the thick adherend shear test (TAST).

3.6.3 Evaluation of Mechanical Properties of Adhesives

The principal mechanical properties of adhesives include: (a) lap shear strength, (b) tensile strength and modulus, (c) shear strength and modulus, (d) flexural strength and modulus, and (e) the glass transition temperature T_g. To evaluate some of these properties and compare with manufacturer's specifications, the candidate carried out a small number of adhesive tests at the University of Glamorgan Structural Laboratories. The Exchem Resifix 31, a typical plate bonding adhesive system on the UK market, were tested to determine the flexural strength and modulus, as well as the Poisson's ratio and the shear modulus, in accordance with BS 6319, Part 3 (1990). A four-point load configuration was used as shown in Figure 3.5.

Figure 3.5 Four-point Load Configuration of Adhesive Tests

Four specimens of 288 mm length with 25 mm by 25 mm were prepared and load tested to failure. The effective span of each sample was 264 mm, with two point loads applied at each end. The two supports were located at the third span positions, or 88 mm from the point loads. This configuration enables more accurate results to be computed than having the supports at the ends of the beam. Initially, the specimens were loaded to strain value of 0.00022 (220 μ), to determine the lower and upper load levels N1 and N2, in the absence of numerical value for the ultimate loaded. Deflection readings are taken, within four loading-unloading cycles, before the samples were loaded to ultimate failure.

Longitudinal and lateral strains were recorded at every stage corresponding to particular values of load and deflection. Once satisfactory variations of the strains were verified, the gradients of best linear regressions were measured and hence the Poisson's ratio ν was calculated as the lateral strain divided by the longitudinal strain. The shear modulus, G, was then determined using the standard elastic theory (Gere *et al*, 1991) by the expression: $G=0.5E/(1+\nu)$. The results of these tests are shown in Table 3.5.

Table 3.5 Summary of Tests of A Typical Plate-Bonding Adhesive

Specimen Reference	**Flexural modulus E_a** GN/m^2	**Poisson's ratio** mm/mm	**Shear modulus G_a,** GN/m^2	**Flexural Strength f_a** N/mm^2
PAH1	9.80	0.2664	3.84	25.83
PAH2	8.82	0.2542	3.52	26.10
PAH3	8.81	0.2650	3.48	23.82
PAH4	7.90	0.2663	3.12	21.30
Average	**8.83**	**0.26**	**3.50**	**24.26**

The results were closely matched with the manufacturer's specifications. It was shown that these simple tests were reliable and the designers should obtain confirming test data whenever possible. Tests on other mechanical properties of adhesives may be carried out in accordance with BA 30/94 (1994) and BS 6319 (1990), in the absence of more specific guides for FRP bonding adhesives.

3.7 SURFACE TREATMENT PRIOR TO FRP BONDING

Surface preparation plays an extremely important role in influencing the joint strength of an adhesive bonded assembly. Mays and Hutchinson (1992), and Hutchinson and Quinn (1999) presented in detail the theories and methods on adhesion and surface treatment for various materials. It was pointed out that adhesion, in essence, was the result of interfacial molecular forces between the adhesive and the adherend acting across the interface and attaching their surfaces within a layer of molecular dimension.

3.7.1 Adhesion and Surface Free Energy

According to Mays and Hutchinson (1992), adhesives join materials by attaching to their surfaces within a thin layer of 0.1-0.5 nm, so that interatomic forces may be generated. The adhesive has to spread over the adherend surface, penetrating into the irregularities, displacing air and any contaminants for interfacial contact to be established. They listed the ideal conditions of good adhesion as follows:

- Surface free energy of the adherend should be higher than that of the liquid adhesive;
- The liquid adhesive should exhibit a zero or near zero contacting angle with the adherend;
- The adhesive's viscosity should be relatively low at some time during the bonding process;
- The joint should be closed in good time to assist air displacement;
- There should be an extended time before adhesive setting;
- An external pressure should be applied.

The extent of the intermolecular forces between a solid surface and an adhesive may be referred to as wettability of the solid (Rahimi, 1996). Good wettability is a prerequisite of strong and durable adhesive bond. The surface tension of liquid can be used as a direct indication of the intermolecular forces. At the surface of a liquid, there is an imbalance of attractive forces between neighbouring molecules, and work has to be done to bring these molecules to the surface. Surface molecules therefore possess a

higher energy than that of the bulk liquid. This extra energy is termed surface free energy or surface energy. Similarly, solid surfaces also posses surface energies. The surface energy of a solid is approximately proportional with its Young's modulus.

The basic requirement for good adhesion is to provide an intimate contact between the adhesive and the adherend substrate without any weak or contaminated surfaces. To achieve this, the surface tension (energy) of the liquid adhesive must be lower than the surface free energy of the adherends to be bonded, in this case, the FRP composites and the concrete element.

The typical values of surface energies of FRP composites and surface tension of epoxy adhesives are listed in Table 3.6 (Mays and Hutchinson, 1992; Rahimi, 1996). It can be seen that the surface tension of the epoxy adhesive is compatible and slightly lower than most of the FRP materials' surface energies. This is due to the similarities in composition of the epoxy adhesive and the epoxy-based matrix for FRP. Strong adhesion is therefore assured if any surface contamination is removed from the FRP composites prior to bonding.

Table 3.6 Typical Values of Surface Free Energies for FRP Bonding Materials

Type of Surface	**Surface Free Energy (mJ/m^2)**
Water*	72
Epoxy Adhesive*	45
CFRP (Vinylester matrix with peel ply)	64
CFRP (Epoxy matrix, heavily abraded)	58
CFRP (Vinylester matrix, solvent degreased)	51
GFRP (Polyester matrix, corona treated)	57
GFRP (Polyester matrix, heavily abraded)	55
GFRP (As moulded)	38-40
Steel	>50

* Surface tension.

3.7.2 Surface Pretreatment for Concrete

In order to ensure a perfect bonding between the concrete and FRP composite, which is critical for a successful strengthening design, it is essential that surface preparation be carried out on the surfaces of concrete beams to be bonded. Due to the complex physical and chemical nature at the concrete surface, it is impossible to measure the surface free energy of concrete, although as a rule of thumb, its constituents have much higher surface free energy than the surface tension of epoxy adhesives.

The aggregates are believed to have a surface free energy of greater than 100 mJ/m^2 (Rahimi, 1996), far more than that of epoxies. It is therefore desirable to expose the small to medium sized pieces of aggregates on the sub surface of the concrete structure, which will enhance the mechanical interlocking as well as chemical reaction. Surface contaminants, if any, such as dusts, oil and greases, should be cleaned, preferably by water blasting or steam cleaning using a suitable detergent. Sand-blasting and wire-brushing may be used to remove the loose and unsound particles and laitence. High-powered vacuum cleaning should be used finally to remove any residual dust. The concrete surface should be dried as much as possible, but surface water content should in any case be controlled to be less than 4% (Gaul, 1984). Indicative checks can be carried out by simply holding absorbent papers against the concrete surfaces, or using a polythene tape on part of the surface and noting the underside of the paper for condensation (Mays and Hutchinson, 1992).

A review of surface treatment techniques was carried out by Rahimi (1996), the frequently used methods are briefly described as follows.

3.7.2.1 Sand blasting, shot-blasting and grit blasting

This method is by far the most commonly used to remove concrete surface contaminants. A large variety of blast media such as alumina, chilled iron grit and sand are used. The finished concrete surface is highly dependent on the blast media used, the media sizes and types of equipment deployed and the blast pressure applied. Generally speaking, a microrough but macrosmooth concrete surface is preferred for FRP plate bonding, since an excessively rough concrete surface would affect the adhesive

thickness and thus adversely influence the joint strength. The particles from the blast media may be left embedded in the concrete surface, and must be removed prior to bonding. Wet blasting may be considered but the wet concrete surface must be dried before bonding.

3.7.2.2 Bush-hammering (Kango-hammering)

This method uses pneumatically propelled chisels or other blunt tools to remove contaminants from the concrete surface. It was used by Oehlers and Moran (1990) and Triantafillou *et al* (1992) in their studies. Great care must be taken when using this approach as it is possible that while removing surface debris, it may also damage the aggregates and fracture the sub-surface of the concrete.

3.7.2.3 Wire brushing

This can be performed manually or a powered wire brush may be used. It is a simple technique but it is labour intensive. A regular surface finish may be created, although the brushing depth is limited. This surface treatment approach is more suitable for application to relatively new and sound concrete, as was used in all surface preparation work in the laboratory tests of the present study.

3.7.2.4 Other methods for concrete surface treatment

Other available surface treatment methods include water jetting, flame blasting, chipping (Fleming and King, 1967) and acid-etching. Whatever method it is chosen, it is important to leave a sound and dry concrete surface that is free of any dirt, contaminants or weak layers before the bonding process.

3.7.3 Surface Treatment for FRP Composites

A set of comprehensive guidelines is available on the question of preparing FRP plate for adhesive bonding. These include ASTM (1984), Mays and Hutchinson (1992), Clarke (1996), Rahimi (1996) and Hutchinson (1997). The main techniques of FRP surface preparation are as follows:

- *Surface Solvent Degreasing* – This can be used to remove the soluble greases or mould releasing agents on the FRP surface. A suitable solvent such as acetone or methyl ethyl ketone (MEK), or 1,1,1,-trichloroethane (Genklene) is used, sometimes after mechanical treatment.

- *Mechanical Abrasion* – This can be done by grinding, sanding, light grit blasting or silicon carbide abrasion, the treated surface should be textured, dull and lustreless.

- *Peel-ply Technique* – A peel-ply is a non-composition layer of the FRP composite. It is usually a thin layer of either nylon or polyester, of around 0.2 mm thickness, placed at the utmost surface of the FRP composite during the manufacturing process and cured together with the composites. The peel-ply can be manually "peeled off" just before bonding, leaving a clean and uniformly rough surface that is effectively an imprint of the patterned peel-ply, which enhances the mechanical interlocking between the adhesive and the FRP plate.

FRP composites with peel-ply generally exhibit higher values of surface free energies as shown in Table 3.6, and thus good initial joint strength is assured. For this reason, the peel-ply technique seems to be obviously the best choice and is widely used. However, researchers have reported concerns in using the peel-ply method. Hart-Smith *et al* (1993) carried out extensive tests on the peel-ply technique for FRP composites. Epoxy based fibre composites were bonded with nylon peel-ply layers and cured together at 120°C and 180°C. With the help of microscopy, they found that under the higher temperature of 180°C, residual nylon pieces were left on the composite surface after the peel-ply was removed, and as a result, the bonded joint failed prematurely. However, under the lower temperature of 120°C, no similar problems were detected. These findings clearly suggest that higher temperature resisting polyester is probably a better choice for peel-ply composites. Hutchinson (1997) has discussed this subject more fully, and concluded that peel-ply represented an important aspect of surface treatment technology.

3.8 THE BONDING OPERATION

Correct selection of FRP materials and suitable adhesive systems, together with good surface preparations, are the prerequisites of a strong and durable adhesive joint. The process of bonding FRP composite to the concrete elements is a key element in a successful strengthening project, and it must be performed by appropriately trained personnel to ensure good quality of work on which the strengthening design is based. Many experts have given detailed commentaries on this important aspect of FRP strengthening technique (Mays and Hutchinson, 1992; BA 30/94, 1994, Clarke, 1996; Hutchinson, 1997; Clarke, 2000). The following is a brief summary of the bonding process.

3.8.1 Storage and Handling of Materials

The light unit weight of FRP composites makes it possible to store these materials in great length in coiled form. They must be kept in a dry and well-ventilated space and protected from surface scratching which may damage the fibres near the surface. There should be no drilling in the FRP composites plates as this will damage the fibres and may lead to premature splitting and delamination of the composites. The adhesives should be stored in cool and dry conditions, out of direct sunlight and away from sources of ignition.

3.8.2 Surface Preparation

As discussed in Section 3.7, surface preparation of both concrete and FRP composites should be carried out. Although this part of the operation is perhaps the more difficult one to control in the bonding process, especially if the bonding surfaces are overhead or vertical, it is essential that surface preparation is carried out to the appropriate standard. According to the manufacturer's specification for the Resifix 31 adhesive used in the present study (Exchem, 2000), the variation in surface levels can be checked using a 2 metre straight edge, the maximum permissible deviation is ±5 mm over a distance of 2 metres in any direction. Uneven surfaces that are out of this requirement must be reprofiled using a compatible repair material before FRP bonding can be carried out.

3.8.3 Working and Service Environment

Most adhesive systems seen in the UK have an application temperature range of between 5°C and 30°C. It is important for the ambient temperature and the temperature of the bonding surfaces to be within the specified range in order that a proper cure can take place. The working environment should be enclosed, and heater should be used to maintain the suitable temperature.

Most adhesives have a glass transition temperature T_g of between 40-60°C. The current BA 30/94 (1994) guidelines specify a minimum T_g of 40°C. If the ambient temperature is higher than the glass transition temperature, the bond strength may be adversely affected. Pang *et al* (2000) carried out an experimental investigation in which CFRP bonded full size RC beams were subjected to boiling water for 7 days, and then tested to ultimate failure. It was shown that the strengthened beams exhibited almost no strengthen increase over the control specimens. Although in practical applications, such high temperature environment is unlikely, it indicates the potential degradation of the strengthened structures when the temperature is raised above the glass transition range. Due care should therefore be taken in selecting an adhesive of appropriate T_g for the expected service temperature.

3.8.4. Adhesive Mixing and Application

Correct mixing of adhesives in accordance with the manufacturer's instructions is essential in ensuring a good quality bonding. During the experimental investigation in the present study, it was found that the two-part epoxy adhesive systems should not be over mixed, or the pot life may be reduced and excessive heat would be generated. For the application, it is important to ensure that both concrete and FRP surfaces are covered with the adhesives. It was recommended (Exchem 2000) that a 1 mm thick adhesive be applied to the concrete, and then 1-2 mm thick to the FRP plate with approximate 3 mm at the centre. Small plastic thickness gauges of the design-specified value (usually 2 mm) should be placed between the concrete and FRP surface, to maintain the correct adhesive thickness. There exists no specific guidance as to the size and location of thickness gauges. The current study recommends that these gauges

should be preferably 5 mm wide by 25 mm long, and be placed at regular intervals of say, 500 mm on the flat concrete surface in the longitudinal direction and near the edges of the FRP plates. This is to minimise the disturbances of the thickness gauges to the adhesive bonding layer as they will be permanently left in place. Sufficient pressure should be applied to hold the plate in position, continue until resin squeezes out evenly around the plate and all air is removed. For the Resifix 31 adhesive used in the current study, the final adhesive thickness should be 2 mm, and the surplus at the plate edge should be removed.

3.8.5 Durability and Fire Resistance

The FRP composites materials are durable materials if appropriately protected from accidental damage or vandalism (Clarke, 2000). The durability of adhesive joints and FRP strengthened element have been addressed in details by Hutchinson and Quinn (1999) and Hutchinson and Hollaway (1999). Apart from the initial work in Switzerland (see Chapter 1), research data on fire resistance of FRP strengthened structure are currently limited. It is believed that fire resistance may be enhanced by high fibre content, and fire retardant fillers may also be used to improve the FRP performance in case of fire.

Other concerns on the long-term durability issues of FRP composite strengthened structures have also been raised by financiers and owners of structures. One such concern is that the high voltage power lines over FRP strengthened bridge structures may generate electrical current in the conductive FRP composites, strong enough to destroy the polymer matrix and thus result is malfunction the FRP materials (Bell, 2000). Although there is no evidence to support any such claims, it is important, and in the interest of all concerned, that research in this area and other durability issues such as fire resistance of FRP strengthened structures be conducted. Only then can definitive conclusions on FRP composites' long-term durability performance be drawn.

3.9 SUMMARY

There are a large variety of FRP composites which are available for use as reinforcing and strengthening materials for RC elements. The strength, stiffness and other mechanical properties of FRP composites are influenced by the type of fibres used, fibre orientation, fibre content and the composition of the polymer matrix used. The ductile, low strength of epoxy or other similar thermosetting polymers used as bonding matrix for the various fibres, and the properties of the resulting composite materials are therefore influenced by the matrix.

Currently, the designers tend to "choose" whatever FRP composite material that are available to them, without clear appreciation as to what are the best suited FRP material properties for the specific strengthening applications. This issue can only be addressed after the strengthening requirements are clearly identified and the design process carried out. More discussions and examples on this will be presented in Chapters 5 and 8.

There are also many quality structural adhesive systems available for bonding FRP composites to the concrete. Appropriate selection of adhesives and good surface preparation will ensure that strong and durable joints are achieved, and failure modes in strengthened elements such as the FRP debonding from the concrete surface due to inadequate bond adhesion can therefore be prevented.

CHAPTER 4

Flexural Behaviour of RC Beams Strengthened by FRP Composites

4.1 INTRODUCTION

Flexural strengthening of reinforced concrete (RC) members using fibre reinforced polymer (FRP) composites has been studied by many researchers as reviewed in Chapter 2. Up to 430% of increase in flexural capacity of FRP strengthened beams has been reported in the literature (Bonacci, 1996, He *et al* 1997a). The FRP strengthening technique seems remarkably convincing as a natural substitute of the conventional steel plate bonding method. Yet after ten years of research and four years since its first application in the UK, it is still regarded by many as a new and innovative technique. Nevertheless, few researchers and consultants worldwide who are closely involved in this field have any doubts in their mind that FRP composites can effectively strengthen new and mechanically degraded RC structures. The main question that remains to be asked now is not "whether FRP is suitable for structural strengthening" but how best to make this technique a reliable and safe one, and readily acceptable to all involved in the structural maintenance industry.

Partly due to the insufficient information and design aids available, and partly due to their unfamiliarity of the FRP strengthening method, many structural design engineers are still somewhat reluctant or even sceptical at times in considering FRP as a

strengthening option. As a result the number of site applications adopting these advanced composite materials and strengthening method, although increasing, is still rather limited. In fact, the designers' concerns are by no means unjustified. To the contrary, these specialists who are entrusted by the state and the general public to design safe buildings and structures are still faced with far too many inconclusive words such as "seems", "appears", "probably" and "likely" etc., used by many researchers in their study conclusions. These concerns are a clear indication that a great deal more academic research should be conducted, and should be co-ordinated with the practical strengthening applications utilising the FRP composites.

In flexural strengthening of RC elements incorporating FRP composites, the principal issues that need to be addressed are as discussed in Sections 1.6.4 and 2.3. This Chapter presents an experimental investigation on the CFRP strengthened or reinforced concrete beams. Discussions will be focused on the following aspects of beam behaviour:

- Failure modes at ultimate limit state.
- Strength and stiffness enhancement.
- Prediction of failure loads.
- Under- and over- strengthening.

4.2 EXPERIMENTAL PROGRAMME

4.2.1 Beam Reinforcement Layout and Loading Configuration

For the experimental study, a total of thirty full sized, simply supported and four two-span continuous beams were cast for testing at the Concrete and Structural Laboratories of the University of Glamorgan. This Chapter will deal with all simply supported beams, which were 2.6 metres long, 200 mm deep by 100 mm wide. Four-point load configuration was chosen, with the length of the constant bending zone being 1.25 metres, thus enabling sufficient flexural data to be obtained. The load was applied using a hydraulic load jack, at the rate of 0.125 kN per second throughout the tests. The geometrical and loading configuration for all beams is shown in Figure 4.1.

The reinforcement cage was constructed and placed into a wooden mould before casting. The formwork was greased and checked for dimensions, soundness and cleanliness. A nominal cover of 15 mm was kept by placing plastic spacers at the bottom of the reinforcement cage. The beams were all under reinforced, having low reinforcement ratio of 0.79%. The reinforcement configuration is shown in Figure 4.2.

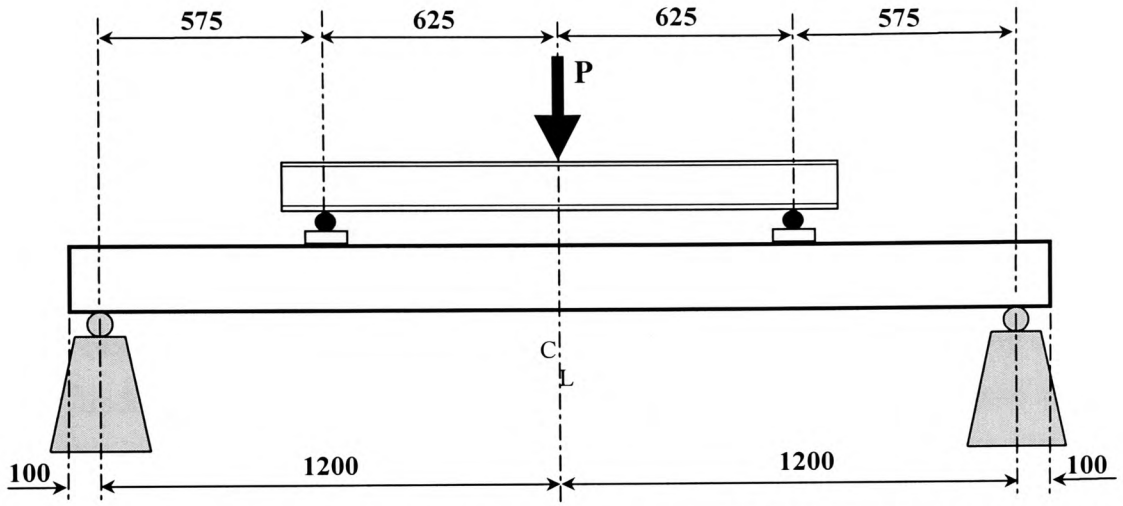

All unit of length are in mm. Seven deflection dial gauges were placed along the beam including two on the supports, to monitor the elastic deformation of the A-shaped steel supporting frames.

Figure 4.1 Loading Configuration for All Simply Supported Beams

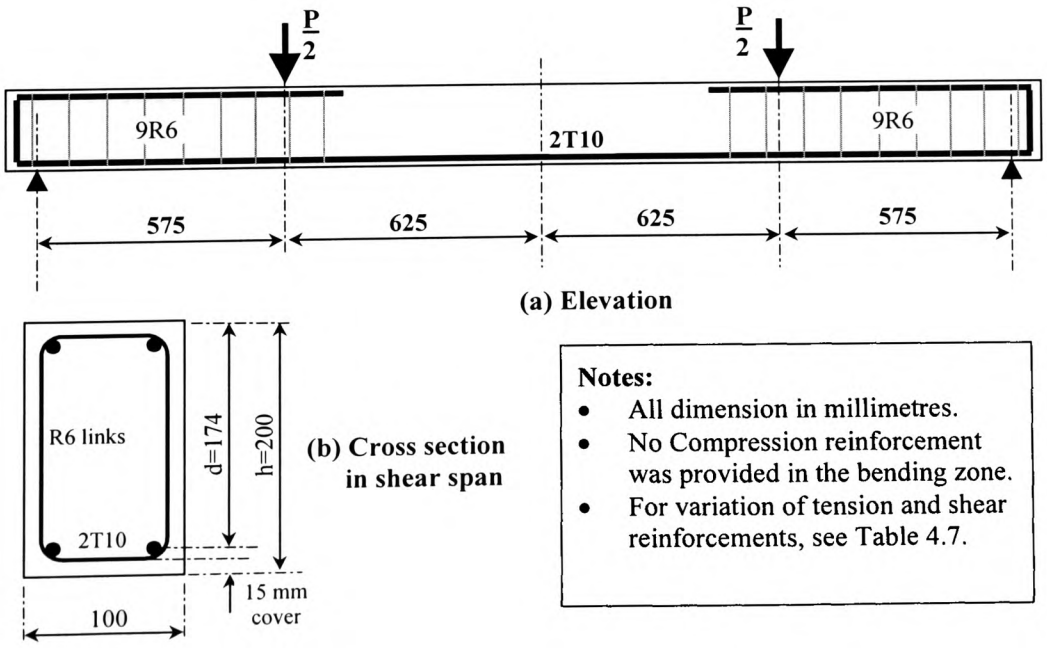

Figure 4.2 Typical Internal Reinforcement Configuration

4.2.2 Materials Properties

4.2.2.1 Concrete

All concrete materials used were produced from the same mix design, with the proportion of water, cement, sand and aggregates by weight being **0.5**:**1.0**:**3.0**:**3.0** for series A and series B tests. For the rest of the beam tests (series C, D and M), these ratios were modified to **0.5**:**1.0**:**2.0**:**4.0**. Ordinary Portland Cement was used with minimum cement content of 350 kg/m^3. Natural sand (fine aggregates) and crushed gravel (coarse aggregates) with maximum size of 12.7 mm were used. These mix designs were considered typical of those used by ready mixed concrete manufacturers, although no plasticisers or other additives had been used in the present study.

For each beam cast, six 100 mm concrete cubes and two 150 mm diameter by 300 mm length cylinders were made from the same batch of concrete. The average cube strength and the characteristic value of various batches of concrete mixings in series A and series B tests are as listed in Table 4.1. It was apparent that the concrete mixed in the summer of 1998 had much lower strength compared with others. This was partly due to the changes in the quality of raw materials supplied, the moisture content of the sand and aggregates, which was not taken into account in the mix design, was noted to be much higher than that of the previous batches. In the subsequent tests of series C, series D and series M beams, this deficiency was corrected and more consistent results of concrete compressive strength were achieved.

In the determination of characteristic strength, a few obviously abnormal readings (5 N/mm^2 above or below the mean value) have been discarded in the standard deviation and final strength calculations, as indicated in Table 4.1. However, in order to assess realistic beam behaviour, the actual concrete strengths, used for predicting the beam failure load in this thesis, are the mean values. The influences of concrete strength on the behaviour of the FRP composites strengthened beams are discussed in Chapter 5. An analytical model is used to predict the beam failure load, FRP failure stress and the maximum beam deflection with the variation of concrete compressive strength, f_{cu}. (Section 5.8.3, pp 205-205).

Table 4.1 Characteristic Strength of Concrete for Series A and B Beams

Beam Ref. (Original Casting Date)	**Cylinder Strength** (N/mm^2)		**Test Cube Strength** (N/mm^2)		**Characteristic Strength f_{cu}** (kN/mm^2)	**Elastic Modulus E_c** (kN/mm^2)
R1 (Control 1) (27/11/96)	Cylinder 1	31.04	Cube 1	47.30	**42.34** av = 47.23 (σ = 2.98)	35.1 35.8^a 34.5^b
			Cube 2	49.30		
			Cube 3	47.80		
			Cube 4	49.00		
	Cylinder 2	32.66	Cube 5	45.30		
			Cube 6	44.70		
R2 (Control 2) (23/01/97)	Cylinder 1	-	Cube 1	47.10	**40.33** av = 48.14 (σ = 4.76)	- 35.4^a 34.1^b
			Cube 2	49.70		
			Cube 3	51.60		
			Cube 4	45.70		
	Cylinder 2	-	Cube 5	46.60		
			Cube 6	*41.40**		
R3 (Control 3) (30/01/97)	Cylinder 1	-	Cube 1	46.78	**43.38** av = 46.97 (σ = 2.19)	- 36.2^a 27.3^b
			Cube 2	*41.53**		
			Cube 3	47.80		
			Cube 4	44.67		
	Cylinder 2	-	Cube 5	48.63		
			Cube 6	-		
A2, A6 (02/03/98)	Cylinder 1	37.98	Cube 1	45.28	**41.98** av = 44.60 (σ = 1.60)	33.8 35.6^a 34.4^b
			Cube 2	45.14		
			Cube 3	44.86		
			Cube 4	46.03		
	Cylinder 2	34.05	Cube 5	42.02		
			Cube 6	44.30		
A4, A5 (12/03/98)	Cylinder 1	39.45	Cube 1	50.13	**47.07** av = 49.60 (σ = 1.54)	39.8 37.7^a 35.4^b
			Cube 2	46.44		
			Cube 3	51.15		
			Cube 4	50.56		
	Cylinder 2	41.28	Cube 5	50.32		
			Cube 6	49.16		
A1 (20/03/98)	Cylinder 1	44.11	Cube 1	52.60	**47.73** av = 54.96 (σ = 4.41)	38.4 37.9^a 35.5^b
			Cube 2	*46.09**		
			Cube 3	56.05		
			Cube 4	57.51		
	Cylinder 2	41.32	Cube 5	52.33		
			Cube 6	56.34		
A3, A7 (31/03/98)	Cylinder 1	39.06	Cube 1	47.87	**42.54** av = 48.90 (σ = 3.88)	37.5 35.9^a 34.5^b
			Cube 2	48.96		
			Cube 3	50.58		
			Cube 4	50.00		
	Cylinder 2	37.30	Cube 5	50.88		
			Cube 6	45.12		
B4 (30/07/98)	Cylinder 1	26.1	Cube 1	32.62	**27.10** av = 31.68 (σ = 2.80)	32.4 28.6^a 31.4^b
			Cube 2	32.67		
			Cube 3	29.19		
			Cube 4	32.74		
	Cylinder 2	27.2	Cube 5	29.37		
			Cube 6	33.50		

Table 4.1 (continued) Characteristic Strength of Concrete for Series A and B Beams

Beam Ref. (Original beam casting date)	Cylinder Strength (N/mm^2)		Test Cube Strength (N/mm^2)		Characteristic Strength f_{cu} (kN/mm^2)	Elastic Modulus E_c (kN/mm^2)
A8	Cylinder 1	42.2	Cube 1 Cube 2 Cube 3	68.96 68.55 66.56	**64.35** av = 66.93	41.8 44.1[a]
(22/10/98)	Cylinder 2	42.6	Cube 4 Cube 5 Cube 6	67.04 64.15 66.10	(σ = 1.57)	38.8[b]
A9, A10	Cylinder 1	46.9	Cube 1 Cube 2 Cube 3	68.52 68.32 69.01	**68.08** av =68.67	42.3 45.4[a]
(19/11/98)	Cylinder 2	45.2	Cube 4 Cube 5 Cube 6	69.27 68.32 68.58	(σ = 0.36)	39.6[b]
B1	Cylinder 1	-	Cube 1 Cube 2 Cube 3	37.80 36.50 35.90	**35.92** av =36.71	- 32.9[a]
(15/10/99)	Cylinder 2	-	Cube 4 Cube 5 Cube 6	35.90 37.00 37.20	(σ = 0.48)	33.2[b]
B2	Cylinder 1	-	Cube 1 Cube 2 Cube 3	47.60 45.12 47.05	**44.45** av = 46.29	- 36.7[a]
(29/10/99)	Cylinder 2	-	Cube 4 Cube 5 Cube 6	45.53 47.38 45.31	(σ = 1.12)	34.9[b]
B3, B8	Cylinder 1	-	Cube 1 Cube 2 Cube 3	44.50 46.26 43.54	**42.61** av = 44.24	- 35.9[a]
(12/11/99)	Cylinder 2	-	Cube 4 Cube 5 Cube 6	44.28 43.30 43.56	(σ = 0.99)	34.5[b]
B7	Cylinder 1	36.5	Cube 1 Cube 2 Cube 3	43.30 45.60 47.50	**41.36** av = 46.46	34.8 35.4[a]
(24/10/96)	Cylinder 2	37.8	Cube 4 Cube 5 Cube 6	47.50 48.40 *36.70**	(σ = 3.11)	34.3[b]
B5, B6	Cylinder 1	27.27	Cube 1 Cube 2 Cube 3	*24.09** 30.69 32.11	**29.52** av = 33.10	31.1 27.8[a]
(21/09/99)	Cylinder 2	26.49	Cube 4 Cube 5 Cube 6	34.01 34.73 33.97	(σ = 2.18)	31.9[b]

* These were discarded in the normal distribution calculations. [a] Tangent modulus evaluated from BS 8110 equation 5.5 $\sqrt{\frac{f_{cu}}{\gamma_m}}$ where the material partial factor of safety γ_m is taken as 1. [b] Secant modulus evaluated from BS 8810, Part 2, equation $E_o = (20 + 0.2f_{cu}) \pm 6$ (maximum).

4.2.2.2 Steel reinforcement

The main steel reinforcements used are of typical cold-worked high-yield deformed type II bars, with characteristic strength of 460 N/mm^2. Confirmatory site tensile tests were performed at the Mechanical Engineering Laboratory at the University of Glamorgan. Although the main reinforcement was intended to be of circular cross section, it was found during the tests that some of the bars were actually of near square section. The actual area was therefore measured and used in the determination of yield strengths. The results indicated an actual ultimate tensile strength of 599.9 N/mm^2, and a yield stress of around 473.9 N/mm^2 as shown in Table 4.2 and Figure 4.3. The shear reinforcements were either 6.0 mm mild steel or 8.0 mm high-yield steel links. The beams were over designed in shear unless specified otherwise, to ensure a ductile flexural failure at ultimate limit state.

Table 4.2 Mechanical Properties of Tension Steel Reinforcement

Specimen No.	Section Properties*				Load		Elongation		Stresses	
	d_1 mm	d_2 mm	ϕ_e mm	Area mm^2	Yield (kN)	Peak (kN)	Yield (mm)	Failure (mm)	Yield N/mm^2	UTS N/mm^2
R1	9.91	9.85	11.1	96.7	46	59	0.70	2.82	475.7	610.1
R2	9.92	9.93	11.2	98.5	47	59	1.00	2.92	477.2	599.0
R3	9.96	9.95	11.2	99.1	46	60	0.86	3.06	464.2	605.4
R4	9.90	9.92	11.2	98.2	47	57.5	0.80	2.50	478.6	585.5
Average	**9.92**	**9.91**	**11.2**	**98.1**	**46.5**	**58.9**	**0.84**	**2.83**	**473.9**	**599.9**

* The bar cross section area was the measured actual area; d1 and d2 are the apparent dimension of the bars and ϕe was the equivalent diameter of a circular section of the same cross sectional area; The standard gauge length was 200 mm.

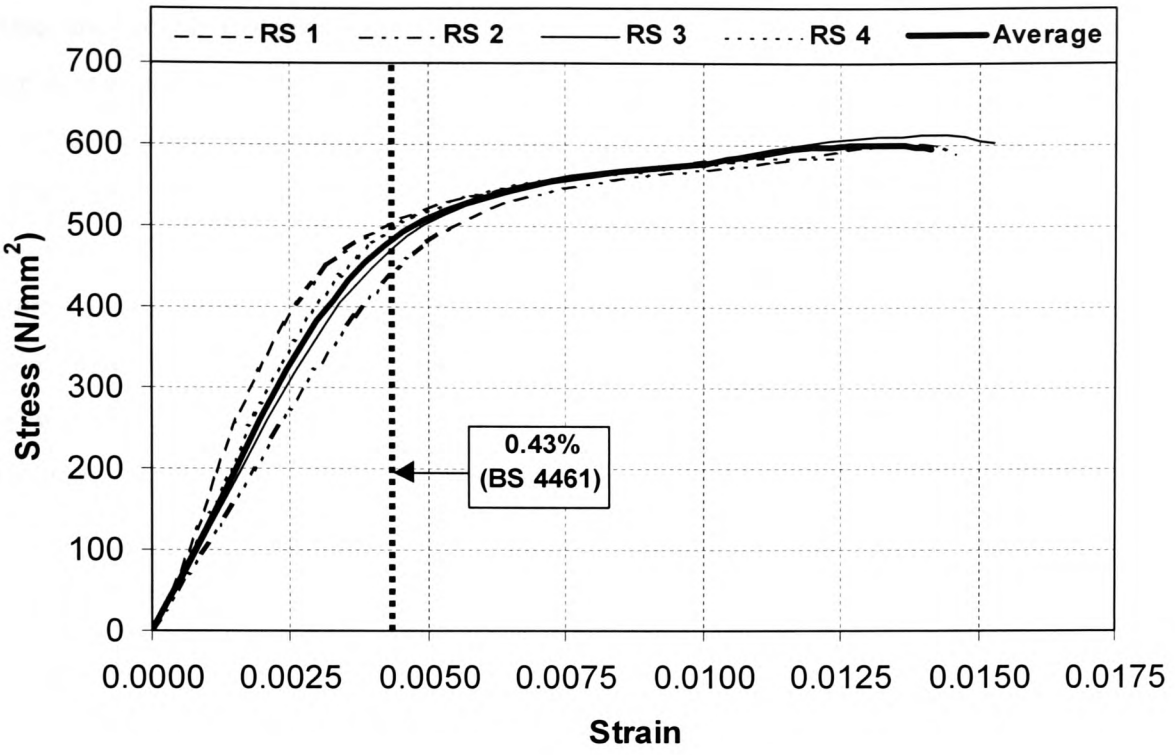

Figure 4.3 Stress Strain Curves of Reinforcement Samples

4.2.2.3 CFRP composites

Three types of CFRP composites were used, two being prelaminated pultruded CFRP plates and the other unidirectional CFRP fabric sheets, all supplied by a leading UK based company closely involved in construction repair in association with a major composites manufacturer. The plate "Type A" was of medium strength. They were made by pultrusion from vinylester resin with a combination of unidirectional carbon fibres, non woven polyester fleece and woven carbon fabric. The total fibre content was approximately 65% by volume. The tensile strength as specified by the manufacturer was 1500 N/mm^2 with a tensile modulus of 150 kN/mm^2 and interlaminar shear strength of 11 N/mm^2. The manufacturer had commissioned tensile tests elsewhere and results indicated that the strength variation was between 1365 and 1673 N/mm^2 with a tensile modulus of 145 - 188 kN/mm^2. The specific density was 1.5, and all plates used were 80 mm wide with an average thickness of 1.60 mm. CFRP plate "Type B" had an ultimate tensile strength of 2950 N/mm^2 and its elastic modulus was 184 - 196 kN/mm^2. The plates were unidirectional with carbon fibre content of 65% by volume, and a nylon peel-ply was used. The plate's net thickness after the removal of the peel-ply was

measured to be 1.5 mm (manufacturer specified 1.4 mm), and the maximum strain at break was 1.4%. Other properties were the same as that of plate type A. Type of CFRP composite used was the fabric tow sheet having a thickness of 0.145 mm per sheet which had similar properties as those of plate type A. A high strength and high modulus CFRP sheet (type D) was also used in series B beams, while a GFRP sheet (type G) was used to strengthen two beams B7 and B8. The main mechanical properties of various types of CFRP composites used in the study are summarised in Table 4.3, which includes the AFRP (type G) used in the continuous beam M3, as discussed in Chapter 7. These data are supplied with the manufacturers' technical data sheets.

Table 4.3 Mechanical Properties of CFRP Composites Used in Current Study

UD CFRP Composites	Thickness (mm)	Tensile Strength (N/mm^2)	Tensile Modulus (kN/mm^2)	Elongation at Failure (%)	Density (g/cm^3)
Plate Type A (A)	1.60	1500	125	1.4	1.45
Plate Type B (B)	1.40	2900	185	1.6	1.50
CFRP sheets (C)	0.145	1750	125	1.4	1.80
CFRP sheets (D)	0.145	4900	230	2.0	1.80
GFRP sheets (G)	0.165	3450	73	4.5	2.60
AFRP sheets (K)	0.165	2900	100	2.9	1.45

4.2.2.4 Epoxy adhesives

The adhesives used in the present study for plate bonding was the Resifix 31 system obtained from Exchem Mining and Construction Ltd, a UK based adhesives manufacturer and supplier. It is an epoxy based, two-part thixotropic adhesive originally developed for steel plate bonding. It comprises specially formulated epoxy resin and thixotroping organic fillers as a white base component, which is activated by a black coloured thixotropic hardener. The hardened adhesive has a specified tensile strength of 24 N/mm^2 and a minimum lap shear strength of 6 N/mm^2. Other physical properties of this adhesive are as shown in Table 4.4. These data have been verified against BA30/94 guidelines, and were reported elsewhere (Exchem, 1993).

Table 4.4 Properties of Plate Bonding Adhesive Used in Current Study (Resifix 31)

Property	Manufacturer Specification	BA 30/94 Requirement	Actual Value
Lap Shear @ 20°C (to steel) (N/mm^2)	11	8	16.4
Flexural Strength (N/mm^2)	55	-	-
Tensile Strength (N/mm^2)	24	12	34.3
Flexural Modulus (kN/mm^2)	6.5	4-10	8.8 [(1), (2)]
Shear Modulus (kN/mm^2)	-	-	3.50
Poissons Ratio	-	-	0.26[(2)]
Density (kg/m^3)	1500	-	1500
Glass Transition Temperature (°C)	-	40	42[(1)]

Notes: (1) Tested by the University of Nottingham for Exchem M & C Ltd (1993).
(2) Tested by the candidate for Exchem M and C Ltd (2000).

For hand lay-up of FRP sheets, the bonding system used was the Exchem Carbofibe Primer and the Carbofibe Laminating Resin (Exchem, 2000). The primer is a solvent free two pack epoxy material with low viscosity, thus enabling good penetration into the porous surface of the concrete. The laminating resin consists of a liquid epoxy resin and two alternative setting time hardeners. It has been formulated as a solvent-free, thixotripoc system, which allows easy mixing and fibre inpregnation, with minimum drainage and sag on vertical surfaces. The properties of the Carbofibe laminating resin are listed in Table 4.5.

During the application in the present tests, it was found that a ratio of FRP fabrics to mixed resin weight of approximately 2 to 1, was reasonable to ensure a thorough wetting of the concrete surface as well as the fabric sheets. The pot life of the fast-hardener resin was about 20 minutes. This could be extended to 40 minutes if a standard hardener was used. It was found necessary not to mix excessive amounts of resin which could not be used up during its pot life. A large container is preferred as the mixing vessel, as it helps dissipate the heat generated from the resin chemical reactions and thus enable increased working time.

Table 4.5 Properties of Laminating Resins Used in Current Study for Wet Lay-up

Property	Primer	Laminating Resin
Appearance	yellow liquid	green liquid
Hardener appearance	red liquid	red liquid
Mixed system appearance	orange	dark green
Resin to hardener ratio	100 : 47 (by weight) 2 : 1 (by volume)	100 : 45 (by weight) 2 : 1 (by volume)
Resin viscosity	640 cps @ 25°C	700 cps @ 25°C
Hardener viscosity	140 cps @ 25°C	350-400 cps @ 25°C
Gel time	-	20-40 minutes
Bond strength	>4.6 N/mm^2	-
Application temperature (°C)	10-30	10-30
Glass Transition Temperature (°C)	59	66

Both Resifix 31 and the Carbofibe Laminating Resin were specified to cure at ambient temperatures. In the present study, the strengthened beams were left for at least 7 days at ambient temperature of around 20°C before they were load tested. While this is the time required for the properties to be realised substantially (>95%), it is believe that the full cure cycle for the laminating resin can take up to 4 weeks according to the manufacturer's instruction sheets. It is thus prudent to ensure that strengthened structures are not loaded to design capacity until 4 weeks after the completion of strengthening work.

4.2.3 Instrumentation

Extensive instrumentation was used to monitor the performance of test beams during various loading stages. The large amount of data recorded for each beam included vertical deflection at various points along the beam profile; the strain readings in the constant moment bending zone; the crack propagation process and crack pattern and the failure mode. Six rows and up to six columns of Demec discs were mounted on both sides of the beam web in the pure bending zone, as shown in Figure 4.4. Two Demec gauge readers were used, one mechanical and the other digital. Both gauges were calibrated regularly in the Structural Laboratory of the University, and the stress-strain tests are UKAS (formerly NAMAS) accredited (No. 1014). The strain conversion factor for the mechanical and digital gauge readers were 0.801×10^{-5} and 0.403×10^{-5} respectively.

The vertical deflections of the test beams were recorded using the deflection dial gauges along the beam profile, and a Linear Variation Displacement Transducer (LVDT) was used at the mid span of the beam to monitor the maximum span deflection. Two further dial gauges were used at each of the two beam supports to monitor any elastic settlement. The arrangement of the deflection dial gauges is shown in Figure 4.5.

During the late part of the experimental study, a "System 5000" data logging system was purchased and used to record the deflections of the beam profile automatically. LVDT were placed at ten locations along the beam soffit and the deflection readings under each load increment were electronically stored via the 10 input channels into a controlling computer.

The strain variations in the FRP composites along the plate were measured in Series B beams, 12 Demec gauges were placed on the surface along the 2.2 metres long FRP layers, and the readings under each load increment was measured and recorded automatically into a computer spread sheet program.

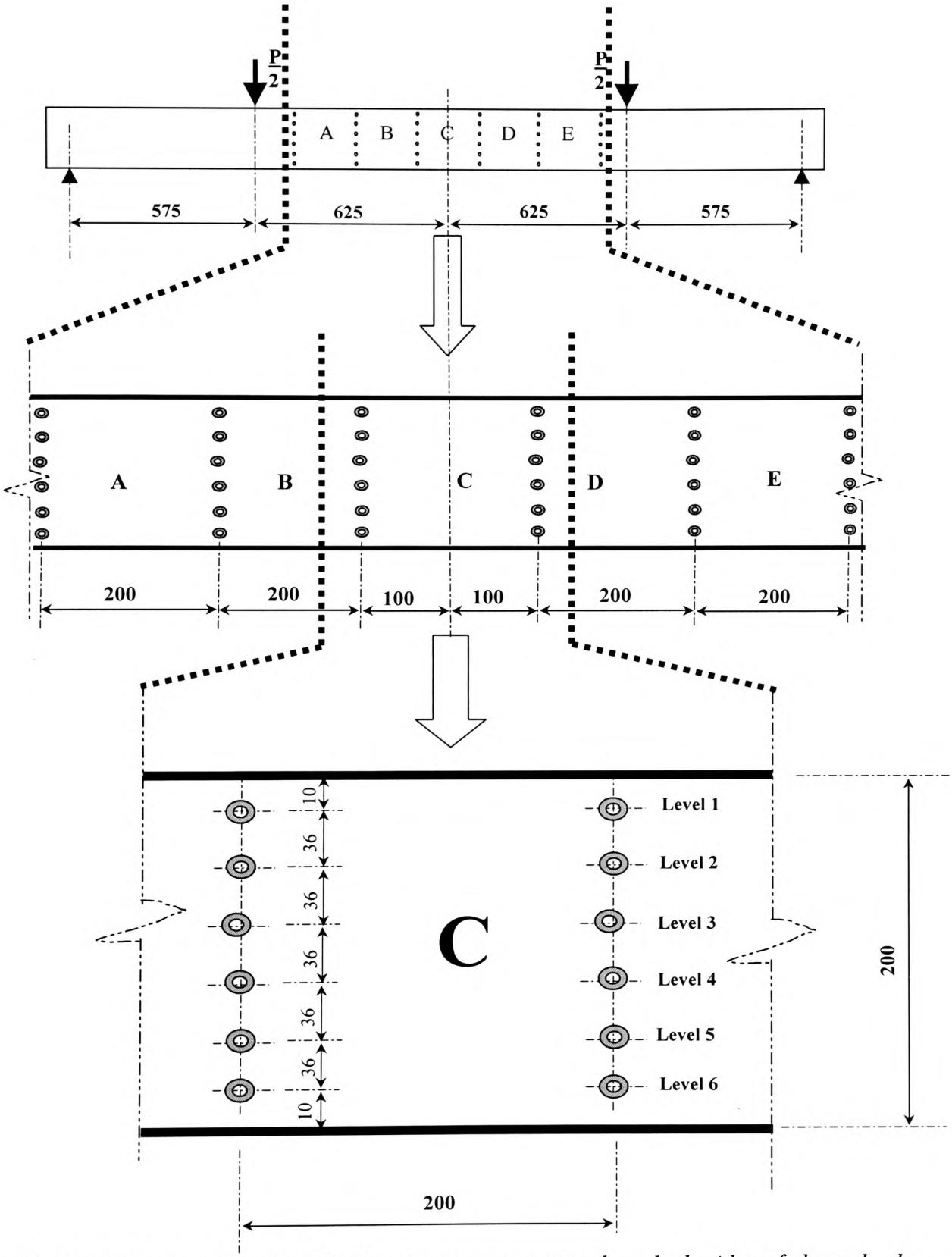

All dimensions in millimetres. Strain gauges were mounted on both sides of the web, the measurement regions at the rear face of the beams were identified with A', B', C, D, and E'.

Figure 4.4 Instrumentation – Location of Demec Strain Gauges

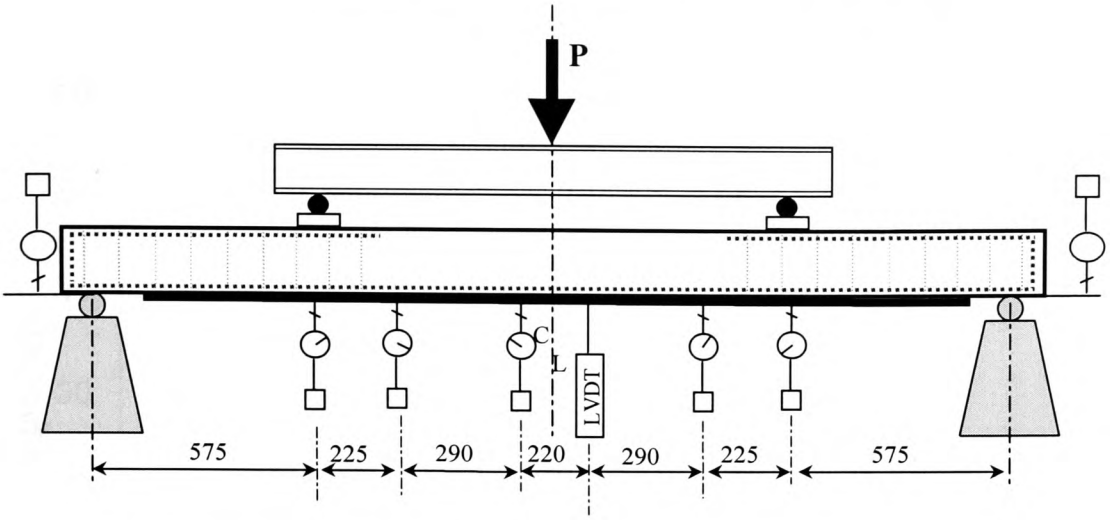

Figure 4.5 Instrumentation – Location of Deflection Gauges

4.2.4 Test of Control Beams

Three conventionally reinforced control beams were loaded to ultimate failure. These were used as reference beams for generating data for comparison with FRP strengthened beams. A summary of the test results for the control beams is listed in Table 4.6.

Table 4.6 Test Results of the Control Beams

Beam Ref.	f_{cu} (N/mm^2)	Tension Steel, A_s (mm^2)	Links A_{sv} (mm^2)	Max. Load (kN)	Max. Deflection δ (mm)	Failure Mode
R1 (DG4)	43.1	157.0	56.5	48.8	30.5	All beams failed by steel yielding first, and followed by concrete crushing.
R2 (DG7)	40.6	157.0	56.5	47.6	31.3	
R3 (DG10)	42.2	157.0	56.5	47.2	33.7	
Average	**41.9**	**157.0**	**56.5**	**47.9**	**31.8**	

It can be seen that the three control beams had near identical behaviour. For convenience, the average of these three beams was taken for subsequent comparative purposes in the present study. Shown in Figure 4.6 is the load-deflection behaviour of the control beams.

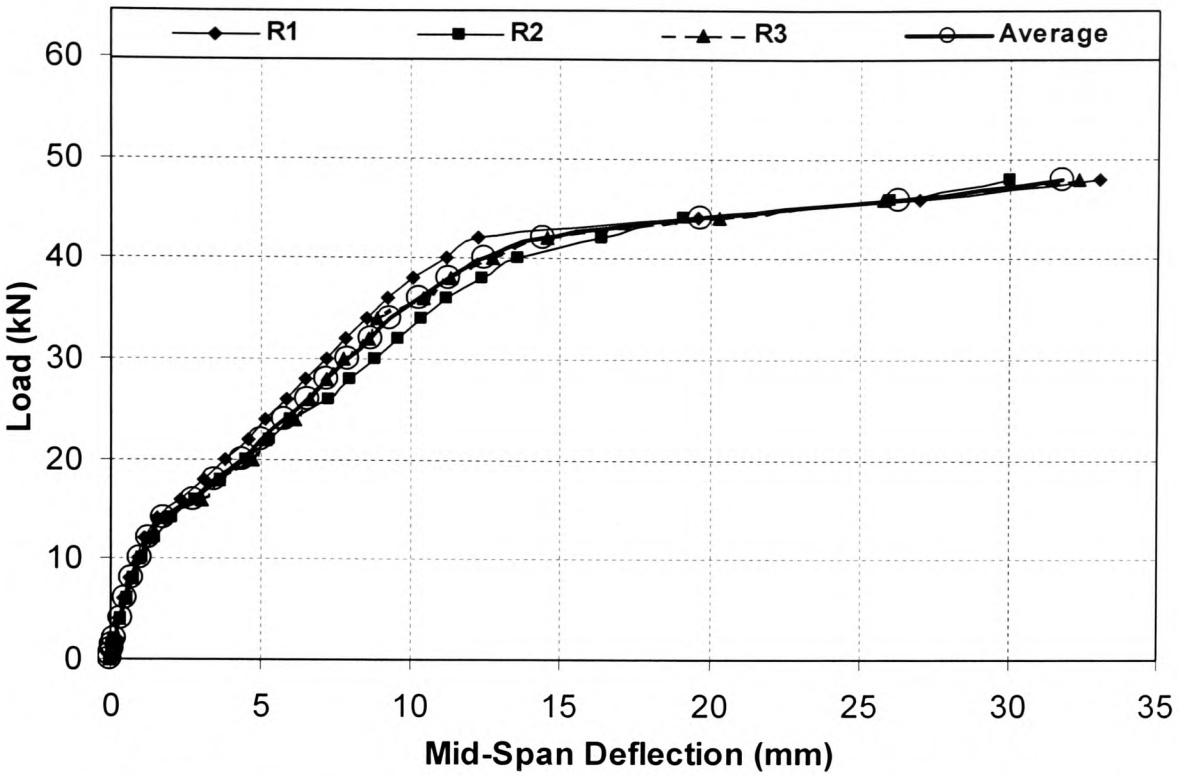

Figure 4.6 Load –Deflection Behaviour of the Unstrengthened Control Beams

4.2.5 Mechanical Degradation (Precracking) of Test Beams

Strengthening works are usually carried out on existing structures that are normally cracked under the service load. In order to simulate a RC element more realistically, it was decided to pre-load the test specimens to the expected "working load" level, when service cracks would have been induced.

Six beams (A1, A2, A4, A5, A6 and A8) were loaded to around their serviceability limit state. The serviceability limit state could be defined in different ways according to the specifically required functions of the structure, and it also depends on the design codes of practice which tend to have different requirements from country to country. For the most common type of reinforced concrete building structures, deflection and crack width are the two important serviceability limit states. In BS 8110, these are defined as follows:

- The maximum span deflection reaches 1/350 of the effective span (6.8 mm) under the live load, or 1/250 of the effective span (9.6 mm) under the combined total dead and live load.

- The maximum surface crack width reaches 0.30 mm. A set of standard feeler gauges was used to monitor the surface crack width at various loading stages. In the current study it was found that the deflection limit was the prevailing one, at which stage the typical crack width were observed to be around 0.1-0.15 mm.

During the precracking of the test beams in the current study, loading was stopped shortly after the maximum span deflection reached 1/300 of the span (or 8.0 mm). This was believed to be a reasonable simulation of real structures, since most structures that could be strengthened have not necessarily reached the serviceability limit state. The load deflection curves of the precracked beams, together with that of the control beam, are shown in Figure 4.7, while Figure 4.8 shows the same set of curves at the early loading stage. It can be seen that these beams showed similar load-deflection trend as that of the control beam.

4.2.6 Strengthening Procedure

Having been loaded to around the normal service load and the service cracks become visible, the beams were then strengthened using the CFRP plates/fabrics, and the Resifix 31 or Carbofibe laminating resin adhesive systems. The mixing of the two part adhesive had been carried out using a low speed electric drill and a paddle. Once a uniform colour was achieved, it was mixed for a further minute in accordance with the manufacturer's instructions.

The tension surface of the concrete beams was prepared for CFRP plate bonding. A wire brush was attached to a standard electrical drill and used to remove contaminants and create a rough interface on the concrete surface. All debris were removed, and a high power vacuum was used to clean the concrete surfaces of dust. The epoxy adhesive was then applied to the prepared surface to approximately 2.0 mm thick, a fine

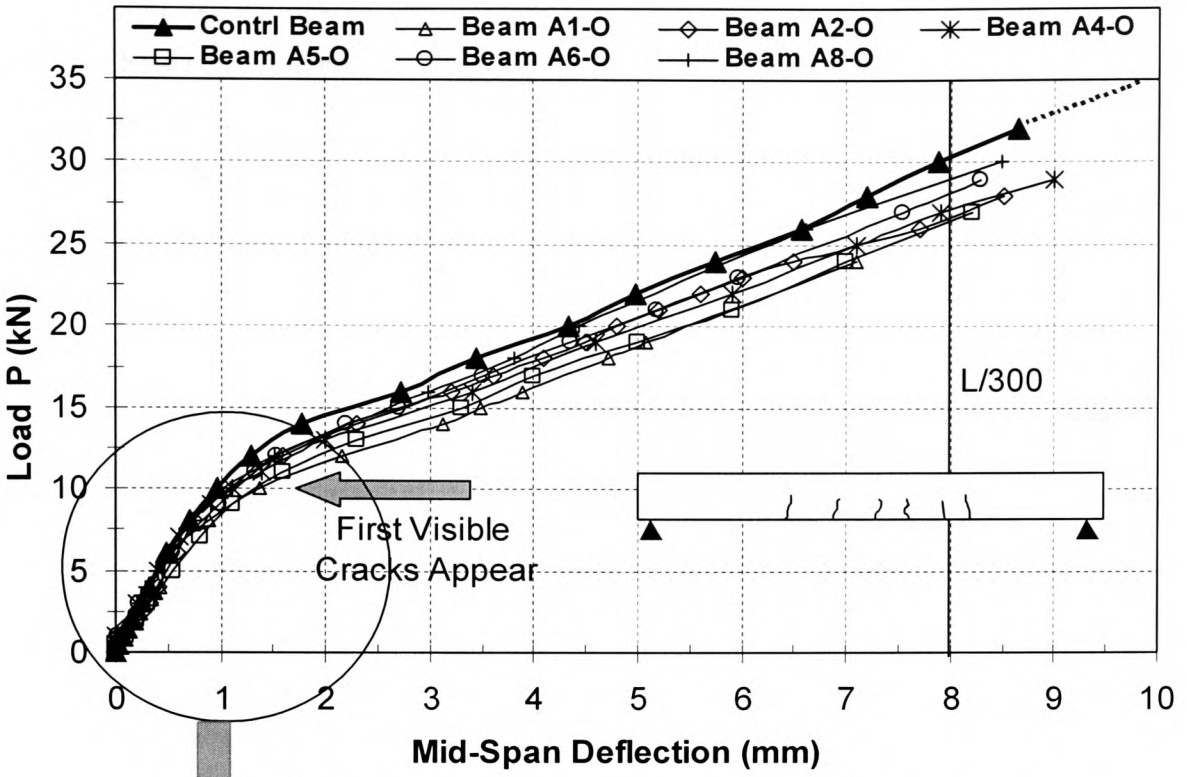

Figure 4.7 Precracking of Test Beams (Original) in Series A

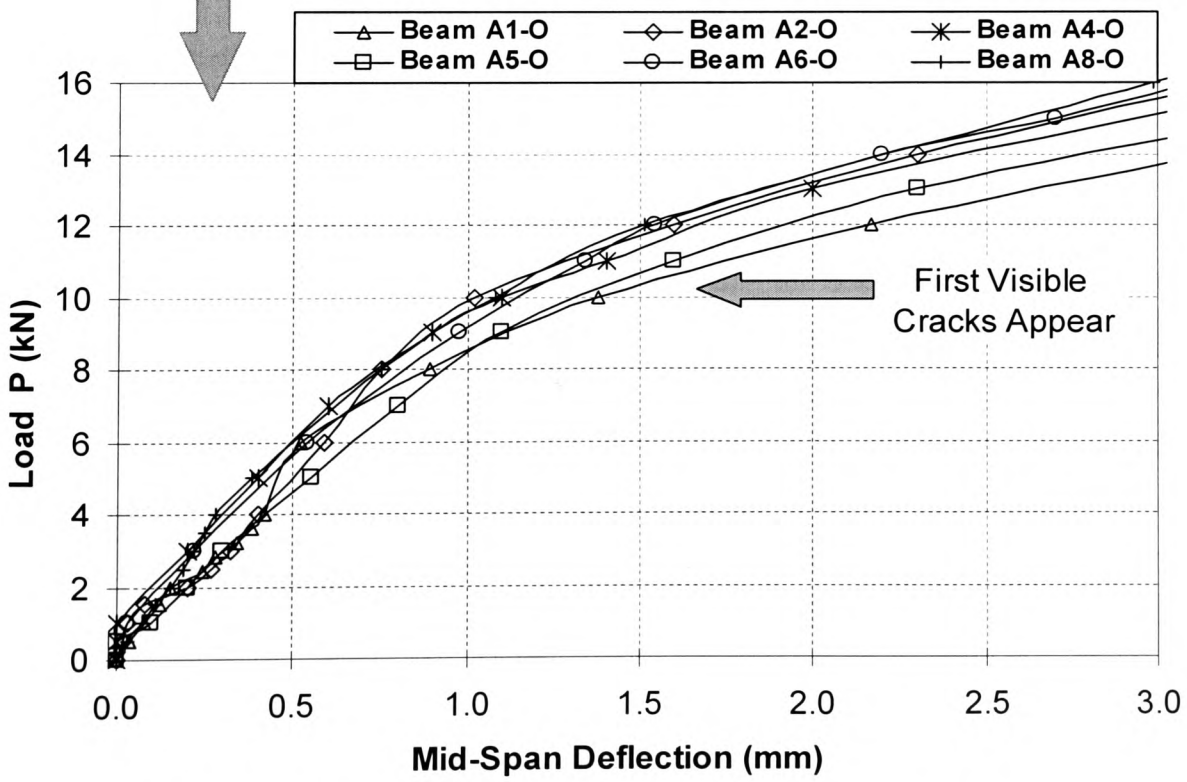

Figure 4.8 Precracking of Test Beams (Early Loading Stages)

layer of the mixed adhesive was also applied to the CFRP plate surface to ensure perfect bonding between concrete and the CFRP plates. The plate was then hand pressed onto to the concrete tension surface, and the excess adhesive was then wiped off from both edges of the plate. The overall thickness of the adhesive layer was controlled to be 2.0 mm, using plastic thickness gauges at various locations of the beam. The bonded beam was then left to cure for a minimum 7 days before testing. The FRP plates and internal steel reinforcement details are listed in Table 4.7, and also shown in Figure 4.9.

For two beams (Beam A8 and A9), a small and uniform pressure was applied to the plate for one day after CFRP plate bonding. This was to ensure adequate setting of the adhesive and later to allow comparisons with the other beams without such a confining pressure. This pressure was applied by placing a piece of timber strip of the same width as the CFRP plate, and two G clamps were placed and lightly tightened at one-third span of the timber strip.

There was no evidence to suggest that the confining pressure during the initial cold curing of the adhesive had helped improve the bond between the CFRP plate and the concrete. In fact the two beams failed at a premature manner, by debonding of the CFRP plate from the concrete beam.

It must be pointed out, however, that all beams prepared for the present test series had been turned "upside down" for convenience of applying the adhesives in the laboratory conditions. This is obviously unrealistic when a real structure is strengthened on site, as the working surfaces are most likely to be overhead or vertical, except where sagging moment over the supports is encountered. When wet lay-up of FRP sheets are used, these working surfaces will not present great difficulties, provided that the resin used is sufficiently viscous so that dripping is avoided. When bonding prelaminated FRP plates, however, it is essential to ensure that full contact between the concrete and the plate surfaces are achieved by applying sufficient pressure to hold the FRP plate in position. Although not absolutely required, it may be advisable to apply a confining pressure, wherever possible, to the FRP plates such as by means of temporary propping for the duration of the installation process.

Table 4.7 Steel Reinforcement and FRP Strengthening Details (Series A and B)

Beam Code	Concrete f_{cu} (N/mm^2)	Internal Steel Reinforcement**		Externally Bonded FRP Composites		
		Tension A_s (mm^2)	Shear A_{sv} (mm^2)	FRP type *	A_p (mm^2)	Length l_p (mm)
A1-O	54.9	157	56.5	-	-	-
A1	54.9	157	56.5	A	128	2200
A2-O	44.6	157	56.5	-	-	-
A2	44.6	157	56.5	A	128	2200
A3	48.9	157	56.5	A	128	2200
A4-O	49.9	157	56.5	-	-	-
A4	49.6	157	56.5	A	128	2200
A5-O	49.6	157	56.5	-	-	-
A5	49.6	157	56.5	A	128	2200
A6-O	44.6	157	100.5	-	-	-
A6	44.6	157	100.5	A	128	1000
A7	48.9	157	100.5	A	128	1000
A8-O	66.9	157	100.5	-	-	2200
A8	66.9	157	100.5	A	128	2200
A9	68.7	157	100.5	A	128	2200
A10	68.7	157	100.5	A	128	2200
B1	36.7	157	56.5	D	14.5	2200
B2	46.3	157	0.0#	B	112	2200
B3	44.2	157	56.5	D	14.5	2200
B4	31.7	157	56.5	C	14.5	2200
B5	33.1	157	56.5	D	14.5	2200
B6	33.1	157	56.5	C	14.5	2200
B7	46.5	157	56.5	G	16.5	2200
B8	44.2	157	56.5	G	16.5	2200

* See Table 4.3 for details.

** All tension reinforcing bars were high yield type II, 2T10; shear reinforcement - mild steel, single R6 or T8 links @ 100 mm cross centres.

\# No internal shear links were provided in beam B2.

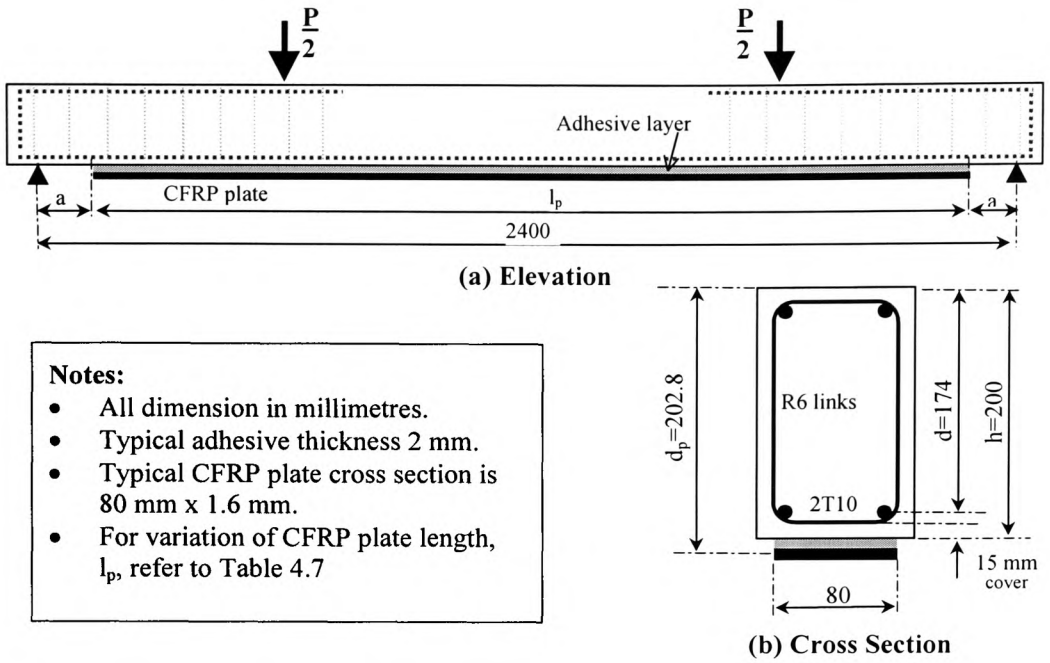

Figure 4.9 Details of Externally Bonded CFRP Composites

4.2.7 Testing of FRP Strengthened Beams to Ultimate Failure

All tests were carried out under load-controlled conditions and the post peak load-deflection relationship therefore was not obtainable. The reason for this choice rather than displacement control is that in practice, most structures are subject to gravitational load, which usually does not increase dramatically as the structure deforms. If a real structure is overloaded then it collapses immediately and the post peak load behaviour will never occur. This is especially important if ultimate deflection is used for the determination of deformability and ductility indices (Lees, 1997, see Chapter 7).

The re-testing of the repaired beams was carried out 7 to 14 days (except for beams A9 and A10) after the plate bonding procedure had been completed. The minimum setting time of the Resifix 31 epoxy specified by the manufacturer was 3 to 7 days for 90% of the strength to be reached. During the reloading process, any new cracks were identified and marked with the corresponding loading value.

At ultimate failure, no debonding at the concrete FRP interface was observed in all but two beams (A9 and A10). The bonding between the CFRP plate and concrete had remained strong. On some occasions the actual carbon fibre plate had been delaminated, but the bonding between the plate and the concrete surface remained intact.

The debonding problems observed in the tests were thought to be the result of inappropriate mixing of the adhesive systems. In this case, the mixing of the two-part adhesive was manually performed using a spatula. CFRP plates were bonded to two non-precracked RC beams (A9, A10), using this particular mixing with an average of 1.5 – 2.0 mm adhesive thickness. These beams were tested at 4, and 6 days respectively after the bonding, and "peeling off" of the plates was observed before ultimate failure, after which the beams behaved similarly to a non-strengthened beam. The failure load of these beams remained at about 15 - 20% over control beams. Subsequent checks on the adhesives on beam A9 revealed that small parts of the epoxy resin in the bond layer had not been fully hardened yet, suggesting an unsatisfactory mixing procedure. It also indicates that the thickness of the bonding layer perhaps should not have been less than 2.0 mm. These two beams were therefore not considered to be representative of typical behaviour. It highlights, however, the importance of a good mixing of the two components of the adhesive to achieve a suitable final product. Since these beams were tested less than 7 days after the bonding operation, it may also have been a contributory factor that the full bonding strength had not yet been achieved and thus the beams failed prematurely.

4.2.8 Summary of Test Results

Extensive test data including deflections and strain readings, crack propagation process and failure load have been recorded for each beam. Table 4.8 includes the main characteristic behaviour of all beams in series-A tests.

Table 4.8 Summary of Test Results for Series-A Beams

Beam Reference	Load at specific stages (kN)			Ultimate Load Increase %	Deflection @ failure (mm)	Failure Mood
	First crack	SLS (δ=9.6mm)	Ultimate Failure			
Control	12	34.7	47.9	-	31.7	SY-CC
A1	*	50.0	76.2	59.1	18.2	PTC
A2	*	47.2	73.8	54.1	18.9	PTC
A3	20	51.8	89.9	87.7	20.9	PTC
A4	*	45.4	74.4	55.3	19.8	PTC
A5	*	52.0	82.0	71.6	19.4	PTC
A6	*	47.0	62.0	29.6	13.0	PTC
A7	12	-	59.1	21.3	10.7	PTC
A8	*	45.0	68.8	43.6	16.84	DB-CC
A9	12	49.8	58.1	24.9	10.66	DB
A10	12	46.5	55.6	16.1	11.40	DB

Notes: * Precracked; SY-CC = Steel yielding followed by concrete crushing; CC-Concrete crushing; PTC – Premature tearing-off of concrete cover;

All beams repaired or strengthened by CFRP plates failed typically by tearing-off of the concrete cover at the internal steel reinforcement level, and in some occasions the concrete in the compression zone was crushed simultaneously.

For each of the test beams, approximately 1,500 to 1,800 strain data readings were taken within the pure bending region. From these recorded data, load versus strain diagrams can be plotted at every loading increment. The experimental values of the neutral axis depth at each load were determined from the diagrams of strain against the beam depth. Since there are many sets of related data, which are taken under an "identical loading zone" and in theory, should be equal, any "unusual" set of readings are then double-checked against those of their peer group readings, and if necessary an average value may then be calculated.

Table 4.9 Summary of Test Results for Group B Beams

Beam Reference	Load at specific stages (kN)			Ultimate Load Increase %	Deflection @ failure (mm)	Failure Mood
	First crack	SLS (δ=9.6mm)	Ultimate Failure			
Control	12	35.0	47.9	-	31.7	SY-CC
B1	14	37.5	70.0	40.3	34.8	CC
B2	14	58.2	92.5	93.1	19.0	Shear
B3	10	39.5	68.4	42.8	23.0	CC
B4	12	34.8	72.5	51.4	35.4	FF-CC
B5	12	39.0	76.2	59.1	32.9	CC
B6	10	29.8	62.5	30.5	34.9	FF-CC
B7	*	37.5	40	-16.5	10.4	BRF
B8	14	37.5	67.5	40.9	32.6	BD

Notes: SY-CC = Steel yielding followed by concrete crushing; CC = Concrete failure in compression zone; FF = Fibre failure; DB = Debonding of FRP; * Beam B7 was precracked; BFR = Brittle reinforcement failure.

In series B, a total of eight FRP strengthened beams were tested. Beam B2 was plated with the high strength type B CFRP plate. Five beams, namely, B1, B3, B4, B5 and B6 were strengthened using a single layer CFRP sheet to the full width of the beam and the length of the composite layer was 2.2 metres.

Beam B7 was originally loaded to ultimate flexure at the end of 1996. It was then repaired by removing completely a 500 mm length of damaged concrete section in the constant moment zone and replacing with new concrete. The yielded reinforcing bars were cut and two new bars were butt welded to the existing steel. The beam was then strengthened in October 2000, with two layers of type G GFRP sheets bonded to the tension face. The intention was to assess the effect of FRP strengthening on this severely damaged and then repaired member. Beam B8 was similarly strengthened, from new, by two layers of type G GFRP fabric sheets. This was intended to assess the variance of CFRP and GFRP composites on the behaviour of strengthened members, since both materials have vastly different mechanical properties. The FRP fabric sheets were bonded to the pretreated concrete surface using the Exchem two part Cabofibe laminating resin, as discussed in Chapter 3. Table 4.9 lists the main results for the series-B beams.

4.3 DISCUSSION AND ANALYSIS OF RESULTS

4.3.1 Redefinition of Debonding and Peeling Failure

Apart from the commonly expected flexural and shear failure modes, FRP strengthened RC elements often fail prematurely due to either tearing-off of the concrete cover, debonding, delamination or peeling off. It is therefore necessary to clearly define the terminology to avoid possible confusion:

- **Debonding of FRP plates** - The term was originally used in the steel plate bonding technique, where the plates become separated from the adhesive layer or the plate-adhesive is separated from the concrete surface at any location within the bondline. This type of failure is usually due to the weak bonding strength of the adhesive system, or the lack of mechanical gripping at the steel plate surface. Poor surface preparation of either concrete or plates may naturally result in such failure. It can happen at any position of the bonded length, and the whole plate may "drop off" if no suitable anchorage is provided.

- **Peeling-off of FRP plates** - This is a form of partial debonding, and it usually starts at the ends of the FRP plates as if the plates were "peeled" off the concrete.

- **Tearing-off of concrete cover** - This type of failure is initiated at the plate cut off point due to the great concentration of normal (peeling) and shear stresses which may exceed the lateral shear strength of the concrete. It occurs at the internal steel reinforcement level, and the FRP plate is usually still well bonded to the separated concrete cover. This is by far the most common type of "premature" failure as observed in the current study as well as reported by others (Chapter2). It is often referred to as "peeling-off" by other researchers, but the candidate feels this term may be misleading, as tearing-off at the reinforcement level is fundamentally different from a peeling failure due to weak adhesive bonding.

- **Delamination** – This condition refers to the physical separation of the FRP composites layers in the prelaminated plates or wet lay-up FRP sheets. It is usually

due to the poor FRP fabrication or application process, and this type of failure may be combined with the tearing-off failure mode.

4.3.2 Beam Failure Mode

4.3.2.1 Series-A beams

Typical failure mode of series A beams is illustrated in Figure 4.10. During the laboratory tests, it was observed that for beams A1-A5 in series-A, which were fully strengthened by 2.2 metre long CFRP plates, the typical failure mode was the premature tearing-off mechanism. These occurred at the internal steel reinforcement level, where the concrete cover was torn off with the CFRP plate still well bonded to it. As discussed earlier, the candidate suggests that such a failure mode may be referred to as "Tearing-off" of concrete cover rather than "peeling failure" due to weak bonding strength. Such tearing-off failure occurs prior to the CFRP plate reaches its design strength, and is thus described as premature.

It indicates that there exists a level of strengthening at which high specific strength and stiffness of the FRP composite can no longer be fully utilised. This leads to the concept of over strengthening, which may result in brittle and premature failure as was seen in group A beams. The prediction of ultimate failure load for these beams, based on the flexural theories, is therefore expected to be over estimated. It is important to point out that the development of any theory for predicting ultimate failure load must first ensure that a correct failure mode is to be reasonably expected. Further discussions on over and under strengthening will be presented in Chapter 5.

For beams A6 and A7, the 1.0 metre length strengthening CFRP plates were bonded centrally between the two point loads. The plate length is 0.25 m shorter than that of the constant moment zone. As was observed, the stiffness enhancement for these two beams was initially small but increased substantially to approach that of the full length strengthened beams. The final failure mode of these two beams was still the tearing-off of the concrete cover at the plate cut-off point, rather than a full flexural failure as expected to occur at the same position within the constant moment zone.

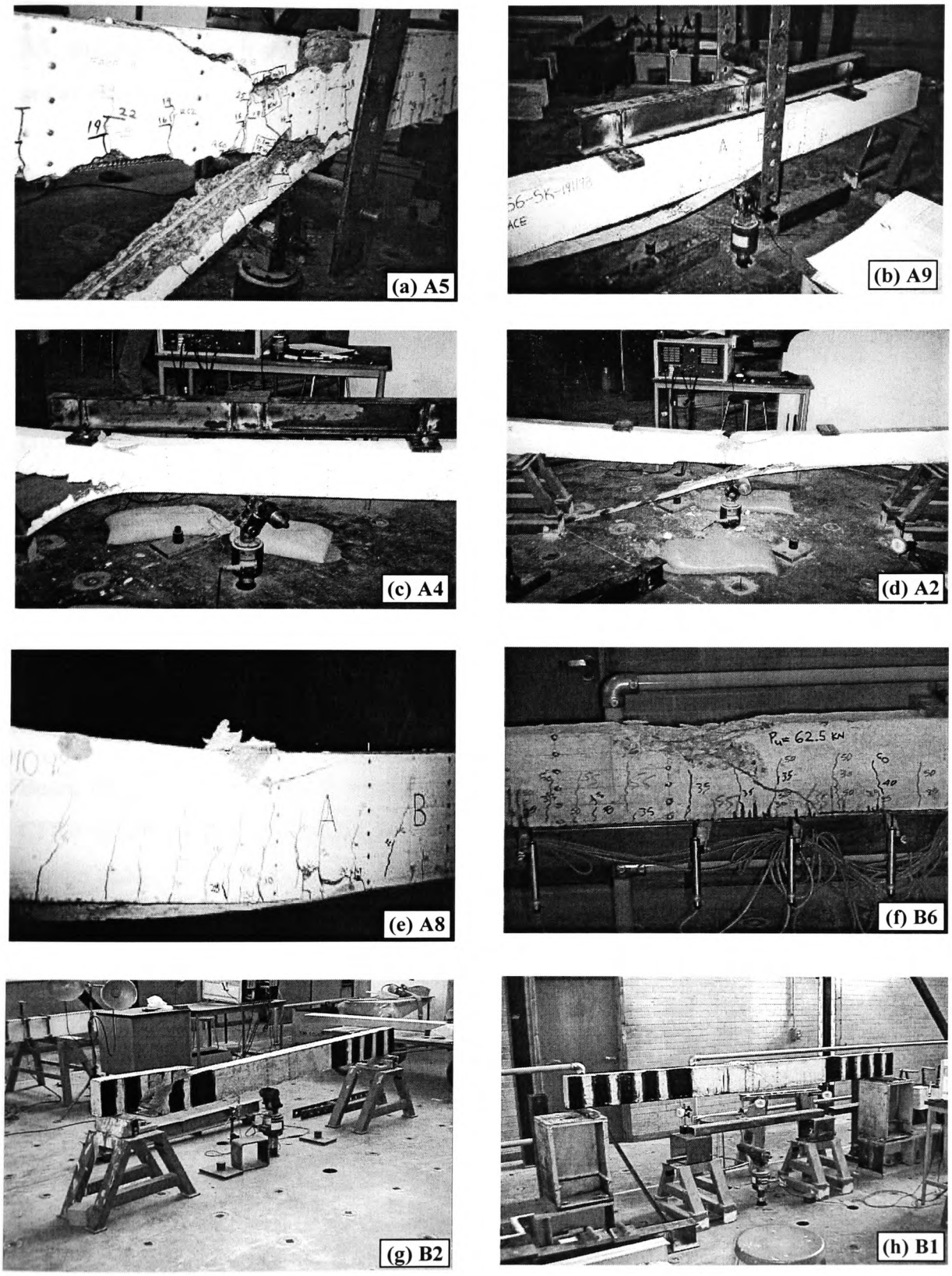

Figure 4.10 Typical Failure Modes of Series A and Series B Beams

The length of the tearing-off failure was proportionally smaller than that of beams A1 to A5, and did not reach mid span of the beam. The actual failure, albeit still brittle, was not as dramatic as the full length CFRP strengthened beams.

Beams A8-A10 were made of higher strength concrete. It was intended that these beams would sustain higher ultimate load that those of beams A1 to A5, since the concrete strength was over 50% higher, and the CFRP plates were shown to have further tensile capacity to be mobilised than had been reached in beams A1 to A7. Beam A8 also failed by combined tearing-off and compression failure, while beams A9 and A10, failed by premature debonding of the CFRP plate from the concrete surface, followed by concrete crushing at the top of the compression zone.

4.3.2.2 Series-B beams

Some typical failure modes of series B beams are included in Figure 4.10. Beam B2 was strengthened with the high strength CFRP plate (type B). It had no internal steel shear links and shear enhancement was provided by external wrapping of the CFRP fabrics (type C) within the shear spans. This beam failed in shear at 94.2 kN.

Beam B1, B3 and B5, which were strengthened by the higher strength and modulus CFRP sheets (type D), all failed by concrete crushing, and the CFRP layer seemed to remain elastic where there were not any apparent signs of imminent failure.

In beam B4, the type C CFRP fabric layer failed first, rattling sound in the fabrics were heard, accompanied by partial snapping of the fibres. This was followed gradually by the crushing of the concrete in compression which led to the ultimate failure of the beam.

The concrete strength for beam B6 was lower than the other beams in the group. This was reflected by the load-deflection relationship as discussed in the following section. The above beam failed by the crushing of concrete in the compression zone, and the type C CFRP sheet seemed to remain elastic. It was found that after the beam had failed, the final deflections observed were much smaller than the values recorded before

the failure, indicating that part of the elastic deformation had recovered as discussed in the following section.

Beams B7 had performed normally until the load reached 40 kN, a number of new cracks appeared at the load of 30 kN, when the existing cracks also widened up to around 0.15-0.2 mm. However, at loads just in excess of 40 kN, the beam suddenly failed in the constant moment zone within the total replacement concrete. It broke into two separate sections, with the GFRP sheets partly peeled-off during the failure process. Subsequent inspection revealed that the welded joints in the internal reinforcement bars had failed. It is therefore concluded that the repair and replacement of any damaged internal reinforcing bars is not normally recommended in the location where maximum bending moment is likely to occur. If it is unavoidable, the replacing should ideally be carried out by welding an extra section of steel bars to the existing steel and with sufficient over lap length. Under no circumstances should a "butt" welded joint be used.

Beam B8 failed by debonding of the GFRP at the plate end. Under the point load near the failed end, signs of a tearing-off failure were also evident. This suggested that even if the partial debonding of GFRP did not occur, the premature tearing-off failure was imminent. This beam was over strengthened by default, since the GFRP used has a low elastic modulus of 73 kN/mm^2 with a high strength of 3450 N/mm^2. This was expected to result in a depth of neutral axis depth of less than 0.1h for a fully balanced section (refer to Chapters 5 and 8 for detailed discussions).

It is concluded that for this type of GFRP composites, the FRP will never reach its design strength. If a high partial factor of safety is also used, it will result in a substantially low material efficiency. It is therefore suggested that there is no need to have a material with inordinately high strength if the elastic modulus is low. In other words, it does not mean that the higher failure strain of an FRP composite will lead to a better strengthening performance, as has been the belief among some FRP material manufacturers.

4.3.3 Load Deflection Behaviour

The vertical deflections along the length of all test beams were recorded including the elastic deformation at the supports. A typical set of deflection profiles (Beam A1) at various loading stages is shown in Figure 4.11. Hereafter, all reported deflections have been corrected after taking account of initial support settlement.

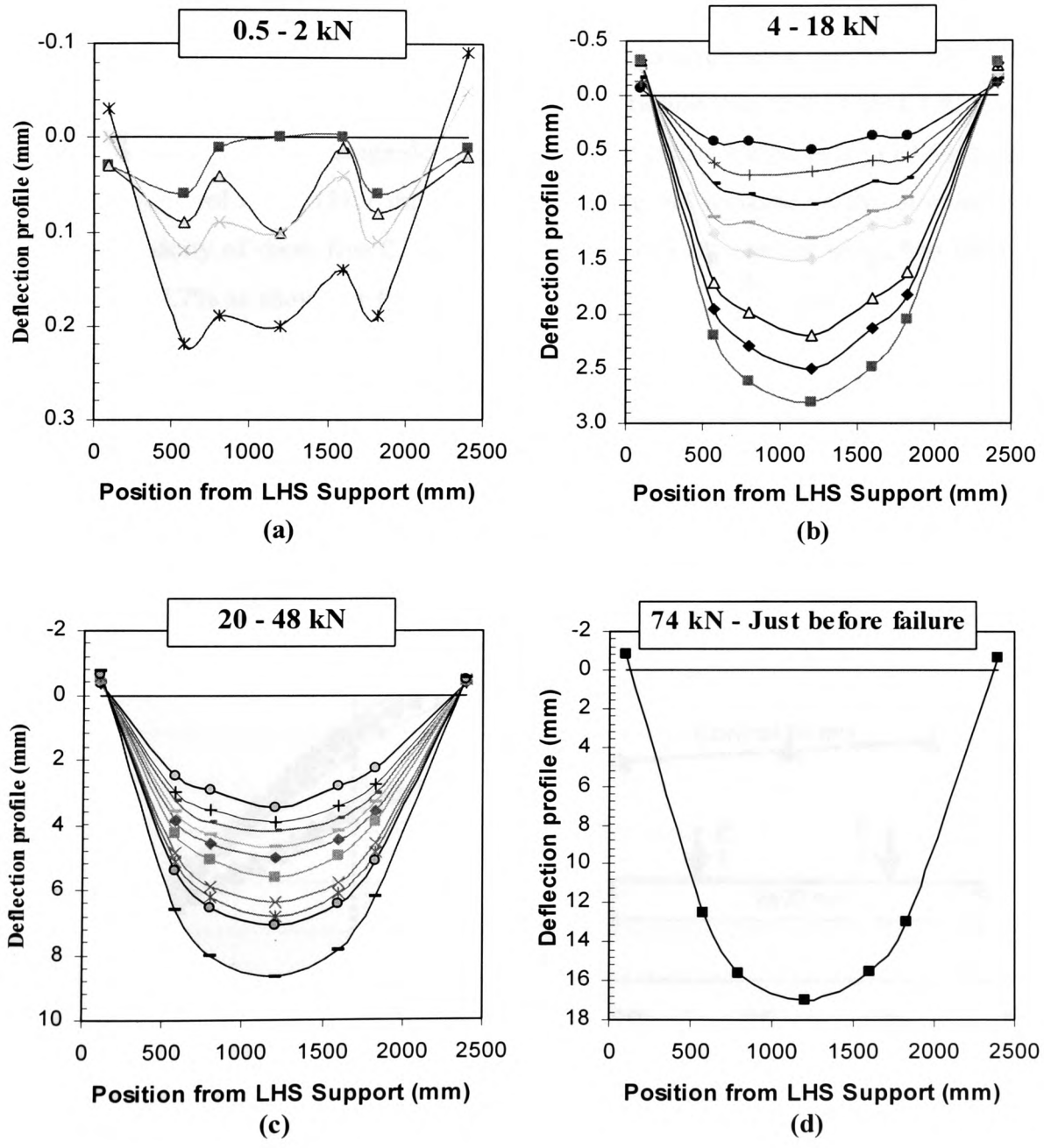

Figure 4.11 Deflection Profiles for Beam A1

The load to maximum span deflection relationships of CFRP plated beams A1, A2, A3, A4 and A5, together with that of the generic, unplated control beam are represented in Figure 4.12. It is apparent that all CFRP strengthened beams show an increased ultimate load capacity as well as stiffness enhancement.

At the serviceability limit of deflection (9.6 mm), the average load of the CFRP strengthened beams was increased by 43% above that of the conventional RC beams. This trend continued until the CFRP plated beams reached their ultimate limit state, at which point the corresponding load increase over the control beam was 68 – 100%. The control beam exhibited a much greater deflection at failure than that of the CFRP plated beams, with the ratio of average deflection at failure of the plated beam (19.44 mm) to that of the control beam (31.7 mm) being 0.61. The net increase of the ultimate load carrying capacity of these five CFRP plated beams over the control beam was between 54.1% and 87.7% as shown in Table 4.8.

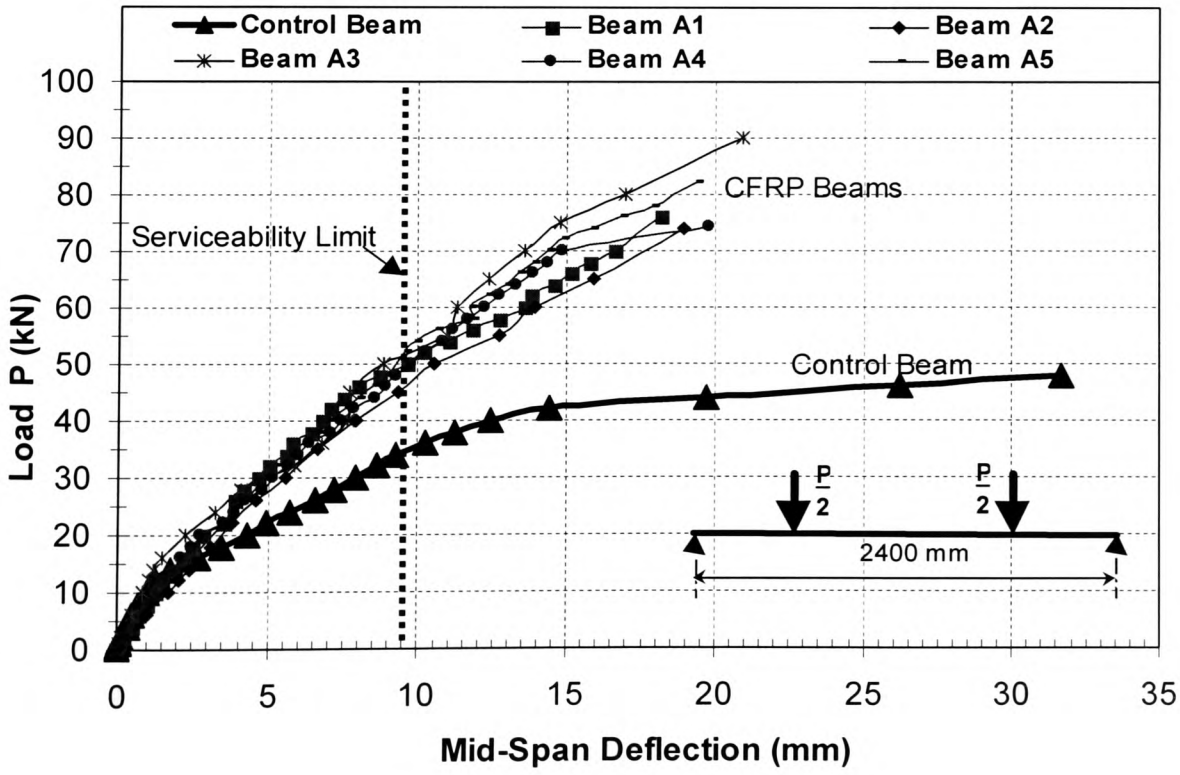

Figure 4.12 Comparison of Load Deflection Behaviour of Beams A1, A2, A3, A4 and A5 with the Control Beam at Ultimate Limit State

Figure 4.13(a) shows the load deflection relationships of these beams up to the serviceability limit state. While the average load increase of the strengthened beams at this stage was 43%, the precracked beam A2 had the lowest increase of 32%. This could be partly due to the lower concrete characteristic strength (41.98 N/mm^2), although at the precracking stage, there was no indication that beam A2 was weaker than others as can be seen from Figure 4.8. Beam A5, which was also precracked, had the maximum load increase of 49%. This was slightly higher than that for beam A3, which was plated from its "pristine state" under perfect conditions with no preloading applied.

Of the five plated beams A1 – A5, the precracked ones (A1, A2, A4 and A5) generally showed a more ductile behaviour under load than beam A3 did. The latter generally exhibited higher stiffness during various loading stages. However, the load deflection curve for beam A3 also showed apparent hardening at a number of locations as can be seen from the enlarged curves shown in Figure 4.13(b). There are two possible reasons for this behaviour. Firstly, a small amount of slippage might have occurred in the adhesive bonding layer, which resulted in an increase of the deflection measurement. Secondly the possibility of an inaccurate original data entry, however small, cannot be completely ruled out. Subsequent moment-curvature analysis of each beam using the strain data, suggests that the latter was more likely.

It is interesting to note that at the early loading stage up to around 15 kN, all the CFRP plated beams which were precracked before being strengthened, had shown lower stiffness than those of the control beam and the uncracked beam A3. The first point at which the directions of tangent changes in a load-deflection curve is of significance when studying the behaviour of a RC element. The decrease of tangent of the load-deflection curve usually signals that the concrete tensile strength has been reached, and it is the end of elastic behaviour. The first crack in concrete can be detected at this stage.

Shown in Figure 4.13(b) is the enlarged initial part of the load deflection curves for all beams in the A series. It can be seen that there were no apparent early kinks in these curves for all of the precracked beams A1, A2, A4 and A5. A near linear load-deflection

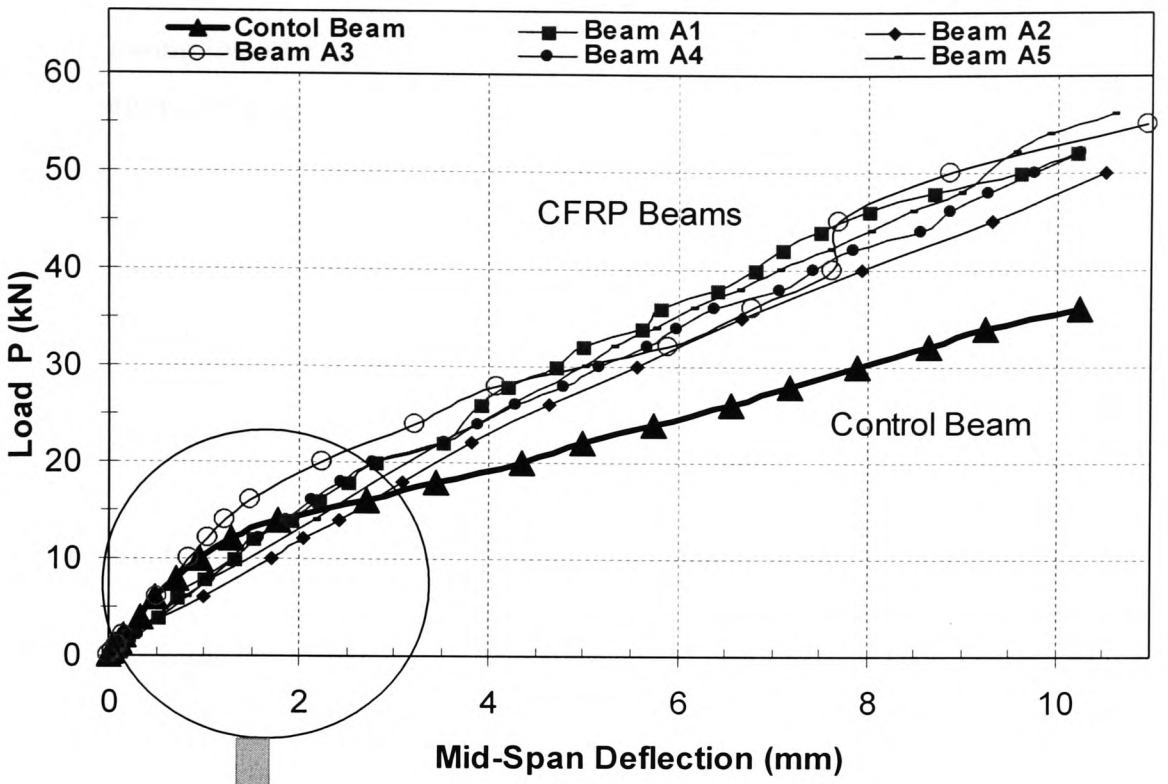

(a) At Serviceability Limit State

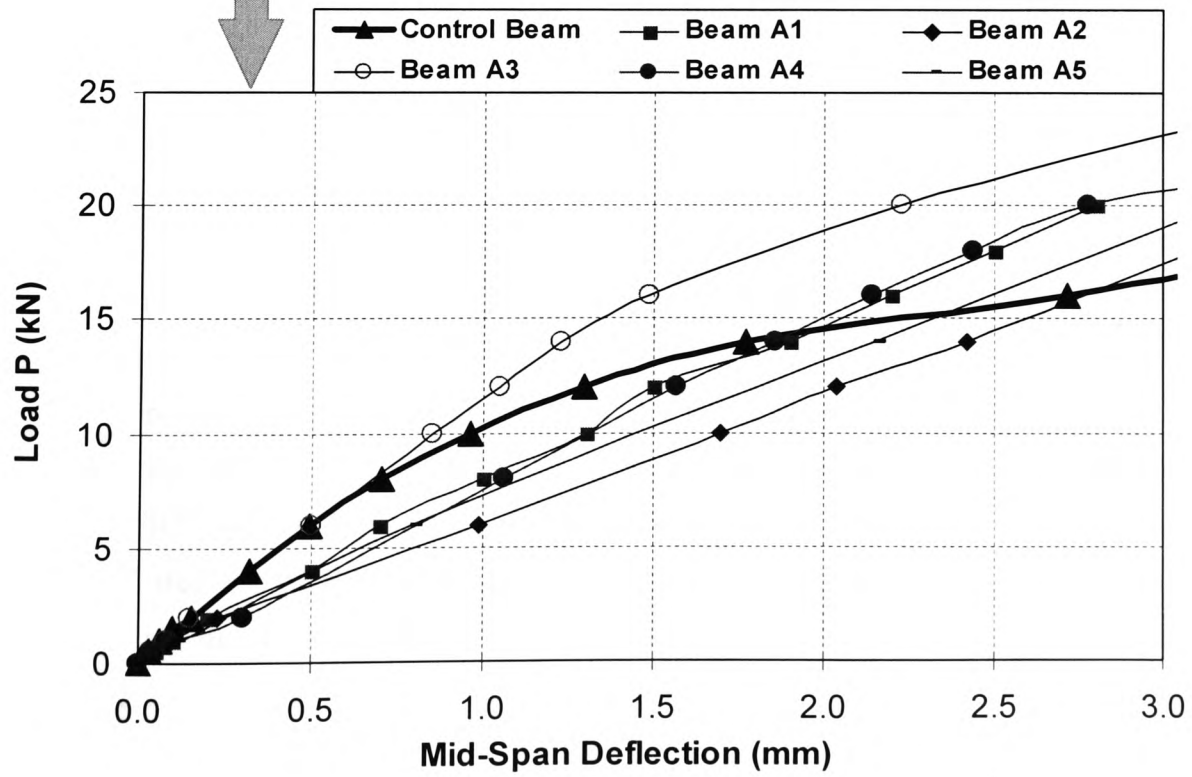

(b) At Initial Loading Stage

Figure 4.13 Load Deflection Behaviour of Beams A1, A2, A3, A4 and A5 at SLS

behaviour was evident. Based on the experimental results, the candidate has suggested the following hypothesises for this observed behaviour. He also intends to verify these assumptions using the analytical modelling, to be presented in Chapter 5.

Hypothesises on the precracked, CFRP strengthened RC beams:

- The strengthened section exhibits pseudo linear load deflection behaviour up to the serviceability limit of deflection, after which the reduction of tangent slope is still relatively small in comparison with the conventional RC beams.

- Such behaviour, apart from the tension stiffening effect, is due to most of the transfer of tensile stresses (in the precracked loaded concrete beam) to the internal steel and external CFRP plate reinforcement, which have elastic characteristics.

- New cracks are expected not to appear in the precracked beam until at least the reloading exceeds the maximum original precracking load.

The last statement was in fact already observed to be valid during experimentation. None of the precracked, CFRP strengthened beams showed any more new cracks until after the original serviceability limit. The old cracks, which were a result of the preloading to the originally designed serviceability limit, appeared to widen just prior to any new cracks emerging.

It was interesting to note that the maximum crack width generally occurred at about half the height on the surface of the beam web on both sides, while the cracks at the bottom near the FRP bonding layer showed just visible hairline magnitudes. This is a clear indication that for FRP strengthened flexure members, the number of cracks will increase, as the corresponding crack width decreases, in comparison with the unstrengthened element under the same service load.

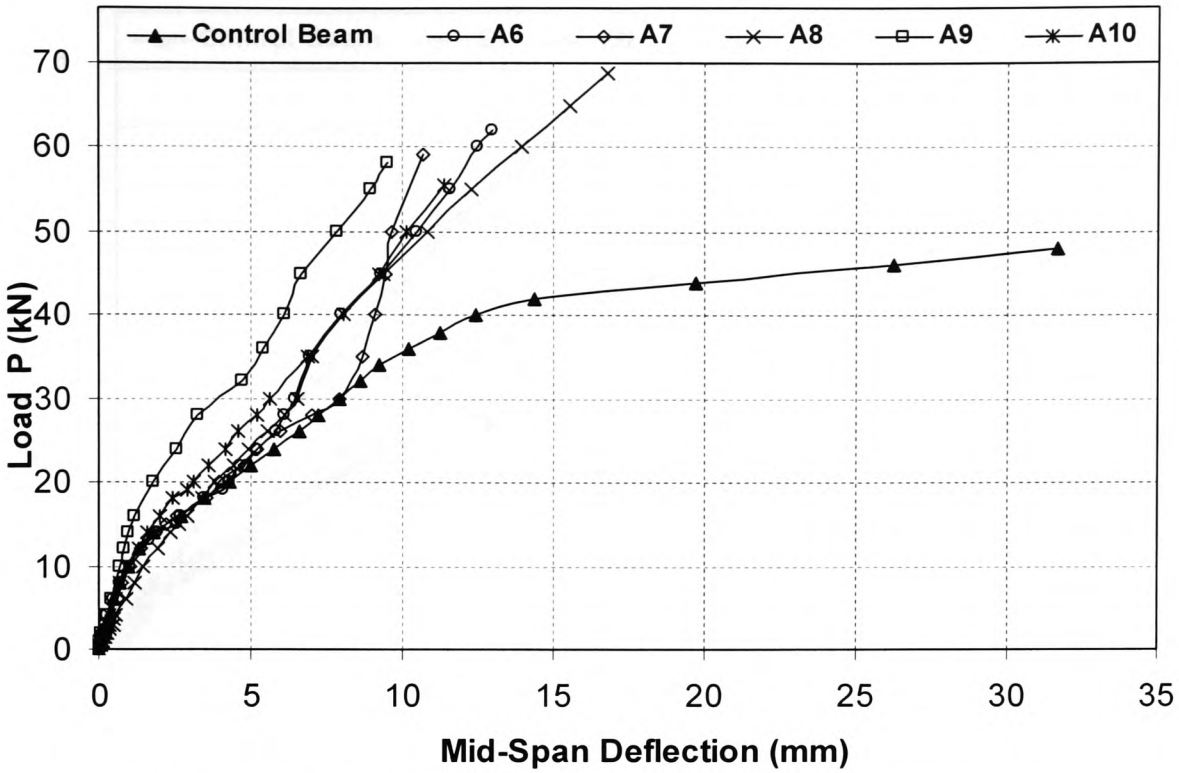

Figure 4.14 Comparison of Load Deflection for Beams A6-A10

For beams A6-A10, the load deflection relationship is shown in Figure 4.14. Beams A6 and A7, both were strengthened with 1.0 metre type A CFRP plate in the constant moment zone, the load-deflection responses were almost identical to that of the control beam, until a load of 26 kN (55% of the ultimate load of control beam). After this load, both beams exhibited a "leap" in the stiffness increase, suggesting that the stress transfer to the FRP had a sudden increase. Both beam A6 and A7 failed by tearing-off of concrete cover. This was somewhat unexpected, since the length of FRP was shorter that the constant moment zone, and it was expected the beams would fail shortly after the load had reached the ultimate level of the unstrengthened control specimens.

The load-deflection behaviour of beams B1 to B6 is shown in Figure 4.15. The high strength and high elastic modulus of type B CFRP plate resulted in a significant strength increase (91%) as well as stiffness enhancement for beam B2. This beam was over strengthened, as were all the beams in series A-tests.

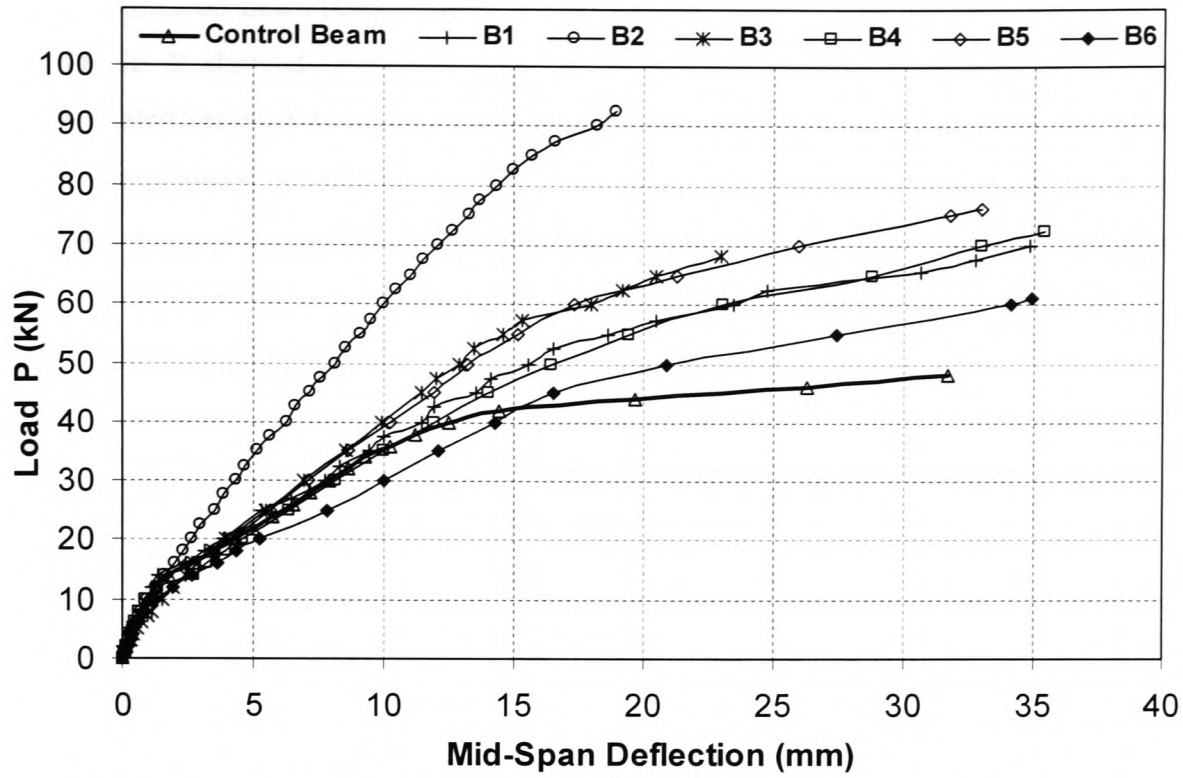

Figure 4.15 Comparison of Load-Deflection Behaviour for Beams B1 to B6

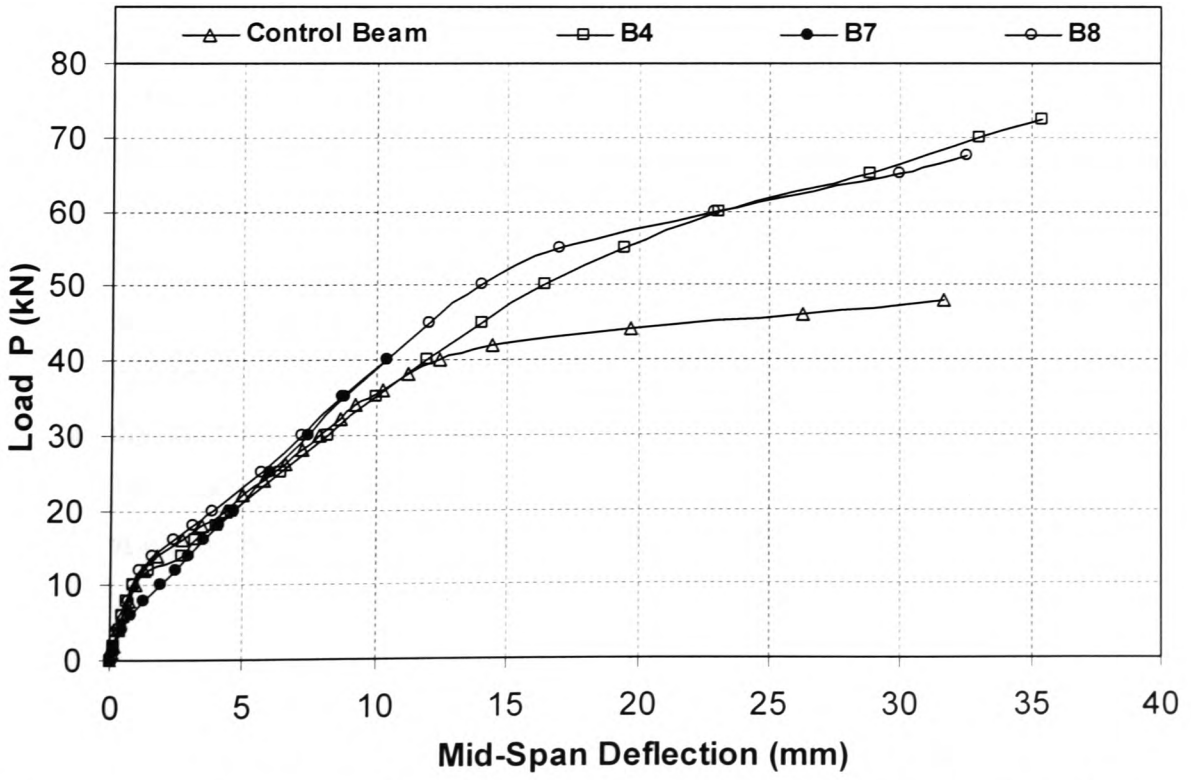

Figure 4.16 Comparison of Load Deflection Behaviour of GFRP Strengthened Beams B7 and B8 with CFRP Strengthened Beam B4 and the Control Beam

It is reconfirmed that FRP strength cannot be efficiently utilised, and the failure mode was brittle. It showed "improvements" in its ultimate load increase over the type A CFRP plated series-A beams, but the failure mode was brittle. On the other hand, the CFRP fabric sheets strengthened beams were considered to be lightly strengthened with an FRP cross sectional area of 14.5 mm^2 (ρ_p = 0.73%). These beams exhibited a more ductile behaviour in comparison, the strength enhancement achieved was between 27 – 59% as summarised in Table 4.9.

Although the extent of ultimate load increase is relatively low, the ductile behaviour of these CFRP sheets strengthened beams is considered to be a great benefit in comparison with the brittle behaviour of the over strengthened beams.

Figure 4.16 demonstrate the load-deflection relationship of the two GFRP sheets strengthened beams, together with that of the control beam and CFRP strengthened beam B4. It is clear that beam B7 failed suddenly and prematurely due to the failure of internal steel reinforcement as discussed previously. Beam B8 showed similar behaviour to the CFRP sheet strengthened beams. When compared with B4, which is under strengthened with one layer of the type C CFRP sheet and had 51% ultimate load increase, the performance of beam B8 was see to be inferior at a 41% load enhancement.

This difference in behaviour between the two types of FRP materials clearly demonstrate that the CFRP materials with a lower strength and higher elastic modulus can out perform the GFRP sheets with higher strength but lower elastic modulus. It may be initially concluded that an ideal FRP material for RC strengthening should have medium ultimately tensile strength of, say, around 1500 – 2000 N/mm^2, and the minimum elastic modulus of such FRP composites should be of the order of 120 -150 kN/mm^2.

4.3.4 Strain Distribution

4.3.4.1 Strain distribution across section depth

The concrete strains in the constant moment zone were recorded using the Demec gauge discs as illustrated in Figure 4.4. The Demec gauge recordings were processed in tabulated and graphical form. They were then compared to identify any data that appeared to significantly differ from the general trend. If an obviously incorrect data entry was made as was found on a few occasions, that reading was then discarded. Shown in Figure 4.17(a) is the distribution of concrete surface strains across the depth of the control beam (R3). As can be seen, under the initial low load, the strain measurements appeared to fluctuate slightly. As the load increased, the strain distribution exhibited near perfect linear variation, indicating that plane sections remained plane during the loading process. This was generally true for the CFRP plated beams as well. Shown in Figures 4.18 and 4.19 are the typical strain distribution beam A1 and the CFRP plated beam A3. Figures 4.20 – 4.21 show the strain distribution of the CFRP and GFRP sheets strengthened beams respectively. It was clear that under a given loading level, the control beam showed the greatest concrete surface strain.

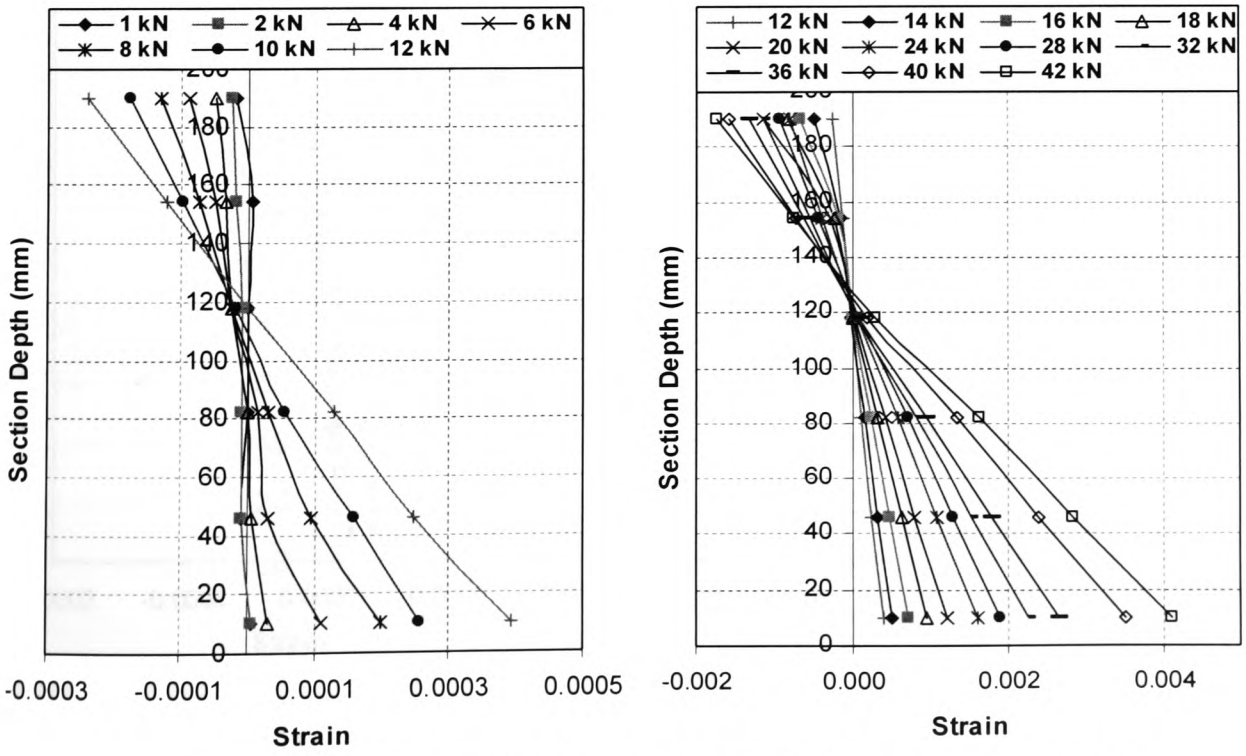

Figure 4.17 Strain Distribution at Mid-span of the Control Beam (R3)

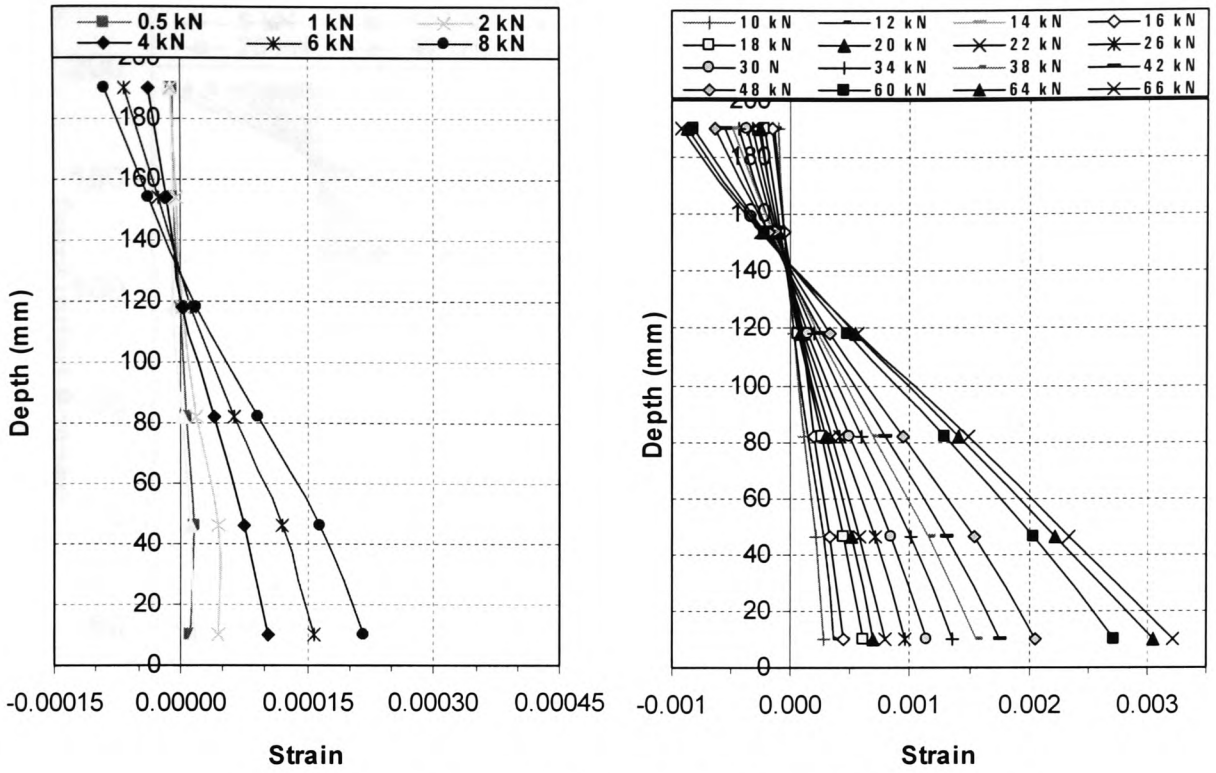

Figure 4.18 Strain Distribution at Mid-span for Beam A1

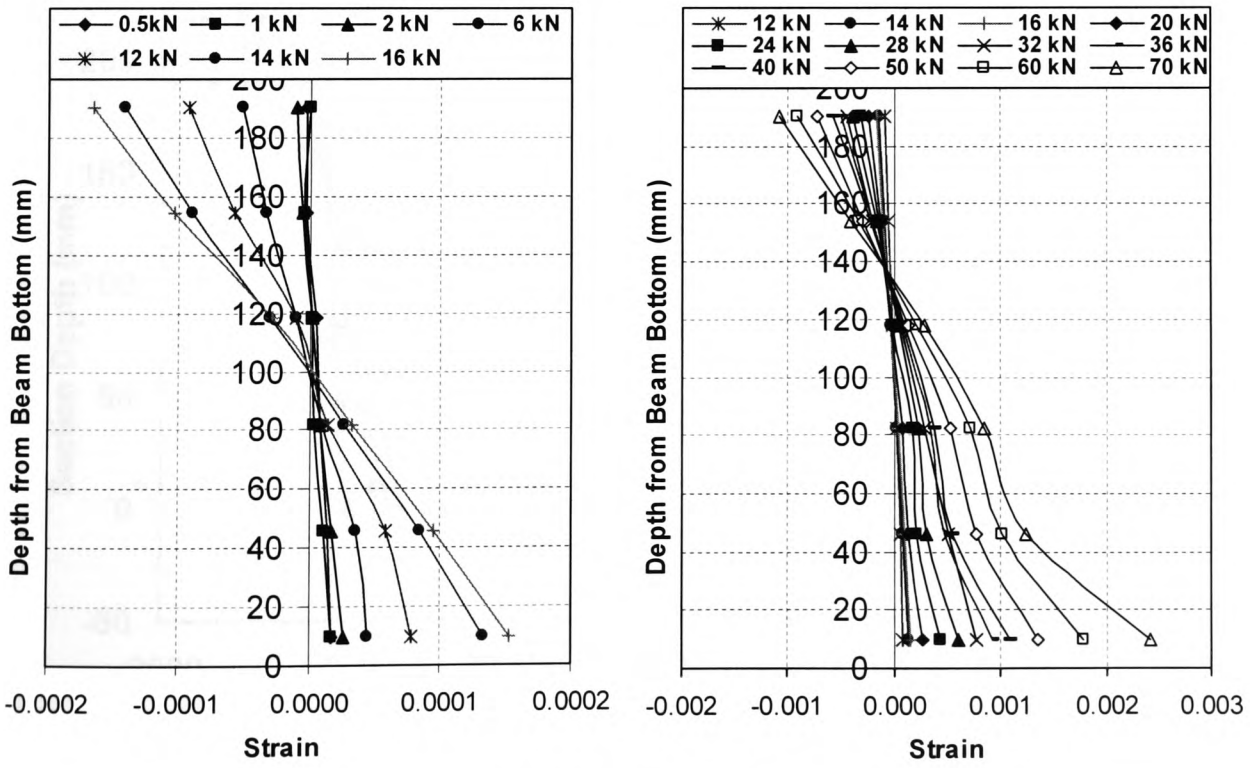

Figure 4.19 Strain Distribution at Mid-span for Beam A3

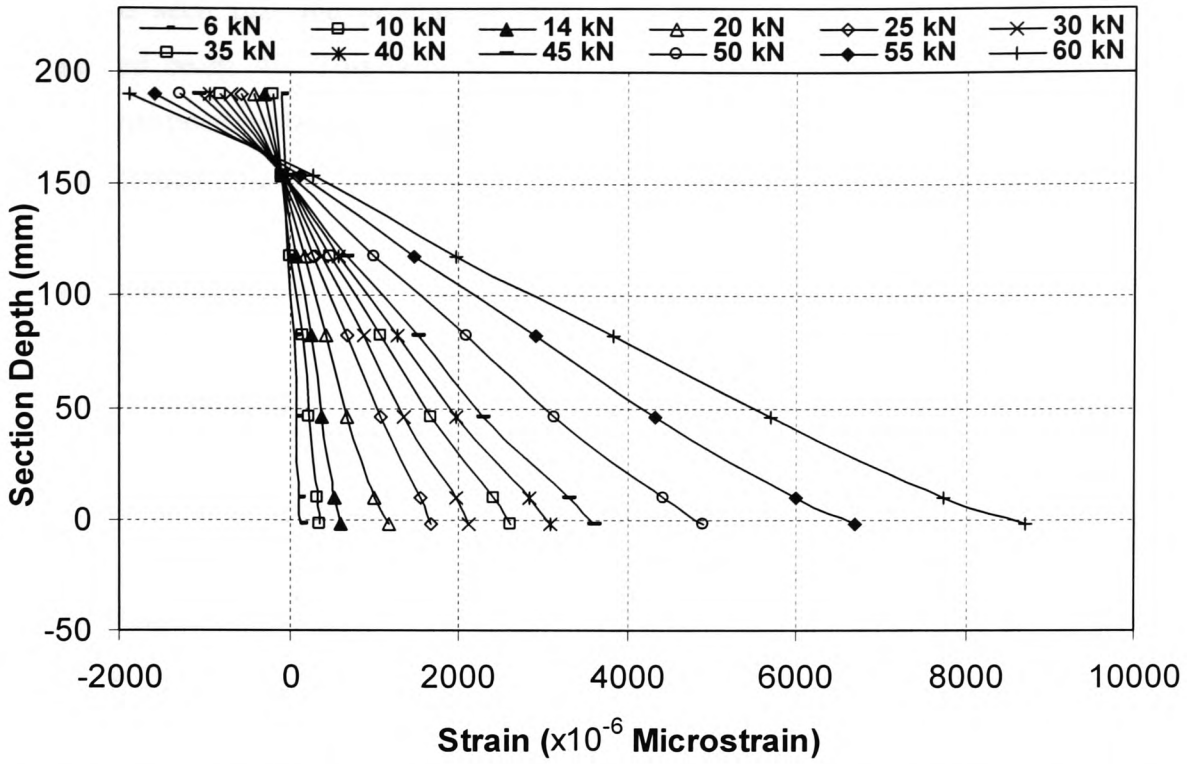

Figure 4.20 Typical Strain Distribution of CFRP Strengthened Beams (B6)

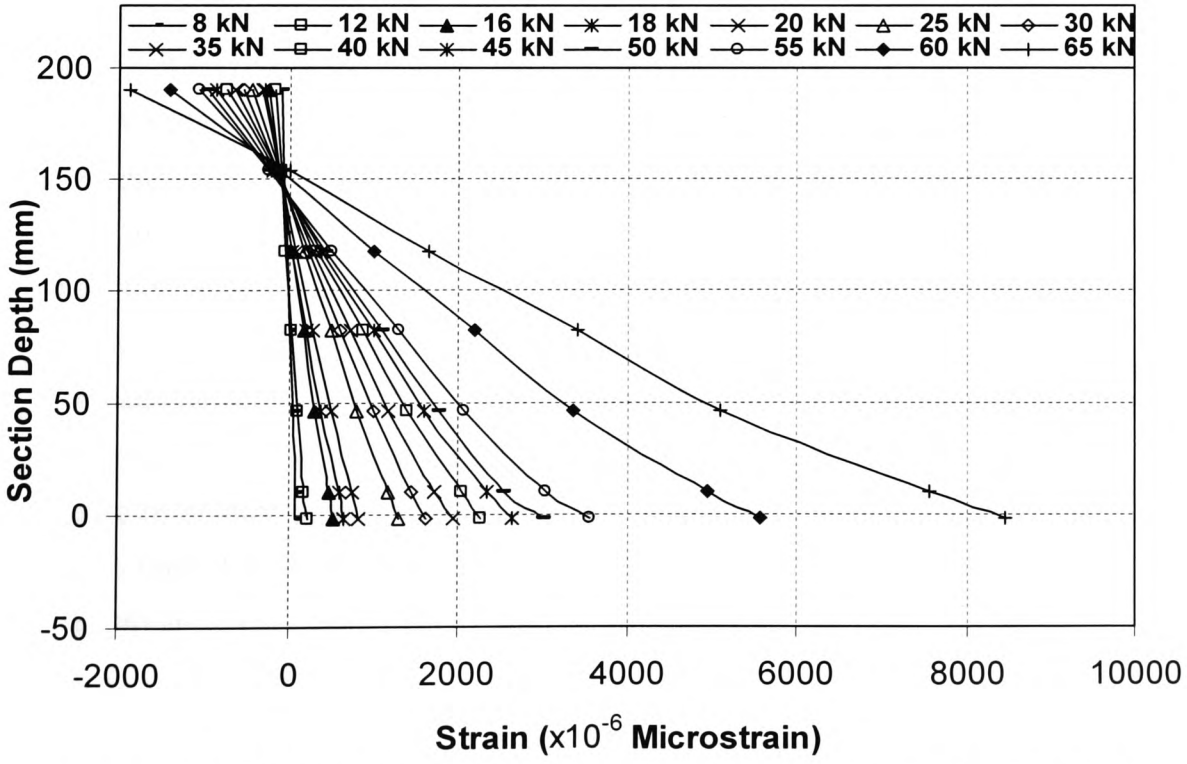

Figure 4.21 Typical Strain Distribution of GFRP Strengthened Beams (B8)

It can be seen that the precracked beam A1 showed greater strain than the non-precracked beam A3. This is because the presence of existing cracks resulted in the neutral axis position being slightly moved upwards, which in turn leads to a reduction of second moment of area.

Although with a much lower elastic modulus, the GFRP strains in beam B8 was much lower than the strains in the CFRP sheet of beam B6 under the same load level. However, at just before ultimate failure, both beams showed similar values of FRP strains at around 8500 microstrain.

4.3.4.2 Load strain relationship

For the control beam, the maximum surface strain near the bottom fibre in the tension zone was recorded to be 4100 microstrain at a load of 42 kN (approximately 85% of the ultimate failure load). The corresponding compressive strain at the top of the beam was 1740 microstrain, as shown in Figure 4.22.

The latter was just 50% of the ultimate concrete compressive strain value of 0.003500, which is a BS 8110 design specification. Although the actual failure strain is usually much lower than this figure (say, 0.002200-0.002600), this fact suggests that during the last loading stage just before the beam failed in steel yielding followed by concrete crushing, the concrete strains in the compression zone underwent rapid increment. A large portion of the value of the ultimate strains was caused by the last 15% of the applied load. Beam A1 and other precracked beams followed the strain values of the control beam, with comparable orders of magnitude. Beam A3 underwent the lowest strain variation at the initial loading stage. However, there appeared to be little difference from other precracked CFRP plated beams as it approached the ultimate limit state. The typical load versus strain relationships for the FRP strengthened beams (A1, A3 and B6) are shown in Figures 4.23-4.25.

It can be seen that strains in beam B6 started to increase more rapidly at 50 kN, suggesting that a ductile failure is possible, while the plated beams A1 and A3 did not show any indication of the imminent brittle and premature failures associated with these series of tests.

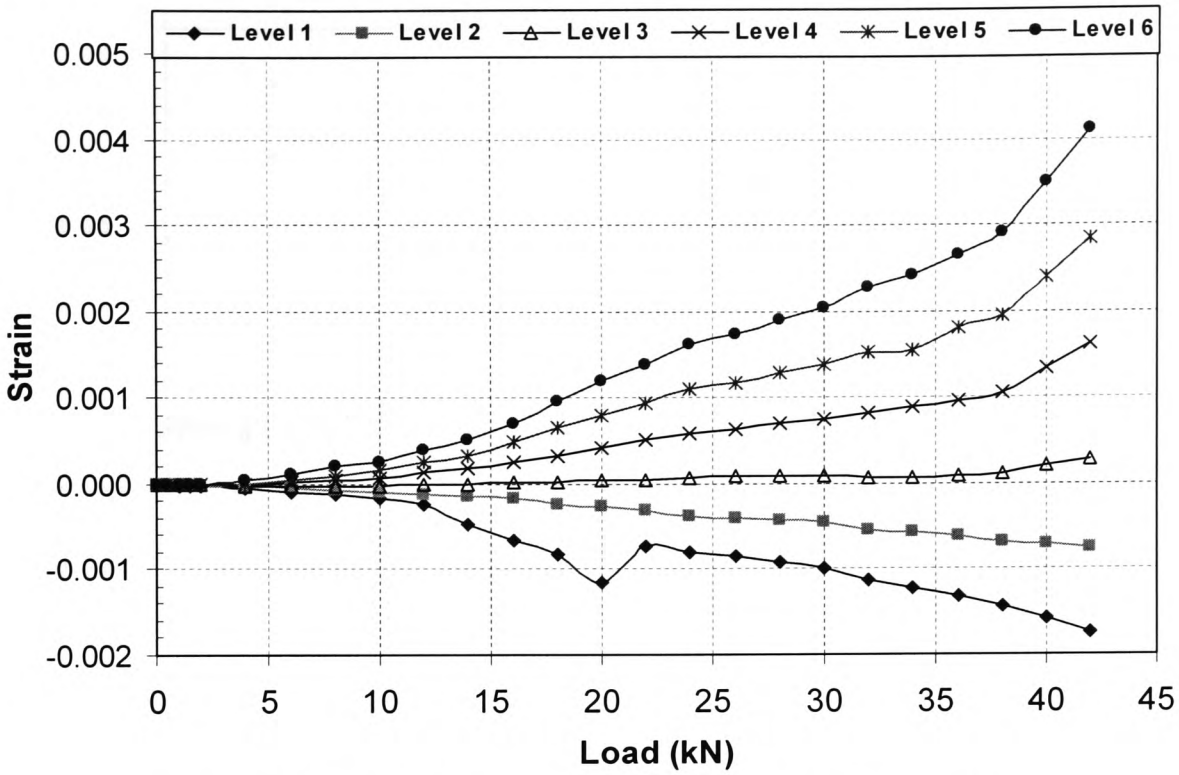

Figure 4.22 Load vs. Strain for Control Beam (Control-R3)

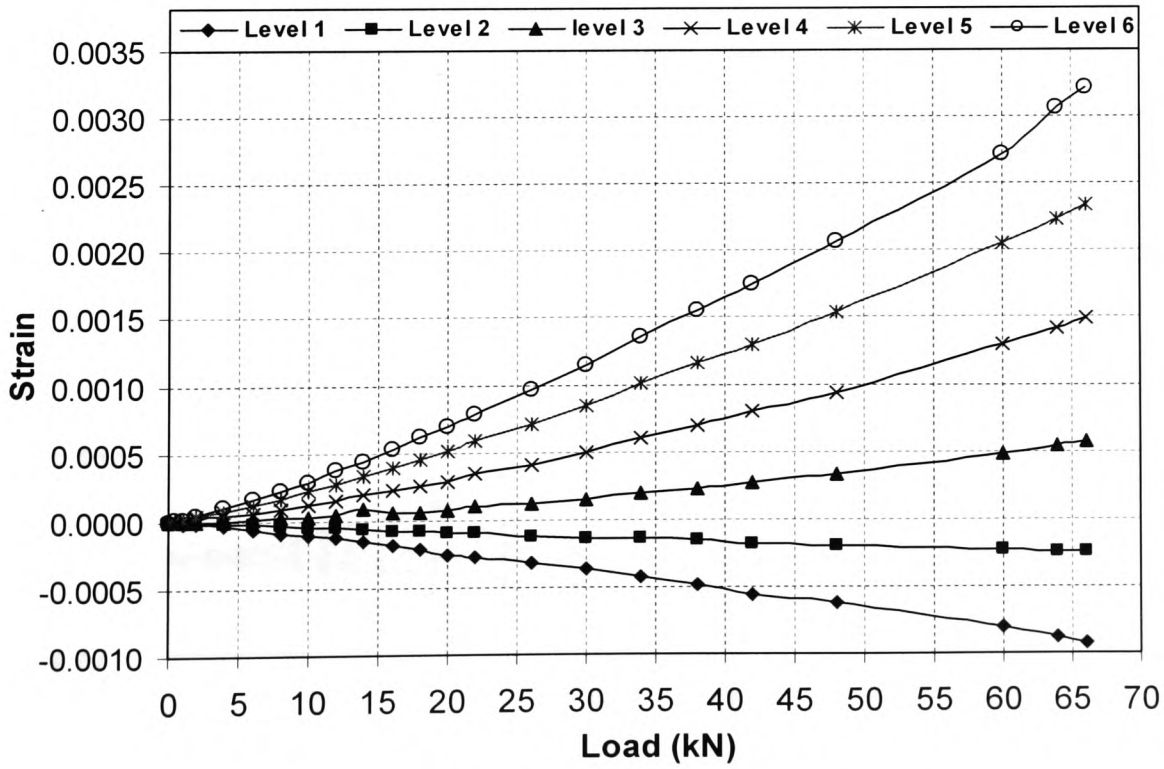

Figure 4.23 Load vs. Strain for Beam A1

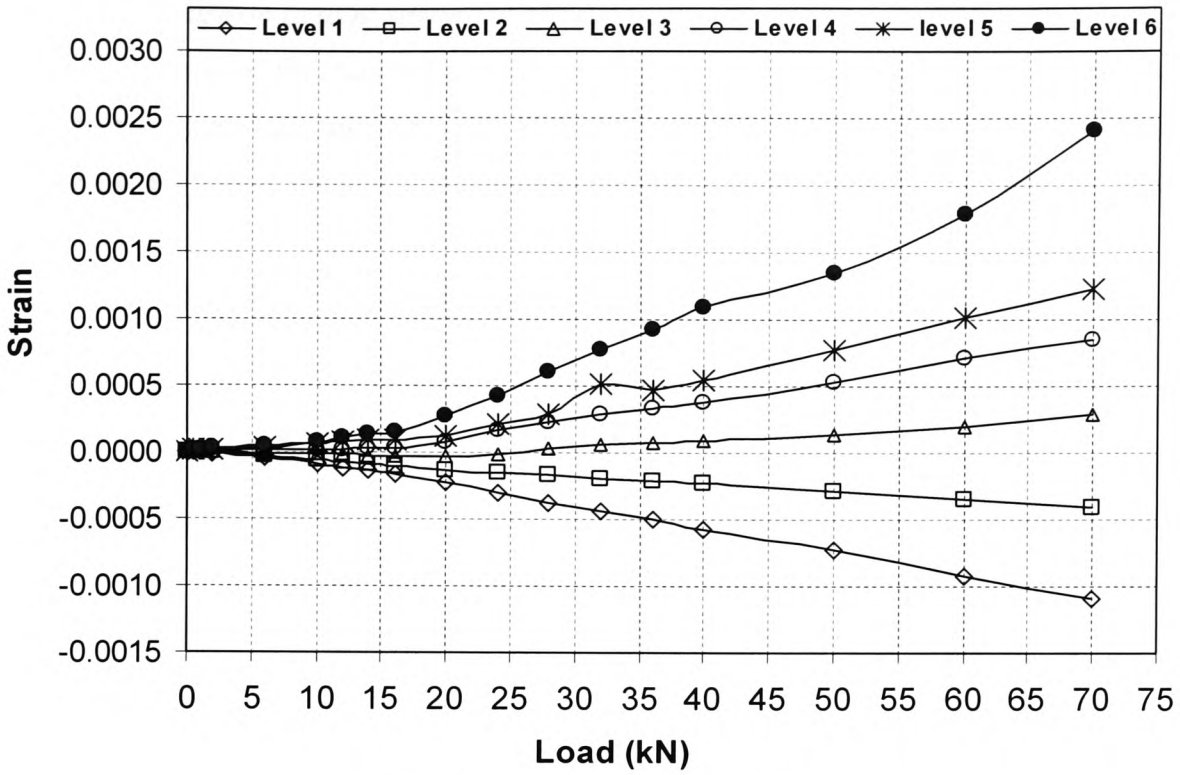

Figure 4.24 Load vs. Strain for Beam A3

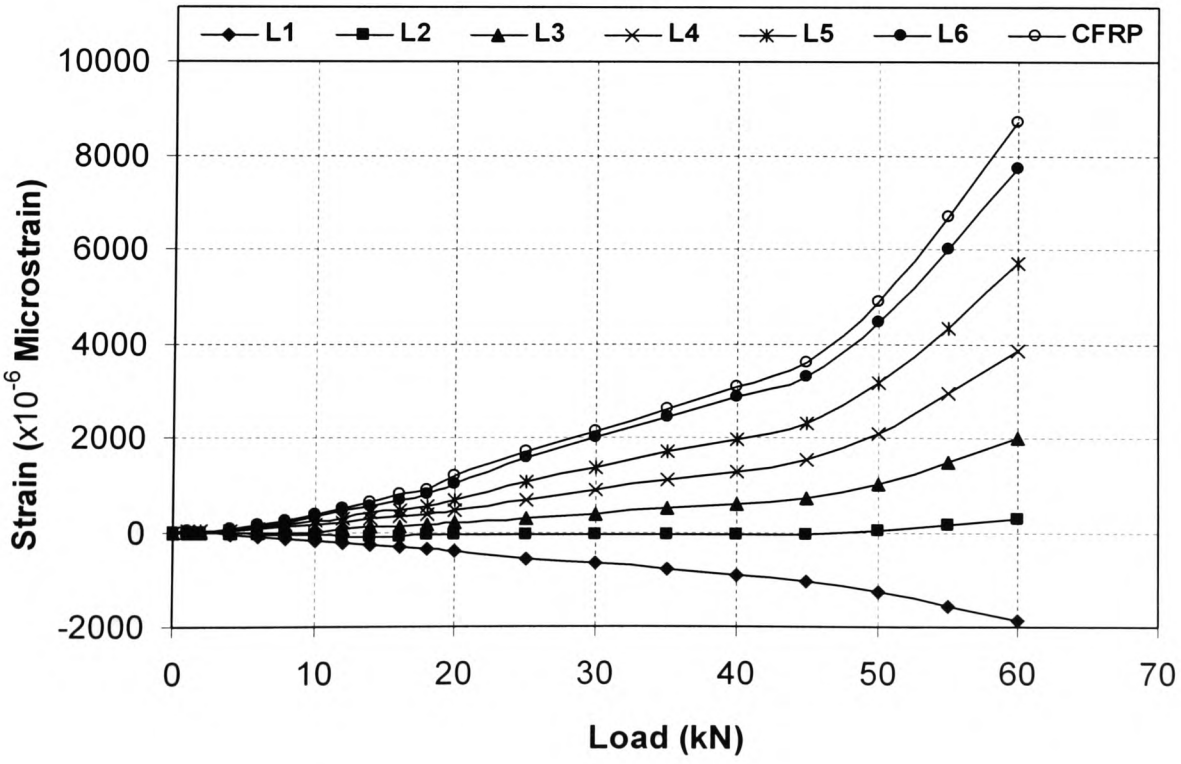

Figure 4.25 Load vs. Strain for Beam B6

4.3.4.3 Comparison of load strain variations

The comparison of the maximum surface strains at failure of beams A3, B6 and B8 is shown in Figure 4.26 together with that of the control beam. It can be seen that the CFRP plated beams showed much smaller strains at failure. This is because the failure mode for these plated beams was premature and brittle due to the large area of FRP provided, and the flexural capacity of neither the FRP nor the concrete was fully used.

In contrast, the single layer CFRP sheet strengthened beam B6 showed a similar trend of load strain relationship as the control beam initially, and the strain was much further extended as the loading was increased towards the ultimate value. The much higher strain values at a load of 60 kN (or 83% of ultimate failure load) indicates that at the final failure, it is most likely that the concrete and FRP strains in beam B6 had reached the ultimate value of 0.003500 and 0.014000 respectively. Beam B8 also showed a similar behaviour as B6, although its strain at beam failure would not have reached the ultimate value of 0.045000 since this beam with two layers of high strength GFRP sheets was considered to be over strengthened.

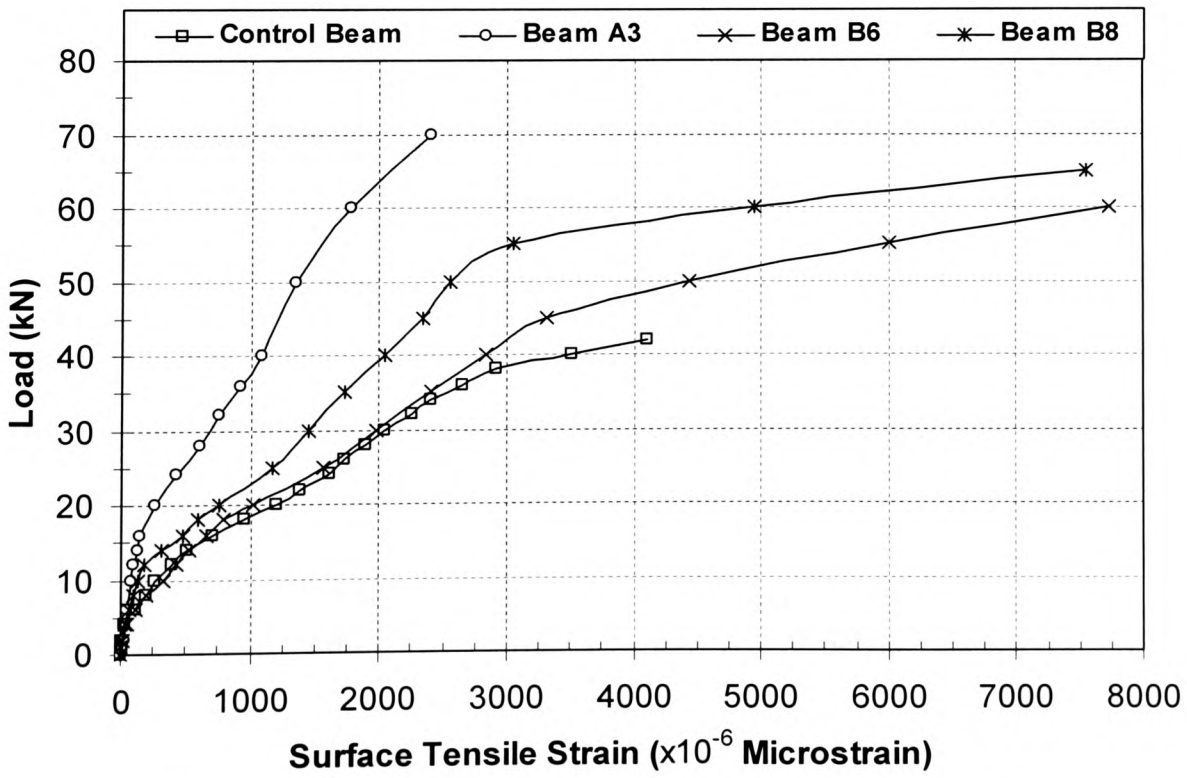

Figure 4.26 Comparison of Load vs. Maximum Tensile Strain

4.3.4.4 Behaviour of precracked beams before serviceability limit

There is a distinctive difference in the strain behaviour between the CFRP plated beams and their original counterparts. Similar to the load-deflection relationships, the strain variations of these beams, as shown in Figure 4.27, also showed the pseudo linear behaviour of the plated beams. This is a clear indication of the composite action between concrete and the FRP materials, the tensile stress transfer through the adhesive layer to the CFRP composites in the strengthened beams took place as soon as the load is applied.

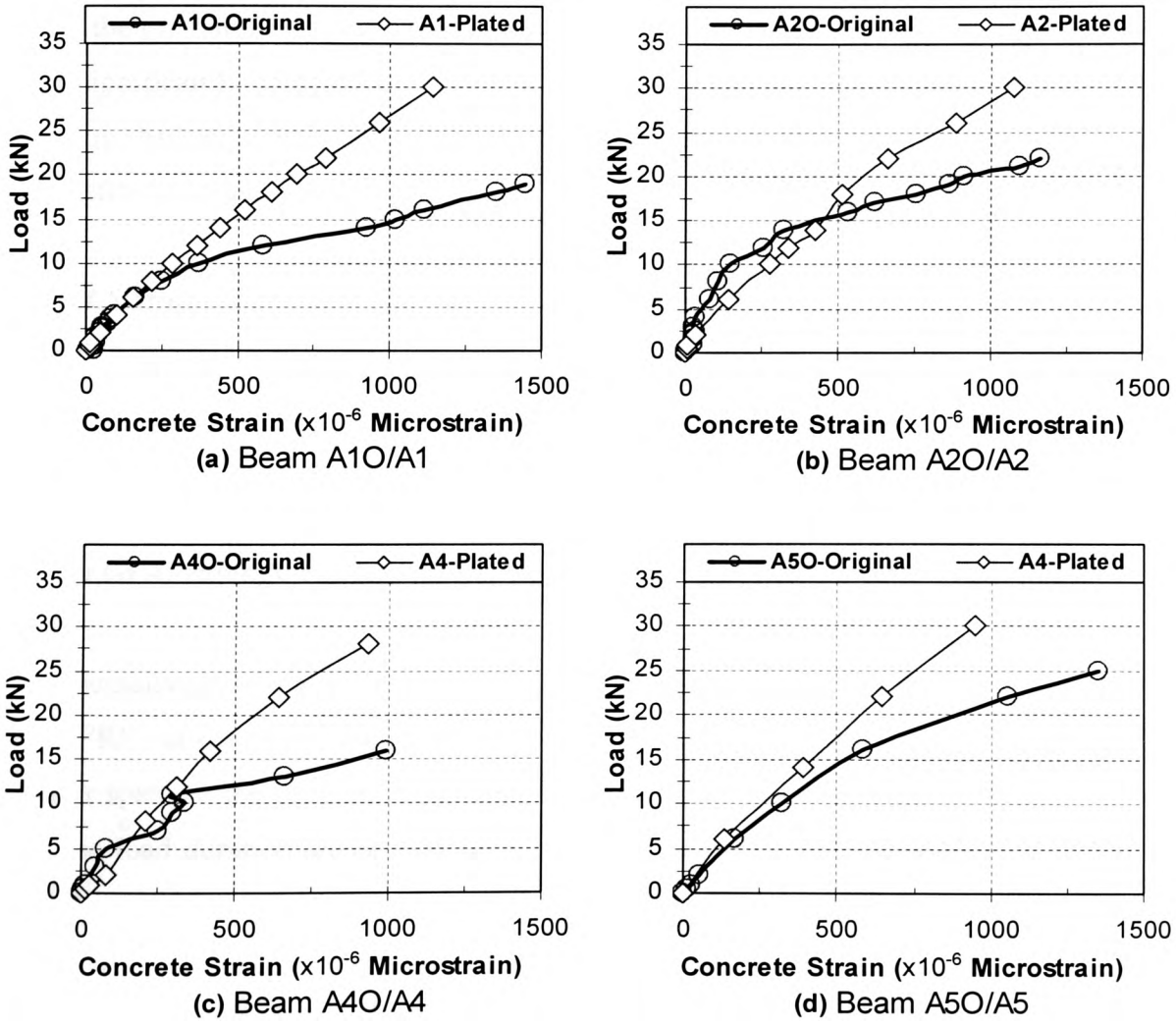

Figure 4.27 Comparison of Strains between the Precracked and the Plated Beams at the Early Loading Stage

At a load of 30 kN, which is just under the normal service load of the control beam, all plated beams exhibited similar strain values as shown in Figure 4.28. Beam A3 showed slightly smaller strains in comparison with the precracked ones, while the control beam underwent the largest strain deformation as expected.

It is interesting to note that, under their respective service load conditions, all beams including the CFRP plated and the control beam, exhibited similar strain distribution as shown in Figure 4.29. It is important to point out that the service load for the strengthened beams were estimated to be 67% of their corresponding actual failure load observed in the experiments. Since the failure mode of these CFRP strengthened beams was the premature tearing-off of concrete cover, it is possible that the service load could be significantly increased if suitable measures were taken to prevent the premature failure. Subsequently, the maximum tensile strains in the strengthened beams would therefore increase accordingly.

4.3.4.5 Strain distributions in the FRP composites

Strains along the FRP surface were recorded in series B tests. Figure 4.30 shows the strain variation in the single CFRP layer at each load increment, while Figure 4.31 displays the load strain relationship at various locations from the end to the mid-span for same beam. These varations are also shown in Figures 4.32 and 4.33 for the two-layer GFRP strengthened beam B8, where the same trends are clearly identified.

As demonstrated in these graphs, the FRP strain increases as the distance increases from the FRP cut-off point toward the mid-span, this trend continues up until the end of the shear span. In the pure bending zone, the FRP strain remains largely constant for most of the load duration. At approaching the ultimate load, the FRP strain in the mid-span tends to increase with loading more rapidly in comparison with positions elsewhere.

This behaviour confirms the assumption of perfect bonding between the concrete and FRP, and the full composite action is ensured. It is also significant in providing information for the prediction of premature tearing-off failure load, which is to be discussed in Chapter 6.

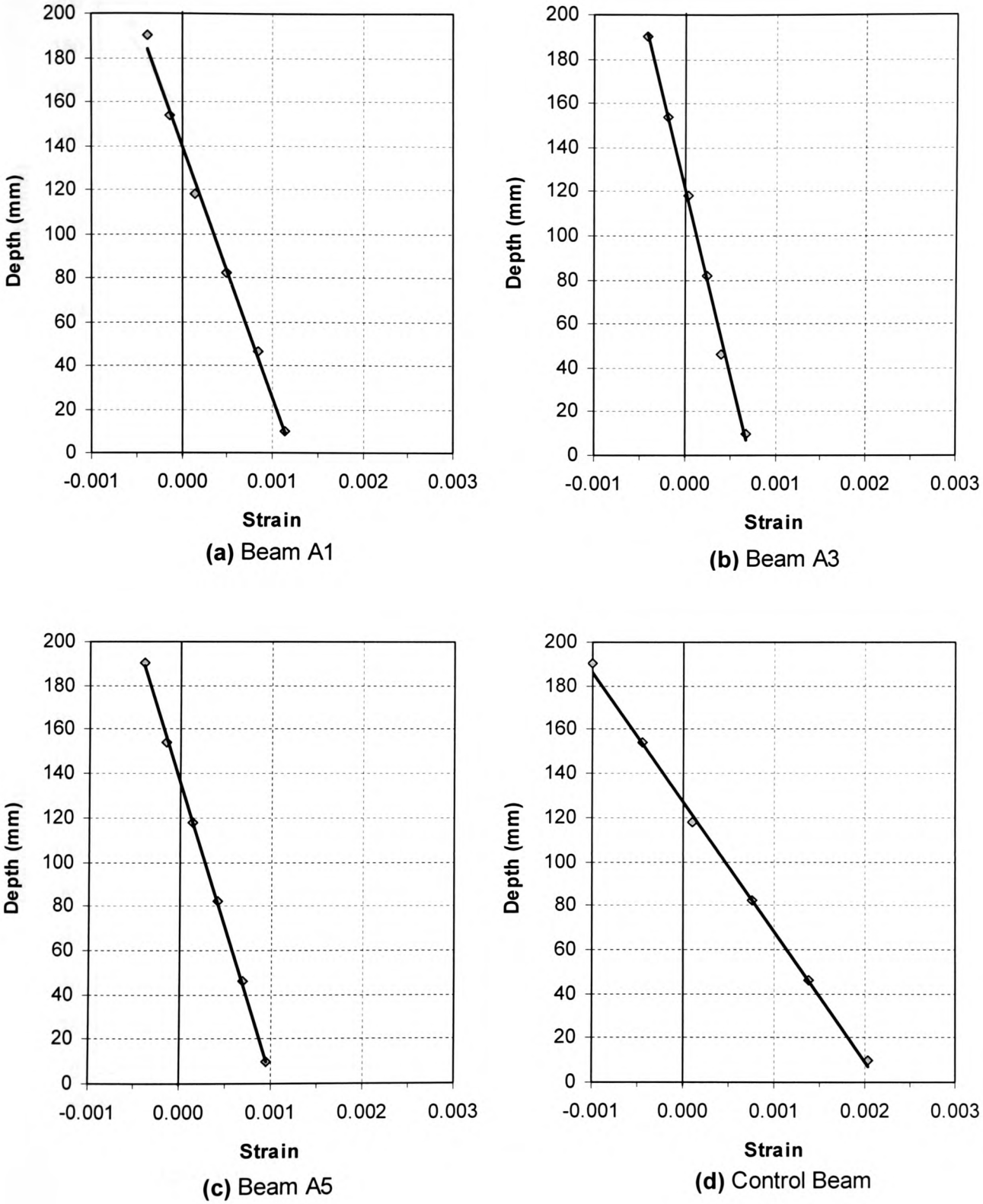

Figure 4.28 Comparison of Section Strains at the Service Load of the Control Beam (30 kN)

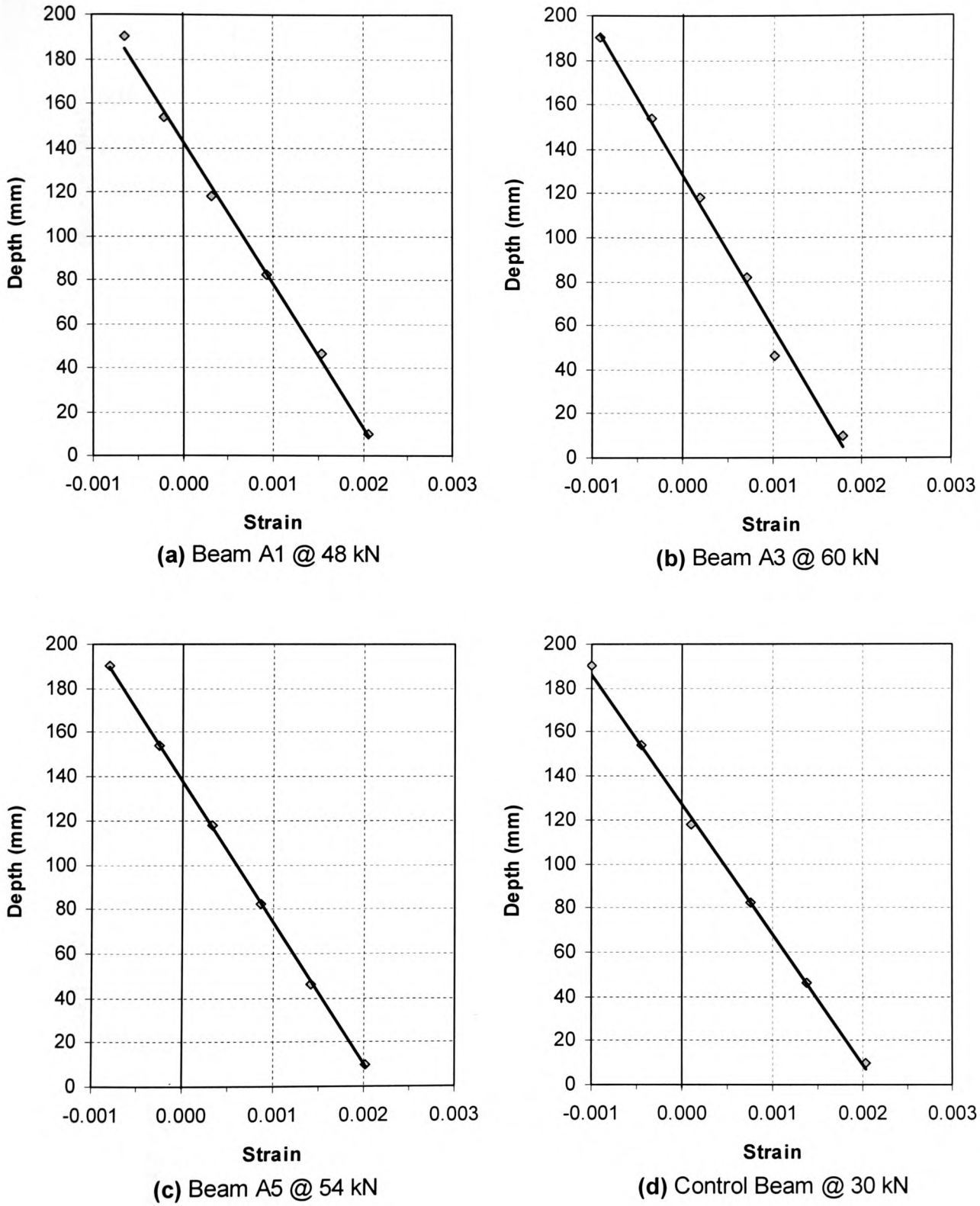

(a) Beam A1 @ 48 kN

(b) Beam A3 @ 60 kN

(c) Beam A5 @ 54 kN

(d) Control Beam @ 30 kN

Figure 4.29 Comparison of Section Strains at the Service Load for Each Beam

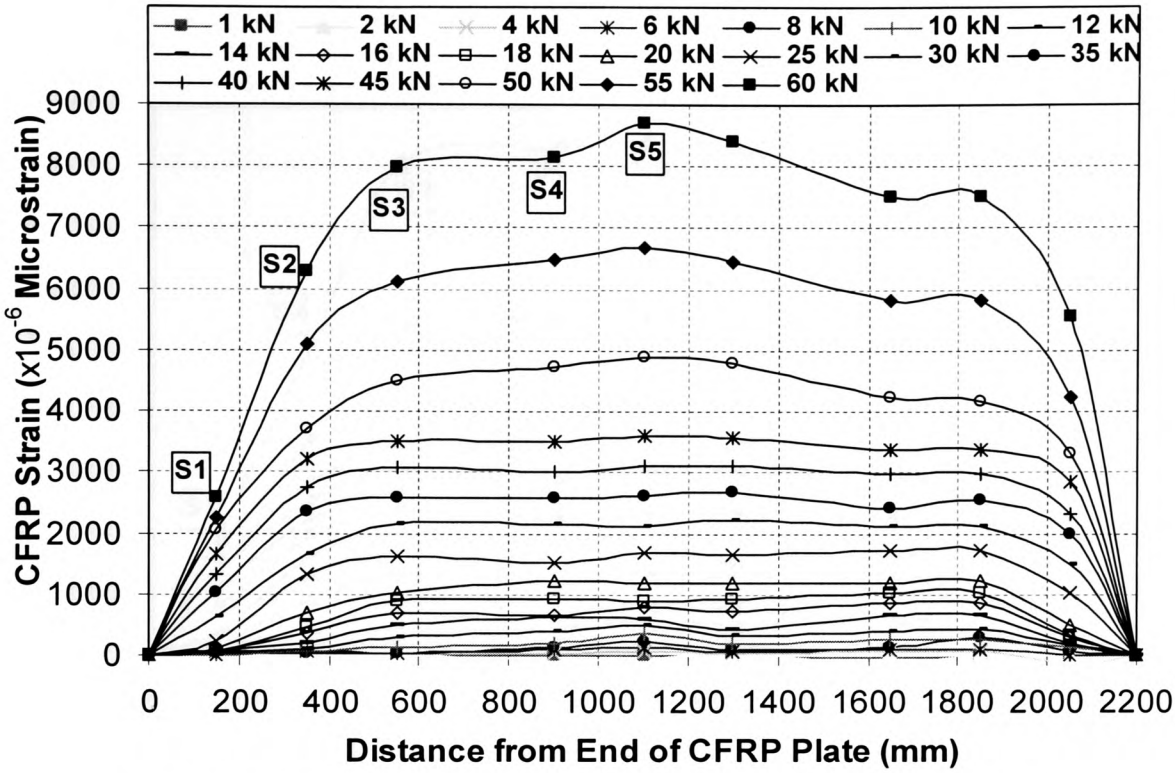

Figure 4.30 Strain Distribution Along the CFRP Length in Beam B6

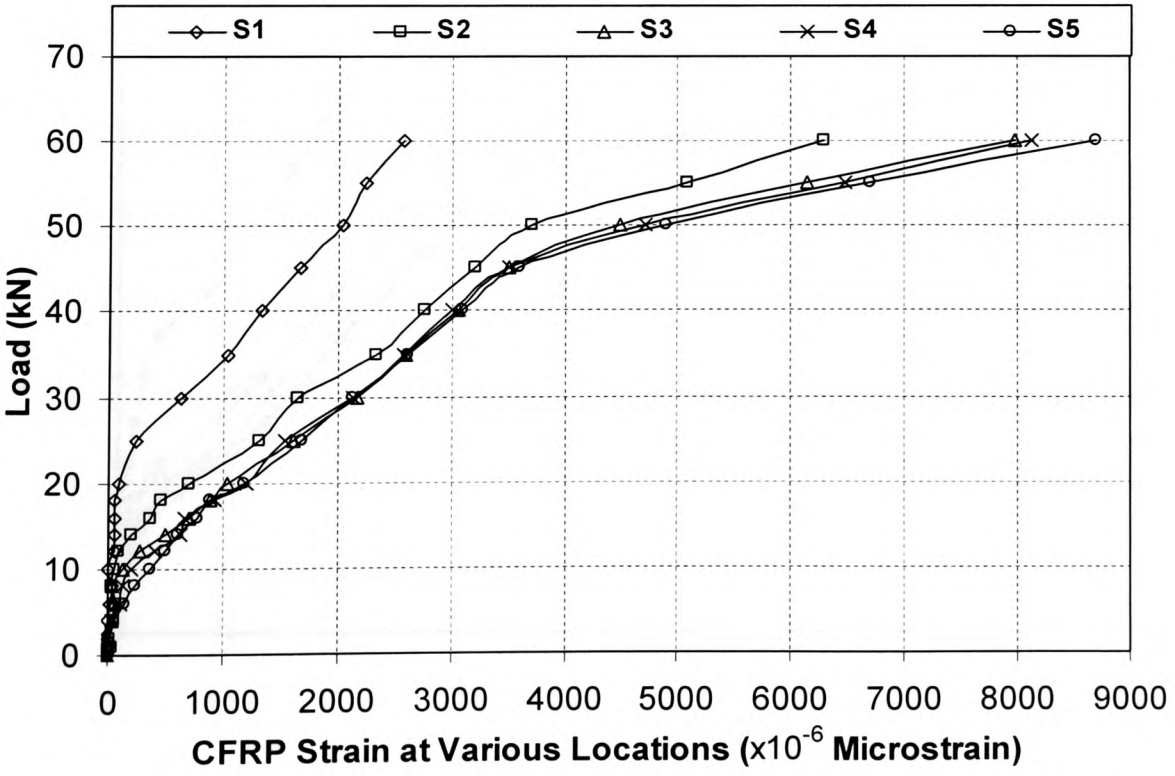

Figure 4.31 Load-Strain Variation in the CFRP Composite Layer of Beam B6

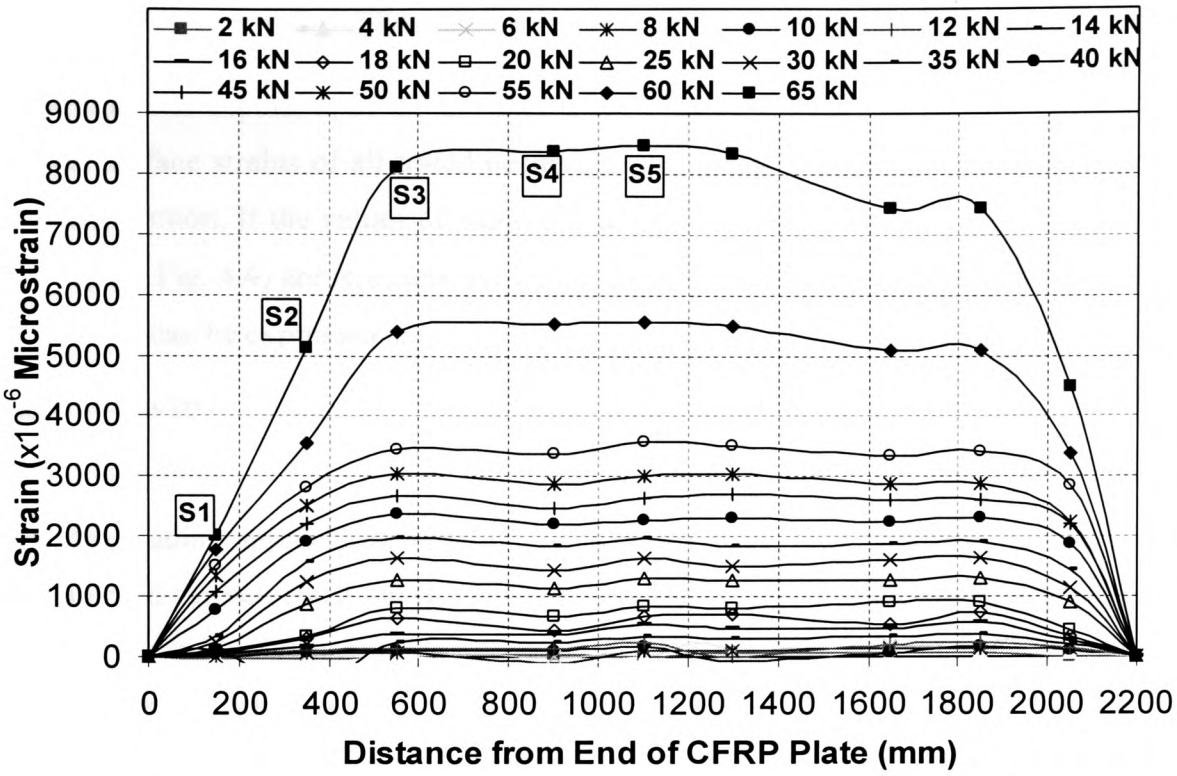

Figure 4.32 Strain Distribution Along the GFRP Length in Beam B8

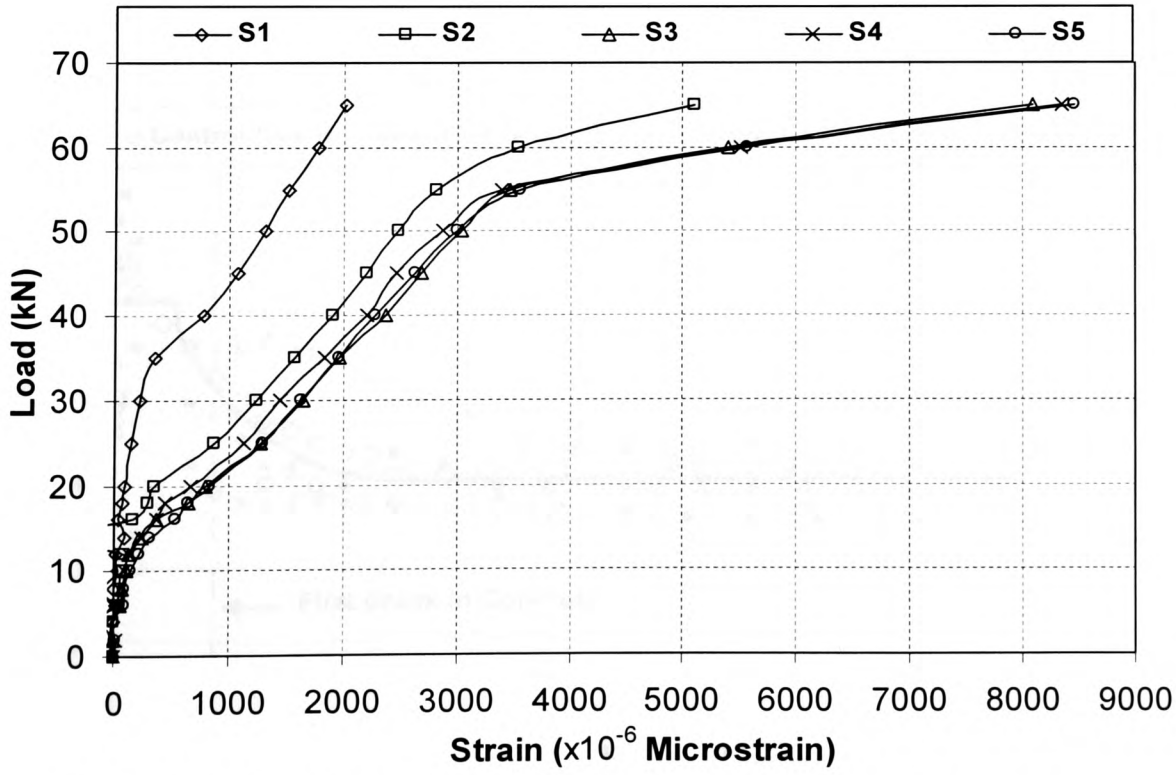

Figure 4.33 Load-Strain Variation in the GFRP Composites for Beam B8

4.3.5 Neural Axis Depth

The neural axis depths, x, of all test beams were experimentally evaluated. Firstly the concrete surface strains of all tested beams showed linear variation as discussed in the preceding section. If the values of strain under a given load at level 1 (top) and level 6 (bottom, see Fig. 4.4) are represented by ε_1 and ε_6 respectively, the neural axis depth, in millimetres, can be expressed as:

$$x = \frac{180}{(1+\frac{\varepsilon_6}{\varepsilon_1})} + 10 \qquad (4.1)$$

When the loading approached the ultimate limit, the strain measurements were ceased. The observed surface crack depth gave a reasonably good indication of the neutral axis position. The typical values of the maximum crack depth in the constant moment zone, at just before ultimate loading, were found to be between 150 – 160 mm for all series A beams. This indicated a typical neutral axis depth of around 40 - 50 mm at just before ultimate failure. Figure 4.34 displays the load versus neutral axis depth relationships for all series-A beams. Although the data appear to be scattered, the general trend is clear. The neutral axis depth will be modelled and further analysed in Chapter 5.

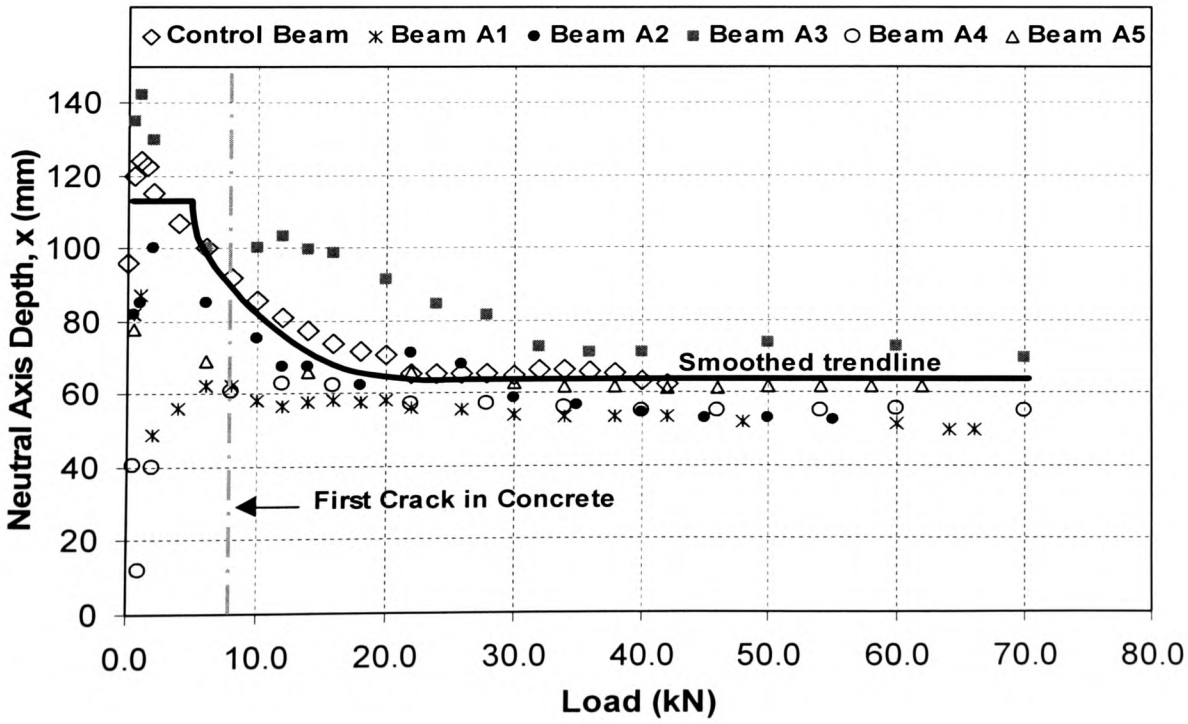

Figure 4.34 Load versus Neutral Axis Depth

4.4 Moment Curvature Relationship and Strength Utilisation

4.4.1 Moment Curvature

The experimental moment curvature relationships for all beams were derived by two different methods from two independent sets of test data. Firstly, the recorded surface strain values of the beams were used to calculate the curvature under the corresponding load. Once the position of neutral axis was determined from the section strain distribution data, as discussed in the preceding section, the curvature κ, was then obtained from the following equation using the classical elastic theory (Gere and Timoshenko, 1991).

$$\frac{M}{EI} = \frac{1}{R} = \kappa = \frac{\varepsilon}{y} \tag{4.2a}$$

In the above equation, y is the variable distance from the neutral axis to the point where the strain, ε, is used to determine the curvature κ for that section. For the current study, the strain values at level one (10 mm from the top extreme fibre in the beam compression zone) were used, and the curvature was thus obtained by dividing these strains by a value of (x-10).

The second approach utilized the maximum span deflection data based on the principle that for a given beam geometrical and load configuration, the relationship between the deflection and the curvature must be a unique one. The four point loading configuration results in the bending moment diagram for the simply supported test beams in the present study as shown in Figure 4.35.

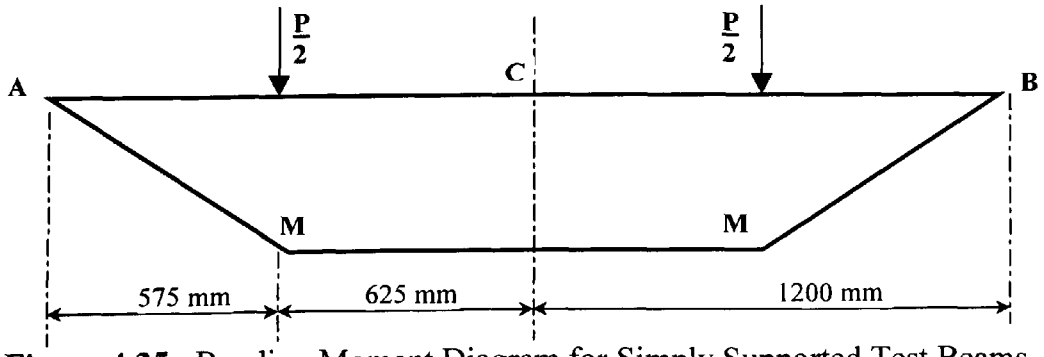

Figure 4.35 Bending Moment Diagram for Simply Supported Test Beams

The maximum mid-span deflection, δ, can be determined by applying the second Area-Moment theorem from point A to point C as follows:

$$-EI\delta = \frac{M}{2} \times 575 \times \frac{2}{3} \times 575 + 625M \times (575 + \frac{625}{2}) = 664895.83M \quad (4.2b)$$

The above relationship is only correct if a constant flexural rigidity EI is achieved throughout the beam. However, for reinforced concrete beams of the present test configurations, the values of EI in the constant moment zone and within the shear span are different due to the different neutral axis depths. Deflection results from Equation (4.2b), therefore, are expected to be greater than the true deflection, since a reduced EI of the constant moment zone is used to represent the whole beam. Nevertheless, the mid-span curvature determined this way, may be used for indicative purposes upon comparison with the strain-based values, as defined by Equation (4.1). By combining Equations (4.2 a & b), the deflection based curvature is then estimated as:

$$\kappa = -\frac{\delta}{c} \quad (4.3)$$

where c is the constant which defines the unique deflection-curvature relationship. For the load configuration of the simply supported test beams used in the present study, this constant c is 664895 as shown in Equation (4.2b).

The moment curvature curves of beams A1 to A5 together with that of the control beam, derived from strains and deflections respectively, are shown individually in Figure 4.36. It can be seen that these graphs, as results of the two different methods, match well for most beams despite the approximation used to derive Equation (4.3). The difference of curvature values, derived from the two sets of independent data, is generally within 2.5-3.0 % with the exception of beam A3. At the final loading stage, no strain recordings were available thus comparisons could not be made. For beam A3, some discrepancies were apparent at the two points where the beam deflection displayed some stiffening characteristics. As discussed previously, this may be attributed to possible inaccuracies in original deflection data reading. The comparison of moment curvature relationship for all beams in series-A is represented in Figures 4.37 and 4.38, and Figures 4.39 and 4.40 show the same for series B beams. These four sets of graphs were all based on the measured maximum span deflections, and were evaluated using Equation (4.3).

These moment curvature relationships demonstrated the same behaviour of the FRP strengthened beams as discussed in the analysis of deflections and strains, they also reflect the stiffness characteristics of these beams as discussed in the following section.

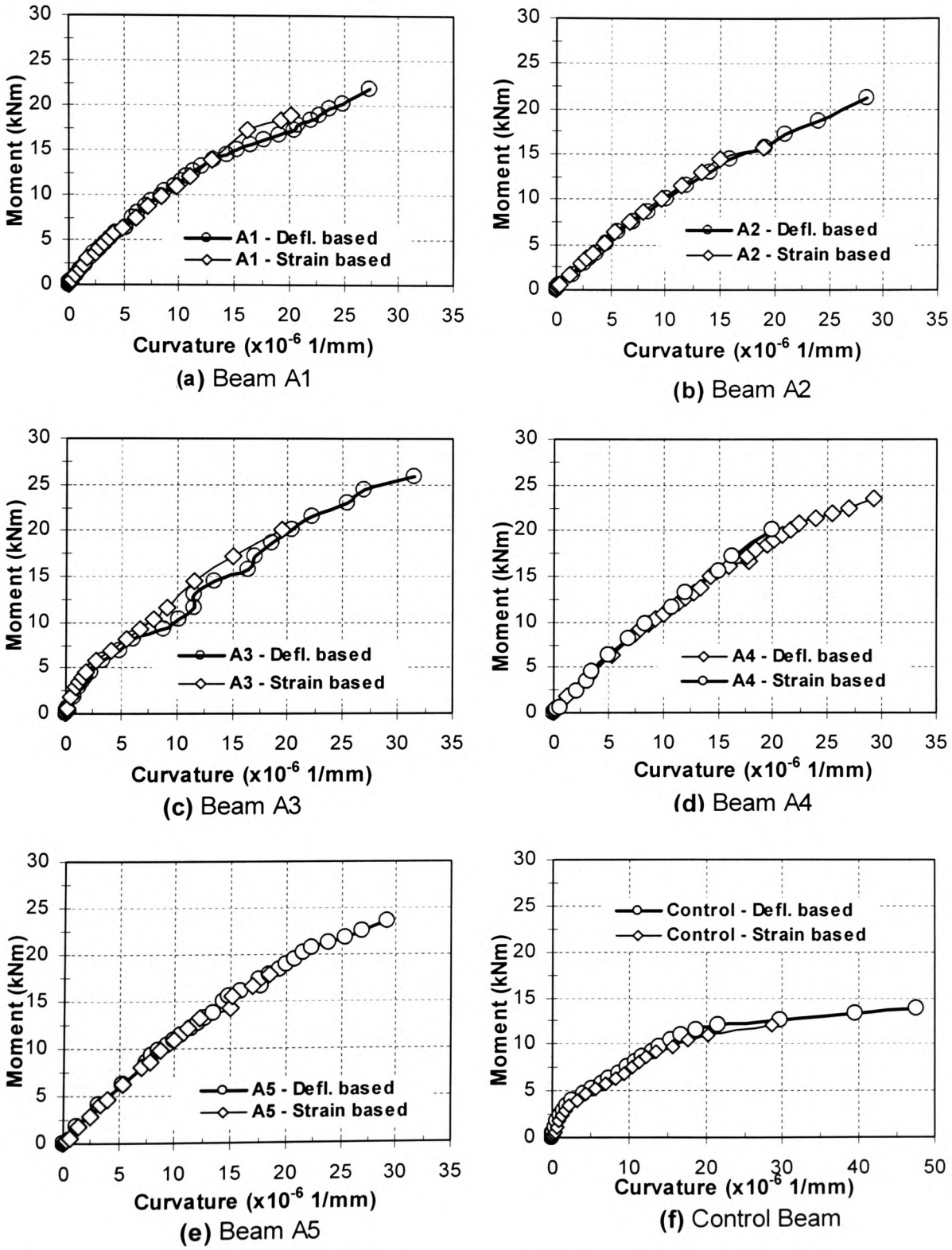

Figure 4.36 Experimental Moment vs. Mid-span Curvature Relationships

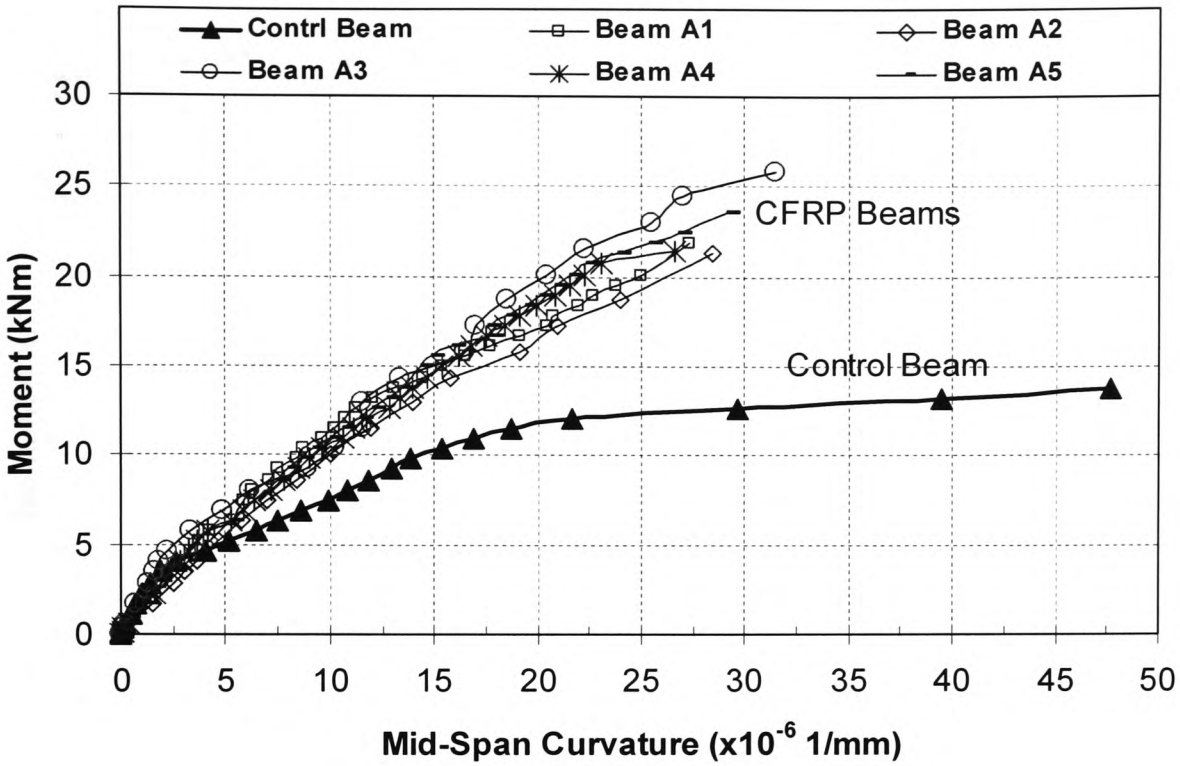

Figure 4.37 Comparison of Moment Curvature Relationships for Beams A1 – A5.

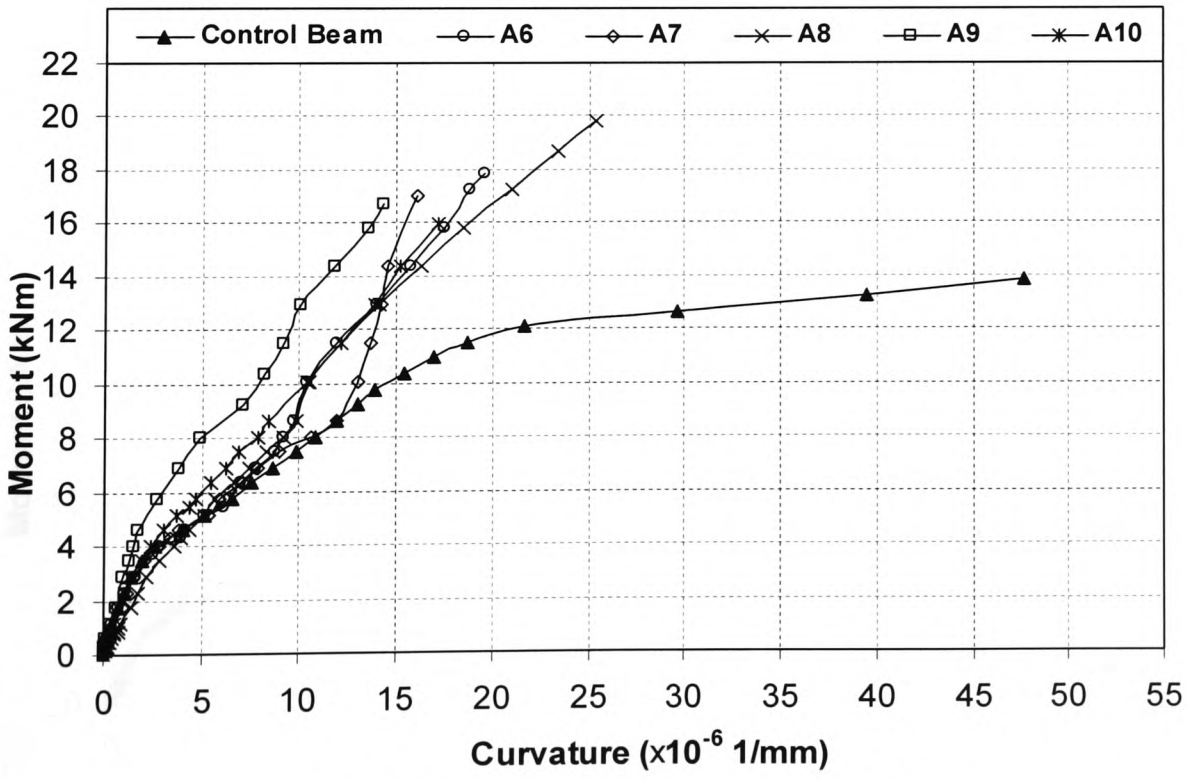

Figure 4.38 Moment Curvature for Beams A6-A10

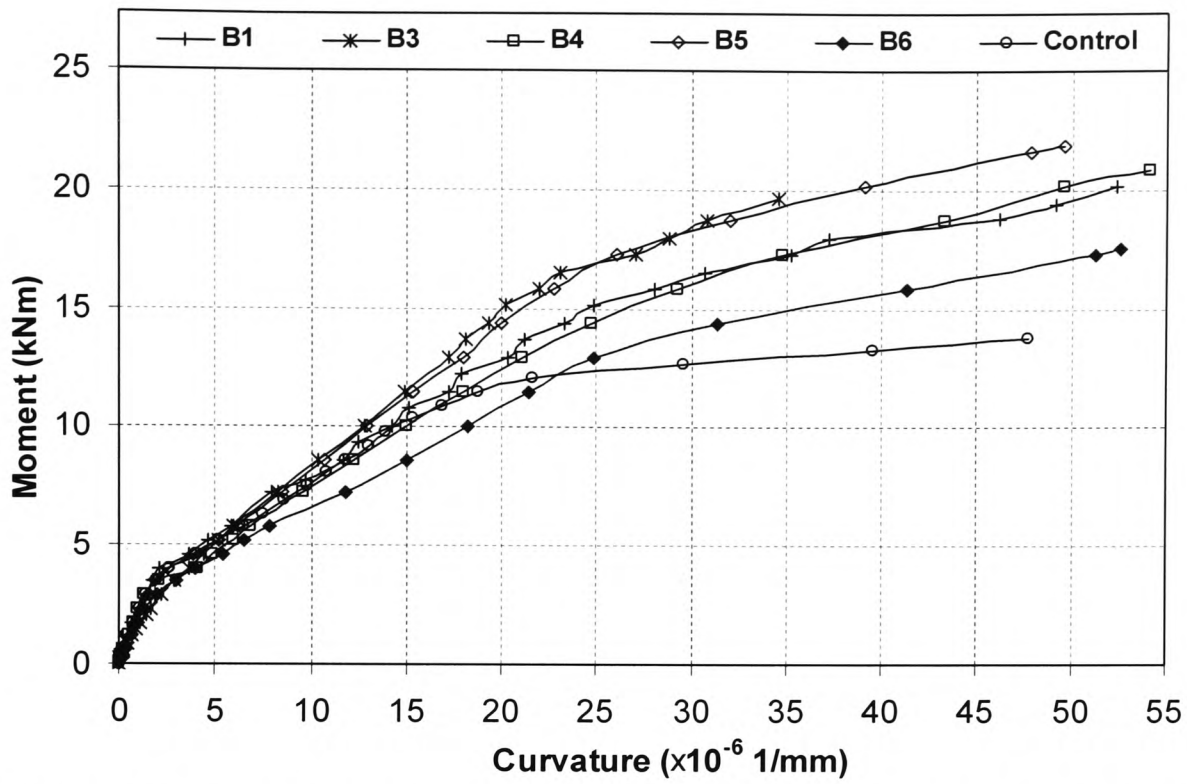

Figure 4.39 Comparison of Moment Curvature Relationships for Beams B1, B3 to B6.

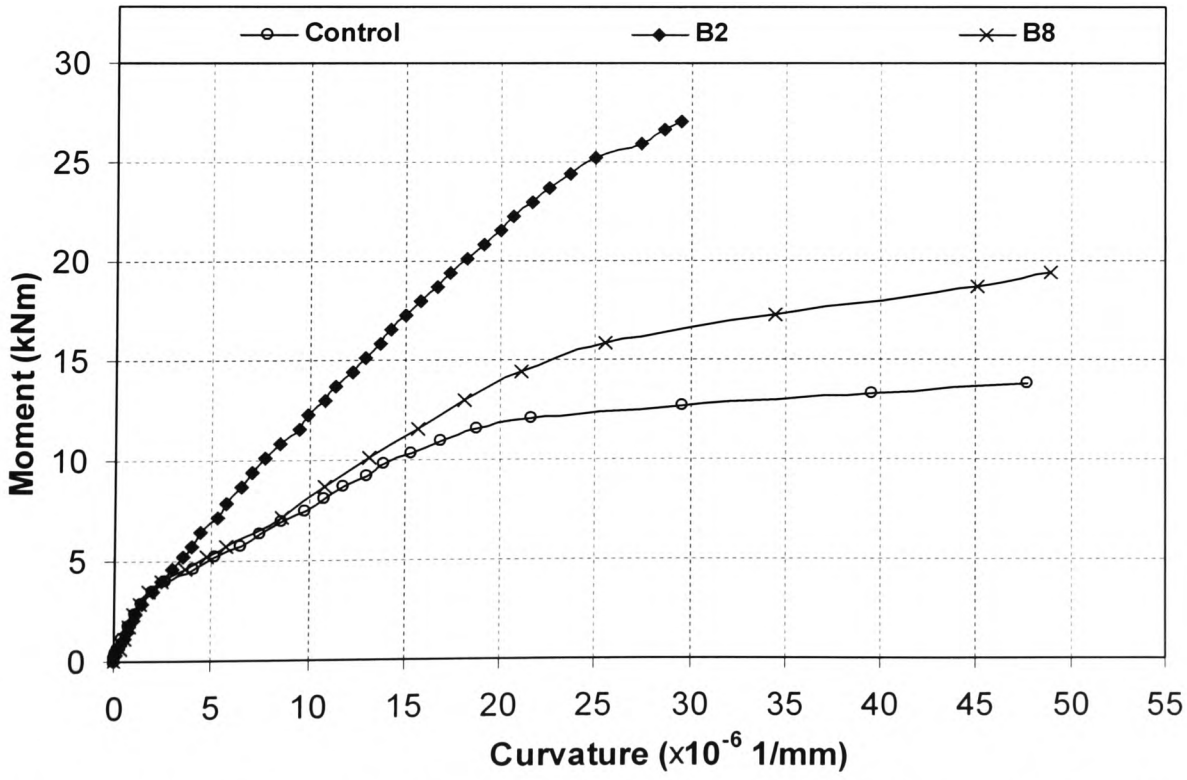

Figure 4.40 Comparison of Moment Curvature Relationships for Beams B2 and B8

By examining the moment curvature relationship in Figures 4.36 to 4.40, comparisons can be made between the series A and series B test beams. The major configuration difference between these two groups of beams is that the former were heavily strengthened by CFRP plates, while the latter were "lightly" strengthened by single or double layer of FRP fabric sheets. It can be seen that for group-A beams and beam B2, there exists no apparent yield plateau associated with the steel reinforcement. The only apparent slope changes occurs at the initial concrete cracking stage, at a moment of around 2.5-3.5 kNm, and corresponding load of 8.50 -12 kN. After this initial change of slope in the moment curvature curves (also the load-deflection), the beam behaves almost "linearly" until sudden failure. Although reasonably large deflections are detectable, the failure mode was observed to be very sudden and brittle during the laboratory tests. For group B beams (except B2), whilst the initial change of slopes on the moment curvature also takes place at about the same load level as group A beams, a change of slope is also evident at a curvature of around 20 x 10^{-6} mm^{-1}. This corresponds to a mid span deflection of 13.0 mm, or $1/185^{th}$ of the beam effective span, which is beyond the serviceability of deflection of 1/250 of span. From the structural design view point, the behaviour of group B beams is more desirable than group A beams, as it shows more ductile characteristics.

4.4.2 FRP Strength Utilisation

The composite strength utilisation ratio, defined as the CFRP stress at beam failure divided by its ultimate tensile strength, can be calculated based on the actual beam failure load and the BS 8110 simplified rectangular stress block. For the two groups of beams the comparison is made as follows in Table 4.10.

Table 4.10 Comparison of Estimated Composite Stress at Failure

Beam Reference	Est. Average CFRP Stress at Beam Failure* (Strength) (N/mm^2)	Composite strength utilisation ratio	Effective margin of safety
A1-A5	750 (**1750**)	0.43	1/0.43 = **2.32**
B1, B3, B5	1035 (**4900**)	0.21	1/0.21 = **4.76**
B2	835 (**2950**)	0.28	1/0.28 = **3.57**
B4, B6	1500 (**1500**)	1.00	1.0/1.0 = **1.0**

* Estimation based on the measured plate strains at just before failure, for theoretical determination of plate stress under any load level, please refer to Chapter 5.

4.5 STRENGTH AND STIFFNESS ENHANCEMENT

4.5.1 Strength Enhancement

It was observed that all the CFRP strengthened beams exhibit improved overall stiffness. Shown in Figure 4.41 is the variation of the maximum span deflection of beams A1 – A5 against the ultimate load increase over the control beam. As can be seen, the ultimate load capacity increased by nearly 50% when the deflection of the CFRP strengthened beam reached 60% of the final deflection.

The 60% of ultimate deflection for the CFRP strengthened beams, falls within a range of 10.8 to 13.2 mm, which is just beyond the BS 8110 specified serviceability limit state of deflection of 1/250 of the span (9.6 mm). It is therefore realistic to conclude that for the current test beam configuration , an increase of approximately 50% of the working load can be expected.

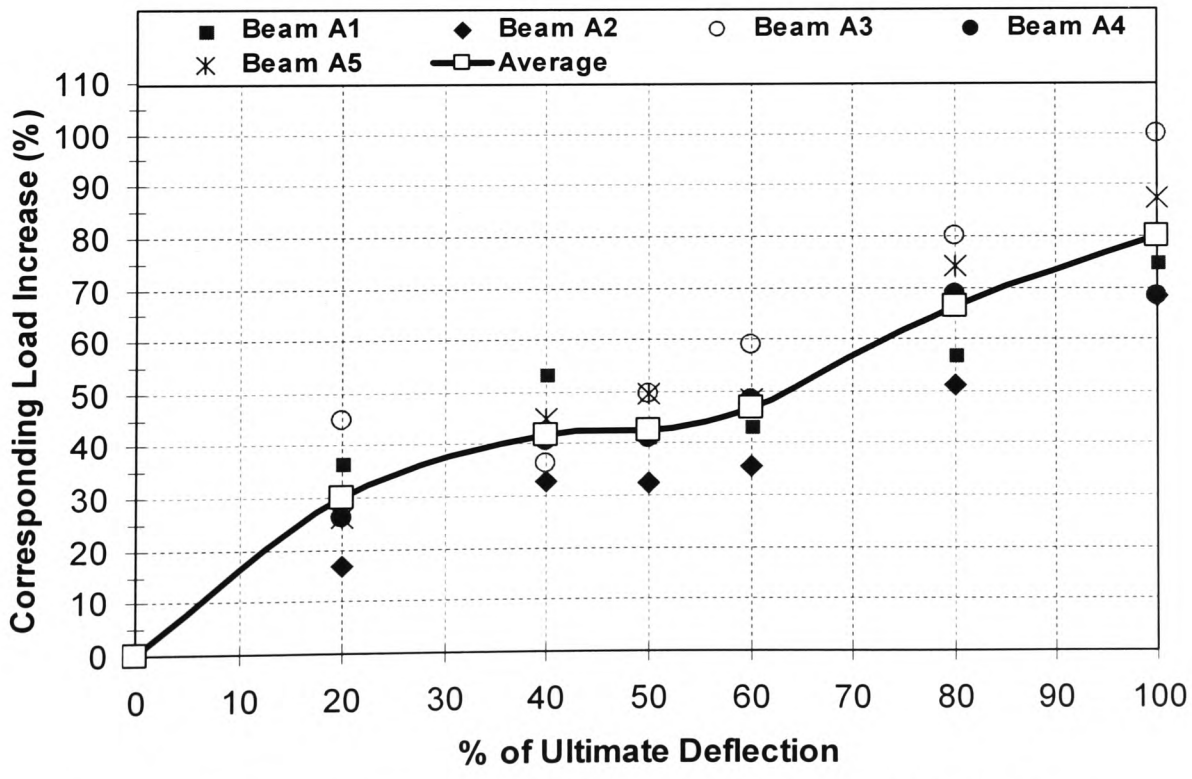

Figure 4.41 Load Increase over Control Beam at Various Deflection Stages

4.5.2 Stiffness Enhancement

The actual stiffness enhancement can be determined from the moment-curvature relationships that were presented in the preceding section. Listed in Table 4.11 are the experimental stiffness values for two distinct stages. These corresponding to reaching the maximum span deflection of 5.0 mm (span/480) and the serviceability limit state of deflection (span/250). The average stiffness values at 5.0 mm deflection increased by 35.5% over the control beam for all nine beams strengthened by the 2.2 m CFRP plates, namely, A1-A5, A8-A10 and B2. The corresponding figure for the serviceability limit of deflection of 9.6 mm is 45.7% for the same group of beams.

The two beams (A6 and A7) strengthened by the 1.0 m long CFRP plates within the constant moment zone, showed a much lower stiffness enhancement at lower deflection (only 6.3% average at 5.0 mm deflection). This suggested that the overall beam stiffness is closely dependent on the "participation" length of the strengthening plate. If the length of the strengthening plate is shorter than the length of the constant moment zone, then the stiffness improvement at early loading stage is rather limited. However, under the serviceability limit state, a 38% of stiffness enhancement was achieved, comparing with the 45.7% for the fully strengthened beams.

For group B beams (except B2), which are strengthened by the single layer CFRP fabrics, the average stiffness increase of around 1.5% at both the 5.0 mm deflection and the serviceability limit state is negligible. This clearly demonstrates that the thickness of the strengthening plate plays an important role in the beam overall stiffness performance. As expected, the CFRP plates contribute more than the thin layer of CFRP fabrics to the stiffness of the strengthened beams.

The elastic modulus of the strengthening composites also influences the overall stiffness behaviour. As demonstrated by the high modulus CFRP strengthened beam B2, its stiffness enhancement ratios (59.1% and 66.5%) are much higher that of the respective averages (35.5% and 45.7%) for series B beams as discussed above. The low modulus GFRP strengthened beams (two sheets) B7 and B8 only showed similar stiffness increase as their single layer CFRP sheet strengthened counterparts.

Table 4.11 Stiffness Increase Up to Serviceability Limit

Beam Ref.	At Deflection of 5.0 mm (Span/480)		At Deflection of 9.6 mm (Span/250 - SLS)	
	Stiffness ($x10^9$ Nmm^2)	% Increase over control beam	Stiffness ($x10^9$ Nmm^2)	% Increase over control beam
Control	844	-	694	-
A1	1210	43.4	993	43.1
A2	1060	25.6	916	31.9
A3	1155	36.8	1028	48.1
A4	1106	31.0	986	42.1
A5	1152	36.5	1038	49.5
A6	900	6.7	937	35.0
A7	893	5.8	979	41.1
A8	933	10.5	916	31.9
A9	1280	51.6	1159	67.0
A10	1053	24.8	924	33.1
B1	920	9.0	708	2.0
B2	1342	59.1	1155	66.5
B3	907	7.5	778	12.1
B4	820	-2.9	680	-2.0
B5	867	2.7	764	10.0
B6	760	-9.9	583	-15.9
B7	812	-3.5	776	11.8
B8	888	5.2	775	11.8

4.5.3 Benefit of Stiffness Enhancement

For mechanically degraded or damaged beams, the member stiffness usually suffers a reduction from the original design level. The strengthening of such members with FRP composites therefore provides a recovery and enhancement measure for the member stiffness. However, it is not always necessary or even beneficial to over increase the flexural stiffness of a RC member. Greater stiffness results in reduced deformations and hence less warning prior to the ultimate failure of the member. It can be seen from Table 4.11 that different types of FRP properties and sectional area provided will greatly influence the overall stiffness of the strengthened RC beams. It is possible to control the increase of stiffness through proper design. This is discussed with the ductility issues in Chapter 7.

4.5.4 Under- and Over- Strengthening

Group B beams (except B2) were regarded as under strengthened in comparison with group A beams. The cross sectional area and the thickness of CFRP plates in group A are approximately 9 times those of single layer CFRP fabric sheets. However, the increase over the control beam in ultimate load carrying capacity has been up to 59.1% in group B beams. This group of beams did not experience any tearing-off type of premature failure as seen in group A, and in general the failure was observed to be much milder and less brittle than that of the heavily strengthened group A beams.

It is therefore reasonable to conclude that under strengthened sections enable the CFRP composites to be more fully utilised than over strengthened sections, and the associated structural characteristics of the under strengthened sections are more acceptable in structural design. Further discussions on under and over strengthening will be presented in Chapter 5.

4.5.5 Ductility

An important observation from the results is that the CFRP strengthened beams, if properly designed, can exhibit suitable ductility and thus avoid catastrophic type of brittle failure. The maximum span deflection at just before ultimate failure was found to be typically between span/120 for the CFRP plated beams and span/80 for the beams strengthened by CFRP fabric sheets. This is reasonably easy to be detected and thus provide an acceptable level of warning for appropriate measures to be taken to prevent ultimate failure. For steel only reinforced RC beams, this figure is slightly higher, and more apparent plastic deformation usually follows. Nevertheless, the high magnitude of deflection does not necessarily lead to high ductility. The structural ductility of FRP strengthened elements is a complex issue which needs to be addressed more fully, and more discussions on this topic will be presented in Chapter 7.

4.6 BEAMS WITH EXTERNAL CFRP REINFORCEMENT ONLY

4.6.1 Overview

The technique of FRP strengthening usually involves strengthening of concrete structural elements, which were already conventionally reinforced by some nominal amount of steel reinforcement in most cases. The primary objective of the strengthening process is to enhance the structural capability of the elements to be strengthened. The candidate has been rather intrigued with the idea as to what would happen if a flexural member were to be externally reinforced only with FRP composites without any internal steel reinforcement. The prerequisite, naturally, is that a perfect bonding between the concrete and the FRP plate must be achieved, and this is perfectly viable with the development of adhesive technology today as discussed in Chapter 3. On the practical aspect of structural engineering, there may be occasions where, due to various design or workmanship errors, a structural concrete element is in use without proper, or even no tension reinforcement at all. There is even the argument that there is no need for any internal steel reinforcement if sufficient and well-bonded external FRP composites were provided.

Shown in Figure 4.42 is a flight of precast concrete staircase in a Lincolnshire school. The treads of the staircase had been installed in place upside down, and hence there were effectively no tension reinforcement provided in these members, upon which there could be school children running, and jumping. The possible consequence of this error could be a catastrophic and even a tragic one! Fortunately, the problem was identified when cracks were noted, and before any structural failure occurred. A simple strengthening solution was used to rectify the problem. CFRP plates were bonded to the soffit of each tread to act as external tension reinforcement, as shown in the photograph. A total of 80 metres of CFRP plates were utilised in this project and disruption to normal school activities was minimised.

However, there still remain questions to be answered. Is such a strengthening solution, where no minimal internal tension steel was provided, safe and reliable? And in general, can external CFRP reinforcement in any flexural member act effectively with the

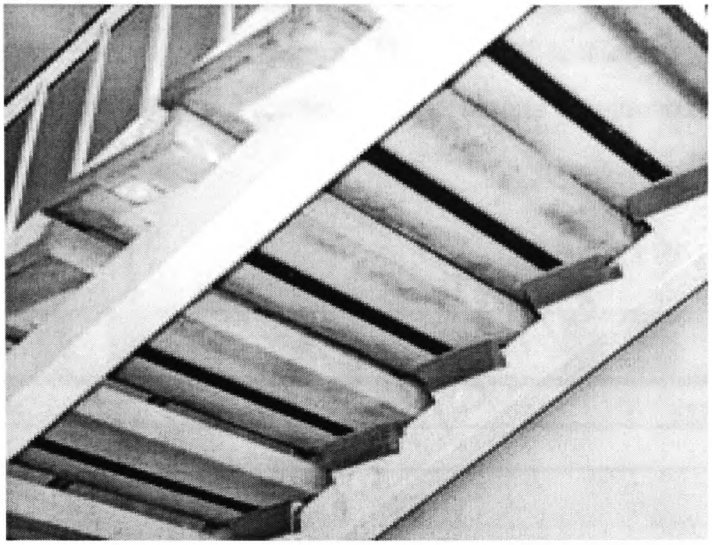

Figure 4.42 CFRP Strengthening of Concrete Staircases in Yarborough School, Lincoln (Courtesy of Sika UK Ltd)

concrete without any internal steel reinforcement? This section intends to address these important questions by conducting an experimental investigation.

4.6.2 Experimental Set-up

Six mass concrete beams C1 to C6, of the same size as the series A beams, were cast without any internal steel reinforcement. Beams C1 to C5 were then externally strengthened in flexure by bonding the type A CFRP plates to the soffit. The same type of adhesive, that is Resifix 31, was used, and similar surface treatment procedures were followed. All plates were again 2.2 m long, 80 mm wide by 1.6 mm thick, similar to those used in series A tests. The shear reinforcement of beams C1 to C4 was provided using 16 number of 200 mm by 80 mm by 1.6 mm CFRP plates, vertically bonded to the beam web, at 100 mm clear spacing. Internal steel links were also provided in Beam C5 at 100 cross centres. Beam C6 was reinforced in both flexure and shear using externally bonded single layer CFRP fabrics. The design thickness of the CFRP fabric layer was 0.145 mm. The length of the CFRP fabric for flexural strengthening was kept at 2.2 metres, while the full width of the beam was covered using the Exchem laminating resin. The external shear reinforcement of beam C6 was provided using the

same fabrics that were cut into 500 mm length strips, and bonded in U-shapes within the shear span at a clear spacing of 100 mm. The general test configuration of series C beams is shown in Figure 4.43, and the reinforcing details are shown in Table 4.12.

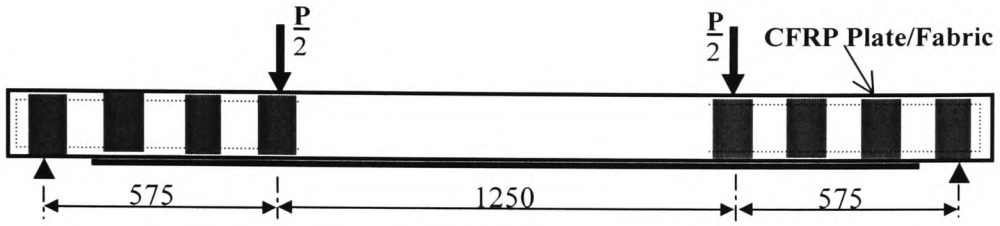

Section 1-1

Notes:

1. No internal tension reinforcement was provided in any series "C" beams.
2. Beam C5 had internal shear links, of mild steel, R6@100mm.

Figure 4.43 General Configuration for Series "C" Test Beams

Table 4.12 Reinforcing Details of Group C Beams

Beam Code	Concrete f_{cu} (N/mm^2)	Internal Steel Reinforcement**		Externally Bonded CFRP Composites	
		Tension A_s (mm^2)	Shear A_{sv} (mm^2)	A_p (mm^2)	Length l_p (mm) (type)
C1	37.9	0	CFRP plate	128	2200 (A)
C2	33.6	0	CFRP plate	128	2200 (A)
C3	38.5	0	CFRP plate	128	2200 (A)
C4	38.1	0	CFRP plate	128	2200 (B)
C5	35.8	0	56.5 & CFRP~	128	2200 (B)
C6	36.0	0	CFRP#	14.5	2200 (C)

~ Internal shear links R6@200 mm and external CFRP fabric U-shape wrapping.
\# Externally bonded CFRP U-shaped fabric strips as shear reinforcement with no internal links provided.

4.6.3 Test Results

All six beams in series C tests failed in a brittle manner. The load at first visible crack ranged from 10 to 14 kN. This is largely in line with that of the standard internally reinforced control beam. The summary of the test results is listed in Table 4.13. It can

be seen that none of the FRP externally reinforced beams reached the ultimate load capacity of the control beam, which is the same as that used in series-A tests. The external FRP plates for beam C1 to C5 had much greater tensile capacity than the steel reinforcement of the said control beam.

Table 4.13 Summary of Test Results for Series C Beams

Beam Reference	Load at specific stages (kN)		Ultimate Load decrease %	Deflection @ failure (mm)	Failure Mode*
	First crack	Ultimate Failure			
Control	12.0	47.9	0	31.7	SY-CC
C1	10.0	28.0	-42	6.8	BFF
C2	10.0	28.0	-42	9.4	BFF
C3	14.0	20.0	-58	4.1	BFF
C4	12.0	30.0	-37	7.6	BFF
C5	10.0	30.0	-37	11.2	BFF
C6	12.0	14.0	-71	2.8	BFF

*SY-CC: steel yield followed by concrete crushing; BFF: Brittle Flexural Failure.

For beams C1 to C5, the ultimate load capacity suffered large reductions of between 37% and 58% in comparison with the control beam. The load deflection curves for all six beams are shown in Figure 4.44. Beam C6, which was reinforced with only one layer of external CFRP fabric, exhibited the lowest stiffness. There was not any apparent kink of the P-Δ curve, and the beam failed suddenly at a low loading of 14 kN before the CFRP fabric layer reached its design strength, and shortly after the first visible crack appeared.

The comparison of the C beams with the control beam is shown in Figure 4.45. It is interesting to note that beams C1 to C2 broadly follow the load-deflection trend of the control beam at the early loading stage up to around the crack load, while beam C6 was apparently less stiff than the control beam.

The failure mode of all beams was similar. Shortly after the concrete tensile strength was reached and the first visible cracks appeared, the tensile stress was transferred to

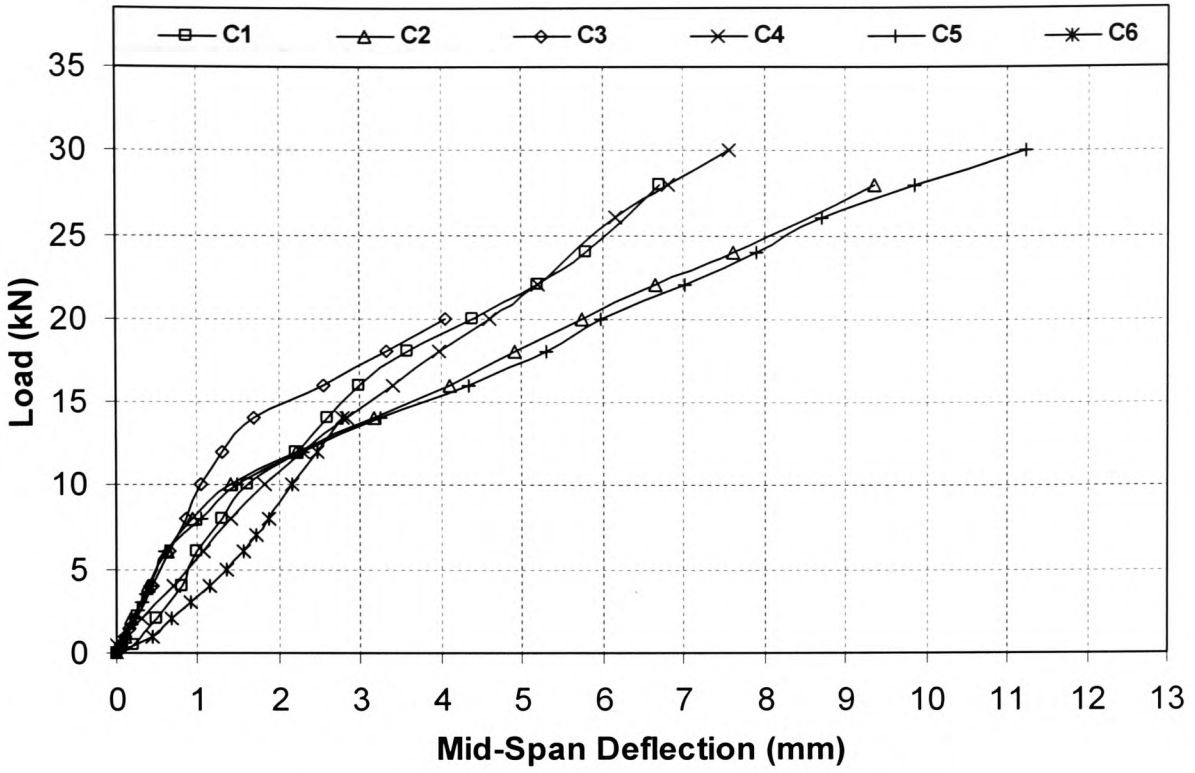

Figure 4.44 Load-Deflection Curves of Series "C" Beams

the CFRP plate. At this stage, it is conventionally expected that the CFRP composites will act to resist all the principle tension forces in the beam, and continue to act with the concrete in a composite manner. However, whether or how the CFRP plates/fabrics can act with the cracked concrete, with no internal steel reinforcement, in resisting further load seems to be somewhat unpredictable. It was observed that even though the bond between the concrete surface and the FRP plate/fabric was well maintained and of the same high quality as those in series A beams, premature failure occurred in all beams. The number of cracks at beam failure was observed to be very small, with an average crack spacing of around 300-400 mm. In the case of one layer CFRP fabric bonded beam C6, only one major crack was noted. The beam failed in tension at that crack position, where the crack was seen to have reached the top of the compression zone and the beam was effective split into two halves. The CFRP fabric layer however, still remained elastic. The estimated CFRP stress at the beam failure load is only about 60 N/mm^2, far below its design strength. The failure mode of beams C1-C5 is shown in Figure 4.46.

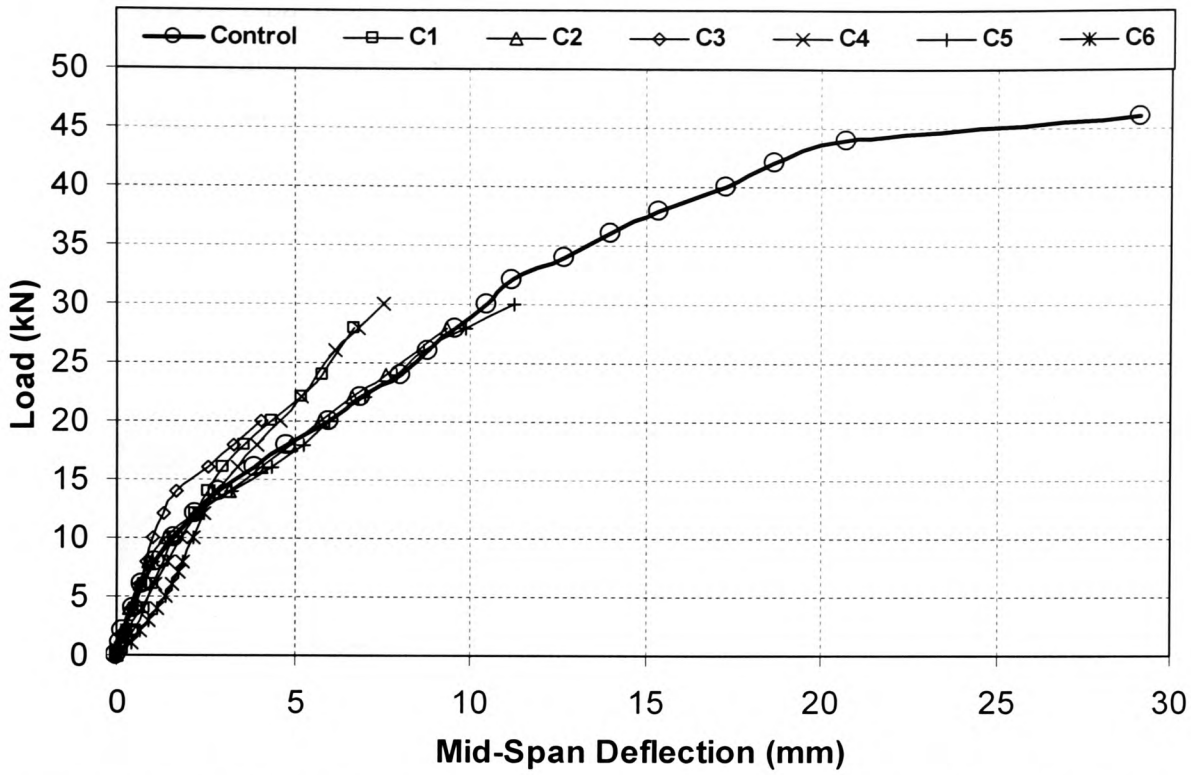

Figure 4.45 Comparison of Series C Beams with Steel Reinforced Control Beam

4.6.4 Suitability of FRP Composites as External Reinforcement

It is clear that FRP externally reinforced concrete beams with no internal steel reinforcement do not behave in the same way as conventional steel reinforced concrete flexural elements. The former develops into premature brittle failure under light load conditions shortly after the formation of concrete tensile cracks. As a result, the high specific strength of the FRP composites cannot be utilised, and the beams fail at much lower load compared with concrete beams internally reinforced with steel bars.

It is therefore concluded that a mass concrete element should only be strengthened externally by FRP composites, which are treated as members of relatively minor structural importance such as lintels. For mass concrete beams and slabs, it is not realistic to expect externally bonded FRP composites to act in lieu of the internal steel bars, and behave in the same way as conventional RC members without the actual presence of any internal steel reinforcement. This statement may be justified as follows: the lack of internal steel reinforcement in the FRP externally strengthened beams results

in wider cracks than those seen in the conventional RC beams under the same load level. This is because that in conventional RC members, the bond between the concrete and steel bars controls the development of the pattern and width of the cracks. In the FRP strengthened mass concrete elements, however, concrete cracks develop rapidly and after the concrete tensile strength is reached, thus the members fail prematurely in a brittle manner before the tensile stress can be transferred to the FRP composites as shown in Figure 4.46.

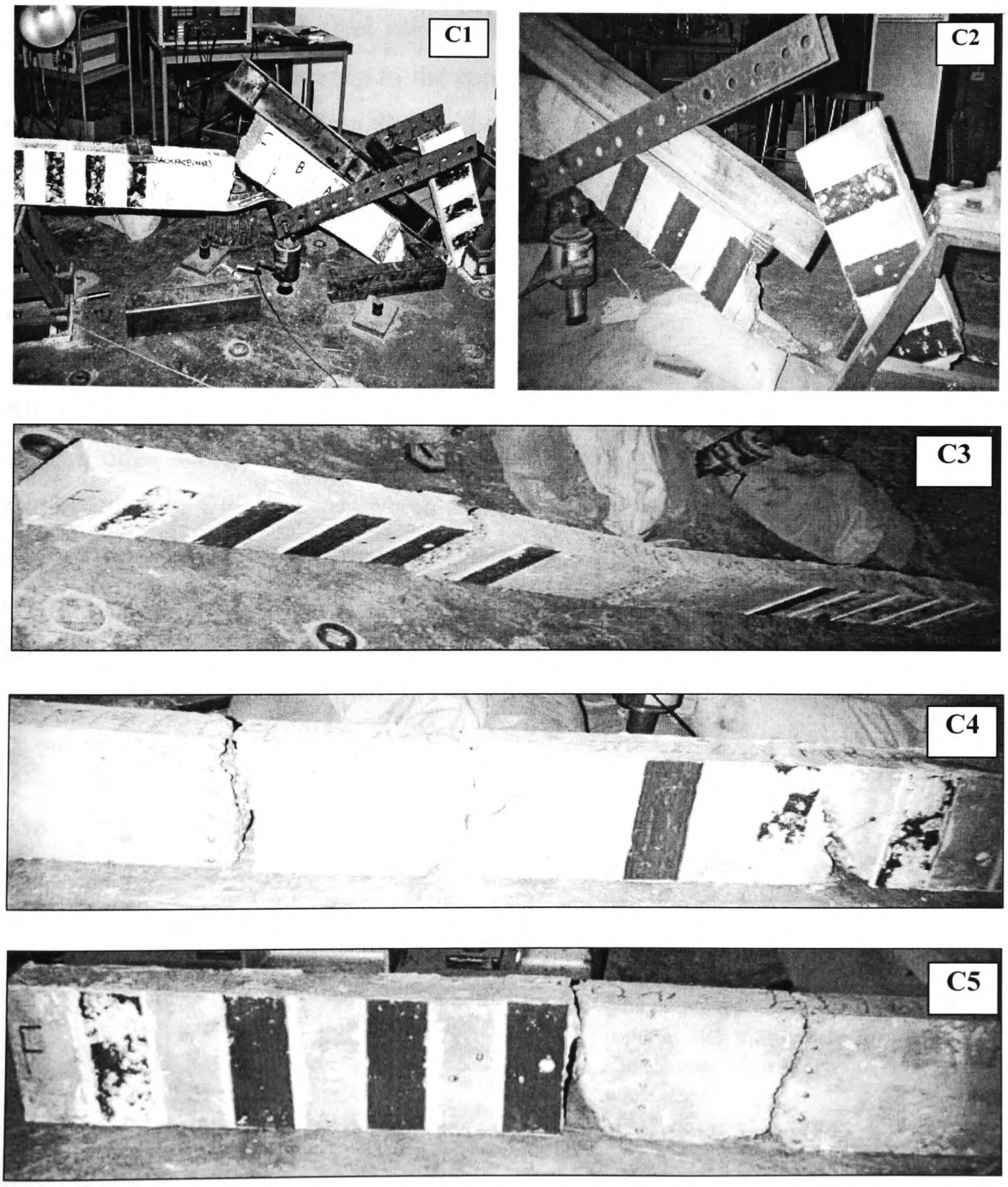

Figure 4.46 Typical Failure Mode of Series C Beams

4.7 BEAMS INTERNALLY REINFORCED WITH CFRP STRIPS

As discussed in the preceding sections, the over strengthened CFRP plated RC beams are likely to fail prematurely before the full flexural strength can be developed. In order to assess the differences in performance of FRP strengthened beams to those of FRP reinforced ones, a further experimental study was performed. Five concrete beams were reinforced in tension with narrow type A CFRP strips only, and then loaded to ultimate failure. This section attempts to investigate the potential application of CFRP strips as an alternative to internal steel reinforcement. If the idea is viable, then the contact perimeter of a thin CFRP strip to the concrete is much greater than a round bar of the equivalent cross sectional area, hence, the bond strength between the concrete and FRP reinforcement may be enhanced.

4.7.1 Loading and Reinforcement Details

All five beams have the same standard geometrical properties and load configuration as used in other series of simply supported beam tests of the present study. They were reinforced with CFRP strips, which were of 20mm width by 1.6mm thickness. The stirrups for all beams consisted of high yield 6 mm diameter steel bars at 100 mm centres. Figure 4.47 shows the general test arrangement. The material properties for each beam are listed in Table 4.14.

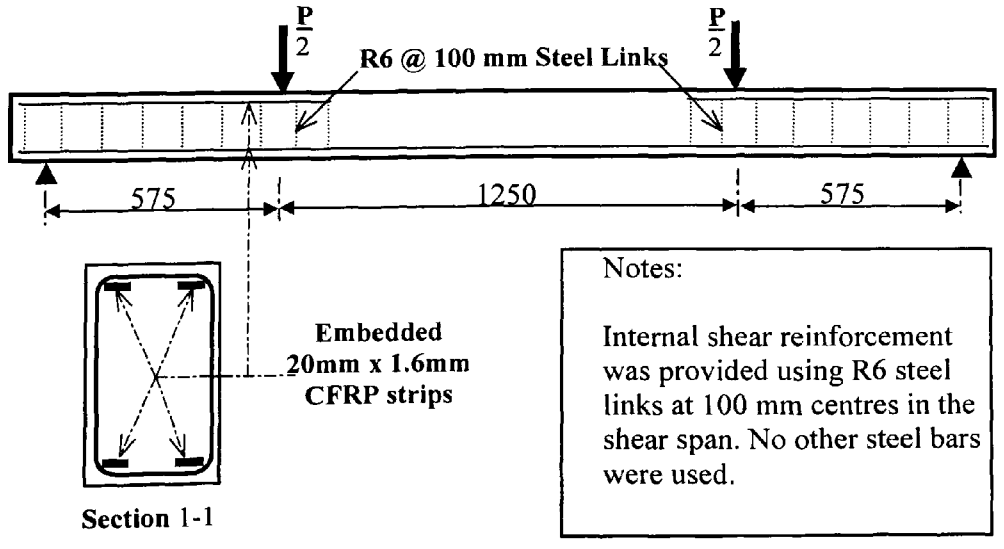

Figure 4.47 General Configuration for Series "D" test Beams

Table 4.14 Reinforcing Details of Series D Beams

Beam Reference	Concrete f_{cu} (N/mm^2)	Internal FRP Reinforcement		Remarks
		Tension A_s (mm^2)	Shear A_{sv} (mm^2)	
D1	34.2	64 (CFRP)	56.5 (steel)	Not any form of external reinforcement was provided.
D2	34.2	64 (CFRP)	56.5 (steel)	
D3	29.7	64 (CFRP)	56.5 (steel)	
D4	29.7	64 (CFRP)	56.5 (steel)	
D5	32.8	128 (CFRP)	56.5 (steel)	

4.7.2 Test Results and Discussions

Table 4.15 shows the main characteristics of all beams during the loading process. A reference beam with similar configuration as the control in series-A tests was used (f_{cu}= 42 N/mm^2). The CFRP strips reinforced beams appeared to have slightly lower first crack load than other beams in the study. The crack distribution appeared to be evenly within the bending zone, at an average spacing of around 130 mm, and with a typical depth of 160 mm at just before failure. It was observed that the crack widths of CFRP reinforced beams were slightly greater than that of the steel reinforced beams at the same load level. This is because the CFRP strips had lower elastic modulus than that of steel bars and thus results in larger strains under the same load level.

Table 4.15 Summary of Test Results for Series D Beams

Beam Reference	Load at specific stages (kN)			δ at 0.95P_u (mm)	Av. Crack Spacing at ULS (mm)
	At first crack	At SLS (δ=7.0 mm)	At ultimate failure		
Control	12	22.0	51.2	32.0	80
D1	10	14.5	28.7	17.1	128
D2	8	11.9	29.6	9.7	106
D3	10	16.5	52.7	20.2	116
D4	8	13.2	32.0	14.2	106
D5	10	15.1	43.5	14.7	123

The deflections of these CFRP reinforced beams, as shown in Figure 4.48, were observed to be much greater than those of the control beam. At the serviceability limit, the load carried by the control beams was 50% higher than the average load carried by the CFRP strips reinforced ones, which exhibited stiffing behaviour before failure.

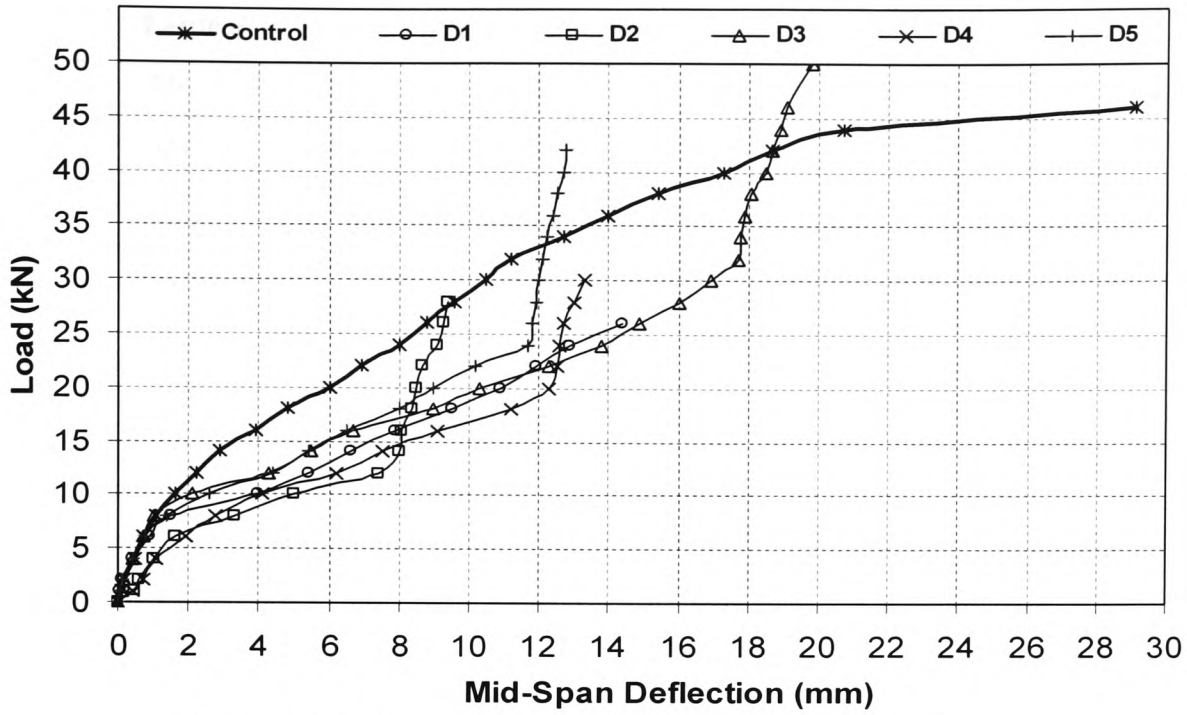

Figure 4.48 Load Deflection Curves for Beams D1 – D5

All CFRP strips reinforced beams failed in a similar manner by combined bending and shear. Failure always occurred near one of the point load positions, where initial flexural cracks were observed. As the load increased, these cracks under the point loads developed diagonally towards the centre of the beam, to be followed by ultimate failure. Shown in Figure 4.49 shows the failure mode of beams D2 and D4, which is typical of the CFRP reinforced beams. The predicted failure moment of all beams based on BS 8110, and the actual values of moment at failure are listed in Table 4.16.

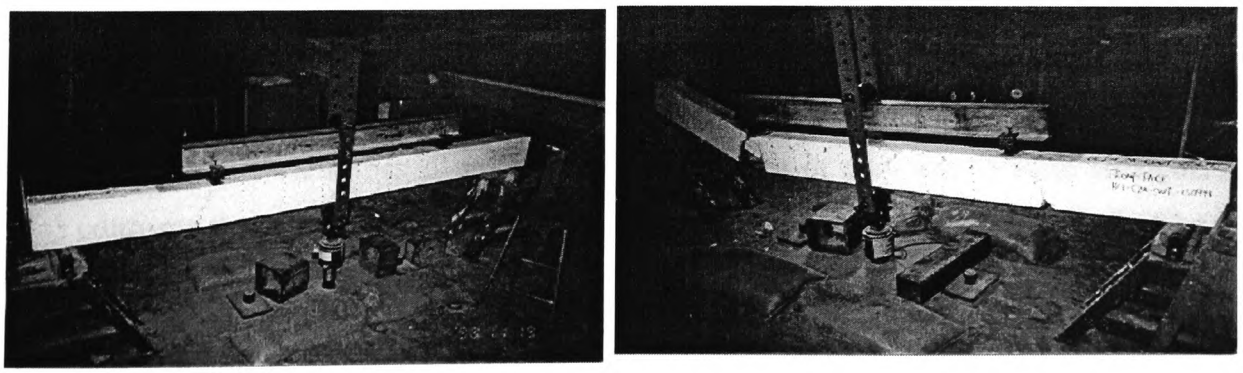

Figure 4.49 Failure Mode of beams D2 and D4

Table 4.16 Failure Moment and Failure Mode of Group D Beams

Beam Code	M_{cr} (kNm) (1)	M_{u-p} * (kNm) (2)	M_{u-exp} (kNm) (3)	(3)/(1) (4)	Failure Mode
Control	3.45	12.84	14.72	4.26	Steel yielding followed by concrete crushing.
D1	2.88	14.75	8.25	2.86	Combined bending and shear, at point load.
D2	2.30	13.28	8.50	3.69	Same as D1, with severe failure at point load.
D3	2.88	11.98	15.15	5.26	Shear and minor bending failure at point load.
D4	2.30	15.21	9.20	4.00	Same as D1.
D5	2.88	11.18	12.51	4.34	Same as D1, and with mild compression failure.
D6	2.88	16.08	11.70	4.06	Same as D1, but with greater crack width.

* The predicted M_{u-p} values were based on BS 8110, for the control beam it was assumed that the steel bars reached the yield strength first. For the CFRP reinforced beams, compression failure of concrete was assumed, and the maximum x/d ratio of 0.26 was used. All factors of safety had been removed in these calculations.

As can be seen from Table 4.16, most of the CFRP strips reinforced beams did not reach the predicted value of moment at failure. It is therefore concluded that neither the CFRP strips, nor the concrete in compression had reached the ultimate strength. In the current tests, the maximum contact perimeter between the four CFRP strips and concrete is 172.8 mm, or 3.1 times of the perimeter for two equivalent 4.5 mm diameter round bars. However, the bonding strength between the CFRP strips and concrete need to be fully investigated for any design formulae to be developed. Based on the limited number of tests carried out in this report, the following observations can be summarised:

It is potentially viable to use CFRP narrow strips as an alternative to the steel tension reinforcement. The CFRP strips reinforced beams exhibit greater ductility at the earlier loading stage when compared with conventionally reinforced beams of similar configuration. The failure load of most CFRP reinforced beams was significantly less than the predicted value based on the full development of concrete flexural strength. This confirms that shear force is an important contributor in the final failure mode. The CFRP strips must be so placed, with the flat surfaces perpendicular to the plane of bending to avoid any possible out of plane instability. The current BS 8110 design formulae should not be directly applied to design CFRP strips reinforced beams. Extensive further tests need to be carried out to provide sufficient data for developing suitable design formulae.

4.8 CONCLUSIONS OF THE EXPERIMENTAL STUDIES

As was demonstrated in the experimental studies, the technique of strengthening RC elements using external bonded FRP composites is undoubtedly an effective method of upgrading the capabilities of structurally deficient members. However, the failure mode of such beams needs to be further studied so that influencing parameters can be controlled in the design process.

The following conclusions can be drawn from these experimental investigations:

(i) CFRP composite plates can be effectively bonded to the tensile face of mechanically deficient elements, and strengthen the ultimate load carrying capacities of such conventionally reinforced concrete beams.

(ii) The final stresses in the CFRP plates in the current series of beams tested were observed to be below 1000 N/mm^2. It is believed that even if a higher strength of CFRP material had been used, the ultimate failure load of the RC beams would not have been significantly increased.

(iii) For CFRP strengthened RC beams and considering a "balanced" section analysis (based on the BS 8110 simplified rectangular stress block and using CFRP properties specified in this project), it would imply that the ratio of neutral axis to beam depth (x/h) would have to be limited to around **0.25**. This figure, compared with the limit of x/d to 0.5 for conventional RC beams, is practically too low, which leads to the conclusion that the high strength of CFRP plates is unlikely to be fully utilised.

(iv) The high strength of CFRP plates can only be utilised if the modulus of elasticity is increased proportionally. However, the increase in the modulus will also compromise the beam ductility.

(v) It is suggested that the most suitable CFRP plates for strengthening RC beams would be those with a characteristic strength of around 1300 to 2000 N/mm^2, based on an elastic modulus of approximately 150 kN/mm^2. These characteristics are compatible with grade 40 concrete and high yield deformed type II bars typically used in the UK. The factor of safety for materials resulted from such a combination will be greater than 1.5.

(vi) The current material factor of safety for steel reinforcement specified by the BS 8110 is 1.05. It is suggested that the CFRP composite material manufacturers specify an appropriate factor of safety for their products, to enable the designers to use appropriate design strengths. Given the complexity in the process of manufacturing the CFRP composites, a factor of safety for materials of 1.5 may be considered as suggested as above. However, a greater partial factor of safety for materials does not necessarily lead to a better safety margin. In fact, an unnecessarily large material factor of safety could result in over strengthening and thus lead to the undesirable and even dangerous brittle failure mode at ultimate limit state.

(vii) The adhesive used for pre-laminated plate bonding in the current study was Resifix 31, a thixotropic epoxy resin with a matching hardener. This adhesive system is considered to be pertinent and effective for bonding CFRP plates to concrete elements. It is recommended that care is taken to prepare a satisfactory mixing and correct portions of the two adhesive components, and appropriate pre-treatment of concrete surface to be bonded should be carried out. The latter could be ensured by means of mechanical wire brushing and cleaning among other methods as discussed in Chapter 3.

(viii) The crack patterns of beams strengthened with CFRP plates, which have already reached or nearly reached the serviceability limit before plate bonding, are similar to the original ones. The lengths of the original cracks tend to increase when the load reaches about 90% of the original serviceability level. Only a small number of new cracks were then observed. Beams that were strengthened under perfect conditions, were not loaded before the completion of plate bond

setting. The visible initial crack load (around 20 kN) tends to be delayed in comparison with the non-strengthened beams (at around 10-12 kN).

(ix) The failure mode of the CFRP plates strengthened beams is rather brittle. The ultimate failure occurred within the flexural region as expected, at the interface between the internal main steel reinforcement, and the concrete cover between the CFRP plates to the steel bars. This is typical longitudinal shear failure of the concrete and the bond failure of the steel reinforcement. The adhesive bonding between the external CFRP plates and the concrete was shown to be adequate. At the ultimate failure, most of the bonding layer between CFRP plates and the concrete remained intact. The failure mode is thought to be influenced by the adhesive, concrete, reinforcement and composite properties. Further analysis on the brittle tearing-off failure will be presented in Chapter 6.

(x) The behaviour of mass concrete beams with no internal reinforcement, and which were externally bonded by CFRP plates, differs greatly from that of the conventionally reinforced concrete beams. Concrete beams which were reinforced only by externally bonded CFRP plate/fabrics, fail in a sudden and brittle manner at much lower ultimate load than beams with minimum internal steel reinforcement. It is therefore important to conclude that FRP composite strengthening should only be applied to such members which already contain minimum internal steel reinforcement.

(xi) Concrete beams internally reinforced with narrow CFRP composite strips behave differently to the conventional RC members. Such members exhibit lower stiffness, and the full tensile strength of CFRP composites could not be developed before the beams fail prematurely in combined flexure and shear.

CHAPTER 5

Analytical Modelling of FRP Strengthened RC Elements

5.1 INTRODUCTION

In the preceding chapter, the behaviour of CFRP strengthened RC beams was experimentally investigated. The results showed clearly the viability and effectiveness of this new strengthening technique using CFRP composites. However there are always limitations, of either physical or economical nature, with any experimental studies. One such significant limitation in the current study is that the geometrical configuration and steel reinforcement ratio of the test beams had been kept constant. This was due to practical difficulties but was also intended to generate a clear indication of behaviour for the given set of loading and geometrical parameters with the least possible changes in influencing factors.

A parametric study is nevertheless essential to correlate the experimental results, and thus quantify the general structural behaviour. This chapter introduces the development and application of a non-linear analytical model for predicting the behaviour of FRP strengthened flexural members. The current method deployed is different from the conventional finite element techniques such as those carried out by He *et al* (1997b), which were found to have many limitations. The results of the modelling process will be compared with that of the current test data and conclusions will be presented.

5.2 MATERIAL CONSTITUTIVE LAWS

In order to predict the structural behaviour of the strengthened elements with reasonable accuracy, the actual material properties should be clearly defined. In the present study, the well-established material constitutive laws were reviewed and compared with the results of the in-house tests. The variations that best matched the test results were then chosen to develop an analytical model for the prediction of the composite strengthened section behaviour. The following paragraphs describe these models.

5.2.1 Flexural Concrete in Compression

The stress-strain relationship of concrete in compression is a factor that influences the element behaviour critically. Many national and international design codes such as BS 8110: Part 1 (1997) and EC 2 (1992) use a simplified rectangular stress block for concrete in bending at the ultimate limit state as shown in Figure 5.1.

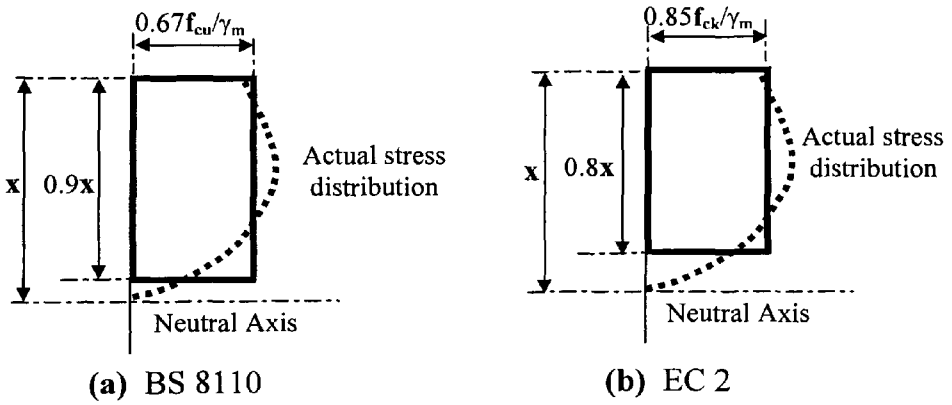

Figure 5.1 Simplified Rectangular Models for Concrete in Compression

This simplified rectangular representation of compressive stress blocks is shown in Figure 5.1. The maximum compressive stress that can be attained in a flexural member is well understood to be 80% of the concrete characteristic cube strength f_{cu} (Kong & Evans, 1989). BS 8110 uses a factor of 1.2 which takes account of the difference between the parabolic and rectangular stress blocks, the design strength is therefore $0.67f_{cu}$ divided by the material factor of safety γ_m, which is 1.5 for concrete in bending. In BS 8110: Part 2 (1985), as well as in EC 2, a more accurate stress-strain curve was

defined for concrete in compression as in Equation 5.1. Both codes use the same constitutive law with only slight difference in the factor η.

$$\sigma_c = 0.8 f_{cu}\left[\frac{k\eta - \eta^2}{(k-2)\eta}\right] \qquad (5.1)$$

where $k=1.4E_o/f_{cu}$, and $\eta= \varepsilon/\varepsilon_o$. ε_o is the concrete strain at peak stress, and has a value of 0.002200. The ultimate strain of ε_{cu}, at which the concrete starts to disintegrate, is taken as 0.0035 as specified by BS 8110, Part1 (1997).

In the present study, the accurate stress-strain curve of BS 8110 Part 2 was used. A typical curve for a concrete compressive strength of 45 N/mm^2, which was approximately the same as that of beam A2 and A2-O (44.6 N/mm^2), is shown in Figure 5.2. The modulus of elasticity, E_o, was determined from cylinder test results and compared well with the values determined by other means as listed in Table 5.1. The E_o values were also evaluated from the experimentally obtained moment-curvature curves as presented in Section 4.4. Firstly the flexural rigidity EI was determined from the initial slope of the M-κ curves, and E_o was then obtained by dividing EI by the second moment of area of the transformed section. These values agree well with the cylinder test results and those determined by BS 8110 and EC2 methods.

Table 5.1 Comparison of Elastic Modulus for Concrete (kN/mm^2)

f_{cu} (N/mm^2)	**BS8110, Part 1** $E_c=5.5(f_{cu})^{0.5}$	**BS 8110, Part 2*** $E_c=20+0.2f_{cu}$	**EC2** $E_c=9.5(f_{ck}+8)^{1/3}$	**Cylinder Test**	**Derived from moment curvature**
47.4 (Control)	**37.8**	29.5	32.4	35.1	32.5
54.9 (A1)	**40.7**	30.9	35.1	38.4	33.4
44.6 (A2)	**36.7**	28.9	33.5	33.8	31.7
33.1 (B6)	**31.6**	26.6	31.0	31.1	30.7

It was therefore decided that the following equation, given by BS 8110, Part 1, would be used in the present study for determining the E values of concrete, with the material factor of safety γ_m being removed.

$$E_o = 5.5\sqrt{\frac{f_{cu}}{\gamma_m}} \qquad (5.2)$$

5.2.2 Flexural Concrete in Tension

Although the tensile strength of concrete is usually ignored in the design of RC flexural members, the concrete in between the cracks does contribute to the beam stiffness, and hence influences the moment-curvature relationship. Many studies have dealt with the question of concrete constitutive model in tension. Tamai *et al* (1988), at the University of Tokyo, first proposed the following equations, which were subsequently confirmed by Hsu and his co-researchers at the University of Houston experimentally and theoretically (Hsu & Zhang 1996, Belarbi and Hsu, 1994).

$$\sigma_t = f_{ct}\,\varepsilon_t \qquad (\varepsilon_t < \varepsilon_{ct}) \qquad (5.3a)$$

$$\sigma_t = f_{ct}\left(\frac{\varepsilon_{ct}}{\varepsilon_t}\right)^{0.4} \qquad (\varepsilon_t > \varepsilon_{ct}) \qquad (5.3b)$$

$$f_{ct} = 0.31\sqrt{f_{cu}} \qquad (5.3c)$$

where ε_{ct} is the average tensile strain, at which the first concrete crack occurs. Its value is 0.000080 (80 Microstrain). The factor of 0.4 is a coefficient representing the characteristic bond of deformed steel bars with concrete (Sato *et al*, 1999). The variation of concrete tensile strength, f_{ct}, was recommended by Belarbi and Hsu (1994), as given in Equation (5.3c).

Shown in Figure 5.3 is a typical concrete tensile stress-strain curve as defined by Equations (5.3a-c). The concrete material involved was the same as described in the compression model in Figure 5.2.

5.2.3 Steel Reinforcement

To take account of the tension stiffing effects, a model, in which the behaviour of reinforcement embedded in concrete differs from that of the bare steel rod in tension, is deployed. The most important difference is the lowering of the yield stress to below the yield strength f_y of bare bar in tension. Belarbi and Hsu (1994) reported that the concrete tensile strength and the ratio of steel reinforcement were the major factors, which influence the magnitude of this difference. Let the apparent yield strength of the embedded steel bars be f_y^*, then this stress can be estimated by the following equation.

$$\frac{f_y^*}{f_y} = 1 - \frac{4}{\rho}\left(\frac{f_{ct}}{f_y}\right)^{1.5} \qquad (5.4)$$

where ρ is the tension steel reinforcement ratio, f_{ct} is the concrete tensile strength [see Equation (5.3c)], and f_y the yield strength of bare bar in tension. For the current study, the following typical values were taken: (i) concrete tensile strength f_{ct} of 2.0 N/mm^2 (based on a typical lower boundary modulus of elasticity of 25,000 N/mm^2 and a crack strain ε_{ct} of 80μ), and (ii) the typical steel reinforcement ratio ρ_s = 0.785%. The apparent yield stress f_y^* in the reinforcement was therefore estimated to be 0. 852f_y = 403 N/mm^2 for f_y = 560 N/mm^2.

Based on the above discussion, a tri-linear model was developed for the current study with the apparent yield stress being 400 N/mm^2, and an ultimate strength of 560 N/mm^2. The model is shown in Figure 5.4 together with the averaged and back analysed experimental stress-strain curve. It was apparent that the experimental curve showed a lower Young's modulus than the standard and manufacturer specified value of 200 kN/mm^2. This was thought to be untypical and may have been due to experimental error. In order to finalise a generic representation, the tri-liner model used in the current study, was thus modified to E_s = 200 kN/mm^2 in accordance with BS 8110 (1997).

5.2.4 FRP Composites

The CFRP composites have linear stress-strain relationships up to failure, which can thus be expressed by the standard Hook's Law.

$$\sigma_p = E_p \varepsilon_p \qquad (5.5)$$

The subscript "p" in the above equation indicates that the property is related to FRP composites. For most of the available medium strength CFRP products for the construction market, the typical tensile strain at failure is around 1.4 - 1.6%. The FRP manufacturers usually specify material properties including the ultimate tension strength, the break strain and the elastic modulus. It is often found that these specifications do not match the relationship defined by Equation (5.5). For example, the Sika CFRP strips were specified to have an elongation at break of 1.4% with an elastic modulus of 150 kN/mm^2, which should result in an ultimate tensile strength of 2100 N/mm^2. However, the company specified an actual minimum tensile strength of 2400 N/mm^2 (Sika, 1998). This is thought to be the result of under specified failure strain. Such a strain at break of pultruded FRP plates is especially difficult to quantify. Although it is recognised that FRP fails in a brittle manner, the actual failure process usually initiates at partial snapping of the fibres, a complete failure of the whole cross section is accompanied by large final break strains as the bonding polymer matrix under goes plastic deformation. It is thus prudent to specify a lower bound value for the FRP failure strain. In over strengthened sections, however, the behaviour of the strengthened elements will not be influenced by the ultimate strength and strain of the fibre composites, since the concrete will have failed before the FRP reaches the design strength.

Figure 5.5 shows the stress-strain curves for the three types of CFRP composites that were used in the current study. The tensile modulus for type A CFRP plate was determined to be 125 kN/mm^2, while E_p was 185 and 230 kN/mm^2 for type B plate and the type D CFRP fabric respectively.

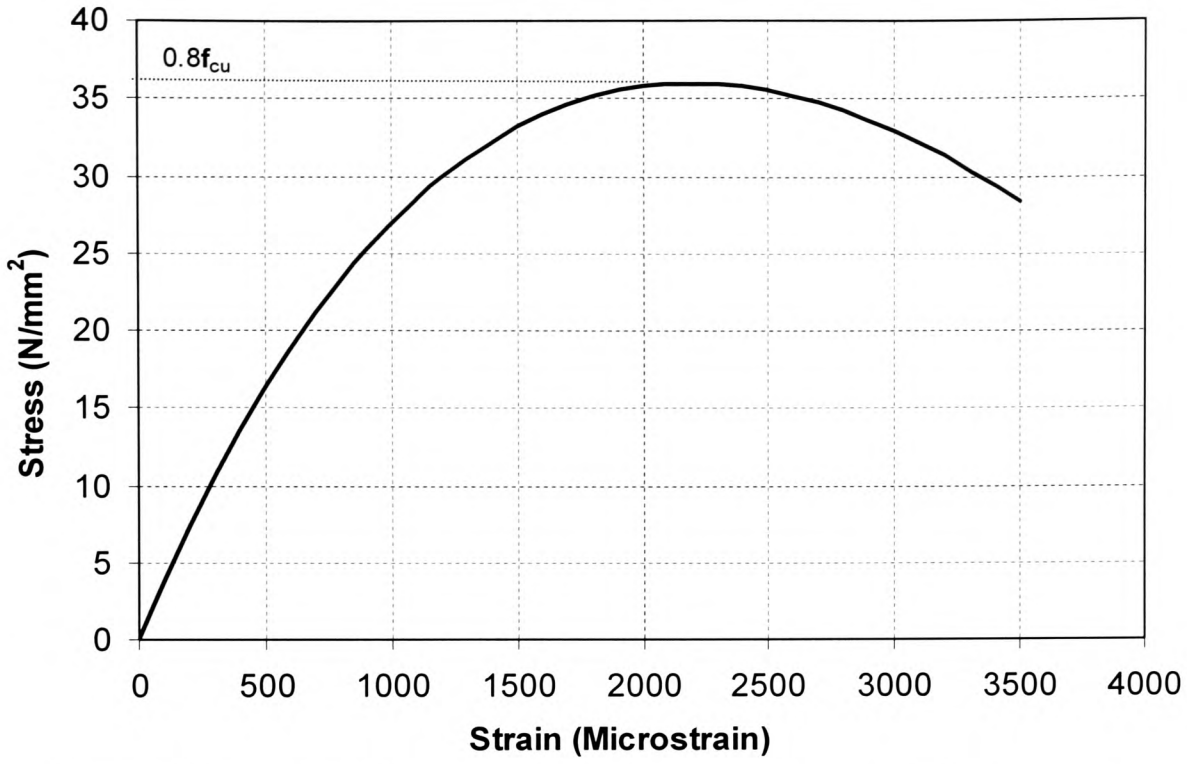

Figure 5.2 Short Term Stress-Strain Relationship of Concrete in Compression used in the Current Study (f_{cu} = 45 N/mm^2, Beam A2)

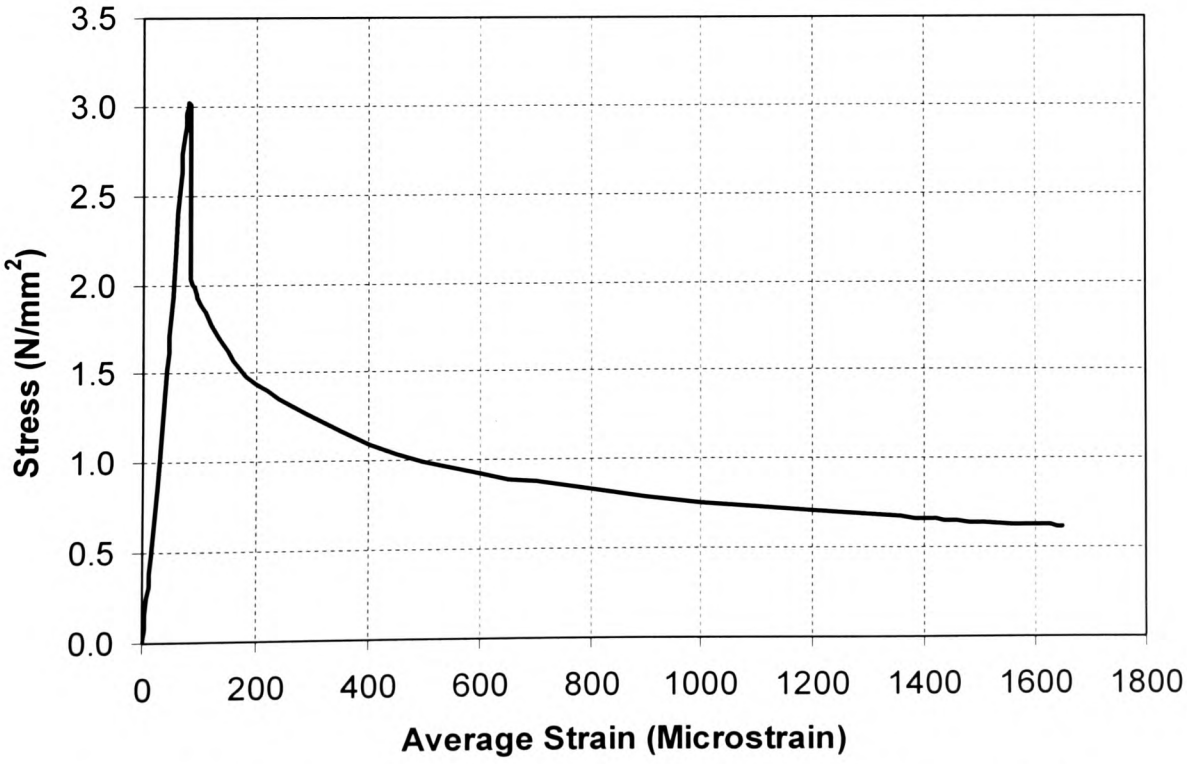

Figure 5.3 Typical Tensile Constitutive Model Used in the Current Study (f_{cu} = 45 N/mm^2)

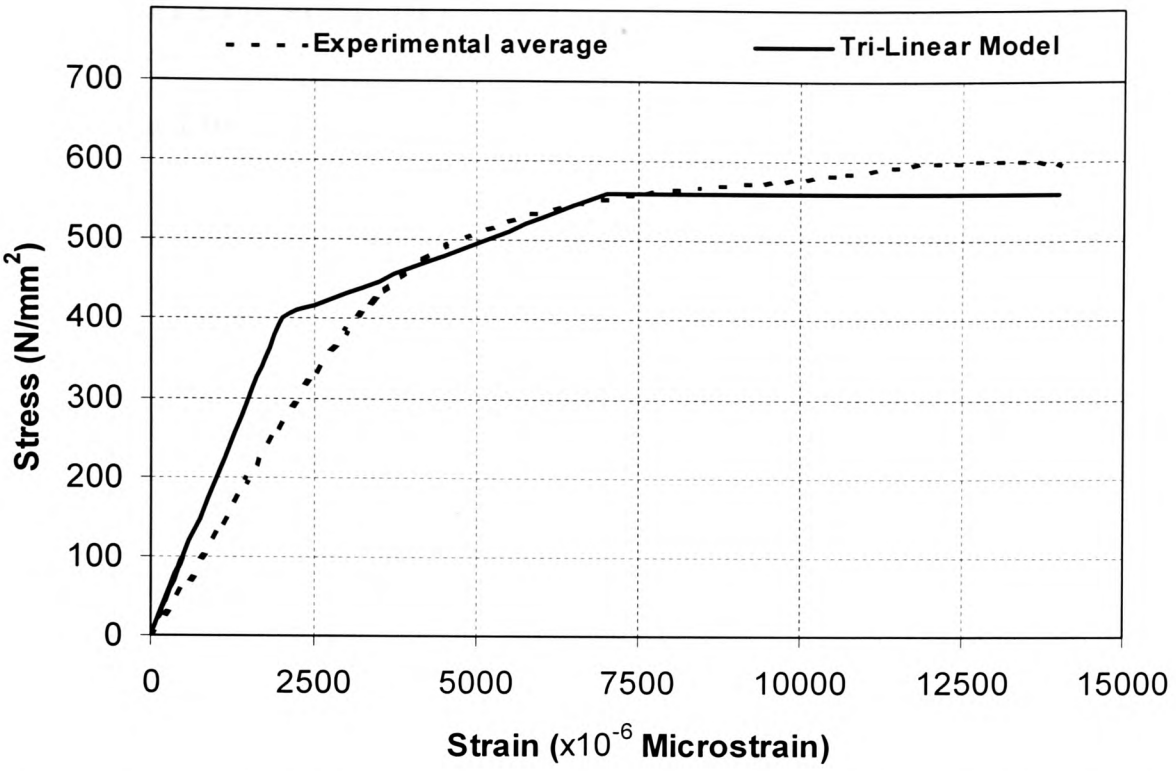

Figure 5.4 Modified Tri-linear Representation of Stress-Strain Relationship of Steel Reinforcement Embedded in Concrete

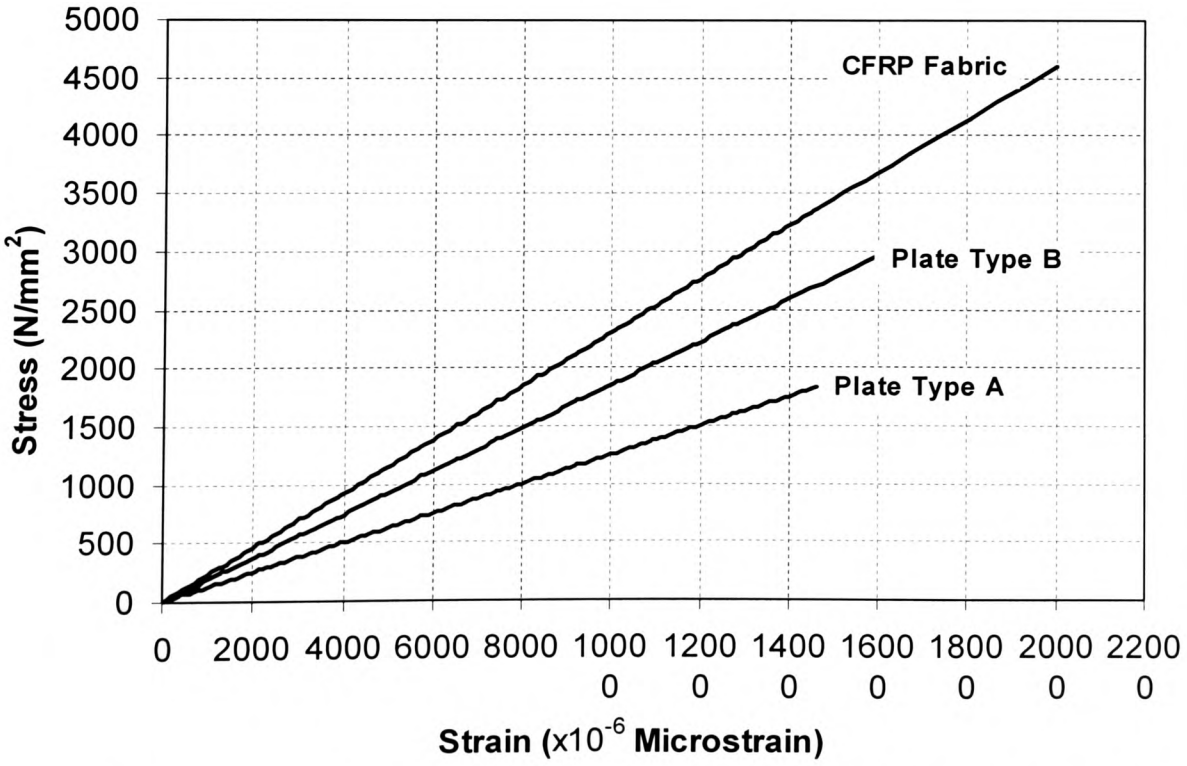

Figure 5.5 Stress-Strain Relationship of CFRP Composites Used in Current Study

5.3 ANALYTICAL MODEL FOR FLEXURAL MEMBERS

5.3.1 Model Development

A non-linear analytical model for FRP strengthened rectangular beams subjected to bending was established based on the materials properties discussed above. The section stress strain distribution is shown in Figure 5.6. Unlike most other analytical methods proposed by other researchers as discussed in Chapter 2, which only deal with the elements at ultimate failure, the current model was intended to predict the element's behaviour during the whole loading process.

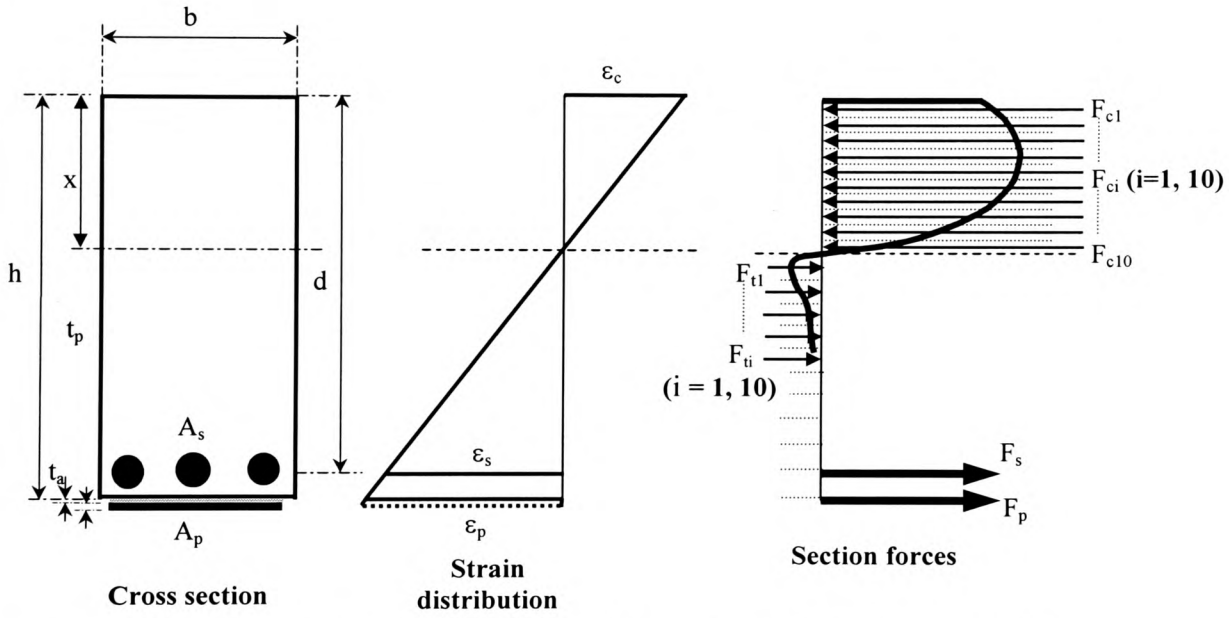

Figure 5.6 Analytical Model - Section Stress Strain Distribution for Singly Reinforced, FRP Strengthened Rectangular Beams

It was thus possible to compare the proposed analytical model with the experimental results. This was intended to provide an accurate predictive model to assess the behaviour of CFRP strengthened elements under loading.

The principle assumption made was that plane sections remain plane before and during deformation. The strain distribution across the section depth exhibited linear characteristic, this was confirmed by the test results as discussed in Chapter 4. The adhesive bonding layer was not included in the model. Instead, perfect composite action

between concrete and the FRP, as a result of the adhesive bonding, was assumed. This assumption was considered to be reasonable as no failure in the actual adhesive bonding layer, or on the concrete-adhesive and/or adhesive-FRP interfaces had been observed in the current loaded beam tests.

5.3.2 Solution Procedure

A numerical integration technique was used to determine the concrete compression and tensile forces. Both the compression and tension zones were divided into a finite number of narrow strips, and each force component was then determined as the product of the strip area and the corresponding stress. Since the beam depth of 200 mm in the current test configuration is relatively small, it was decided to use 20 strips in the model, namely 10 each in the compression and tension zones respectively.

The strains in the steel bars ε_s, and FRP plates ε_p, were expressed in terms of the concrete compressive strain, ε_c, as follows.

$$\varepsilon_s = \frac{d - x}{x}\varepsilon_c \tag{5.6}$$

$$\varepsilon_p = \frac{h + t_a + \frac{t_p}{2} - x}{x}\varepsilon_c \tag{5.7}$$

The concrete tensile strain at the soffit of the beam, ε_t, can be expressed in terms of x and ε_c in a similar manner by the following equation.

$$\varepsilon_t = \frac{h - x}{x}\varepsilon_c \tag{5.8}$$

The resultant concrete compressive and tensile forces can then be determined by the following equations, where f_{ci} and f_{ti} are the compressive and tensile stresses at the i^{th} strip, as defined by Equations (5.1) and (5.3) respectively.

$$F_c = F_{c1} + F_{c2} \ldots + F_{c10} = \frac{bx}{10} \sum_{i=1}^{10} f_{ci} \qquad (5.9)$$

$$F_t = \frac{b(h-x)}{10} \sum_{i=1}^{10} f_{ti} \qquad (5.10)$$

The tensile forces in the internal steel reinforcement and the external CFRP composite can be determined respectively as follows.

$F_s = f_s A_s = E_s \varepsilon_s A_s$ (ε_s<0.002) (5.11a)

$f_s = [400 + 32000(\varepsilon_s - 0.002)]A_s$ (0.002<ε_s<0.007) (5.11b)

$f_s = 560$ ($\varepsilon_s \geq 0.007$) (5.11c)

$F_p = f_p A_p = E_p \varepsilon_p A_p$ (5.12)

Consider the section force equilibrium:

$F_c + F_t + F_s + F_p = 0$ (5.13)

Substitute Equations (5.9) – (5.12) into Equation (5.13), the neutral axis depth x can therefore be determined for a given concrete compressive strain ε_c. Successive iterations were used to determine the precise value of x. A computer program, using Visual Basic Macros and the Microsoft Excel spreadsheet, was developed to perform the numerical operations. The computer program interface and typical results are shown in the Appendix B.

The moment of resistance of the CFRP strengthened section was then derived by taking moment contribution of all forces about the neutral axis, as defined by the following equation.

$$M = \sum_{i=1}^{n} F_i(x_i - \frac{x}{20}) + \sum_{i=1}^{n} F_{ti}(x_{ti} + 10 - \frac{x}{20}) + F_s(d - x) + F_p(h + t_a + \frac{t_p}{2}) \quad (5.14)$$

where, x_i - the distance from the top of the i^{th} compressive strip to the neutral axis.

x_{ti} - the distance from the bottom of the i^{th} tensile strip to the neutral axis.

The curvature value for a given load can now be determined from the concrete compressive strain and the neutral axis depth using the following equation.

$$\kappa = \frac{\varepsilon_c}{x} \quad (5.15)$$

5.4 FRP SECTION ANALYSIS

5.4.1 The Fully Balanced Section

Firstly, consider a "partially balanced section" in an FRP strengthened flexural member, ignoring the presence of steel reinforcement, the stress at failure of the FRP composites can be evaluated from the strain compatibility condition and expressed in terms of ultimate concrete compressive strain ε_{cu}.

$$f_{pu} = \frac{h + t_a + \frac{t_p}{2} - x}{x} \varepsilon_{cu} E_p \quad (5.16)$$

Solve Equation (5.16), the neutral axis depth for such a balance section can be determined, with no partial factors of safety, as:

$$x_{pb} = \frac{h + t_a + \frac{t_p}{2}}{(1 + \frac{f_{pu}}{\varepsilon_{cu} E_p})} \quad (5.17)$$

The neutral axis value must be less than the value determined from the above equation if FRP is to fail before the concrete reaches its crushing strength.

From the principle of similar triangles, it can be seen that the tensile strains in the steel reinforcement and the FRP composite have the following relationship.

$$\varepsilon_{pu} = \frac{h + t_a + \frac{t_p}{2} - x}{d - x} \varepsilon_{su} \tag{5.18}$$

where ε_{pu} and ε_{su} are the ultimate strains of FRP composite and steel reinforcement respectively. If both materials were to reach their ultimate strength simultaneously, then the following equation must be satisfied.

$$x = \frac{d\varepsilon_p - (h + t_a + \frac{t_p}{2})\varepsilon_s}{\varepsilon_p - \varepsilon_s} \tag{5.19}$$

If the neutral axis depth x at the ultimate load is less than that determined by the above equation, then the steel reinforcement will yield before the FRP composites. In the current study, the steel reinforcement reached its ultimate tensile strength at a strain of 0.007000. Substitute h (200mm), d (174mm), t_a (2mm), t_p (1.6mm) and a typical FRP ultimate failure strain ε_p (1.4%) into Equation (5.19), x is evaluated to be 0.83d (145.2 mm).

This indicates that the neutral axis depth must be greater than or equal to 0.83d for the FRP composite to reach failure strain before, or simultaneously with, the steel reinforcement reaching its ultimate tensile strength. The neutral axis for the steel-reinforced-only sections is less than 0.83d, which can be evaluated as follows:

$$x_{sb} = \frac{d}{(1 + \frac{f_y}{\varepsilon_{cu} E_p})} \tag{5.20}$$

Substitute d (174 mm), f_y (560 N/mm^2), E_p (200000N/mm^2) and ε_{cu} (0.0035) into the above equation, x_{sb} is found to be 0.556d (96.6 mm).

Practically this means that for the tests performed using the materials in the current tests, it was ensured that the steel reinforcement would always yield first before the FRP composites. This would be true no matter how small the area of FRP provided is. This was indeed observed to be the case in both the experiments and the analytical model. Generally speaking, whether FRP or steel reinforcement fails first depends on the failure strains of the two materials. For a "fully balanced section" where steel reinforcement, FRP composites and the concrete in compression fail simultaneously, then the following condition can be defined by equating Equations (5.19) and (5.20) for strain compatibility, the following equation must be satisfied.

$$\frac{d\varepsilon_p - (h + t_a + \frac{t_p}{2})\varepsilon_s}{\varepsilon_p - \varepsilon_s} = \frac{d}{(1 + \frac{\varepsilon_s}{\varepsilon_{cu}})} \tag{5.21}$$

Let $\beta = d/(h + t_a + t_p/2)$, Equation (5.21) can be rewritten as:

$$\frac{\varepsilon_p - \frac{1}{\beta}\varepsilon_s}{\varepsilon_p - \varepsilon_s} = \frac{\varepsilon_{cu}}{\varepsilon_{cu} + \varepsilon_s} \tag{5.22}$$

The candidate suggests that the factor β be called "Reinforcement Position factor" since it defines the relative positions of the internal steel and the external FRP reinforcements. Its value depends on the thickness of the nominal concrete cover, and the thickness of the adhesive layer as well as the FRP plates. The range of β is from 0.8 for relatively small beams to 0.95 for larger sections. For the size configuration used in the present study, $\beta = 174/202.8 = 0.858$.

Solving Equation (5.22), the FRP strain for a fully balanced section, ε_{pb}, can now be expressed as follows:

$$\varepsilon_{pb} = \frac{\varepsilon_{cu} + \varepsilon_s}{\beta} - \varepsilon_{cu} \tag{5.23}$$

For the typical high-yield steel reinforcement used in the UK, BS 8110:Part 1 (1997) recommends a bi-linear stress-strain curve and a design strength of f_y/γ_m, where the characteristic strength f_y is 460 N/mm^2 and the material partial factor of safety for steel, γ_m, is taken as 1.05. The yield strain of steel reinforcement is therefore:

$$\varepsilon_s = (\frac{460}{1.05}) \div 200000 = 0.002190$$

Substitute the above ε_s into Equation (5.23), and for typical β value of 0.85, the FRP balance strain ε_{pb} is found to be 0.003130. This figure is far less than the ultimate failure strain of most CFRP composites, which is in the order of 1.4%. For the present study - where the steel strain for the corresponding ultimate tensile strength of 560 N/mm^2 was evaluated to be 0.007000 - the value of ε_{pb} was found to be 0.008730, again much smaller than 0.014000. It can therefore be generally concluded that:

For FRP composite strengthened flexural RC elements, the steel reinforcement will always fail before the external FRP reinforcement. This behaviour will not be affected by the amount of FRP composites provided.

The above statement has significance in design for FRP strengthening, since it is usually desirable for the steel to fail before the FRP composites and the concrete, to ensure a reasonably ductile failure mode. This will be discussed further in Chapter 8.

5.4.2 Under- and Over- Strengthened Sections

5.4.2.1 Definitions

Similar to the concept of "under-reinforced section" in the design of flexural RC elements, FRP strengthened RC elements should also be designed so that the sudden and brittle failure of concrete in compression will be avoided. The actual design issues will be addressed in Chapter 8, the following sections discuss the actual boundary between under- and over-strengthened section for FRP strengthened RC members. Firstly the definitions are given as follows:

Over-strengthening – A section is considered to be "over-strengthened" if the area of FRP composites provided is such that the concrete will reach its crushing strength before the FRP reaches its ultimate tensile strength. In such cases the failure will be sudden and brittle, and should be avoided if possible.

Under-strengthening – If the area of FRP composites provided in an FRP strengthened section is such that the steel reinforcement will yield first, followed by the rupture of the FRP composites before the concrete in compression reaches its ultimate strength, the section is then considered to be under-strengthened. Under-strengthened elements exhibit better ductility characteristic and the failure is usually proceeded with sufficient warning.

5.4.2.2 Maximum Area of FRP

Based on the analysis in Section 2.4, the area of FRP that should be provided to ensure an under-strengthened section can now be defined. The force equilibrium expressed in Equation (5.13) at the ultimate limit state can be expanded as:

$$F_{tp} = F_c - F_{tc} - F_s = \Omega f_{cu} bx - F_{tc} - f_y A_s = f_{pu} A_p,$$

where Ω is a shape factor of the stress-strain curve for concrete in compression, and is found to be 0.6626 for the present model based on an equivalent rectangular stress block with full neutral axis depth of x. For an under-strengthened section, the maximum area of FRP provided should therefore be limited to:

$$A_{p\max} = \frac{\Omega f_{cu} bx - F_{tc} - f_y A_s}{f_{pu}} \qquad (5.24)$$

The neutral axis depth x in the above equation should be determined by Equation (5.17). Equation (5.24) does not incorporate any partial factors of safety for practical design purposes, which will be discussed in Chapter 8.

For a typical beam strengthened by the type A CFRP plate in the current test series, the following properties were used: f_{pu}=1750 N/mm^2, f_{cu}= 45 N/mm^2, f_y = 560 N/mm^2, A_s =

157 mm^2. The neutral axis depth value x and the concrete tension resistance F_{tc} at ultimate limit state were determined to be 40.56 mm and 1026.34 N from the analytical model. Substituting these figures into Equation (5.24), the maximum area of CFRP plate to be provided for an under-strengthened section is found to be **13.65** mm^2. This is approximately one layer of the CFRP fabric in the current testing series.

Since all the type A CFRP plates have a cross sectional area of 128 mm^2, the beams strengthened by this type of plate were therefore all over-strengthened, and the concrete would be expected to fail before the composite plate.

The analytical model actually predicts that the tensile stress in the FRP plate at the ultimate beam failure is 827 N/mm^2, at a strain of 0.006618, far less than the ultimate tensile strength of 1750 N/mm^2 and break strain of 0.014000 for the CFRP composites.

5.4.3 Modelling of the Control Beam

The analytical model was first applied to simulate the unplated control beam. All structural parameters including stresses, strains, deflection and neutral axis depth were computed. The curvature was then determined from the compressive strain for a given load. Figure 5.7 contains the normalised moment-curvature curves of the control beam, derived from both the analytical model and the experimental data. M_u and k_u are the ultimate moment of resistance and curvature resulted from the analytical model. It can be seen that the analytical model and the experimental results generally agree well. The experimental failure moment is 98.2% of the analytical value, however, the corresponding ultimate curvature ratio is only 0.45. This large discrepancy can be attributed to the experimental set up. In the present study, all beam tests were performed using force control, as soon as the beam starts to deflect "rapidly", the control system automatically shuts off the hydraulic jack at peak load. As a result, only "Pre peak load" load-deflection behaviour is recorded, whereas the post peak load behaviour was not available.

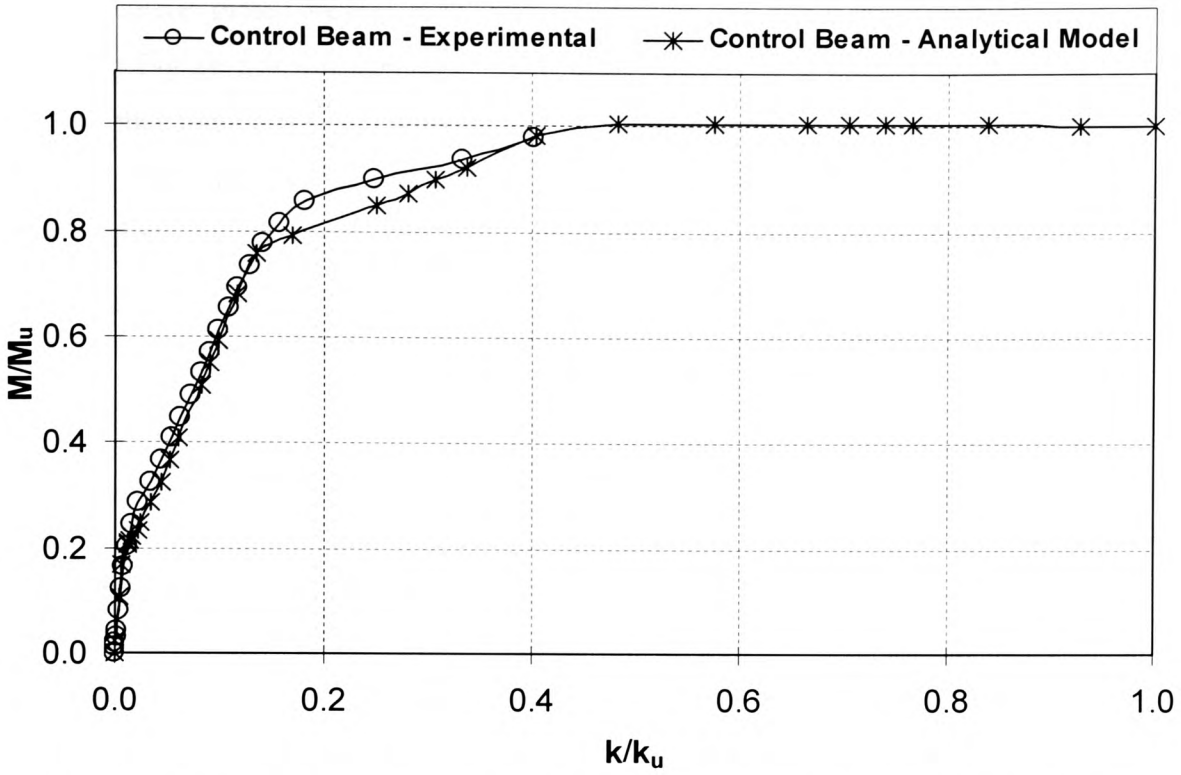

Figure 5.7 Comparison of Moment-Curvature Relationship of the Control Beam

At just after the apparent steel yield point, the analytical model shows up to be 6% lower than the experimental moment capacity, although it increases almost linearly with the curvature to beyond the experimental line, before reaching the plateau. This behaviour seemed to be directly related to the tri-linear representation of the steel reinforcement, indicating that the steel reinforcement governs the structural behaviour after yielding.

5.4.4 Analysis of Section Stresses

The concrete stress distribution across the section, at various strains, was computed and plotted against the section depth. Figure 5.8 shows the stress distribution for the unplated control beam. The stresses exhibit linear variation up to a load level of around 8kN, when first tensile cracks appear in the concrete at a tensile strain of 80 microstrain. At the ultimate limit state, the average tensile resistance provided by the concrete is 1.69 kN, this is 1.92% of the average tension in the steel reinforcement.

For the CFRP plated beams that were pre-loaded and cracked before strengthening, shown in Figure 5.9, the stresses in the steel reinforcement and FRP composites are much higher than that of the control beam. An extract of comparison of stresses in the concrete, steel, and FRP is presented in Table 5.2. It can be seen that the differences of stress values in the steel and FRP composites between the precracked and non-precracked models decreases with the increase of concrete strain. The two models converge eventually with very little difference in the ultimate stress magnitude.

Table 5.2 Comparison of Stresses in Concrete, Steel and FRP*

	ε_c=100 με f_c = 3.76		ε_c=1000 με f_c = 25.66		ε_c=2250 με f_c = 33.57		ε_c=3500 με f_c = 33.54		Failure Load kN
	f_s	f_p	f_s	f_p	f_s	f_p	f_s	f_p	
Control Beam	16.7	-	425.6	-	560.0	-	560.0	-	48.8
Precracked	45.4	34.0	387.3	292.3	560.0	603.5	560.0	827.5	108.7
Non-Precracked	16.5	13.5	369.8	279.9	560.0	593.4	560.0	827.3	108.4

* All units in N/mm^2 unless otherwise stated.

In Figure 5.10, stress distribution for the non-precracked CFRP strengthened model is shown. Its initial stress is lower than that of the control beam, this is expected since the external FRP plate also shares the load from the very beginning.

The maximum concrete tensile resistance seen is 18.8 kN from the control beam at a tensile strain of 0.000315, when the corresponding compressive strain and the applied load are 0.000180 and 11.1 kN respectively. For the non-precracked CFRP plated beams, the concrete tensile contribution peaks at 18.8 kN, at a tensile strain of 262 με and an applied load of 13.3 kN. This tensile resistance reduces to 1.98 kN at ultimate failure, which accounts for 2.2% and 1.8% of the forces in the steel reinforcement and FRP composites respectively. It is interesting to note that the precracked model give a slightly higher ultimate failure load than the non-precracked model, this is because the neutral axis depth in the precracked model is slightly lower, thus resulting in a higher stress in the FRP plate than the tension stiffening model.

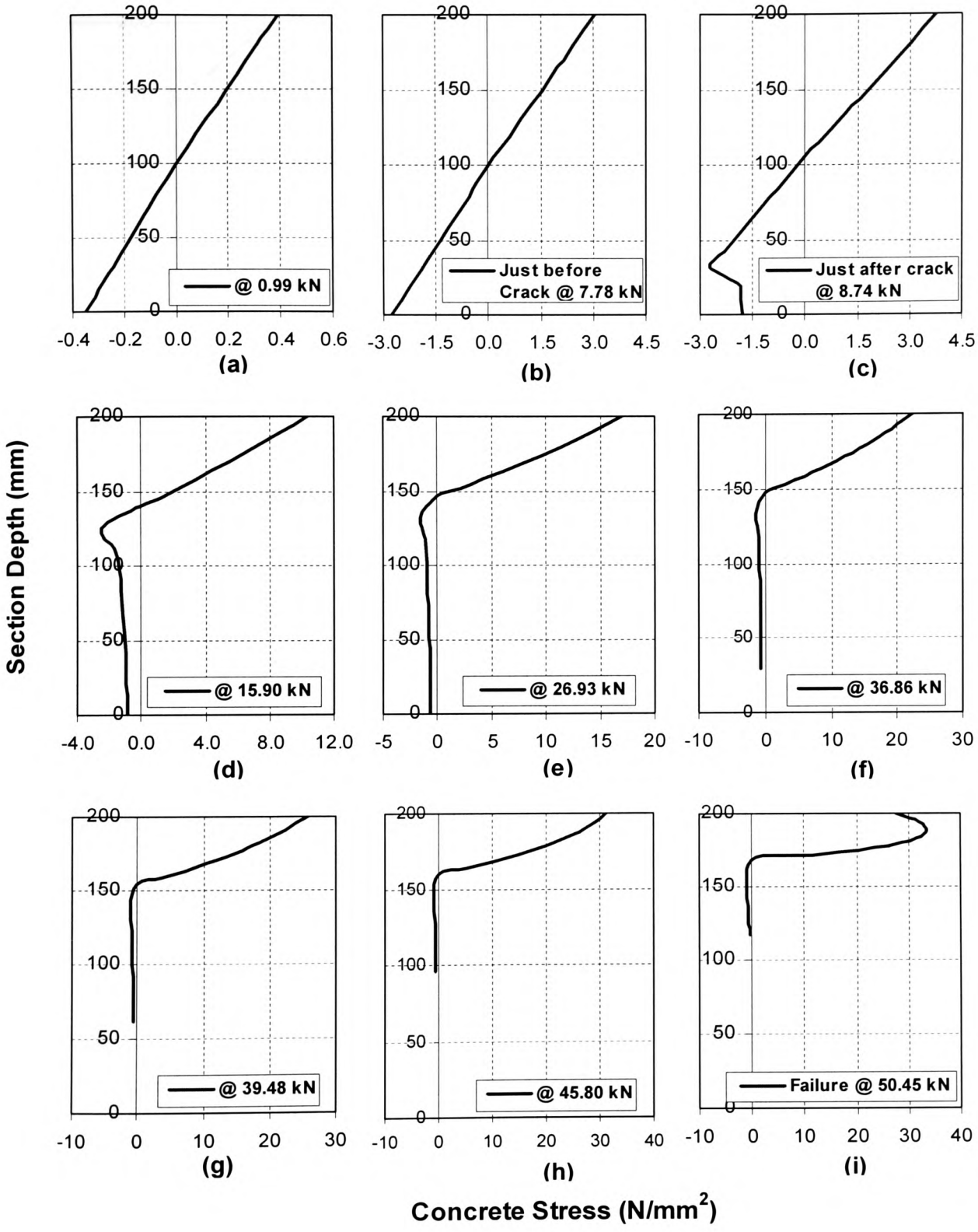

Figure 5.8 Concrete Stress Distribution for Unstrengthened Control Beams at Various Compressive Strains – With Tension Stiffening
(a) At 10 με, **(b)** – 80 με, **(c)** – 100 με, **(d)**- 300 με, **(e)** – 550 με, **(f)** – 800 με, **(g)** – 1000 με, **(h)** – 1500 με, **(i)** – at failure3500 με.

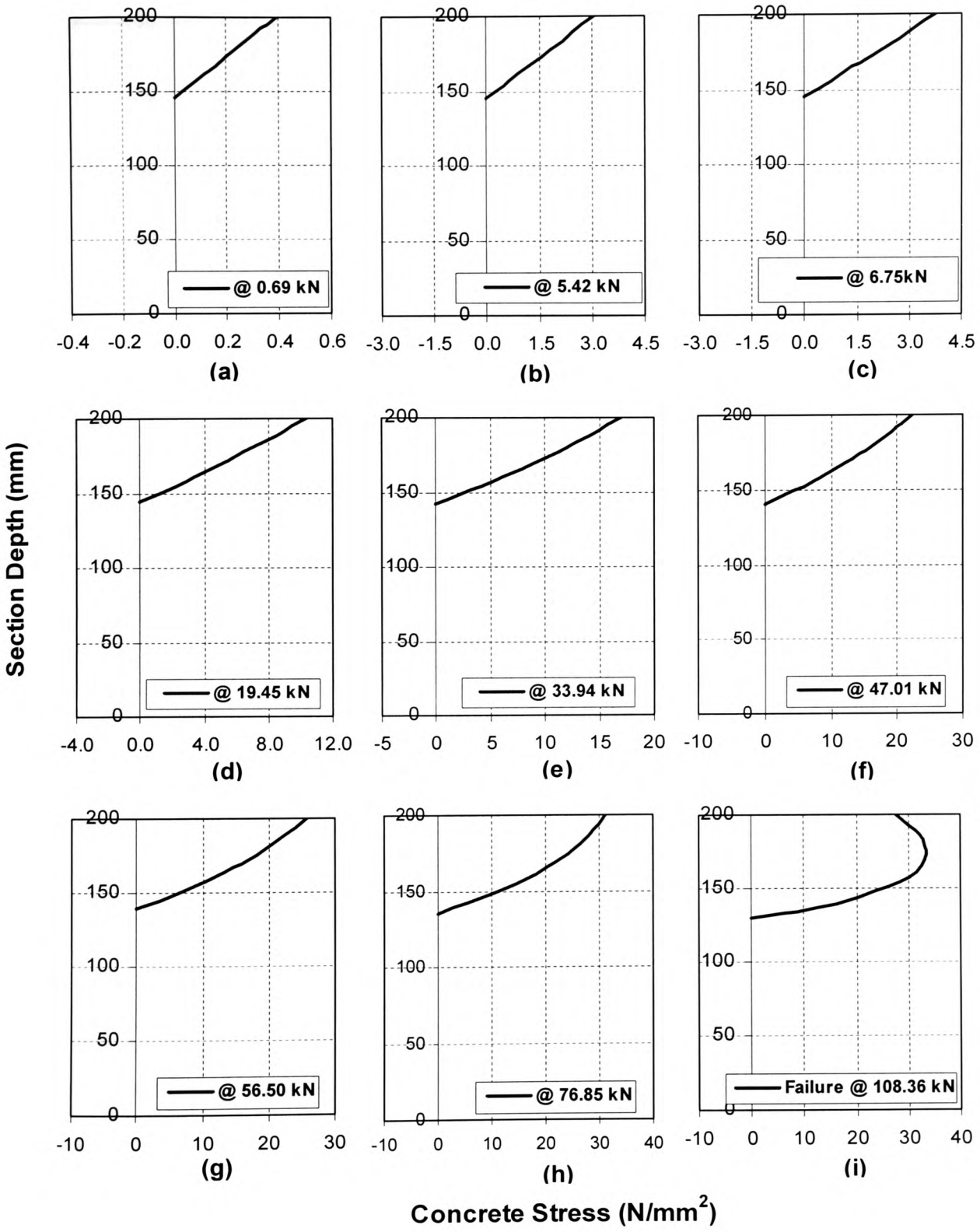

Figure 5.9 Concrete Stress Distribution for CFRP Strengthened Beams at Various Compressive Strains – The Precracked Model
(b) At 10 με, **(b)** – 80 με, **(c)** – 100 με, **(d)**- 300 με, **(e)** – 550 με, **(f)** – 800 με, **(g)** – 1000 με, **(h)** – 1500 με, **(i)** – at failure3500 με.

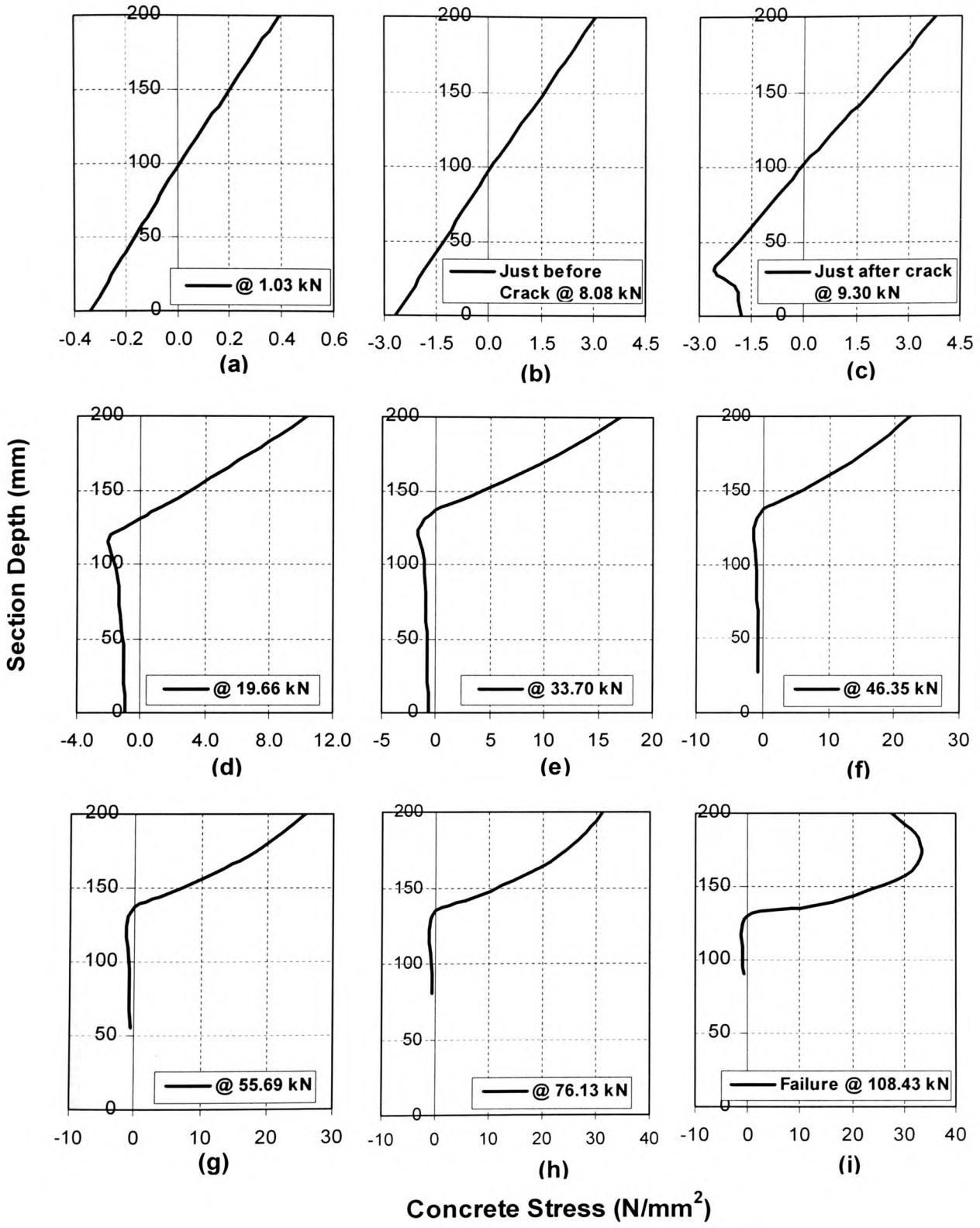

Figure 5.10 Concrete Stress Distribution for CFRP Strengthened Beams at Various Compressive Strains – Non-precracked "Virgin" Model **(c)** At 10 με, **(b)** – 80 με, **(c)** – 100 με, **(d)**- 300 με, **(e)** – 550 με, **(f)** – 800 με, **(g)** – 1000 με, **(h)** – 1500 με, **(i)** – at failure3500 με.

5.5 THE NEUTRAL AXIS DEPTH

5.5.1 The Control Beam

Figure 5.11 shows the load-neutral axis depth (P-x) variation for the control beam. The graph can be divided into four distinctive sections. Firstly, the reinforced concrete section behaves linearly elastic under the small load up to 9.2 kN, corresponding to an applied moment of 2.64 kNm. The concrete tensile strength was found to be 3.0 N/mm^2 at the crack initiation strain of 80 με. The neutral axis depth remains a constant at just below the half depth of the beam.

The moment at cracking, M_{cr}, can also be obtained from simple bending theory, in which the transformed equivalent concrete section is shown in Figure 5.12. The modular ratio is taken as 5.7. Taking the first moment of area about the top of the beam, the value of x is thus determined to be 102.6 mm. The second moment of area is then calculated as:

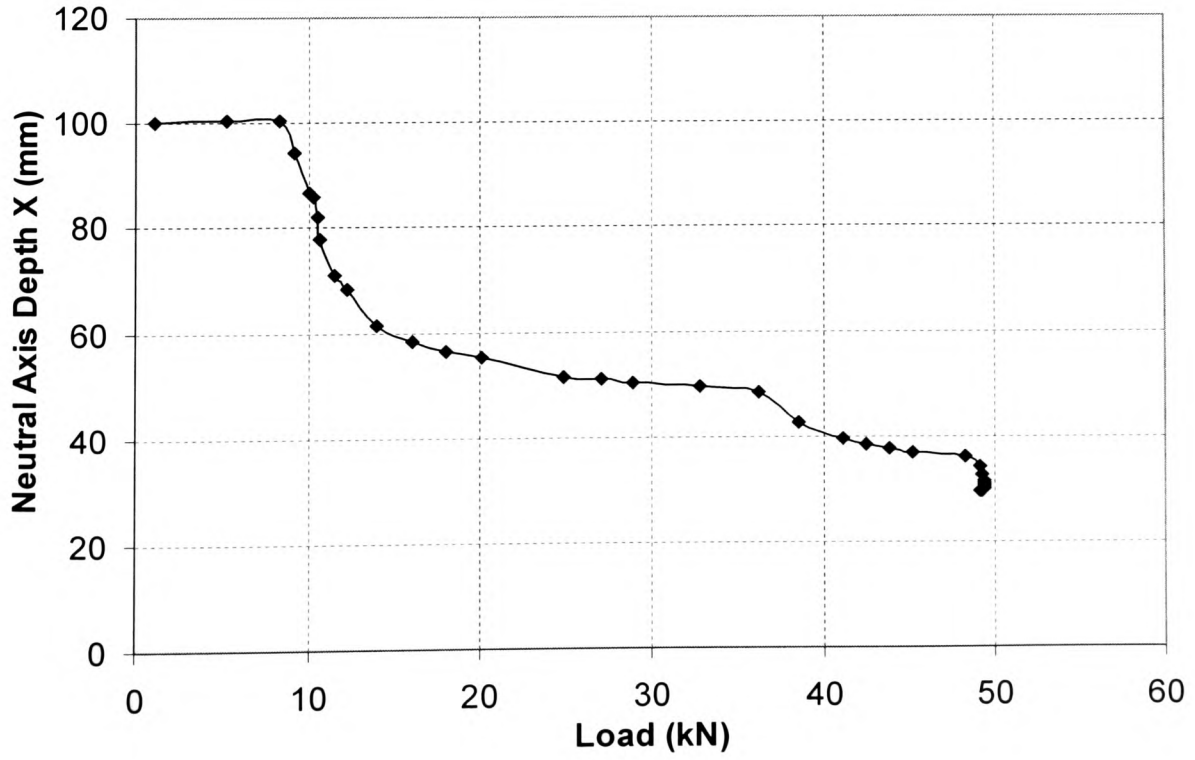

Fig 5.11 Load vs. Neutral Axis Depth for Control Beam

$I = b[(x^3+(200-x)^3]/3+(\alpha-1)A_s(d-x)^2$

$= 70.56x10^6\ mm^4.$

The cracking moment can therefore be calculated as:

$M_{cr} = f_{ct}I/(200-x) = 2.8x70.56/97.4 = 2.03$ kNm.

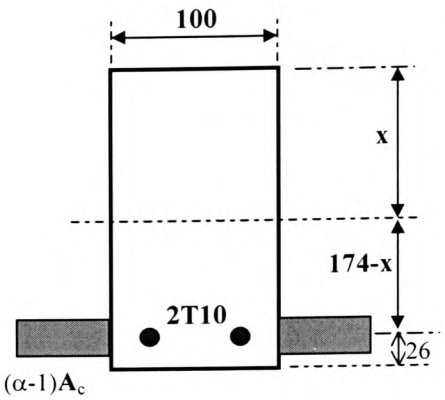

Figure 5.12 Transformed Section of Control Beam

This is about 9% less than the 2.24 kNm from the analytical model as discussed above. The analytical model is considered to be more accurate. The modulus of elasticity of concrete is not a major influencing factor for this difference, since even if E_c is reduced to an unrealistically low value of just 20 kN/mm^2 with α increased to 10, the M_{cr} value determined this way would still be 2.17 kNm.

The second distinctive variation of the P-x curve starts from the first crack and ends at a load of around 38 kN, when the steel reinforcement reaches its yield stress, which is represented in the second part of the tri-linear model for the reinforcement as shown in Figure 5.4. In this range, the neutral axis depth value decreases rapidly at just after the crack moment, indicating that stress transfer to the steel bars has taken place. The total concrete tensile resistance, however, does not reach the peak until a tensile strain of 370 με with a corresponding compressive strain of 200 με, and the applied load at this stage is 11.7 kN. The actual tension contribution at this point from the concrete and the tension reinforcement is 19.1 kN and 9.4 kN respectively, indicating that steel bars contributes approximately 33% towards the tensile resistance of the section, while the concrete provides the remaining 67%, and reaches its maximum tensile capacity.

These results agree well with the experimental data. During the laboratory testing work, the surface tensile cracks of the control became visible in the constant moment zone at around 11-12 kN, which suggests that the concrete had reached its full tensile capacity, and the tensile resistance would start decreasing rapidly until it became negligible. The very first crack, which was modelled to have occurred at around 8 kN, was not observed

in the experiments. This was because the micro cracks are usually undetectable to the naked eye.

The normalised tensile resistance contribution from the concrete against the load increase is indicated in Figure 5.13. It is apparent that concrete tensile strength plays a significant role in the total tension resistance of the section. At the service load, assumed to be around 65% of the ultimate load, the concrete tensile contribution to tension resistance is still over 15% of the total tension. However, at the ultimate limit state, the tensile contribution from the concrete is effectively zero.

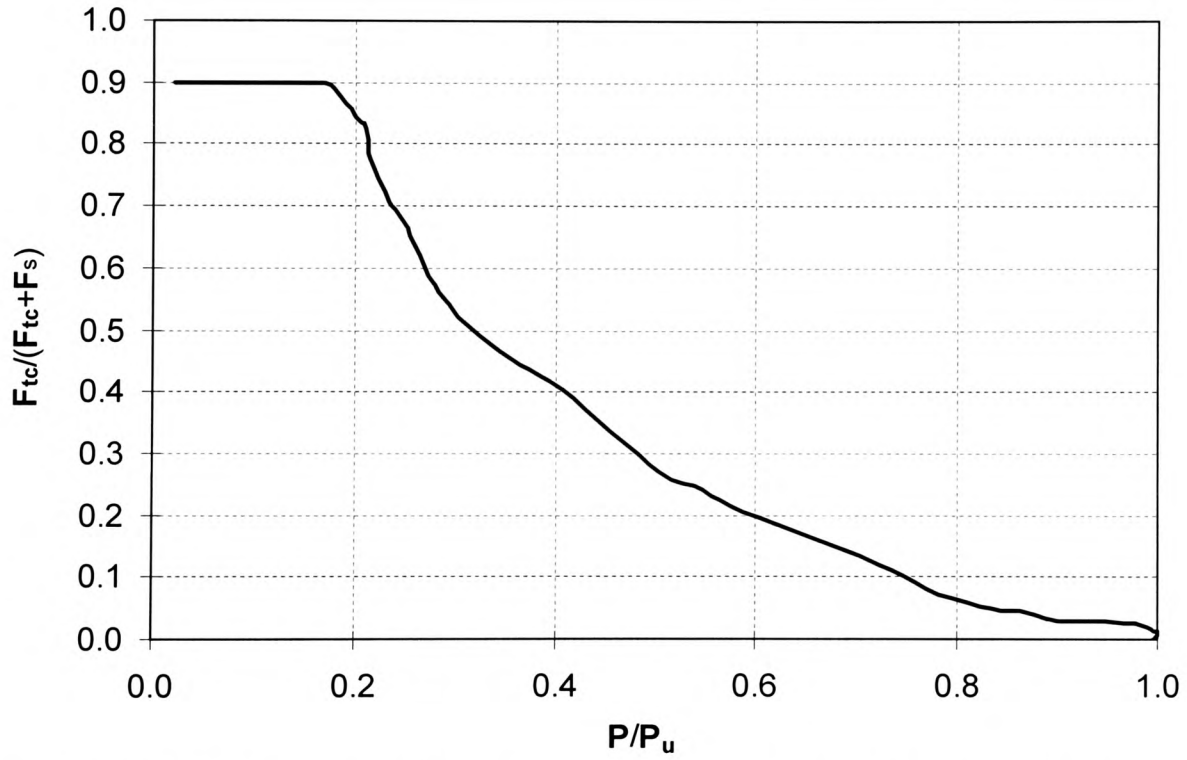

Figure 5.13 Normalised Concrete Tensile Contribution of the Control Beam

Once the steel reinforcement reaches its apparent yield stress, the P-x curve starts descending again. This forms the third distinctive stage of the curve. The trend continues until the reinforcement reaches its full ultimate tensile strength at a strain of 0.007000. At the last part of the P-x curve, the tensile force in the steel reinforcement remains constant, and the applied load increases slightly until after the concrete compression reaches its peak value at a strain around 0.002200. The applied load then

decrease slightly until it reaches the ultimate failure at a concrete compressive strain of 0.003500. The neutral axis depth at the last loading stage also decreases as the concrete compressive strain approaches its ultimate value.

5.5.2 FRP Strengthened Beams

For the FRP strengthened beams, two models were used to predict the neutral axis depth, namely the "Precracked Model" and the "Tension Stiffening" (Non-Precracked) Model. For the precracked model, the residual tensile strength of the cracked concrete beam was completely ignored for the entire loading sequence, whilst in the non-precracked models account is taken of the concrete tensile strength before cracking as well as the post cracking stiffening effects of concrete between the cracks.

Figure 5.14 shows the P-x curves for the two models for an over-strengthened RC beam using CFRP plate, together with a regression line of the P-x relationship that was derived from the experimental data. It can be seen clearly that the concrete tensile strength has a significant influence on the neutral axis depth at the early loading stage, up to a load of 25 kN, which is approximately 23% of the beam ultimate load. The neutral axis depth in the non-precracked model decreases rapidly after the first crack, until the total concrete tensile contribution reaches the peak. This behaviour, although not to the same extent, follows a similar trend to the influence of concrete tensile strength of the unplated concrete control beam.

For the cracked model, the neutral axis depth gradually increases, from 54 mm to 64.5 mm, until a loading of 78 kN is reached. This is the load level at which the steel reinforcement reaches its ultimate tensile strength of 560 N/mm^2, while the stress in the CFRP plate is about 600 N/mm^2. The levelling-up of x depth continues until the concrete at the extreme fibre reaches its compressive strength at the peak strain of 2200 microstrain. The position of the neutral axis now has to descend again until the ultimate failure, at which x is recorded to be 70 mm, compared to 70.4 mm for the non-precracked model and 32.6 mm of the control beam.

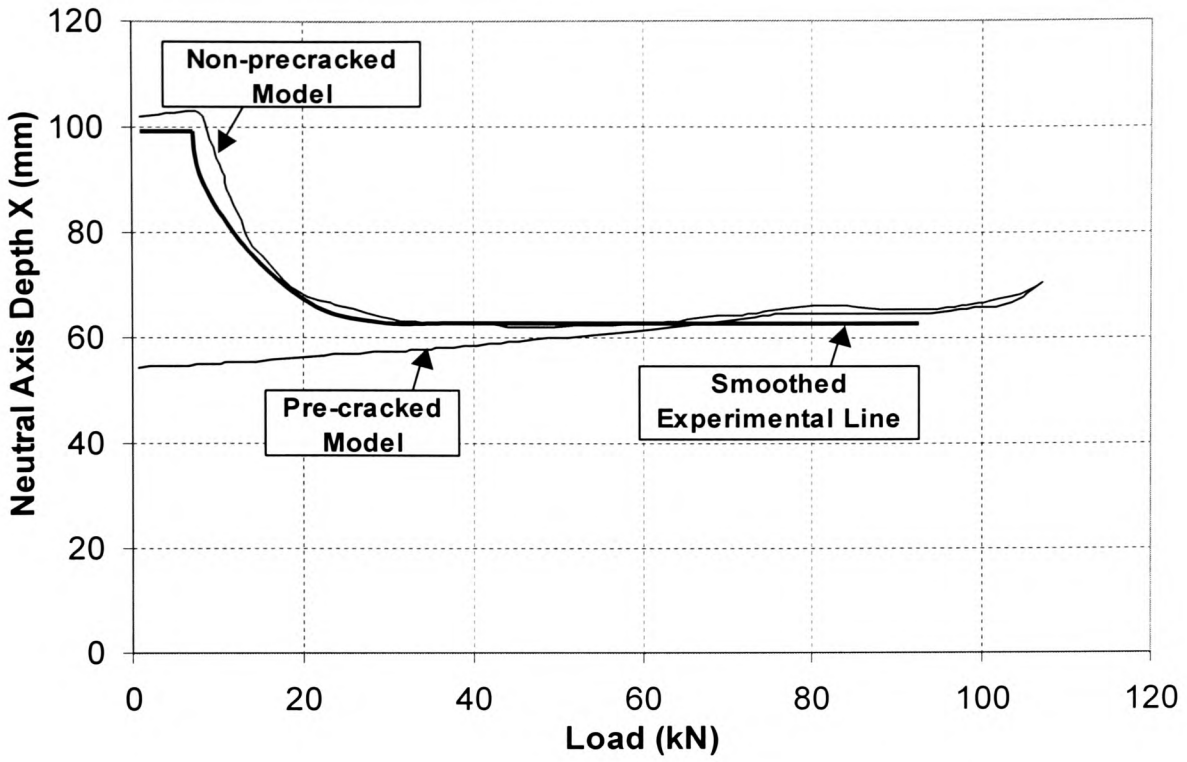

Figure 5.14 Load vs. Neutral Axis Depth for Over-Strengthened Sections

5.6 MOMENT CURVATURE RELATIONSHIPS

The moment curvature (M-κ) relationships of the two models are plotted in Figure 5.15. Unlike the M-κ relationship for the control beam, these curves do not show the apparent plateau after the steel reinforcement reaches the ultimate tensile strength. This is because the CFRP plate remains elastic at the ultimate failure of the beam, with a relatively low stress of 827 N/mm^2 as discussed previously. As a result, changes in steel characteristics have a combined influence with the elastic behaviour of the FRP plate, and therefore appear to be indistinct. At the early loading stage, the influence of the concrete tensile strength and the tension stiffening action is clearly demonstrated by the apparent differences in the slope of the M-κ curves as shown in Figure 5.16. The cracked model exhibits an almost perfect linear variation of the moment curvature, even though the cracked concrete should behave non-linearly. This phenomenon can be referred to as the "**pseudo-linear**" behaviour of the degraded RC elements strengthened by FRP composites.

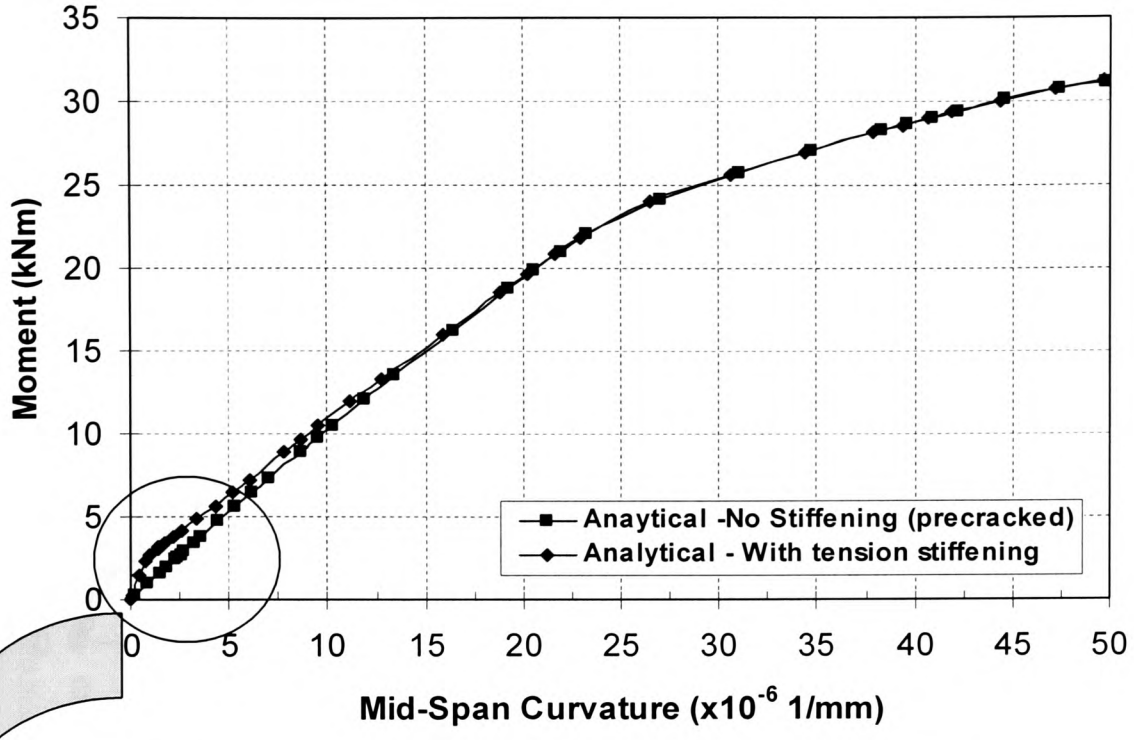

Figure 5.15 Moment-Curvature Relationship for Over-strengthened Section

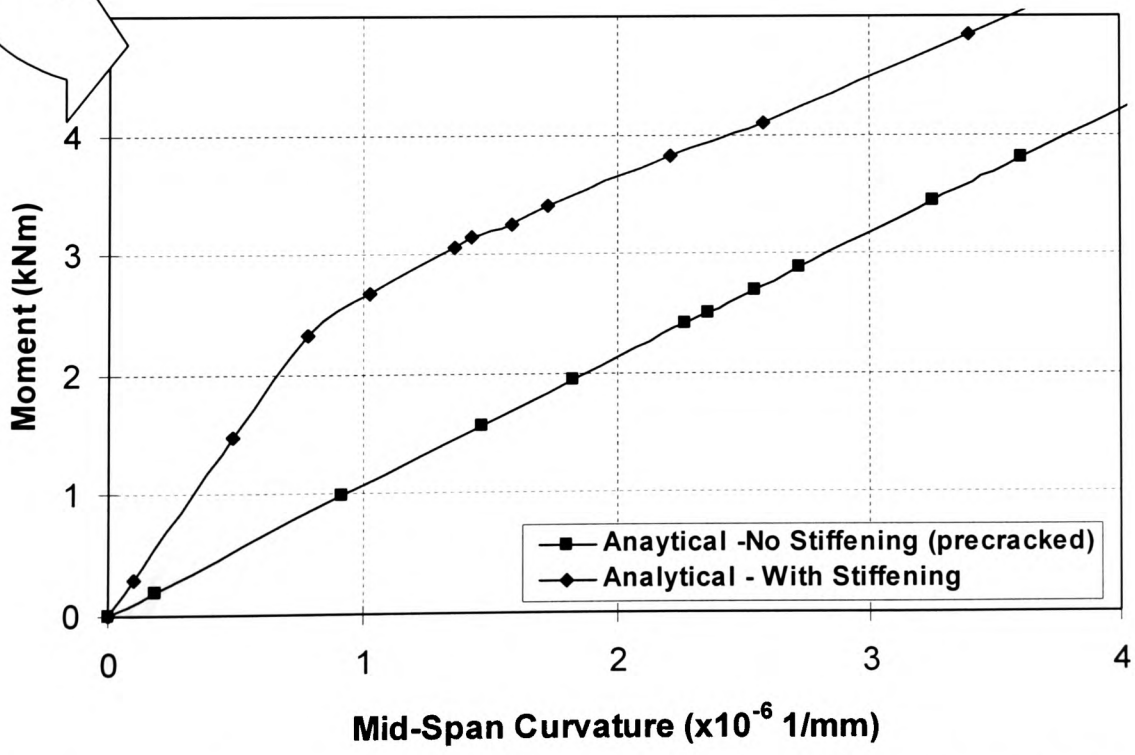

Figure 5.16 Comparison of Moment-Curvature Relationship at Early Loading Stage

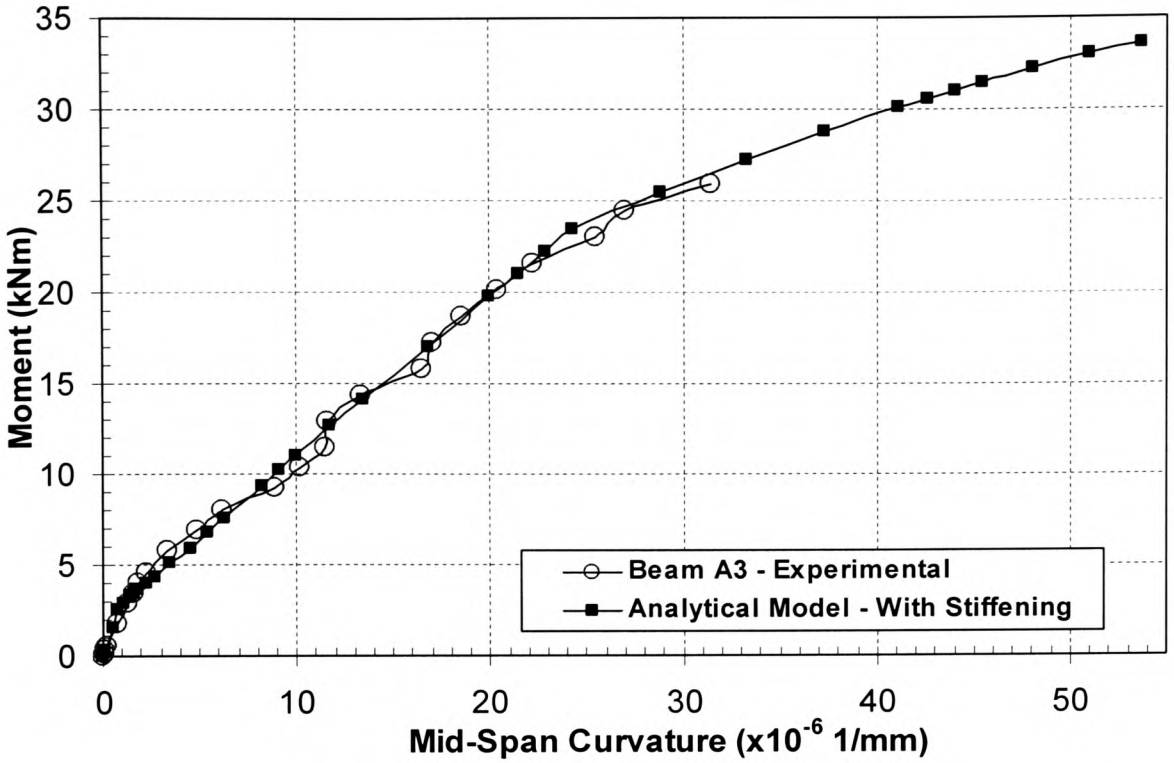

Figure 5.17 Comparison of Theoretical and Experimental Moment-Curvature Relationships (Beam A3)

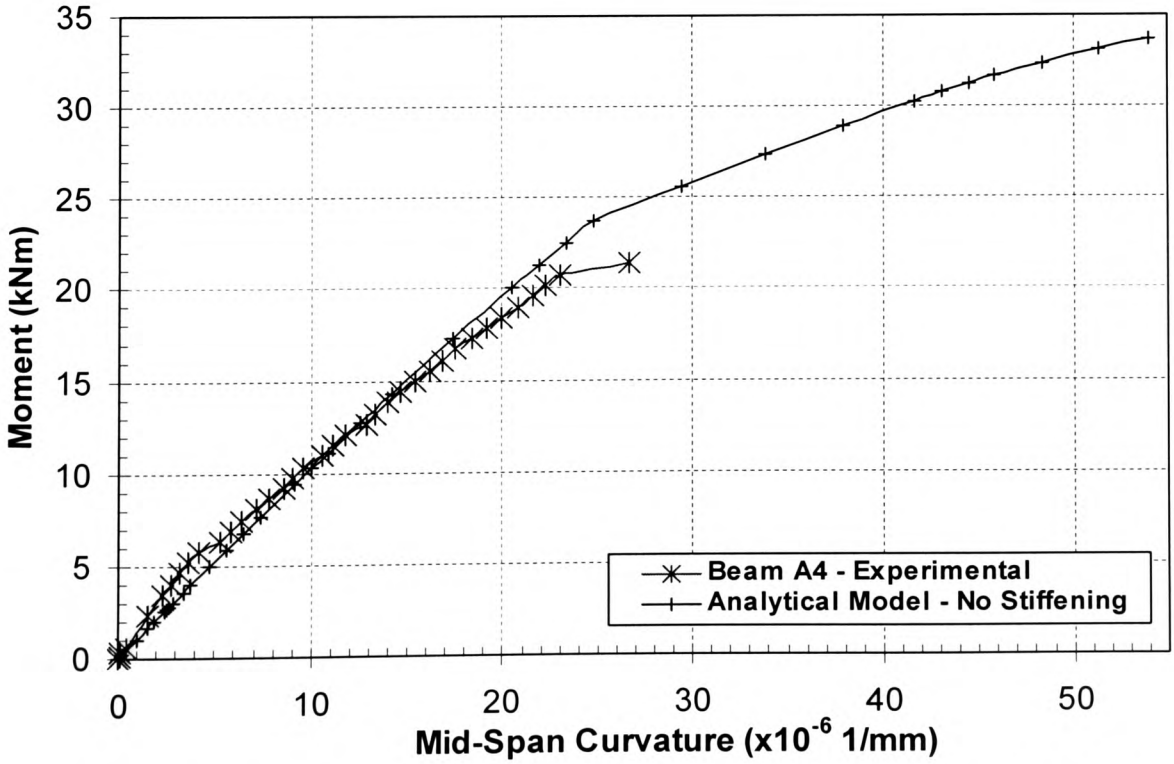

Figure 5.18 Comparison of Theoretical and Experimental Moment-Curvature Relationships (Beam A4)

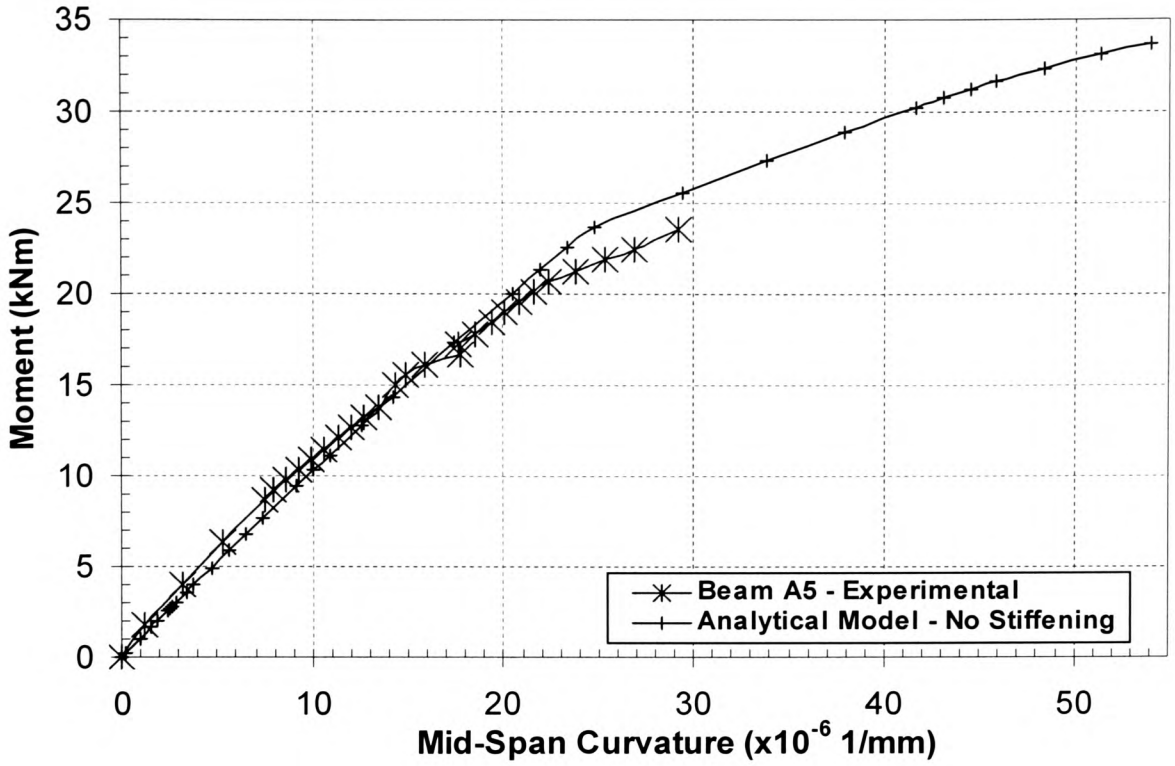

Figure 5.19 Comparison of Theoretical and Experimental Moment-Curvature Relationships (Beam A5)

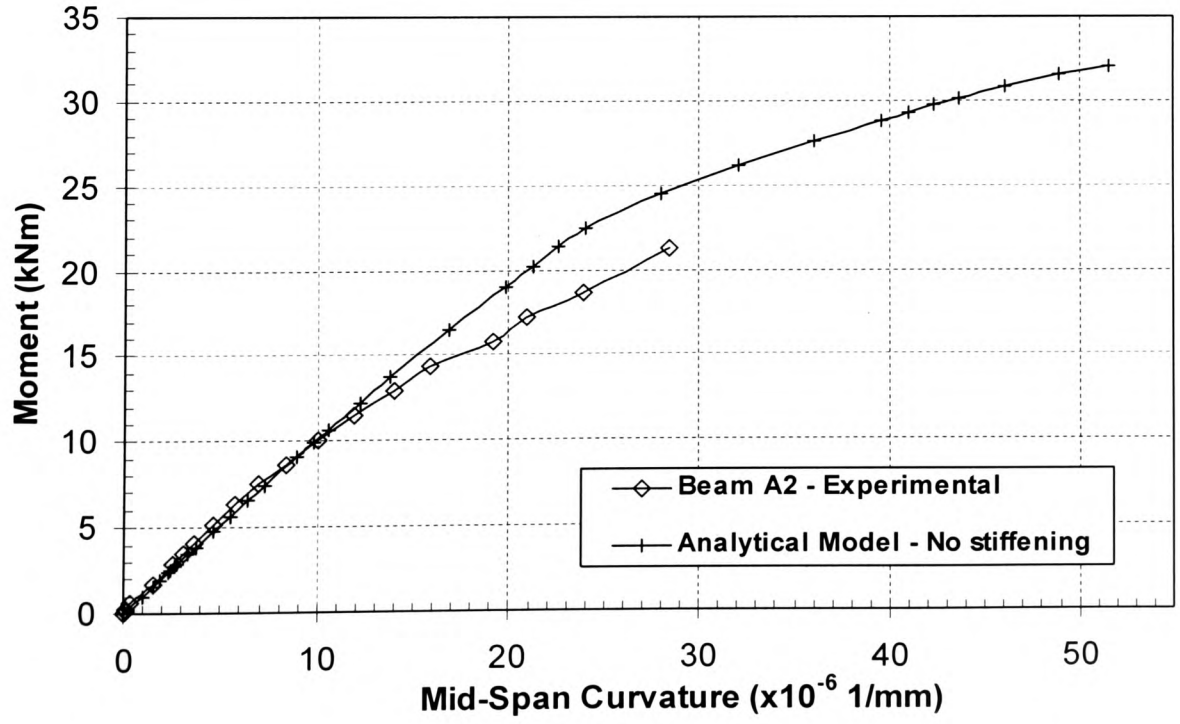

Figure 5.20 Comparison of Theoretical and Experimental Moment-Curvature Relationships (Beam A2)

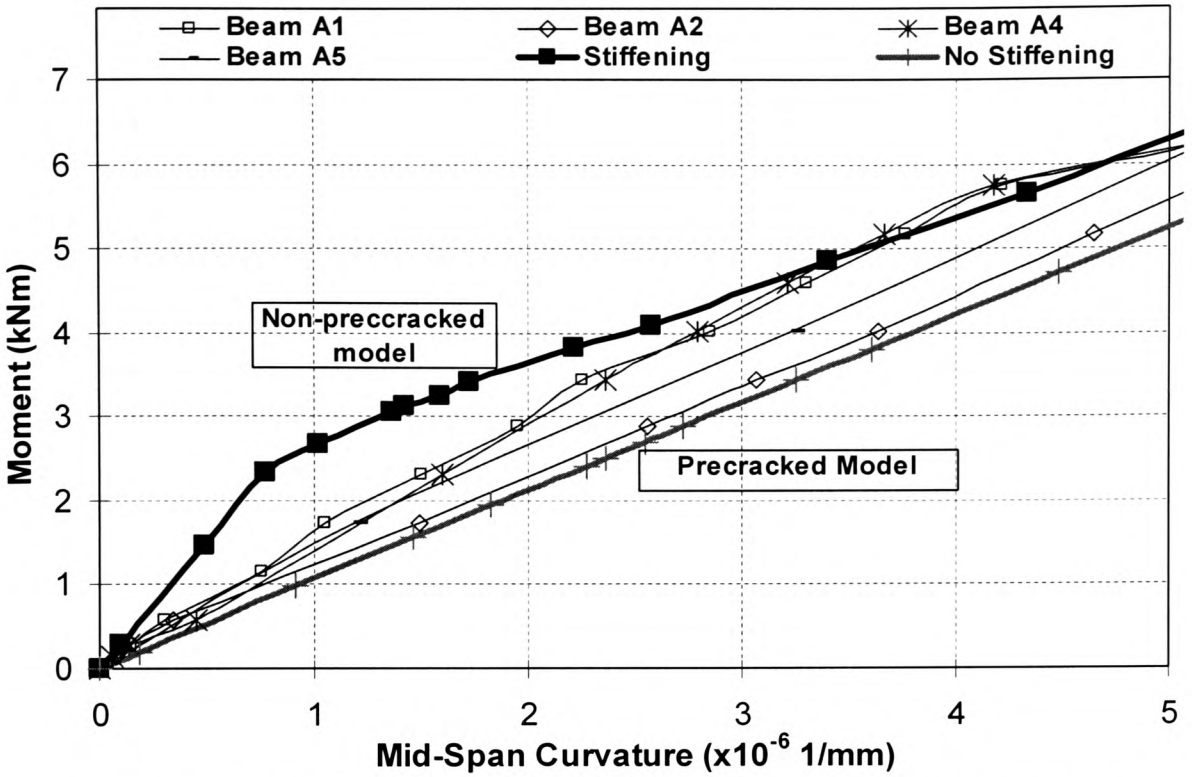

Figure 5.21 Comparison of Moment Curvature of Beams A1-A5 with Analytical Model at Early Loading Stages

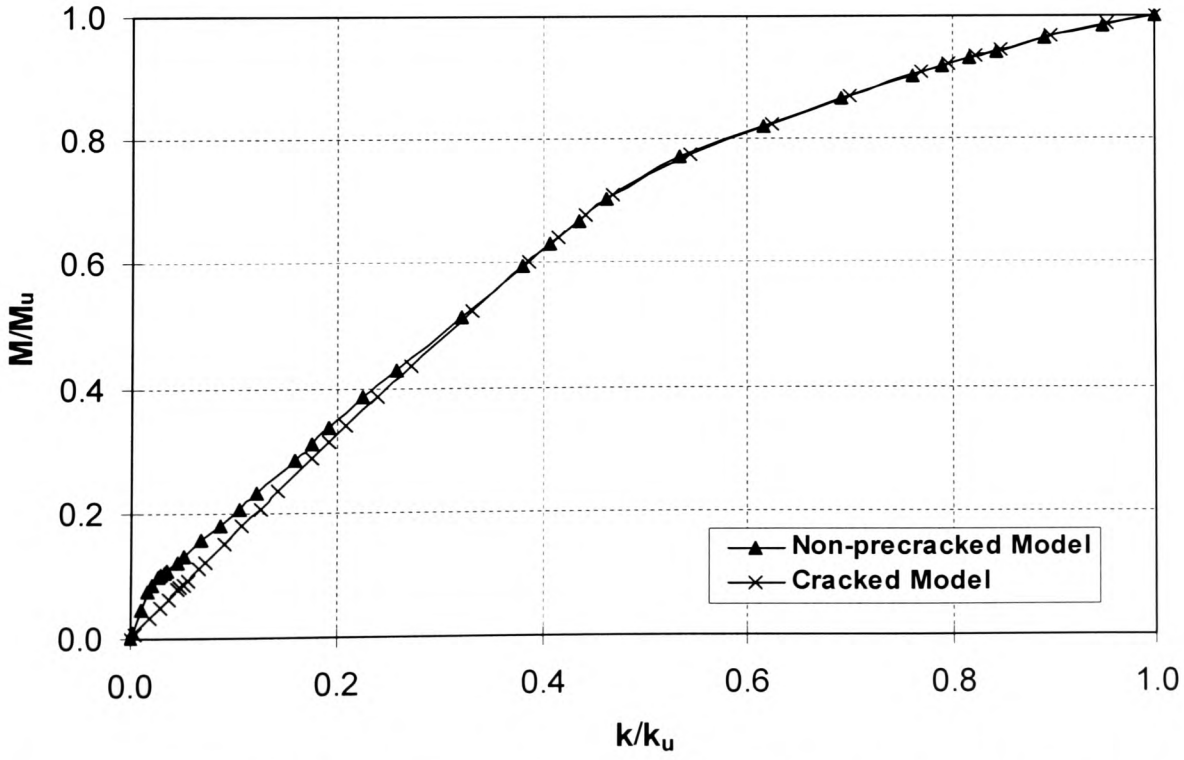

Figure 5.22 Normalised Moment-Curvature Relationships of the Analytical Models

5.7 COMPARISON OF ANALYTICAL EXPERIMENTAL RESULTS

5.7.1 Moment Curvature

Figure 5.17 shows the comparison of the moment curvature relationship derived from the non-precracked model against that of the experimental results of beam A3. The experimental M-k curve was deflection based, and generally matches the model well up to the actual ultimate failure, although the experimental failure load is seen to be only 83% of the predicted value. This difference is attributed to the premature failure of debonding or tearing-off of concrete cover, which is discussed in Chapter 6.

Shown in Figures 5.18 – 5.20 are the comparisons of moment curvature relationship for the precracked model against three sets of experimental data from beams A4, A2, and A5. Again it can be seen that the model generally matches the experimental results well up to the actual failure, indicating the reliability of the model and the premature nature of the failure modes. It is interesting to observe that all beams seem to fail at the same curvature of around $30x10^{-6}$ 1/mm. This suggests that there exists a constant strain level at which premature failure will occur. (Please refer to Chapter 6 for further discussions).

Figure 5.21 is the comparison of M-k curves from the four precracked beams in experimental series A with those of the two analytical models at early loading stages. The precracked and the non-precracked models form the lower and upper boundaries respectively. It can be seen that all the experimental data from the precracked beams fall between the two boundaries. This again confirms the reliability of the two models, and indicates that some of the precracked beams were left with higher residual concrete tensile strength than others.

5.7.2 Section Stiffness

The pseudo-linear behaviour of the precracked and CFRP strengthened sections confirms the fact that concrete tensile strength and its post-cracking tension stiffening influence the flexural rigidity, **EI**. The value of EI is readily obtainable from the moment curvature relationship, based on the classic theory of bending as follows:

$\kappa = \frac{1}{R} = \frac{M}{EI}$, and EI may therefore be obtained as:

$$EI = \frac{M}{\kappa} \tag{5.25}$$

For the precracked and CFRP strengthened section, EI suffers a considerable reduction from the non-precracked level up to 30% of the ultimate load. The normalised non-dimensional stiffness value in this table is defined as EI_{norm}, and may be determined by the following equation.

$$EI_{norm} = \frac{M / M_u}{\kappa / \kappa_u} \tag{5.26}$$

The results are given in Table 5.3. It can be seen that initially the stiffness of the precracked section is only 52% of that of the non-precracked section, whilst at about 70% of the ultimate load, the difference between the precracked and non-precracked models has little influence on the section stiffness values.

Table 5.3 Stiffness Reduction of Precracked Model*

M/M_u	Non-Precracked Model		Precracked Model		% Reduction of EI
	k/k_u	EI_{norm}	k/k_u	EI_{norm}	
0.01	0.002	5.04	0.004	2.62	48.1
0.05	0.009	5.04	0.018	2.63	47.8
0.08	0.015	4.98	0.029	2.60	47.9
0.12	0.044	2.79	0.065	1.88	32.5
0.15	0.067	2.28	0.089	1.72	24.5
0.18	0.086	2.08	0.106	1.68	18.9
0.20	0.103	1.98	0.123	1.65	16.3
0.28	0.156	1.81	0.173	1.63	9.8
0.31	0.173	1.77	0.189	1.62	8.6
0.38	0.222	1.71	0.237	1.60	6.2
0.42	0.255	1.66	0.268	1.59	4.7
0.51	0.318	1.60	0.327	1.56	2.8
0.59	0.377	1.56	0.384	1.54	1.9
0.63	0.406	1.55	0.411	1.52	1.4
0.66	0.433	1.53	0.438	1.51	1.2
0.70	0.459	1.52	0.464	1.50	1.1
0.76	0.536	1.43	0.543	1.41	1.3
0.82	0.618	1.32	0.623	1.31	0.7
0.86	0.694	1.24	0.698	1.23	0.6
0.90	0.764	1.18	0.768	1.17	0.5

* Based on the same material properties as described in Table B-1 (Appendix B).

The graph in Figure 5.23 represents variation of normalised load against the percentage reduction in stiffness EI of the precracked section in comparison with the non-precracked model.

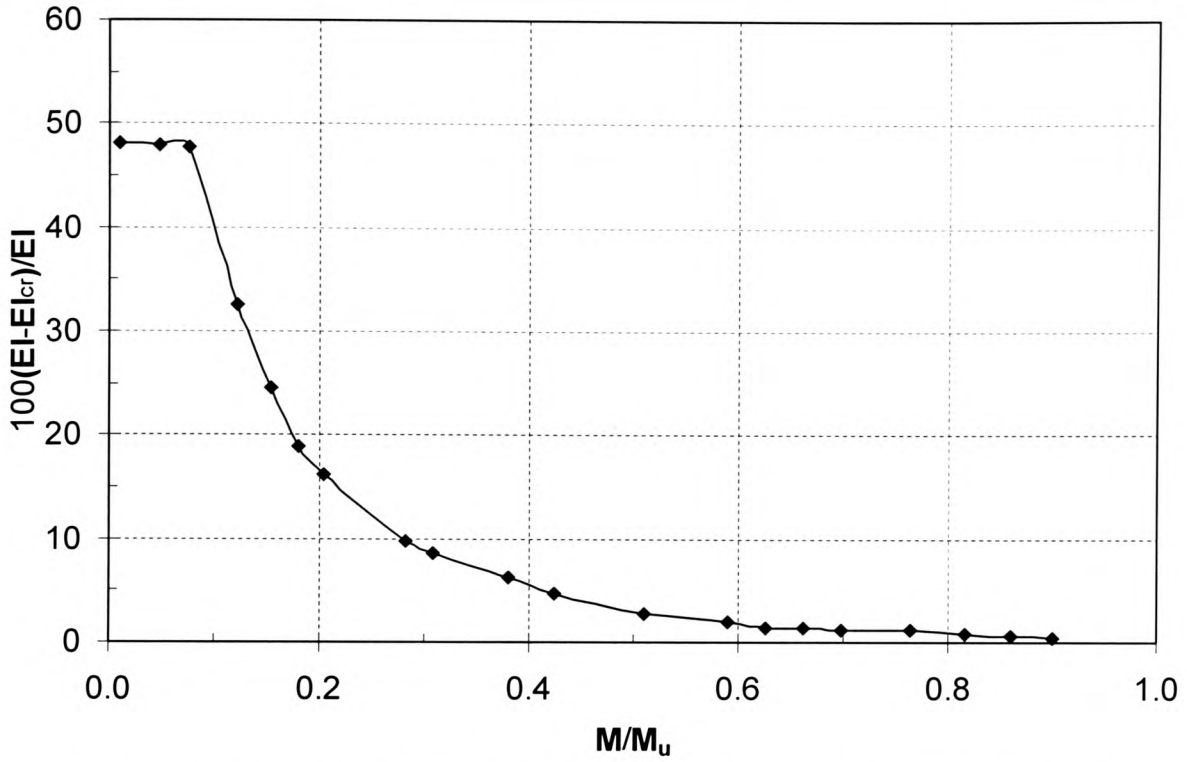

Figure 5.23 Variation of Load vs. Stiffness Reduction for the Precracked Model

This graph shows why in many national standards for the design of RC members at the ultimate limit state, the tension stiffening effect is ignored. It also demonstrates the fact that under "permanent" load, which is often deemed to be dead load plus 25% of the imposed load, the tension stiffening action affects the member stiffness considerably, and hence, it should be taken into account when estimating the deflections.

However, the tensile contribution of concrete towards the total section tensile resistance does not stop at 60% of the ultimate load. Figure 5.24 shows the variation of the ratio of the average concrete tensile force to the total section tensile resistance, with the load increase for both control and the CFRP strengthened beams. It shows that at 60% of the ultimate load, the concrete still shares 6% and 18% of the total tensile resistance for the CFRP strengthened and the control beams respectively.

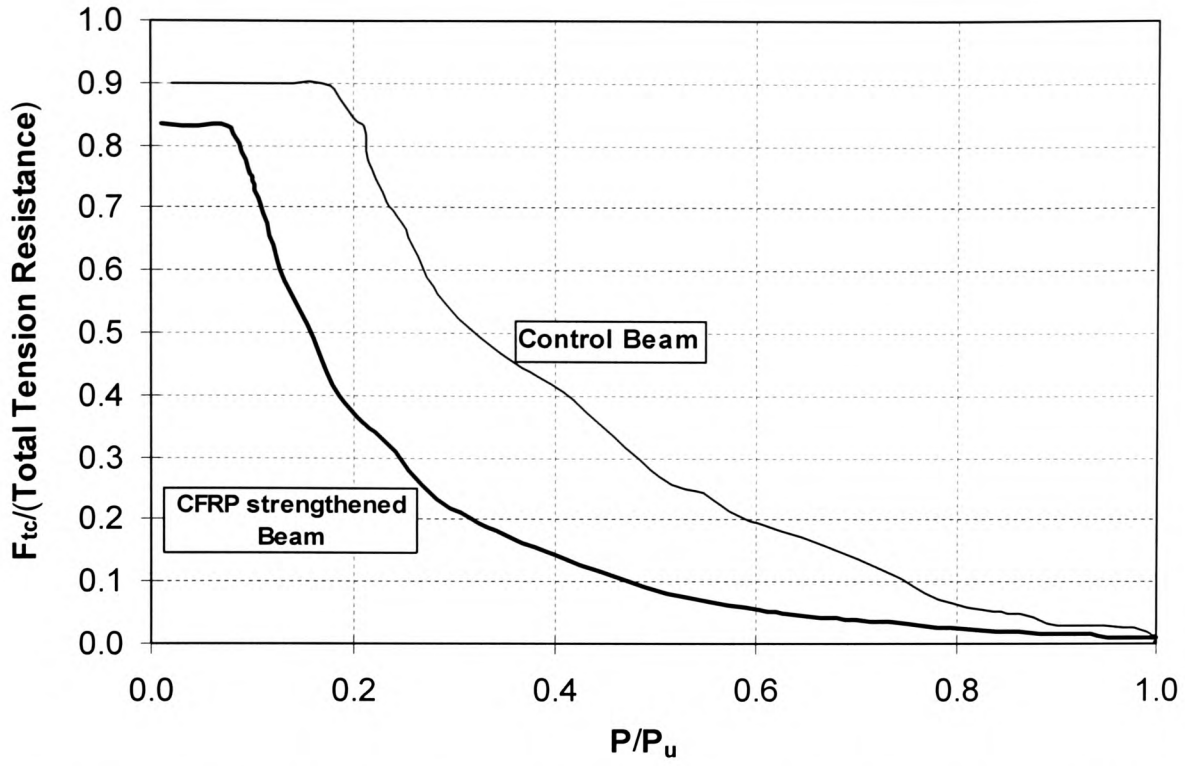

Figure 5.24 Comparison of Concrete Tensile Contribution vs. the Total Section Tensile Resistance for the Control and CFRP Plated Beams

5.7.3 Deflections and Strains

The deflection of the CFRP strengthened beams is determined from the curvature value for a given load. Having already achieved close agreement of the moment curvature relationships, the experimentally recorded deflections are expected to match the predicted values well. Figure 5.25 shows a typical load deflection curve for beam A5. Although the predicted deflection value at ultimate failure load is 75% higher than the experimental failure deflection, the two lines match well before the observed beam collapse, which again suggests that a premature failure has occurred.

The load - strain relationships follow the same trend as those of moment-curvature and load-deflection. Figure 5.26 shows the load versus strain curves for beam A5. It can be seen that the predicted and experimental strain values display good agreement before the beam failure.

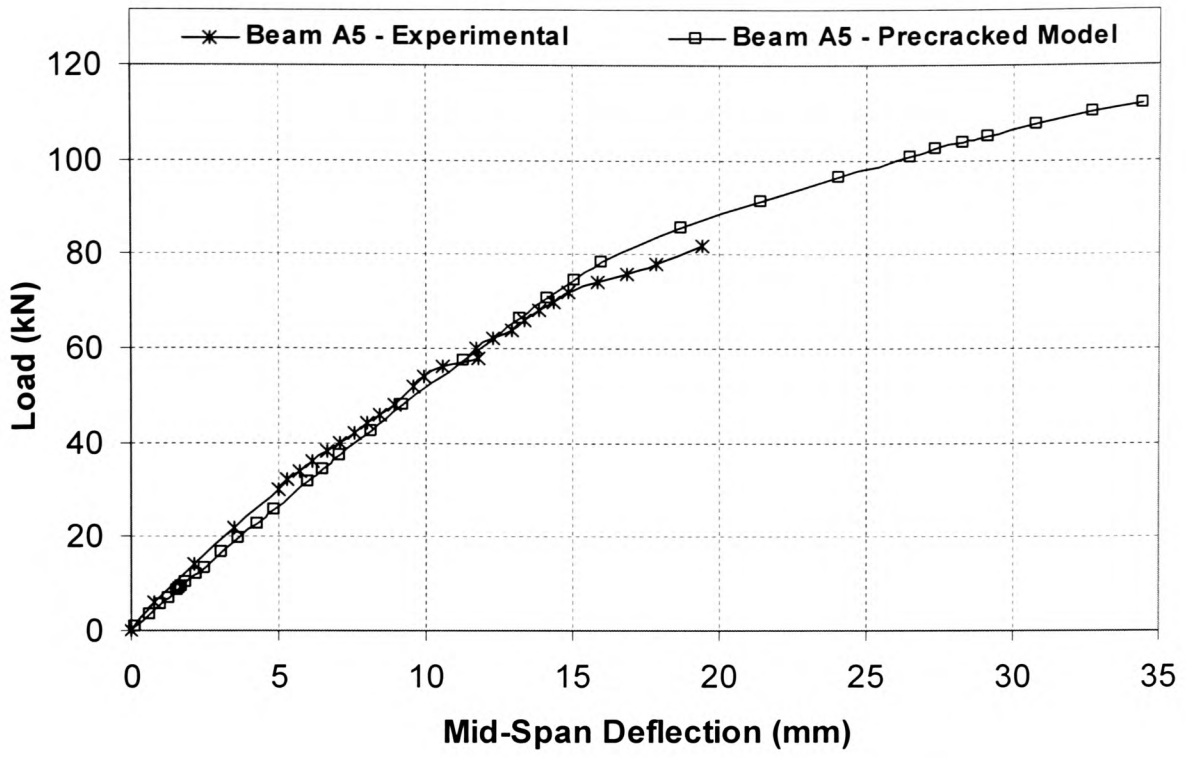

Figure 5.25 Comparison of Experimental Deflection with Predicted Values of Beam A5

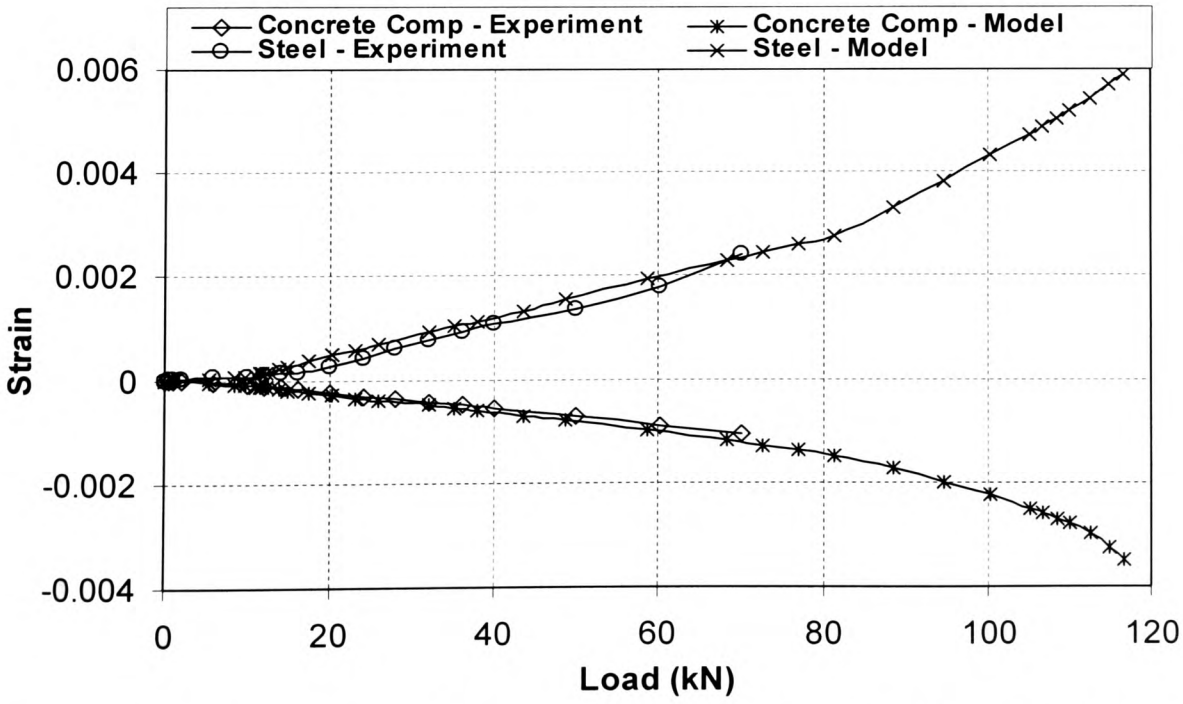

Figure 5.26 Comparison of Concrete Compressive and Steel Reinforcement Strains

5.8 Factors Influencing Flexural Behaviour

The analytical models have been shown to give a satisfactory representation of the actual behaviour as observed in the experiments. A parametric study is now desirable to determine the influences of various factors that affect the flexural behaviour of CFRP strengthened beams. The factors will be discussed in the following sections and include:

- Area of CFRP composites provided.
- Percentage of internal steel reinforcement.
- Young's modulus of concrete.
- Concrete compressive and tensile strength.
- Tensile strength of steel reinforcement and CFRP.

5.8.1 Area of FRP Composites

The area of composites plays a significant role in the behaviour of FRP strengthened RC beams. It governs the failure mode of the strengthened beam. Over strengthened sections will fail in a brittle manner, and it is advisable that all flexural strengthening work should be carried out such that the members are under strengthened if possible. The neutral axis depth x is one of the most important parameters that directly influence the element flexural behaviour, and is chosen here to demonstrate the effects of the amount of FRP provided.

Figure 5.27 shows the load versus the neutral axis depth of a standard test specimen under various percentage areas of CFRP composites. The x values at the final loading stage are of particular interest to designers. For the under-reinforced and unstrengthened control beam, x decreases just before ultimate failure, indicating that no more tensile contribution is available. At the same time, concrete compression is still increasing thus the neutral axis moves upwards. For the balanced section, the P-x curve remains flat just before failure, indicating that the concrete compression force and the total tensile resistance of the section are truly in equilibrium, and the neutral axis position remains unchanged during this stage.

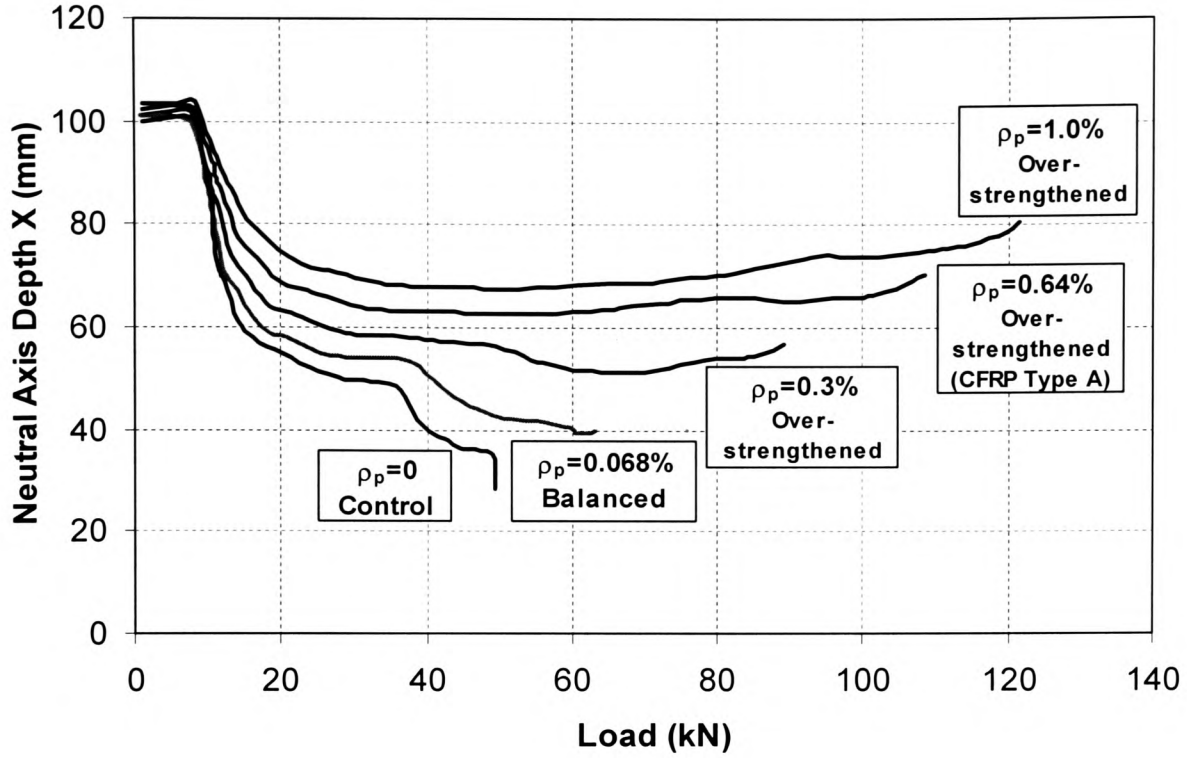

Figure 5.27 Load vs. Neutral Axis Depth for Various CFRP Area Percentages

(f_{yu} = 560 N/mm^2, f_{cu} = 45 N/mm^2, f_{pu} = 1750 N/mm^2, b=100 mm, h = 200 mm
E_s = 200 kN/mm^2, E_c = 36.8 kN/mm^2, E_s = 200 kN/mm^2, ρ_p=A_p/bh)

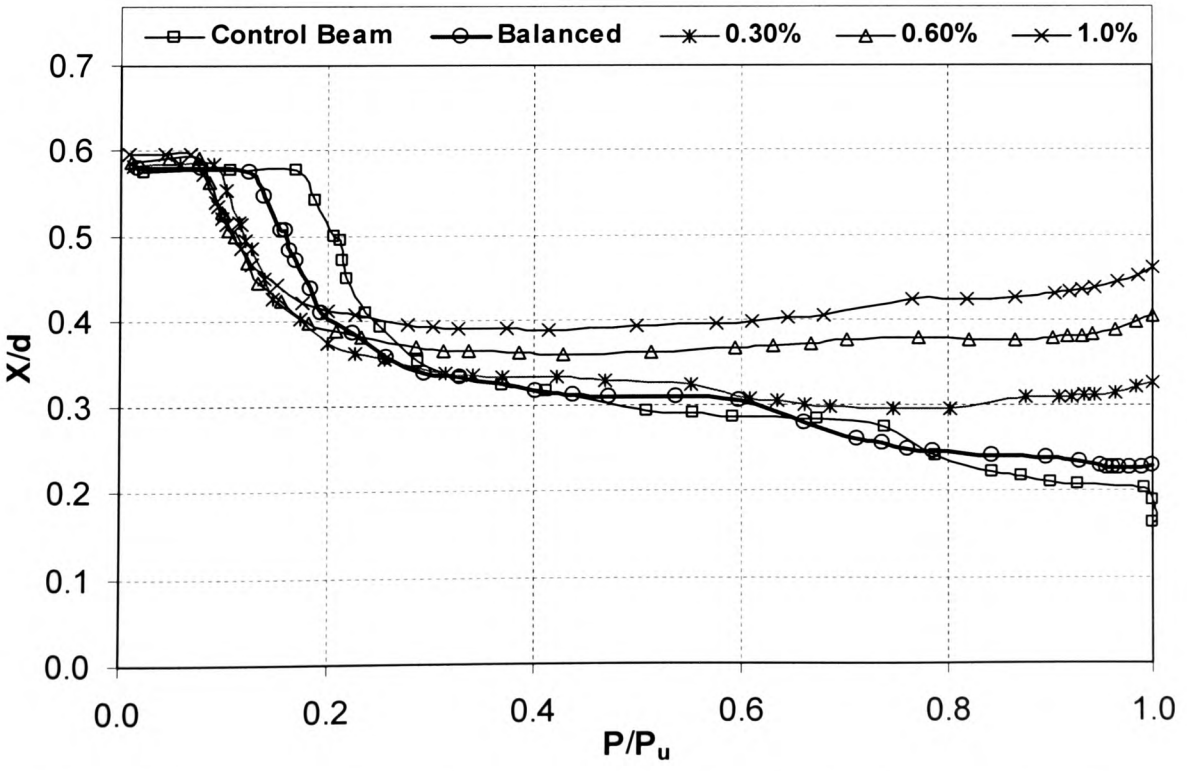

Figure 5.28 Normalised Load-Neutral Axis Relationship for Various Percentage ρ_p

For the three over-strengthened sections shown, the corresponding x values increase at the final loading stage, suggesting that neutral axis position moves downwards. This is because the tension resistance in the CFRP composite still increases with the increase of strain, as it has not yet reached its ultimate tensile strength. As a result, the concrete will fail first by brittle crushing.

A normalised P-x graph is shown in Figure 5.28. All sections have the same effective depth of **d**. The ultimate failure load P_u used was for each individual case, and hence a generic trend comparison is achieved. The balanced section has a neutral axis depth of around 0.23d at ultimate failure, this is the same as the value determined by using Equation (5.17). It is interesting to observe that the concrete cracking load appears to be within a well defined range, and does not vary significantly with the amount of externally bonded CFRP composites. Table 5.4 shows the comparison of the cracking load and moment for various CFRP ratios. It can be seen that actual crack load only increases slightly with the large increase of CFRP area. However, the crack load as a percentage of the ultimate value decreases from 16% of the control beam to 7.3% for an over-strengthened section with ρ_p of 1 percent. (Defined as A_p/bh).

Table 5.4 First Crack Load for Various Percentages of CFRP Area

	Load at first Crack (kN)	**Cracking Moment** (kNm)	**$100(P_{cr}/P_u)$**
Control Beam (ρ_p=0%)	7.83	2.25	16.0
Balanced (ρ_p=0%)	8.03	2.31	12.4
Over-strengthened ((ρ_p=0.3%)	8.21	2.36	9.2
Over-strengthened ((ρ_p=0.64%)	8.49	2.44	7.8
Over-strengthened (ρ_p=1.0%)	8.90	2.56	7.3

The maximum span deflection under load is another important indicator of flexural behaviour for the CFRP strengthened beams. In general, it is found that the span deflection decreases with the increase in area of externally bonded CFRP composites. Figure 5.29 shows the influence of CFRP area provided on the maximum span deflection at both ultimate failure and at the service load level.

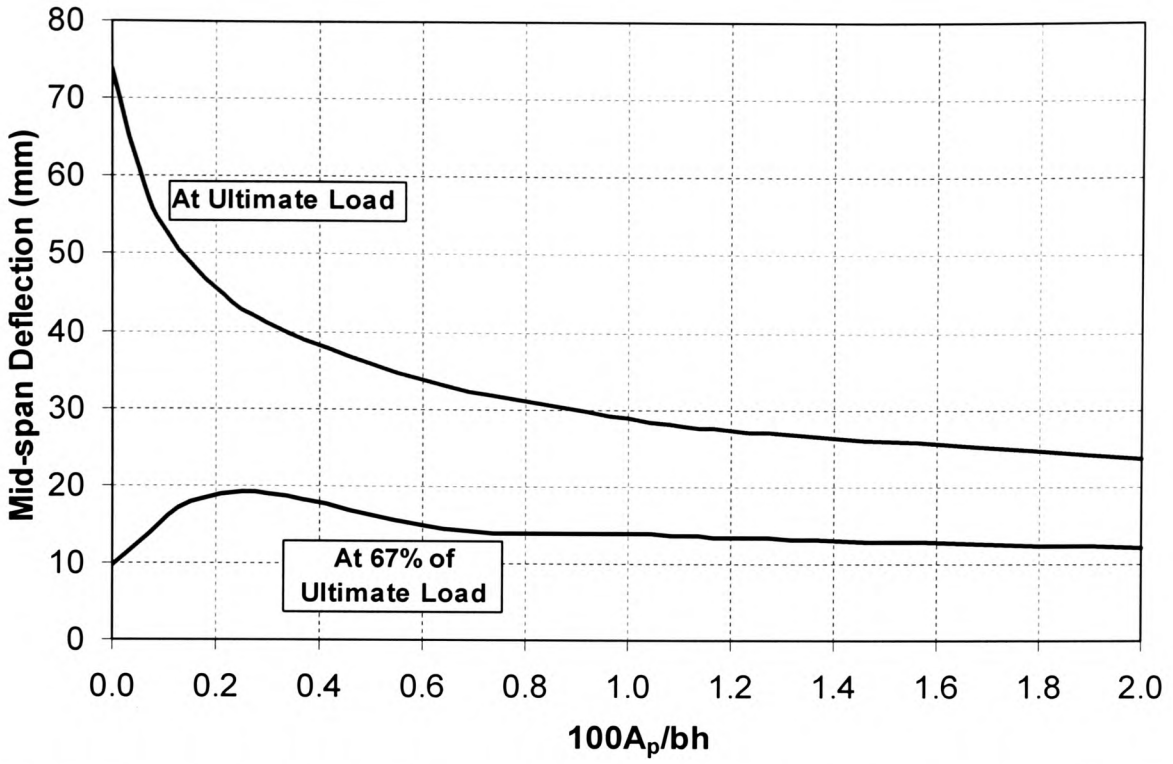

Figure 5.29 Effects of Cross Section Area of CFRP on the Maximum Span Deflection

It is interesting to note that for lower CFRP ratios, the deflection at ultimate failure decreases rapidly with the increase of ρ_p. At the service load level - defined to be approximately 67% of the ultimate load, (assuming equal proportion of dead and imposed load) – the span deflections of CFRP strengthened beams increase with the ρ_p ratio of up to 0.3%. This is because the presence of CFRP composites greatly enhances the ultimate load carrying capacity over the unplated control beam, and the corresponding service loads are much greater than that of the control beam, with increased span deflection accordingly. After 0.3% of ρ_p, however, the rate of stiffness enhancement reduces, and the ratio of ultimate deflection to the deflection at service load, δ_u/δ_s, remains almost constant at a value of round 2 as shown in Figure 5.29.

Figure 5.30 shows the percentage reduction and increase of deflection over the control beam, at the ultimate limit state and the service load level respectively, with the increase of CFRP ratio. From a design view point, the closer these two curves in relation to each other, the more ductile the CFRP strengthen section will remain.

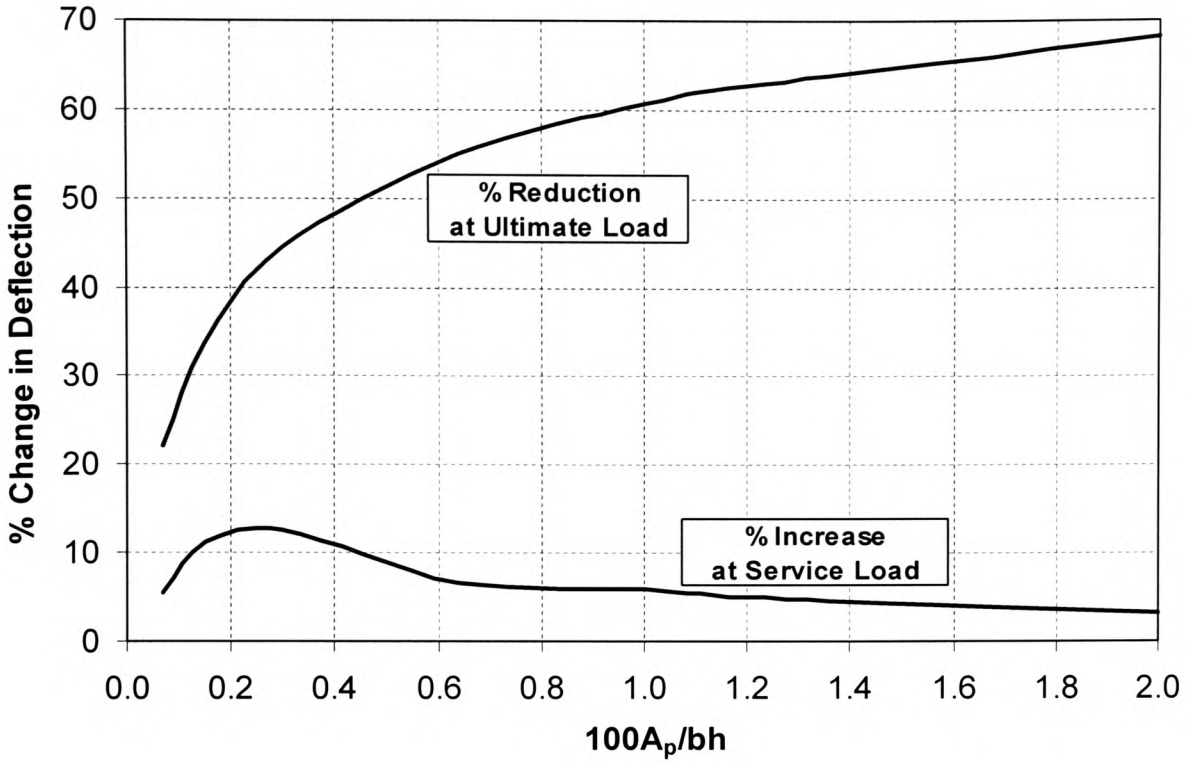

Figure 5.30 Effect of CFRP Area on Percentage Change of Deflection

It can be seen from Figure 5.30, that after ρ_p of 0.3%, the gap between the reduction of deflection at the ultimate limit state and the increase in deflection at service load widens. This characteristic is important and should be taken into consideration when deciding what degree of strength and stiffness enhancement is to be achieved in the design for strengthening works.

In Figure 5.31, the actual ultimate load is shown of a CFRP strengthened beam, modelled on beam A3, against the increase in CFRP cross sectional area. It can be seen that the load increases with the increase of CFRP area, but not linearly. The lower ratios of CFRP prove to be more effective, since the stresses in the fibres are closer to the CFRP strength than those sections where higher CFRP ratios are used. Figure 5.32 shows the percentage variation of ultimate load increase verses the CFRP ratio. For the tests in series A, a maximum increase of around 120% is shown to be achievable, provided that premature failure is avoided. For the lower CFRP ratio of 0.0725%, as used in series B tests, the load increase is only under 40%, but beams so strengthened appear to exhibit much better ductility characteristics.

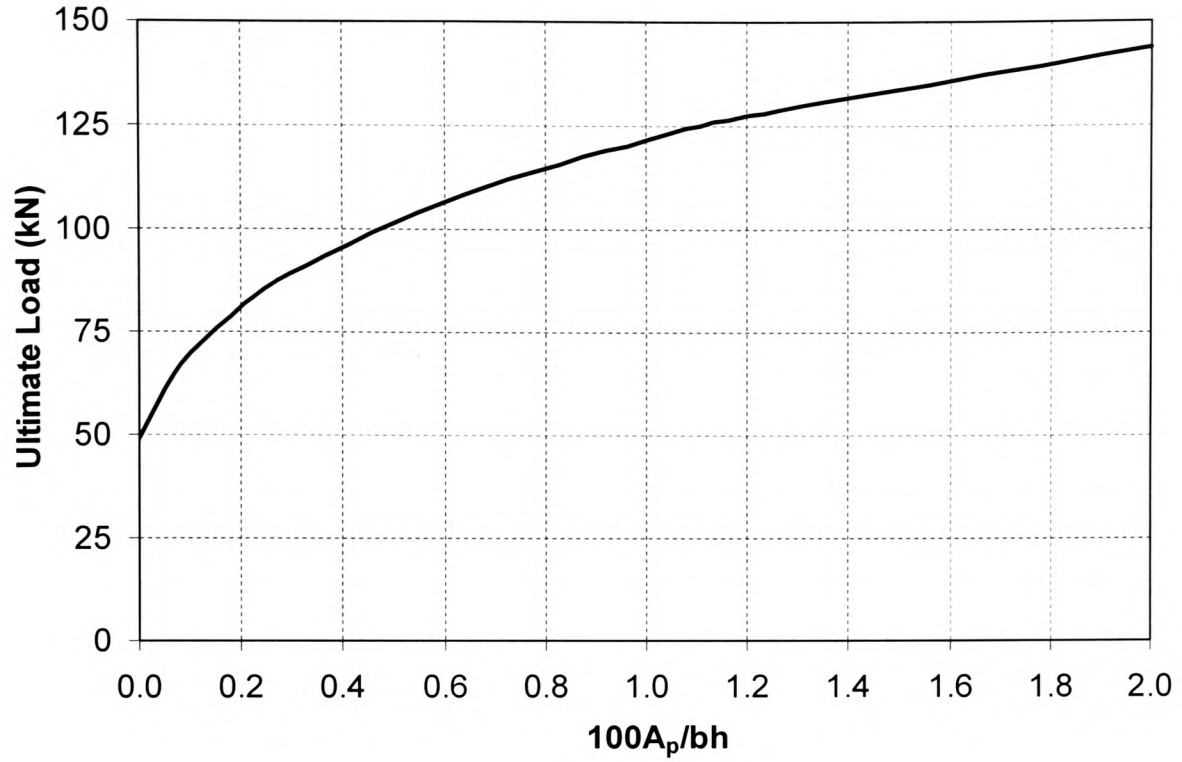

Figure 5.31 Ultimate Load Increase vs CFRP Area

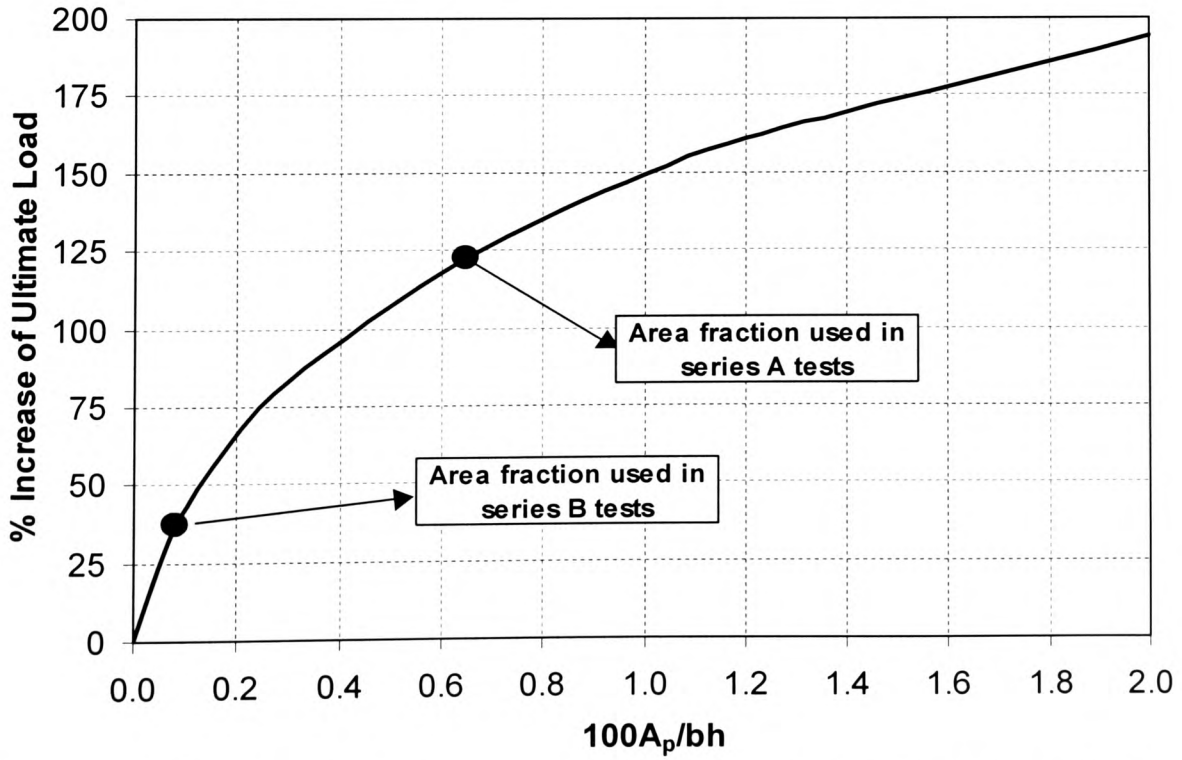

Figure 5.32 Effect of CFRP Area Ratio vs. Percentage Increase in Ultimate Load

5.8.2 Strength and stiffness of FRP composites

As discussed in Section 5.2.1.4, CFRP composites exhibit linear stress-strain behaviour. The two most important material parameters are therefore the tensile modulus and the ultimate strain. For all of the CFRP composites used in the present study, the material manufacturer has specified a maximum strain at failure of 1.4%. This is in line with most of the CFRP composites available in the construction market.

One of the greatest advantages of FRP composites is the high specific strength as discussed in previous chapters. For CFRP composites, the maximum tensile strength available could be as high as 5500 N/mm^2. There is, however, a misconception that the higher the strength of composite, the better suited it is for concrete strengthening works. It is thus important to quantify the influence of FRP strength, and identify if possible, the optimum strength range that is suited for RC strengthening. Based on the present experimental data and the analytical model, a parameter study was carried out to investigate the influence of the composite strength on the performance of strengthened beams. All material properties used are the same as discussed in preceding section, the only variation was the change of tensile modulus of CFRP composites.

Figure 5.33 shows the results of analytical modelling. It is important to note that these modelled beams were over strengthened, as in experimental series A tests, with the area fraction of CFRP being 0.64%. In Figure 5.33(a), the curves indicate that the plate stress at failure increases with the tensile modulus, and as a result, the ultimate load capacity of CFRP strengthened beam also increases with the increase of tensile modulus of the plate, as shown in (b). The reduction of deflection with the increase of modulus is clearly represented in (c), while the increase in flexural rigidity, EI -which can be evaluated by dividing the moment by the corresponding curvature value k –is shown in Figure 5.33(d).

From the outset, these graphs indeed confirm the conventional believe that higher CFRP modulus, and hence higher ultimate plate strength, generally results in better structural behaviour of the strengthened beams.

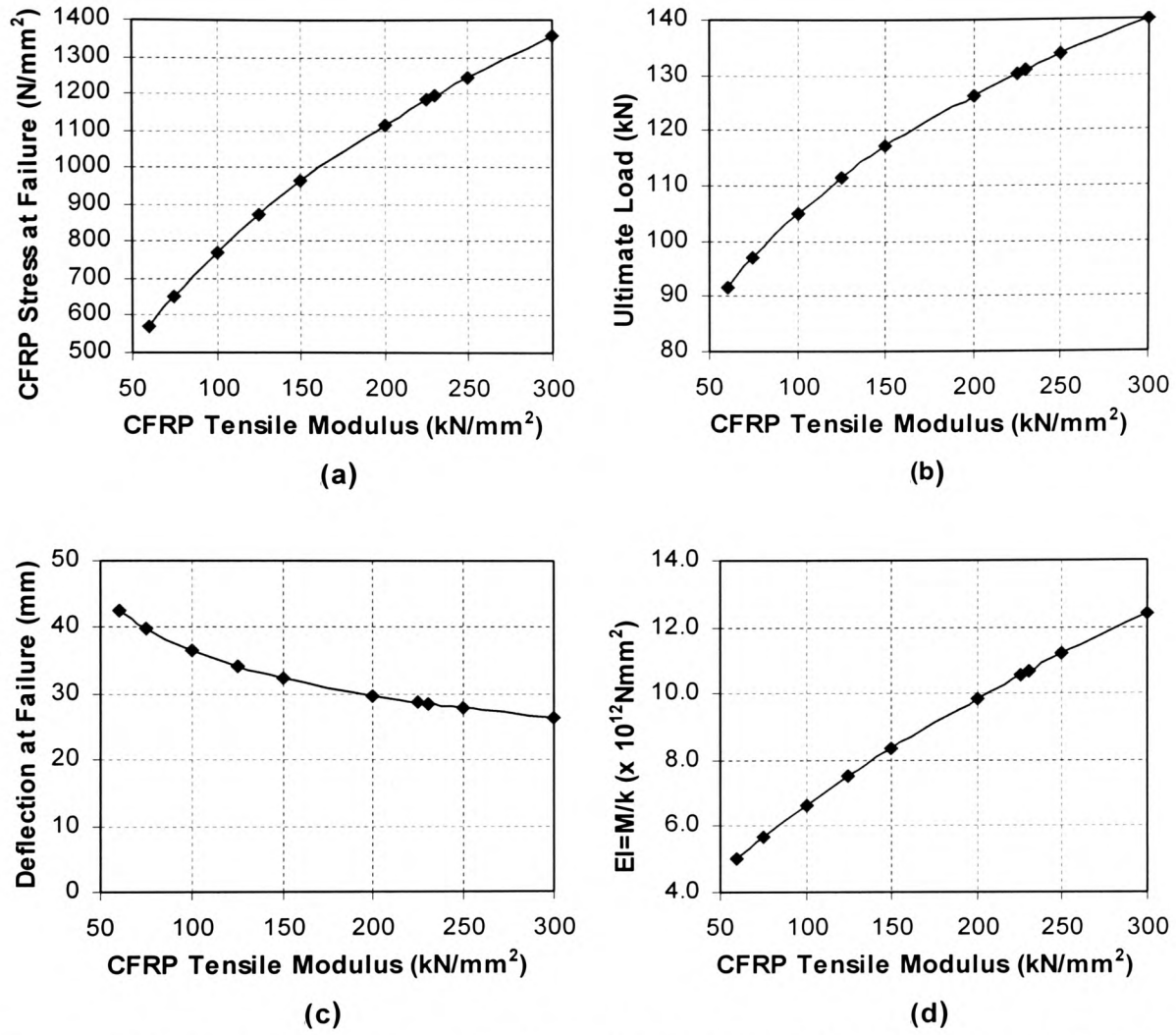

Figure 5.33 Variation of Beam Behaviour with CFRP Modulus for Over-strengthened Sections (with $\rho_p = 0.64\%$, $f_{cu} = 45$ N/mm^2)

However, the degree of performance enhancement will not increase proportionally with the increase in plate ultimate strength. Shown in Figure 5.34 is the CFRP plate strength against the actual plate failure stress for an over-strengthened RC beam (with ρ_p = 0.64%, f_{cu} = 45 N/mm^2). It is clearly shown that for a given area of CFRP provided, low CFRP ultimate strength can be more fully utilised, whilst the very high plate strength, although resulting in some load capacity increase as shown in Figure 5.33(b), contributes only a low percentage of its capacity. This phenomenon is mainly due to the plane section of the strengthened beam remaining plane during its loading process, when the strain distribution in the section follows a linear variation.

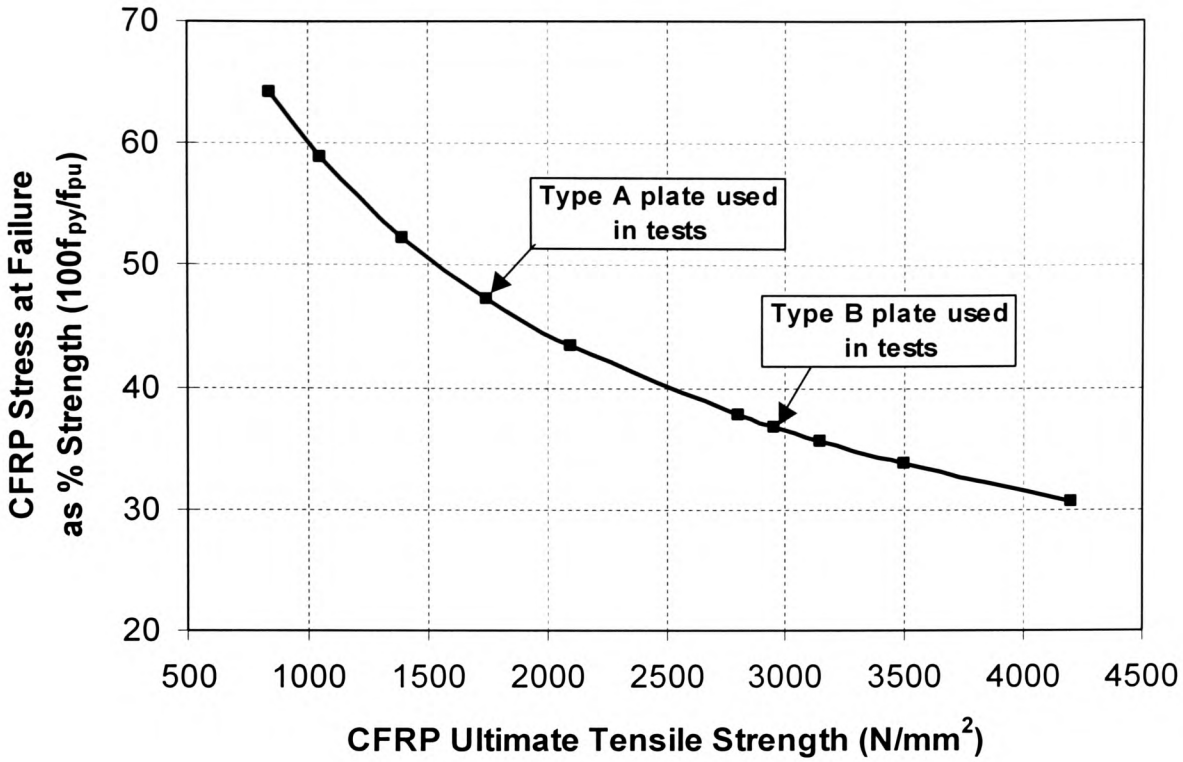

Figure 5.34 Plate Stress at Failure against Ultimate Tensile Strength

It is therefore reasonable to conclude that for an over strengthened section, there is no apparent advantage in using very high strength/high modulus FRP composites, since a material typical as above will never reach its tensile strength. The higher the CFRP plate ultimate tensile strength, the lower the percentage of strength utilisation rate at final failure. Experimental data in the present test series A confirm the above statement. In all tested beams, none of the CFRP plates had shown any signs of reaching or approaching its tensile strength at ultimate load.

5.8.3 Strength of Concrete in Compression

The concrete compressive strength appears to be influencing the behaviour of CFRP strengthened beams more significantly than the FRP tensile strength. Consider the over strengthened beams as discussed in previous sections, it was found that a 100% increase in concrete compressive strength from 15 to 30 N/mm^2 results in approximately 54% increase in ultimate load, with 42% in the corresponding deflection at failure, as shown in Figure 5.35.

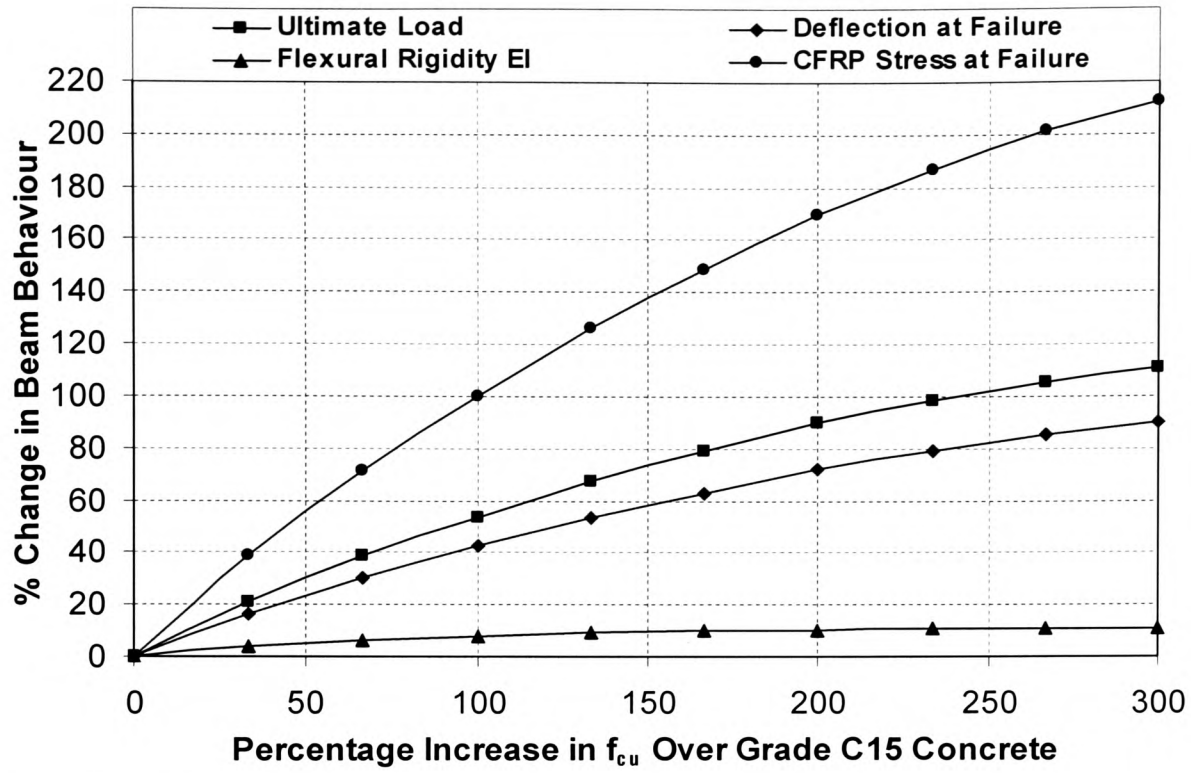

Figure 5.35 Effect of Concrete Compressive Strength on Beam Behaviour

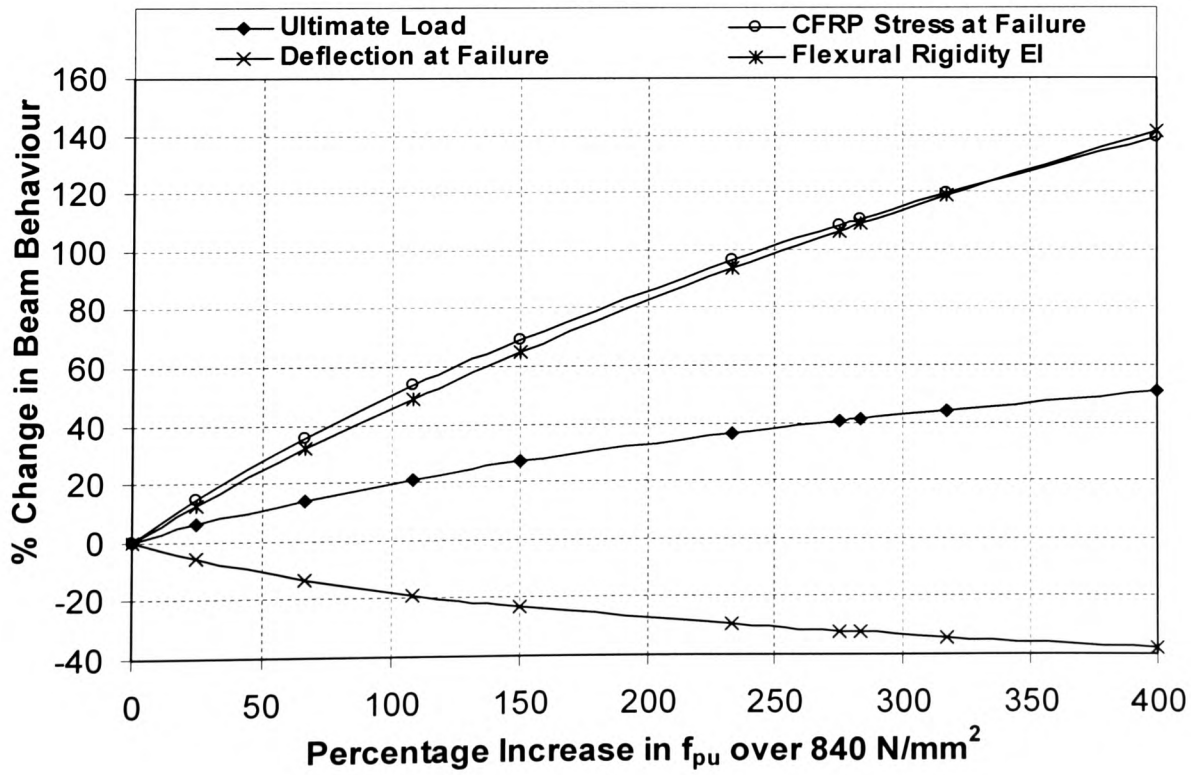

Figure 5.36 Effects of CFRP Strength on Beam Behaviour

A similar study was made to compare the influence of the increase in CFRP strength on the beam behaviour, the modelling results are shown in Figure 5.36. It is seen that a 150% increase of CFRP strength from 840 to 2100 N/mm^2, only results in 27% increase in ultimate load. The stiffness of the strengthened beam increases rapidly with CFRP strength, whilst the concrete compressive strength has relatively little influence on the flexural rigidity. Consequently, RC beams strengthened with higher strength CFRP plate exhibit lower failure deflection. At a CFRP strength of 4200 N/mm^2, the failure deflection is reduced by 38% from that of the same beam strengthened by a CFRP plate of 840 N/mm^2, as can be seen from Figure 5.36.

The greater increase in flexural rigidity EI, due to the higher strength of CFRP plate, can be explained in conjunction with the load-neutral axis depth (P-x) curve as discussed in preceding sections. Generally speaking, in an over-strengthened section, the higher the CFRP strength, the lower the neutral axis position will be in the beam. The part of second moment of area **I** for the cracked section, due to the concrete in compression only, can be determined as ($\mathbf{bx^3/3}$). As a result, the increase in **x** value leads to a much stiffer section with greater enhancement in flexural rigidity EI, followed by reduced span deflections.

The increase in concrete compressive strength, on the other hand, only influences the neutral axis position marginally. The EI values are only enhanced by up to 10% over a 300% increase in concrete strength from 15 to 60 N/mm^2, as shown in Figure 5.35.

The CFRR stress at beam failure, ultimate load, final deflection and the flexural rigidity variation of the plated beams, are plotted against the grades of concrete as shown in Figure 5.37 (a)-(d) respectively. It is interesting to compare these diagrams with those in Figure 5.33. Clearly, the beam overall behaviour is more sensitive to the increase in concrete grade than would be caused by the change of CFRP properties. It is therefore reasonable to conclude that:

FRP composites can strengthen all concrete beams with minimum residual strength and stiffness, but it is much more effective to strengthen a member with high grade of concrete.

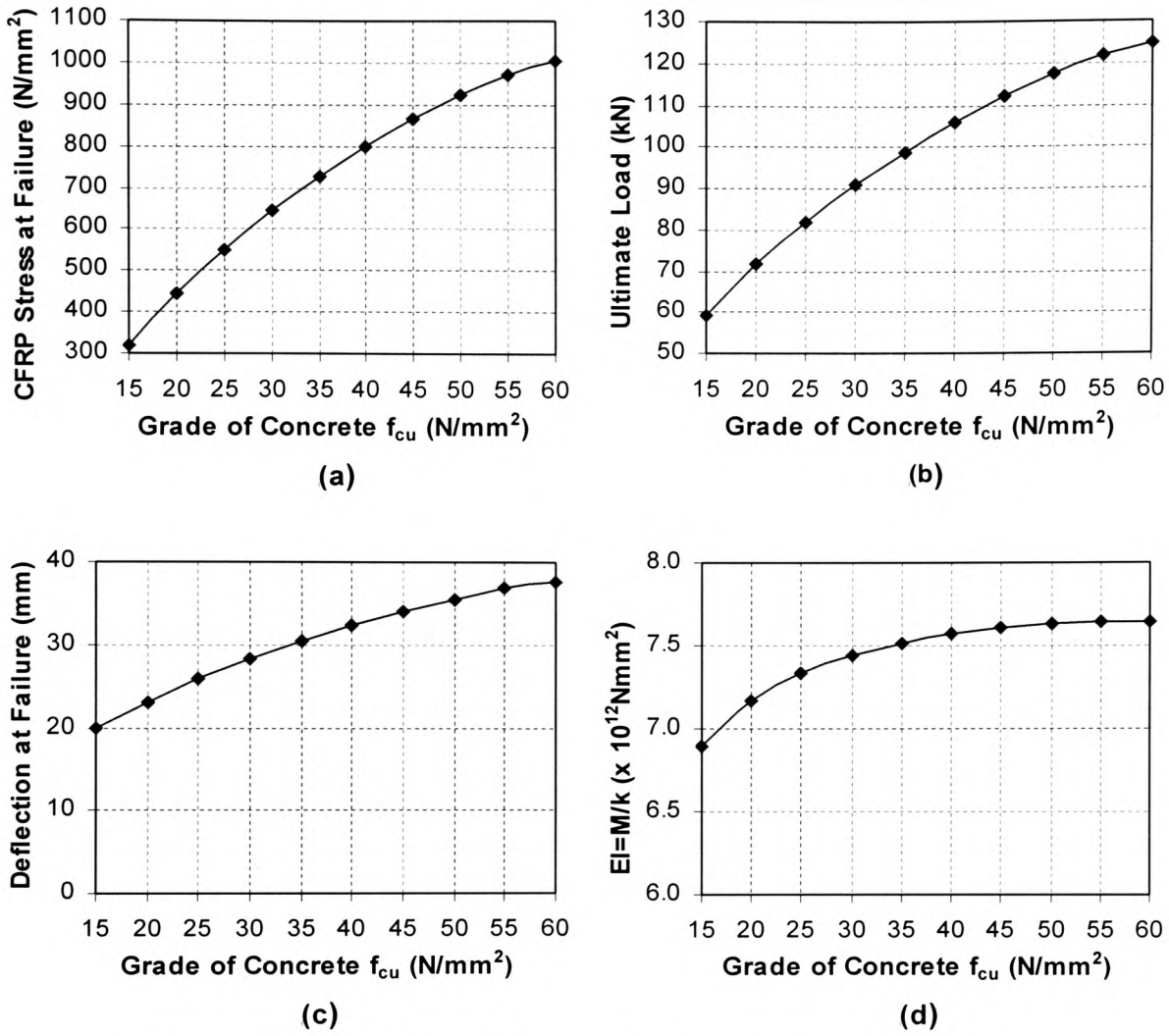

Figure 5.37 Variation of Beam behaviour vs. Concrete Grades

5.8.4 Area of Internal Steel Reinforcement

The amount of existing internal steel reinforcement plays a critical role in determining the boundary between under- and over-strengthened sections, as defined by Equation (5.24). In general, all existing reinforced concrete flexural members have been designed as under-reinforced sections in accordance with most national or international design codes such as BS 8110 and EC 2. It is the candidate's view that doubly reinforced section should not be strengthened by FRP composite, unless suitable enhancement in compression is also accomplished. This argument will be more clearly demonstrated in the design related Chapter 8. This section deals with members where the existing steel

reinforcement provided has not reached the maximum area allowed for a singly reinforced section with tension steel only. The maximum steel area for a singly reinforced section can be defined as follows:

$$A_s = \frac{K' f_{cu} b d^2}{f_{yd} z} \tag{5.27}$$

where $\mathbf{f_{yd}}$ and **z** are the design strength of the reinforcement and the lever arm respectively. The factor **K'** may be defined as $0.4(\beta_b\text{-}0.4) - 0.18(\beta_b\text{-}0.4)^2$, as in BS 8110, it equals to 0.155 if no moment redistribution is considered, and β_b is the moment redistribution factor which usually ranges between 0.7 and 0.9.

In the present study, most of the beams (unless otherwise stated) have been reinforced with 2T10 bars (A_s = 157 mm^2, ρ_s = 0.785%) whilst the maximum allowed area for a singly reinforced section could be up to 320 mm^2 (ρ_s = 1.6%), assuming a grade 40 concrete. The parametric study is therefore performed for a maximum steel area of 1.6%. Based on the analytical model and all other material properties kept the same as in the preceding sections, various steel reinforcement ratios have been used to investigate the influence of steel area on the behaviour of CFRP strengthened beams.

Shown in Figure 5.38(a)-(d) are the results of the modelling of various steel reinforcement ratios on the influence of beam behaviour. There are a number of significant aspects that are different from the earlier results relating to concrete and CFRP. Firstly, contra to the increase in concrete or CFRP strength, the increase in steel area does not result in any increase in the CFRP stress. In fact, the opposite is true. When the area is increased to the maximum of 320 mm^2 (1.6%), the failure stress in the CFRP plate is only 548 N/mm^2 as shown in (a). Similar to the influence of FRP plate, the increase of reinforcement area results in significant reduction of span deflection at failure as shown in (c). This is because the additional area provided will lead to the neutral axis moving downwards, and hence the flexural rigidity EI is increased as a result, which is shown in (d). The ultimate load also increases with the increase in steel area, but to a lesser degree than that resulted from the increase of FRP and concrete strength, as shown in (b).

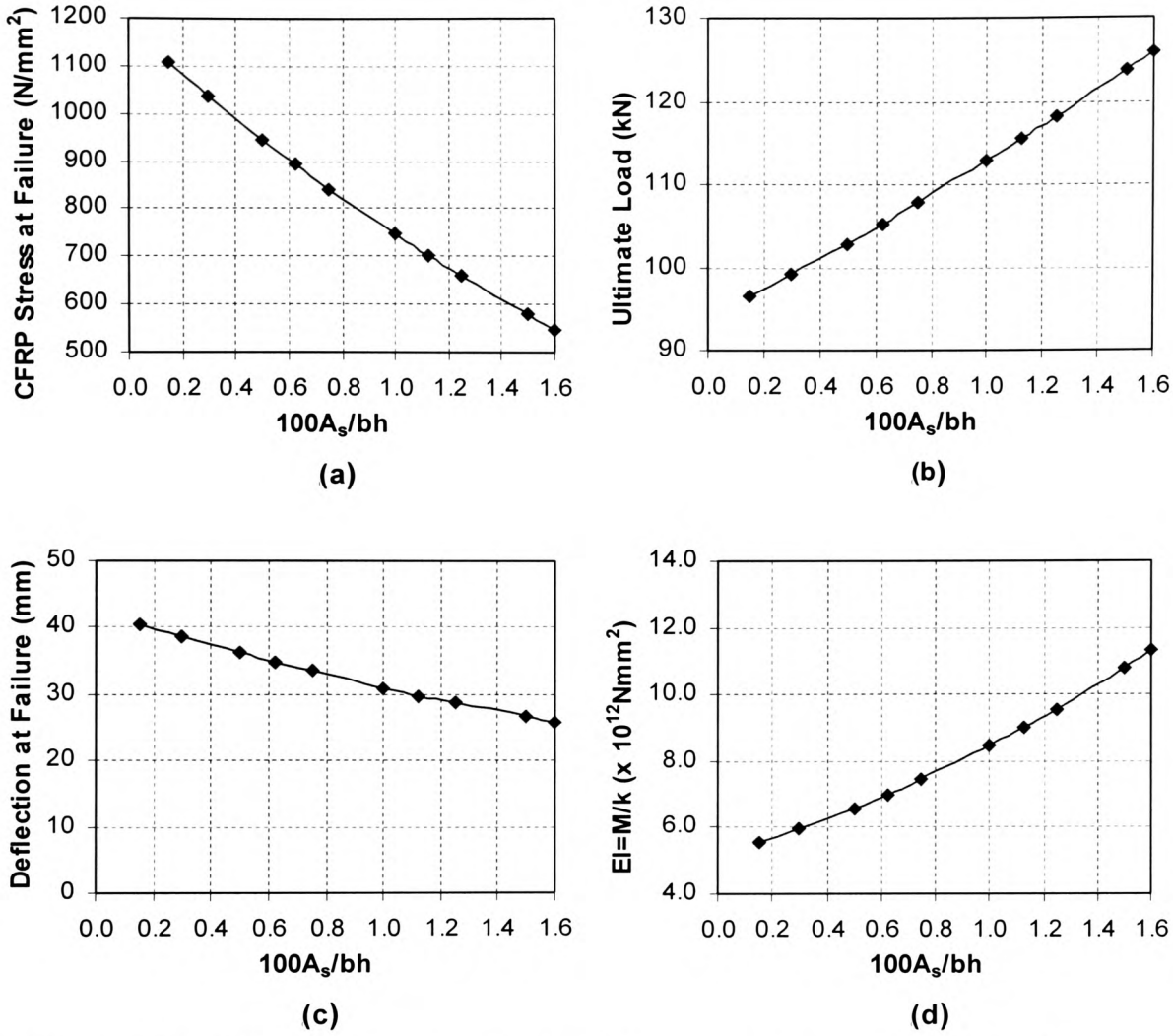

Figure 5.38 Effect of Increasing Steel Reinforcement Area on Beam Behaviour

Figure 5.39 illustrates the percentage influence on beam behaviour due to the change in steel reinforcement area. It is clear that both CFRP stress at failure and the ultimate deflection decrease with the increase of reinforcement area. The comparison of beam behaviour under various factors is shown in Table 5.5.

Table 5.5 Comparison of Beam Behaviour at 300% Increase in Properties

	% Change in Ultimate Load	% Change in Deflection
300% Increase in A_s	+ 8.5	- 13.0
300% Increase in f_{pu}	+ 42.5	- 33.0
300% Increase in f_{cu}	+ 110.0	+ 90.0

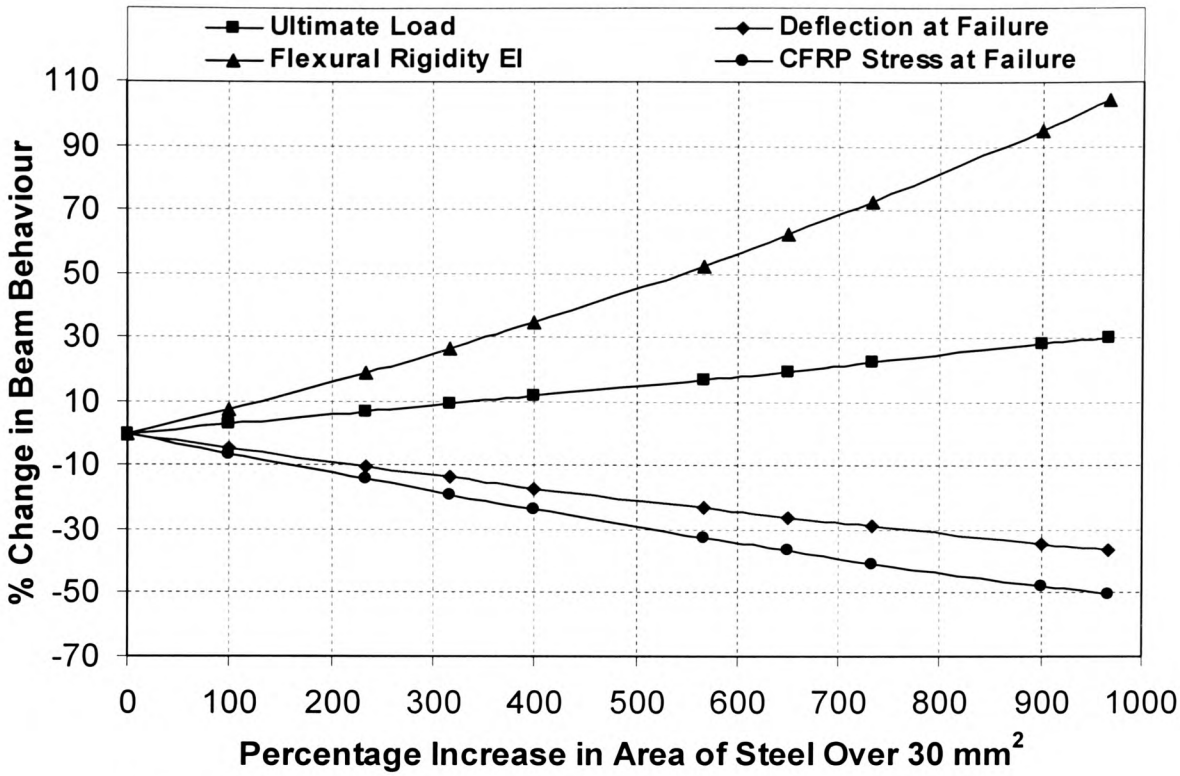

Figure 5.39 Effect of Steel Reinforcement Area on Beam Behaviour

It can also be seen from Table 5.5 that, if all other factors are kept constant, the change of steel reinforcement area has the least influence on the beam behaviour. This is followed by the increase of CFRP ultimate strength. The increase in concrete compressive strength is, by far, the most sensitive influential factor for an over strengthened RC element. This behaviour can be interpreted as the interaction between the internal steel reinforcement and the externally bonded CFRP plate is highly complementary. The increase in steel area automatically decreases the CFRP stress.

The increase in the concrete compressive strength, however, results in the increase of CFRP stress at failure, and hence the composites can be more fully utilised. It can be generally concluded that for strengthening RC elements, which have low-grade concrete strength, only low strength FRP composites need to be used. On the other hand, the higher strength CFRP materials may be applied to strengthen concrete members with higher residual strength, say, of greater than 45 N/mm^2 in compressive strength. A design recommendation in this regard is made in Chapter 8.

5.9 ANALYSIS OF SURFACE CRACK WIDTH

5.9.1 Crack Width of Conventional Members

The average crack width due to flexure in a RC beam is a function of the reinforcement strain. For conventionally reinforced concrete beams, BS 8110, Part 2 (1985), uses the following equation to determine the average crack width, w_{cr}, provided that the stress in the reinforcement is less than its design strength.

$$W_{cr} = \frac{3a_{cr}\varepsilon_m}{1+2(\frac{a_{cr}-c_{\min}}{h-x})} \qquad (5.28)$$

where a_{cr} is the distance from the location where crack width is being considered to the surface of the nearest longitudinal bar, and ε_m is the average strain at the level of the crack width being considered, after taking into account the concrete tension stiffening effects.

It is clear from equation (5.28) that the maximum surface crack width is likely to occur at the soffit between the main reinforcement or at the bottom corner as shown in Figure 5.40(a). The average tensile strain ε_m is at its maximum value at the soffit and the distance a_{cr} is the greatest at that level. For relatively deep beams, the location at mid-way between the neutral axis and the reinforcing bars is also of significant interest when crack width is determined.

For FRP strengthened RC beams, however, the above approach has to be modified. Provided that the FRP plate is well bonded to the concrete surface, the maximum crack width will not occur at the soffit level. The cracks between the FRP plate and the internal steel reinforcement are likely to be of small "diamond" shape as shown in Figure 5.40(b). In beams where no internal steel reinforcement is provided the maximum crack width is likely to be occurring at the web surface mid way between the neutral axis and the longitudinal bars as shown in Figure 5.40(c).

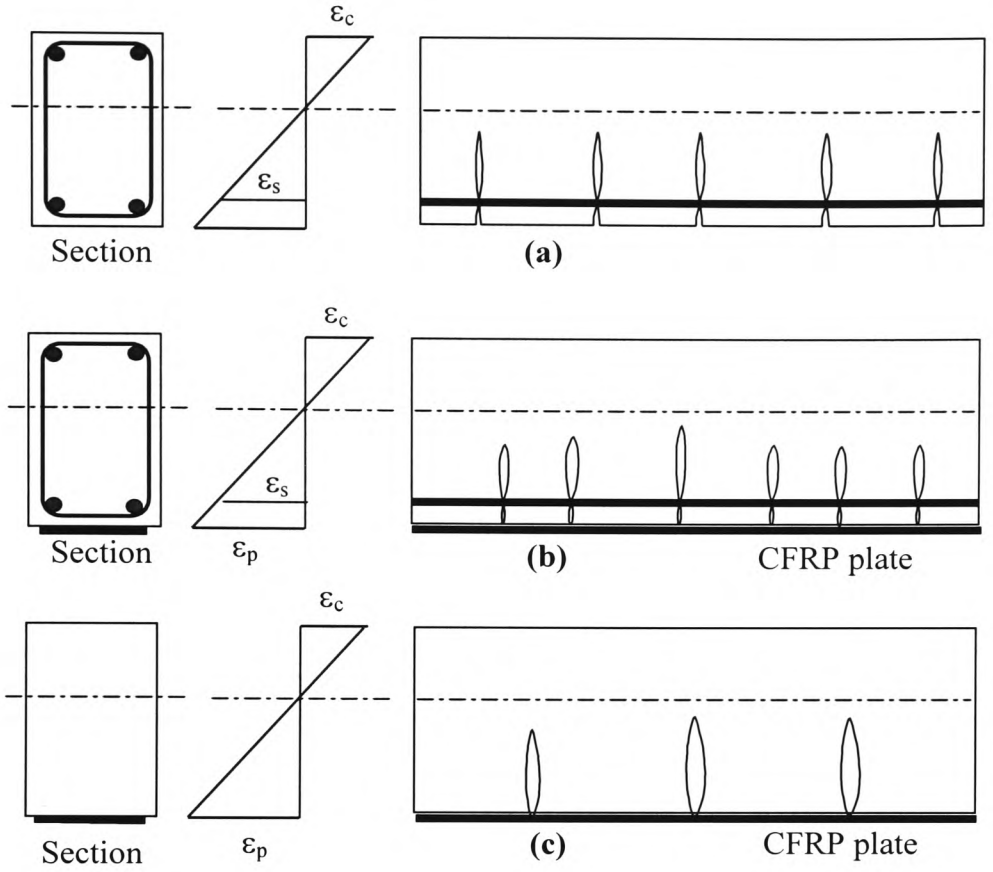

Figure 5.40 Schematic of Crack Propagation in Flexural Elements
(a) Conventionally Reinforced Concrete Beam; **(b)** FRP Strengthened RC Beam;
(c) Concrete Beam with External FRP Reinforcement Only.

5.9.2 Determination of Crack Width for FRP Strengthened RC Beams

In FRP strengthened flexural members, the amount of composites plate or fabric sheets influence the magnitudes of the strains in the tension reinforcement and hence the crack width and distribution. The influence of the FRP may be taken into account by transform it to the equivalent steel area. If suitable surface preparation has been carried out on the FRP surface (eg. peel-ply protection), and the adhesive is properly mixed and applied in accordance with manufacturer's instructions, then a strong bond between the concrete and the FRP is ensured as discussed in Chapter 3. This will lead to the crack width at the adhesive-FRP interface being of very small values, similar to these cracks at the internal reinforcement-concrete interface as shown in Figure 5.40(a). The conventional BS 8110 approach, as developed by Beeby (1979) therefore need to be

modified, since it recognises that the maximum cracks width are likely to occur at the soffit and at the corners of the beam, as the average tensile strains usually reach maximum at these locations. The maximum crack width for an FRP externally reinforced section with no internal steel reinforcement, is likely to occur at a location where the product of the concrete surface strain, ε_c, and the distance to the nearest reinforcing bar a_{cr}, results in the maximum value, as shown in Figure 5.41. The concrete surface strains in the tension zone can be approximately expressed in terms of FRP strain , ε_p as follows:

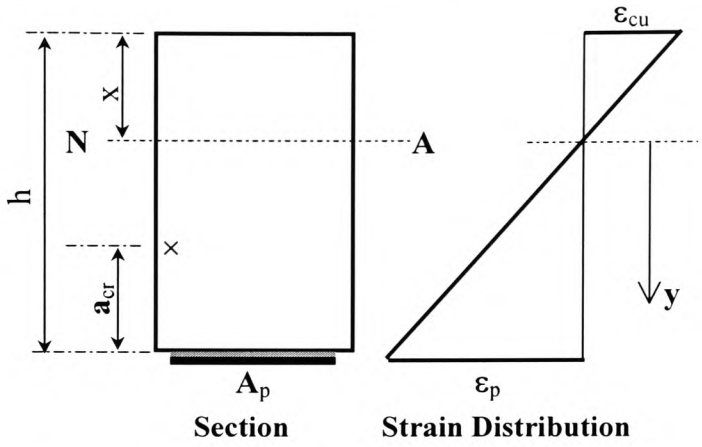

Figure 5.41 Location of Maximum Crack Width in FRP Strengthened Beam

$$\varepsilon_c = \varepsilon_p \frac{y}{(h-x)}$$

Differentiate the product of $\varepsilon_c(y-h+x)$ and let the expression be referred to zero, the distance from the beam soffit to a point where the surface crack is likely to sustain its maximum value, is determined to be 0.5(h-x), or approximately half way between the neutral axis and the FRP composite.

Substituting $a_{cr} = 0.5(h-x)$, and $\varepsilon_c = 0.5\varepsilon_p$ into Equation 5.28, the modified equation for determining the maximum surface crack width in FRP strengthened beams (with no internal steel bars) can therefore be expressed in the simple form of:

$$W_{cr} = 0.75(h-x)\varepsilon_p \qquad (5.29)$$

For FRP strengthened RC sections, strains in the steel reinforcing bars will control the crack width just as is the case for the conventionally reinforced concrete beams. However, the crack width magnitude in FRP strengthened RC beams is expected to be smaller, and the number of cracks greater, than that of the conventional RC beams. This is due to the presence of the bonded FRP at the beam soffit. The reduction of crack width may be taken into account by modifying Equation (5.29), where the overall beam

depth h is replaced by the effective depth d, to reflect the position of internal steel reinforcement. The value of ε_p should be replaced by the average effective reinforcement strain, ε_m, as used in Equation (5.28). However, the above method is an over simplification in the determination of crack width for FRP strengthened concrete beams. Although correct in principle, these simple approaches have to be further developed and validated before they can be used by designers. Currently, there are insufficient experimental data on surface cracks to carry out a rigorous analysis. It is therefore suggested that extensive further work be carried out in this important aspect of FRP strengthen design.

5.10 SUMMARY

A non-linear analytical model, based on material constitutive laws, was developed to predict the flexural behaviour of FRP strengthened RC elements. The predicted value of ultimate load for the control beam was within 2% of the actual failure load. This was achieved when the FRP area A_p was set to zero in the modelling process. For series B beams (except B2), close agreement between the predicted failure load and the experimental values was also observed.

However, the predicted ultimate load was generally much higher when compared with the actual failure value of the over strengthened beams in the series-A tests. This is because the current model is based on the assumption that complete flexural failure is achieved at ultimate limit state, while series-A beams in fact all failed in some form or another in a premature tearing-off manner (see Chapter 6). Nevertheless, the predicted beam behaviour, whether it is load-deflection, strains or moment-curvature relationship, all closely matched that of the experimental results up to the actual failure point. It is therefore concluded that the present analytical model can accurately predict the behaviour of FRP strengthened beams, if measures are taken to prevent premature failure of these elements.

Using the present model, a parametric study was carried out. The influence of various factors including the properties of concrete, steel and FRP composites, on the behaviour of FRP strengthened elements was investigated. It was found that:

- Precracked beams strengthened by FRP composites exhibit a pseudo-linear behaviour until about 50% of the ultimate load. Their non-precracked counterparts still show clear change of slope on the load-deflection curves, at the load that causes the first crack in concrete.
- There is negligible difference in the ultimate load behaviour between the pre-cracked and non pre-cracked beams. This is because the concrete tension stiffening effect only counts less than 3% of the total tension resistance at ultimate limit state.
- The value of neutral axis depth, x, of the FRP over-strengthened sections, tends to increase with the increase of applied load.
- For the non-precracked beams, the neutral axis depth value remains constant until the first crack in the concrete appears, after which it decrease rapidly, and then develops a similar trend as the precracked members.
- For fully balanced or under strengthened sections, the neutral axis depth decreases as the applied load is increased, while at between 40% of the ultimate load and service load, the neutral axis position tends to be stabilised without much change.
- The maximum span deflections decrease rapidly with the increase of FRP area when the FRP area fraction is less than 1%, after the reduction in deflection still occurs as the FRP area increases, but at a much reduced rate.
- Under the service load, the corresponding span deflections increase with the increase of FRP fraction until it reaches a value of 0.4%, after which the percentage increase of span deflections remains almost constant.
- The ultimate load level increases with the increase of FRP area, provided that complete flexural failure is ensured.
- For over strengthened sections, higher FRP modulus of elasticity results in increased ultimate load capacity and enhanced stiffness. The failure stress in the FRP composite also increases, and is accompanied with a reduction in span deflection.
- The higher the ultimate tensile strength of FRP, the lower the FRP failure stress in over strengthened sections will be.
- Higher concrete compressive strength leads to improved structural behaviour of FRP strengthened elements in every aspect.
- The higher the existing reinforcement ratio is, the lower the FRP stress and span deflection at failure becomes, but the ultimate load and stiffness will increase.

CHAPTER 6

Premature Tearing-off Behaviour of FRP Strengthened RC Beams

6.1 INTRODUCTION

The adjective "premature" in the context of "premature failure", clearly suggests that such failures occur prior to the commonly expected or predicted failure load. The word also comes with hints that such a failure mode should be avoided or prevented from taking place. Conventional RC beams are usually designed to be under-reinforced so that ultimate failure starts with the yielding of reinforcement and is then followed by the crushing of concrete in compression. Broadly speaking, any failure mechanisms in a beam, which takes place before the steel reinforcement or concrete reaches their design strength may be regarded premature. These are often characterised as sudden and brittle, such as shear failure in beams with insufficient shear resistance.

In FRP strengthened RC beams, a predominant type of failure mechanism is the debonding of the concrete cover at the reinforcement level, with the FRP composite still well bonded to the concrete. In the current testing of series A, nearly all CFRP plate strengthened beams had failed in such a manner. In order to distinguish this typical premature failure mode from the actual debonding of the FRP plate at the adhesive layer, the candidate suggests that such a debonding failure of concrete cover should be referred to as "tearing-off of concrete cover" or "tearing-off" failure for short.

Figures 6.1 shows a typical tearing-off failure mechanism of a CFRP plate strengthened beam in the "series A" tests. The plate anchorage length, l_a, which may be defined as the

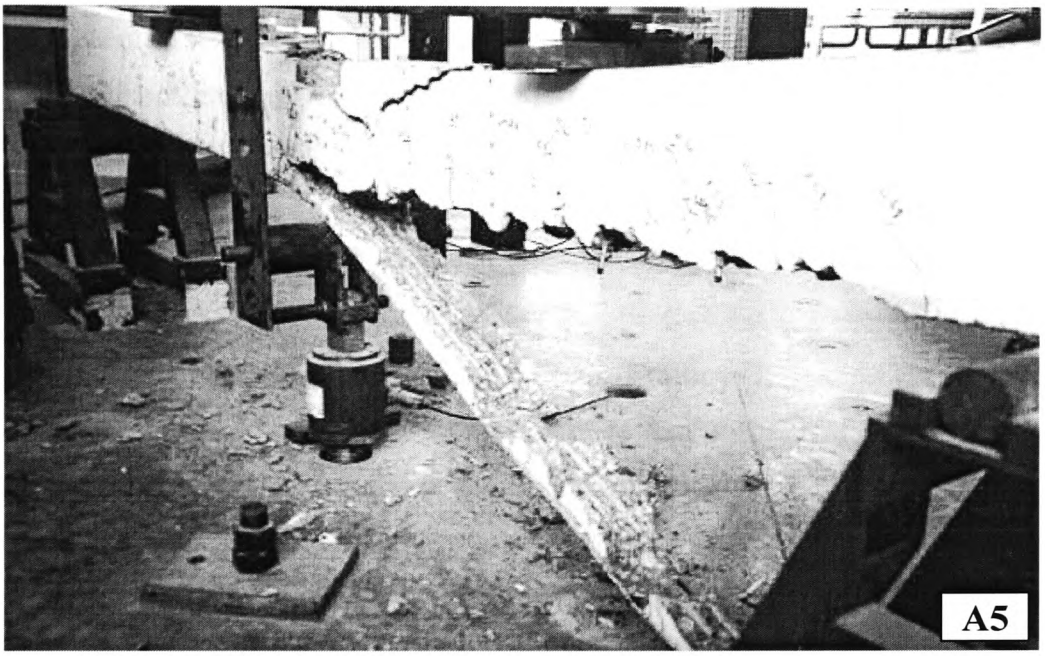

Figure 6.1 Typical Tearing-off Failure of CFRP Plated Beam
(Beam A5, length of CFRP plate: 2.20 m)

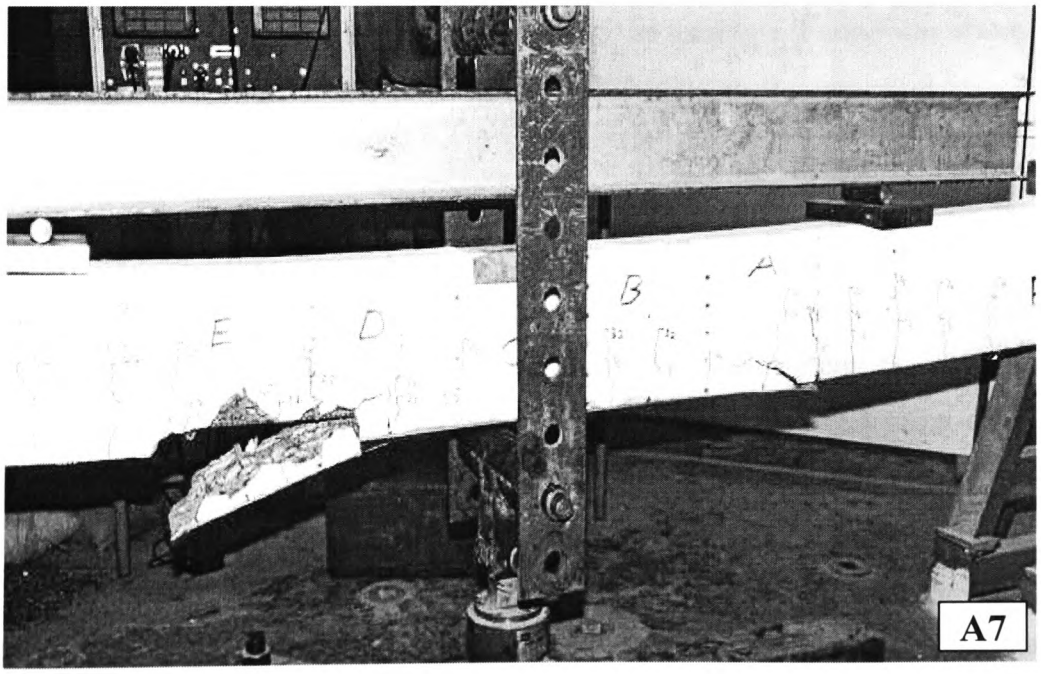

Figure 6.2 Typical Tearing-off Failure of CFRP plated Beam
(Beam A7, CFRP plate terminated within the constant moment zone, plate length: 1.00 m)

distance from the end of the constant moment zone to the plate cut off point, is 475 mm for beam A7 as the 2.2 metres long plate was terminated 100 mm away from the supports. This configuration was kept the same for most other simply supported beams in the present test series unless otherwise specified. Such an anchorage mechanism, however, did not prevent the severely brittle tearing-off failure as shown in the picture. The concrete cover of half of the length of the beam effective span had been torn off suddenly in an explosive and catastrophic manner, leaving the steel reinforcing bars fully exposed, while the CFRP plate was still well attached to the concrete surface.

Shown in Figure 6.2 is another typical tearing-off failure. In this case, the same CFRP plate with a shorter length of 1.0 m was bonded to the soffit of the beam within the constant moment zone. The distance between the two point loads was 1250 mm as seen in Chapter 4. It was intended that such a plate configuration would trigger a conventional flexural failure within the unstrengthened part (250 mm) of the constant moment zone, at a load not much higher than that of the control beam. It was thus somewhat surprising to note that beam A7 actually failed at 59.1 kN, or about 23% higher than the failure load of the control beam. From Figure 6.2, it was observed that the beam still failed by tearing-off of the concrete cover. However, in this case it was much more "mild-mannered" in that the length of the tearing-off zone was about 25% of the plate length at approximately 250 mm.

Many renowned researchers - including Roberts (1989); Saadamanesh *et al* (1998); Raoof *et al* (1995, 1997, 2000); Oehlers *et al* (1990, 1992, 1998); Swamy *et al* (1999); Quantrill *et al* (1996); (Aiello, 1999) and Ali *et al* (2000) - have reported the tearing-off type of failure. They recommended various methods in estimating the so-called plate "peeling-off" stresses that would cause such premature tearing-off failure. Unfortunately this topic still appears to be inconclusive today, few of these methods seem to give any definitive and convincing solutions.

The aim of this Chapter is to apply and compare the available theories in estimating the parameters such as the plate-end normal and shear stresses together with the failure load, and correlate these parameters with the current test results. A modified semi-empirical approach for estimating the failure load will be suggested.

6.2 APPROACHES FOR IDENTIFICATION OF PREMATURE FAILURES

6.2.1 Concept of Passive Joint Failure

Reinforced concrete has been used widely and successfully in the construction industry for over a hundred years, and it is often forgotten that it is a composite material itself. The composite action of concrete is achieved by a combination of chemical reaction and mechanical interlocking between the main ingredients of cement, water, sand and aggregates. In reinforced concrete, this composite action is the result of bond strength between the embedded reinforcement and the concrete. For RC members externally strengthened by FRP composites, two types of new materials are involved, namely FRP composites and the adhesives. A strengthened element is essentially, therefore, a new composite material derived from a composite construction strengthened by another composite. The expected role of a suitable adhesive system is to bond the FRP composite to the RC member. The bonding layer will transfer the stresses (tensile and shear) from the concrete to the strengthening FRP plate and ensure a full composite action between the concrete and the strengthening laminates. This principle has been proven realistic with steel plate bonding systems. A good adhesive system would result in full composite action at the interface of plate and concrete, and prevent plate "peeling-off" type of failure. Any peel-off of FRP plate is most likely to be a result of poor workmanship during mixing or application of the adhesives.

Many commercial products of epoxy adhesives that are available to the construction industry are in fact rather strong and stiff materials in their own right. They are manufactured to the then Department of Transport specification BA 30/94 as discussed in Chapter 3. The minimum tensile strength of plate bonding epoxy adhesives is specified to be 12 N/mm^2 in the guidance document, while in practice the actual tensile strength could reach as high as 40 N/mm^2 such as the "Resifix 31" adhesive used in the present tests. As a result, it is rare to see an actual bond failure if proper surface preparation (Chapter 3) has been carried out and correct bonding procedure followed.

In the adhesive joint of a loaded CFRP plated beam, three components are directly involved to form the composite action, namely, concrete, adhesive and the FRP plate.

Once the ultimate strength of the joint is reached, the weakest member of the three will fail first, and for the observed failure modes in the current test series, this weakest member is undoubtedly concrete.

However, most of the tearing-off failure mechanisms seen in the tests are not, strictly speaking, direct joint failures, since the CFRP composites are still well bonded to the concrete cover as shown in Figures 6.1 and 6.2. The candidate suggests that tearing-off failure is indeed a concrete failure, due to the great strength in the adhesive joint, rather than the actual joint failure. It may be regarded, at most, as a passive joint failure.

In the light of the above, the following hypothesis may be made:

The concrete properties and the applied load, directly influence the tearing-off of concrete cover failure mode, while the mechanical properties of the adhesive and FRP composites may be regarded as secondary influencing factors. There exists a critical thickness and area of FRP plate provided, above which the premature tearing-off failure will always occur at a much lower load than the otherwise expected ultimate load, which is based on the normal flexural failure mechanism.

This critical FRP area is the area required for an FRP strengthened beam which has a fully balanced section, as defined in Chapter 5.

6.2.2 Peeling-off and Tearing-off Stresses

The candidate feels that it is important to distinguish these two types of stresses. The so-called peeling-off stresses, at the interface between the concrete and the FRP plate at the plate cut-off region, comprise the normal and shear stresses. There are differences between the peeling-off stresses and the tearing-off stresses.

For the former, peeling-off will occur if the bond stress between the FRP and the adhesive, or between the adhesive and the concrete, exceeds the bond strength. What follows is debonding of the FRP from the strengthened concrete element, with the

adhesive layer still attached to either the FRP plate or the concrete. Such a plate peeling-off failure mechanism is rare. The cause of it is either poor quality of adhesive material, or poor workmanship in applying it as previously mentioned.

The second type, the tearing-off stresses, are directly related to the tearing-off failure mechanism. One approach in identifying the mechanical characteristics of such failure is to evaluate the plate end shear and normal stresses under a given load, and to ensure that these stresses are within the limit of the concrete tearing-off resistance. The concrete resistance to tearing-off, however, is a new concept specific to FRP plate bonding. It is likely to be the result of a combination of concrete tension, shear and flexural resistance, and, to date, there exists no definite guide for the determination of its value.

In order to determine such a "new" concrete structural property, the experimental tearing-off stresses at the premature failure load will be determined in Section 6.3, using the experimental data and various existing theories.

6.2.3 Determination of Premature Failure Load

One other approach in dealing with the premature failure of concrete cover tearing-off, is to determine directly the load that causes such a failure. Design guidelines are then prepared to ensure that the applied load does not exceed the specified limit. Raoof and his associates (Zhang *et al*, 1995, Raoof and Zhang 1997, Raoof and Hassanen, 2000) developed a theory based on the minimum stabilised cracking spacing, in which the upper and lower bounds of the failure load are determined. The current experimental results will be used in Section 6.3 to show the validity or otherwise of this method.

6.3 COMPARATIVE STUDY OF EXISTING THEORIES

6.3.1 Plate-end Stresses Based Theories

Roberts and Haji-Kazemi (1989) reported a theoretical study on the topic of debonding of steel plate from a concrete beam. They used linear elastic theory to demonstrate that the elastic shear and normal stresses in and adjacent to the adhesive layer increase rapidly towards the end of the steel plate. Roberts (1989) also presented a simplified method for estimating the plate end stresses, as reviewed in Chapter 2, Equations 2.4 and 2.5. It was shown that the stiffness of the adhesive joint, the thickness of the steel plate and its point of termination play a major role in influencing the plate end shear and normal stresses.

In a following up discussion, Oehlers (1989) argued that the main failure modes could be separately identified as shear peeling and flexural failure at the tension reinforcement level, and the plate peeling-off at the bondline was normally attributable to bad workmanship. Oehlers and Moran (1990) carried out further experimental and analytical studies, and proposed that the failure moment at the plate end for cases where the plate is terminated with in the constant moment zone, could be evaluated by

$$M_{up} = \frac{(EI)_{cp} f_t}{0.474 E_s t_p} \tag{6.1}$$

where $(EI)_{cp}$ is the flexural rigidity for the strengthened concrete cracked section based on the assumption that concrete tensile strength f_t is zero and the materials still behave linearly. E_s is the Young's modulus of steel plate and t_p is the plate thickness.

In a subsequent paper, Oehlers (1992) addressed the issue of shear peeling and the interaction between shear peeling and flexural peeling of steel plated beams. Various plate lengths were used such that the plate end, located in the shear span, was terminated with different moment to shear force ratios, M/V. It was demonstrated that there was strong interaction between flexural and shear peeling, and a failure envelope was suggested.

$$\frac{M_p}{M_{up}} + \frac{V_p}{V_{uc}} \leq 1.17 \qquad (6.2)$$

where M_p ($<M_{up}$) is the moment at the plate end when peeling occurs, M_{up} is the moment when peeling occurs at the plate end when V = 0 as given by Equation (6.1); V_p ($<V_{uc}$) is the shear force at the plate end when peeling takes place and V_{uc} is the shear strength of RC beam without shear links.

This seems a simple equation, which can be easily incorporated into design codes. However, this equation was derived under the condition that V_p must be less than V_{uc}. It has therefore severely limited the use to virtually a very small range of application. The FRP strengthened beam should certainly exhibit much greater shear resistance than the unplated beams for any strengthening in flexure to be effective without suffering a premature shear failure.

Theoretical and finite element modelling work carried out by Täljsten (1997), confirmed that the shear and normal stresses are at their maximum at the end of the plate and diminish quickly as the distance from the plate end increases. The maximum shear stress τ_{max} is determined by:

$$\tau_{max} = \frac{G_a P}{2 t_a E_c Z_c} \frac{(l_p + a - b)}{\frac{l_p}{2} + a} \frac{(a\lambda + 1)}{\lambda^2} \qquad (6.3a)$$

$$\lambda^2 = \frac{G_a b_p}{t_a} \left(\frac{1}{E_p A_p} + \frac{1}{E_c A_c} + \frac{z_o}{E_c Z_c} \right) \qquad (6.3b)$$

where l_p is the length of the plate; P is the applied load; Z_c is the section modulus of concrete; z_o is the lever arm; a and b are the distances from the plate end to the nearest support and the point load respectively; and λ is the relational constant. All other symbols have their usual meaning.

The maximum plate end normal stress σ_{max} is then expressed as:

$$\sigma_{max} = \frac{E_a}{t_a}\{\frac{P}{4\beta^3}\frac{l_p+a-b}{\frac{l_p}{2}+a}[\frac{a\beta+1}{E_cI_c}(1-\eta)+\frac{\beta\lambda^2-\lambda^3}{(\lambda^4+4\beta^4)}\frac{ab_p}{t_aE_pI_p}$$
$$(\frac{E_a\eta}{E_cI_c\lambda^2}+\frac{G_at_p}{2E_cZ_c})+\frac{G_ab_pt_p}{2t_aE_pI_pE_cZ_c}\frac{a\lambda+1}{\lambda^2}]$$
$$+\frac{P}{2E_cI_c}\frac{l_p+a-b}{\frac{l_p}{2}+a}\frac{\eta a}{\lambda^4}-\frac{P}{2}\frac{ab_p}{t_aE_pI_p(\lambda^4+4\beta^4)}\frac{l_p+a-b}{\frac{l_p}{2}+a}(\frac{E_a\eta}{E_cI_c\lambda^2}+\frac{G_at_p}{2E_cZ_c})\} \quad (6.4a)$$

and the two constants η and β are determined by the following equations respectively.

$$\eta = \frac{G_ab_pz_o}{t_aE_cZ_c\lambda^2} \quad \text{and} \quad \beta = \sqrt[4]{\frac{E_ab_p}{4t_aE_pI_p}} \quad (6.4b)$$

Täljsten pointed out that the magnitude of the plate end stresses was influenced not only by the geometrical and material parameters of the beam, but also by the properties of the adhesives and the strengthening plates.

Similar closed form analysis of plate end stresses was carried out by Saadatmanesh and his associates (Malek *et al*, 1998). They assumed linear elastic and isotropic behaviour of all four materials of concrete, steel, adhesive and FRP composites. The following equations were used to calculate the maximum shear stress at the plate cut off point.

$$\tau_{max} = t_p(b_3\sqrt{A}+b_2) \quad (6.5a)$$

$$A = \frac{G_a}{t_at_pE_p},\ b_1 = \frac{y'a_1E_p}{I_{tr}E_c},\ b_2 = \frac{y'E_p}{I_{tr}E_c}(2a_1L_0+a_2), \text{ and}$$

$$b_3 = E_p\{\frac{y'}{I_{tr}E_c}(a_1L_0^{\ 2}+a_2L_0+a_3)+2b_1\frac{t_at_p}{G_a}\} \quad (6.5b)$$

where y' is the distance from the neutral axis to the centre of FRP plate; L_o is the distance from the plate cut-off point to the origin of x; I_{tr} is the second moment of area of the transformed section.

The bending moment at any section is expressed by:

$$M(x) = a_1x^2 + a_2x + a_3 \quad (6.5c)$$

and the polynomial coefficients can be determined from this equation by comparing it with the actual bending moment.

The co-existing maximum normal stress is determined by

$$\sigma_{max} = \frac{K_n}{2\beta^3}\left(\frac{V_p}{E_pI_p} - \frac{V_c + \beta M_0}{E_cI_c}\right) + \frac{qE_pI_p}{b_pE_cI_c} \quad (6.6)$$

where $K_n = E_a/t_a$, is the unit stiffness of adhesive; $\beta = (K_nb_p/4E_pI_p)^{0.25}$; q is the load, M_o and V_o are the bending moment and shear force at the plate end due to external applied load; V_p and V_c are the shear force in the FRP plate and concrete beam, respectively, after taking account of interfacial shear stresses, where they are determined as follows.

$$V_c = V_o - b_py't_p(b_3\sqrt{A} + b_2) \quad (6.7a)$$

$$V_p = -\tfrac{1}{2}b_pt_p^2(b_3\sqrt{A} + b_2) \quad (6.7b)$$

6.3.2 Application of Plate End Stresses Theories

In order to assess the applicability of the above discussed theories, the test results of two typical CFRP plated beams A5 and A7 (shown in Figure 6.1 and 6.2) are used to evaluate the plate end shear and normal stresses that caused the premature failure of

concrete cover tearing-off. The relevant physical properties of the two beams are listed in Table 6.1.

Table 6.1 Details of Beams A5 and A7

Beam Ref.	f_{cu} (E_c)	f_y (E_s)	f_p (E_p)	G_a (E_a)	l_p	l_o	t_a	t_p	x_t	P_t (kN)
A5	47.1 (37.7)	560 (200)	1750 (125)	3.50 (8.8)	2000	100	2.0	1.6	62.7	82.0
A7	45.3 (37.0)	560 (200)	175 (125)	3.50 (8.8)	1000	700	2.0	1.6	61.3	68.0

Units: f_{cu}, f_y, f_p – N/mm^2, E_c, E_s, E_p – kN/mm^2, all other units in mm unless otherwise stated.
$\mathbf{x_t}$ is the neutral axis depth at the instance of premature tearing-off failure, derived from the analytical model in Chapter 5.
P_t is the experimental premature failure load.

Based on these details, the maximum plate end stresses are determined using the above discussed equations.

The calculation results are listed in Table 6.2.

Table 6.2 Comparison of Various Theories on Maximum Plate-end Stresses

Beam Reference	τ_{max} (N/mm^2)			σ_{max} (N/mm^2)		
	Roberts	Täljsten	Malek	Roberts	Täljsten	Malek
A5	2.71	2.39	5.09	1.74	27.8	N/A*
A7	6.12	1.99	4.28	3.93	22.6	N/A*

* The coefficient b_3 is calculated to be 20.1 by Equation (6.5b), where L_o is 100 mm, and a2 is 41000 and 34000 respectively. This resulted in a negative value of the concrete shear force V_c in Equation (6.7a), which is physically impossible.

Of the three methods presented in Table 6.2, Roberts' theory has been widely quoted and regarded by many as the most authoritative formulation for estimating plate end stresses. Although all the authors had presented well-matched results in the original papers and established the general trend of plate end stress distribution, the application of these methods to the present test results have led to drastically unconvincing and, in

the case of normal stress by Täljstein's theory, obviously wrong results. This was despite many repeated and careful numerical operations. In a recent review, Mukhppadhyaya and Swamy (1999) also confirmed that Robert's theory led to widely scattered results. They concluded that there was a need to develop a reliable design tool, in order to predict the plate end stresses in a more consistent manner and for a wide range of FRP or steel properties.

The reason for such large discrepancies may be attributed mainly to the lack of detailed parametric study. Each theory seemed to be applicable only to a particular type of material, load and beam geometrical configuration. Although all methods were based on linear elastic theory, the final results were certainly expected to be influenced by the non-linearity of the cracked concrete. The complex and somewhat non-unique nature of these methods in determining plate end stresses makes it highly unlikely for these equations to be adopted for practical design purposes.

6.3.3 Theories on Determination of Failure Load

Oehlers theory -Equation (6.1), for determining the premature failure moment of strengthened beams with plate terminated in the constant moment zone- is applied to evaluate the failure load for beam A7. It gives a lower failure load, of 47 kN, than that of the unplated control beam, and the actual premature failure load was underestimated by 45%.

Raoof and his associates at Loughborough University carried out another piece of pioneering work on this topic (Zhang *et al*, 1995, Raoof *et al*, 1997, 2000). They argued that the axial stress in the strengthening plate at the instance of failure was the controlling criteria for determining the load, which caused the premature tearing-off failure. And the magnitudes of these axial stresses in turn, depended on the stabilised crack spacing in the concrete cover. Since the crack spacing has a large variation say, by a factor of 2, in practice, there exists no unique solution to the failure load. A lower bound and upper bound approach was thus recommended.

Based on the classical theory of concrete cracking, first proposed in 1943 by Watstein and Parsons (1943), Raoof used the following equations to determine the minimum and maximum crack spacing l^p_{min} and l^p_{max} respectively.

$$l^p_{min} = \frac{A_e f_t'}{u(\sum 0_{bars} + b_p)} \tag{6.8a}$$

$$l^p_{max} = 2l^p_{min} \tag{6.8b}$$

where u is the average bond strength between the steel plate and the concrete which may be determined as $0.28(f_{cu})^{0.5}$ in the case of steel plate-concrete bond (Mosley *et al* 1999); f_t' is the cylinder splitting tensile strength which may be determined as $0.36(f_{cu})^{0.5}$ as recommended by BS 8110 (1997); $\sum 0_{bars}$ is the total perimeter of tension reinforcing bars; b_p is the plate width; and A_e is the area of concrete in tension as defined by Nawy (1992). For the current test beam configuration, A_e of 2100 mm^2 is determined as the beam width (100 mm) times the distance from the tensile face of the concrete to the centroid of the tensile reinforcement (21 mm).

Raoof treated the cracked concrete cover in the shear span as individual teeth, acting effectively as separates cantilevers under lateral shear stress at the plate-concrete interface as shown in Figure 6.3.

Once the maximum tensile stress at the reinforcement level (point A) reaches the concrete tensile strength, f_t', the brittle plate tearing off starts to initiate. The stress σ_A can be readily evaluate using the simple bending theory.

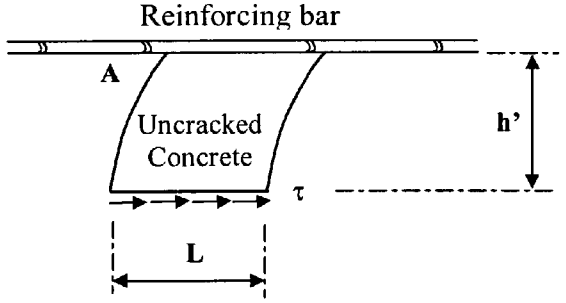

Figure 6.3 Concrete Tooth Between Two Stabilised Cracks (After Raoof *et al*, 2000)

$$\sigma_A = \frac{M_A(L/2)}{I_A} \tag{6.9}$$

where $I_A = bL^3/12$, and $M_A = \tau L b_p h'$.

At the instance of plate tearing failure, σ_A equals the concrete tensile strength f_t'. The shearing stress, τ, can therefore be expressed as:

$$\tau = \frac{f_t' Lb}{6h'b_p} \tag{6.10}$$

The ultimate shear stress sustained by the concrete between two adjacent cracks is proportional to the crack spacing L. Furthermore, the mean shear stress within the shear span is balanced by the axial stress in the plate. The effective length l_p of the plate in the shear span (Raoof and Zhang 1997) is given by the lower of the actual plate length in mm in the shear span, and the value $l_{p,2}$, which can be calculated from the following semi-empirical equations – whichever is smaller.

$l_{p,2} = l_{min}^p (21\text{-}0.25\, l_{min}^p)$, when $l_{min}^p \leq 72$ mm (6.11a)

$l_{p,2} = 3.0 l_{min}^p$, when $l_{min}^p > 72$ mm. (6.11b)

For FRP plates, these equations may be modified as:

$l_{p,2} = l_{min}^p (24\text{-}0.5\, l_{min}^p)$, $l_{min}^p \leq 40$ mm (6.11c)

$l_{p,2} = 4.0 l_{min}^p$, $l_{min}^p > 40$ mm. (6.11d)

The lower bound of the FRP plate tensile stress, $\sigma_{s(min)}$ can therefore be determined by

$$\sigma_{s(min)} = \frac{A_e (f_t')^2 L_p b}{6h' t_p (u \sum 0_{bars} + u_p b_p) b_p} \tag{6.12}$$

and the maximum plate axial stress $\sigma_{s(max)} = 2\sigma_{s(min)}$.

Assuming the average plate axial stress, σ_s, to be $1.5\sigma_{s(min)}$ and by rearranging Equation (6.12), Raoof recommended the following equation for determining the FRP effective plate length l_p.

$$L_p = \frac{15.47\sigma_s h' b_p t_p (u\sum 0_{bars} + u_p b_p)}{h_p b^2 f_{cu}} \qquad (6.13)$$

Raoof's approach provides an encouraging new path for understanding the premature failure behaviour. It is simple and realistic. It seems such a method has great potential to be incorporated into design guidelines. The downside of the method is that the difference between the two bounds, although appearing to have covered the actual failure load range, is too wide.

Consider beam A5 again, for example, the minimum axial stress in the CFRP plate is evaluated to be 234.8 N/mm^2 using Equation 6.12, and assuming an FRP-concrete bond strength of 1.0 N/mm^2. The average axial plate stress is therefore 1.5 times 234.8 N/mm^2, which leads to 352.2 N/mm^2. This stress is then used in conjunction with the non-linear material constitutive law based analytical model, which was developed in Chapter 5, to calculate the premature failure load. The above theoretical failure load is found to be 70.8 kN, while the actual recorded experimental value was 82 kN. It is worth noting that the maximum plate axial stress of 2 x 234.8 = 469.6 N/mm^2, would have resulted in a premature failure load of 86.4 kN, while the minimum plate axial stress would lead to a much lower failure load of 47.8 kN. This figure is approximately the same as the failure load of the unplated control beam. The actual failure load (82 kN) of beam A5, and indeed all other beams with tearing-off failure mode, is well within the range of the upper (86.4 kN) and lower (47.8 kN) bounds, but approaching the higher limit.

From a practical design point of view, such a wide scatter, although indicative and therefore helpful, does not provide sufficiently accurate and useful information for the prediction of premature failure load. It is therefore essential to find ways of narrowing down the bounds considerably.

6.4 EVALUATION OF FRP-CONCRETE BOND STRENGTH

6.4.1 The Need for The Test

For the method as outlined in Equations 6.12 and 6.13, an important unknown parameter is the bond strength, $\mathbf{u}_p$, between the FRP plate and concrete, For the natural bond strength between steel reinforcing bars and concrete, the value of **u** can be determined as $0.28(f_{cu})^{0.5}$ (Mosley *et al*, 1999). However, there exists no reported equivalent simple relationship for the FRP plate-concrete bond. To this end, an experimental investigation was carried out, in which 9 specimens were tested to evaluate this important property.

Currently there are no specific guidelines for determining the bond strength at the concrete FRP plate interface. BA 30/94 (1994) has a section on the method for determining the lap shear strength of adhesives to bright mild steel at a range of temperatures including –25°C, +20°C and +45°C. It states that the average minimum lap shear strength at 20°C should be 8 N/mm^2. The total bonding area is 4 × 40 × 25 = 4000 mm^2 as shown in Figure 6.4. This is a relatively small figure and the test results will not show any direct representation of the concrete FRP bond strength.

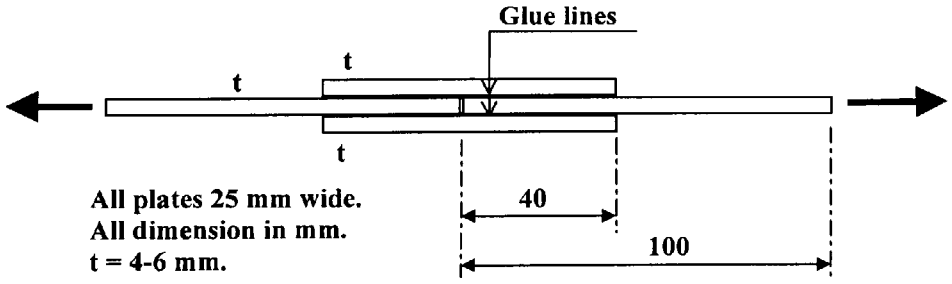

Figure 6.4 Lap Shear Test Overlap Joint (After BA 30/94, 1994)

In fact the manufacturer of Resifix 31 plate bonding adhesive system, which was used in the present test series, specified a lap shear strength to grit blasted steel of 14 N/mm^2 (Exchem, 1999). This is thought to be a rather high value, and for FRP plate to concrete bonding, a much lower bond strength is expected.

6.4.2 Experimental Evaluation

Figure 6.5 shows the schematic arrangement of the current testing mechanism, which was developed at the University of Glamorgan and adopted by the Concrete Society as a standard test configuration (Concrete Society, 2000). CFRP plates were bonded directly to the two concrete prisms, and a steel tension frame with large end bearing area was made to ensure that no local concrete shear failure would take place.

Similar to the BA 30/94 double lap shear test, there are 4 bond areas, each was strictly controlled to have a net contact area of 8000 mm^2. This was achieved by placing clear tapes at the edges of the bonding zone.

All bonding surfaces were wire brushed to remove any dirt and debris, and a high powered vacuum cleaner was then used to clear off the dust before bonding took place. The nine specimens were divided into three groups, with each group having an adhesive

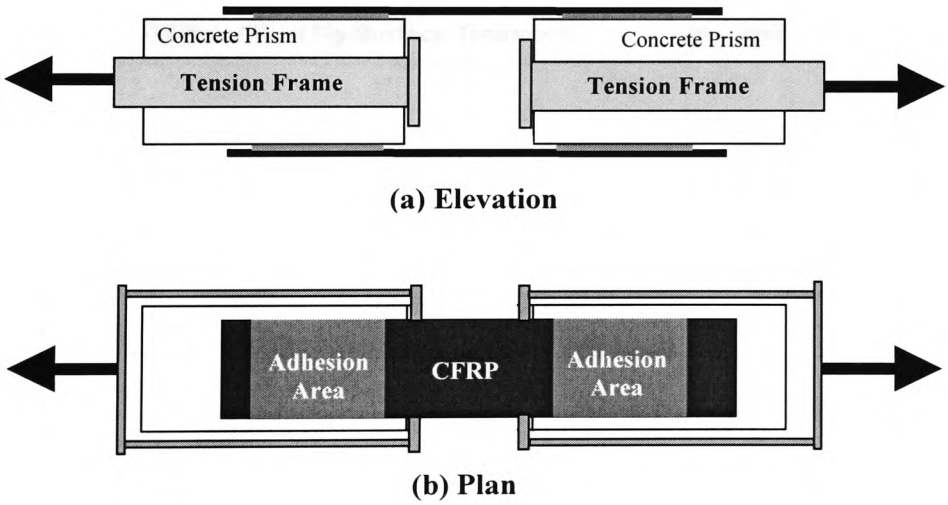

Figure 6.5 Schematic FRP-Concrete Bond Strength Test Configuration

thickness of 1.0, 2.0 and 3.0 mm respectively. Perspex thickness gauges were used outside each end of the bonding zone to ensure correct adhesive thickness, thus a total of 8 gauges were used for each specimen. The details of all test prisms are listed in Table 6.3.

Table 6.3 Details of FRP-Concrete Bond Strength Tests*

Specimen Ref.	Adhesive Thickness** (mm)	Type of CFRP Plate	Failure Load (kN)	Average Bond Strength (N/mm^2)
L1-1	1.0	B	44.63	1.39
L2-1	1.0	B	55.94	1.74
L3-1	1.0	A	37.18	1.16
L4-2	2.0	B	54.09	1.69
L5-2	2.0	B	58.86	1.84
L6-2	2.0	A	47.44	1.48
L7-3	3.0	B	59.56	1.86
L8-3	3.0	B	59.20	1.85
L9-3	3.0	A	46.97	1.47

* The characteristic strength of all concrete prisms is 39.4 N/mm^2. The elastic modulus of the type A and type B CFRP plates are 125 and 185 kN/mm^2 respectively. Type B plate had a 0.2 mm thick nylon peel ply on both surfaces, these were peeled off just before applying the adhesives.

** The epoxy adhesive system used was the Resifix 31, the properties of which were discussed in Chapter 3.

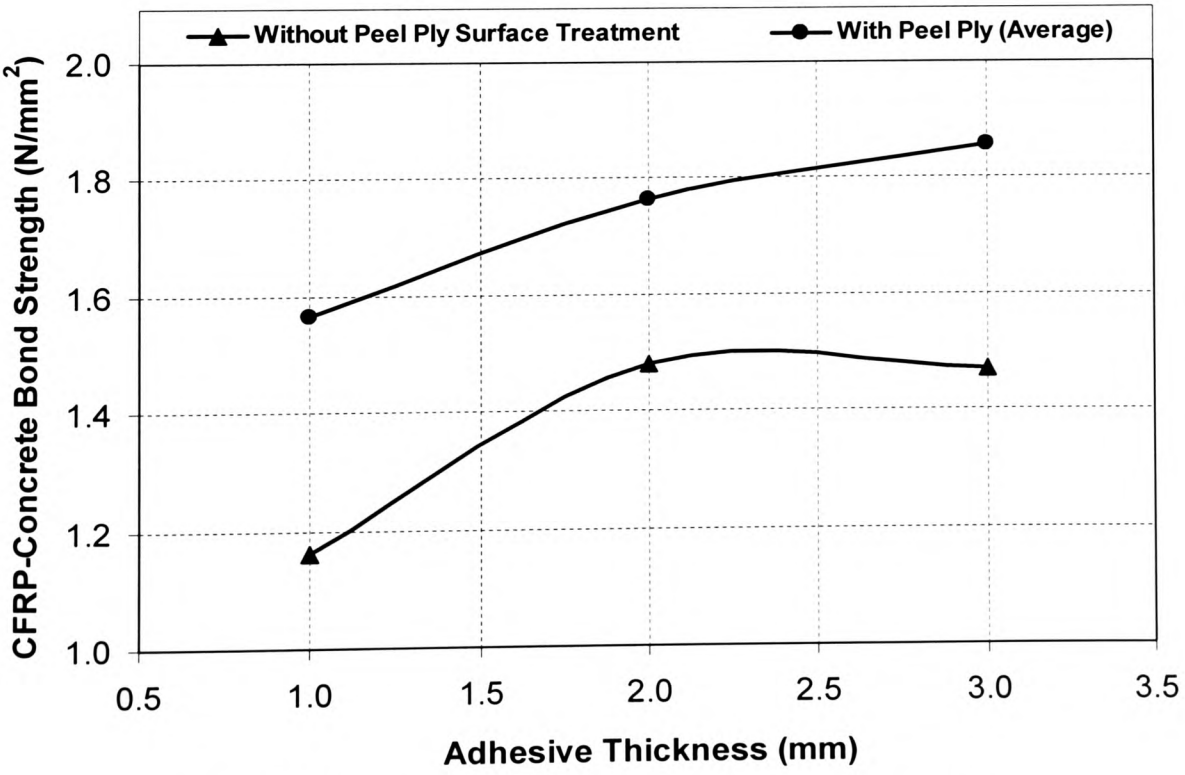

Figure 6.6 Comparison of FRP-Concrete Bond Strength

From these results, it can be seen that CFRP plates with peel-ply generally had higher bond strength to the concrete surface than those without peel ply surface treatment. Shown in Figure 6.6 is the comparison of bond strength for the two types of CFRP plates, the strength increase as a result of peel-ply surface treatment is 34%, 20% and 26% for the three adhesive layer thickness of 1.0 mm, 2.0 mm and 3.0 mm respectively.

From Figure 6.6, it is also apparent that the adhesive thickness influences the FRP plate-concrete bond strength. For both types of CFRP plates, the 1.0 mm adhesive thickness resulted in the lowest bond of 1.16 and 1.56 respectively. The strength increases with the thickness, but not directly proportional. It appears that for the non peel-ply plate, an adhesive thickness of 2.0 mm gives the highest bond strength, whilst for the peel ply plates, the highest bond strength was achieved when the bond layer was 3.0 mm thick. Although the 9 tests are rather limited in number, the results have clearly shown the influences of the adhesive thickness, and the advantage of peel ply surface treatment technique for FRP plates. The detailed study on this topic is out of the scope of the present research and will be carried out elsewhere in the future. Based on the observations of the current tests, and in the absence of more substantial data and more rigorous analysis, the following equations are suggested for determining the CFRP plate-concrete bond strength.

For CFRP plate without peel ply surface treatment protection:

$$u_p = 0.18\sqrt{f_{cu}}(t_a)^{0.25} \quad (t_a \leq 3) \tag{6.14a}$$

For CFRP plate with peel ply,

$$u_p = 0.22\sqrt{f_{cu}}(t_a)^{0.25} \quad (t_a \leq 3) \tag{6.14b}$$

For a typical concrete strength of 45 N/mm^2 in the present study, and with non peel ply CFRP plate, Equation (6.14a) produces a bond strength of 1.44 N/mm^2 for an adhesive thickness of 2.0 mm.

It is interesting to note that Raoof and Hassanen (2000) recommended a bond strength $\mathbf{u_p}$ of 0.8 N/mm^2, which is also the value recommended by BS 5400 (1990) as the allowable shear stress between the *in-situ* and the precast concrete surfaces for grade 40 concrete or greater. These figures appear to be too low, the impact of which is that the minimum plate axial stress, as determined by Equation 6.12, will increase with the reduction of $\mathbf{u_p}$. The bond strength value of 0.8 N/mm^2 is almost certainly the lowest possible, provided of course, that proper concrete surface pretreatment had been carried out and the correct adhesive bonding procedure had been followed. Any increase of FRP-concrete bond strength over and above 0.8 N/mm^2 will result in reduced plate axial stress, and thus the reduction in the predicted premature failure load. The lower bound is then further lowered down to, perhaps, even more unrealistic levels.

6.5 A NEW METHOD FOR DETERMINING FAILURE LOAD

In Raoof's method, the axial plate stress and hence the premature failure load is essentially governed by the spacing of the stabilised cracks. The value of such spacing is variable and depends on the steel reinforcement-concrete and FRP plate-concrete bond strength among many other factors. According to equation (6.8a), the minimum spacing of cracks is around 25 mm, this figure is much smaller than what is found in the present study. For all the CFRP plate (type A) strengthened beams tested in the present study, it was found that the number of flexural cracks in the constant moment zone varied from 20 to 30. This gives a cracking spacing of between 42 and 63 mm, far greater than the 25-50 mm predicted by the Watstein and Parson (1943) theory, which was originally developed for embedded steel reinforcement only. For external FRP plate bonding this equation may be modified as follows.

$$l_{\min}^{p} = \frac{A_e f_t^{'}}{(u\sum 0_{bars} + \alpha_p u_p b_p)} \qquad (6.15)$$

where α_p is the modification factor to take account of differences in the bond mechanism between externally bonded and internally embedded reinforcements. For the

present testing series, it seems that a value of 0.4 is appropriate, and will result in typical crack spacing of around 35 mm in the constant moment zone.

It is also worth noting that without external FRP plate, Watstein's equation predicts a minimum crack spacing of 44 mm for the current test beams. In other word, the externally bonded CFRP plate (without peel ply) should result in seven more cracks, on average, than the unplated control beam within the constant moment zone. This seems indeed to be the case for the five beams (A1 – A5) which were plated with 2.2 m long non peel ply CFRP plate as discussed in Chapter 4.

Based on the above discussions, Raoof's lower bound theory is suggested to be replaced by an average axial plate stress approach. The average axial stress is, as recommended by Raoof, 1.5 time of the minimum axial stress. Equation (6.12) may therefore be modified as follows for non peel ply CFRP plated RC elements.

$$\sigma_{p,av} = \frac{0.25A_e(f_t')^2 L_{pe} b}{h' t_p (u\sum 0_{bars} + 0.18\alpha_p \sqrt{f_{cu}}(t_a)^{0.25} b_p) b_p} \qquad (6.16)$$

and for CFRP plate with peel ply surface treatment,

$$\sigma_{p,av} = \frac{0.25A_e(f_t')^2 L_{pe} b}{h' t_p (u\sum 0_{bars} + 0.22\alpha_p \sqrt{f_{cu}}(t_a)^{0.25} b_p) b_p} \qquad (6.16b)$$

The effective length L_p in Raoof's original equation should, however, be replaced by the new effective length L_{pe}, which is taken as:

$$L_{pe} = \omega L_{cm} - b \qquad (6.17)$$

where L_{cm} is the length of the constant moment zone, b is the beam width, and ω is the effective length factor depending on the point load location and the actual FRP plate length. For the current test beam set out, ω is suggested to be 0.5 for the 2.2 m long plates and 0.40 for the 1 m long plates that terminate in the constant moment zone.

In Raoof's equations, L_p is defined as the plate length in the shear span, ie, from the point of plate termination to the nearest point load application position, or as defined by Equation 6.1 whichever is smaller. This condition would severely restrict the application scope of the theory. For instance, if the plate is terminated at a very short distance outside the constant moment zone, the resulting axial stress in the plate would be very small. As a result, the predicted failure load could be as low as, or even lower than that of the unplated control beam, which is obviously not the case.

6.6 VALIDATION OF THE MODIFIED SEMI-EMPIRICAL METHOD

The validity of the above proposed method was tested, using data from the seven beams that failed by tearing-off of concrete cover in the laboratory tests. In Raoof's original theory, only the axial stress range was estimated, and not the actual failure load. The non-linear material constitutive law based model developed in Chapter 5 was therefore used to calculate the premature failure load. The results are listed in Table 6.4.

Table 6.4 Comparison of the Actual and Predicted Premature Failure Load*

Beam Ref.	f_{cu} (N/mm^2)	Actual Failure Load (kN)	Predicted ** Failure Load **(Raoof's Lower Bound)**		Predicted ** Failure Load **(Present study)**	
			$\sigma_{s(min)}$ (N/mm^2)	P_u (kN)	$\sigma_{p,av}$ (N/mm^2)	P_u (kN)
A1 (2.2 m plate)	54.9	76.2	193.1	41.8	402.1	77.1
A2 (2.2 m plate)	44.6	73.8	181.1	39.5	363.1	69.2
A3 (2.2 m plate)	48.9	89.9	182.3	39.7	380.3	72.8
A4 (2.2 m plate)	49.6	74.4	191.8	41.5	383.0	73.6
A5 (2.2 m plate)	49.6	82.0	191.8	41.5	383.0	73.6
A6 (1.0 m plate)	44.6	62.0	186.9	40.4	280.1	58.2
A7 (1.0 m plate)	48.9	59.1	186.9	40.4	301.9	59.7

* Material properties used: t_a = 2.0 mm; t_p = 1.6 mm; A_e = 2100 mm^2; h'= 21 mm; L_{cm} = 1.25 m; α_p = 0.4; u = $0.28(f_{cu})^{0.5}$; f_t'=$0.36(f_{cu})^{0.5}$; b = 100mm; u_p from Equation 6.14a; b_p = 80 mm; ω = 0.5 for 2.2 m plate; ω = 0.40 for 1.0 m plate.

** The predicted failure loads were evaluated based on the non-linear model developed in Chapter 5, and using the axial plate stress from Raoof's lower bound theory, and the current modified semi-empirical approach respectively.

It can be seen from these results that the modified semi-empirical approach leads to more realistic results than Raoof's original predictions. There is still however a need to check the validity of the new approach extensively against further laboratory test results with variations of all major parameters.

6.7 PREVENTION OF PREMATURE TEARING-OFF FAILURE

The preceding sections discussed and established some semi-empirical methods in determining the plate tearing-off stresses, and the load that causes such premature failure. It was shown that the linear elastic theory based approaches do not necessarily predict plate end stresses to a satisfactory level of accuracy. The determination of failure load by the proposed semi-empirical method, although leads to more realistic predictions of failure load, still lacks the accuracy required for practical design purposes. On the other hand, even if the premature failure load is accurately determined, it does not solve the whole problem. This is because no preventative measures will be identified by predicting just the failure load. A common solution is to extend the FRP plate to as close to the supports as possible, thus the long anchorage length is expected to "prevent" the premature failure of concrete cover tearing-off. However, current tests have shown that this method was not reliable. The anchorage length for beams A1 to A5 was essentially the maximum value possible, with only 100 mm distance from the centre of supports at both ends, but this maximum anchorage did not prevent these beams from premature failure.

It is therefore essential to analyse why premature tearing-off occurs, and whether or how it could be prevented, or, at least, delayed.

Consider a section of a strengthened concrete beam in the shear span as shown in Figure 6.7, the stresses at all three interfaces are shown. The normal stresses are expected to be of small magnitude as the flexural stiffness of the FRP and the adhesive layer is insignificant in comparison with that of the concrete beam. If any of the interfacial shear stresses due to the applied load exceeds the concrete tensile strength, the tearing-off failure is expected to initiate.

As explained by Raoof's "tooth theory" (Raoof and Hassanen, 2000), the maximum shear stress is likely to occur at the "fixed-end" of the cantilever, that is, at the embedded steel reinforcement level, or τ_3 in Figure 6.7.

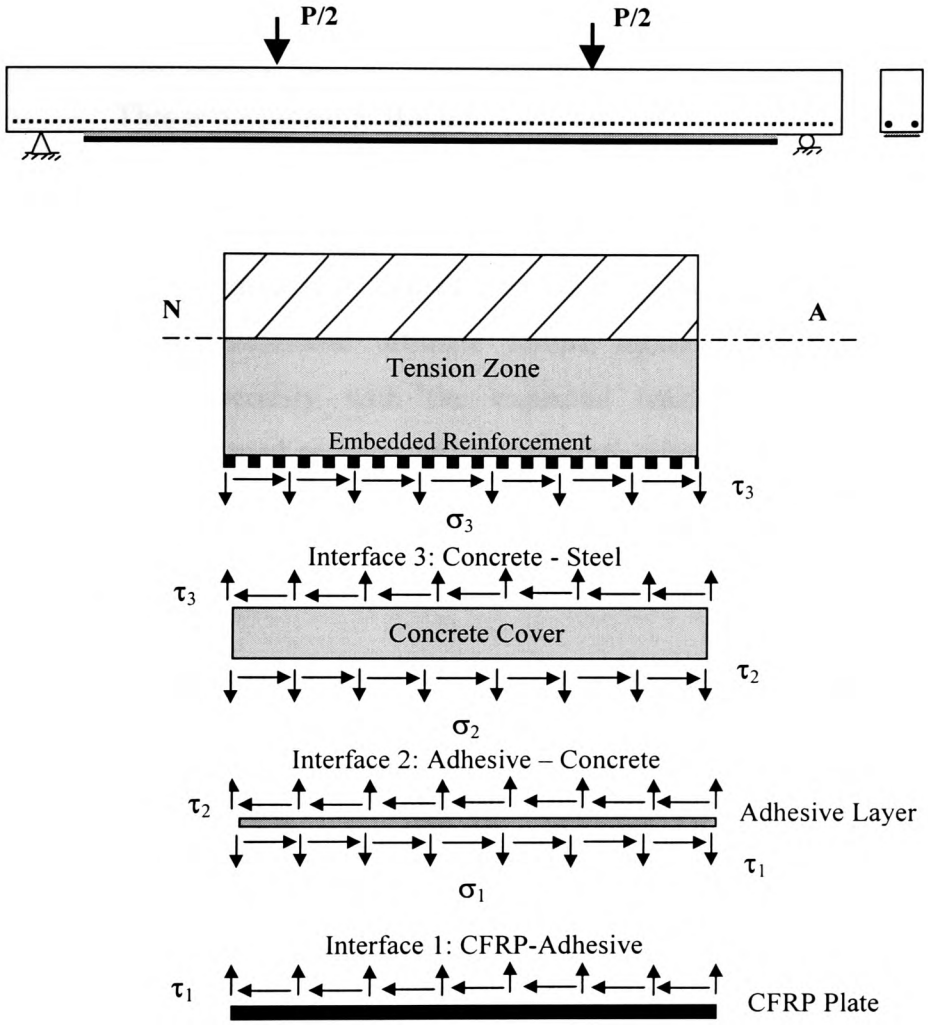

Figure 6.7 Interfacial Normal and Shear Stresses in CFRP Strengthened Beam

In order to prevent the premature tearing-off failure, there are three possible options to be considered in design:

(a) *Passive Prevention* – As discussed in the preceding section, the failure load is predicted based on semi-empirical approaches. Various parameters including the FRP anchorage length is optimised to achieve

the greatest value of failure load, and the design ultimate load is then limited to this value.

(b) *Delay or Change of Failure Mode* – By applying a plate end anchorage system, which either delays the premature failure mechanism, or changes it to another failure mode such as crushing of concrete in compression. This is discussed in the following section.

(c) *Optimised Design Approach* – In such cases the elements are strengthened such that no premature failure will occur. In other words, the conventional ultimate failure mode will take place **before** or simultaneously with the expected tearing off failure. The under-strengthened sections will satisfy this criterion, as is discussed in design related Chapter 8.

6.8 EFFECT OF END WRAPPING ANCHORAGE

In steel plate bonding, bolts are usually used at the plate ends to help hold the heavy plate in place, and also to act as end anchorage so that premature tearing-off type of failure is prevented. The bolting mechanism is effective but the process involves extensive labour. In some cases where the internal reinforcing bars are closely arranged, it may also damage the structural integrity of the existing member due to the requirement of drilling bolt holes. In FRP composite strengthening, bolt anchorage is not viable. This is not because there is no need for it, but because of the unidirectional structure of the FRP plates, which is not suitable for drilling. The out-of-plane shear resistance of FRP plates or fabric layers may be regarded as negligible, thus no shear transfer along the longitudinal fibre interface can take place.

Wrapping the FRP prelaminated plates or the wet-lay fabric layers at the cut-off ends using the FRP fabrics is then considered an alternative. In the present study, the three continuous beams (M2, M3 and M4), and seven simply supported beams (A6, B1-B6) were wrapped using either single layer CFRP or Kevlar fabrics at the plate cut-off

positions. None of these beams had shown any similar drastically brittle failure mechanisms as seen in most of the group A beams.

Shown in Figure 6.8(a) is the failure mode of beam A6. The one metre length CFRP plate within the constant moment zone was wrapped around with two layers of continuous Kevlar sheets at both ends. The adhesive used was the same as applied in the plate bonding, namely, Resifix 31. It should be noted that Resifix 31 should normally be applied only to prelaminated FRP plate. In this case, it was used instead of the wet-lay epoxy resin. The purpose of the end wrapping was to delay the brittle tearing-off failure, and enable the large elastic energy stored in the plate-end vicinity to be gradually released. The composite wrapping "holds" the plate in place so that an artificial "buffer zone" may be created. The adhesive thickness was about 1.0 mm and no prestress was applied to the 100 mm wide Kevlar fabric sheet. It was observed that a single, large tearing-off shear crack was developed at the plate end just before the ultimate failure. As the load increased, the crack propagated further and the Kevlar wrapping was seen to gradually peel off the adhesive. As can be observed from the picture, the final failure mode was mild and gradual, which was in direct contrast to beam A7 that failed in a very brittle manner as discussed earlier.

In Figure 6.8(b) the final failure mode of beam B1 is shown. The beam was wrapped with singly layer U-shaped CFRP fabrics, and the adhesive used was the "Selfix Carbofibe laminating Resin" specifically developed for wet-lay FRP fabric bonding to

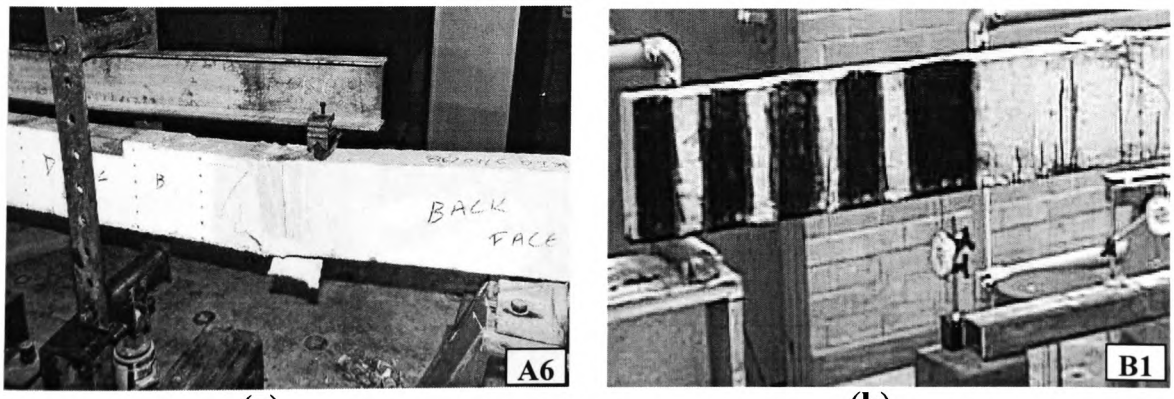

(a) (b)

Figure 6.8 End Wrapping at plate cut-off locations
(a) Kevlar round wrapping; (b) CFRP U-shaped wrapping

concrete surfaces. No buffer zone was available at the concrete FRP interface. It can be seen that the tearing-off failure mode did not materialise, instead, the beam failed by the crushing of concrete in the compression zone. The presence of well bonded U-shaped CFRP strips influenced the distribution of the normal and shear stresses at the plate cut off vicinity, and changed what may have been a tearing-off failure mode into a compression failure mechanism.

In essence, the function of the FRP wrapping strips is not dissimilar to that of the bolts in steel plate bonding. The normal (tearing) stress component induced in the flexural plate is partially transferred to the wrapping FRP strips. The transverse shear stress is resisted mainly by the FRP composites if the they are wrapped around in closed and overlapping loops. In this case, the four corners of the wrapped beam seemed to attract most stress concentration, as was seen in beam M3 (see Chapter 7) where the wrapping CFRP strips actually failed in tension at these corners. However, in practice it is not always possible to wrap around an existing beam. The U-shaped wrapping has to be introduced, in which case the transverse shear is resisted by the FRP composites as well as the concrete layer closest to the web surface through the adhesive bonding. At ultimate failure, the FRP strips appeared to be intact but a new form of tearing-off can be seen. Shown in Figure 6.9 are two CFRP strips taken off beam B2 after its ultimate failure in its shear span, it can be seen clearly that a thin layer of concrete is well attached to the CFRP strips, indicting that a concrete transverse shear failure had occurred.

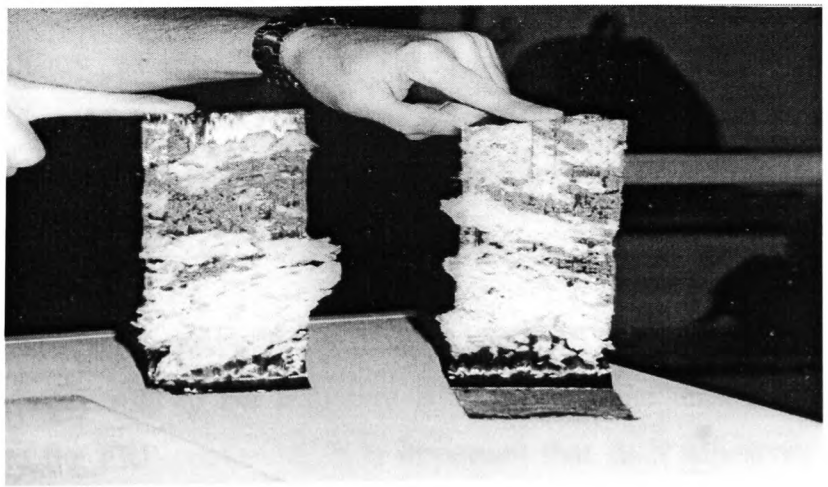

Figure 6.9 Failure mode of U-shaped CFRP Wrapping Strips (Beam B2)

6.9 CONCLUSION

Tearing-off of concrete cover at the reinforcement level is a major type of failure mechanism for FRP strengthened RC beams. It is brittle, sudden and often drastic as seen in the laboratory tests, and should therefore be avoided and prevented in strengthening design. Such a failure mode is rather different from that of a peeling-off of FRP plate, which is usually due to weak adhesive layer. The principle causes for the brittle tearing-off failure mode can be summarised as follows:

For a loaded beam strengthened by FRP plate, the over strengthened section will result in a large amount of stored elastic energy. The stress concentration at the plate cut-off location leads to high magnitude of normal and shear stresses at the adhesive joint. The weakest member among concrete, adhesive and FRP composite will fail once its "tearing" strength is reached. The cracked concrete segments in the cover layer may be treated as individual cantilevers with the fixed-end at the steel reinforcement level, where the concrete horizontal stress is at its maximum, as discussed in Section 6.3.3. It is therefore natural that tearing-off failure should initiate in concrete at the internal steel reinforcement level, if the adhesive layer has higher tensile and shear strengths than those of the concrete.

The strength of a bonded joint will be determined by the strength of its weakest component, which should generally be designed to be the adhesive layer (Mays and Hutchinson, 1992). However, the typical FRP plate bonding adhesives used today in the construction industry, as shown in Table 6.5, have much higher tensile and shear strengths than that of the concrete. Mismatch of the properties at the bond line inevitably results in large interfacial stress concentration, and thus the occurrence potential tearing-off failure.

It is therefore essential to ensure that a suitably specified adhesive is used for a given case. As the primary role of the adhesive is to transfer the tensile stress from the concrete beam to the FRP composite, it is important that such adhesives exhibit high tensile and shear strengths. In order to achieve a compromise between the requirements of high strength and acceptable flexibility, so that elastic energy may be partially

released to avoid excessive stress concentration, it may be desirable to use a layer of primer as one component of the adhesive joint. The primer may be designed to act as the weakest link in the joint.

Table 6.5 Comparison of Typical Material Properties for RC Strengthening

Property	Epoxy Adhesives	Concrete	Mild Steel	UD CFRP Composites
Young's Modulus (kN/mm^2)	1-10	15-40	200	150-230
Tensile Strength (N/mm^2)	12-40	1.5-4.0	460	1500-4500
Tensile Strain at Break (%)	1-4	0.16	10-30	1.2-2.0
Relative Density	1.3	2.3	7.8	1.5
Coefficient of Thermal Expansion ($10^{-6}/°C$)	35	10	11	0.3

Based on the experimental evidence and the discussions presented in this Chapter, the following conclusions may be drawn.

- The few existing theories in predicting the stress concentration values for FRP bonded RC beams seem to produce vastly variant and unrealistic results. Consequently these theories cannot be used for design purposes. The main reason for the resulted inaccuracies can be attributed to the existing theories all assuming elastic behaviour of the adhesive joint. It is clear that cracked concrete does not behave elastically, and the adhesive bonded joint of concrete and FRP composite should exhibit non-linear characteristics.

- The failure load of a "tearing-off" mode may be reasonably estimated using the modified semi-empirical approach as discussed in Section 6.5.

- The premature tearing-off failure mode is influenced by the amount of FRP cross section area provided. Tearing-off is more likely to occur in over strengthened sections than in under strengthened beams.

- The end wrapping of the main strengthening FRP composites with the FRP fabric sheets, either in closed loops or U-shaped wrapping, can delay and contain the tearing-off failure mode, and make the failure appear effectively more ductile than those beams without end wrapping.

- Wrapping around the plate end can also change the failure mode from the very brittle tearing-off to a less brittle compression failure of concrete. However, such concrete crushing failure mode is still unacceptable and should be avoided if possible.

- Over strengthened sections result in large amount of stored elastic energy, and when suddenly released at the premature failure, leads to explosive type of brittle failure as seen in the laboratory tests. It is therefore important to avoid, whenever possible, over strengthened sections in order to ensure that the strengthened beams exhibit acceptable ductility.

CHAPTER 7

Ductility and Moment Redistribution of FRP Strengthened RC Beams

7.1 DUCTILITY

The word ductility comes from its Latin origin *ductilis*, which is described by the Chambers Science and Technology Dictionary as the "ability of metals and alloys to retain strength and freedom from cracks when shape is altered." Today it is being interpreted to describe the ability of any material to sustain plastic deformation before fracture. In this chapter, the term "ductility" strictly refers to the structural ductility of RC elements or FRP strengthened RC members. Concrete itself is a rather brittle material, nevertheless, it is generally accepted that conventionally reinforced concrete members can attain suitable ductile behaviour by proper design and detailing of steel reinforcement. The yield point of steel is thus treated as an important datum beyond which inelastic deformation of the RC member takes place, thus enabling the full stress and strain capacity of concrete to be developed before ultimate failure.

Since the early 1990s, the viability of using non-metallic FRP reinforcement instead of the conventional steel reinforcing bars has been widely researched (Clarke, 1993). It is recognised that FRP reinforced concrete members behave differently from the steel

reinforced counterparts, due to the linear elastic stress-strain characteristics of the composites up to failure. The question of ductility for FRP reinforced concrete elements has, naturally, been a topic of debate among many researchers (Saadatmanesh *et al,* 1994; Naaman *et al*, 1995; Swamy *et al*, 1996; Grace *et al*, 1998; Mirmiran *et al* 1999). Despite these attempts to address the issue, there is, to date, still a distinctive lack of general agreement as to how the ductility characteristics of such elements may be quantified and analysed.

As for the ductility of FRP strengthened RC elements, there have been relatively fewer research activities focused on this important area (Razaqpur *et al* 1996; Aridome *et al*, 1998; Pisanty *et al*, 1998; Grace *et al*, 1999). Yet, consideration of structural ductility is of predominant importance to any structural designer, as all appropriately designed structures must attain sufficiently ductile behaviour under ultimate design loads. This is to ensure the redistribution of internal forces in a statically indeterminate structure when part of the structure reaches its ultimate capacity, and to provide sufficient warning so as to prevent the structure from sudden and brittle failure.

7.2 TRADITIONAL METHODS FOR DUCTILITY CALCULATION

From a structural design view point, ductility has been traditionally defined as the ability of a structure to sustain deformation before its failure under ultimate load (Park and Paulay, 1975). Kemp (1998) described ductility as the "inelastic rotations through which critically stressed regions of a beam can deform in flexure before a loss of moment capacity occurs".

It has been generally accepted that ductility can be measured by a dimensionless factor, often referred to as the ductility index, in several different forms within two broad categories.

7.2.1 Deformation Based Methods

Firstly, the deformation-based approach, which has been widely used, can be summarised as follows. The ductility index (φ) of a structural element is determined as the ultimate deformation (Δ_u) divided by the corresponding values of deformation at the material yield point (Δ_y), and may be expressed as:

$$\varphi = \frac{\Delta_u}{\Delta_y} \tag{7.1}$$

The yield point, in the case of RC elements, is the point when the steel reinforcement starts yielding for under reinforced sections. The broad term of deformation is a generic description of deflection, rotation, curvature or compressive strain.

Aburawi (1997) also used a different form of curvature ductility index, suggested by Professor Swamy of Sheffield University, which is defined as follows:

$$\varphi = 1 + \frac{M_u - M_y}{\chi M_y} \tag{7.2a}$$

$$\chi = \frac{(EI)_2}{(EI)_1} \tag{7.2b}$$

where χ is the ratio of flexural rigidity after yielding $(EI)_2$ divided by the pre-yielding value $(EI)_1$ as shown in Figure 7.1.

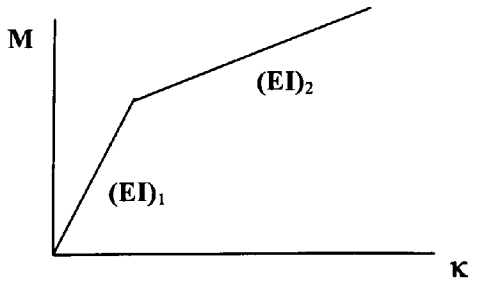

Figure 7.1 Simplified Moment-Curvature Relationship

7.2.2 Energy Based Approach

The second approach is energy based, whereby the total energy of a deformed element is divided by a reference value at an arbitrary reference point, such as 75% of the ultimate load as suggested by Aburawi (1997):

$$\varphi = \frac{E_{total}}{E_{0.75P_u}} \tag{7.3}$$

The quantity of energy may be obtained by integrating the area under the load deflection curves of the beam considered. This method is in fact a variant of the deformation based approach, and is only valid if the materials of the structural element exhibit elastic-plastic behaviour. The reference point of 75% of the ultimate load is, nevertheless, somewhat arbitrary.

7.3 DEFORMABILITY AND DUCTILITY

7.3.1 The Need for a New Definition of Deformability Index

For concrete elements reinforced by internal FRP reinforcement, or RC members strengthened by external FRP composites, the structural ductility can no longer be expected to be reasonably assessed by any of the above methods as prescribed by Equations (7.1) – (7.3). Consider beams A3 and A5 in the current study, for example, the respective ductility indices, using these equations, would be as listed in Table 7.1, together with that of the unplated control beam.

Table 7.1 Comparison of Ductility Index by Conventional Methods

Beam Ref.	Deflection Based φ_δ	Strain Based φ_{strain}	Curvature Based φ_c
Control	2.82	1.97	6.12
A3	1.41(*1.87*)	1.25 (*2.12*)	3.78
A5	1.50 (*2.14*)	1.31 (*2.18*)	3.83

* Values in brackets are predicted maximum achievable if premature tearing-off failure was avoided.

In Table 7.1, the values of deflection and strain based ductility indices were obtained using Equation (7.1), while the curvature based values were calculated using Equation (7.2), which appear to provide much higher values than the figures in the first two columns. Had Equation (7.1) been used for curvature based ductility, these answer would be of similar order as the deflection based values. The yield point of the control beam was conveniently located from the load deflection and moment curvature graphs as presented in Chapter 4. For the CFRP plated beams, A3 and A5, however, there is no apparent yield point, and the identification of Δ_y values is difficult. For the purpose of comparative calculations in Table 7.1, the internal steel reinforcement yield point was identified, using the non-linear model developed in Chapter 5. The values of the corresponding load, and hence the deflection, strain and curvature were then calculated to derive the ductility indices.

As can be seen from these results, the "ductility indices" of the CFRP strengthened beams appear to be of acceptable level in comparison with the under reinforced control beam. The implication of it is that these beams should fail in a ductile manner under ultimate load. However, the actual failure mechanisms of these beams were very sudden and brittle as described in Chapter 4. This was because the relatively large deformation in the beams was not inelastic, and a great amount of elastic strain energy had been stored in the strengthened beams. Although the cracking of concrete in the tension zone, and some plastic deformation had dissipated part of the elastic energy, a substantial amount still remained in the system until the ultimate failure, as shown in Figures 7.2 and 7.3. The elastic energy is the area subtended by curve **A'BC**. Such a large amount of unconsumed energy, when released at beam failure, would naturally result in the brittle and catastrophic type of failure as illustrated in Figure 6.1.

Based on the relatively large beam deformation at failure, it has been claimed (Razaqpur *et al*, 1996) that FRP strengthened elements exhibit good ductility characteristic. This is only partly true and could lead to serious misconception, and indeed a rather dangerous one. The large deformation may be due to the lower modulus of elasticity of FRP composites, but the energy stored in the system remains largely elastic. To consider ductility of FRP strengthened RC elements in the traditional context is no longer suitable.

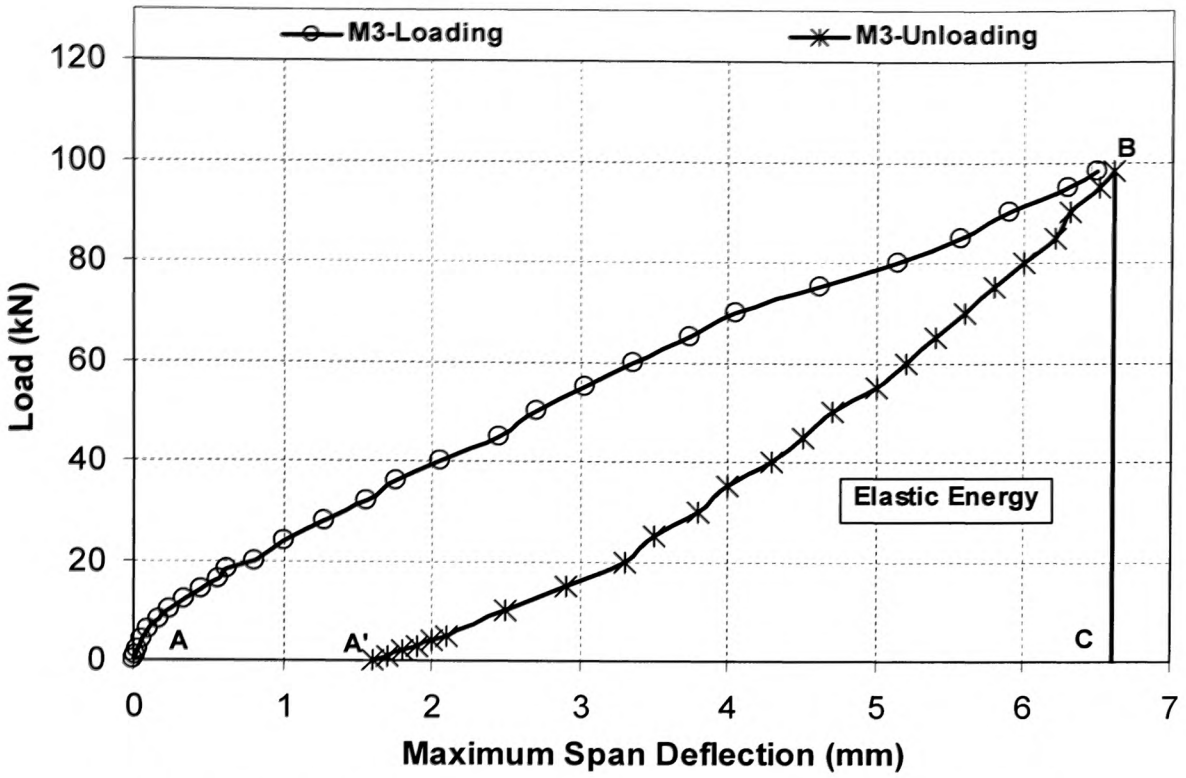

Figure 7.2 Loading-Unloading Cycle of Beam M3 (up to 98.6 kN)

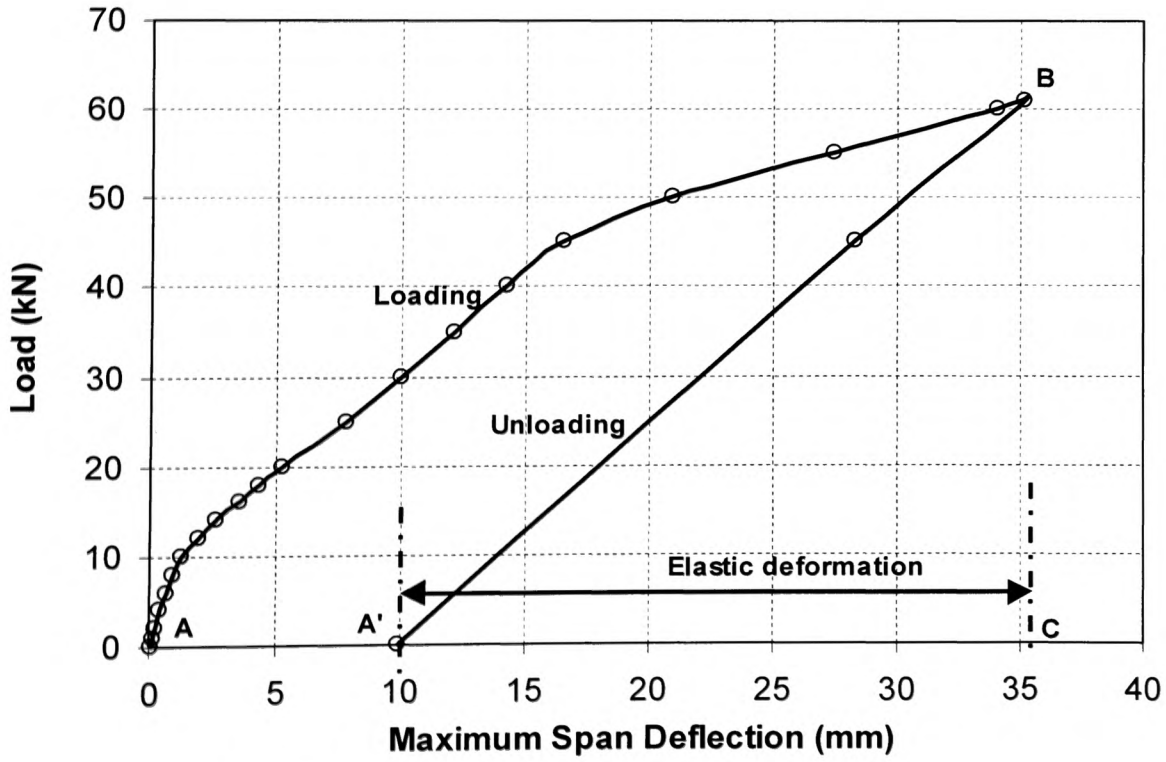

Figure 7.3 Loading-Unloading Cycle of Beam B6

An alternative terminology must be used to difine the deformation characteristics of FRP strengthened beam. Lees (1997) used the term "rotational capacity" to distinguish deformation from ductility. However, the word rotation could be misleading in that it may be interpreted as to refer only to rotating of the beam and not deflection or strain deformation.

A more appropriate description is therefore needed for use with FRP strengthened elements undergoing large deformation under load but not necessarily high ductility. The candidate suggests that the term "deformability index" should be used. Deformability index, φ_{df}, may be defined as the ratio of ultimate deformation to the deformation at a reference point as follows:

$$\varphi_{df} = \frac{\Delta_{0.95P_u}}{\Delta_s} \tag{7.4}$$

where $\Delta_{0.95Pu}$ is the generic deformation at 95% of the pre-peak load, which may include deflection, rotation, curvature or compressive strains, and Δ_s is the corresponding value of deformation at the reference point.

The figure of 95% of pre-peak load is suggested. This is because it has been observed during the laboratory tests that the ultimate deflection in the beams could be greatly influenced by the load rate and general configuration of the testing system, and may not accurately reflect the mechanical characteristics of the beam. The ductility index at 100% of ultimate load could be up to as high as 4-5 times that of the same beam at 95% of failure load. For the tests performed in this study, the load-control configuration was used, and deformation corresponding to 95% of the ultimate load was found to be more representative than the actual final load-deflection reading, which depends heavily on the actual failure position and mode.

As for the reference point for deformation, there exists no apparent yield point for the strengthened beam. Even though the yield point of the steel reinforcement may be identified through instrumentation or analytical modelling, the overall load-deflection response curves of FRP strengthened beams do not show any easily identifiable "kinks" at steel yielding. This is due to the higher strength of the strengthening composites,

which "overwrites" the steel yield characteristics through its own increase in stress to "make up" for the lost capacity, after the steel has yielded. At first, the deformation at the serviceability limit state was considered, for example, BS 8110 (1997) recommended maximum beam deflection at $\frac{1}{250}$ of the effective span was used as Δ_y (Tann and Delpak, 1999, 2000) to evaluate ductility index. However, the serviceability requirements vary with different national codes and boundary conditions, and thus may not objectively reflect the beam deformability or ductility. After careful consideration and comparison it was found that the deformation corresponding to the service load is best suited to be the denominator for the deformability index calculation, and the service load W_s is unfactored as defined by:

$$W_s = \frac{(1+\varpi)}{3} W_u \tag{7.5}$$

and $\varpi = \frac{Q_k}{G_k}$ is the ratio of imposed load to dead load. For the special case of $\varpi = 1$, then W_s is 67% of the design ultimate load W_u, which is defined as $W_u = 1.4G_k + 1.6Q_k$ in accordance with BS 8110.

For typical concrete buildings (e.g., office blocks, schools and other commercial concrete structures), if the imposed load is assumed to be around 60% of the dead load, then $\varpi = 0.6$, and W_s is still approximately 67.8% of the ultimate design load. It is therefore reasonable to define the reference deformation Δ_s as the corresponding values of deflection, rotation, curvature or strain at two thirds of the maximum ultimate design load.

7.3.2 Ductility for FRP Strengthened Beams

Clearly, deformability is not necessarily ductility. There is a need to establish a new methodology for determining a ductility index for FRP strengthened RC elements. Consider an idealised load-deflection response as shown in Figure 7.4. The total energy

$\mathbf{E}_{tot}$ and the elastic energy $\mathbf{E}_{el}$ are the work done under the total and elastic deformation respectively. For a maintained level of deformation Δ_u, this can be written as:

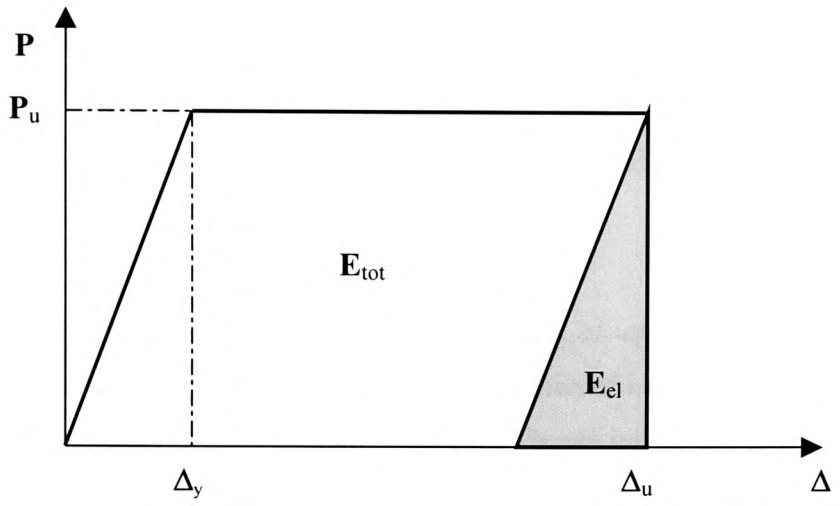

Figure 7.4 An Idealised Load-Deformation Relationship (Loading-Unloading Cycle)

$$E_{tot} = P_u\Delta_u - \tfrac{1}{2}P_u\Delta_y \qquad (7.6a)$$

$$E_{el} = \tfrac{1}{2}P_u\Delta_y \qquad (7.6b)$$

Combining Equations (7.6a) and (7.6b), the ratio of total energy to the elastic energy is therefore:

$$\frac{E_{tot}}{E_{el}} = \frac{P_u\Delta_u - \frac{1}{2}P_u\Delta_y}{\frac{1}{2}P_u\Delta_y} = 2\frac{\Delta_u}{\Delta_y} - 1 \qquad (7.6c)$$

Substitute the traditional definition of $\varphi = \dfrac{\Delta_u}{\Delta_y}$ into Equation (7.6c) and rearrange the equation, the new form of energy based ductility index, φ_{du}, can now be expressed as:

$$\varphi_{du} = \frac{1}{2}\left(\frac{E_{tot}}{E_{el}} + 1\right) \qquad (7.7)$$

This method was first published by Naaman and Jeong (1995). For an ideal elastic-plastic material, Equations (7.7) and (7.1) lead to exactly the same value, whilst for a material such as FRP composites with linear stress-strain responses up to failure, Δ_u equals to Δ_y, and the ductility index becomes unity, indicating that the element possesses virtually no ductility.

Grace *et al* (1998) used an "energy ratio" method to quantify ductility of FRP reinforced beams. The energy ratio is defined as the ratio of inelastic energy to the total energy. If the energy ratio is 75% or greater then the beam will exhibit a ductile failure. Fundamentally, there is no difference to the above procedure, Grace's method is in effect a reversed form of the Naaman and Jeong (1995) approach. If the energy ratio is 75%, than, E_{tot}/E_{el} would be $\frac{1}{(1-0.75)} = 4$, and the ductility index as determined by Equation (7.7) would be 2.5, which is naturally a indication of acceptable ductility.

It is therefore recommended that the Naaman and Jeong (1995) method should be used in determining structural ductility for FRP strengthened RC members. However, there are practical difficulties in identifying the elastic stored energy for such members. The only definite measure is to load test the beam, and then unload at just before failure.
Yet it is not always possible to predict when the exact failure will occur, especially given that premature failure is difficult to predict as shown in Chapter 6. Naaman and Jeong suggested that the elastic energy could be estimated using an equivalent triangle area under the load-deflection curve. The two initial slops S_1 and S_2 of the load-deflection curve were weighted to define slope S for the equivalent unloading response. Consider beam M3 again for example, the original load-unload cycle (Figure 7.2) is replaced in Figure 7.5, and the equivalent unloading slope is determined using the following equation:

$$S = \frac{P_1 S_1 + (P_2 - P_1) S_2}{P_2} \qquad (7.8)$$

It can be seen the equivalent elastic energy (area of triangle A"BC) is approximately the same as the actual unloading area subtended by A'BC.

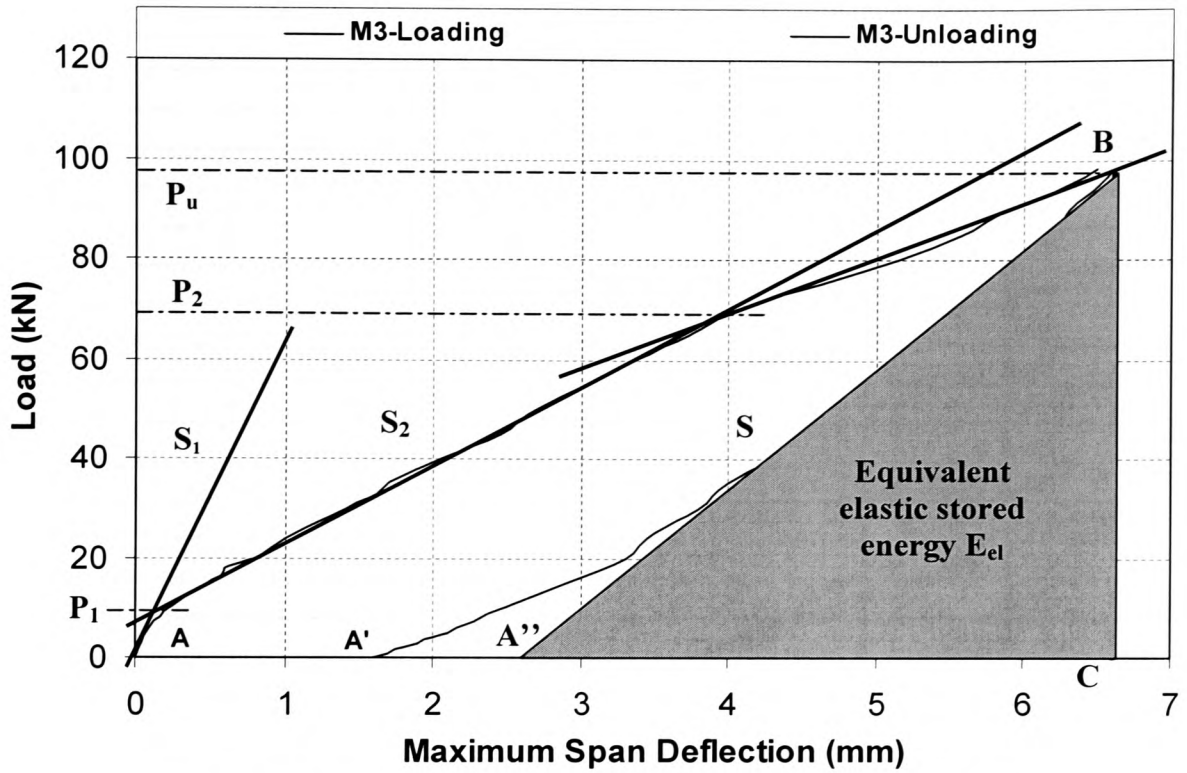

Figure 7.5 Determination of Elastic Stored Energy (Beam M3)

This method of estimating the elastic stored energy, therefore, appears to be realistic, and the candidate suggests that it should be used as a standard method in the determination of the energy-based ductility index if no actual load-unload cycle data are available.

7.3.3 Deformability and Ductility Indices of Test Beams

The maximum span deflections of all beams at 95% and 67% of the ultimate load were obtained from the load-deflection curves. Using equations 7.4 and 7.5, the deformability indices of series A and B beams can be conveniently calculated, and are listed in Table 7.2.

Table 7.2 Proposed Method for Deformability Index φ_{df} (Equations 7.4 & 7.5)

Beam Ref.	$\delta_{0.95Pu}$ (mm)	δ_s (mm)	φ_{df}
Control	26.3	8.6	**3.10**
A1	16.8	10.1	**1.66**
A2	17.7	10.4	**1.70**
A3	18.8	11.2	**1.68**
A4	14.9	9.5	**1.57**
A5	16.9	10.3	**1.64**
A6	12.0	8.1	**1.48**
A7	10.5	9.0	**1.17**
A8	15.6	9.5	**1.64**
A9	9.0	5.8	**1.55**
A10	10.6	7.4	**1.43**
B1	31.9	13.9	**2.29**
B2	16.7	10.2	**1.64**
B3	23.0	11.5	**2.00**
B4	31.2	15.3	**2.04**
B5	27.5	13.4	**2.05**
B6	32.4	15.1	**2.15**

It can be seen that for all beams strengthened by the prelaminated CFRP plates (A1-A10 and B2), the deformability index ranges from 1.17 to 1.70. This indicates that under service load, these beams can be expected to sustain further deformation of between 17% and 70% of the corresponding values at service load level, before ultimate failure occurs. For the five beams (A1-A5) which had similar failure mode, the variation is narrowed down to 1.57 to 1.70, with an average of deformability index of 1.65.

At an average deformability index of 1.65, beams A1 and A5 failed in the brittle premature tearing-off mode. While group B beams (except B2) has an average deformability index of 2.11, and these beams failed relatively more mildly even though concrete compression failure occurred in some of them (please refer to Chapter 4). This indicates that in order to avoid the extremely brittle failure mode, a minimum deformability index of 2 is desirable.

The ductility index of the same groups of beams was also determined using the energy based method discussed in the previous section, these are listed in Table 7.3.

Table 7.3 Determination of Energy Based Ductility Index* (φ_{du})

Beam Ref.	P_1 kN	P_2 kN	P_u kN	δ_1 mm	δ_2 mm	δ_u mm	S_1 kN/m	S_2 kN/m	S kN/m	δ_y mm	E_{tot} kNmm	E_{el} kNmm	φ_{du}	$\frac{\varphi_{df}}{\varphi_{du}}$
Control	10	38.0	48.0	1.0	11.3	31.7	10000	2718	4634	10.36	1129	248.6	**2.77**	**1.12**
A1	12	54.0	76.2	1.5	11.0	18.2	8253	4400	5256	14.50	792	552.4	**1.22**	**1.36**
A2	12	60.0	73.8	1.6	13.9	18.9	7500	3902	4622	15.97	786	589.2	**1.17**	**1.46**
A3	14	75.0	89.9	1.2	14.8	20.9	11382	4495	5780	15.55	1115	699.0	**1.30**	**1.29**
A4	12	68.0	74.4	1.6	14.3	19.8	7643	4399	4971	14.97	910	556.7	**1.32**	**1.19**
A5	12	72.0	82.0	1.6	14.7	19.4	7500	4580	5066	16.18	921	663.5	**1.19**	**1.37**
A6	10	62.0	62.1	1.0	13.0	13.0	9901	4337	5234	11.86	436	368.4	**1.09**	**1.35**
A7	10	59.1	59.1	1.0	10.7	10.7	9804	5072	5872	10.06	339	297.4	**1.07**	**1.09**
A8	10	50.0	68.8	1.5	10.9	16.8	6667	4278	4755	14.47	643.8	497.6	**1.15**	**1.43**
A9	12	58.1	58.1	1.0	9.5	10.7	12000	5404	6766	8.59	370.6	249.4	**1.24**	**1.25**
A10	10	55.6	55.6	0.9	11.4	11.4	11111	4343	5560	10.00	348	278.0	**1.13**	**1.27**
B1	10	47.5	70.0	1.4	14.1	34.8	7143	2953	3834	18.25	1588	638.9	**1.74**	**1.31**
B2	12	80.0	92.5	1.3	14.4	19.0	9231	5191	5796	15.96	1007	738.0	**1.18**	**1.39**
B3	12	55.0	68.4	1.9	14.6	23.0	6283	3388	4020	17.02	954	581.9	**1.32**	**1.51**
B4	12	50.0	65.9	1.9	16.4	28.8	6316	2615	3503	18.81	1178	619.8	**1.45**	**1.41**
B5	12	50.0	76.2	1.3	13.3	32.9	9231	3167	4622	16.49	1616	628.1	**1.79**	**1.15**
B6	10	50.0	62.0	1.2	16.4	34.9	8333	2632	3771	16.44	1498	509.6	**1.97**	**1.09**

*** Notes:**

1. For φ_{df} values please refer to Table 7.2.
2. δ_y is the elastic deformation, and is determined as P_u/S.
3. φ_{df} is determined using Equation 7.7.
4. $E_{tot} = 0.5P_1\delta_1 + 0.5(P_1+P_2)(\delta_2-\delta_1) + 0.5(P_2+P_u)(\delta_u-\delta_2)$.
5. $E_{el} = 0.5P_u\delta_y$.

The results from Table 7.3 clearly show that the energy based ductility indices reflect the beams structural ductility more realistically as these values take account of the unconsumed, elastic stored strain energy at the failure stage. Comparing with Table 7.2, it is apparent that ductility index is generally of smaller value than the deformability index. Beams with large deformability index such as that of beam B3, do not necessarily behave in a ductile manner, as the ductility index could be much lower (φ_{du} = 1.32 for B3).

Considering a pure elastic material such as FRP composites which behaves linearly until ultimate failure, the ductility index is unity since the elastic portion of the strain energy equals the total energy at failure. For all group A beams (plus beam B2), the ductility index ranges from 1.07 to 1.32 with an average of 1.18. This relatively low figure suggests that brittle failure should be expected, and it was indeed the case that all group A beams as well as beam B2 failed in a extremely brittle manner.

The single CFRP fabric layer strengthened beams (B1 and B3-B6) have an average ductility index of 1.65, which is 40% higher than the group A average. This confirms the laboratory observations that failure in this group of beams, as expected, was much less brittle than that of group A beams. It can be considered as near ductile behaviour and the candidate suggests that a ductility index of 1.65 can be accepted as the minimum value in practical structural strengthening design. Shown in Table 7.4, is the general comparison of deformability and ductility for the two groups of beams.

Table 7.4 Comparison of Deformability and Ductility Indices

Beam Group	φ_{df}	φ_{du}	Failure Mode
Control Beam	3.10	2.77	Ductile
Group A (Plus. B2)	1.56	1.18	Extremely Brittle
Group B (Ex. B2)	2.11	1.65	Acceptable but still considered brittle

It is clear that for FRP strengthened beams, whether plated or strengthened by fabric sheets, it is not possible to sustain the ductility level of the original unstrengthened

elements. However, suitably designed element, such as these of group B beams, can possess acceptable ductile characteristics.

It is important to distinguish deformability index from ductility index. High deformability is a prerequisite rather than a sufficient condition for good ductility characteristics. Ductile elements possess high deformability, while members with high deformability alone could still fail in a very brittle manner. Nevertheless, high deformability does provide some warning in that large elastic deformation may be observed before ultimate failure, and in order to achieve good ductility, deformability must first be ensured.

It must be emphasised that the absolute values of the deformability or ductility index is less significant than the relative comparison of these values with that of a control beam. It is not advisable to compare ductility index values derived from one method with those determined from a different approach, since the reference point is often arbitrarily defined if no apparent yield point of the loaded element is found.

One argument against using a ductility index for an FRP strengthened beam was presented by DiTommaso *et al* (1996). The authors argued that it should be solely the amount of inelastic energy that is used to quantify ductility, and the proportion of elastic energy to total energy is not important. In principle this statement is correct. However, the candidate suggests that ductility index is an important parameter for design consideration. The actual amount of inelastic energy varies in each element with different geometry, reinforcement and load configuration. It would be impossible to compare and determine which element is more ductile without the provision of ductility indices for all members.

The present proposed concept of deformability index seems to be pertinent for application to FRP strengthened RC beams. The greatest merit of this method is its design based approach and ease of use. The deformability values also clearly indicate the possible further deformation scope after the service load and before the ultimate failure conditions.

7.3.4 Enhancing Deformability and Ductility

7.3.4.1 FRP confinement

The ductility of reinforced concrete beams may be increased by external FRP confinement. Laboratory tests were performed on 8 standard 150 mm x 300 mm concrete cylinders wrapped with single layer FRP fabric sheets that were used for the strengthening of series B beams. Shown in Figure 7.6 is a typical comparison of the

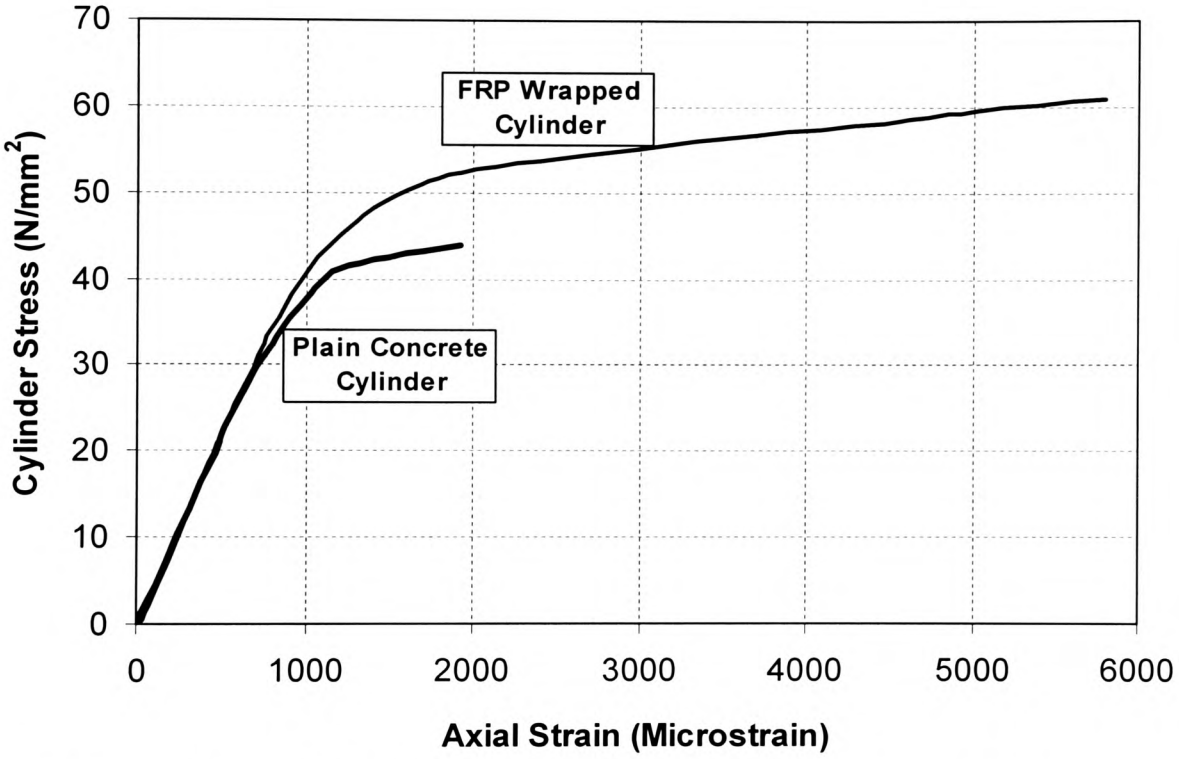

Figure 7.6 Stress-Strain Comparison of Plain and CFRP Wrapped Cylinders

average standard concrete cylinder test results against that of cylinders wrapped around with a single layer of CFRP fabric sheets. The CFRP confined cylinders exhibited an ultimate strain at peak stress 3 times that of the plain concrete cylinders. Although the overall beam ductility would have undoubtedly been influenced by the strength and ratio of the internal steel reinforcement as well as other factors such as concrete properties, it is reasonable to conclude that FRP wrapped RC beams will possess better ductile characteristics than those without external wrapping. This was demonstrated by group B beams which were partially wrapped in the shear spans.

7.3.4.2 The influence of under and over strengthening

Although confinement of concrete in compression does improve the ductility of FRP strengthened RC beams, the major influencing parameters are the material properties and cross sectional area of the strengthening FRP composite. From what had been observed in the laboratory tests, the FRP under strengthened sections possess greater deformability and ductility behaviour as demonstrated by group B beams.

Using the numerical model developed in Chapter 5, the relationship between the area of FRP provided and the beam deformability or ductility index can be established, albeit the determination of deformability index, as proposed in the preceding section, is a more straight forward process. Figure 7.7 illustrates the variation of the cross sectional area of the three types of strengthening CFRP composites with the deformability index for a typical test beam used in the present study.

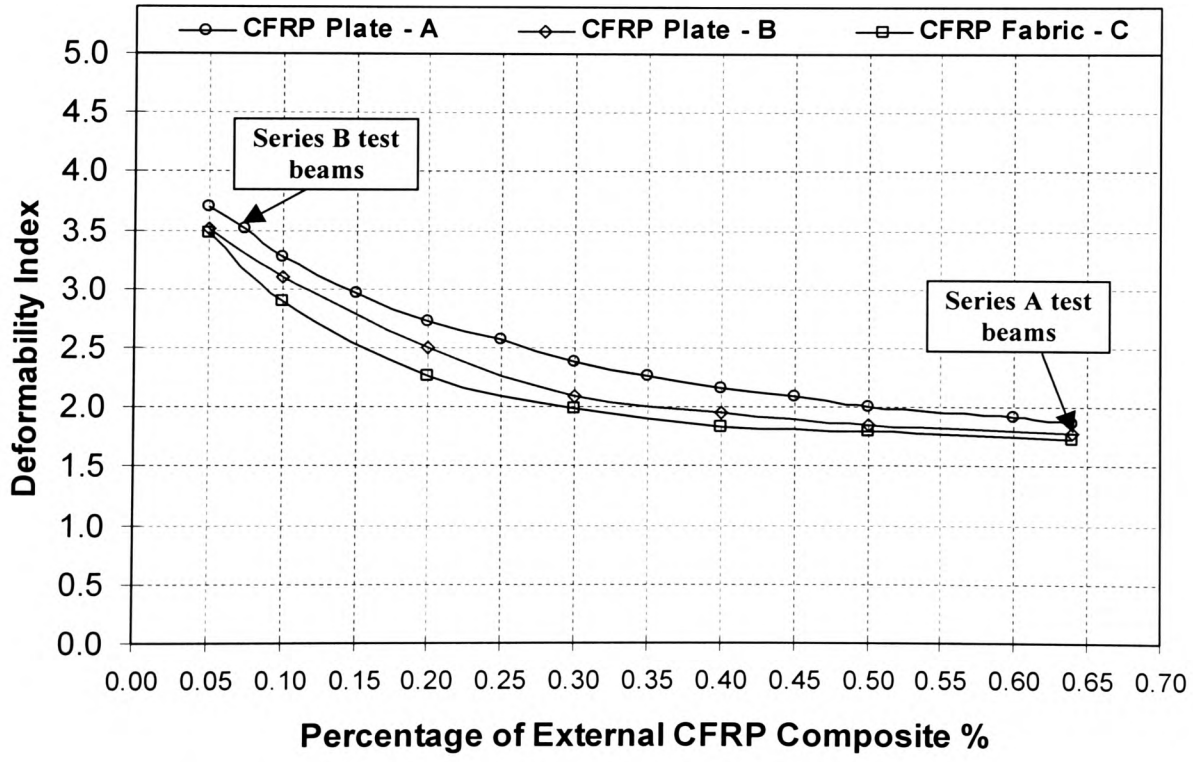

Figure 7.7 Variation of CFRP Ratios with Deformability Index

The deformability index values in Figure 7.7 were determined using Equation (7.7). Maximum span deflections under 95% and 67% of the ultimate load were derived respectively using the non-linear analytical model developed in Chapter 5. The main

assumption in this calculation is that adequate measures have been taken to ensure that no tearing-off or any other type of premature failure would occur in the FRP strengthened beams.

The graphs clearly demonstrate that the deformability index decreases rapidly with the increase of area percentage of the FRP composites However, this trend stops at around 0.4% of the FRP area, after which its increase appears to have reduced influence on the beam deformability.

It is interesting to note that the variation of deformability index among the three types of CFRP composites seems to be rather small, considering the values of elastic modulus of the three materials are very different. This may be attributed to the fact that most of the beams included in Figure 7.7 are over strengthened. Since plane sections remain plane during load, and because the beams are already over strengthened, the application of a higher modulus or higher strength FRP composite does not provide proportionally higher strength and stiffness contribution to the strengthened beam. This again demonstrate that in FRP strengthening design, excessively high strength composites are not necessarily more beneficial than a lower strength counterpart for a given situation.

7.3.4.3 Influence of internal steel reinforcement

The cross section area of the existing internal steel reinforcement of a beam to be strengthened also affects the deformability and ductility of the beam after strengthening. Shown in Figure 7.8 is the variation of steel reinforcement ratio with the deformability index for beams having a CFRP ratio of 0.25%.

It can be seen that when the steel reinforcement ratio is between the minimum of 0.13% and 0.4%, the deformability index improves with the increase in steel area from 2.07 to 2.59, equivalent to a 25% improvement. After this stage the deformability appears to be less sensitive to the increase in steel reinforcement area. This is due to the fact that before this 0.4% of internal steel reinforcement is reached, the 0.25% of CFRP external reinforcement is insufficient in counterbalancing the concrete in compression, and the section is effectively an under strengthened section. At this stage the increase in steel

reinforcement results in greater ultimate load capacity as well as the ultimate deformation, hence the deformability index is also increased.

Once the section becomes over strengthened, the tension force in the beam will be shared between the internal steel reinforcement and the external FRP composites. At this stage only the increase of external FRP will decrease the deformability as demonstrated in Figure 7.7. For a given constant area of FRP, the increase in steel reinforcement appears to have little influence in the deformability behaviour. This however, does not mean that the absolute values of the beam deflection will not change with the increase in reinforcement area. It simply indicates that the deflections at both 95% and 67% of the ultimate load will change accordingly, and hence the ratio, or the deformability index, stays approximately unchanged, which is represented by the portion of graph that is almost horizontal. It is again confirmed that over strengthening of RC section is unnecessary. Not only it does not bring any practical benefit, it may result in large quantity of elastic stored energy which eventually leads to catastrophic brittle failure.

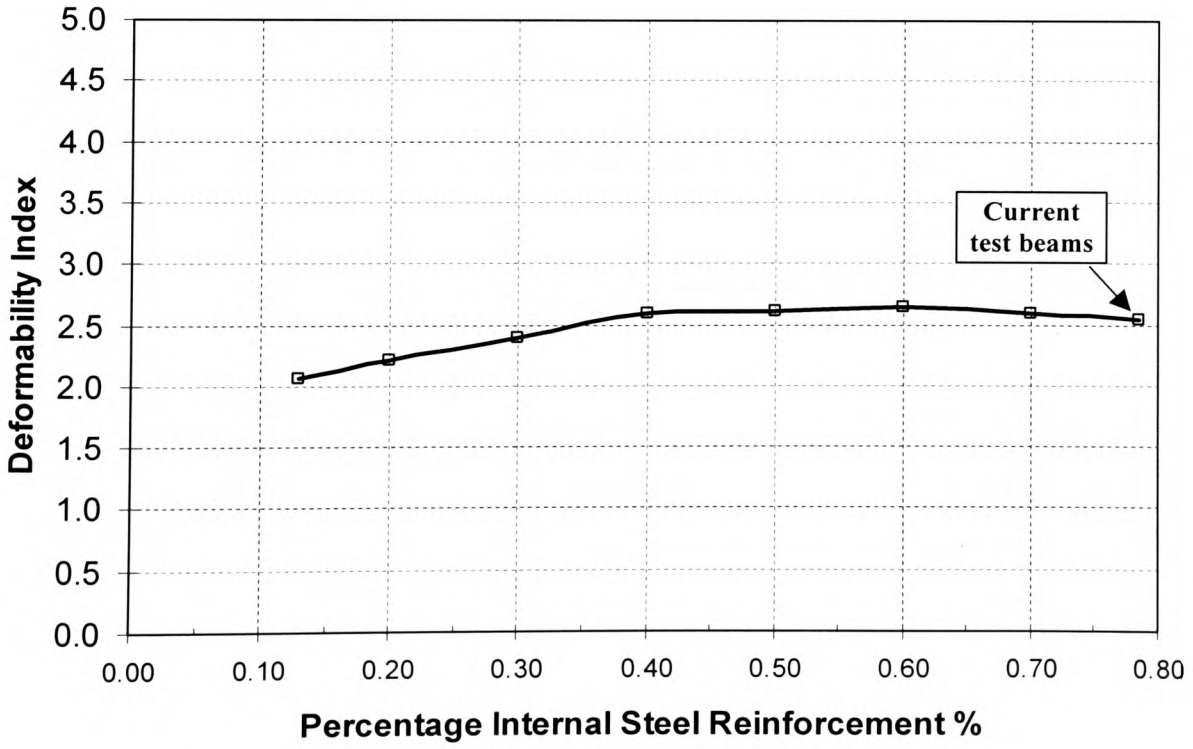

Figure 7.8 Variation of Deformability Index With Internal Steel Reinforcement Ratio

7.3.4.4 Influence of concrete strength

Although engineer's ability to alter the material properties of the existing concrete elements, which are to be strengthened, is limited, it is desirable to determine what influences the existing properties may have on the structural behaviour of the elements after strengthening. This will ensure that an optimum design of strengthening work may be performed. The concrete compressive strength, and hence its elastic modulus, will affect the ductility behaviour of the strengthened member. Figures 7.9 shows how the deformability index may be influenced by the concrete grade. This has been based on a standard over strengthened section used in the current tests with type A CFRP plates.

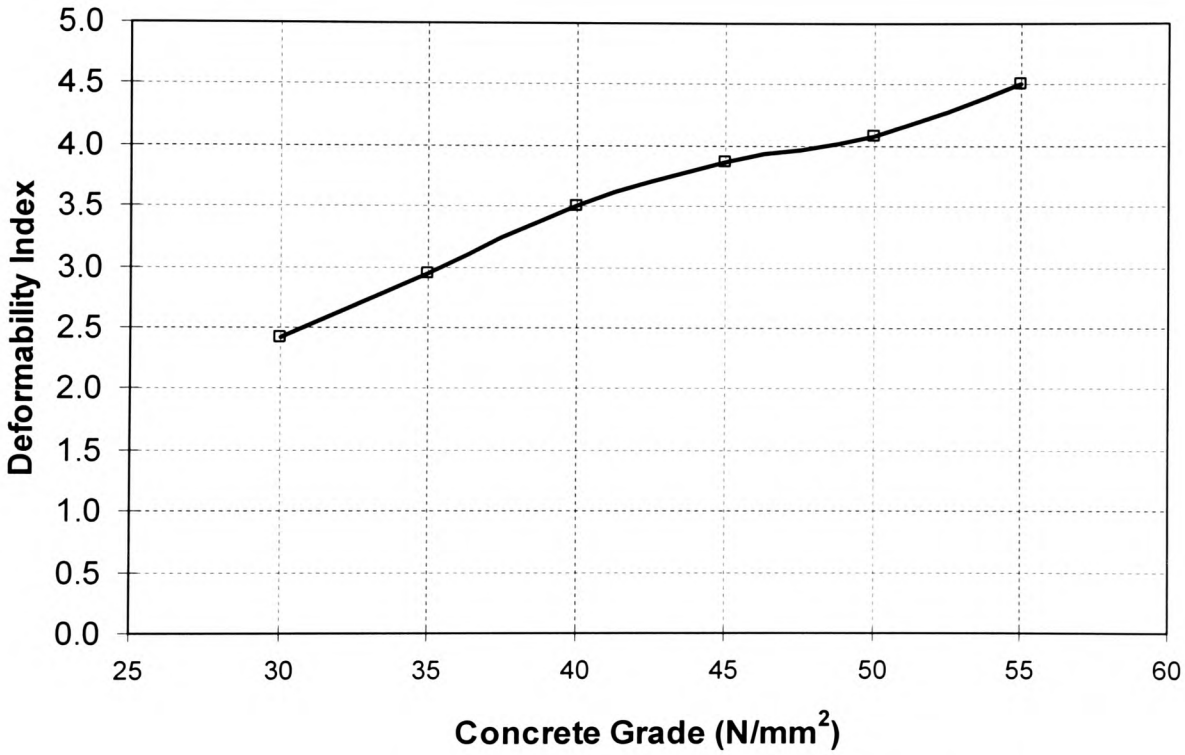

Figure 7.9 Variation of Deformability Index with Concrete Grade

It is interesting to observe that with an increase of concrete grade from 30 to 55, the deformability index improves by 88% from 2.4 to 4.5, this undoubtedly leads to improved ductility behaviour. This observation is of significance in designs for strengthening, as it suggests that strengthening existing concrete structures which have relatively high strength, is more desirable than a similar activity for a concrete with very low compressive strength. Nevertheless, it is perfectly viable and practical to strengthen a concrete structural element with low compressive strength, provided that it should not

be over strengthened and the deformability and ductility behaviour is well considered at the design stage.

7.3.5 Summary on Deformability and Ductility

The amount of inelastic or consumed energy in FRP strengthened beams, rather than the actual amount of deformation, is the determining factor for the ductility behaviour. It can be evaluated from the load-deflection response curves, as the difference between the total energy and the elastic stored energy. The elastic stored energy may be determined as the area subtended by the unloading-deflection curve. However, it is usually difficult to predict the exact failure point of any FRP strengthened beams, and hence impractical to unload at the appropriate time. A simplified approach, as suggested by Naaman and Jeong (1995), was found to be realistic in estimating the elastic part of the energy. The energy based ductility index can therefore be determined, and the candidate suggests that a minimum value of 2.0 should be achieved in a flexural element to avoid the extreme brittle failure mode.

The deformability index is an alternative proposed in the current study, and it is fundamentally different from the ductility index. High deformability will give good warning about the pending failure but it should be considered with the expected failure mode, as the failure may still be brittle. Nevertheless, high deformability is an important condition of achieving good ductility.

It was found that over strengthened sections have low ductility index and are most likely to fail in a brittle manner, while under strengthened sections exhibited acceptable level of ductile behaviour.

The existing reinforcement and concrete material properties influence the ductility of FRP strengthened beams. The ideal conditions correspond to concrete of high compressive strength, the higher the grade of concrete, the greater the ductility. Concrete confinement by FRP wrapping is another means of improving ductility and deformability.

7.4 MOMENT REDISTRIBUTION IN CONTINUOUS BEAMS

7.4.1 Introduction

Moment redistribution method is often used in the design of continuous reinforced concrete flexural members. A key consideration, when using such a design approach, is whether the member is sufficiently ductile to enable the formation of plastic hinges at the maximum moment positions. For this reason, the conventional RC flexural elements are designed as under-reinforced sections, and most design codes including BS 8110 and EC 2 have specific limits for the depth of neutral axis to ensure that acceptable level of ductility exists. For FRP composites strengthened RC beams, however, the ratio of neutral axis to the effective depth, x/d, is usually much lower than conventionally reinforced concrete beams as discussed in Chapter 5. The typical value for a balance section ranges from 0.2 to 0.35, depending on the types of FRP used. This is due to the high characteristic FRP plate strength and its relatively low modulus of elasticity. Consequently, a large number of the FRP plates strengthened RC beams may be potentially over-strengthened, which could lead to the extreme brittle modes of failure described in Chapters 6 and 7 (Sections 7.3 and 7.4).

Current published research work on the ductility of continuous RC beams is limited. It is therefore important to gain an understanding of the moment redistribution behaviour in continuous beams strengthened by CFRP plates. The following sections aim to provide experimental evidence to verify whether full moment redistribution is possible in such beams, and if not, what is the expected percentage of moment redistribution. Such information and knowledge is essential to the designers.

7.4.2 Experimental Investigation of Continuous Beams

In the current test series, four two-span continuous beams were load tested to ultimate failure. All beams were 5.0 metres long and with two 2.4 metres effective spans. The section size and tension reinforcement details were kept the same as the simply supported beams.

7.4.2.1 Reinforcement details and test general configuration

The reinforcement details are listed in Table 7.5 whilst the general configuration of the test beams is shown in Figure 7.10. The beams were so configured so that maximum possible moment redistribution can take place, and both flexural and shear behaviour can be observed during the load tests.

Table 7.5 Reinforcement Details for Continuous Beams

Beam Reference	Tension Reinforcement		Shear Reinforcement	
	Internal	External	Internal #	External
M1	2T10	None	9 T8 @ 100	None
M2	2T10	None	9 T8 @ 100	100 mm wide CFRP sheets at 100 mm clear centre*
M3	2T10	80 mm x1.7 mm CFRP Plates	9 R8 @ 100	100 mm wide CFRP sheets at 100 mm clear centres*
M4	2T10	2 layers of 100mm x 0.165mm AFRP fabrics	None	150 mm wide AFRP sheets at 75 mm clear centres

* 200 mm width CFRP sheets at load points. # Reinforced over 800 mm from all supports.

7.4.2.2 Material properties

All beams were cast in the laboratory using a generic industrial mix design for concrete (Water : Cement : Sand : Aggregates = 0.5:1:2:4) with a minimum cement content of 350 kg/m^3, and average slump of 35 mm. This was different from that of simply supported beam series, and the 28-day compressive strength was between 43.6 – 51 N/mm^2 as listed in Table 7.6.

The main tension reinforcement bars used were the high yield deformed type two bars as used in the simply supported beam series, which were described in Chapter 4.

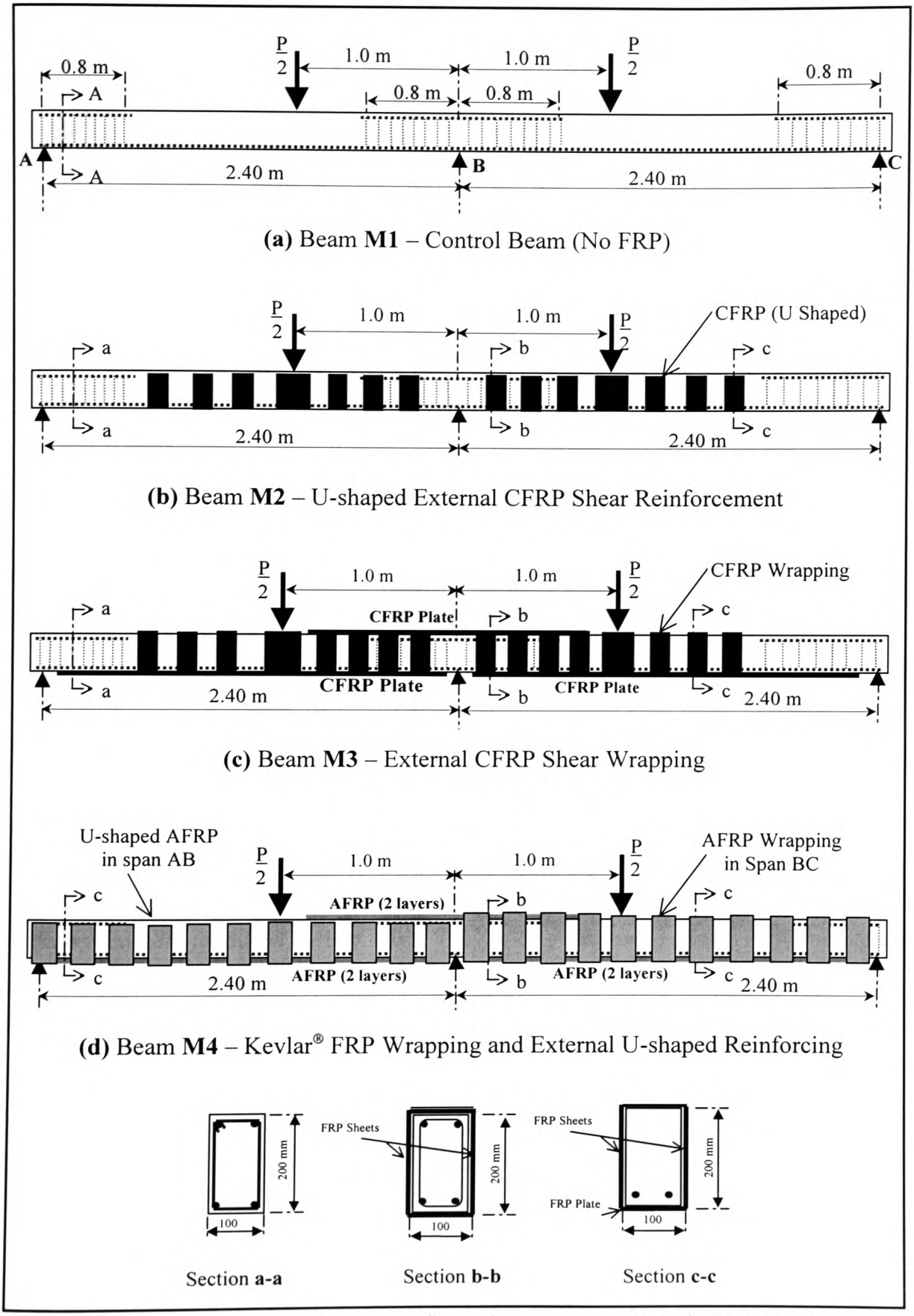

Figure 7.10 Continuous Beam Configurations (**a**)-M1, (**b**)-M2, (**c**)-M3, (**d**)-M4

The unidirectional CFRP plate and fabrics were the same as those used in the tests for simply supported beams, and the Kevlar FRP fabric sheets were those typically available in the UK construction market. The actual material properties are listed in Table 7.6.

Table 7.6 Material Properties

Materials		**Actual Strength** N/mm^2	**Elastic Modulus** kN/mm^2
Concrete	Beam **M1**	f_{cu} = 46.2	37.4
	Beam **M2**	f_{cu} = 43.6	36.3
	Beam **M3**	f_{cu} = 51.0	39.2
	Beam **M4**	f_{cu} = 45.0	36.9
Steel	Tension bars	f_y = 560	200
	Shear links	f_{yv} = 255	200
FRP Composites	CFRP fabric strips (0.14 mm thickness)	f_{pcv} = 1750	125
	CFRP Plates (1.70 mm thickness)	f_p = 2950	185
	AFRP fabrics (0.165mm thickness)	f_p = 2100	125

7.4.2.3 Application of strengthening materials

For Beam M2, single 500 mm long by 100 mm wide CFRP fabric sheets were used as external shear reinforcements at sections where no internal shear links were provided. These fabrics were bonded in a U-shape to the concrete surface, using an epoxy based adhesive system produced by Feb MBT. The CFRP sheets were spaced at 100 mm clear centres, and 200 mm wide sheets were used directly under the point load to act as shear reinforcement as well as containing the compression zone. The concrete surface was wire brushed and cleaned of any dust before the application of composite, no surface primer was used.

Two 2.2 metres long, 80 mm wide and 1.7 mm thick CFRP plates (Type B) were bonded to the soffit of the two spans of Beam M3 using Exchem Resifix 31 plate bonding adhesives, which meets the specifications of BA30/94 guidance. A third plate of 1.80 metres long was bonded to the top surface at the middle support where hogging

bending moment is expected. The CFRP plates were designed to strengthen the bending capacity of the beam to prevent bending failure before the shear damage was expected to occur.

Two days after the plate bonding, CFRP composite fabric sheets were used to wrap around the beam in a similar manner to Beam M2. The CFRP sheets are of same width as used in Beam M2, except that they were 800 mm in length, with approximately 200 mm overlap when wrapped around the plated beam.

The purpose of wrapping CFRP on this beam is three fold: (a) to act as external shear reinforcement in regions where no internal links were provided; (b) to strengthen the shear capacity near the middle support where the mild links were insufficient for the expected load, and (c) to act as end anchorage to the CFRP plates so as to prevent the typical premature tearing-off failure of the strengthened beam as observed in the plated simply supported beams.

No internal shear reinforcement was provided in beam M4. This beam was strengthened in bending using two layers of 2.2 m long, 100 mm wide and 0.165 mm thick AFRP fabrics at the soffit of the two spans, and two 1.8 m long sheets at the top over the middle support. The epoxy adhesive used was the Exchem Carbofibe laminating resin, and matching surface primer was used before the bonding of the fabrics. The whole beam was strengthened in shear by wrapping with one layer of 150 mm wide AFRP strips at 75 mm clear centres. The AFRP fabrics used for shear strengthening were the same as the ones used for flexural strengthening. In span AB the AFRP sheets were of 500 mm in length and were wrapped in U-shapes, whilst in span BC, 800 mm length AFRP sheets were used for full wrapping around, with an overlap of 100 mm at each side of the web was adopted.

7.4.2.4 Test procedure

All beams were loaded at a constant speed of 0.125 kN/second using two 100-kN hydraulic jacks simultaneously. The two spans of each beam were identically configured and loaded. Six rows of Demec strain gauges were fixed on both sides of each beam, three columns at each load position and two columns at the middle support

(minimum number of gauges =112). The control beam, M1, had no FRP composites, and was internally reinforced only. However, no shear reinforcement had been provided for a length of 0.8 m in the middle of the two spans, which enables the actual shear resistance of the beam without links to be determined.

All four beams were loaded to ultimate failure, while beam M3 also went through a number of load-unload cycles. Beam M3, which was strengthened in flexure by CFRP plates at its tension faces, was loaded to the service load.

7.4.3 Test Results

The test results provide strong evidence to show that external bonding or wrapping of CFRP plates and fabrics to the concrete surfaces of continuous RC beams is an effective means of strengthening. The flexural as well as shear capacities of the beams were enhanced. Although the two spans of these beams were identically loaded and the load deflection behaviour very similar, without exception the ultimate failure occurred only in one of the spans. Shown in Table 7.7, is the summary of the main data for all four beams.

Table 7.7 Summary of Main Results

Beam Ref.	Max. Load (kN)	Max. Deflection (mm)	Maximum Surface Strain at Point Load		Failure Mode
			Tensile	Comp.	
M1	68.2	9.10	$0.004570^{\#}$	$0.000956^{\#}$	Brittle shear failure in one span near the load point.
M2	80.2	20.2	0.005150^{*}	0.001250^{*}	Flexure failure after the formation of plastic hinges at the middle support and in span AB.
M3	180.6	21.2	0.007580^{-}	0.002080^{-}	Combined flexure and shear failure at point load position in span BC.
M4	116.9	19.8	0.006560^{+}	0.001950^{+}	Failed by premature debonding of the AFRP composite (top)

Corresponding to: $^{\#}$ load of 60 kN; * load of 70 kN; $^{-}$ load of 160 kN; $^{+}$ load of 100 kN;

The load deflection curves for all four beams are shown in Figure 7.11. It can be seen that beams M1 and M2, neither of which was strengthened in bending, had almost identical load-deflection responses until beam M1 failed. The former failed prematurely in shear at a load of 68.2 kN. The brittle failure occurred in one span between the middle support and the point load, and it was close to the load position where no internal shear reinforcement was provided, as shown in Figure 7.12, together with beams M2, M3 and M4.

The U-shaped CFRP wrapping of beam M2 prevented any premature shear failure as seen in beam M1. This beam failed in flexure in one span at the load position, after the formation of plastic hinges at the middle support and at the load positions in the spans. The plastic hinge was first formed at the middle support, where extensive cracking was observed. It was observed that the plastic hinges in concrete elements are not really ideal "hinges" which usually mean a central point of rotation. A concrete plastic hinge may be more appropriately described as a "yielded" region, and thus this type of hinges can be measured by the length and depth.

The first crack in beam M2 showed a typical sign of concrete tensile failure. It was perpendicular to, and started from, the top surface of the beam. The location of this crack was exactly at the centre of the support, and its depth developed as the load increased. Meanwhile, a large number of cracks were induced after the first, as the load was increased. These cracks appeared to form close locations with an average spacing of around 40 mm. The cracks, away from the centre of the support, tended to be inclined where the respective angle of these cracks to the beam top surface decreased with the increase of distance away from the support. The furthest crack in the hinge from the centre line of the support was about 45 degrees to the horizontal, typical of a shear crack. The shape of the middle support plastic hinge was seen to be approximately in the form of an inverted trapezium, with the maximum hinge depth of 180 mm, and the spread length of the hinge was in the order of 600 mm, or 3.5 times of the beam effective depth. It is shown in Figure 7.13(a). The hinges in the two spans at the load positions were not as apparent as the one over the middle support, since the 150 mm wide CFRP fabrics were bonded at these locations.

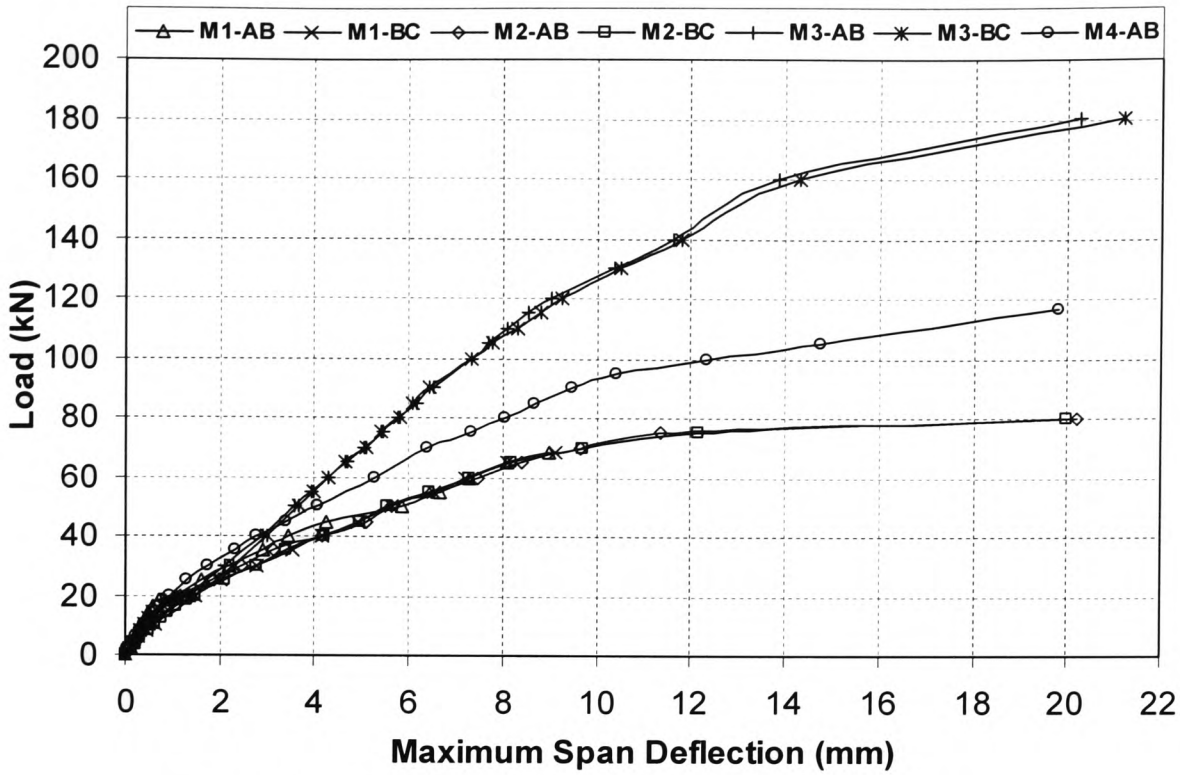

Figure 7.11 Load-Deflection Curves for Continuous Beams

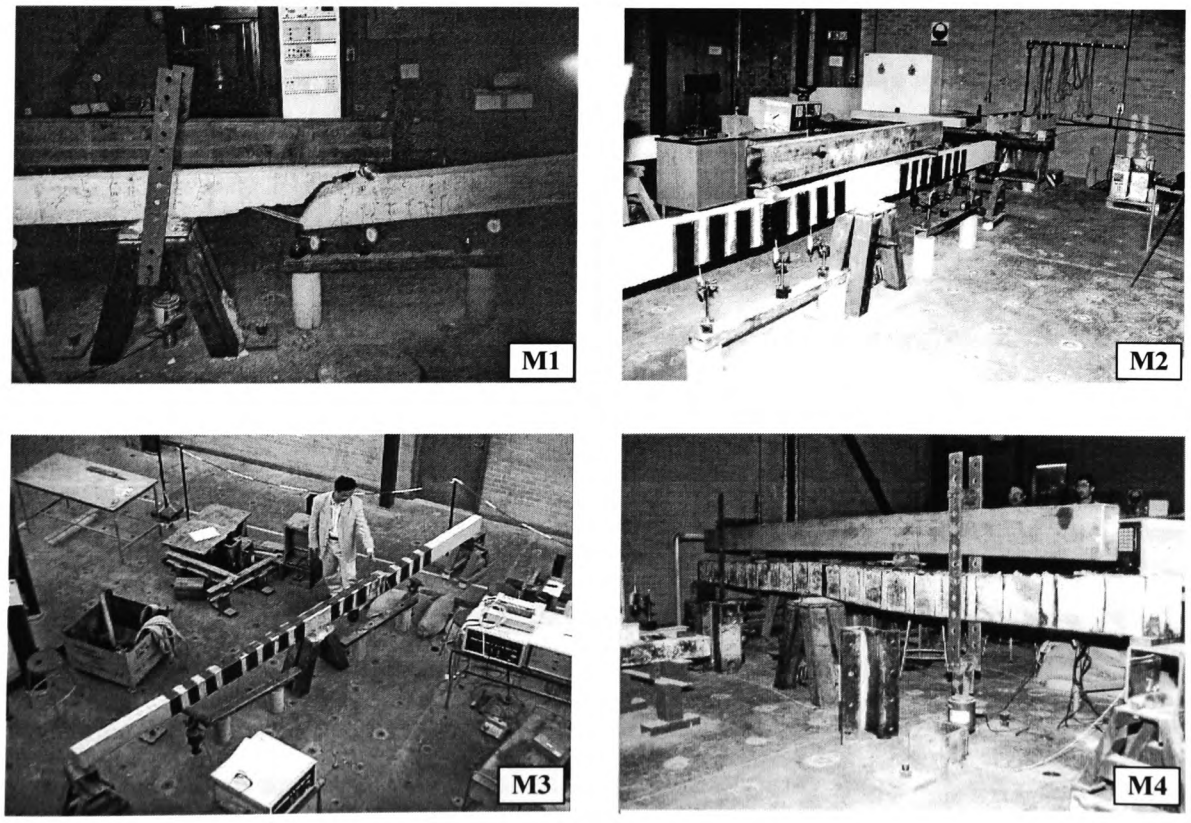

Figure 7.12 Overview of Failure Mode of Continuous Beams

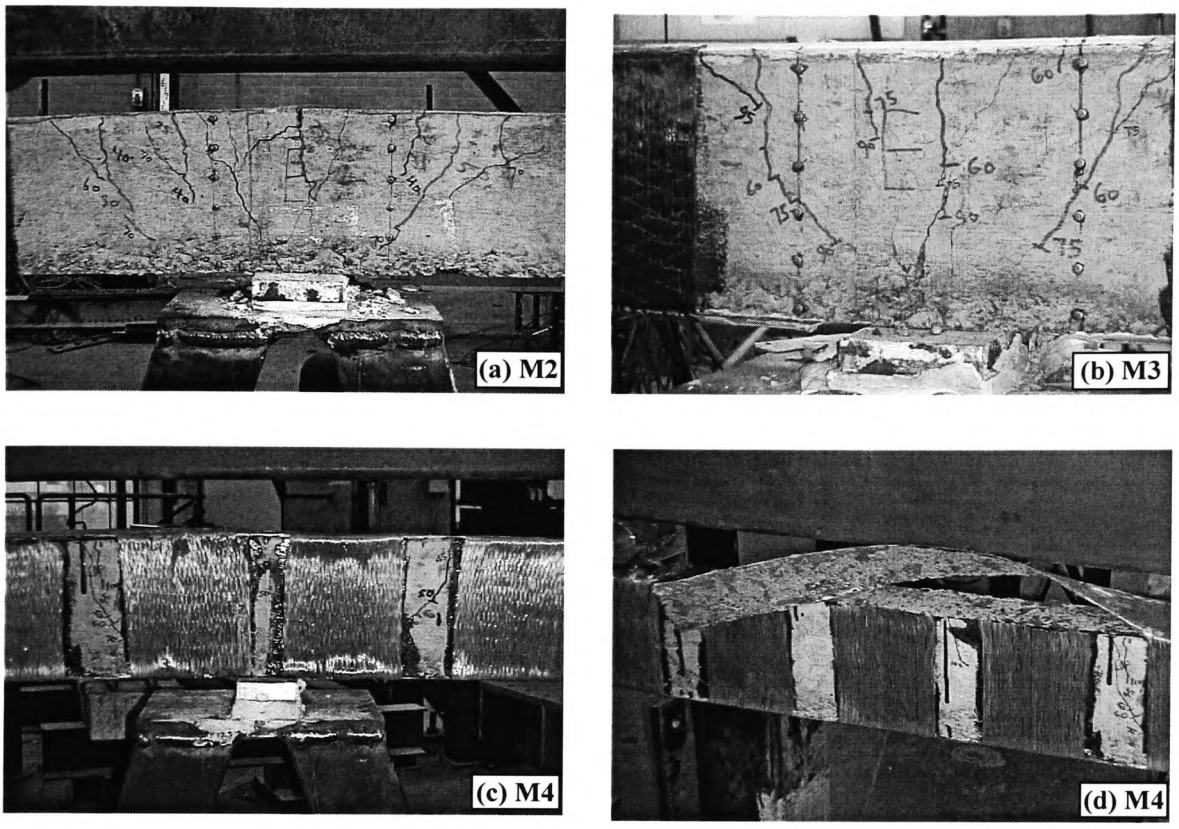

Figure 7.13 Close-up View of Failure Mode of Continuous Beams
(a) M2-Plastic hinge at middle support; (b) M3-Partial plastic hinge at middle support; (c) M4-Partial plastic hinge at middle support; (d) M4-AFRP Debonding in span AB.

Beam M3 was strengthened in flexure with type B CFRP plates. This beam failed at 180.6 kN in one of the spans in combined bending shear at approximately the same position as that of beam M1. A large diagonal shear crack was observed at each of the load position when the load reached 140 kN. The beam behaviour leading to the final ultimate failure was gradual and progressive. Continuous snapping sound of the wrapping CFRP fabrics could be heard as the loading increased, suggesting that the shear stresses in some of the external CFRP wrapping strips were approaching the ultimate tensile strength. There was no indication as to which span the beam would eventually fail in. The final failure was induced by the large shear crack in span BC, the beam failed in shear, and almost simultaneously the concrete at the top of beam where the point load was applied, was crushed. The final failure mode of beam M3 was considered to be mild, there was not any explosive type of brittle tearing-off failure as seen in the simply supported beam series. Although this beam was still over

strengthened in flexure, the CFRP fabric wrapping had helped confine the concrete and the ductility of the beam was evidently greatly improved over beams M1 and M2. The overview failure mode and a close-up view of beam M3 at failure are shown in Figures 7.12 and 7.13(b) respectively. The length of the middle support plastic hinge was much less than the one in beam M2. It was measured to be just under 400 mm, or 2.2 times of the beam effective depth, and the visible cracks were less extensive than can be seen from the plastic hinge in M2 as shown in Figure 7.13(a). All these indicate that a full plastic hinge could not be formed in beam M3. This was due to the presence of FRP strengthening composites, and such plastic hinges in RC structures may be referred to as partial plastic hinges.

Beam M4 failed at 116.9 kN by premature debonding of the AFRP composites layers at the top of the beam (Figure 7.12). The failure occurred in the span where the AFRP strips were wrapped in U-shapes, as illustrated in Figure 7.13(d). There was no sign of debonding in the other span where closed and overlapped AFRP loop wrapping around was deployed. This confirms the assumption that FRP wrapping of the beam web can not only strengthen the beam shear capacity, it can also act to confine the concrete as well as the flexural FRP composites, especially if the wrappings were in closed loops.

Similar to beam M3, the plastic hinge at the middle support of beam M4 was only partially developed, with the length of the hinge measured to be around 400 mm, as shown in Figure 7.13(c). However, the number of cracks was not clearly identifiable due to the wrapping AFRP strips. Nevertheless, they seemed to be again less than that of beams M2 and M3.

One of the important initial observations from these tests of continuous beams is as follows: FRP strengthened continuous RC elements could enhance the flexural as well as shear capacities if appropriately designed, but it seems clear that the presence of bonded FRP composite prevents the full development of plastic hinge. The design implication is that the maximum percentage of redistribution should thus be further limited.

7.4.4 Analysis of FRP Strengthened Continuous Beams

Having established that plastic hinges can only be partially developed in FRP strengthened elements and only some amount of moment redistribution can be carried out, it is now desirable to quantify this amount of moment redistribution. This in turn will provide useful information for developing design guidelines with regard to strengthening continuous RC elements.

7.4.4.1 Maximum possible percentage of moment redistribution

The elastic analysis of the two-span continuous beam was carried out and the bending moment and shear force diagrams are shown in Figure 7.14. This beam is statically indeterminate by one degree. To cause a partial collapse in one span, the minimum number of plastic hinges required is 2. Since the maximum bending moment occurs at the middle support, this is the position where the first hinge will be formed. To achieve the maximum possible moment redistribution in this beam, the elastic hogging moment at the middle support was reduced so that the moment over the support equalises those sagging moments at the point load positions in the two spans. This redistribution was carried out, the maximum moment reduction at the support was found to be **20.2%**, from 230.9P to 184.2P, as shown by the dotted line in Figure 7.14(c).

7.4.4.2 Plastic moment

For beams M1 and M2, the plastic moment of resistance was determined using the actual strength of concrete and steel reinforcement. This leads to a concrete design strength of $0.67f_{cu}$, based on the BS 8110 rectangular stress block. The neutral axis depth, x, is therefore calculated as:

$$x = \frac{f_y A_s}{0.67 f_{cu} \times 0.9b} = \frac{560 \times 157}{0.603 \times 43.6} = 32.8mm$$

This value agrees well with the observed x value for beam M2 at failure. The maximum crack depth, at the middle support and the load points, was recorded to be around 160 to 165 mm. This indicates a neutral axis depth at the ultimate load of 35 – 40 mm.

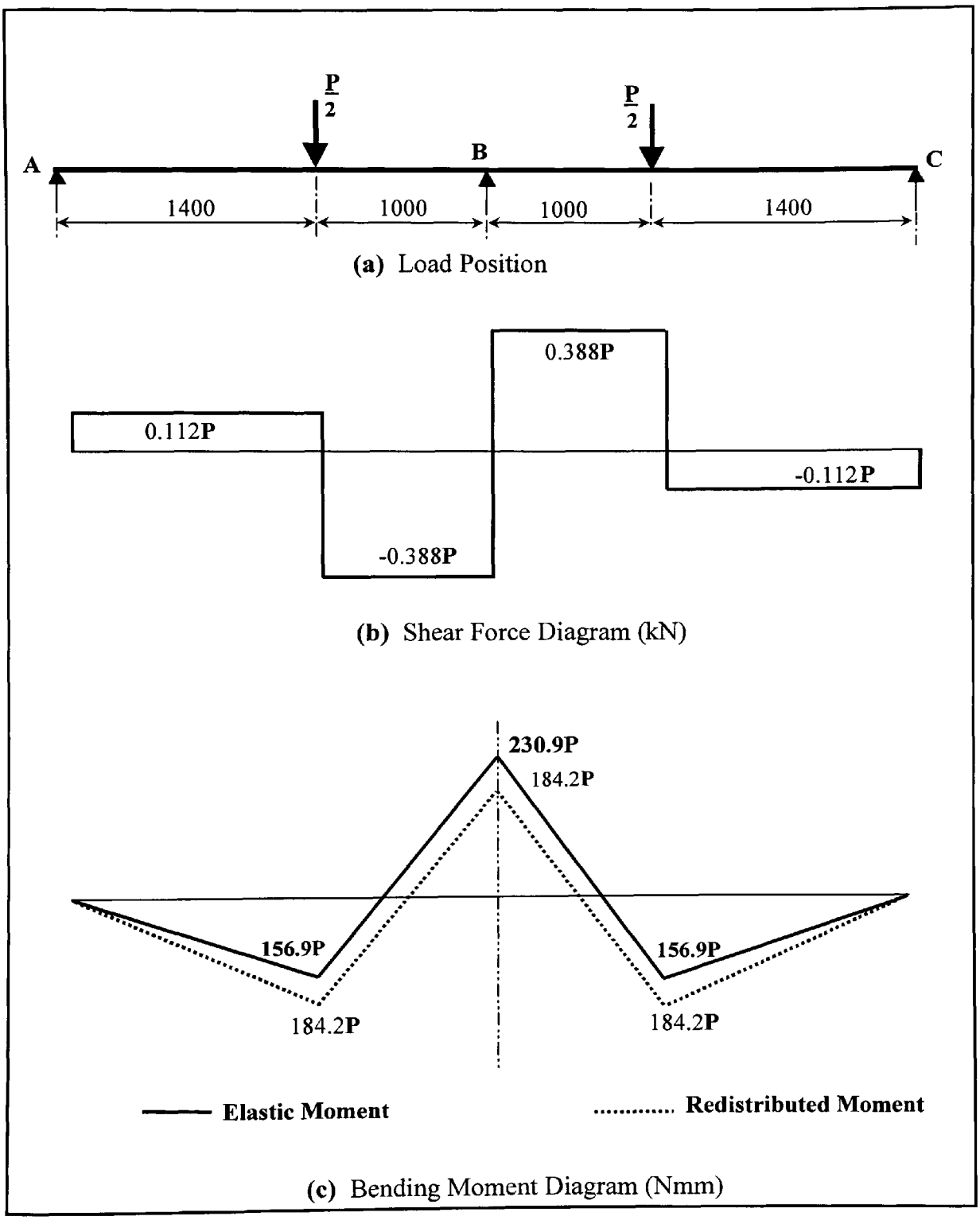

Figure 7.14 Bending Moment and Shear Force Diagrams for Continuous Beams

The lever arm, **z**, can be determined as follows:

$$z = d - 0.45x = 174 - 0.45 \times 32.8 = 159.2mm < 0.95d$$

The section plastic moment can therefore be determined as:

$$M_p = F_s z = 560 \times 157 \times 159.2 \times 10^{-6} = 14.0kNm$$

The actual failure load of beam M2 was 80.2 kN, and the corresponding hogging moment at the support just before the collapse would have been:

$$184 \times 80.2 \times 10^{-3} = 14.7kNm$$

This is the experimental value of plastic moment capacity of the beam section. The magnitude of plastic moment is considered reasonably accurate when compared with the control beams in the simply supported beam series. The failure load of the simply supported control beams, which were similarly reinforced as the continuous beams and had compatible concrete strength, was 48 kN, which corresponds to a failure moment of 13.8 kNm. In the continuous beam M2, the plastic hinge over the support was fully developed over a length of 600 mm, the corresponding plastic moment is therefore expected to have been slightly greater than that of the simply supported beams.

The section plastic moment for beams M3 and M4, however, was more difficult to determine. This is because both sections had been over strengthened, and the FRP composites would not reach the design strength at ultimate failure.

Theoretically, the maximum applied load to cause a "full" plastic hinge may be determines as follows. Assuming that FRP composites, internal steel reinforcement and the concrete in compression reach the respective design strengths at the formation of the plastic hinge, the total compression in the concrete must balance the total tension in the steel and FRP composites. This condition can be generally expressed by the following equation:

$$0.603 f_{cu} bx = f_y A_s + f_p A_p \qquad (7.9)$$

This equation does not take into account any factors of safety for material strength. The factor 0.603 is based on BS8110 rectangular stress block where factors of safety have been removed. For beam M3, f_{cu} = 51 N/mm^2, f_p = 2950 N/mm^2 and A_p = 136 mm^2. Substitute these figures into Equation (7.9),

$$x = \frac{f_y A_s + f_p A_p}{0.603 f_{cu} b} = \frac{560 \times 157 + 2950 \times 136}{0.603 \times 51 \times 100} = 159mm = 0.91d$$

This value is completely unrealistic, it is impossible for the neutral axis depth x to reach this high magnitude at ultimate failure. It can therefore be concluded that there exists an optimum level of FRP area provided in a strengthened RC section, beyond which a full plastic hinge cannot be developed since it would not be possible for the FRP composites to reach the full design strength at failure. This statement echoes the discussions regarding over and under strengthening as presented in Chapter 5.

Consider a "fully balanced" FRP strengthened section and assuming that concrete reaches its ultimate compressive strain, the neutral axis depth **x**, as defined in Equation (5.17), can now be used to determine the applied load that causes the formation of a full plastic hinge for a non-over strengthened section. The plastic moment may be expressed by the following equations:

$$M_p = F_s(d - 0.45x) + F_p(h + t_a + \tfrac{t_p}{2} - 0.45x) \qquad (7.10)$$

$$x = \frac{h + t_a + \frac{t_p}{2}}{(1 + \frac{f_{pu}}{\varepsilon_{cu} E_p})} \qquad (7.11)$$

$$F_p = F_c - F_s = 0.603 f_{cu} bx - f_y A_s \qquad (7.12)$$

The maximum area of FRP to be provided is therefore:

$$A_{p\max} = \frac{0.603 f_{cu} bx - f_y A_s}{f_{pu}} \qquad (7.13)$$

The above equation is a different form of Equation (5.24) where concrete tension stiffening effects have been ignored, and the shape factor Ω has been taken as 0.603, based on BS 8110 simplified rectangular stress block.

In order that the plastic hinges can be fully developed in the continuous beams, the plastic moment of resistance of the two beams M3 and M4 at fully balanced condition are evaluated, using Equations (7.10) - (7.12), to be 16.7 kNm and 15.2 kNm respectively. These figures are based on the maximum area of FRP provided to be limited to 8 and 4 mm^2 respectively, which are obviously notional values. The actual FRP area in beams M3 and M4 was 136 and 29 mm^2. These figures suggest that full plastic hinge, and hence full moment redistribution, will not occur in FRP strengthened continuous beams.

7.4.4.3 Maximum moment of resistance of over-strengthened sections

The maximum moment of resistance for an over strengthened RC section depends on how the premature failure would occur. There are four distinctive possibilities of failure mechanisms:

(a) Crushing of concrete in the compression zone;
(b) Premature debonding of FRP composites from concrete surface;
(c) Premature tearing-off failure;
(d) Shear failure.

In the current tests, beam M3 failed by combined shear and concrete in compression, whilst beam M4 failed by premature debonding. The only way to determine the section moment of resistance at failure is to utilise the collected strain data and carry out a back analysis in order to estimate the actual stress in the FRP composites before beam failure. Due to safety concerns, the strain measurement activities were usually stopped before the ultimate failure thus the valuable FRP strain data at the instance of beam failure were not recorded. Nevertheless, the last recorded strains at just before failure were still

expected to give a good indication of the beam's behaviour at ultimate limit state. Shown in Figure 7.15 is the strain distribution across the section depth at the point load position in one of the spans of beam M4. The recorded maximum strain was 0.006560 at 100 kN. In Figure 7.16, the strain distribution in the top AFRP fabric along the beam is shown, and the maximum strain was noted to be 0.007080 at 100 kN.

This shortcoming can be overcome by utilising the deflection data, based on which the moment curvature relationship was established. The maximum crack depth in beam M4 was measured to be 155 mm at the span and 160 mm at the middle support, indicating a neutral axis depth of 45 and 40 mm at these positions respectively. The x values were then used to determine the FRP strain of the beams at failure from the moment-curvature relationships shown in Figure 7.17. For beam M4, the curvature at the point load position under the failure load was 61.6 x 10^{-6}, the corresponding concrete compressive strain at failure load of 116.9 kN should therefore be:

$$\varepsilon_c = \kappa x = 61.3 \times 10^{-6} \times 45 = 0.002470.$$

This strain has exceeded the concrete peak strain of 0.002200, indicating that concrete failure in compression would occur shortly. This predicted ultimate strain value is about 26% over the strain value of 0.001950 at a load of 100 kN. The strain in the AFRP composites at beam failure can now be determined, based on the principle of plane sections remaining plane, as follows:

$$\varepsilon_p = \frac{h + t_a + \frac{t_p}{2} - x}{x} \varepsilon_c = \frac{200 + 2 + 0.17 - 45}{45} \times 0.00247 = 0.008630.$$

This is 31% over the strain value at 100 kN. The stress in the bottom AFRP composite when beam M4 failed is therefore estimated to be:

$$f_p = \varepsilon e_p E_p = 0.00863 \times 125000 = 1078.7 N/mm^2.$$

This stress value is 51% of the AFRP ultimate tensile strength.

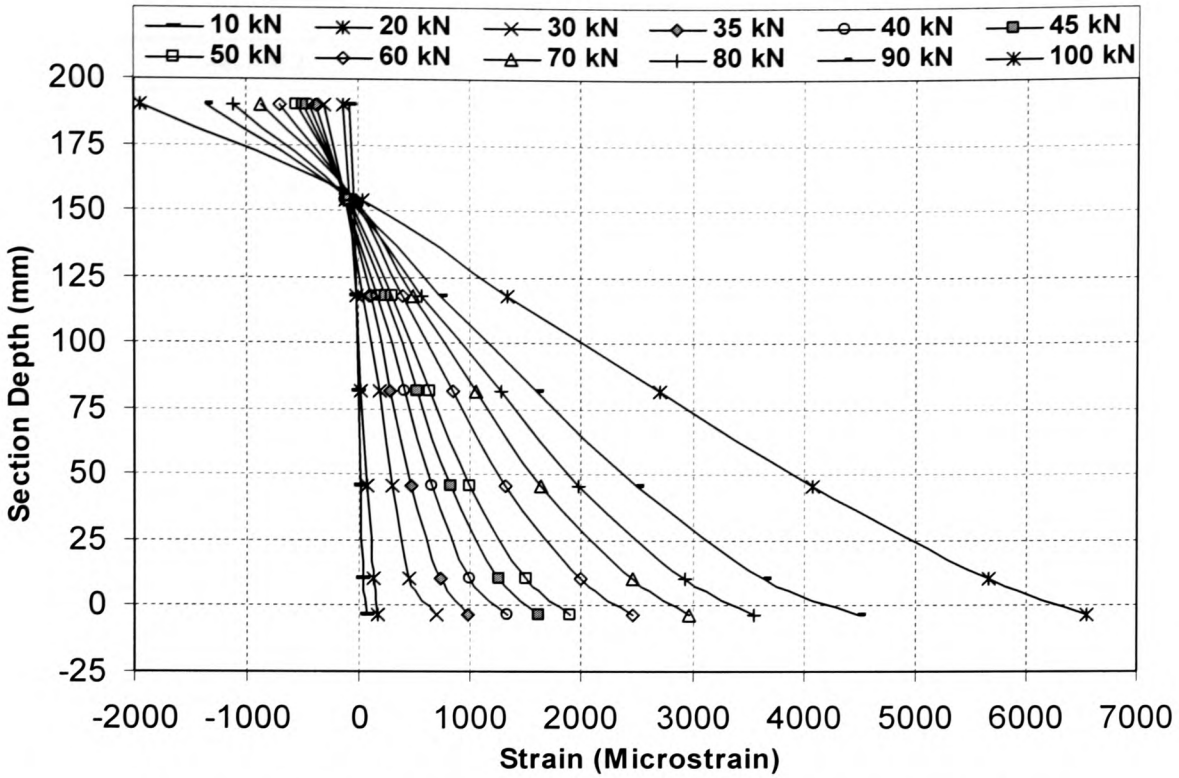

Figure 7.15 Strain Distribution of Beam M4 at Point Load Position

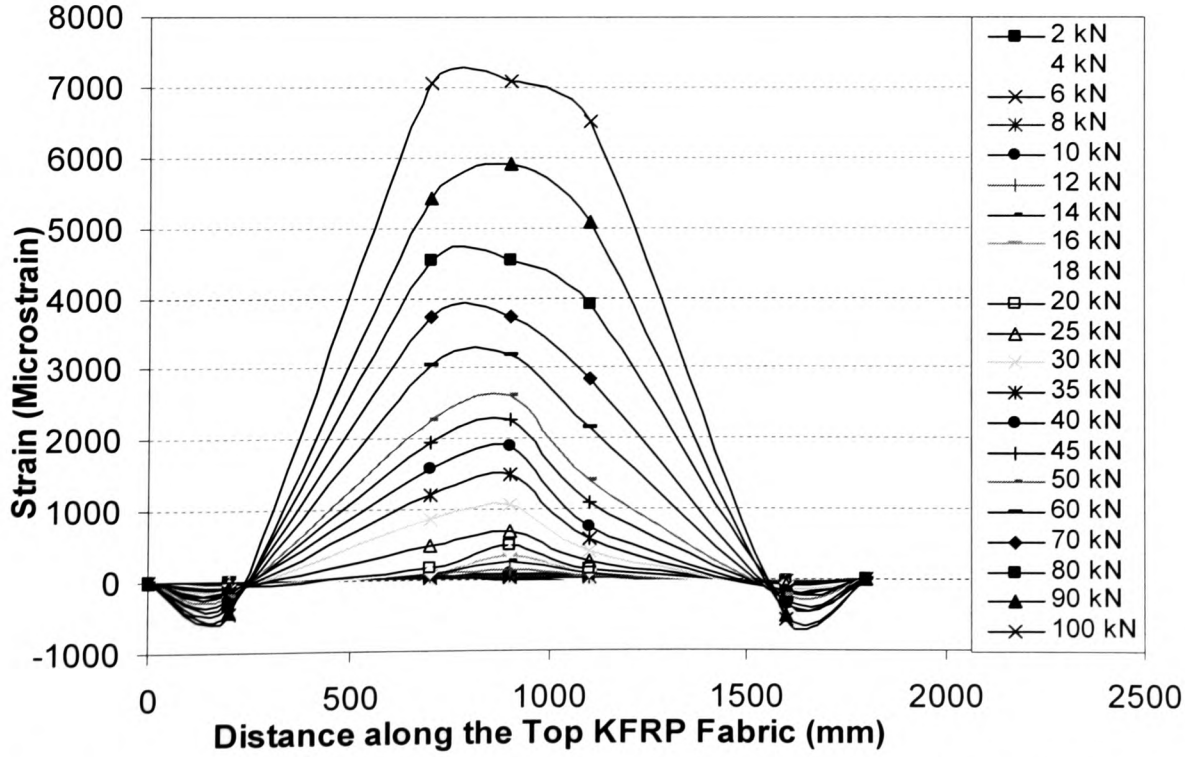

Figure 7.16 Strain Distribution of Top AFRP at Various Load Stages (M4)

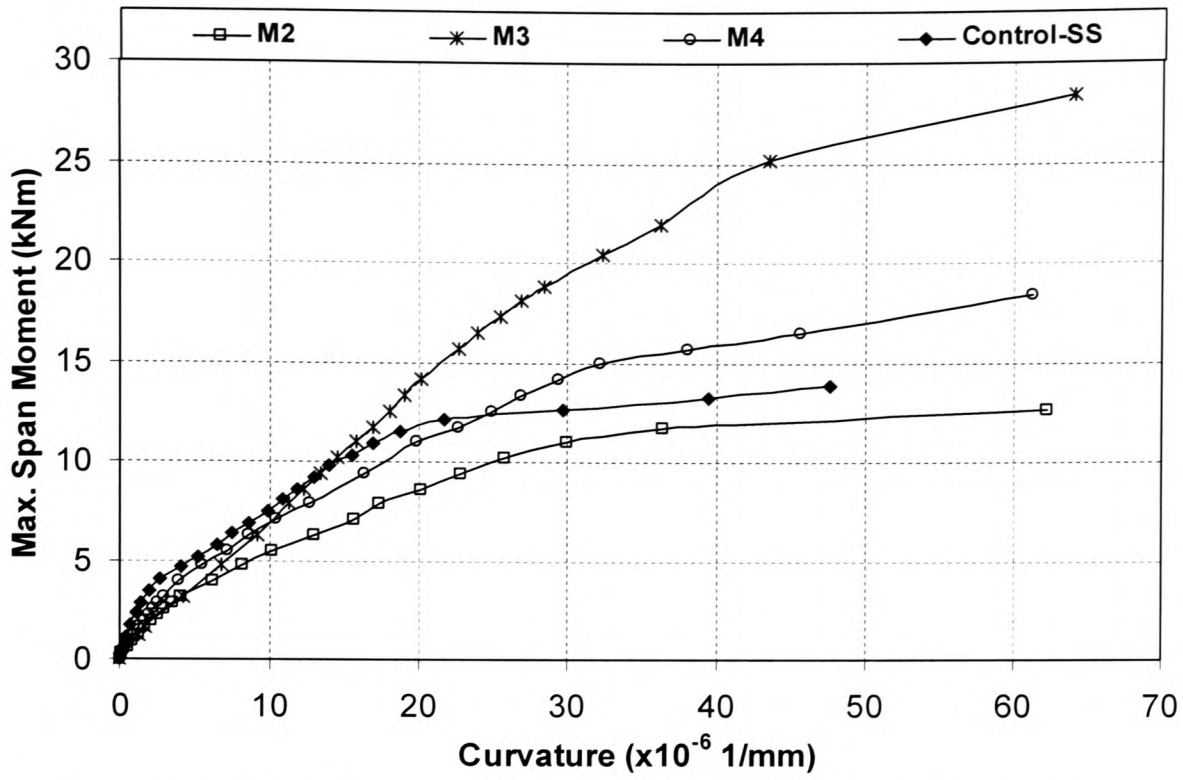

Figure 7.17 Deflection Based Moment Curvature Curves for Continuous Beams

The maximum moment of resistance at the point load position in the span of beam M4 can now be estimated by the following equation:

$$M = f_p A_p (h + t_a + \tfrac{t_p}{2} - 0.45x) + f_y A_s (d - 0.45x) \qquad (7.14)$$

Substituting all known parameters into Equation (7.14), the moment of resistance in the span is evaluated to be **24.5** kNm. Similarly the moment of resistance at the middle support is determined to be **26.1** kNm.

Based on the elastic analysis of the continuous beam, the bending moment at the middle support at beam failure is 230.9P = 230x116.9/1000 = 26.9 kNm. Comparing with 26.1 kNm, this suggests that at the support, the elastic moment had hardly been reduced. Inspection of the strain distribution (Figure 7.16) also confirmed that at least no moment reduction had taken place before 100 kN, since the strains were still increasing with the increase of load.

However, the moment in the span appeared to have substantially increased from the value of elastic analysis of 18.3 kNm at the failure load. This indicates that although no full plastic hinge could be formed at the middle support, partial moment redistribution did occur in the beam. The middle support could therefore be referred to as a "partial plastic hinge" which could still take further loading without reduction in moment resistance.

7.4.4.4 Deformability and ductility index of continuous beams

The deformability and ductility indices of FRP strengthened continuous beams can be determined using the methods discussed in previous sections of this Chapter. Listed in Table 7.8 are the deformability index values for the four continuous beams.

Table 7.8 Deformability Index of Continuous Beams

Beam Reference	Deformability Index φ_{df}	Ductility Index φ_{du}	Failure Mode
M1	1.60	1.08	Brittle
M2	2.68	2.43	Mild
M3	1.88	1.52	Brittle
M4	2.15	1.95	Mild

It can be seen that the AFRP fabric strengthened beam M4 exhibited suitable ductility, and this beam failed, although with premature debonding, in a ductile manner similar to beam M2. The greatly over strengthened beam M3, even though sufficient warning signs were observed, still failed in shear, which was considered brittle.

7.5 SUMMARY

The apparent lack of structural ductility in FRP strengthened RC elements is one of the most important issues in the design of strengthening works. This chapter has highlighted the misconception that high deformation in FRP strengthened elements leads to great ductility. It has shown that members with sufficient deformation can still fail in a very

brittle manner. A new design-based method of quantifying structural deformability has been proposed and was shown to represent the behaviour well. High deformability is considered a prerequisite of good ductility, and is therefore desirable. However, a significant amount of elastic stored strain energy, in over strengthened members, will result in extreme and brittle failure mechanisms when the energy is released at failure. The deformability of an FRP strengthened member was found to be influenced by the area fraction of FRP provided, the concrete strength and the existing steel reinforcement ratio. It was found that a deformability index of at least 2.0 tends to lead to reasonably ductile failure mode, as seen in the series B test beams.

It was found that full plastic hinges could not be developed in FRP over strengthened sections, since the ultimate strength of the FRP composites could not be reached. Therefore no moment redistribution in the traditional sense was envisaged to have taken place. However, it was evident that some moment redistribution in the strengthened system did occur. The redistribution process was therefore considered to be fundamentally different from the traditional concept of moment redistribution, which only takes place after the full formation of a plastic hinge.

CHAPTER 8

Development of Design Guidelines

8.1 INTRODUCTION

As discussed in Chapter 1, in the UK and many other developed countries, there is now an appreciable number of bridges, building structures and other facilities that have been strengthened using externally bonded Fibre Reinforced Polymer (FRP) composites. The trend is growing as this new strengthening technique becomes better understood and appreciated, and the material and project costs are reduced. Nevertheless, few national design standards or codes of practice for FRP strengthening of concrete structures or other general design guides exist (Chaallal, *et al* 1998). The first independent design guidance developed by the Concrete Society in the UK (Concrete Society, 2000) was recently published. However, this document is only regarded as an interim guidance and it is still open for discussion and recommendation.

Based on the current experimental and numerical studies, this chapter proposes a set of design guidelines and equations for flexural and shear strengthening of RC beams and slabs using externally bonded FRP plates or fabric sheets. The design equations are derived based on the criteria that the strengthened structures, under certain conditions, still exhibit acceptable level of ductility. The principles used include linear strain compatibility theory. The well established stress-strain relationships were applied to all

materials present in the section. The symbols used are based on the current British codes of practice BS8110 and Eurocode EC2. Design examples are presented, and experimental verification has been carried out. The test results show good agreement with the proposed design formulae.

8.2 FAILURE MECHANISMS OF FRP STRENGTHENED SECTIONS

For FRP composites strengthened reinforced concrete elements, there exist the following types of possible failure modes:

1. Concrete crushing in compression zone;
2. Tension steel reinforcement yield, followed by concrete compression failure;
3. Shear failure;
4. Peeling or debonding of FRP composites from concrete;
5. Tearing-off of concrete cover where FRP composites remain bonded;
6. Delamination of FRP prelaminated plate;
7. Rupture of FRP laminates/fabrics;
8. Combination of any of the above.

Of these failure mechanisms, some are not commonly seen and can be avoided. The peeling and debonding of FRP composites from the concrete surfaces can be easily prevented if a suitable adhesive system is used, and appropriate surface treatment is carried out prior to plate bonding. The shear failure is due to the insufficient shear resistance from the existing internal shear reinforcement. It is viable and effective to bond FRP fabrics externally to enhance the shear capacity, as demonstrated in the C and M series of beam tests. More details on shear strengthening design is presented later in this Chapter. The delamination of FRP plate occurs very rarely, it may be attributed to the manufacturing quality control of the composites, or the plate thickness.

The rest of the flexural failure modes may be summarised into three categories, which are typical as seen in the current laboratory tests and reported in literature. These are shown in Figure 8.1.

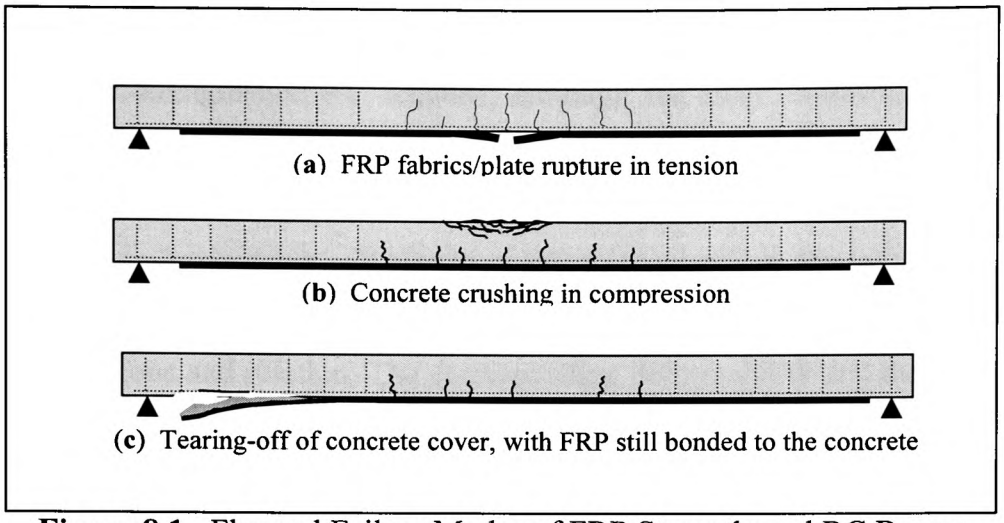

Figure 8.1 Flexural Failure Modes of FRP Strengthened RC Beams

At the Ultimate Limit State (ULS), the FRP strengthened elements fail, but the manner in which these failures occur is drastically different. It is important to identify which type of failure mode is considered acceptable so that a design method can be devised accordingly. The deciding factor for an "acceptable" failure mode is whether it is sufficiently ductile. A ductile structural failure takes place gradually, and the associated large deformation can thus serve as a pre failure warning.

8.2.1 Steel Yield, FRP Rupture followed by Concrete Crushing

This type of failure mode is considered to be most readily acceptable among all typical failure mechanisms seen in FRP strengthened sections. It is characterised by the apparently large deflections due to the yielding of internal steel reinforcement at service load, as discussed in the following section. At the pre-failure stage, a snapping sound in the FRP fibres could be heard when fabric sheets were used. This is taken as a definite indication of the imminent failure, so that necessary actions can be taken.

For beams strengthened by prelaminated FRP plates, the sections may often become over strengthened. The tensile strains in the system may thus result in a large amount of strain energy being accumulated in the FRP composites. Consequently, the failure will exhibit very brittle characteristics, as the stored strain energies are released.

8.2.2 Concrete Crushing with FRP Remaining Elastic

In greatly over strengthened RC sections, although the steel reinforcement will still yield at and after service load, the magnitude of these strains will be greatly reduced (please see Section 8.3.3). As the strain in the concrete in compression increases, the value of the neutral axis depth will also increase to accommodate the large tension force in the FRP. As a result, the strains in the FRP composites will be decreased, which leads to small deflections and rotation. The corresponding deformability and ductility indices will be small, and when the concrete reaches the ultimate strength, the beam will fail suddenly in a brittle manner. In such cases, no sufficient pre-failure warning such as large deflection or excessive cracking will be present, hence this type of failure is considered unacceptable and should be avoided.

8.2.3 Tearing-off and Debonding Failure

As discussed in Chapter 6, the tearing-off of concrete cover at the internal reinforcement level is extremely brittle and should be prevented. This can be achieved by optimising the design so that the tearing-off stresses at the plate cut-of position are small enough to ensure that flexural failure occurs first.

The principal function of an adhesive system in FRP strengthening is to ensure composite action between the FRP composites and the concrete so that the tensile stresses may be effectively transferred to the FRP. This role can be readily fulfilled by a number of epoxy-based plate bonding adhesives such as Resifix 31 and other epoxy laminating resins used in the current project. It may also be desirable for a "smart" adhesive system to be developed, which will not only transfer the stresses to the plates, but may actually, together with the FRP plate, form a part of confinement of the over stressed concrete. As suggested in Chapter 6, a primer can be considered to act as a buffer agent between FRP and concrete. When the interfacial stresses at the bondline reach the concrete strength, the primer lay will gradually "yield" to enable the release of part of the large amount of strain energy accumulated in the system, and the failure mode will be much milder when it eventually occurs.

8.3 PARTIAL FACTORS OF SAFETY

8.3.1 Partial Safety Factor for Materials Strength

Until very recently, there had been no commonly accepted values for the partial factors of safety with respect to FRP composite materials, γ_m. Since there are a number of distinctive methods for manufacturing composites, the FRP mechanical properties are greatly influenced by the these methods. In the latest official design guidelines published by the Concrete Society (2000), it was recommended that these partial safety factors should be a function of the type of fibre and the manufacturing process as presented by Clarke (1996) in the EUROCOMP Design code. The final value of partial factor of safety for composite material is expressed by the following equation.

$$\gamma_{mF} = \gamma_{mf} \times \gamma_{mm} \qquad (8.1)$$

where the factor γ_{mf} depends on the type of FRP composites used, as shown in Table 8.1, while the factor γ_{mm} takes account of the various manufacturing process as shown in Table 8.2.

Table 8.1* Partial Factors of Safety for Material Strength for FRP

Material	Partial factor of Safety γ_{mf}
Carbon FRP	1.4
Aramid FRP	1.5
Glass FRP	3.5

* Reproduced from the Concrete Society Design Guidance (Concrete Society, 2000)

The product of γ_{mf} and γ_{mm} for various carbon FRP composites could therefore range from 1.54 for pultruded plates to 1.96 for the in-situ wet lay-up sheets. For prefabricated hand-held sprayed Glass FRP shell, however, the factor of safety could be as high as 7.7. There is certainly a need for the composites manufacturers, the consultants and the

Table 8.2 Partial Factor of Safety for FRP Manufacturing Methods (Clarke, 1996)

Type of System (and method of application or manufacture)		**Additional Partial Factor of Safety** γ_{mm}
Plates	Pultruded	1.1
	Prepreg	1.1
	Preformed	1.2
Sheets or Tapes	Machine-controlled application	1.1
	Vacuum infusion	1.2
	Wet lay-up	1.4
Prefabricated (factory-made) Shells	Filament winding	1.1
	Resin transfer moulding	1.2
	Hand lay-up	1.4
	Hand-held spray application	2.2

researchers to study the possibility of reducing the high values of safety factor. There are a number of major disadvantages if an excessively high value of material safety factor is applied in strengthening design. The following points apply:

- Firstly, it is obviously not economical. The material manufacturers need to find ways of improving the quality and reliability of the FRP, especially GFRP products.
- Secondly, it may be dangerous, since high safety factor may lead to great underestimation of composite strength. As a result, an intended under strengthened or balanced section could indeed be greatly over strengthened, which may result in sudden and brittle failure at ultimate limit state.

The suitability of some of the current range of GFRP products as RC flexural strengthening materials, therefore, needs to be further investigated. These GFRP composites with high factors of safety may be more suitable as shear strengthening materials, as the failure strain in the shear wrapping strips are usually much lower than the ultimate strain. Naturally, it must be ensured that the strengthened elements are designed such that shear failure is not expected before any flexural failure.

8.3.2 Partial Safety Factors for Elastic Modulus

Another partial factor of safety for composite is related to the elastic modulus. Since it is recognised that the long-term value of the elastic modulus for FRP material changes with time, a safety factor, γ_{mE}, of 1.1 for CFRP and AFRP composites should be used. This is as recommended by the Institution of Structural Engineers (1999) and adopted by the Concrete Society Design Guidance, while this partial safety factor may be taken as 1.8 for Glass FRPs.

8.3.3 Reinforcement Stress Under Service Load of FRP Strengthened Sections

Once strengthened by FRP composites, the ultimate load carrying capacity of a RC beam will be increased, and the service load will also increase accordingly. However, the amount of existing internal steel reinforcement could not be altered. Consequently, steel reinforcement may yield under the new service load, leaving permanent deformation in the strengthened structure.

The Concrete Society Design Guidance recommends increasing the partial factor of safety from 1.05 to 1.25. For many older structures where an assumed grade 230 reinforcing bars were used, it was recommended that the service steel stress be increased to 1.0 f_y, provided that other factors such as crack widths and concrete quality do not preclude this approach to strengthening (Concrete Society, 2000).

It is naturally undesirable for any structure to sustain permanent deformation under service load. For FRP strengthened RC flexural elements, however, it may not be effective to simply increase the factor of safety for steel reinforcement, some amount of permanent deformation is a "side effects" of FRP strengthening and it may be inevitable.

Assume that the original ultimate load capacity of the unstrengthened member to be $\mathbf{P}_{uo}$, whereupon to be increased to $\mathbf{P}_{uf}$ after strengthening work has taken place. Considering that service load is approximately two-third of the ultimate load, there may exist a misguided view that the steel reinforcement will remain elastic after strengthening if the

new ultimate load P_{uf} is limited to $1.5P_{uo}$ or effectively limiting the enhancement ratio of load carrying capacity for a strengthened flexural element to 50%. This is based on increasing the steel stress under service load to 1.0 f_y. However, this may not necessarily be the case. Even a relatively small percentage increase, say between 30-50%, in ultimate load carry capacity, may result in the existing reinforcement yielding. This is mainly because the strain and stress distribution in the FRP strengthened section is different from that of the unstrengthened member. The concrete compressive strain will be increased and the neutral axis depth will be altered, which is likely to lead to the increase in reinforcement strain when the new service load is increased accordingly. This condition can be represented by the non-linear analytical model presented in Chapter 5.

Table 8.3 lists the values of concrete and reinforcement strains under the increased service load for FRP strengthened sections. These calculations are all based on typical testing beam configurations, in the current study, without factors of safety. The parameters used are: b = 100 mm, h = 200 mm, cover to reinforcement = 15 mm; f_{cu} = 45 N/mm^2, f_y = 560 N/mm^2, f_p = 1500 N/mm^2 and E_p = 125 kN/mm^2.

A major assumption in these calculations is that any form of premature failure will be prevented and the concrete in compression will reach its ultimate strain of 0.003500. The service load is then estimated at around two third of the ultimate load. It was found that the level of strain in the steel reinforcement was largely influenced by two factors, these are:

(a) the existing steel reinforcement ratio;
(b) the area of FRP strengthening composites provided, and hence the maximum percentage increase of ultimate load.

Figure 8.2 shows the variation of the percentage of ultimate load increase with the theoretical level of reinforcement strain at service load. For the four different reinforcement ratios used, it can be seen that the steel bars in the original lightly reinforced sections exhibited large magnitudes of strain under the service load of the newly strengthened sections. When a 10 mm^2 CFRP sheet is bonded to the tension face

Table 8.3 Steel Strains at Service Load for FRP Strengthened Sections*

Area of FRP A_p (mm^2)	Ultimate load (kN)	Service load (kN)(#)	% increase at ULS	Neutral axis depth x (mm)	Concrete comp. strain	Steel bars strain
2T6 bars, A_{sp}=56.5 mm^2						
0	18.7	12.8 (68)	-	43.4	0.0004	0.001212
10	40.4	26.9 (67)	116.0	24.9	0.0013	**0.007831**
20	51.2	34.3 (67)	178.2	28.1	0.0015	**0.007847**
40	65.6	42.8 (65)	250.8	34.5	0.0015	**0.006103**
60	75.8	49.0 (65)	305.3	39.4	0.0015	**0.005159**
80	83.9	54.1 (65)	348.6	43.4	0.0015	**0.004539**
100	90.6	58.4 (64)	384.5	46.9	0.0015	**0.004089**
128	98.4	63.5 (65)	426.2	51.2	0.0015	**0.003625**
160	105.8	69.3 (66)	465.7	56.4	0.0015	**0.003152**
2T8 bars, A_{sp} = 100.5 mm^2						
0	32.5	21.9 (67)	-	44.5	0.0005	0.0016
10	48.5	31.2 (64)	49.2	44.2	0.0008	**0.002365**
20	58.1	38.9 (67)	78.8	44.7	0.0010	**0.002912**
40	71.3	48.1 (67)	119.4	48.3	0.0012	**0.003147**
60	80.8	54.2 (67)	148.6	51.0	0.0013	**0.003157**
80	88.4	60.2 (68)	172.0	53.5	0.0014	**0.003178**
100	94.7	62.8 (66)	191.3	55.5	0.0014	**0.003012**
128	102.1	69.6 (68)	214.2	58.7	0.0015	**0.002966**
160	109.1	73.3 (67)	235.6	61.6	0.0015	**0.002762**
2T10 bars, A_{sp} = 157 mm^2						
0	49.2	32.1 (65)	-	51.9	0.0007	0.001659
10	60.3	40.4 (72)	22.5	52.2	0.0009	**0.002123**
20	68.1	44.9 (66)	38.4	53.3	0.0010	**0.002283**
40	79.4	54.3 (68)	61.3	55.8	0.0012	**0.002558**
60	87.8	60.1 (68)	78.4	58.2	0.0013	**0.002608**
80	94.7	62.3 (66)	92.5	59.9	0.0013	**0.002496**
100	100.4	68.1 (68)	104.1	61.9	0.0014	**0.002552**
128	107.2	70.9 (66)	117.8	64.2	0.0014	**0.002417**
160	113.7	77.6 (68)	131.1	67.2	0.0015	**0.002405**
2T12 bars, A_{sp} = 226 mm^2						
0	68.0	45.6 (67)	-	59.1	0.0009	0.001750
10	75.3	49.6 (66)	11.2	60.1	0.0010	**0.001913**
20	80.1	53.7 (67)	17.8	60.7	0.0011	**0.002001**
40	90.1	60.2 (67)	32.5	63.2	0.0012	**0.002125**
60	97.2	65.8 (67)	42.9	65.2	0.0013	**0.002189**
80	103.0	69.0 (67)	51.5	66.9	0.0014	**0.002175**
100	108.0	73.3 (68)	58.8	68.7	0.0014	**0.002163**
128	113.9	75.6 (66)	67.5	70.6	0.0014	**0.002070**
160	119.6	80.1 (67)	75.9	72.7	0.0014	**0.002025**

- As a percentage of ultimate load.

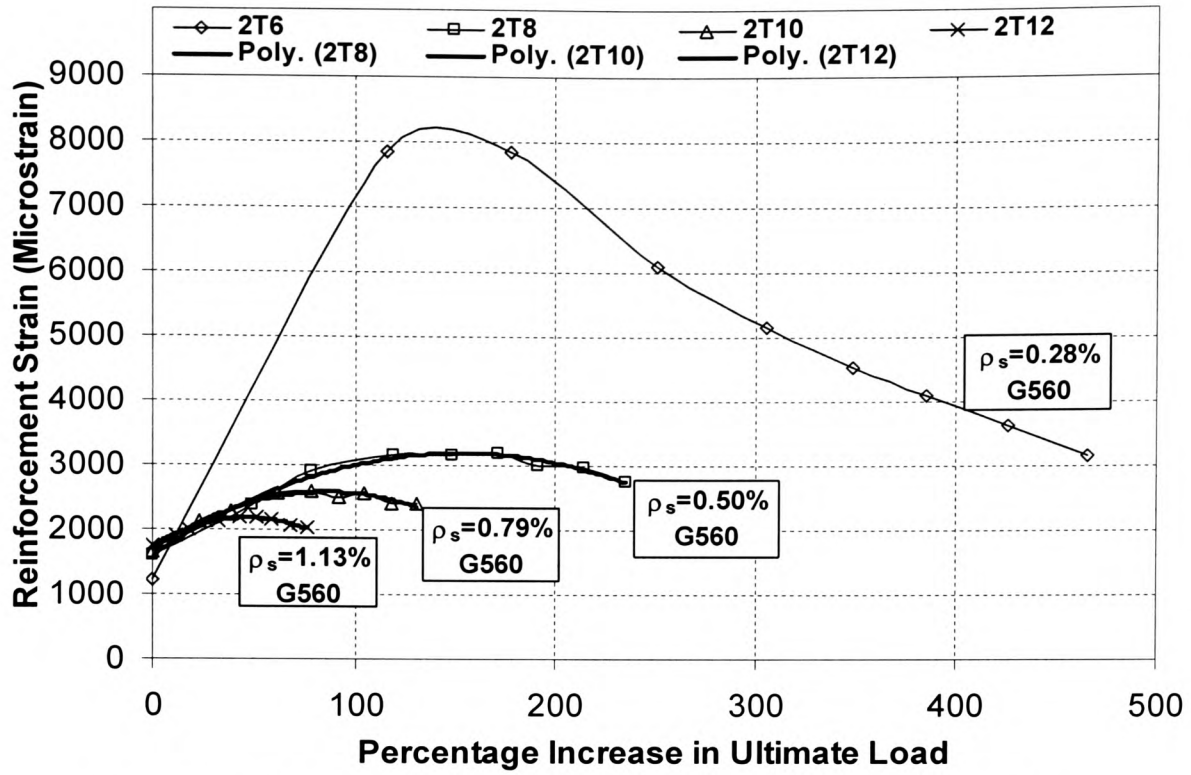

Figure 8.2 Influence of Ultimate Load Increase on Reinforcement Strain
(For actual steel yield strength 560 N/mm^2)

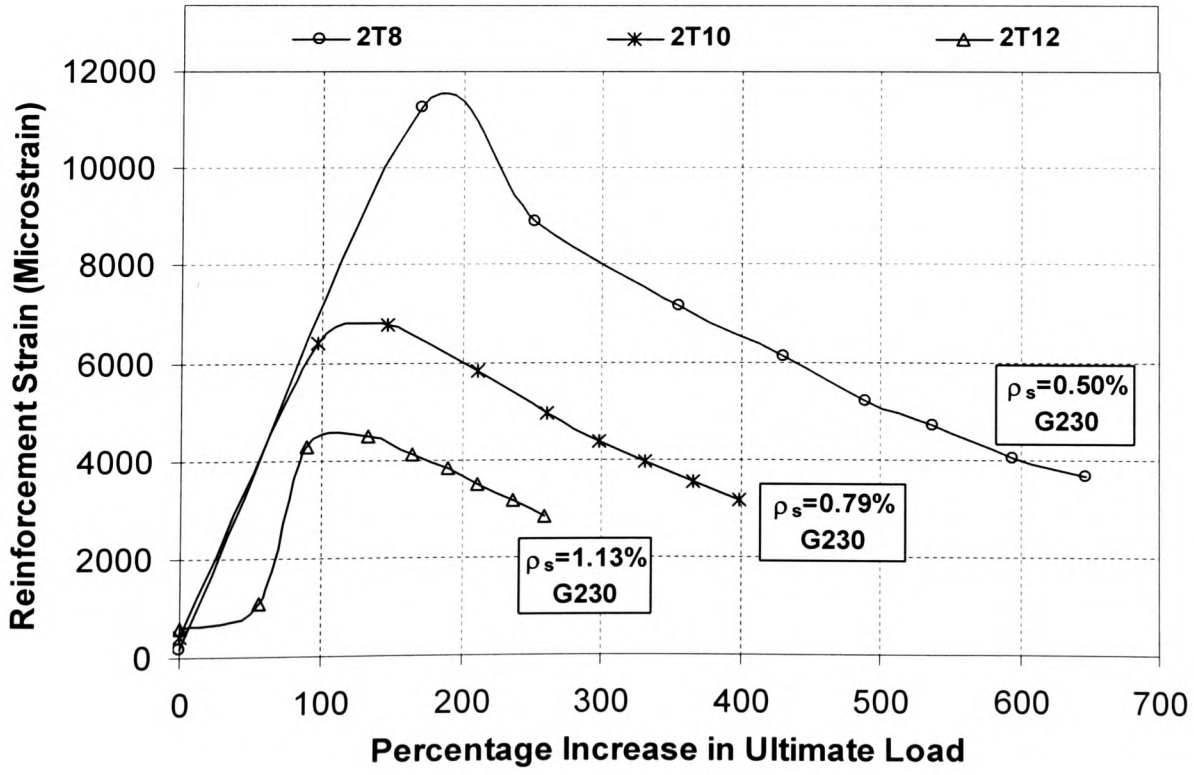

Figure 8.3 Load Increase vs. Steel Strain for the Older Grade 230 Bars

of the beam, which results in a 110% increase in the beam ultimate load capacity, the increase in steel strain at service load could reach as high as 6.5 times of the unstrengthened beam. It may therefore be concluded that for FRP strengthened RC section which are originally lightly reinforced, the strains in the internal steel reinforcement will be yielded under the new increased service load. A partial safety factor of 1.25 cannot therefore be considered effective or sufficient to ensure elastic behaviour in the steel reinforcement.

For beams with higher original reinforcement ratio, the increase in steel strains is in a much smaller scale as shown in Figure 8.2. It is still most likely that the reinforcement will yield under new service load, if typical high yield steel bars are used, which have a yield strain of approximately 0.00219 as specified by the BS 8110 (1997).

There exists a peak level in the percentage of ultimate load increase, after which the reinforcement strains will start to decrease. It can be seen that the higher the original reinforcement ratio, the lower this level will be. This percentage load increase at which the steel strain peaks, may be recommended to be a realistic limit of strengthening work. For example, the maximum percentage of load enhancement for a beam with an original steel reinforcement ratio of 1.13%, may be limited to around 50%. The descending branches of the graphs in Figure 8.2 indicate that the large area of FRP provided, impose a lowering of the neutral axis depth, in order to balance the increased FRP tensile force. As the x value increases, the strains in the reinforcement naturally, will decrease. This in turn, is expected to lead to a potentially brittle and extremely dangerous failure mode. The concrete will fail as the compression zone increases, and the deflection in the strengthened beam will be of very small magnitude due to the small strains in the steel and FRP. The deformability and ductility indices will be small and thus brittle failure is ensured.

Another important consideration is the Grade 230 steel reinforcement used in many older structures. The variation of percentage load increase with the steel strain is shown in Figure 8.3. It is clear that steel strains will far exceed the 0.001500 yielding level under the new service load, and this need not be a worrying factor. The presence of FRP composite will result in increased number of cracks and hence the crack widths will not

in fact increase dramatically over the unstrengthened level. An area of 30 mm^2 of CFRP composites, or approximately a maximum 2 layers of the standard CFRP sheets, will results in 130% (with ρ_s of 1.13%) to 170% (with ρ_s of 0.5%) increase in ultimate load capacity. This confirms the validity and rationality of the earlier recommendation that the percentage at which strain peaks be used as the strengthening limit.

8.4 DESIGN FOR FLEXURE

8.4.1 Stress Strain Distribution

The ultimate concrete compressive strain, ε_{cu}, at the extreme fibre of a flexural member may vary between 0.003600 for C15 concrete and 0.002800 for grade 60 concrete. For design purposes, BS 8110 (1997) recommends this value to be 0.003500. The strain distribution and the simplified rectangular stress block of BS 8110 has been in use widely for many years, and is shown here in Figure 8.4. Other material models such as that of Eurocode 2 (1992) may also be used with only slightly different results.

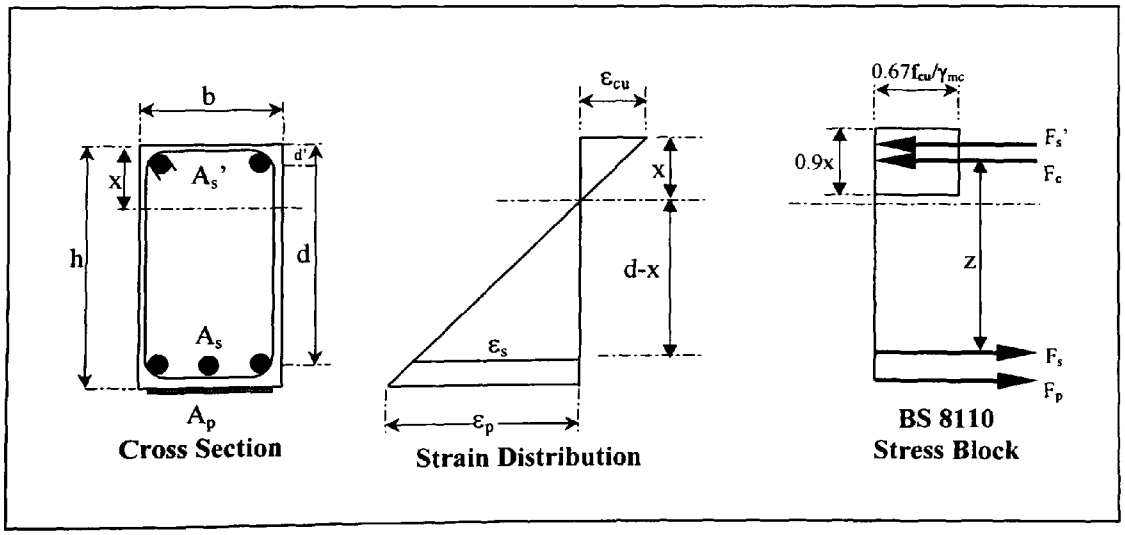

Figure 8.4 Cross Section and Stress Strain Distribution

Based on the assumption that plane sections remain plane during deformation, the strains in the steel bars ε_s, and FRP plates ε_p, can be expressed respectively as:

$$\varepsilon_s = \frac{d - x}{x}\varepsilon_{cu} \tag{8.2}$$

$$\varepsilon_p = \frac{h + t_a + t_p - x}{x}\varepsilon_{cu} \tag{8.3a}$$

Since $h >> (t_a, t_p)$, hence ε_p can be approximated as:

$$\varepsilon_p \approx \frac{h - x}{x}\varepsilon_{cu} \tag{8.3b}$$

For an existing load carrying section strengthened by FRP composites, the strain in the bonded composites should be adjusted by first subtracting the initial strain ε_o, due to the dead load or any minimal imposed load at the time of bonding FRP composites. This can be determined by:

$$\varepsilon_o = \kappa_o x = x(M_o/EI). \tag{8.4}$$

The design strength of FRP plates/fabrics can be expressed as:

$$f_{pd} = f_{pu}/\gamma_{mF}. \tag{8.5}$$

FRP composites usually exhibit linear elastic behaviour until failure. By combining Equations (8.3) and (8.5), the stress in the composites at just before failure can be determined as:

$$f_p = \varepsilon_p E_p \tag{8.6}$$

$$f_{pd} = \frac{h - x}{x}\varepsilon_{cu}E_p = \frac{f_{pu}}{\gamma_{mF}} \tag{8.7}$$

The neutral axis depth for a balanced section, x_{sb}, can therefore be evaluated as:

$$x_{sb} = \frac{h}{1 + \frac{\frac{f_{pu}}{\gamma_{mF}}}{0.0035 \frac{E_p}{\gamma_{mE}}}} \qquad (8.8)$$

For a typical pultruded CFRP plate used in the current study, the ultimate tensile strength f_{pu} and the elastic modulus E_p are 1500kN/mm^2 and 125 kN/mm^2 respectively. Substituting these values into Equation (8.8) and using partial safety factors γ_{mF} of 1.54 and γ_{mE} of 1.1, the neutral axis, x_{sb} is determined as:

$$x_{sb} = 0.289h \qquad (8.9a)$$

A CFRP plate which has an ultimate tensile strength f_{pu} of 2950 N/mm^2 and an elastic modulus E_p of 185 kN/mm^2 respectively, the neutral axis for a balanced section is:

$$x_{sb} = 0.235h. \qquad (8.9b)$$

For high strength CFRP fabric sheets, which are suitable to be used in wet lay-up applications, the strength and elastic modulus are 4900 N/mm^2, and 230 kN/mm^2 respectively. With an increased partial safety factor γ_{mF} of 1.96, the neutral axis of the fully balanced section, x_{sb}, is evaluated to be:

$$x_{sb} = 0.226h. \qquad (8.9c)$$

These figures are relatively small in comparison with the x = 0.615d for the high yield steel reinforced sections. To ensure an under-strengthened section, it is suggested that the above x values should be limited to **0.25h** for type A CFRP plate, and **0.20h** for the type B CFRP plate and type C CFRP fabrics. This effectively means that excessively high strength of FRP can never be utilised, since the area of FRP composites will have to be kept very low, as discussed in Chapter 5, to satisfy this balanced condition.

8.4.2 Under Reinforced Sections

8.4.2.1 Singly reinforced rectangular sections

The derivation of equations in this section is based on the principle that are under strengthened rectangular section is adopted so that the reinforcement will yield first, followed by the rupture of FRP composites and concrete failure in compression.

Consider the strengthening of a singly reinforced section, the force equilibrium at the cross section is expressed as:

$$F_c = F_s + F_p \tag{8.10}$$

$$0.4f_{cu}bx_{sb} = 0.95f_yA_s + 0.65f_{pu}A_p \tag{8.11}$$

Here, γ_{ms} of 1.05 has been taken for steel reinforcement, and γ_{mc} of 1.50 for concrete, as recommended by BS 8110 (1997), and if the section is to be designed as fully balanced, then the maximum FRP plate area can de determined by the following equation.

$$A_{p\max} = \frac{0.08 f_{cu} bh - 0.95 f_y A_s}{0.65 f_{pu}} \tag{8.12}$$

When A_p in Equation (8.12) becomes negative, it indicates that the strengthened section should not be treated as an under reinforced design. Hence for the newly strengthened section, the ultimate load carrying capacity can be readily determined. The minimum lever arm z for a balanced section is, assuming that h = 1.1d,

$$z = d - 0.45x_{sb} = d - 0.45 \times 0.2 \times 1.1d = 0.9d. \tag{8.13}$$

Taking moments about the concrete compression, the maximum moment that a balanced section can resist is therefore:

$$\begin{aligned} M_{max} &= 0.95f_yA_s \times 0.9d + 0.65f_{pu}A_p \times (1 - 0.45 \times 0.2) \times 1.1d \\ &= d(0.85f_yA_s + 0.65f_{pu}A_p). \end{aligned} \tag{8.14}$$

For a given applied moment of M, if $M<M_{max}$, the FRP area required can therefore be determined as:

$$A_{pr} = \frac{M - 0.85 f_y A_s d}{0.65 f_{pu} d} \tag{8.15}$$

The increase over the original design moment of resistance is:

$$M_{incr} = M - 0.95 f_y A_s z \tag{8.16}$$

where z is the original lever arm from the centroid of steel reinforcement to the resultant concrete compression force, z = d - 0.45x, and x is the neutral axis depth before strengthening, which can be determined as follows:

$$x = \frac{0.95 f_y A_s}{0.4 f_{cu} b} < 0.5d \tag{8.17}$$

The original lever arm z has a minimum value of 0.775d. The condition of applying the above equation is that the new neutral axis depth for the FRP strengthened section is less than the original neutral axis before strengthening.

8.4.2.2 Doubly reinforced sections

For existing doubly reinforced sections, assuming that the compression steel reinforcing bars reach the design strength of $0.95f_y$, then,

$$F_s' + F_c = F_s + F_p \tag{8.18}$$

$$0.40 f_{cu} b x_{sb} + 0.95 f_y A_s' = 0.95 f_y A_s + 0.65 f_{pu} A_p \tag{8.19}$$

$$A_{pmax} = \frac{0.08 f_{cu} bh - 0.95 f_y (A_s - A_s')}{0.65 f_{pu}} \tag{8.20}$$

Take moment about the concrete compression, the ultimate moment of resistance for the FRP strengthened, doubly reinforced section, is therefore:

$$M = 0.95f_yA_s \times 0.9d + 0.65f_{pu}A_p \times (1-0.45\times0.2) \times 1.1d - 0.95f_yA_s' \times (0.45\times0.2\times1.1d-d')$$
$$= d(0.85f_yA_s + 0.65f_{pu}A_p) - 0.95f_yA_s'(0.1d-d'). \quad (8.21)$$

For the special case of d' = 0.1d, the moment of resistance can be simply approximated to:

$$M = d(0.85f_yA_s + 0.67f_{pu}A_p) \quad (8.22)$$

This equation has the same form of Equation (8.14). In order to ensure that the compression steel yields, the compressive in the compression reinforcement, ε_s', must reach 0.002185 (0.95*460/200000), or:

$$\varepsilon_s' = 0.0035(1-d'/x) = 0.002185. \quad (8.23)$$

From which d'/x is found to be 0.375. The d'/x ratio therefore, must be limited to 0.375, or d' < 0.075h when x = x_{sb} = 0.2h.

If d'/x >0.375, the compression steel will not yield, and Equation (8.20) has to be modified to:

$$A_{p\max} = \frac{0.08f_{cu}bh + 0.95f_{ys}'A_s' - 0.95f_yA_s}{0.65f_{pu}} \quad (8.24)$$

where f_{ys}' is the actual stress in the compression bars, which can be determined as:

$$f_{ys}' = 700(1-d'/x) \quad (8.25)$$

The above equations are suitable for application of strengthening conventionally under reinforced sections, and the strengthened sections will remain under reinforced. The failure mode therefore will be starting with the yielding of internal tension

reinforcement followed by the rupture of the external CFRP reinforcement, and finally leads to concrete failure in the compression zone.

The compression steel reinforcement will also yield if d' is less than 0.1d. However, if the doubly reinforced section was originally designed so that the difference of tension and compression steel, A_s-A_s', equals to the maximum reinforcement area provided for a singly reinforced section, then Equation (8.20) will yield to the same value as that of Equation (8.12) for the singly reinforced sections. This indicates that FRP strengthening work beyond the area limit as determined by Equation (8.20), should not be carried out, unless suitable enhancement to the compression zone is also ensured at the same time. The reason for this is simply: for the additional steel reinforcement provided in the concrete compression zone, an equivalent amount of steel must have been provided in the tension zone to maintain the force equilibrium.

8.4.2.3 Critical reinforcement ratio

The percentage increase in the ultimate load capacity for singly reinforced concrete elements, largely depends on the amount of the original steel reinforcement provided. If the original steel reinforcement was designed to resist the maximum applied moment, e.g., $M=0.155f_{cu}bd^2$, then the area of steel provided was already the maximum for a singly reinforced section. The beams in such a case should not be strengthened since acceptable ductile characteristics will not be achieved. A ductile failure is ensured only if the area of FRP composites provided is less than the values defined in Equations (8.12), (8.20). Reorganising Equation (8.12) and dividing the area of steel by the product of **bh**, the maximum steel reinforcement ratio, ρ_{scr}, beyond which strengthening should not normally take place, can be expressed as:

$$\rho_{scr} = \frac{0.4x_{sb}f_{cu}}{0.95f_y h} \tag{8.26}$$

This ratio may be referred to as the critical reinforcement ratio for under strengthening. Figure 8.5 shows a typical relationship of the maximum percentage of possible increase in ultimate load capacity against the steel reinforcement ratio for grade 45 concrete and

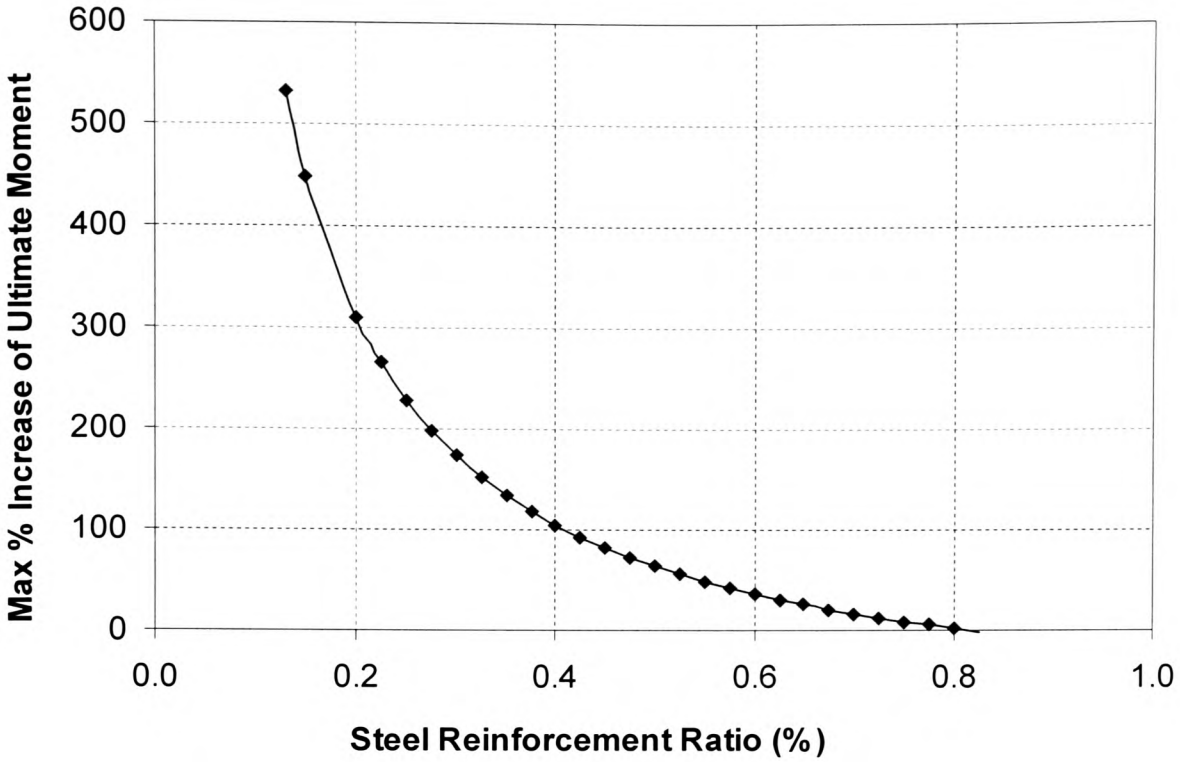

Figure 8.5 Maximum Possible Percentage Increase in Ultimate Moment of Resistance vs. Existing Steel Reinforcement Ratio

high yield reinforcement. It is clear that if the reinforcement ratio exceeds the critical value of 0.824, then a "ductile strengthening" is no longer possible.

It can be seen that for an existing reinforcement ratio of between 0.2 – 0.6%, the maximum possible percentage increase in ultimate load capacity for the FRP strengthened section is between 310% and 40%.

These relatively low reinforcement ratios are more typically used in solid RC slabs rather than in beams. For example, for a 200 mm thick slab with 10 mm diameter bars at 200 mm centres, the corresponding reinforcement ratio is just under 0.2%, and the maximum possible increase in ultimate load capacity could be up to 310% after strengthening. It is therefore reasonable to suggest that RC slabs are more suitable for FRP strengthening, since an under strengthened section can be easily ensured and the sudden and brittle failure mode will be prevented.

8.4.3 Over Strengthened Sections

The range of critical reinforcement ratios for FRP under strengthening, as defined by Equation (8.26), although usual for RC slabs, are practically at the lower end of reinforcement ratios commonly used in RC beams. For most reinforced concrete beams, the typical tension reinforcement ratio ranges from 0.5% to 1.5%. This effectively means that for most RC beams, over strengthening is inevitable.

It is thus likely that the area of FRP composites provided, exceeds the maximum values as determined by Equations (8.12), (8.20) and (8.24). In such cases, the concrete in the compression zone is likely to fail in a sudden and brittle manner, unless some other premature failure occurs first.

8.4.3.1 Over strengthened singly reinforced sections

The maximum moment of resistance for over strengthened, singly reinforced sections can be determined by taking moments about the FRP at the bottom face. The adhesive and FRP thickness may be ignored:

$$M_R = 0.4 f_{cu} bx(h - 0.45x) - 0.95 f_y A_s (h - d) \qquad (8.27)$$

The neutral axis depth x in the above equation, will be greater than the balanced value of 0.2h as defined in the preceding section, since the strains in the CFRP plates will not reach the ultimate failure value. The section force equilibrium is written as:

$$0.4 f_{cu} bx = 0.95 f_y A_s + f_p A_p \qquad (8.28)$$

where the stress in the FRP, f_p, will be less than the design strength. The FRP area A_p will be greater than that defined by Equations (8.12), (8.20) and (8.24). The stress in the steel reinforcement is assumed to have reached the design strength at the ultimate limit state. As the Grade 460 high yield reinforcement used in the UK has a design strength of $0.95 f_y$, the corresponding yield strain is 0.002190. The above assumption is therefore

confirmed as demonstrated in Figures 8.2 and 8.3, where all the reinforcement strain values of FRP strengthened section exceed this limit even under service load.

Since $f_p = E_p\varepsilon_p$, and $\varepsilon_p = \varepsilon_{cu}(h-x)/x$, Equation (8.28) may be rewritten as:

$$0.4f_{cu}bx = 0.95f_yA_s + \varepsilon_{cu}\frac{h-x}{x}E_pA_p \qquad (8.29)$$

This leads to the following quadratic equation:

$$0.4f_{cu}bx^2 + (\varepsilon_{cu}E_pA_p - 0.95f_yA_s)x - \varepsilon_{cu}hE_pA_p) = 0 \qquad (8.29a)$$

The solution of the neutral axis depth, x, for a given area of FRP composite A_p, for the over-strengthened section is therefore:

$$x = \frac{0.95f_yA_s - 0.0035E_pA_p + \sqrt{(0.95f_yA_s - 0.0035E_pA_p)^2 + 0.0056hE_pA_p}}{0.8f_{cu}b} \qquad (8.30)$$

The moment of resistance is then evaluated by substituting x into Equation (8.27).

For a given applied moment M, where $M > M_{max}$ as defined by Equation (8.14), Equation (8.27) should be used and it may be rearranged as follows:

$$0.18f_{cu}bx^2 - 0.4f_{cu}bhx + M + 0.95f_yA_s(h-d) = 0 \qquad (8.31a)$$

$$x = \frac{0.40f_{cu}bd + \sqrt{0.16f_{cu}^2b^2d^2 - 0.72Mf_{cu}b}}{0.36f_{cu}b} \qquad (8.31b)$$

The area of FRP required for an "over-strengthened" section can then be determined as follows:

$$A_p = \frac{(0.4f_{cu}bx - 0.95f_yA_s)x}{\varepsilon_{cu}(h-x)E_p} \qquad (8.32)$$

Such a strengthening strategy, however, should only be applied with caution. In other words, there should be a limit of percentage increase in the ultimate load carrying capacity over the unstrengthened beam. Excessive demand of strength enhancement will result in a large area of FRP required, which in turn will lead to very brittle failure mode at ultimate load. The concrete in such cases will be suddenly crushed in the top compression zone of the beam, while the presence of large areas of FRP materials will prevent any acceptable level of deformability and ductility of the strengthened system.

It is impossible, nevertheless, to specify a generic standard of "suitable" degree of strength enhancement, since it greatly depends on the existing reinforcement details and the concrete strength. One reasonable limit for strengthening of RC beams is as recommended in Section 8.3.1.3, i.e., whenever the steel reinforcement strains start to decrease under the new service load of FRP strengthened sections, the corresponding percentage increase in ultimate load at that point should be the strengthening limit.

In the current Concrete Society Design Guidance document, there exists no specific guidance on the maximum percentage of strength enhancement. Instead, a maximum limit on the neutral axis depth is recommended to be 0.45d. The reason given for this limit is that the tensile steel should reach the yield strength under ultimate load, and at a strain of 0.004000, this is ensured. However, as discussed in Chapter 5 and also in Section 8.3.1.3, there need not be any concern over the yielding of steel reinforcement, since it is almost a guaranteed occurrence in most cases (See Figures 8.2 and 8.3). The limit of x to 0.45d is considered to be much too relaxed in comparison with the balanced x/h ratio of around 0.25. The danger of this will be a greatly over reinforced section, and an extremely brittle failure mode under ultimate load is guaranteed. The candidate recommends that the neutral axis depth of FRP strengthened sections should be kept as close to the balanced ratio as possible, and in no case should it exceed 0.35h.

It is also recommended that for strengthening flexural members, a 100% increase in ultimate load capacity, i.e., doubling the original design capacity, may be considered a practical upper limit in any strengthening case.

8.4.3.2 Doubly reinforced sections

All doubly reinforced concrete sections are designed such that the compression reinforcement play a role of "helping" the concrete in compression. The additional amount of compression resistance provided by the compression steel, is usually balanced by the provision of the additional tension reinforcement over and above the maximum for a singly reinforced section.

It is therefore a simple concept that any addition of FRP strengthening composites in the tension zone, must be accompanied by providing extra resistance in the compression zone if the same neutral axis position is to be maintained. Without the corresponding strengthening in the compression zone, the neutral axis position will move toward the tension zone, and the concrete compressive strain will increase. This will inevitably lead to the concrete being crushed in a brittle manner, while the stress and strain in the FRP are still at relatively low respective magnitude for a given load.

Strengthening for a doubly reinforced section is therefore by implication over strengthening, and should only be used with extreme caution and consideration of the expected failure mode. The maximum percentage increase for strength enhancement may be recommended to be between 20 to 30 %. This will result in a reduced safety margin against concrete crushing. Existing elements with high concrete strength in such cases have a distinctive advantage for strengthening over the relatively low concrete strength of, say, below 25 N/mm^2.

The section force equilibrium for an over strengthened, doubly reinforced section can be derived from Figure 8.2 as follows:

$$0.4f_{cu}bx + f_y'A_s' = 0.95f_yA_s + f_pA_p \qquad (8.33)$$

and the moment of resistance may be evaluated by taking moment about the FRP composites at the bottom face:

$$M_R = 0.4f_{cu}bx(h-0.45x) + 0.95f_y\{A_s'(h-d') - A_s(h-d)\} \qquad (8.34)$$

The value of x may be evaluated by equating M_R with the applied moment, but in this case it is guaranteed to have a larger value than 0.5d. This is because all the doubly reinforced sections are already designed such that the x/d ratio is at the limit of 0.5 if no redistribution of elastic moment is carried out. With the addition of FRP composite in the tension face, the neutral axis position will inevitably move further toward the tension zone and hence guarantee a value of x greater than 0.5d. The consequence of this change in neutral axis position is that the concrete strain will increase as the applied load increases, and eventually result in brittle failure.

It is therefore reasonable to suggest that doubly reinforced concrete beams should NOT be strengthened by FRP composites if the same safety margin needs to be maintained. However, at the expense of a reduced safety margin against concrete crushing, a maximum of 20% to 30% load capacity enhancement may be considered, provided that the expected possible brittle failure mode is fully investigated and provision for the aforementioned eventuality is in place.

8.5 NUMERICAL CASE STUDIES

8.5.1 Design Case One – Flanged Beams

Consider a simply supported reinforced concrete T beam. The beam has an effective span of 8.0 metres, and was originally designed to support an ultimate load of 67.5 kN/m. The section and reinforcing details are shown in Figure 8.6. It is proposed to increase the ultimate load by 20% to 81 kN/m by bonding CFRP plates to the soffit of the beam. Determine the area of CFRP composite required given the following design data, and specify the strengthening limit.

Material properties: f_{cu} = 45 N/mm^2, f_y = 460 N/mm^2, f_{pu} = 1500 N/mm^2, E_p = 150 kN/m^2.

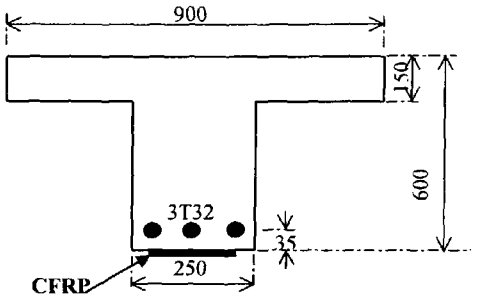

Figure 8.6 T- Section Details

Firstly, in order to secure a ductile failure mode, the original reinforcement ratio must be less than the critical ratio of reinforcement ρ_s as defined by Equation (8.26).

$$\rho_{scr} = \frac{0.4 x_{sb} f_{cu}}{0.95 f_y h} = \frac{0.4 \times 0.2 \times 600 \times 45}{0.95 \times 460 \times 600} = 0.824\%$$

The existing reinforcement area, A_s = 2412 mm^2, hence,

$$\rho_s = \frac{A_s}{bh} = \frac{2412}{900 \times 600} = 0.446\% < 0.824\%, \text{ OK.}$$

Next, the original applied moment is evaluated to be 540 kNm, and the minimum moment of resistance to be increased by is:

$$M = \frac{(81 - 67.5) \times 8^2}{8} = 108 kNm$$

Substituting M into Equation (8.15) the area of CFRP required is determined as:

$$A_p = \frac{M - 0.85 f_y A_s d}{0.65 f_{pu} d} = \frac{648x10^6 - 0.85 \times 460 \times 2412 \times 565}{0.65 \times 1500 \times 565} = 209.1 mm^2$$

From Equation (8.11), the neutral axis depth may be evaluated as:

$$x = \frac{0.95 f_y A_s + 0.65 f_{pu} A_p}{0.4 f_{cu} b} = \frac{0.95 \times 460 \times 2412 + 0.65 \times 1500 \times 209.1}{0.4 \times 45 \times 900} = 77.6 mm$$

77.6 mm < 0.2h = 120 mm, OK.

Provide 2 No 80mm wide by 1.5 mm thick by 7800mm long CFRP prelaminated plates, evenly spaced and bonded to the soffit of the beam using a suitable adhesive system (e.g. Resifix 31). Alternatively, unidirectional CFRP fabric sheets may be used, for a typical sheet of 0.145mm thickness and of similar specification. Six layers will be needed across the full web width of the beam. Wet lay-up is recommended using a suitable epoxy based adhesive system such as the MBT or Exchem laminating resins.

Finally, the maximum area of CFRP composite that could be provided for this beam is determined using Equation (8.12):

$$A_{p\max} = \frac{0.08 f_{cu} bh - 0.95 f_y A_s}{0.65 f_{pu}} = \frac{0.08 \times 45 \times 900 \times 600 - 0.95 \times 460 \times 2412}{0.65 \times 1500} = 912.8 mm^2$$

The corresponding moment of resistance for the strengthened beam is evaluated by Equation (8.14):

$M_{max} = d(0.85 f_y A_s + 0.65 f_{pu} A_p)$

$= 565 \times (0.85 \times 460 \times 2412 + 0.67 \times 1500 \times 885.5) \times 10^{-6}$

$= 1035.7$ kNm

This figure represents a maximum possible increase of 92% in the moment of resistance over the unstrengthened section. However, to provide an area of 912.8 mm^2 of CFRP plates in a narrow width of 250 mm for a T-beam may be impractical and unrealistic. The maximum increase in ultimate load capacity for this particular T beam is therefore recommended to be limited to around 20% as shown in this example.

8.5.2 Design Case Two – Singly Reinforced Rectangular Sections

Determine various strengthening options for a series of reinforced concrete beams of 400 mm width by 800 mm overall depth for the given material properties.

The results are tabulated in Table 8.4, with various steel reinforcement ratios, starting from the minimum ratio of 0.13%. The limit of a "ductile strengthening" can be defined based on the existing area of steel reinforcement provided. Since this ratio depends on the design strength of concrete and steel reinforcement, the limit in this example is determined to be 0.824%, identical to that in the case one example.

Column {1} is the maximum cross sectional area of a given FRP material, which could be provided for the existing steel reinforcement details as shown in columns {3} and {4}. The original design for the moment of resistance, listed in column {5}, is based on the steel reinforcement yielding, and the neutral axis depth x is smaller than the design value of 0.5d. For the strengthened section, the new maximum neutral axis depth used is the design value of 0.2h for the specified CFRP material. The moment of resistance for the strengthened section, as given in column {7}, is therefore still less than the maximum value of $0.155f_{cu}bd^2$, which is the maximum design moment of resistance for a balanced section, as determined assuming the concrete will reach its design compressive strength.

It is clear from column {9}, that the maximum possible percentage increase of ultimate load capacity for the given beams, could be increased by more than 5 times over the original design capacity, provided only minimum reinforcement is provided at the outset. If the section is reinforced with 3 T32 bars, the maximum percentage of increase

Table 8.4 Design Examples for a Series of 400mm x 800mm Beams

Maximum area of FRP to be provided - A_{pmax} (mm^2)		Original steel reinforcement		Original moment of resistance M_o (kNm)		Moment of resistance after strengthening M_R (kNm)		Increase over and above original design (%)	
With FOS {1}	*Without FOS* {2}	A_s (mm^2) {3}	ρ (%) {4}	**With FOS** {5}	*Without FOS* {6}	**With FOS** {7}	*Without FOS* {8}	**With FOS** {9}	*Without FOS* {10}
970.21	*1024.43*	416	0.130	**137.0**	*144.9*	**866.6**	*1299.9*	**532.6**	*797.4*
942.24	*1004.80*	480	0.150	**157.7**	*1669*	**864.4**	*1296.6*	**448.1**	*677.0*
872.32	*955.73*	640	0.200	**209.1**	*221.6*	**858.8**	*1288.1*	**310.8**	*481.3*
837.36	*931.20*	720	0.225	**234.5**	*248.8*	**855.9**	*1283.9*	**265.0**	*416.0*
802.40	*906.67*	800	0.250	**259.8**	*275.9*	**853.1**	*1279.7*	**228.4**	*363.9*
767.44	*882.13*	880	0.275	**284.9**	*302.8*	**850.3**	*1275.5*	**198.4**	*321.2*
732.48	*857.60*	960	0.300	**309.9**	*329.7*	**847.5**	*1271.3*	**173.4**	*285.6*
697.52	*833.07*	1040	0.325	**334.8**	*356.4*	**844.7**	*1267.0*	**152.3**	*255.5*
662.56	*808.53*	1120	0.350	**359.4**	*383.1*	**841.9**	*1262.8*	**134.2**	*229.7*
627.60	*784.00*	1200	0.375	**384.0**	*409.6*	**839.1**	*1258.6*	**118.5**	*207.3*
592.64	*759.47*	1280	0.400	**408.4**	*436.0*	**836.2**	*1254.4*	**104.8**	*187.7*
557.68	*734.93*	1360	0.425	**432.6**	*462.3*	**833.4**	*1250.1*	**92.7**	*170.4*
522.72	*710.40*	1440	0.450	**456.6**	*488.5*	**830.6**	*1245.9*	**81.9**	*155.1*
487.76	*685.87*	1520	0.475	**480.6**	*514.5*	**827.8**	*1241.7*	**72.3**	*141.3*
452.80	*661.33*	1600	0.500	**504.3**	*540.5*	**825.0**	*1237.5*	**63.6**	*129.0*
417.84	*636.80*	1680	0.525	**527.9**	*566.3*	**822.2**	*1233.2*	**55.7**	*117.8*
382.88	*612.27*	1760	0.550	**551.4**	*592.1*	**819.3**	*1229.0*	**48.6**	*107.6*
347.92	*587.73*	1840	0.575	**574.7**	*617.7*	**816.5**	*1224.8*	**42.1**	*98.3*
312.96	*563.20*	1920	0.600	**597.9**	*643.2*	**813.7**	*1220.6*	**36.1**	*89.8*
278.00	*538.67*	2000	0.625	**620.9**	*668.5*	**810.9**	*1216.4*	**30.6**	*81.9*
243.04	*514.13*	2080	0.650	**643.7**	*693.8*	**808.1**	*1212.1*	**25.5**	*74.7*
208.08	*489.60*	2160	0.675	**666.4**	*718.9*	**805.3**	*1207.9*	**20.8**	*68.0*
173.12	*465.07*	2240	0.700	**689.0**	*744.0*	**802.5**	*1203.7*	**16.5**	*61.8*
138.16	*440.53*	2320	0.725	**711.3**	*768.9*	**799.6**	*1199.5*	**12.4**	*56.0*
103.20	*416.00*	2400	0.750	**733.6**	*793.8*	**796.8**	*1195.2*	**8.6**	*50.6*
68.24	*391.47*	2480	0.775	**755.7**	*818.5*	**794.0**	*1191.0*	**5 .1**	*45.5*

f_{cu} =45 N/mm^2, f_y =460 N/mm^2, f_{pu} =1500 N/mm^2, γ_{mF} = 1.5, γ_{mc} = 1.5, γ_{ms} = 1.05, γ_{mE} = 1.1, b = 400 mm, h = 800 mm, d = 765 mm

in its ultimate load capacity is only around 8% in order to achieve a reasonably ductile failure mode. This clearly shows that ductile FRP strengthening is most suitable for

slabs or flanged beams where the reinforcement ratios are usually lower compared with rectangular beam sections.

Table 8.4 contains the listings of the calculations with all factors of safety removed from these calculations, including those for the original design, the results are shown in italic form. It is seen that the critical ratio of ρ_s could be increased to 1.76%, creating a much wider scope for ductile strengthening of existing structures. This indicates that the present design methodology has a reasonably large safety margin to ensure that the strengthened members will exhibit an acceptable level of ductility.

8.5.3 Design Case Three – Doubly Reinforced Rectangular Sections

The beam section shown in Figure 8.7 is to resist an applied moment of 165 kNm. The materials strengths are: f_{cu} = 30 N/mm^2 and f_y = 460 N/mm^2.

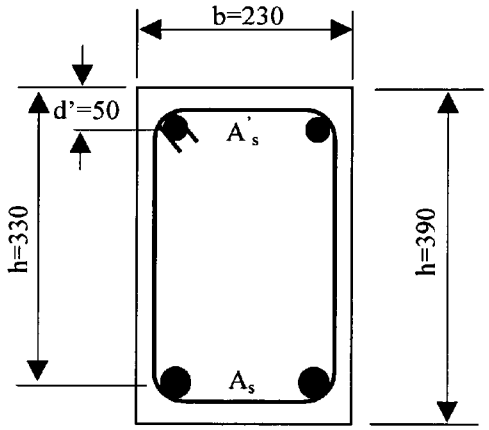

Figure 8.7 Doubly Reinforced Section Details

This original example is taken from a standard text of reinforced concrete design (Mosley *et al*, 1999).

The area of compression and tension reinforcement required can be determined using the standard design equation of BS 8110, Part 1 (1997), and are calculated to be 391 mm^2 and 1440 mm^2 respectively. Two T20 bars (A_{sp}' = 628 mm^2) are provided as compression reinforcement, while tension bars provided are two T32 bars (A_{sp} = 1610 mm^2).

Suppose that a 50% of ultimate load increase has taken place, and the section is now required to resist an applied bending moment of 250 kNm. The FRP strengthening options are as discussed as follows.

Firstly, this will be an over strengthening job by default, since no additional compression strengthening is involved. Substituting the value of bending moment into Equation (8.34),

$$250\times10^6 = 0.4f_{cu}bx(h-0.45x)+0.95f_y\{A_s'(h-d')-A_s(h-d)\}$$
$$= 0.4\times30\times230x(390-0.45x)+0.95\times460\times\{628\times(390-50)-1610\times(390-330)\}$$

The neutral axis depth value x can be solved from the above equation:

x = 267 mm = 0.81d, and strain in the FRP can be determined as:

$$\varepsilon_p = \frac{0.0035}{267}(390-267) = 0.001600.$$

Assuming that type B of CFRP plates are to be used (f_{pu}=2950 N/mm^2, E_p=185 kN/mm^2). This will result in a required CFRP area of 1040 mm^2, through substitution of relevant values into Equation (8.33). The results suggest an equivalent of 9 number of 80 mm wide by 1.6 mm thick plates, or a 230 x 5.0 mm thick plate!

It is clearly unrealistic to use such a large area of CFRP plates for strengthening at such a low stress of 296 N/mm^2 (0.001600 × 185000).

It must be noted that in the Concrete Society Design Guidance there is no specific reference to the limit of x/d ratio for doubly reinforced section. However, it does not appear to distinguish the singly and doubly reinforced sections with respects to the neutral axis positions, and this may lead to the designers falsely thinking that 0.5d in x value is the limit as is in the conventional RC design.

In the above example, if x is limited to 0.5d (165 mm), the corresponding FRP strain would be 0.004900, and the area of CFRP required (type B plates) can be determined by Equation (8.33) as 29 mm^2. The corresponding moment of resistance, using Equation (8.34) is thus determined as 195 kNm. The stress in the CFRP would be 906 N/mm^2

(0.004900 × 185000). The increase in ultimate load capacity in this case, however, is just over 18%.

This confirms the earlier suggestion that doubly reinforced sections should not normally be strengthened by FRP composite, and if the strengthening work has to be carried out, the percentage increase of load capacity should be limited to 20-30%, while the neutral axis depth should be limited to 0.5d.

8.5.4 Design Case Four – Solid RC Slabs

Solid RC slabs usually have relatively low reinforcement ratios, and are best suited for FRP strengthening as discussed previously. Consider a continuous RC slab (Mosley *et al*, 1999) as shown in Figure 8.8. The four-span slab supports a live load of 3.0 kN/m^2 and a total dead load, including self-weight, of 5.05 kN/m^2. The material strengths are f_{cu} = 30 N/mm^2 and f_y = 460 N/mm^2.

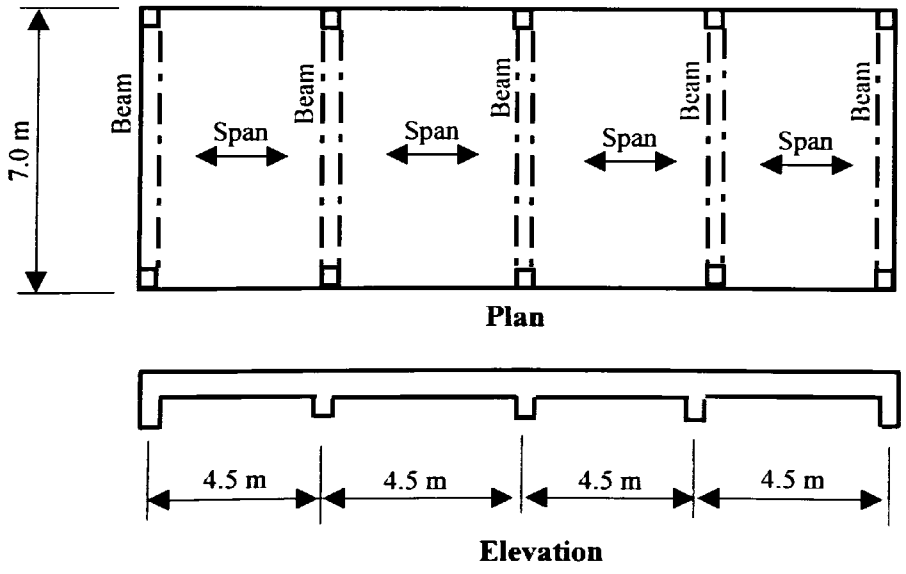

Figure 8.8 Continuous RC Slabs

The original slab is designed to be 170 mm thickness with an effective depth of 140 mm. It is subjected to a maximum bending moment of 20.8 kNm (Using Table 3.12 of BS 8110, Part 1) at the first interior supports and at the end spans. The calculated

required area of tension reinforcement at these positions is 357 mm^2, and T10 bars at 200 mm centres are provided, with A_p equals to 393 mm^2.

Suppose that, due to a drastic change of use, the floor slab is now required to resist an increased live load of 6.0 kN/m^2. The FRP strengthening option is discussed as follows.

Firstly, the increase in load will result in a new ultimate design moment of 29.1 kNm, which is a net 40% increase over the original design value. The critical reinforcement ratio, as defined by Equation (8.26) is:

$$\rho_{scr} = \frac{0.4 x_{sb} f_{cu}}{0.95 f_y h} = \frac{0.4 \times 0.2 \times 170 \times 30}{0.95 \times 460 \times 170} = 0.55\%$$

Th existing reinforcement ratio is 0.23%, therefore it is viable to have an under strengthened section. Using Equation (8.15), and assuming CFRP fabrics sheets are used (f_{pu}=1500 N/mm^2, E_p=125 kN/mm^2). The area of FRP required to strengthen the section is:

$$A_{pr} = \frac{M - 0.85 f_y A_s d}{0.65 f_{pu} d} = \frac{29.1 \times 10^6 - 0.85 \times 460 \times 393 \times 140}{0.65 \times 1500 \times 140} = 55.6 mm^2$$

Providing a single layer of 100 mm wide by 0.145 mm thick CFRP fabric sheets at 150 clear spacing, the area provided is 58 mm^2.

This example supports the earlier suggestion that FRP strengthening is best suited for RC slabs and other elements which are usually lightly reinforced. One important consideration of slab strengthening is the clear spacing of composites. This needs further investigation. Until more specific research and guidelines are developed, it is recommended that a maximum clear spacing of 1.5 times of the width of the FRP plates or sheets may be used. Alternatively, a "secondary layer", similar to the function of distribution steel reinforcement in slabs, may be used at the perpendicular direction to, and before the bonding of, the main strengthening composites.

8.6 SHEAR STRENGTHENING

8.6.1 Experimental Evidence

It has been shown in the current experimental investigation that external FRP shear wrapping provides effective additional shear resistance to concrete beams. The simply supported Beams B2 and two continuous beams M1 and M3 all failed in shear in a brittle manner, at ultimate limit state, as shown in Figure 8.9. The failures occurred at positions where no internal steel shear reinforcement was provided and the shear resistance was provided by the concrete beam and the externally bonded FRP wrapping.

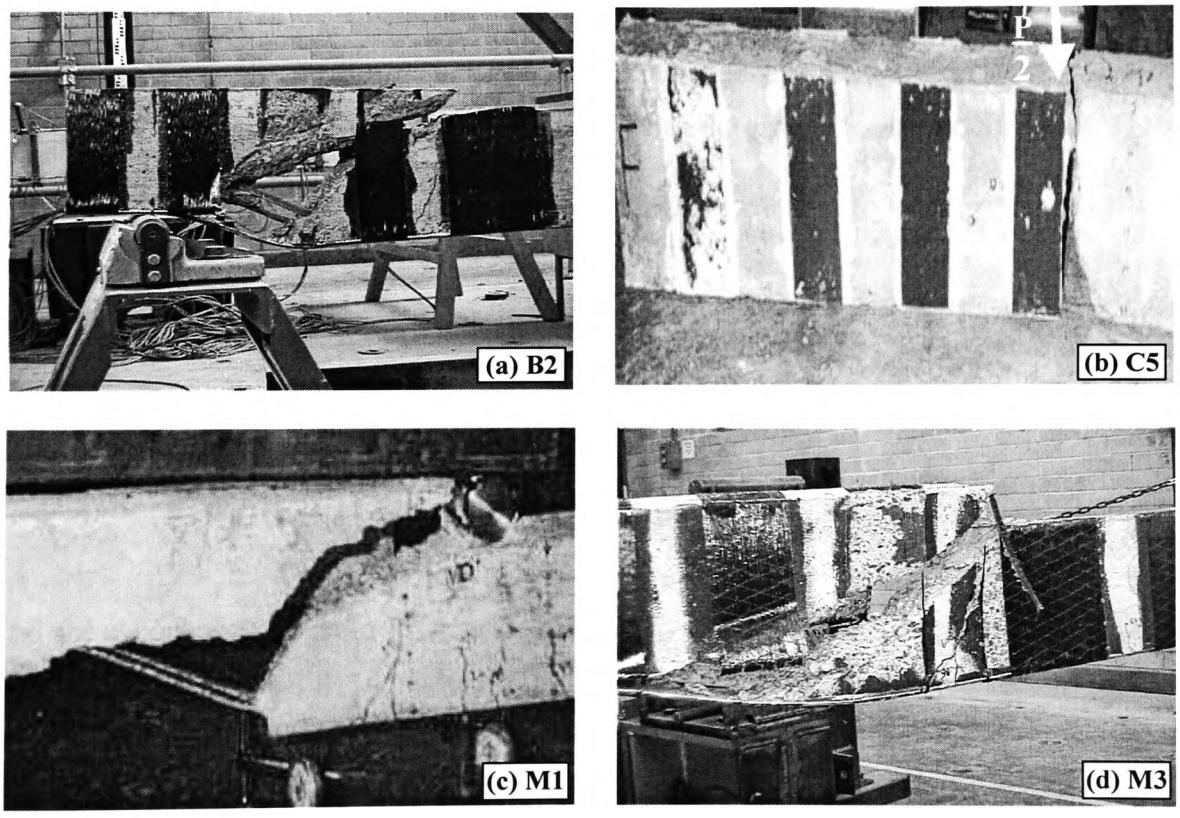

Figure 8.9 Typical Shear Failure Mode of Simple and Continuous Beams

Beams in series C failed in the flexural region due to the lack of internal tension reinforcement. The shear spans were externally reinforced by CFRP plates, and no shear cracks were observed at the ultimate failure (Figure 8.9b).

8.6.2 Evaluation of Shear Resistance

The shear resistance of a RC flexural member consists three parts:

(1) Design concrete shear stress, v_c;
(2) Contribution from shear links, v_l;
(3) Contribution from FRP composites, v_p.

If the combined shear resistance of concrete and the steel links is less than the applied shear force, then FRP composite may be provided to strengthen the shear capacity, in the form of external shear strips, shear wings or U-jackets.

The design concrete shear stress v_c and the resistance provided by any internal steel links, v_l, may be determined by the standard procedure as recommended in BS 8110: Part 1: 1997, by the following equations.

$$v_c = \frac{0.79}{\gamma_m}\left(\frac{100A_s}{b_v d}\right)^{\frac{1}{3}}\left(\frac{400}{d}\right)^{\frac{1}{4}}\left(\frac{f_{cu}}{25}\right)^{\frac{1}{3}} \tag{8.35}$$

$$v_l = 0.95 f_{yv} A_{sv} \frac{d}{S_v} \tag{8.36}$$

The shear contribution from FRP strips may be evaluated using a similar truss analogy as that deployed by BS 8110, shown in Figure 8.10. Let A_{pv} be the cross section area of each FRP shear strip.

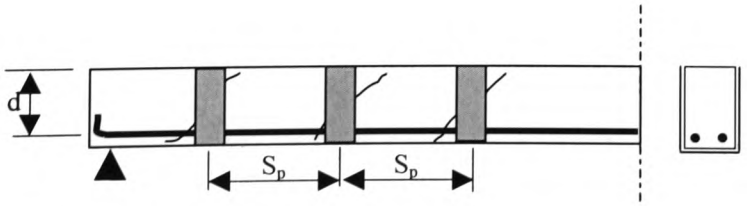

Figure 8.10 FRP Strip Shear Reinforcement

The total area of A_{pv} that intersects a full shear crack is $A_{pv}\frac{d}{s_p}$. The shear resistance can be expressed, in BS 8110 format, as this area multiplied by the design strength of FRP composites, using the following equation:

$$v_p = \frac{f_p}{\gamma_{mF}}\frac{A_{pv}}{S_p b} \tag{8.37a}$$

If the strengthening FRP is inclined at an angle β to the longitudinal axis of the strengthened member, the FRP shear contribution may be rewritten as:

$$v_p = \frac{f_{pf}}{\gamma_{mF}}\frac{A_{pv}}{S_p b}\sin\beta(1+\cot\beta) \tag{8.37b}$$

The stress in the FRP strips at failure, f_{pf}, depends on many factors including the bonding condition and the shape of wrapping. The Concrete Society Design Guidance recommends a limit FRP strain of 0.004000. Previous published work (Triantafillou, 1998; Khalifa *et al* 1998; Maeda *et al*, 1997) have shown that the failure strain in the FRP strips is influenced by the axial rigidity of the sheet. It could be much smaller than the average ultimate strain due to stress concentrations at sharp corners. The following equations were used by Khalifa *et al* (1998) and Khalifa and Nanni (2000) to estimate the FRP failure strain ε_{pe} due to the stress concentration at corners and the bond failure between FRP and concrete:

$$\varepsilon_{pe} = e_{pu}\{0.5622(\rho_p E_{pu})^2 - 1.2188(\rho_p E_{pu}) + 0.778\} \quad (\text{If } \rho_p E_{pu} < 1.1 \text{ N/mm}^2) \tag{8.38}$$

$$\varepsilon_{pe} = 0.0042\{0.835 f_{cu})^{2/3} W_{pe}\}/\{(E_p t_p)^{0.58} d\} \tag{8.39}$$

where W_{pe} is the effective width of FRP (mm), and equals to $(d-L_e)$ if FRP is in the form of a U-jacket, and $d-2L_e$ where FRP is bonded to side faces. L_e is the effective bond length which may be defined as $461.3/(t_p E_p)^{0.58}$, and ρ_p is the FRP shear

reinforcement ratio, $\rho_p=(2t_p/b)(w_p/s_p)$ for beams strengthened with FRP strips, and $2t_p/b$ for beams where continuous FRP sheets are used.

The predicted failure strains for the beams in the current test series were evaluated and listed in Table 8.5.

Table 8.5 Predicted Failure Strains of FRP Shear Strips in Current Tests

Materials	FRP Shear Reinforcement Details	Stress concentration failure strain Eqn. (8.38)	Bond failure strain Eqn. (8.39)
CFRP plates (A)	200 mm by 80 mm by 1.6 mm plates bonded to web sides at 100 clear spacing.	n/a ($E_{pu}\rho_p>1.1$)	0.001700
CFRP sheets (C)	U-jacket and round wrapping of 100 mm wide by 0.145 mm thick sheets at 100 clear spacing.	0.008400	0.004100
AFRP sheets (K)	U-jacket and round wrapping of 150 mm wide by 0.29 mm thick sheets at 75 mm clear spacing.	0.007300	0.003900

The member will fail in shear when any of these limiting strains are exceeded. The Concrete Society Design Guidance recommends the design strain should be the lesser of 0.004000 and those determined from Equations (8.38) and (8.39). The failure strain due to bond failure determined by Equation (8.39) appears to be more critical than that due to stress concentration at corners. For the shear strengthening configurations used in the current tests, the failure strains were thus limited to 0.001700, 0.004000 and 0.003900 respectively. The FRP stress at failure can therefore be evaluated as the respective product of these strains and the corresponding elastic modulus of the FRP materials.

Taking account of shear resistance from all contributing components, the combined shear resistance of an FRP shear strengthened RC element may be written as:

$$V_R = (v_c + v_l + v_p)b_v d \qquad (8.40)$$

For an applied shear stress, v, if $v_e < v < 0.8f_{cu}$ (or 5 N/mm^2), where $v_e = v_c + v_l$ is the existing shear resistance before strengthening, the required external FRP shear strengthening can be determined using the following equation of BS 8110 format:

$$\frac{A_{sp}}{S_p} = \frac{b(v - v_e)\gamma_{mF}}{f_{pf}} \tag{8.41}$$

where γ_{mF} is the partial safety factor for material strength as discussed in section 8.3.1. The FRP design strength f_{pf} may be initially assumed to be $0.004E_{pu}$, once the area and spacing of FRP are determined, the actual failure strain in the strips may be evaluated as recommended by the Concrete Society Design Guidance (Concrete Society, 2000).

The predicted and actual failure shear stresses for the current test beams that failed in shear are listed in Table 8.6. These are the average shear stresses, which are equal to the shear force divided by $b_v d$, where b_v is effective width in resisting shear and equals to b for a rectangular section, d is the standard effective depth to the tension reinforcement.

Table 8.6 Comparison of Average Shear Failure Stresses

Beam Reference	Shear FRP Details	v_c (N/mm^2)	v_p (N/mm^2)	Predicted v_{pri} (N/mm^2)	Actual failure stress v_{at} (N/mm^2)	% of under estimation
B2	CFRP (B)	1.05 *(1.31)*	0.37 *(0.73)*	1.42 *(2.04)*	2.71	-47.6 *(-24.7)*
M1	n/a	0.88 *(1.01)*	n/a	0.88 *(1.01)*	1.52	-42.1 (-33.5)
M3	CFRP (B)	1.05 *(1.31)*	0.37 *(0.73)*	1.42 *(2.04)*	4.02	-64.7 (-49.3)
C1	CFRP (A)	1.01 *(1.26)*	0.88 *(1.36)*	1.89 *(2.62)*	0.80	n/a
C5	CFRP (A)	1.01 *(1.26)*	0.88 *(1.36)*	1.89 *(2.62)*	0.86	n/a

Notes:
1. No internal shear reinforcements were used in any of these beams, thus $v_l = 0$.
2. Beams C1 and C5 were only reinforced externally by CFRP plates, these beams failed at the point load position under combined maximum bending and maximum shear force.
3. *Values* in brackets are derived without material partial safety factor.

The design concrete shear stress, v_c, was determined using Equation (8.35) with f_{cu} being limited to 40 N/mm^2 (BS 8110, 1997). The flexural strengthening FRP composites were accounted for by the transformed equivalent steel area. This approach is obviously conservative and underestimates the actual shear resistance, as is demonstrated by the figures relating to beam M1. This beam had neither external FRP strips, nor internal shear links at the failure position, and the actual failure shear stress was about 0.5 N/mm^2 (33.5%) higher than that defined by BS 8110. As observed from beams B2 and M3, the predicted average shear failure stresses also appeared to be underestimated, suggesting that there is scope for allowable FRP strain values to be increased.

The typical CFRP ultimate strain, ranges from 1.4 –2.0%, which is 3.5-5.0 times of the current recommended value of 0.004000 for failure strains in shear strengthening. This, together with the material partial safety factor γ_{mF} (e.g., 1.96 for wet lay-up CFRP sheets, see Section 8.3.1), effectively limits the stress in the FRP shear strips to about 10-14% of the ultimate tensile strength. However, before more substantial laboratory test data are available, it seems prudent to limit the FRP strain to 0.004000 or those derived from Equations (8.38) and (8.39) if lesser, as recommended by the Concrete Society Design Guidance (Concrete Society, 2000).

8.7 CONSIDERATIONS OF TEARING-OFF OF CONCRETE COVER

The tearing-off of concrete cover type of failure is premature, extremely brittle and should be avoided. The existing theories, as discussed in Chapter 6, in predicting the tearing-off stresses or the corresponding failure load cannot yet be directly applied in general strengthening design since these results seem to be highly case dependent. One reason for the failure of the existing theories to produce generic design guidelines is that most of them are based on the elastic theory, while clearly a non-linear behaviour in the adhesive joint region is more realistic. The modified semi-empirical approach proposed in the current study is only a small step toward a better understanding of the beam behaviour, and is not ready to be used as design guidance before a substantial confirmation process is carried out. The current study does highlight the ways on how to prevent the tearing-off of concrete cover type of premature failure, and suggests that an

under reinforced section is the key to solving this problem. Moreover, a "smart" adhesive may be developed to cause deformation before the weaker concrete reaches the tearing off strength, so that part of the strain energy accumulated in the strengthened system may be released and a more ductile failure ensured.

In the current Concrete Society Design Guidance (Concrete Society, 2000), it is recognised that the FRP plate aspect ratio (b_p/t_p) is an influencing factor in the tearing-off behaviour. Based on the research work of Garden (1997), it recommended that an aspect ratio of far greater than 50 should be acceptable. It should be pointed out that all beams seen with the tearing-off failure mode in the current tests had FRP aspect ratio of 50. It is also recommended that the FRP strain should be limited to between 0.6-0.8% to avoid debonding failure. However, it is felt that this may be an over simplification since the strains in the FRP composites clearly, are influenced by the amount of FRP area provided, as demonstrated in Figures 8.2 and 8.3. The large FRP area provided may result in decreased strain values, yet there is no evidence to suggest that greater FRP area will contribute to the reduced likelihood of FRP debonding. It may therefore be stated that debonding behaviour is more likely to be influenced by: (a) the workmanship on the mixing and application of adhesives, (b) the surface treatment procedure and (c) the properties of the adhesive system.

CHAPTER 9

Conclusions and Suggestions for Further Work

9.1 FOREWORD TO CONCLUSIONS

During the course of the current research programme, the general awareness and the application of Fibre Reinforced Polymer (FRP) composites, as structural strengthening materials, has developed rapidly. There are now an appreciable number of bridges and other structures that have been strengthened (including some in the UK) using these advanced composites.

The main purpose of this research was to achieve a fuller understanding of the behaviour of reinforced concrete (RC) flexural elements strengthened by FRP composites, and make recommendations for design guidelines on flexural strengthening. This aim was satisfactorily fulfilled through an experimental investigation combined with analytical modelling applied to FRP strengthened RC beams. New findings, regarded to be significant by the candidate, have been highlighted and design recommendations have been presented. It is hoped that the data from this work will be an innovative contribution towards the current state of information and knowledge on FRP strengthening of RC structures. The following sections are intended to present a summary of the main observations, as well as to serve suggestions for future research.

9.2 SUMMARY OF MAIN CONCLUSIONS

The sub sections concerned, although appearing separate, are interrelated.

9.2.1 Ultimate Load Capacity

- **Experimental evidences have shown that FRP strengthened RC flexural members can definitely enhance the ultimate load carrying capacity significantly.**

This is a confirmation of what has been reported by a large number of previous researchers as reviewed in Chapter 2. In the current study, the increase of ultimate load over the control beams for the simply supported beam test series was up to a maximum 88%. For the continuous beams tested in the present study, the increase was up to 165%.

- **The actual level of increase in ultimate load carrying capacity of FRP strengthened elements is greatly influenced by the existing properties of the original members.**

The existing material properties such as the strength of concrete and steel, and especially the reinforcement ratio, greatly influence the failure mode and hence the ultimate load of the strengthened members. The typical existing tension reinforcement ratio used in the present study was 0.79%. It is believed that the lower the existing reinforcement ratio is, the greater the percentage of ultimate load enhancement that can be achieved through FRP strengthening can become.

- **Although FRP composites exhibit linear stress-strain behaviour until the failure, FRP strengthened RC elements need not have the same brittle characteristics.**

This is because the FRP strengthened element is no longer just FRP but an additional entity, which is a new composite material as a result of combination with the existing

concrete and reinforcement. If designed appropriately, the new material will exhibit much improved overall ductility behaviour (Please refer to the following section on ductility).

- **In typical FRP strengthened RC flexural elements, the steel reinforcements will always yield before the possible rupture of FRP composites. This condition will not be influenced by the amount of FRP provided.**

The above statement is significant in preparing for the design guidelines. There have been doubts among the designers as to whether the steel reinforcement will yield before the rupture of FRP composites. This was discussed and analysed in Chapter 5. Most of the known flexural elements are designed such that the sections are under reinforced. The typical yield strain for high yield reinforcement is 0.002190, and the typical ultimate strains of FRP composites range from 1.2 - 2.5%. It was shown that due to the strain compatibility conditions, the reinforcement must yield first before it is possible for the ultimate strain of FRP to be reached. Neither the area of reinforcement nor that of FRP composites will alter this failure sequence.

9.2.2 Failure Mode

- **Of all typical failure modes observed in FRP strengthened sections, the mechanism of steel yielding, followed by FRP rupture or near rupture, and then concrete crushing, may be considered the most acceptable with respect to ductility.**

This desirable sequence is due to the deformability and possibly the ductility index in such members, which may be greater than that corresponding to any other failure modes. Since the FRP composites will reach or nearly reach the design strength at the ultimate failure, the deformation is usually high. In unidirectional FRP sheets strengthened RC elements, all fibres do not necessarily fail at the same time. Some fibres in the strengthening layers may reach the ultimate strength first thus enabling the gradual release of stored strain energies in the composite. This phenomenon was

observed in the series B and M test series when fibre snapping sound was heard well before the ultimate failure, and partial failure of the FRP fabrics was observed.

In over strengthened sections, the concrete crushing failure mode is likely. This type of failure is very sudden and brittle, the deformations before the ultimate failure are limited. The tearing-off of concrete cover at the internal reinforcement level is an extremely brittle failure mode and should be avoided as discussed in Chapter 6. Ultimate shear failure can usually be avoided by providing sufficient external shear strengthening strips or U-jackets.

- **The debonding of FRP from concrete failure mode may also be considered to be an alternatively acceptable failure mechanism, since it is usually less brittle.**

Currently, the separation of FRP composites from concrete surface type of failure is likely to be a result of unfavourable surface treatment or poor mixing and workmanship during the application of adhesive systems. Consequently, the ultimate failure load in such cases is usually low. However, if this type of plate debonding can be controlled by design, it may be an acceptable failure mode. For example, the plate may be designed to partly and gradually separate from the concrete element when the elastic stored energy reaches a high level, without release of which, the premature tearing-off failure will be imminent. This may be achieved by using a "smart" adhesive in which the primer layer is designed to be more flexible and energy absorbing than the main resin. The advantage of this approach is that it will avoid the extremely brittle failure of concrete cover tearing-off.

9.2.3 Suitability of FRP Composites for Strengthening RC Structures

- **The FRP strengthening is most suited for application to floor slabs, car parks floors and bridge decks. It is also viable to strengthen singly reinforced concrete beams.**

This is because the existing steel reinforcement ratios in these members are likely to be low. For a typical 200 mm floor slab with T10 bars at 150 mm spacing, the

reinforcement ratio is just 0.26%. Singly reinforced beams may also be strengthened by FRP composite, while still retaining the main characteristics of an under reinforced section.

The addition of FRP composites in the tension zone of these members can therefore act to supplement the existing steel reinforcement, while still remaining under strengthened. The ultimate failure mode can thus still exhibit acceptable ductility. However, the new neutral axis depth of the FRP strengthened sections will be reduced from that of the original unstrengthened members. This effectively limits the area of maximum FRP composite area that can be provided in order to maintain an acceptable level of deformability and ductility behaviour of the strengthened elements.

- **The balanced neutral axis depth ratio of FRP strengthened flexural elements depends on the FRP material properties. For typical FRP composites, this figure is between 0.2 - 0.3. An under strengthened section is always recommended, which effectively limits the neutral axis depth at ultimate failure to around 0.2h.**

The neutral axis depth of a fully balanced section in FRP strengthened flexural elements, depends on the ultimate strain values of the composites. Although for slab elements it is often possible to design an under strengthened section which leads to a more ductile failure mode, it may be more difficult to apply this limit to singly reinforced beams if the existing reinforcement ratio is relatively high. In such cases, the neutral axis depth ratio should be constrained to remain as close to the value for a fully balanced section as possible.

The current Concrete Society Design Guidance recommends a x/d limit of 0.45. This is regarded a little too relaxed. The consequence of this is that the sections could be over strengthened with large areas of FRP composites. At ultimate failure, the stress and strains in these composites will have a low value and the failure mode will be sudden and brittle. The present study suggests a maximum limit of 0.4d.

- **FRP strengthening is not suitable for doubly reinforced concrete beams if the same safety margins as that of the original elements against brittle concrete failure is to be maintained. The addition of tension composite will lead to concrete being crushed in compression.**

The main reason for this restriction, as discussed in Chapter 8, is that all doubly reinforced members are designed such that the neutral axis is limited to $(\beta_b$-0.4)d, where β_b is the ratio of moment redistribution. Therefore the depth of neutral axis, x, in any doubly reinforced concrete flexural member is designed to be 0.5d when no elastic moment redistribution is accounted for or if it is less than 10%. The addition of FRP in the tension zone without corresponding enhancement in the compression zone can only increase the neutral axis depth, where a sudden and brittle failure in the concrete by compression is thus ensured.

- **Over strengthened section will result in decreased ductility and the strains in the reinforcement and the FRP composites will reduce with the increased area of FRP provided. As a consequence large amount of elastic energy will be stored in the strengthened system and the ultimate failure mode will be extremely brittle when the unconsumed energy is released.**

It is therefore recommended that, if possible, all sections should be under strengthened. This effectively limits the maximum level of strength enhancement as discussed in Chapter 8. The maximum area of FRP composites provided for an under strengthened section can be determined for a given material. There exists a critical reinforcement ratio as defined in Chapter 8, which depends on the concrete and steel reinforcement properties, beyond which an under strengthened section is no longer possible.

- **The use of very high strength of FRP materials is not necessarily beneficial in RC strengthening, neither is high ultimate FRP failure strain. High FRP failure strain is not necessarily an advantage.**

As discussed in Chapters 5 and 8, the very high strength and ultimate strain will never be reached unless they are used for under strengthened section. It may be considered

suitable that an FRP composite with an ultimate tensile strength of around 2000 N/mm^2, and minimum elastic modulus of round 150 kN/mm^2 should be used as the preferred strength and modulus range for flexural strengthening. The FRP elongation at failure is preferred to be between 1.2% and 1.7%. High FRP ultimate failure strain is not necessarily an advantage, as it is usually the result of low elastic modulus, which leads to small values of neutral axis depth.

- **Excessively high partial factors of safety for FRP composite materials do not necessarily make the strengthened elements safe.**

This is because greatly reduced FRP strength from the realistic value will lead to large FRP areas being required, and thus result in members being over strengthened. The FRP manufacturers and researchers should jointly develop a confidence level in defining consistent specification of the FRP composite properties. The material partial factors of safety for wet lay-up FRP sheets and GFRP products, for example, may be reduced from those recommended by the Concrete Society Design Guidance once the manufacturing and application techniques are improved and the characteristic strength well specified.

9.2.4 Ductility, Deformability and Moment Redistribution

- **Deformability index is a convenient means of measuring the level of warning prior to ultimate failure, the higher the deformability index, the more noticeable deformations present will be.**

A new deformability index was proposed as discussed in Chapter 7. It is defined as the ratio of the beam deformation at 95% of the ultimate load to the corresponding values under the service load. A deformability index of at least 2.0 is recommended, which should ensure that sufficient pre-failure warning could be obtained. It must be noted, however, that a high deformability index does not necessarily lead to a ductile failure mode. If the unconsumed strain energy in the FRP strengthened section is high, the failure mode can still be very brittle and catastrophic at ultimate failure.

- **Ductility of FRP strengthened flexural section can only be measured using the energy approach.**

The traditional method of evaluating ductility of steel reinforced elements is not applicable to the FRP strengthened sections, since there exists no apparent yield point in the FRP. The yielding of steel reinforcement in FRP strengthened RC sections is "overwritten" by the presence of FRP composite. Ductility of an FRP strengthened section is directly proportional to the amount of consumed energy. Ductility index may be determined using the total energy and the elastic stored energy concepts as discussed in Chapter 7.

- **Redistribution of elastic moment in FRP strengthened beams does occur but is different from the conventional concept. Plastic hinges cannot be fully developed in over strengthened elements.**

Since the ultimate strength of FRP composites cannot be reached in the over strengthened sections, full plastic hinges in the conventional sense will never be developed. Theoretically, no moment redistribution can therefore be carried out. However, the FRP strengthened section is a new composite contribution to the RC section, in which the concrete part is able to develop a partial plastic hinge as seen in Chapter 7. When the load is increased, the concrete in the partial plastic hinge cannot any longer sustain higher stress, but the FRP plate stress may still increase. As a result, the span moment may increase over the elastic analysis value. However, more experimental evidence is required before the quantification of the actual percentage of redistribution can be carried out.

9.2.5 Adhesive Suitability

- **A strong and durable adhesive system is essential for a successful strengthening project. Appropriate surface treatment should be carried out prior to plate bonding. Peel-ply protection of prelaminated FRP plates is recommended whenever possible.**

As discussed in Chapter 3, the presently available structural adhesive systems are specified to the BA 30/94 guidelines. The strength properties of adhesives generally exceed those of concrete adherent. In an FRP-adhesive-concrete system, the weakest member is usually the concrete, which may lead to the brittle premature tearing off failure as discussed in Chapter 6. It may be advisable for a more flexible adhesive to be developed, for example, by using suitable additives and fillers, so that a partial energy release may be achieved before the ultimate brittle joint failure.

9.2.6 Concrete Beams with FRP Reinforcement Only

- **FRP composite strengthening is not effective in mass concrete elements without any internal steel reinforcement.**

There should be a minimum percentage of existing internal steel reinforcement in RC flexural members before FRP strengthening can be performed, as discussed in Chapter 4. This is because the lack of any internal steel reinforcement in concrete members will result in large cracks within the concrete, and premature lateral bucking may thus follow even though the members are strengthened externally by FRP composites. FRP composites in such cases do not develop to the full strengthening potential. In practice, however, the requirements of converting mass concrete elements as high load-carrying structural members may be rare, but if it arises, external FRP strengthening should not be an option.

- **Prelaminated CFRP narrow strips may be used as internal reinforcement, replacing steel reinforcement.**

In contrast to the above point, FRP strips may be used as main internal reinforcement in stead of steel bars, which will help solve the problem of steel reinforcement corrosion in an aggressive environment. In the present study, only preliminary work was carried out as discussed in Chapter 4. The results showed that FRP strips as internal tension reinforcement is viable, but the full strength of the composites did not appear to be developed. The bond between the flat surface of FRP and the concrete need to be further investigated. Due to the lower elastic modulus of the FRP strips used, the overall

stiffness of the FRR reinforced beams were observed to be much lower than that of conventionally reinforced concrete beams of equivalent configuration.

9.2.7 Premature Tearing-off failure

- **Premature tearing-off failure is brittle and catastrophic, and must be prevented.**

To prevent the above condition, over strengthening should be avoided. The FRP plate aspect ratio should be as large as possible. This type of failure has been observed in the current tests when the aspect ratio of the plates was 50. No premature tearing-off failure was observed when the sections were under strengthened with one layer of CFRP fabric sheet, and when the CFRP aspect ratio was increased to around 680.

FRP fabric U-jacket end anchorage should be provided for beams, whenever possible, as a routine practice. This will not only enhance the member's shear resistance but also prevent or delay the premature failure, and increase the impact resistance.

- **The strengthening FRP composite should be bonded as close to the support as possible, and at a distance of approximate 0.6d away from the surface of the support. This may be used in conjunction with the U-jacket FRP wrapping.**

This method seems to be effective. It was observed that none of the beams configured in this manner had failed by the premature tearing-off mode.

9.2.8 FRP Shear Strengthening

- **Shear strengthening using external FRP strips or U-jacket is an effective means of increasing shear capacity.**

The actual contribution of FRP strips or U-jacket to the member's shear resistance is dependent on the failure strain in the FRP composites, which in turn is influenced by the bond strength between the concrete and FRP. The Concrete Society Design Guidance

recommends a limiting strain of 0.004000 or those as determined by Equations (8.38) and (8.39) if lesser. This approach is reasonable and the results seem to be on the conservative side as discussed in Chapter 8.

- **Strain monitoring devices should be installed on the FRP composites immediately after the completion of strengthening work, to monitor the strain development of FRP under long term load.**

Simple and practical strain monitoring devices such as Demec discs should be installed on the FRP plates or fabrics at suitable positions after the completion of strengthening work. This is to ensure that the composite strain values can be regularly obtained under the increased service load, and act as a reliable pre-warning mechanism should the strain level become alarmingly high.

9.3 SUGGESTED FURTHER WORK

Despite the present series of extensive laboratory tests carried out, there are, as usual, many partially or unanswered questions which should be addressed. The existing reinforcement used was kept at a constant ratio of 0.79%. Although analytical modelling and a parametric study were carried out to address this issue, it is desirable to test greater cross section sizes of RC beams with various reinforcement ratios. This will confirm the influence of reinforcement ratio on the behaviour of strengthened elements.

The non-linear material based analytical model correlates well with the experimental results, but it does not consider the influence of the shear stress in the cross section, and can only be applied in the constant moment zone. It is desirable to develop a model, which will also take account of the shear force combined with the varying bending moment in the shear span.

During the course of the current study, the candidate attempted to use a 3-D non-linear finite element package, DIANA, to model the flexural behaviour of FRP strengthened members, but it failed to produce any satisfactory results in relation to the experimental

results. Extensive FEA numerical modelling needs to be performed, and the results should be correlated with all the available experimental data. The candidate feels it may be necessary to calibrate the existing commercially available FEA packages against the latest and extensive experimental data of FRP strengthened RC elements, to take account the non-linear behaviour of such members. The existing packages such as ANSYS and DIANA, although they have been widely used and acclaimed to be accurate, were developed before the FRP strengthening technique was introduced. Such software packages were mostly calibrated against the conventionally reinforced concrete elements, which behave fundamentally differently to the FRP strengthened counterparts.

More experimental studies on the premature tearing-off of concrete cover type of failure mode need to be carried out on different sizes and general configurations to the current test samples. This will confirm the validity or otherwise of the present conclusion that such brittle failures will not occur in under strengthened sections.

Laboratory investigations on the surface crack width and crack density need to be performed, and hence form the bases on which a more rigorous theoretical determination of crack width in FRP strengthened elements may be established and validated.

9.4 CONCLUDING REMARKS

It has been shown in the present study that FRP strengthening technology is viable and effective. Many shortcomings and problems associated with the traditional steel plate bonding technique can be overcome by the application of FRP composites. However, it has also been highlighted in the study that an appropriate design methodology is the most important first step to ensure full success of any strengthening project. The potential brittle failure at ultimate limit state can be prevented if a suitable design and strengthening strategy is deployed.

Due to the high specific strength and stiffness of FRP composites, as well as the high profile that this technique has enjoyed in the past two years, the application scope and effectiveness of FRP strengthening may, on occasions, be conveniently exaggerated. It must be understood by the structure owners that the FRP strengthening method is not the wonderful elixir that will cure all their problems with minimum effort. For example, if a concrete highway bridge has a 10-ton weight restriction placed upon it, it may be unrealistic to expect that the bridge can be upgraded to 40-ton load carrying capacity simply by FRP strengthening.

To this end, the candidate would like to refer back to the "doctor-patient" analogy made in the opening remarks. The FRP composites strengthening technology may be likened to the invention of the Penicillin antibiotics in the medical field. Although it is an excellent medicine, it would only be effective if prescribed by qualified doctors for treating certain correctly diagnosed illness. Inappropriate or overdosing could lead to undesirable and even tragic consequences. For structural engineers, FRP strengthening techniques have started a new era in structural retrofitting of mechanically degraded or over loaded RC members. With prudent and professional design and practice, this new era may well be referred to, by the future generations, as the era of composites.

REFERENCES

ACI Committee 440 (1996), State of the Art Report on Fibre Reinforced Plastics (FRP) Reinforcement for Concrete Structures (ACI 440R-96), American Concrete Institute, Farmington, Mich., USA, 65pp.

Aiello, M. A. (1999), "Concrete cover failure in FRP reinforced beam under thermal loading," ASCE J. Composites for Construction, V.3, No.1, pp46-52.

Alexander, J. G. S. and Cheng, J. J. R. (1996), "Field application and studies of using CFRP sheets to strengthen concrete bridge girders," Proc. Int. Conf. Advanced Composite Materials in Bridges and Structures, Ed., El-Badry, M. M., Canadian Society for Civil Engineers, Montreal, Canada, pp465-472.

Ali, M. S. M, Oehlers, D. J. and Bradford, M. A. (2000), "Shear Peeling of steel plates adhesively bonded to the sides of reinforced concrete beams," Proc. Institution of Civil Engineers, Structures and Buildings, V.140, Aug., pp249-259.

Al-Sulaimani, G. J., Sharif, A., Basunbul, I. A., Baluch, M. H. and Ghaleb, B. N. (1994), "Shear repair for reinforced concrete by fibreglass plate bonding," ACI Structural J., V.91, No.3, pp458-464.

An, W., Saadatmanesh, H. and Ehsani, M. R. (1991), "RC beams strengthened with FRP plates II: Analysis and parametric study. ASCE J. Structural Engineering, V.117, No.11, pp3434-3455.

Andreou, E. and Delpak, R. (2000), Kevlar Strengthening of RC Structures, Internal Research Report, University of Glamorgan.

Arduini, A., DI Thommaso A. and Manfroni, O. (1995), "Fracture mechanisms of concrete beams bonded with composite plates," in Non-Metallic (FRP) Materials for the Reinforcement and Prestressing of Concrete, Ed., Taerwe, E & FN Spon, London, pp484-491.

Arduini, A., DI Thommaso A. and Nanni, A. (1997), "Brittle failure in FRP plated and sheet bonded beams," ACI Structural J., Vo,94, No.4., Jul./Aug., pp363-370.

Arduini, M. and Nanni, A. (1997), "Behaviour of precracked RC beams strengthened with carbon FRP sheets," ASCE J. Composites for Construction, V.1, No.2, pp63-70.

Aridome, Y., Kanakubo, T., Furuta, T. and Matsui, M. (1998), "Ductility of T-shape RC beams strengthened by CFRP sheet," Transaction of Japan Concrete Institute, V.20, pp117-124.

ASCE (1998), "1998 Report Card for America's Infrastructure," American Society of Civil Engineers, 202/789-2200, Washington DC.

ASTM D2903 (1984), Standard Practice for Preparation of Surfaces of Plastics Prior to Adhesive Bonding, American Society for Testing and Materials, Philadelphia, USA.

BA 30/94 (1994), "Strengthening of concrete highway structures using externally bonded plates," Design Manual for Roads and Bridges, Volume 3, Highway Structures: Inspection and Maintenance, Section 3, Repair and Strengthening, Department of Transport, London.

Ballinger, C. A. (1997), "Strengthening of engineering structures with carbon fibre reinforced plastics – An overview of history and current world wide usage," Proceedings 42nd Int. SAMPE Symposium, Anaheim, California, USA, Eds., Haulik, T., Bailey, V. and Burton, R., 4-8 May 1997, pp927-932.

Baluch, M. H., Ziriba, Y. N., Azad, A. K. and Sharif, A. M. (1995), "Shear strength of plated RC beams," Magazine of Concrete Research, V.47, No.173, Dec., pp369-374.

Barns, R. A. and Mays G. C. (1999), "Fatigue performance of concrete beams strengthened with CFRP plates," ASCE J. Composites for Construction, V.3, No.2, pp63-72.

Beeby, A. W. (1979), "The prediction of crack widths in hardened concrete," The Structural Engineer, V.57A, No.1, January, pp9-17.

Belarbi, A and Hsu, T. T. C. (1994), "Constitutive laws of concrete in tension and reinforcing bars stiffened by concrete," ACI Structural J., V.91, No.4, July-August, pp465-474.

Bell, B. (2000), Railtrack Plc, Private communication.

Bonacci, J. F. (1996), "Strength, failure mode and deformability of concrete beams strengthened externally with advanced composites," Proc. Int. Conf. Advanced Composite Materials in Bridges and Structures, Ed., El-Badry, M. M., Canadian Society for Civil Engineers, Montreal, Canada, pp419-426.

British Standards Institution (1985), BS 8110, Structural Use of Concrete, Part 2:1985, Code of practice for special circumstances, London.

British Standards Institution (1990), BS 6319:Part3:1990, Testing of resin and polymer/cement composites for use in construction, Part 3, Methods for measurement of elasticity in flexure and flexural strength, London.

British Standards Institution (1997), BS 8110, Structural Use of Concrete, Part 1:1997, Code of practice for design and construction, London.

Buyukozturk, O. and Hearing, B. (1998), "Failure behaviour of precracked concrete beams retrofitted with FRP," J. Composites for Construction, V.2, No.3, pp138-144.

Buyukozturk, O., Hearing, B. and Gunes, O. (1999), "FRP strengthening and repair: where do we go from here?" Proc. 8th Int. Conf. Structural Faults and Repair, 13-15 July 1999, London.

Chaallal, O., Nollet. M. J. and Perraton, D. (1998), "Strengthening of reinforced concrete beams with externally bonded fibre-reinforced-plastic plates: design guidelines for shear and flexure," Canadian J. Civil Engineering, V.25, pp692-704.

Chajes, M. J., Januszka, T. F., Mertz, D. R., Thomason, T. A. and Finch, W. W. (1995), "Shear strengthening of reinforced concrete beams using externally applied composite fabrics," ACI Structural J., V.92, No.3, pp295-303.

Chajes, M. J., Thomason, T. A. and Farschman, C. A. (1995), "Durability of concrete beams externally reinforced with composite fabrics," Construction and Building Materials, V.9, No.3, pp141-148.

Chajes, M. J., Thomason, T. A., Finch, W. W. and Januszka, T. F. (1994), "Flexural strengthening of concrete beams using externally bonded composite materials," Construction and Building materials, V.8, No.3, pp191-201.

Charif, A. (1983), Structural Behaviour of Reinforced Concrete Beams Strengthened by Epoxy Bonded Steel Plates, PhD thesis, University of Sheffield, England.

Ciba-Geige (1993?), Guide to Araldite Bonding, Engineering Data Book, Cambridge.

Clark, L. A. (1999), Chair of the "Thaumasite Expert Group", The thaumasite form of sulfate attack: Risks, diagnosis, remedial works and guidance on new construction. DETR, January 1999, pp.180.

Clarke, J. L. (1996), "FRP reinforced concrete structures," Proc. Int. Conf. Advanced Composite Materials in Bridges and Structures, Ed., El-Badry, M. M., Canadian Society for Civil Engineers, Montreal, Canada, pp41-48.

Clarke, J. L. (2000), "Strengthening of concrete structures with fibre composites," Proc. 10th BCA Annual Conf. Higher Education and the Concrete Industry, University of Birmingham, 29-30 June, pp277-288.

Clarke, J. L. (Ed.) (1996), Structural Design of Polymer Composites, EUROCOMP Design Code and Handbook, E & F N Spon, London.

Clarke, J. L. (Ed.)(1993), Alternative Materials for the Reinforcement and prestressing of Concrete, Blackie A & P, Glasgow, 204pp.

Clarke, J. L. and Waldron, P. (1996), "The reinforcement of concrete structures with advanced composites," The Structural Engineer, V.74, No.17, Sep., pp283-288.

Concrete Society (2000), Design Guidance for Strengthening Concrete Structures Using Fibre Composite Materials, Technical Report No. 55, The Concrete Society, Crowthorne, Berkshire, UK. 71pp.

Crowder, J. R. and Howard, C. M. (1990), "End use performance and time-dependent characteristics," in Polymers and Polymer Composites in Construction, ed. Hollaway, L., Thomas Telford Ltd., London, pp145-146.

Demers, C. E. and Abdelgadir, A. A. (1999), "Research in progress: Fatigue of CFRP composites," Proc. 8th Int. Conf. Structural Faults and Repair, 13-15 July 1999, London.

Department of Transport, Welsh Office, Scottish Office and Northern Ireland Environmental Office report (1987), "The Assessment of Highway Bridges and Structures," January 1987, London.

Deskovic, N., Meier, U. and Triantafillou, T. C. (1995), "Innovative design of FRP combined with concrete: long-term behaviour," ASCE J. Structural Engineering, V.121, No.7, pp1079-1089.

Deskovic, N., Triantafillou, T. C. and Meier, U. (1995), "Innovative design of FRP combined with concrete: short-term behaviour," ASCE J. Structural Engineering, V.121, No.7, pp1069-1078.

DETR (2000),"Transport Statistics Great Britain: 1988-1998: 1999 Edition," ISBN: 0 11 552163 1, Published on 2 May 2000, Great Minster House, 76 Marsham Street, London.

DiTommaso, A. Focacci, F. and Foraboschi, P. (1996), "Driven failure mechanisms in fibre-reinforced-plastic prestressed concrete beams for ductility requirements," Proceedings Advanced Composite Materials in Bridges and Structures, Ed., El-Badry, M. M., Canadian Society for Civil Engineers, Montreal, Canada, pp281-288.

DOT (1997), "Lorry Weights – A Consultation Document," January 1997, 76 Marsham Street, London.

Dry, A. (1997), "The development of the carbon fibre industry," Proc. 42nd SAMPE Symposium, Eds., Haulik, Bailey, V. and Burton, R., Anaheim, California, 4-8 May, pp979-986.

Eberline, D. K. Klaiber, F. W. and Dunker, K. (1988), "Bridge strengthening with epoxy bonded steel plates," Transport Research Record (1180), pp7-11.

El-Badry, M. M. (Ed.) (1996), Advanced Composite Materials in bridges and Structures, Proc. ACMBS-II, Canadian Society for Civil Engineer, Montreal, Canada, 1027pp.

EPSRC (1999), Call for research in CMP, EPSRC Website, www.epsrc.org

Erki, M. A. and Meier, U. (1999), "Impact loading of concrete beams externally strengthened with CFRP laminates," J. Composites for Construction, V.3, No.3, pp117-124.

Exchem Mining & Construction (1993) "Test Report - Plate bonding adhesive tests to advice note BA30/94, Appendix A", Department of Mechanical Engineering, University of Nottingham.

Exchem Mining & Construction (2000), Externally bonded reinforcement systems – Selfix cabofibe pultruded CFRP plates, Technical brochure, Alfreton, Derbys.

FHwA (1997), "The Status of the Nation's Highway Bridges: Highway Bridge Replacement and Rehabilitation Program and National Bridge Inventory," Washington DC.

Fleming, C. J. and King, G. E. M. (1967), "The development of structural adhesives for three original uses in South Africa," Proceedings RILEM Symp. Synthetic Resins in Building Construction, Paris, September 1967, pp75-92.

Forde, M. C. (1997), "Bridge research in Europe," Construction and Building Materials, V.12, No.2-3, pp85-91.

Garden, H. N. (1997), The Strengthening of Reinforced Concrete Members Using Externally Bonded Composites Materials, PhD thesis, University of Surrey, August 1997, England.

Garden, H. N., Hollaway, L. C. and Thorne, A. M. (1997), "A preliminary evaluation of carbon fibre reinforced polymer plates for strengthening reinforced concrete members," Proc. Institution of Civil Engineers, Structures and Buildings, V.123, May, pp127-142.

Garden, H. N., Quantrill, R. J., Hollaway, L. C., Thorne, A. M. and Parke, G. A. R. (1998), "An experimental study of the anchorage length of carbon fibre composite plates used to strengthen reinforced concrete beams," Construction and Building Materials, V.12, pp203-219.

Gaul, R. W. (1984), "Preparing concrete surfaces for coatings," Concrete International, V.6, No.7, pp17-22.

Gere, J. M. and Timoshenko, S. P. (1991), Mechanics of Materials, Chapman and Hall, London.

Grace, N. F., Abdel-Sayed, G., Soliman, A. K. and Saleh, K. R. (1999), "Strengthening Reinforced concrete beams using fibre reinforced polymer (FRP) laminates," ACI Structural J., V.96, No.5, pp865-874.

Grace, N. F., Soliman, A. K., Abdel-Sayed, G. and Saleh, K. R. (1998), "Behaviour and ductility of simple and continuous FRP reinforced beams," ASCE J. Composite for Construction, V.2, No.4, pp186-194.

Hancox, N. L. and Mayer, R. M. (1994), Design Data for Reinforced Plastics, Chapman and Hall, London.

Hart-Smith, L. J. and Brown, D. (1993), "Surface preparations for ensuring that glue will stick in bonded composite structures," Proc. 10th Conf. Fibrous Composites in Structural Design, 1-4 November, Hilton Head Island, S. Carolina, USA, pp1-18.

He, J. H., Pilakoutas, K. and Waldron, P. (1997a), "CFRP plate strengthening of RC beams," Proc. 7th Int. Conf. Structural Faults and Repair, University of Edinburgh, 8-10 July 1997, V.2, pp119-127.

He, J. H., Pilakoutas, K. and Waldron, P. (1997b), "Analysis of externally strengthened RC beams with steel and CFRP plates," Proc. 7th Int. Conf. Structural Faults and Repair, University of Edinburgh, 8-10 July 1997, V.2, pp83-92.

Head, P. R. (1988), "Use of fibre reinforced plastics in bridge structures," Proceedings 13th IABSE Cong. 6-10 June 1988, p.124.

Head, P. R. (1996), "Advanced composites in civil engineering – a critical overview at the high interest, low use stage of development," Proceedings Advanced Composite Materials in Bridges and Structures, Ed., El-Badry, M. M., Canadian Society for Civil Engineers, Montreal, Canada, pp3-15.

Hollaway, L. C. (1993), Polymer Composites for Civil and Structural Engineering, Blackie Academic and Professional, Glasgow, 259 pp.

Hollaway, L. C. (Ed.) (1990), Polymers and Polymer Composites in Construction, Thomas Telford Ltd, London, 275pp.

Hollaway, L. C. and Leeming, M. (Eds.) (1999), Strengthening of Reinforced Concrete Structures Using Externally-Bonded FRP Composites in Structural and Civil Engineering, Woodhead Publishing Ltd, Cambridge, UK, 327pp.

Hsu, T. T. C. and Zhang, L. X. (1996), "Tension stiffening in reinforced concrete membrane elements," ACI Structural J., V.93, No.1, Jan-Feb, pp108-115.

Hutchinson, A. R. (1997), Joining of Fibre-Reinforced Polymer Composite Materials, CIRIA Report No.46, CIRIA, London.

Hutchinson, A. R. and Hollaway, L. C. (1999), Environmental Durability, in Strengthening of Reinforced Concrete Structures Using Externally-Bonded FRP Composites in Structural and Civil Engineering, Woodhead Publishing Ltd, pp156-182.

Hutchinson, A. R. and Quinn, J. (1999), Materials, in Strengthening of Reinforced Concrete Structures Using Externally-Bonded FRP Composites in Structural and Civil Engineering, Woodhead Publishing Ltd, pp46-82.

Hutchinson, A. R. and Rahimi, H. (1993), "Behaviour of reinforced concrete beams with externally bonded fibre reinforced plastics," Proc. 5th Int. Conf. Structural Faults and Repair, University of Edinburgh, V.3, pp221-228.

Hutchinson, A. R. and Rahimi, H. (1996), "Flexural strengthening of concrete beams with externally bonded FRP reinforcement," Proc. Int. Conf. Advanced Composite Materials in Bridges and Structures, Ed., El-Badry, M. M., Canadian Society for Civil Engineering, 11-14 August, Montreal, Canada, pp519-526.

Institution of Structural Engineers, The (1999), Interim Guidance on the Design of Reinforced Concrete Structures Using Fibre Composite Reinforcement, Published by SETO, London, ISBN 1 874266 47 6, 116pp.

Irwin, C. A. K. (1975), "The strengthening of concrete beams by bonded steel plates," Supplementary Report 160, Transport and Road research Laboratory, Crowthorne, 21 pp.

Jones, R. and Swamy, R. N. (1986), "Crack control of reinforced concrete beams through epoxy bonded steel plates," Proc. Int. Conf. Adhesion between Polymers and Concrete, Aix-en-Provence, Champman and Hall, pp542-555.

Jones, R. and Swamy, R. N. and Ang, T. H. (1982), "Under- and over-reinforced concrete beams with glued steel plates," Int. J. Cement Composites and Lightweight Concrete, V.4, No.1, pp19-32.

Jones, R. and Swamy, R. N. and Charif, A. (1988), "Plate separation and anchorage of reinforced concrete beams strengthened by epoxy bonded steel plates," The Structural Engineer, June, V.66, No.5/1, pp85-94. (See discussion by Roberts, T. M., 67(12), pp187-188).

Jones, R. and Swamy, R. N. and Charif, A. (1989), "The effect of external plate reinforcement on the strengthening of structurally damaged RC beams," The Structural Engineer, June, V.67, No.3/7, pp45-56.

Jones, R. and Swamy, R. N. and Salman, F. A. R. (1985), "Structural implications of repairing by epoxy bonded steel plates," 2nd Int. Conf. Structural Faults and Repair, London, pp75-80.

Jones, R., Swamy, R. N., Bloxham, J. and Bouderbalah, A. (1980), "Composite behaviour of concrete beams with epoxy bonded external reinforcement," Int. J. Cement Composites, V.2, No.2, pp91-107.

Kaiser, H. P. (1989), Strengthening of Reinforced Concrete with Epoxy-bonded Carbon Fibre Plastic, PhD thesis, ETH Zurich, Ch-8092 Zurich, Switzerland. (in German).

Karbhari, V. M. (1997), "On the use of composite for bridge renewal: materials, manufacturing and durability," Proceedings 42nd International SAMPE Symposium, Anaheim, California, USA, Eds., Haulik, T., Bailey, V. and Burton, R., 4-8 May 1997, pp915-926.

Kemp, A. R. (1998), "The achievement of ductility in reinforced concrete beams," Magazine of Concrete Research, V.50, No.2, June, pp123-132.

Khalifa, A. and Nanni, A. (2000), "Improving shear capacity of existing RC T-section beams using CFRP composites," Cement and Concrete Composites, V.22, pp165-174.

Khalifa, A., Gold, W J., Nanni, A. and Aziz, M. I. A. (1998), "Contribution of externally bonded FRP to shear capacity of RC flexural members," ASCE J. Composites for Construction, V.2., No.4, pp195-202.

Kim, D. H. (1995), Composite Structures for Civil and Architectural Engineering, E & FN Spon, London, 497pp.

Kong, F. K. and Evans, R. H. (1989), Reinforced and Prestressed Concrete, 3rd ed, Van Nostrand Reinhold, London, 508pp.

Ladner, M. (1983), "Reinforced concrete members with subsequently bonded steel sheets," Proc. IABSE Symposium on Strengthening f Building Structures – Diagnosis and Therapy, Venezia, Final Report, V.46, pp203-210.

Leeming, M. B. and Darby, J. J. (1999), "Design and specifications for FRP plate bonding of beams," in Strengthening of Reinforced Concrete Structures using externally-bonded FRP composites in structural and civil engineering, Eds., Hollaway, L. C. and Leeming, M. B., Woodhead Publishing Ltd., pp242-269.

Lees, J. M. (1997), Flexure of Concrete Beams Pre-Tensioned with Aramid FRPs., PhD thesis, University of Cambridge, England.

Ligday, F. J., Kumar, S. V. and Gangarao, H. V. S. (1996), "Creep of concrete beams with externally bonded carbon fibre tow sheets," Proc. Int. Conf. Advanced Composite Materials in Bridges and Structures, Ed., El-Badry, M. M., Canadian Society for Civil Engineers, Montreal, Canada, pp513-518.

Luke, P. S., Leeming, M. and Skwarski, A. J. (1999), "The use of advanced composites in strengthening existing structures and for new build," Proc. 8th Int. Conf. Structural Faults and Repair, 13-15 July 1999, London.

Lynn, D. (1999), "The way we are – report on state of bridges programme," Proceedings of ICE Conference on New Century: New Initiatives – Bridges in the 21st Century, Commonwealth Institute, 25 March 1999, London.

MacDonald, M. D. (1978), "Flexural behaviour of concrete beams with bonded external reinforcement," TRRL Supplementary Report 415, Transport and Road research Laboratory, Crowthorne, UK.

MacDonald, M. D. and Calder, A. J. J. (1982), "Bonded steel plating for strengthening concrete structures," Int. J. Adhesion and Adhesives, V2, No.2, pp119-127.

Maeda, T., Asano, Y. and Sato, Y. (1997), "A study on bond mechanism of carbon fibre sheet," Proceedings 3rd International Symposium on Non-Metallic Reinforcement for Concrete Structures (FRPRCS-3), V.1, Japan Concrete Society, pp279-286.

Malek, A. M. and Saadatmanesh, H. (1998), "Analytical study of reinforced concrete beams strengthened with web-bonded fibre reinforced plastic plates or fabrics," ACI Structural J., V.95, No.3, May-Jun., pp343-352.

Malek, A. M., Saadatmanesh, H. and Ehsani, M. R. (1998), "Prediction of failure load of RC beams strengthened with FRP plate due to stress concentration at the plate end," ACI Structural J., V.95, No.2, Mar-Apr., pp142-152.

Mays, G. C. and Hutchinson, A. R. (1988), "Engineering property requirements for structural adhesives," Proc. Institution of Civil Engineers, Part 2, Sep., pp485-501.

Mays, G. C. and Hutchinson, A. R. (1992), Adhesives in Civil Engineering, Cambridge University Press, England, 333pp.

Mays, G. C. and Hutchinson, A. R. (1992), Adhesives in Civil Engineering, Cambridge University Press, England.

Meier, H. (1999), "The latest R & D in structural strengthening with bonded CFRP plates," Proc. 8th Int. Conf. Structural Faults and Repair, 13-15 July, London.

Meier, U. (1987), "Bridge repair with high performance composite materials," *Mater Technik*, 15, S.125-128 (in French and German).

Meier, U. (1992), "Carbon fibre reinforced polymers: Modern materials in bridge engineering," Structural Engineering international, No.1, pp7-12.

Meier, U. (1993), "Rehabilitation and retrofitting of existing structures through external bonding of thin carbon fibre sheets," in Bridge Assessment management and Design, Eds., Barr, B. I. G, Evans, H. R. and Harding, J. E., Elsevier Science B. V., pp373-378.

Meier, U. (1995), "Strengthening of structures using carbon fibre/epoxy composites," Construction and Building Materials, V.9, No.6, pp341-351.

Meier, U. and Kaiser, H. P. (1991), "Strengtheni 1ng of structures with CFRP laminates," Proceedings Advanced Composite Materials in Civil Engineering Structures, Speciality Conf., Materials Div., ASCE, Las Vegas, Ed., Iyer, S. L., Jan 1991, pp224-232.

Meier, U. and Winistorfer, A. (1995), "Retrofitting of structures through external bonding of CFRP sheets," in Non-Metallic (FRP) Materials for the Reinforcement and Prestressing of Concrete, Ed., Taerwe, E & FN Spon, London, pp465-72.

Meier, U., Deuring, M., Meier, H. and Schwegler, G. (1993), "Strengthening of Structures with advanced composites," in Alternative Materials for the Reinforcement and prestressing of Concrete, Ed., Clarke, J. L., Blackie Academic & Professional, Glasgow, pp153-172.

Miller, B., Nanni, A. and Bakis, C. (1999), "Analytical model for CFRP sheets bonded to concrete," Proc. 8th Int. Conf. Structural Faults and Repair, London, 13-15 July 1999.

Mosley, W. H. Bungey, J. H. and Hulse, R. (1999), Reinforced Concrete Design, 5th Ed., Macmillian Press Ltd, 385pp.

Nanni, A. (1997), "CFRP strengthening," Concrete International, June 1997, pp19-23.

NAO (1996), Highways Agency – The Bridge Programme, National Audit Office, 27 March 1996.

NCE (1983), "Chinese crossing first for plastics pioneers," New Civil Engineer, 14 April 1983.

NCE (1996), "Sticking to the task," New Civil Engineer, 11 July 1996.

Nollet, M. J., Perraton, D. and Chaallal, O. (1999), "Flexural behaviour of CFRP strengthened RC beams under room and freezing temperatures," Proc. 8th Int. Conf. Structural Faults and Repair, 13-15 July 1999, London.

Norris, T, Saadatmanesh, H. and Ehsani, M. R. (1997), "Shear and flexural strengthening of RC beams with carbon fibre sheets," ASCE J. Structural Engineering, V.123, No.7, pp903-911.

NSF (1993), NSF 93-4 Engineering Brochure on Infrastructure, US National Science Foundation, Arlington, VA, USA.

Oehlers, D. J. (1989), Discussion on theoretical study by Roberts and Haji-Kazemi (1989), Proc. Institution of Civil Engineers, Part 2, V.87, Dec., pp 651-663.

Oehlers, D. J. (1992), "Reinforced concrete beams with plates glued to their soffits," ASCE J. Structural Engineering, V.118, No.8, pp2023-2038.

Oehlers, D. J. (1997), Discussion on study by Zhang *et al* (1995), Proc. Institution of Civil Engineers, V.122, Nov., pp493-496.

Oehlers, D. J. and Ali, M. (1998), Discussion on study by Quantrill et al (1996), Magazine of Concrete Research, V.50, No.1, Mar., pp91-92.

Oehlers, D. J. and Moran, J. P. (1990), "Premature failure of externally plated reinforced concrete beams," ASCE J. Structural Engineering, V.116, No.4, pp978-995.

Pang, S. S., Li, G., Ibekwe, S. I. and Williams, D. (2000), Structural degradation of FRP strengthened RC beams subjected to hygrothermal and UV attacks, Proceedings 7th International Conference on Composites Engineering, 2-8 July, Denver, USA, pp 679-680.

Peshkam, V. (1995), "Composite news: Infrastructure," Composite News International, Newsletter, Issue No.18, 18 Jan 1995.

Peshkam, V. and Leeming, M. (1994), "Application of composites to strengthening of bridges: project ROBUST," Proceedings 19th British Plastic Federation Composites Conference, Birmingham, UK, 22-23 Nov. 1994.

Pisanty, A. and Regan, P. E. (1998), "Ductility requirements for redistribution of moments in reinforced concrete elements and a possible size effect," Materials and Structures, V.31, Oct., pp530-535.

Quantrill, R. J., Hollaway, L. C., Thorne, A. M. and Parke, G. A. R. (1996a), "Experimental and analytical investigation of FRP strengthened beam response - Part I," Magazine of Concrete Research, V.48, No.177, pp331-342.

Quantrill, R. J., Hollaway, L. C., Thorne, A. M. and Parke, G. A. R. (1996b), "Predictions of the maximum plate end stresses of FRP strengthened beam - Part II," Magazine of Concrete Research, V.48, No.177, pp343-352. (See also discussions by Oehlers, D. J. and Ali, M. (1998), V.50, No.1, pp91-92).

Rahimi, H. (1996), Strengthening of Concrete Structures with Externally Bonded Fibre Reinforced Plastics, PhD thesis, Oxford Brookes University, England.

Raoof, M. and Hassanen, M. A. H. (2000), "Peeling failure of reinforced concrete beams with fibre-einforced plastic or steel plates glued to their soffits", Proc. Institution of Civil Engineers, Structures and Buildings, V.140, Aug., pp291-305.

Raoof, M. and Zhang, S. (1997), "An insight into the structural behaviour of reinforced concrete beams with externally bonded plates," Proc. Institution of Civil Engineers, Structures and Buildings, V.122, Nov., pp477-492.

Razaqpur, G. A. and Ali, M. M. (1996), "Ductility and strength of concrete beams externally reinforced with CFRP sheets," Proc. Int. Conf. Advanced Composite Materials in Bridges and Structures, Ed., El-Badry, M. M., Canadian Society for Civil Engineers, Montreal, Canada, pp505-512.

Richards, V. M. (1996), "An investigative study of assessment, strengthening and rehabilitation of reinforced and pre-stressed concrete bridges," BEng thesis, University of Glamorgan, May 1996, 135 pp.

Ritchie, P. A., Thomas, D. A., Lu, L. W. and Connelly, G. M. (1991), "External reinforcement of concrete beams using fibre reinforced plastics," ACI Structural J., V.88, No.4, July-August, pp490-500.

Roberts, T. M. (1989), "Approximate analysis of shear and normal stress concentration in the adhesive layer of plated RC beams," The Structural Engineer, V.67, No.12, pp229-233.

Roberts, T. M. and Haji-Kazemi, H. (1989), "A theoretical study of the behaviour of reinforced concrete beams strengthened by externally bonded steel plates," Proc. Institution of Civil engineers, Part 2, V.87, No.2, Mar., pp39-55.

Robery, P. (2001), Maunsell Ltd, Private communications.

Robery, P. and Innes, C. (1997), "Carbon fibre strengthening of concrete structures," Proc. 7th Int. Conf. Structural Faults and Repair, University of Edinburgh, 8-10 July 1997, pp197-208.

Robery, P. and Shaw, J. (1997), "Materials for the repair and protection of concrete," Construction and Building Materials, V.11, No. 5-6, (Jul-Sep 1997), 275-281.

Ross, C. A., Jerome, D. M., Tedesco, J. W. and Hughes, M. L. (1999), "Strengthening of reinforced concrete beams with externally bonded composites laminates," ACI Structural J., V.96, No.2, pp212-220.

Saadatmanesh, H. (1994), "Fibre composites for new and existing structures," ACI Structural J., V.91, No.3, May-June, pp346-354.

Saadatmanesh, H. (1997), "Extending service life of concrete and masonry structures with fibre composites," Construction and Building Materials, V.11, No.5-6, pp327-335.

Saadatmanesh, H. and Ehsani, M. R. (1989), "Application of fibre composites in civil engineering," Proceedings of the Sessions Related to Structural Materials at Structures Congress '89, ASCE, pp526-535.

Saadatmanesh, H. and Ehsani, M. R. (1990a), "Fibre composite plates can strengthen concrete beams," Concrete Int., ACI 12(3), pp65-71.

Saadatmanesh, H. and Ehsani, M. R. (1990b), "Flexural strengthening of externally reinforced concrete beams," Proc. 1st ASCE Material Engineering Cong., pp1152-1161.

Saadatmanesh, H. and Ehsani, M. R. (1991), "RC beams strengthened with GFRP plates I: experimental study," ASCE J. Structural Engineering, V.117, No11, pp3417-3433.

Saadatmanesh, H. and Malek, A. M. (1998), "Design guidelines for flexural strengthening of RC beams with FRP plates," ASCE J. Composite for Construction, V.2, No.4, pp158-164.

Sato, Y., Shouji, K., Ueda, T. and Kakuta, Y. (1999), "Uniaxial tensile behaviour of reinforced concrete elements strengthened by carbon fibre sheets," Proc. 4th Int. Symposium on FRP Reinforcement for Reinforced Concrete Structures (FRPRCS-4), Ed., Dolan, C. W., Rizkalla, S. H. and Nanni, A., American Concrete Institute SP-188, pp697-710.

Sato, Y., Ueda, Y. and Tanaka, T. (1996), "Shear reinforcing effect of carbon fibre sheet attached to side of reinforced concrete beams," Proc. Int. Conf. Advanced Composite Materials in Bridges and Structures, Ed., El-Badry, M. M., Canadian Society for Civil Engineers, Montreal, Canada, pp621-628.

Scalzi, J. B., Podolny, W., Munley, E. and Tang, B. (1999), "Will FRP composites change bridge engineering?," Proc. 8th Int. Conf. Structural Faults and Repair, 13-15 July 1999, London.

Sen, R., Shahawy, M., Mullins, G. and Spain, J. (1999), "Durability of carbon fibre-reinforced polymer/Epoxy/Concrete bond in marine environment," ACI Structural J., V.96, No.6, pp906-914.

Shahawy, M. and Beitelman, T. E. (1999), "Static and fatigue performance of RC beams strengthened with CFRP laminates," ASCE J. Structural Engineering, V.125, No.6, pp613-621.

Sharif, A., Al-Sulaimani, G. J., Basunbul, I. A., Baluch, M. H. and Ghaleb, B. N. (1994), "Strengthening of initially loaded reinforced concrete beams using FRP plates," ACI Structural J., V.91, No.2, March-April, pp160-168.

Sika (1998), "Technology and concepts for structural strengthening," Technical Brochure, Sika Limited, Welwyn Garden City, Herts, England.

Slavid, R. (1993), "Plastic is set to prove a very flexible friend," Construction Weekly, 13 Jan 1993.

Swamy, R. N. and Mukhopadhyaya, P. (1999), "Debonding of carbon-fibre-reinforced polymer plate from concrete beams," Proc. Institution of Civil Engineers, Structures and Buildings, V.134, Nov., pp301-317.

Swamy, R. N., Hobbs, B. and Roberts, M. (1995), "Structural behaviour of externally bonded, steel plate reinforced concrete beams after long-term exposure," The Structural Engineer, 73(16), pp255-261.

Swamy, R. N., Jones, R. and Bloxham, J. W. (1987), "Structural behaviour of reinforced concrete beams strengthened by epoxy-bonded steel plates," The Structural Engineer, 65A(2), pp59-68.

Swamy, R. N., Jones, R. and Charif, A. (1989), "The effects of external plate reinforcement on the strengthening of structurally damaged RC beams," The Structural Engineer, 67(3/7), pp45-56.

Swamy, R. N., Lynsdale, C. J. and Mukhopadhyaya, P. (1996), "Effective strengthening with ductility: use of externally bonded plates of non-metallic composite materials," Proc. Int. Conf. Advanced Composite Materials in Bridges and Structures, Ed., El-Badry, M. M., Canadian Society for Civil Engineers, Montreal, Canada, pp481-488.

Swamy, R. N., Mukhopadhyaya, P. and Lynsdale, C. J. (1999), "Strengthening for shear of RC beams by external plate bonding," The Structural Engineer, V.77, No.12, pp19-30.

Taerwe, L. (ed.) (1995), Non-Metallic (FRP) reinforcement for concrete structures, E & FN Spon, London, 714 pp.

Täljsten, B. (1997), "Strengthening of beams by plate bonding," ASCE J. of Materials in Civil Engineering, V.9, No.4, Nov., pp206-212.

Tamai, S., Shima, H., Izumo, J. and Okamura, H. (1988), "Aversge stress-strain relationship in post yield range of steel bar in concrete," JSCE Concrete Library, No.11, June, pp117-129.

Tann, D. B. and Delpak, R. (1999), "Repair and strengthening of reinforced concrete beams using externally bonded CFRP plates," Proceedings 9th BCA Annual Conference on Higher Education and the Concrete Industry, Cardiff University, July 1999, 195-205.

Tann, D. B., and Delpak, R. (2000), "Ductility of FRP strengthened RC beams", The 7th International Conference on Composite Engineering, 3-8 July, Denver, USA, pp865-866.

Thomas, A. (1989), "Concrete repair," Royal Institute of British Architects Journal, March, pp87-91.

Triantafillou, T. C. (1998), "Shear strengthening of reinforced concrete beams using epoxy-bonded FRP composites," ACI Structural J., V.95, No.2, March-April, pp107-115.

Triantafillou, T. C. and Plevris, N. (1992), "Strengthening of RC beams with epoxy-bonded fibre composite materials," Materials and Structures, V.25, No.148, pp201-211.

Tu, L. and Kruger, D. (1996), "Engineering properties of epoxy resin used as concrete adhesives," ACI Material J., V.93, No.1, pp26-35.

Varastehpour, H. and Hamelin, P. (1996), "Analysis and study of failure mechanism of RC beam strengthened with FRP plate," Proc. Int. Conf. Advanced Composite Materials in Bridges and Structures, Ed., El-Badry, M. M., Canadian Society for Civil Engineers, Montreal, Canada, pp527-536.

Varastehpour, H. and Hamelin, P. (1996), "Experimental study of RC beams strengthened with CFRP plate," Proc. Int. Conf. Advanced Composite Materials in Bridges and Structures, Ed., El-Badry, M. M., Canadian Society for Civil Engineers, Montreal, Canada, pp555-563.

Varastehpour, H. and Hamelin, P. (1997), "Strengthening of concrete beams using fibre-reinforced plastics," Materials and Structures, V.30, Apr., pp 160-166.

Watstein, D. and Parsons, D. E. (1943), "Width and spacing of tensile cracks in reinforced concrete cylinders," J. Res. Nat. Bur. Stand., V.31, No. RP545, pp1-24.

Zhang, S. and Raoof, M. (1995), "Prediction of peeling failure of reinforced concrete beams with externally bonded steel plates," Proc. Institution of Civil Engineers, Structures and Buildings, V.110, Aug., pp257-268.

APPENDIX A

MAIN LABORATORY READINGS OBTAINED FROM THE TESTS OF FRP STRENGTHENED RC BEAMS

Table A-1 Load to Maximum Span Deflection of Beams A1, A2, A3 and the Control

Control		A1		A2		A3	
Load (kN)	Deflection (mm)	Load (kN)	Deflection (mm)	Load (kN)	Deflection (mm)	Load (kN)	Deflection (mm)
0.00	0.00	0.00	0.00	0.00	0.00	0.00	0.00
0.50	0.03	0.50	0.05	0.50	0.05	0.50	0.05
1.00	0.06	1.00	0.10	1.00	0.10	1.00	0.08
1.50	0.10	2.00	0.20	2.00	0.23	2.00	0.15
2.00	0.16	4.00	0.50	6.00	0.99	6.00	0.50
4.00	0.32	6.00	0.70	10.00	1.70	10.00	0.85
6.00	0.49	8.00	1.00	12.00	2.04	12.00	1.05
8.00	0.70	10.00	1.30	14.00	2.42	14.00	1.23
10.00	0.96	12.00	1.50	18.00	3.09	16.00	1.49
12.00	1.29	14.00	1.90	22.00	3.81	20.00	2.23
14.00	1.77	16.00	2.20	26.00	4.63	24.00	3.22
16.00	2.71	18.00	2.50	30.00	5.57	28.00	4.09
18.00	3.45	20.00	2.80	35.00	6.68	32.00	5.90
20.00	4.34	22.00	3.50	40.00	7.93	36.00	6.78
22.00	4.98	26.00	3.90	45.00	9.32	40.00	7.64
24.00	5.74	28.00	4.20	50.00	10.52	45.00	7.70
26.00	6.56	30.00	4.70	55.00	12.74	50.00	8.87
28.00	7.19	32.00	5.00	60.00	13.92	55.00	10.95
30.00	7.89	34.00	5.60	65.00	15.92	60.00	11.29
32.00	8.64	36.00	5.80	74.00	18.92	65.00	12.34
34.00	9.24	38.00	6.40	-	-	70.00	13.57
36.00	10.24	40.00	6.80	-	-	75.00	14.80
38.00	11.25	42.00	7.10	-	-	80.00	16.94
40.00	12.46	44.00	7.50	-	-	89.90	20.90
42.00	14.41	46.00	8.00	-	-	-	-
44.00	19.69	48.00	8.70	-	-	-	-
46.00	26.27	50.00	9.60	-	-	-	-
48.00	31.70	52.00	10.20	-	-	-	-
-	-	54.00	11.00	-	-	-	-
-	-	58.00	12.70	-	-	-	-
-	-	60.00	13.60	-	-	-	-
-	-	64.00	14.60	-	-	-	-
-	-	68.00	15.80	-	-	-	-
-	-	70.00	16.60	-	-	-	-
-	-	76.20	18.20	-	-	-	-

Table A-2 Load to Maximum Span Deflection of Beams A4, A5, A6 and A7

A4		A5		A6		A7	
Load (kN)	Deflection (mm)	Load (kN)	Deflection (mm)	Load (kN)	Deflection (mm)	Load (kN)	Deflection (mm)
0.00	0.00	0.00	0.00	0.00	0.00	0.00	0.00
0.50	0.04	6.00	0.79	0.50	0.03	1.00	0.03
1.00	0.09	14.00	2.15	1.00	0.08	2.00	0.08
2.00	0.30	22.00	3.51	1.50	0.10	4.00	0.25
8.00	1.06	30.00	4.98	2.00	0.14	6.00	0.40
12.00	1.57	32.00	5.31	3.00	0.23	10.00	0.68
14.00	1.86	34.00	5.74	4.00	0.31	12.00	0.84
16.00	2.14	36.00	6.15	6.00	0.50	14.00	0.98
18.00	2.44	38.00	6.63	8.00	0.71	16.00	1.19
20.00	2.78	40.00	7.05	10.00	1.08	20.00	1.78
22.00	3.53	42.00	7.58	13.00	1.70	24.00	2.58
24.00	3.89	44.00	8.00	14.00	1.92	28.00	3.27
26.00	4.27	46.00	8.46	15.00	2.59	32.00	4.72
28.00	4.78	48.00	8.95	16.00	2.74	36.00	5.42
30.00	5.17	52.00	9.54	18.00	3.45	40.00	6.11
32.00	5.68	54.00	9.90	19.00	4.10	45.00	6.68
34.00	5.99	56.00	10.58	20.00	4.30	50.00	7.84
36.00	6.39	58.00	11.79	22.00	4.64	55.00	8.98
38.00	7.07	60.00	11.72	24.00	5.18	58.10	9.53
40.00	7.42	62.00	12.29	26.00	5.85	-	-
42.00	7.84	64.00	12.92	28.00	6.12	-	-
44.00	8.55	66.00	13.36	30.00	6.48	-	-
46.00	8.88	68.00	13.86	35.00	6.93	-	-
48.00	9.28	70.00	14.36	40.00	7.96	-	-
50.00	9.76	72.00	14.86	45.00	9.30	-	-
52.00	10.24	74.00	15.86	50.00	10.50	-	-
54.00	10.79	76.00	16.86	55.00	11.60	-	-
56.00	11.20	78.00	17.86	60.00	12.50	-	-
58.00	11.66	82.00	19.40	62.00	13.00	-	-
60.00	12.22	-	-	-	-	-	-
62.00	12.72	-	-	-	-	-	-
64.00	13.27	-	-	-	-	-	-
66.00	13.83	-	-	-	-	-	-
68.00	14.33	-	-	-	-	-	-
70.00	14.83	-	-	-	-	-	-
74.40	19.80	-	-	-	-	-	-

Table A-3 Load to Maximum Span Deflection of Beams A8, A9, and A10

A8		A9		A10	
Load (kN)	Deflection 9mm)	Load (kN)	Deflection (mm)	Load (kN)	Deflection (mm)
0.00	0.00	0.00	0.00	0.00	0.00
0.50	0.06	0.50	0.05	0.50	0.05
1.00	0.14	1.00	0.10	1.00	0.09
1.50	0.21	1.50	0.15	1.50	0.13
2.00	0.27	2.00	0.20	2.00	0.18
2.50	0.35	2.50	0.25	2.50	0.22
2.80	0.37	3.00	0.30	3.00	0.26
3.00	0.49	3.50	0.32	4.00	0.35
3.50	0.49	4.00	0.39	6.00	0.53
4.00	0.57	6.00	0.63	8.00	0.71
6.00	0.91	8.00	0.77	10.00	0.90
8.00	1.18	10.00	1.02	12.00	1.30
10.00	1.49	12.00	1.41	14.00	1.63
12.00	1.92	14.00	1.87	16.00	2.02
14.00	2.39	15.00	2.24	18.00	2.44
15.00	2.62	16.00	2.56	19.00	2.91
16.00	2.90	18.00	3.56	20.00	3.13
18.00	3.40	20.00	3.94	22.00	3.62
20.00	3.81	21.00	4.31	24.00	4.14
22.00	4.46	22.00	4.76	26.00	4.60
24.00	4.91	24.00	5.21	28.00	5.20
26.00	5.54	26.00	5.99	30.00	5.61
28.00	6.09	28.00	7.02	35.00	6.90
30.00	6.51	30.00	7.91	40.00	8.09
35.00	6.98	35.00	8.65	45.00	9.24
40.00	8.09	40.00	9.09	50.00	10.14
45.00	9.37	45.00	9.42	55.60	11.40
50.00	10.85	50.00	9.65	-	-
55.00	12.27	59.10	10.66	-	-
60.00	13.94	-	-	-	-
65.00	15.59	-	-	-	-
68.80	16.84	-	-	-	-

Table A-4 Load to Maximum Span Deflection of Beams B1, B2, B3 and B4

B1		B2		B3		B4	
Load (kN)	Deflection (mm)	Load (kN)	Deflection (mm)	Load (kN)	Deflection (mm)	Load (kN)	Deflection (mm)
0.00	0.00	0.00	0.00	0.00	0.00	0.00	0.00
1.00	0.05	1.00	0.08	1.00	0.03	0.50	0.03
2.00	0.11	2.00	0.17	2.00	0.17	1.00	0.07
3.00	0.19	3.00	0.25	3.00	0.30	2.00	0.18
4.00	0.28	4.00	0.34	4.00	0.44	3.00	0.30
5.00	0.36	5.00	0.44	5.00	0.59	4.00	0.43
6.00	0.44	6.00	0.53	6.00	0.76	6.00	0.61
7.00	0.72	7.00	0.64	7.00	0.93	8.00	0.79
8.00	0.79	8.00	0.75	8.00	1.11	10.00	1.02
10.00	0.95	10.00	0.99	10.00	1.50	12.00	1.25
12.00	1.15	12.00	1.32	12.00	1.91	14.00	1.71
14.00	1.41	14.00	1.59	14.00	2.42	16.00	2.54
16.00	2.42	16.00	1.98	16.00	2.94	18.00	3.43
18.00	3.12	18.00	2.33	18.00	3.46	20.00	4.10
20.00	3.88	20.00	2.67	20.00	3.97	25.00	5.68
25.00	5.32	22.50	2.95	25.00	5.52	30.00	7.13
27.00	6.49	25.00	3.53	30.00	6.92	35.00	8.60
30.00	7.77	27.50	3.84	35.00	8.54	40.00	10.23
32.50	8.28	30.00	4.34	40.00	9.91	45.00	11.95
35.00	9.45	32.50	4.71	45.00	11.46	50.00	13.26
37.50	10.04	35.00	5.14	47.50	12.05	55.00	15.13
40.00	11.44	37.50	5.66	50.00	12.88	60.00	17.35
42.50	11.93	40.00	6.30	52.50	13.45	65.00	21.30
45.00	13.54	42.50	6.60	55.00	14.61	70.00	26.00
47.50	14.11	45.00	7.18	57.50	15.34	75.00	31.80
50.00	15.53	47.50	7.55	60.00	18.00	76.15	32.96
52.50	16.52	50.00	8.13	62.50	19.20	-	-
55.00	18.64	52.50	8.57	65.00	20.50	-	-
57.50	20.45	55.00	9.13	68.40	23.00	-	-
60.00	23.44	57.50	9.49	-	-	-	-
62.50	24.78	60.00	10.01	-	-	-	-
65.50	30.66	62.50	10.49	-	-	-	-
67.50	32.71	65.00	11.07	-	-	-	-
70.00	34.80	67.50	11.52	-	-	-	-
-	-	70.00	12.13	-	-	-	-
-	-	72.50	12.69	-	-	-	-
-	-	75.00	13.29	-	-	-	-
-	-	77.50	13.71	-	-	-	-
-	-	80.00	14.37	-	-	-	-
-	-	82.50	14.99	-	-	-	-
-	-	85.00	15.69	-	-	-	-
-	-	87.50	16.59	-	-	-	-
-	-	90.00	18.19	-	-	-	-
-	-	92.50	18.99	-	-	-	-

Table A-5 Load to Maximum Span Deflection of Beams B5, B6, B7 and B8

B5		B6		B7		B8	
Load (kN)	Deflection (mm)	Load (kN)	Deflection (mm)	Load (kN)	Deflection (mm)	Load (kN)	Deflection (mm)
0.00	0.00	0.00	0.00	0.00	0.00	0.00	0.00
2.00	0.16	1.00	0.16	2.00	0.19	2.00	0.19
4.00	0.38	2.00	0.25	4.00	0.45	4.00	0.35
6.00	0.52	4.00	0.44	6.00	0.83	6.00	0.50
8.00	0.64	6.00	0.65	8.00	1.29	8.00	0.69
10.00	0.87	8.00	0.90	10.00	1.92	10.00	0.89
12.00	1.41	10.00	1.31	12.00	2.50	12.00	1.15
14.00	2.73	12.00	1.96	14.00	2.96	14.00	1.63
16.00	3.22	14.00	2.63	16.00	3.54	16.00	2.40
18.00	3.97	16.00	3.59	18.00	4.09	18.00	3.14
20.00	4.56	18.00	4.36	20.00	4.65	20.00	3.85
25.00	6.40	20.00	5.23	25.00	6.00	25.00	5.73
30.00	8.17	25.00	7.83	30.00	7.45	30.00	7.21
35.00	10.00	30.00	9.99	35.00	8.83	35.00	8.71
40.00	11.95	35.00	12.12	40.00	10.39	40.00	10.41
45.00	14.05	40.00	14.24	-	-	45.00	12.04
50.00	16.43	45.00	16.54	-	-	50.00	14.02
55.00	19.47	50.00	20.89	-	-	55.00	16.99
60.00	23.10	55.00	27.45	-	-	60.00	22.90
65.00	28.82	60.00	34.10	-	-	65.00	29.97
70.00	33.00	61.00	34.95	-	-	67.50	32.56
72.50	35.40	-	-	-	-	-	-

Table A-6 Load Deflection of Original (Precracking) Beams A1, A2, A4 and A5

A1-O		A2-O		A4-O		A5-O	
Load (kN)	Deflection (mm)	Load (kN)	Deflection (mm)	Load (kN)	Deflection (mm)	Load (kN)	Deflection (mm)
0.00	0.00	0.00	0.00	0.00	0.00	0.00	0.00
0.50	0.04	0.50	0.02	0.50	0.00	0.50	0.00
1.00	0.08	1.00	0.03	1.00	0.00	1.00	0.10
1.50	0.12	1.50	0.08	3.00	0.20	2.00	0.20
2.00	0.15	2.00	0.20	5.00	0.40	3.00	0.30
2.40	0.24	2.50	0.27	7.00	0.60	5.00	0.55
2.80	0.28	3.00	0.32	9.00	0.90	7.00	0.80
3.20	0.34	4.00	0.40	10.00	1.10	9.00	1.10
3.60	0.38	6.00	0.59	11.00	1.40	11.00	1.60
4.00	0.42	8.00	0.75	13.00	2.00	13.00	2.30
6.00	0.52	10.00	1.02	16.00	3.40	15.00	3.30
8.00	0.89	12.00	1.60	19.00	4.60	17.00	4.00
10.00	1.38	14.00	2.30	22.00	5.90	19.00	5.00
12.00	2.17	16.00	3.20	25.00	7.10	21.00	5.90
14.00	3.13	17.00	3.60	27.00	7.90	24.00	7.00
15.00	3.49	18.00	4.10	29.00	9.00	27.00	8.20
16.00	3.90	19.00	4.50	-	-	-	-
18.00	4.73	20.00	4.80	-	-	-	-
19.00	5.09	21.00	5.20	-	-	-	-
24.00	7.10	22.00	5.60	-	-	-	-
-	-	24.00	6.50	-	-	-	-
-	-	26.00	7.70	-	-	-	-
-	-	28.00	8.50	-	-	-	-

Table A-6 (Continued)

A6-O		A8-O	
Load (kN)	Deflection (mm)	Load (kN)	Deflection (mm)
0.00	0.00	0.00	0.00
0.50	0.02	0.50	0.03
1.00	0.03	1.00	0.07
3.00	0.22	1.50	0.11
6.00	0.54	2.00	0.15
9.00	0.98	2.50	0.19
11.00	1.34	3.00	0.22
12.00	1.54	3.50	0.25
14.00	2.20	4.00	0.28
15.00	2.70	5.00	0.38
17.00	3.51	8.00	0.75
19.00	4.35	10.00	1.08
21.00	5.18	12.00	1.51
23.00	5.96	16.00	2.99
27.00	7.54	18.00	3.82
29.00	8.29	20.00	4.43
-	-	26.00	6.62
-	-	30.00	8.48

Table A-7 Load to Maximum Span Deflection of Beams C1, C2 and C3

C1		C2		C3	
Load (kN)	Deflection (mm)	Load (kN)	Deflection (mm)	Load (kN)	Deflection (mm)
0.00	0.00	0.00	0.00	0.00	0.00
0.50	0.20	1.00	0.09	0.50	0.04
2.00	0.50	2.00	0.18	1.00	0.11
4.00	0.80	4.00	0.38	1.50	0.16
6.00	1.00	6.00	0.63	2.00	0.24
8.00	1.30	8.00	0.92	4.00	0.45
10.00	1.60	10.00	1.39	6.00	0.65
12.00	2.20	12.00	2.21	8.00	0.85
14.00	2.60	14.00	3.17	10.00	1.04
16.00	3.00	16.00	4.10	12.00	1.30
18.00	3.60	18.00	4.91	14.00	1.70
20.00	4.40	20.00	5.75	16.00	2.56
22.00	5.20	22.00	6.65	18.00	3.32
24.00	5.80	24.00	7.61	20.00	4.05
28.00	6.70	28.00	9.36	-	-

Table A-8 Load to Maximum Span Deflection of Beams C4, C5 and C6

C4		C5		C6	
Load (kN)	Deflection (mm)	Load (kN)	Deflection (mm)	Load (kN)	Deflection (mm)
0.00	0.00	0.00	0.00	0.00	0.00
0.50	0.01	1.00	0.11	1.00	0.43
2.00	0.31	1.50	0.17	2.00	0.67
4.00	0.70	2.00	0.24	3.00	0.90
6.00	1.07	2.50	0.27	4.00	1.15
8.00	1.41	3.00	0.32	5.00	1.36
10.00	1.82	4.00	0.42	6.00	1.56
12.00	2.30	6.00	0.61	7.00	1.72
14.00	2.83	8.00	1.03	8.00	1.87
16.00	3.41	10.00	1.48	10.00	2.16
18.00	3.98	12.00	2.30	12.00	2.46
20.00	4.59	14.00	3.26	14.00	2.77
22.00	5.19	16.00	4.34	-	-
26.00	6.17	18.00	5.30	-	-
28.00	6.81	20.00	5.97	-	-
30.00	7.56	24.00	7.89	-	-
-	-	26.00	8.70	-	-
-	-	28.00	9.87	-	-
-	-	30.00	11.23	-	-

Table A-9 Load to Maximum Span Deflection of Beams D1 to D5

D1		D2		D3		D4		D5	
Load (kN)	Deflection (mm)	Load (kN)	Deflection (mm)	Load (kN)	Deflection (mm)	Load (kN)	Deflection (mm)	Load (kN)	Deflection (mm)
0.00	0.00	0.00	0.00	0.00	0.00	0.00	0.00	0.00	0.00
1.00	0.05	1.00	0.50	1.00	0.10	1.00	0.40	1.00	0.05
2.00	0.10	2.00	0.60	2.00	0.20	2.00	0.70	2.00	0.10
4.00	0.40	4.00	1.00	4.00	0.40	4.00	1.10	4.00	0.40
6.00	0.90	6.00	1.60	6.00	0.70	6.00	1.90	6.00	0.80
8.00	1.50	8.00	3.30	8.00	1.00	8.00	2.80	8.00	1.40
10.00	4.00	10.00	5.00	10.00	2.10	10.00	4.10	10.00	2.60
12.00	5.40	12.00	7.40	12.00	4.30	12.00	6.20	12.00	4.40
14.00	6.60	14.00	8.00	14.00	5.50	14.00	7.50	14.00	5.40
16.00	7.90	16.00	8.10	16.00	6.70	16.00	9.10	16.00	6.50
18.00	9.50	18.00	8.40	18.00	9.00	18.00	11.20	18.00	8.00
20.00	10.90	20.00	8.50	20.00	10.30	20.00	12.30	20.00	9.00
22.00	11.90	22.00	8.70	22.00	12.30	22.00	12.50	22.00	10.20
24.00	12.90	24.00	9.10	24.00	13.80	24.00	12.60	24.00	11.70
26.00	14.40	26.00	9.30	26.00	14.90	26.00	12.70	26.00	11.80
-	-	28.00	9.40	28.00	16.00	28.00	13.00	28.00	11.90
-	-	-	-	30.00	16.90	30.00	13.30	30.00	12.00
-	-	-	-	32.00	17.70	-	-	32.00	12.10
-	-	-	-	34.00	17.80	-	-	34.00	12.20
-	-	-	-	36.00	17.90	-	-	36.00	12.40
-	-	-	-	38.00	18.10	-	-	38.00	12.50
-	-	-	-	40.00	18.50	-	-	40.00	12.70
-	-	-	-	42.00	18.70	-	-	42.00	12.80
-	-	-	-	44.00	18.90	-	-	-	-
-	-	-	-	46.00	19.10	-	-	-	-
-	-	-	-	50.00	19.80	-	-	-	-

Table A-10 Load to Maximum Span Deflection of Continuous Beams M1 and M2

M1				M2			
Load (kN)	Deflection span AB (mm)	Deflection span BC (mm)	Average (mm)	Load (kN)	Deflection span AB (mm)	Deflection span BC (mm)	Average (mm)
0.00	0.00	0.00	0.00	0.00	0.00	0.00	0.00
2.00	0.13	0.14	0.05	2.00	0.04	0.07	0.06
4.00	0.17	0.19	0.18	4.00	0.14	0.22	0.18
6.00	0.23	0.25	0.24	6.00	0.25	0.33	0.29
8.00	0.29	0.33	0.31	8.00	0.36	0.47	0.42
10.00	0.36	0.41	0.39	10.00	0.48	0.62	0.55
12.00	0.44	0.50	0.47	12.00	0.59	0.77	0.68
14.00	0.50	0.59	0.55	14.00	0.72	0.90	0.81
16.00	0.60	0.79	0.70	16.00	0.86	1.09	0.98
18.00	0.73	0.90	0.82	18.00	0.98	1.31	1.15
20.00	1.09	1.31	1.20	20.00	1.17	1.49	1.33
25.00	1.60	2.00	1.80	25.00	1.85	2.12	1.99
30.00	2.20	2.79	2.50	30.00	2.45	2.79	2.62
35.00	2.91	3.55	3.23	35.00	3.15	3.40	3.28
40.00	3.45	4.14	3.80	40.00	4.15	4.21	4.18
45.00	4.25	4.93	4.59	45.00	5.09	4.96	5.03
50.00	5.88	5.65	5.77	50.00	5.65	5.54	5.60
55.00	6.65	6.55	6.60	55.00	6.50	6.45	6.48
60.00	7.28	7.20	7.24	60.00	7.45	7.29	7.37
65.00	8.10	8.08	8.09	65.00	8.40	8.20	8.30
68.20	9.00	9.00	9.00	70.00	9.65	9.70	9.68
-	-	-	-	75.00	11.35	12.15	11.75
-	-	-	-	80.20	20.00	20.00	20.00

Table A-11 Load to Maximum Span Deflection of Continuous Beam M3

First Time Loading				Second Time Loading			
Load (kN)	Deflection span AB (mm)	Deflection span BC (mm)	Average (mm)	Load (kN)	Deflection span AB (mm)	Deflection span BC (mm)	Average (mm)
0.00	0.00	0.00	0.00	0.00	0.00	0.00	0.00
1.00	0.02	0.01	0.01	8.00	0.35	0.44	0.39
2.00	0.04	0.03	0.04	10.00	0.48	0.61	0.55
4.00	0.06	0.04	0.05	20.00	1.31	1.46	1.38
6.00	0.10	0.10	0.10	30.00	2.09	2.29	2.19
8.00	0.16	0.17	0.17	40.00	2.91	2.99	2.95
10.00	0.23	0.25	0.24	50.00	3.57	3.66	3.62
12.00	0.33	0.35	0.34	55.00	3.93	3.99	3.96
14.00	0.44	0.46	0.45	60.00	4.31	4.30	4.30
16.00	0.55	0.58	0.57	65.00	4.68	4.67	4.68
18.00	0.61	0.64	0.63	70.00	5.04	5.10	5.07
20.00	0.79	0.82	0.81	75.00	5.45	5.42	5.43
24.00	0.95	1.06	1.01	80.00	5.79	5.82	5.81
28.00	1.21	1.34	1.28	85.00	6.18	6.09	6.14
32.00	1.51	1.60	1.56	90.00	6.54	6.43	6.49
36.00	1.70	1.82	1.76	100.00	7.32	7.33	7.33
40.00	2.00	2.11	2.06	105.00	7.68	7.77	7.73
45.00	2.31	2.58	2.45	110.00	8.10	8.31	8.21
50.00	2.61	2.81	2.71	115.00	8.55	8.79	8.67
55.00	2.96	3.11	3.04	120.00	9.05	9.26	9.15
60.00	3.21	3.50	3.36	130.00	10.40	10.49	10.44
65.00	3.58	3.89	3.74	140.00	11.64	11.82	11.73
70.00	3.90	4.20	4.05	160.00	13.86	14.30	14.08
75.00	4.55	4.69	4.62	180.60	20.25	21.20	20.73
80.00	5.05	5.24	5.15	-	-	-	-
85.00	5.45	5.69	5.57	-	-	-	-
90.00	5.84	5.96	5.90	-	-	-	-
95.00	6.18	6.41	6.30	-	-	-	-
98.00	6.41	6.57	6.49	-	-	-	-

Table A-12 Unloading of Continuous Beam M3

Load (kN)	Deflection (mm)	Load (kN)	Deflection (mm)
0.00	1.60	45.00	4.50
1.00	1.70	50.00	4.70
2.00	1.80	55.00	5.00
3.00	1.90	60.00	5.20
4.00	2.00	65.00	5.40
5.00	2.10	70.00	5.60
10.00	2.50	75.00	5.80
15.00	2.90	80.00	6.00
20.00	3.30	85.00	6.20
25.00	3.50	90.00	6.30
30.00	3.80	95.00	6.50
35.00	4.00	98.00	6.60
40.00	4.30	-	-

Table A-13 Load (to Span AB) Deflection of Continuous Beam M4

First Time Loading		Unloading	
Load (kN)	Deflection (mm)	Load (kN)	Deflection (mm)
0.00	0.00	0.00	1.68
2.00	0.05	5.00	2.20
4.00	0.14	10.00	2.70
6.00	0.23	15.00	3.20
8.00	0.33	20.00	3.70
10.00	0.42	25.00	4.08
12.00	0.54	30.00	4.50
14.00	0.64	35.00	4.79
16.00	0.72	40.00	5.10
18.00	0.81	45.00	5.32
20.00	0.94	50.00	5.72
25.00	1.28	55.00	6.15
30.00	1.76	60.00	6.30
35.00	2.32	65.00	6.60
40.00	2.78	75.00	7.32
45.00	3.38	-	-
50.00	4.07	-	-
60.00	5.29	-	-
70.00	6.41	-	-
75.00	7.32	-	-
Reloading		-	-
80.00	8.04	-	-
85.00	8.68	-	-
90.00	9.50	-	-
95.00	10.40	-	-
100.00	12.33	-	-
105.00	14.75	-	-
116.90	20.00	-	-

Table A-14 Measured Surface Strains for Beam A1 ($\times 10^{-6}$)

Zone B (Central)						
Load (kN)	**Level 1**	**Level 2**	**level 3**	**Level 4**	**Level 5**	**Level 6**
0.00	0.00	0.00	0.00	0.00	0.00	0.00
0.50	-8.06	-8.06	0.00	8.06	16.12	12.09
1.00	-12.09	-8.06	-8.06	4.03	12.09	16.12
2.00	-12.09	-4.03	4.03	20.15	44.33	44.33
4.00	-36.27	-16.12	4.03	40.30	76.57	104.78
6.00	-64.48	-24.18	12.09	64.48	120.90	157.17
8.00	-88.66	-36.27	20.15	92.69	165.23	217.62
10.00	-104.78	-48.36	28.21	116.87	217.62	286.13
12.00	-128.96	-52.39	36.27	153.14	274.04	366.73
14.00	-157.17	-60.45	88.66	189.41	326.43	439.27
16.00	-189.41	-76.57	56.42	221.65	382.85	519.87
18.00	-221.65	-84.63	64.48	253.89	443.30	612.56
20.00	-253.89	-100.75	76.57	290.16	507.78	693.16
22.00	-270.01	-100.75	100.75	338.52	584.35	785.85
26.00	-326.43	-116.87	116.87	407.03	705.25	963.17
30.00	-370.76	-132.99	153.14	495.69	846.30	1140.49
34.00	-431.21	-145.08	193.44	600.47	1003.47	1354.08
38.00	-491.66	-157.17	229.71	697.19	1160.64	1555.58
42.00	-556.14	-181.35	261.95	789.88	1301.69	1749.02
48.00	-628.68	-193.44	322.40	938.99	1535.43	2063.36
60.00	-810.03	-225.68	479.57	1289.60	2043.21	2712.19
64.00	-874.51	-241.80	535.99	1414.53	2224.56	3054.74
66.00	-918.84	-249.86	564.20	1491.10	2333.37	3219.97
Zone A						
Load (kN)	**Level 1**	**Level 2**	**level 3**	**Level 4**	**Level 5**	**Level 6**
0.00	0.00	0.00	0.00	0.00	0.00	0.00
0.50	-16.12	-12.09	-8.06	0.00	16.12	-8.06
1.00	-28.21	-16.12	-4.03	4.03	8.06	0.00
2.00	-32.24	-8.06	0.00	12.09	4.03	12.09
4.00	-48.36	-24.18	8.06	24.18	48.36	56.42
6.00	-72.54	-36.27	12.09	32.24	72.54	88.66
8.00	-96.72	-36.27	8.06	48.36	96.72	124.93
10.00	-120.90	-48.36	20.15	72.54	132.99	173.29
12.00	-141.05	-52.39	32.24	88.66	161.20	221.65
14.00	-169.26	-68.51	32.24	96.72	181.35	249.86
16.00	-201.50	-72.54	36.27	112.84	213.59	306.28
18.00	-229.71	-80.60	44.33	132.99	241.80	354.64
20.00	-253.89	-96.72	48.36	149.11	274.04	403.00
22.00	-278.07	-92.69	64.48	213.59	322.40	467.48
26.00	-334.49	-112.84	72.54	213.59	382.85	572.26
30.00	-386.88	-124.93	92.69	261.95	467.48	689.13
34.00	-447.33	-137.02	112.84	314.34	564.20	834.21
38.00	-507.78	-153.14	137.02	370.76	652.86	975.26
42.00	-560.17	-161.20	165.23	419.12	741.52	1104.22
48.00	-648.83	-181.35	210.49	507.78	886.60	1313.78

Table A-15 Measured Surface Strains at Mid Span for the Control Beam R3 ($\times 10^{-6}$)

Load (kN)	Level 1	Level 2	level 3	Level 4	Level 5	Level 6
0.00	0.00	0.00	0.00	0.00	0.00	0.00
0.50	-8.01	0.00	0.00	0.00	-8.01	0.00
1.00	-16.02	8.01	0.00	0.00	-8.01	8.01
1.50	-24.03	-16.02	8.01	0.00	-8.01	8.01
2.00	-24.03	-16.02	-8.01	-8.01	-8.01	8.01
4.00	-48.06	-32.04	-24.03	0.00	8.01	32.04
6.00	-88.11	-48.06	-24.03	16.02	32.04	112.14
8.00	-128.16	-72.09	-24.03	32.04	96.12	200.25
10.00	-176.22	-96.12	-16.02	56.07	160.20	256.32
12.00	-240.30	-120.15	0.00	128.16	248.31	392.49
14.00	-480.60	-136.17	-8.01	176.22	336.42	504.63
16.00	-664.83	-168.21	24.03	256.32	480.60	704.88
18.00	-825.03	-232.29	24.03	336.42	648.81	953.19
20.00	-1145.43	-272.34	32.04	424.53	792.99	1201.50
22.00	-728.91	-320.40	40.05	504.63	929.16	1393.74
24.00	-809.01	-368.46	56.07	592.74	1089.36	1610.01
26.00	-841.05	-392.49	80.10	640.80	1177.47	1730.16
28.00	-929.16	-432.54	80.10	704.88	1289.61	1890.36
30.00	-993.24	-456.57	96.12	752.94	1377.72	2042.55
32.00	-1137.42	-536.67	72.09	817.02	1529.91	2266.83
34.00	-1217.52	-576.72	72.09	881.10	1545.93	2411.01
36.00	-1313.64	-616.77	88.11	961.20	1794.24	2659.32
38.00	-1425.78	-680.85	104.13	1065.33	1946.43	2915.64
40.00	-1577.97	-712.89	200.25	1345.68	2386.98	3508.38
42.00	-1738.17	-744.93	288.36	1626.03	2827.53	4101.12

Table A-16 Measured Surface Strains at Mid Span for Beam A3 ($\times 10^{-6}$)

Load (kN)	Level 1	Level 2	level 3	Level 4	Level 5	Level 6
0.00	0.00	0.00	0.00	0.00	0.00	0.00
0.50	-2.02	-1.94	6.05	8.06	14.11	18.13
1.00	0.00	-4.03	2.02	4.03	12.09	18.12
2.00	-10.08	-6.04	2.02	8.06	18.14	26.19
6.00	-50.38	-32.24	-10.08	10.08	36.27	44.33
10.00	-92.70	-56.42	-10.08	14.11	58.43	78.58
12.00	-124.94	-72.54	-20.15	16.12	68.51	106.79
14.00	-141.06	-88.66	-30.23	26.20	84.63	132.99
16.00	-165.24	-102.77	-28.21	32.24	94.71	153.14
20.00	-233.75	-130.97	-28.21	78.57	126.95	270.01
24.00	-310.32	-149.11	-10.08	171.28	211.57	431.21
28.00	-384.87	-167.25	32.25	227.70	294.19	602.49
32.00	-441.29	-193.44	56.43	282.10	515.84	765.70
36.00	-499.73	-209.56	70.53	332.47	465.46	926.90
40.00	-572.27	-229.71	90.68	384.86	552.11	1083.88
50.00	-729.44	-288.14	141.05	531.96	779.81	1355.88
60.00	-918.85	-342.55	201.50	711.30	1019.88	1786.88
70.00	-1087.99	-415.09	290.17	846.30	1230.88	2411.88

Table A-17 Measured Surface Strains at Mid Span for Beam A5 ($\times 10^{-6}$)

Load (kN)	Level 1	Level 2	level 3	Level 4	Level 5	Level 6
0.50	0.00	0.00	0.00	0.00	0.00	0.00
6.00	-64.48	-28.21	12.09	56.42	92.69	132.99
14.00	-177.32	-72.54	48.36	165.23	286.13	390.91
22.00	-290.16	-112.84	88.66	270.01	463.45	644.80
30.00	-394.94	-149.11	141.05	407.03	681.07	951.08
34.00	-443.30	-153.14	165.23	475.54	789.88	1092.13
38.00	-511.81	-173.29	201.50	556.14	910.78	1269.45
42.00	-576.29	-193.44	237.77	640.77	1043.77	1454.83
46.00	-648.83	-217.62	253.89	705.25	1148.55	1624.09
50.00	-733.46	-245.83	245.83	785.85	1281.54	1817.53
54.00	-810.03	-265.98	322.40	870.48	1418.56	2019.03
58.00	-894.66	-298.22	350.61	951.08	1563.64	2224.56
62.00	-995.41	-326.43	382.85	1043.77	1716.78	2450.24

Table A-18 Measured Surface Strains at Mid Span for Beam B6 ($\times 10^{-6}$)

Load (kN)	Level 1	Level 2	level 3	Level 4	Level 5	Level 6	CFRP
0.00	0.00	0.00	0.00	0.00	0.00	0.00	0.00
1.00	-12.09	-20.15	-8.06	32.24	4.03	-8.06	4.03
2.00	-20.15	-16.12	-12.09	36.27	20.15	-4.03	-20.15
4.00	-52.39	-36.27	-20.15	36.27	36.27	28.21	64.48
6.00	-92.69	-44.33	-20.15	64.48	84.63	108.81	145.08
8.00	-141.05	-72.54	-20.15	92.69	132.99	193.44	233.74
10.00	-181.35	-80.60	0.00	149.11	233.74	330.46	370.76
12.00	-233.74	-100.75	48.36	205.53	298.22	435.24	495.69
14.00	-278.07	-96.72	88.66	265.98	390.91	535.99	604.50
16.00	-330.46	-88.66	124.93	310.31	471.51	660.92	781.82
18.00	-378.82	-80.60	157.17	370.76	556.14	797.94	886.60
20.00	-419.12	-84.63	181.35	439.27	677.04	1015.56	1188.85
25.00	-560.17	-84.63	282.10	673.01	1071.98	1559.61	1680.51
30.00	-685.10	-64.48	382.85	882.57	1366.17	1982.76	2131.87
35.00	-806.00	-64.48	487.63	1084.07	1680.51	2413.97	2623.53
40.00	-930.93	-72.54	572.26	1285.57	1966.64	2841.15	3095.04
45.00	-1043.77	-68.51	693.16	1519.31	2301.13	3308.63	3606.85
50.00	-1273.48	8.06	1003.47	2103.66	3151.46	4433.00	4900.48
55.00	-1571.70	132.99	1479.01	2929.81	4340.31	5996.64	6689.80
60.00	-1886.04	290.16	1978.73	3844.62	5702.45	7733.57	8708.83

Table A-19 Measured Surface Strains at Mid Span for Beam B8 ($\times 10^{-6}$)

Load (kN)	Level 1	Level 2	level 3	Level 4	Level 5	Level 6	GFRP
0.00	0.00	0.00	0.00	0.00	0.00	0.00	0.00
2.00	-28.21	-12.09	-8.06	4.03	12.09	20.15	16.12
4.00	-48.36	-28.21	-12.09	4.03	20.15	48.36	-4.03
6.00	-76.57	-40.30	-24.18	4.03	32.24	68.51	84.63
8.00	-96.72	-52.39	-24.18	16.12	52.39	96.72	96.72
10.00	-116.87	-64.48	-28.21	32.24	72.54	137.02	153.14
12.00	-153.14	-84.63	-32.24	44.33	108.81	185.38	225.68
14.00	-197.47	-100.75	-20.15	96.72	201.50	318.37	322.40
16.00	-237.77	-104.78	28.21	193.44	314.34	475.54	531.96
18.00	-278.07	-100.75	40.30	209.56	394.94	596.44	652.86
20.00	-314.34	-112.84	76.57	290.16	507.78	753.61	830.18
25.00	-431.21	-108.81	177.32	499.72	801.97	1176.76	1305.72
30.00	-527.93	-132.99	233.74	620.62	995.41	1458.86	1624.09
35.00	-624.65	-137.02	286.13	737.49	1176.76	1724.84	1958.58
40.00	-733.46	-153.14	342.55	878.54	1394.38	2039.18	2276.95
45.00	-846.30	-185.38	394.94	1003.47	1612.00	2337.40	2643.68
50.00	-951.08	-205.53	443.30	1116.31	1781.26	2550.99	3010.41
55.00	-1063.92	-229.71	511.81	1297.66	2075.45	3050.71	3566.55
60.00	-1414.53	-104.78	1011.53	2204.41	3373.11	4952.87	5565.43
65.00	-1873.95	16.12	1656.33	3421.47	5093.92	7560.28	8458.97

Table A-20 Measured GFRP Strains along the Soffit of Beam B8 ($\times 10^{-6}$)

Load (kN)	B1	B2	B3	B4	B5	B6	B7	B8	B9
0.00	0.00	0.00	0.00	0.00	0.00	0.00	0.00	0.00	0.00
2.00	-36.27	-24.18	-4.03	24.18	16.12	68.51	68.51	72.54	-12.09
4.00	-4.03	4.03	-16.12	-137.02	-4.03	68.51	78.86	88.66	52.39
6.00	16.12	44.33	56.42	8.06	84.63	84.63	157.17	145.08	128.96
8.00	8.06	60.45	80.60	-104.78	96.72	100.75	149.11	149.11	120.90
10.00	32.24	68.51	112.84	84.63	153.14	-52.39	56.42	169.26	92.69
12.00	24.18	92.69	137.02	128.96	225.68	8.06	209.56	221.65	120.90
14.00	92.69	-556.14	229.71	241.80	322.40	298.22	346.58	354.64	197.47
16.00	44.33	161.20	370.76	370.76	531.96	467.48	463.45	576.29	265.98
18.00	80.60	290.16	648.83	447.33	652.86	701.22	519.87	741.52	330.46
20.00	100.75	350.61	789.88	664.95	830.18	797.94	894.66	902.72	451.36
25.00	141.05	866.45	1277.51	1140.49	1305.72	1281.54	1265.42	1289.60	894.66
30.00	217.62	1241.24	1644.24	1442.74	1624.09	1511.25	1599.91	1628.12	1144.52
35.00	346.58	1571.70	1974.70	1841.71	1958.58	1837.68	1886.04	1894.10	1438.71
40.00	777.79	1906.19	2373.67	2208.44	2276.95	2301.13	2248.74	2309.19	1865.89
45.00	1080.04	2216.50	2688.01	2470.39	2643.68	2700.10	2611.44	2623.53	2208.44
50.00	1325.87	2494.57	3042.65	2877.42	3010.41	3030.56	2893.54	2889.51	2252.77
55.00	1515.28	2816.97	3461.77	3393.26	3566.55	3502.07	3352.96	3405.35	2845.18
60.00	1781.26	3550.43	5400.20	5504.98	5565.43	5500.95	5081.83	5101.98	3381.17
65.00	2015.00	5106.01	8088.21	8350.16	8458.97	8338.07	7435.35	7443.41	4489.42

Table A-21 Measured Surface Strains at Span AB for Continuous Beam M1 ($\times 10^{-6}$)

Load (kN)	Level 1	Level 2	level 3	Level 4	Level 5	Level 6	Soffit
0.00	0.00	0.00	0.00	0.00	0.00	0.00	0.00
2.00	0.00	-4.03	-8.06	-8.06	0.00	12.09	-8.06
4.00	-12.09	-4.03	0.00	0.00	12.09	28.21	-12.09
6.00	-16.12	-12.09	-4.03	0.00	12.09	20.15	-8.06
8.00	-24.18	-12.09	-8.06	0.00	12.09	20.15	24.18
10.00	-28.21	-24.18	-12.09	12.09	32.24	52.39	44.33
12.00	-48.36	-32.24	-8.06	8.06	48.36	96.72	48.36
16.00	-80.60	-48.36	-16.12	36.27	44.33	64.48	60.45
20.00	-132.99	-64.48	0.00	36.27	56.42	64.48	124.93
25.00	-217.62	-80.60	60.45	149.11	225.68	310.31	358.67
30.00	-294.19	-84.63	104.78	189.41	354.64	471.51	572.26
35.00	-378.82	-64.48	205.53	386.88	624.65	834.21	938.99
40.00	-443.30	-72.54	245.83	459.42	753.61	1019.59	1116.31
45.00	-523.90	-72.54	294.19	560.17	906.75	1209.00	1362.14
50.00	-596.44	-68.51	350.61	664.95	1088.10	1430.65	1616.03
60.00	-765.70	-64.48	447.33	850.33	1354.08	1805.44	2039.18

Table A-22 Measured Surface Strains at Span AB for Continuous Beam M2 ($\times 10^{-6}$)

Load (kN)	Level 1	Level 2	level 3	Level 4	Level 5	Level 6	Soffit
0.00	0.00	0.00	0.00	0.00	0.00	0.00	0.00
2.00	12.09	0.00	0.00	-8.06	4.03	8.06	12.09
4.00	-8.06	-20.15	-8.06	-8.06	12.09	12.09	64.48
6.00	-20.15	-24.18	-8.06	0.00	16.12	28.21	112.84
8.00	-36.27	-44.33	-16.12	8.06	24.18	32.24	137.02
10.00	-52.39	-40.30	-12.09	8.06	36.27	56.42	161.20
12.00	-80.60	-56.42	-12.09	24.18	68.51	80.60	229.71
16.00	-120.90	-60.45	8.06	92.69	173.29	225.68	302.25
20.00	-173.29	-84.63	24.18	145.08	241.80	310.31	431.21
25.00	-274.04	-88.66	100.75	278.07	475.54	652.86	862.42
30.00	-350.61	-104.78	96.72	390.91	620.62	902.72	1080.04
35.00	-423.15	-112.84	209.56	491.66	793.91	1071.98	1305.72
40.00	-523.90	-128.96	278.07	640.77	1015.56	1358.11	1607.97
45.00	-616.59	-116.87	346.58	777.79	1241.24	1599.91	1958.58
50.00	-697.19	-116.87	398.97	894.66	1402.44	1882.01	2240.68
60.00	-910.78	-120.90	540.02	1192.88	1849.77	2454.27	2949.96
70.00	-1301.69	-40.30	842.27	1761.11	2712.19	3526.25	3719.69

Table A-23 Measured CFRP Strains at the Top Plate for Continuous Beam M3 ($\times 10^{-6}$)

Load (kN)	T1	T2	T3	T4	T5	T6	T7
0.00	0.00	0.00	0.00	0.00	0.00	0.00	0.00
1.00	-24.03	16.02	24.03	-8.01	-8.01	8.01	-8.01
2.00	-136.17	8.01	24.03	32.04	0.00	16.02	-16.02
4.00	-56.07	8.01	40.05	32.04	8.01	8.01	-64.08
6.00	-112.14	16.02	-8.01	-16.02	8.01	-8.01	-64.08
8.00	-88.11	-8.01	32.04	48.06	16.02	8.01	-32.04
10.00	-120.15	0.00	32.04	48.06	32.04	0.00	-24.03
12.00	-104.13	8.01	40.05	72.09	56.07	0.00	-40.05
14.00	-64.08	0.00	56.07	112.14	64.08	0.00	-32.04
16.00	-104.13	16.02	64.08	120.15	64.08	0.00	-24.03
18.00	-64.08	8.01	88.11	136.17	144.18	16.02	-32.04
20.00	-48.06	24.03	120.15	168.21	104.13	8.01	-32.04
24.00	-48.06	40.05	136.17	256.32	144.18	48.06	-24.03
28.00	-64.08	32.04	184.23	344.43	192.24	56.07	-64.08
32.00	-64.08	56.07	216.27	464.58	176.22	72.09	-56.07
36.00	-48.06	80.10	288.36	600.75	344.43	96.12	-48.06
40.00	-56.07	88.11	360.45	688.86	432.54	112.14	-40.05
45.00	-48.06	112.14	488.61	768.96	552.69	152.19	-40.05
50.00	-64.08	152.19	600.75	1017.27	672.84	192.24	-40.05
55.00	-72.09	192.24	768.96	1169.46	817.02	232.29	-32.04
60.00	-56.07	232.29	841.05	1529.91	953.19	312.39	-40.05
65.00	-32.04	272.34	712.89	1529.91	1113.39	392.49	-32.04
70.00	-48.06	352.44	1009.26	1778.22	1257.57	488.61	-32.04
75.00	-64.08	408.51	969.21	1489.86	1377.72	544.68	-64.08
80.00	-104.13	488.61	1441.80	1826.28	1529.91	648.81	-24.03
85.00	-64.08	568.71	1193.49	1874.34	1698.12	728.91	-24.03
90.00	-64.08	656.82	1706.13	2146.68	1834.29	809.01	-32.04
95.00	-56.07	752.94	1762.20	2362.95	1986.48	913.14	8.01
98.00	-32.04	801.00	1778.22	2290.86	2066.58	977.22	0.00

Table A-24 Measured Surface Strains at Span AB for Continuous Beam M4 ($\times 10^{-6}$)

Load (kN)	Level 1	Level 2	level 3	Level 4	Level 5	Level 6	KFRP
0.00	0.00	0.00	0.00	0.00	0.00	0.00	0.00
2.00	-24.18	-12.09	-4.03	-4.03	0.00	4.03	8.06
4.00	-16.12	-20.15	-8.06	-4.03	4.03	8.06	24.18
6.00	-36.27	-24.18	0.00	0.00	8.06	20.15	44.33
8.00	-48.36	-36.27	-16.12	0.00	12.09	28.21	56.42
10.00	-80.60	-44.33	-20.15	0.00	16.12	32.24	72.54
12.00	-84.63	-56.42	-20.15	0.00	20.15	48.36	80.60
14.00	-84.63	-56.42	-24.18	4.03	24.18	52.39	96.72
16.00	-112.84	-64.48	-24.18	8.06	36.27	60.45	104.78
18.00	-116.87	-76.57	-28.21	8.06	48.36	92.69	141.05
20.00	-145.08	-84.63	-24.18	20.15	68.51	120.90	169.26
25.00	-221.65	-104.78	0.00	84.63	165.23	261.95	407.03
30.00	-314.34	-124.93	36.27	177.32	298.22	447.33	685.10
35.00	-374.79	-120.90	108.81	286.13	463.45	721.37	971.23
40.00	-439.27	-112.84	173.29	407.03	652.86	987.35	1333.93
45.00	-499.72	-96.72	241.80	515.84	826.15	1249.30	1624.09
50.00	-556.14	-84.63	290.16	628.68	991.38	1507.22	1902.16
60.00	-697.19	-48.36	394.94	846.30	1305.72	1982.76	2458.30
70.00	-866.45	-20.15	491.66	1051.83	1636.18	2466.36	2970.11
80.00	-1120.34	-76.57	564.20	1269.45	1970.67	2929.81	3546.40
90.00	-1358.11	-84.63	729.43	1599.91	2498.60	3643.12	4501.51
100.00	-1946.49	36.27	1325.87	2700.10	4078.36	5658.12	6556.81

APPENDIX B

COMPUTER MODELLING PROGRAMS

The numerical operations of the analytical modelling process described in Chapter 5 were performed using a spreadsheet program. Visual Basic macros were created to carry out the iterative procedure. The computer start up screen is shown in Figure B1. The program is specifically designed to perform modelling of the FRP strengthened beams with the load and geometrical configuration used in the current study, but it can be easily extended into a generic modelling program for predicting the flexural behaviour of any FRP strengthened RC elements. The modelling process in the current study started with initial concrete compressive strain being set to 10 microstrain and ultimate strain at 3500. A minimum of 25 steps between these two strains was used. The typical modelling output is shown in Table B-1.

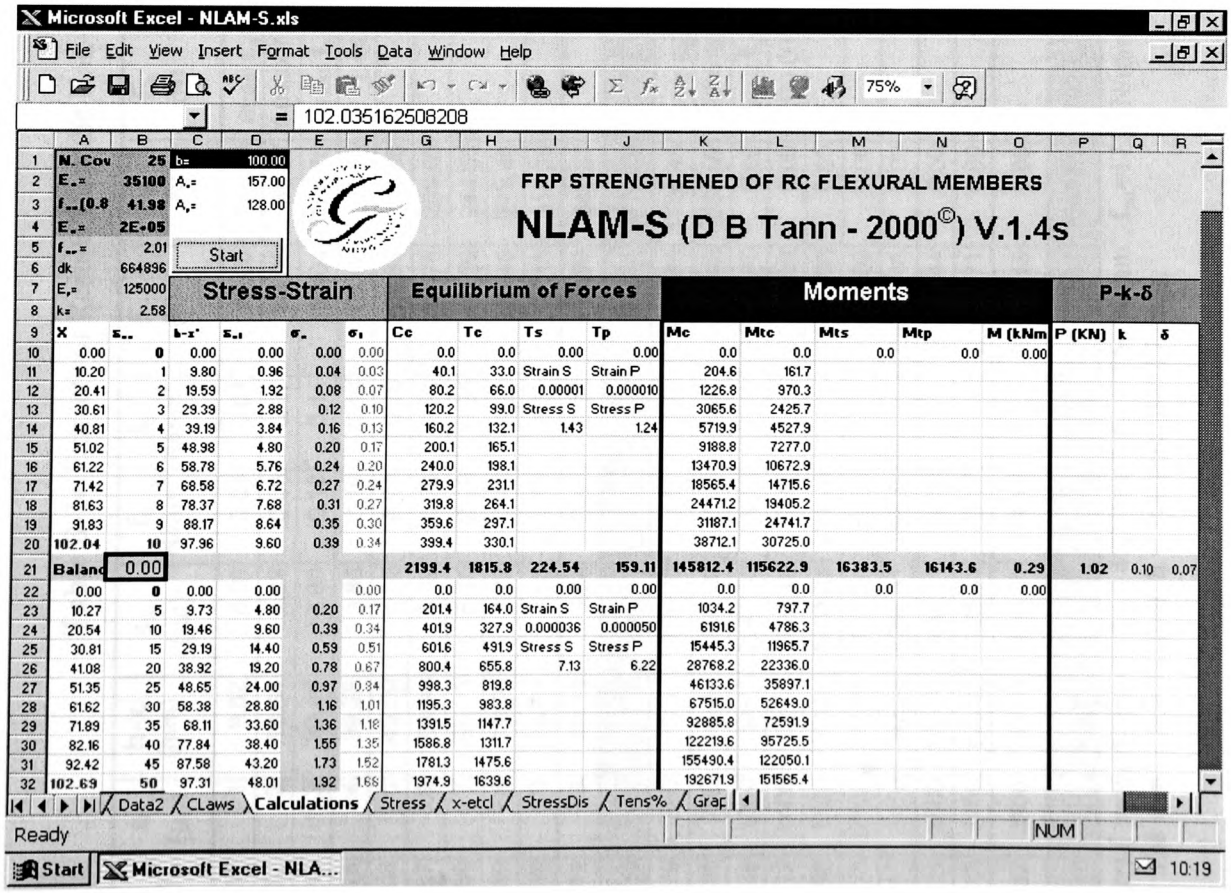

Figure B-1 Typical Computer Start Screen for Analytical Modelling

Table B-1 Extracts of Results from the Non-Precracked Model (at initial and ultimate loading)*

x (mm)	ε_c ($\mu\varepsilon$)	h-x (mm)	ε_{tc} ($\mu\varepsilon$)	f_c N/mm^2	f_{tc} N/mm^2	F_c (N)	F_{tc} (N)	F_s (N)	F_p (N)	M_c (Nmm)	M_{tc} (Nmm)	M_s (Nmm)	M_p (Nmm)	ΣM (kNm)	P (kN)	k (x10^{-6} 1/mm)	δ_{max} (mm)
10.181	1	9.82	0.96	0.04	0.04	42.05	34.93	Strain ε_s	Strain ε_p	214.0	171.5						
20.362	2	19.64	1.93	0.08	0.07	84.06	69.87	0.000007	0.000010	1283.7	1029.0						
30.543	3	29.46	2.89	0.12	0.11	126.04	104.80	Stress f_s	Stress f_p	3208.0	2572.5						
40.725	4	39.28	3.86	0.16	0.14	167.98	139.73	1.44	1.25	5985.8	4802.0						
50.906	5	49.09	4.82	0.21	0.18	209.89	174.66			9616.0	7717.5						
61.087	6	58.91	5.79	0.25	0.21	251.76	209.60			14097.6	11318.9						
71.268	7	68.73	6.75	0.29	0.25	293.60	244.53			19429.4	15606.4						
81.449	8	78.55	7.72	0.33	0.28	335.40	279.46			25610.5	20579.9						
91.630	9	88.37	8.68	0.37	0.32	377.16	314.39			32639.8	26239.4						
101.812	**10**	**98.19**	**9.64**	**0.41**	**0.36**	**418.90**	**349.33**			**40516.1**	**32584.8**				P	k	δ
Balance	**0.00**					**2306.82**	**1921.29**	**225.72**	**159.80**	**152601.0**	**122621.8**	**16520**	**16250**	**0.308**	**1.07**	**0.10**	**0.07**
6.79	350	13.21	680.60	12.51	0.88	8493.86	1166.48	Strain ε_s	Strain ε_p	28845.8	7703.4						
13.58	700	26.42	1361.20	21.66	0.67	14711.52	884.03	0.005518	0.006986	149884.3	17514.2						
20.38	1050	39.62	2041.80	28.13		19108.97	0.00	Stress f_s	Stress f_p	324477.7	0.0						
27.17	1400	52.83	2722.40	32.43		22028.06	0.00	560.00	873.30	523662.9	0.0						
33.96	1750	66.04	3403.01	34.94		23730.06	0.00			725301.8	0.0						
40.75	2100	79.25	4083.61	35.95		24418.09	0.00			912182.8	0.0						
47.55	2450	92.45	4764.21	35.71		24252.48	0.00			1070722.7	0.0						
54.34	2800	105.66	5444.81	34.39		23361.44	0.00			1190058.3	0.0						
61.13	3150	118.87	6125.41	32.17		21848.71	0.00			1261398.1	0.0						
67.92	**3500**	**132.08**	**6806.01**	**29.15**		**19799.18**	**0.00**			**1277550.8**	**0.0**				P_u	k_u	δ_u
Balance	**0.00**					**201752.37**	**2050.51**	**87920.0**	**111781.9**	**7464085.1**	**25217.6**	**9414339**	**15155214**	**32.06**	**111.51**	**51.53**	**34.26**

* Material property input: f_{cu} = 45 N/mm^2, f_{yu} = 560 N/mm^2, f_{pu}=1750 N/mm^2, E_c=36800 kN/mm^2, E_s = 20000 N/mm^2, E_p=125000 N/mm^2, A_s=157 mm^2, A_p = 128 mm^2, **b** =100 mm, **h** = 200 mm, **d** = 174mm.

The design process of design study case two, presented in Chapter 8, was carried out using a spreadsheet program specifically developed for the purpose. It is a generic program that can be applied to any flexural members with any material properties. A typical computer screen is shown in Figure B2.

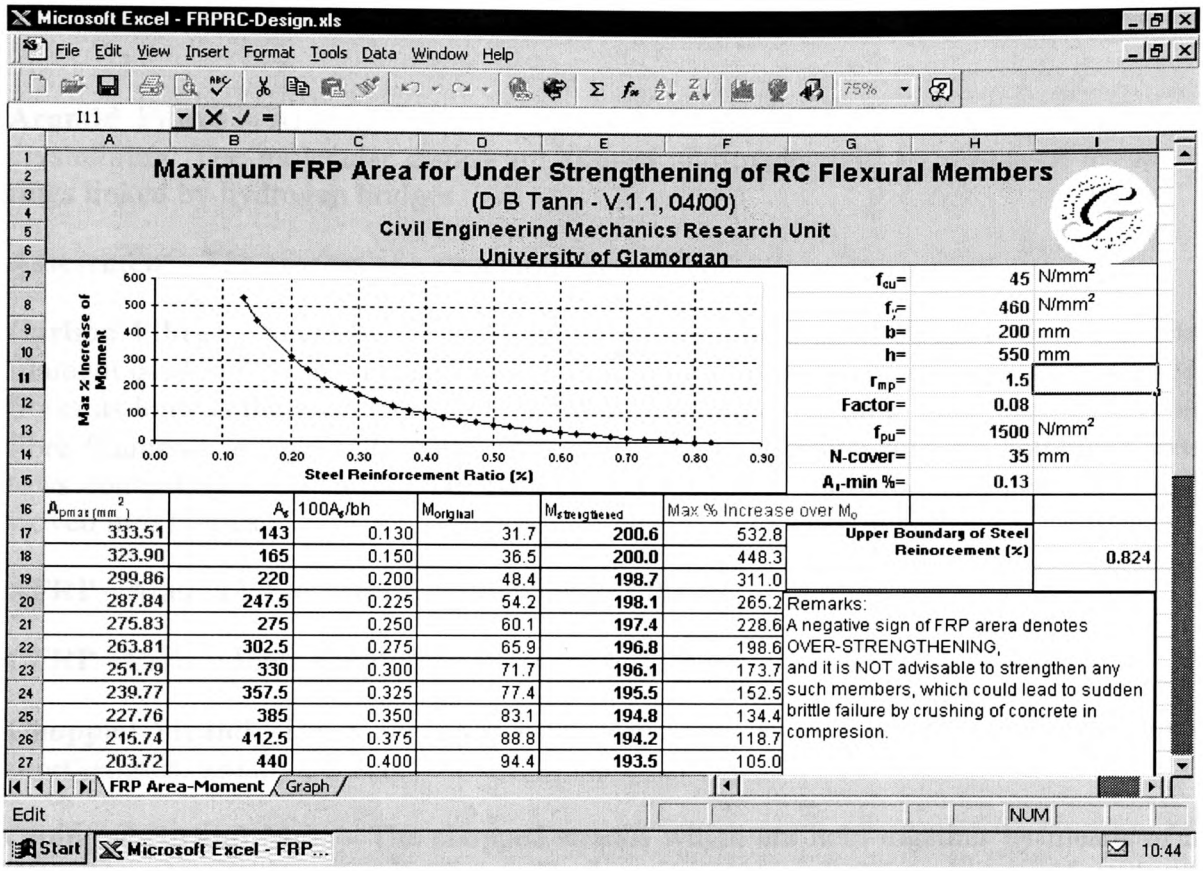

A_{pmax} (mm^2)	A_s	$100A_s/bh$	$M_{original}$	$M_{strengthened}$	Max % Increase over M_o
333.51	143	0.130	31.7	200.6	532.8
323.90	165	0.150	36.5	200.0	448.3
299.86	220	0.200	48.4	198.7	311.0
287.84	247.5	0.225	54.2	198.1	265.2
275.83	275	0.250	60.1	197.4	228.6
263.81	302.5	0.275	65.9	196.8	198.6
251.79	330	0.300	71.7	196.1	173.7
239.77	357.5	0.325	77.4	195.5	152.5
227.76	385	0.350	83.1	194.8	134.4
215.74	412.5	0.375	88.8	194.2	118.7
203.72	440	0.400	94.4	193.5	105.0

Figure B-2 Typical Computer Design Calculations of FRP Strengthened RC Elements

APPENDIX C

FRP COMPOSITE MATERIALS AND REPAIR RELATED TERMINOLOGY

Aramid Fibres - Aramid fibre are organic, man-made fibres with a high degree of crystallinity. The molecular chains are aligned and made rigid by means of aromatic rings linked by hydrogen bridges.

Assessment - The process of a structural appraisal.

Carbon Fibres - Made by carbonising cotton fibres and later, bamboo were the first filament used in Edison's incandescent lamps. Many fibres can be converted into carbon fibres as long as the precursor fibre carbonises instead of melting when heated. Carbon fibre filaments are typically between 5 and 8 μm in diameter and are combined into tows containing 5000 and 12000 filaments. These tows can be twisted into yarns and woven into fabrics.

AFRP - Aramid Fibre Reinforced Polymer (or Plastic)

CFRP - Carbon Fibre Reinforced Polymer (or Plastic).

Chopped Strand -These are made from continuous strands which are chopped into short lengths, usually 50 mm.

Chopped Strand Mats - The chopped strands which are held together by means of a size. The strands are completely randomly orientated and the mats are of uniform thickness. They are produced in various sizes, the most usual being 300 – 400 g/m^2.

Chrystallite - The most rudimentary form of an embryonic crystal that can be identified as a certain species under the microscope.

Continuous Fibre - Continuous fibre may be defined as fibres which are continuous throughout the whole length of the laminate, resulting in the load being applied directly to them; the stress throughout the length of the fibre is constant.

Co-Polymer - An addition polymer of at least two monomers.

Crack Density - Number of visible cracks per unit length.

Critical Length - The critical length of a fibre is the length which is required for the fibre stress to develop its maximum value when under a particular load condition.

Critical Load - The load at which bifurcation occurs determined by theoretical stability analysis.

Damage - Any adverse alterations to the material or mechanical properties of the structural elements. Damages can be broadly classified as material damage, usually caused by environmental loading, and the direct structural damages, caused by overloading.

Delamination - Delamination occurs between layers of a composite laminate and is attributed to the existence of interlaminar stresses which exist in the neighbourhood of a free edge.

Discontinuous FRP - The plastics whose reinforcing fibres have aspect ratios varying between 100 and 5000. The ultimate strength and modulus of short fibre reinforced composites can approach the values for continuous fibre composites, providing that the short filaments can be aligned unidirectionally and that the length is mach greater than the critical length required for shear stress transfer.

E-Glass Fibre - Widely used with polyester and epoxy resins, this low alkali content fibre is the most common glass fibre in the construction industry.

Epoxy - A thermosetting resin, which is widely used in the construction industry. Its toughness is superior to that of the polyester resin and therefore can be operated at higher temperature. Its other advantages include low shrinkage during polymerisation, good adhesion to many substrates, and are especially resistant to alkali attack.

Fibre - Any long and fine material that has a typical aspect ratio of length to transverse dimension of between 1000 and virtually infinity for continuous fibres. The equivalent diameter ranges from 0.001 – 0.5 mm. Such fibres are used in the advanced composite materials.

Fibre Reinforced Concrete - In the concrete industry however, conventional materials with mach smaller aspect ratios such as short, small metal wires, are also used as reinforcing agents. Concrete manufactured this way is now often referred to as "Fibre Reinforced Concrete" or FRC.

Filament - A continuous fibre.

Filament Winding - The oldest mechanical process of manufacturing fibre composites.

FRP - Fibre Reinforced Polymer or Fibre Reinforced Plastic.

Gelcoat - Quick setting resin used in the moulding process to provide an improved surface for the composite, it is the first resin applied to the mould after the mould release agent and provides environmental protection to the composite.

GFRP - Glass Fibre Reinforced Polymer (or Plastic).

Glass fibre - Glass fibre is the only type of inorganic fibre that is being used in the construction industry. It is the common name given to a number of mutually soluble oxides, which can be cooled below their true melting point without crystallization taking place.

Glass Transition Temperature - The temperature at which a sudden change in slope of various physical properties versus temperature curves occurs. It almost approximates the temperature below which a polymer fails in brittle manner and above which it behaves as a leathery or rubbery solid. It is also referred to heat deflection temperature.

Hardner – The curing agent that chemically cross link the resin in the two part system and solidifies the adhesive.

Heat Deflection Temperature – See Glass Transition Temperature

Hybrid - A composite with two or more constituents, for instance, a carbon/glass fibre hybrid. An intralaminar hybrid has plies made from carbon and glass filaments. An interlaminar hybrid has laminates made from two or more different ply materials.

Interface - The interface between the fibre and the matrix is an anistropic transition region that exhibiting a gradation of properties. This is an important region which is required to provide adequate chemically and physically stable bonding between the fibres and the matrix.

Kevlar - An aramid fibre produced by Du Pont

KFRP - Kevlar Fibre Reinforced Polymer, a type of AFRP.

LTR - Localised Total Replacement of degraded concrete material or reinforcement in a damaged element.

Matrix - The parent material, or binders, of fibres (reinforcements) which bonds, contains and protects the fibre reinforcements, and transfers the stress to the reinforcements.

Monomer - A low molecular weight starting material from which a polymer is made. Multidirectional Chopped fibre strands can be placed randomly to obtain isotropic strength.

Off-axes (On-Axes) - Not coincident (Coincident) with the symmetry axis.

PAN - A precursor used in the manufacture of most commercially carbon fibres. PAN is the abbreviation for Polyacrylonnitrile. The carbon fibre conversion yield is 50 to 55%. PAN precursor based carbon fibre generally has a higher tensile strength than a fibre based on any other precursor, due to the lack of surface defects.

Peel Ply - Fabric material usually made of 0.2 mm thick nylon, applied to a laminate to protect the clean, ready-to-use bonding surface and peeled of prior to curing.

Plasticizer - Materials deliberately added to polymers to reduce the stiffness.

PMCM - Polymer Modified Cementitious Mortar, a repair material.

Polymer - A long chain molecule made by connecting many smaller molecules.

Polymerization - The chemical reaction involved when, for example, a liquid polyestaer resin sets to a solid. A comparatively simple chain molecule becomes a highly complex three-dimensional one.

Pre-preg (a pre-impreganated fibre) - An intermediate product consisting of fibres or rows which have been coated with matrix material such as resin.

Prestressing Fibres - Prestressing tendons for concrete as a replacement of high strength steel reinforcing bars.

Pultrusion - Pultrusion is a continuous moulding process. Continuous fibre reinforcement rovings and strand mat are pulled through tanks of resin, a heated forming and curing die to form a completed composite structural shape.

Rayon Precursor - Derived from cellulosic materials, were among the earliest precursors used to make carbon fibre. The significant disadvantage is that only a small part (typically 25%) of the initial fibre mass remains after carbonisation.

Resin – The reactive polymer that is used as the base in an adhesive system, or as the bonding matrix of FRP composites.

Rehabilitation - A generic term referring to any improvement over the current state of a structure, no matter whether such improvement are carried out structurally or for architectural and decorative purposes only.

Repair - The process of restoring the structural capacities of a damaged structure or its elements to the original design specification.

Retrofitting - The combined processes of Repair and Strengthening.

Rod/Bar - Any materials with diameter in the order of 6.4 – 50.0 mm.

S-Glass Fibre - A glass fibre that is stronger and stiffer than the E-glass, which was originally developed for military application.

Strand - This is associated with filaments of fibre, the diameter of a filament is up to 0.0025 mm.

Strengthening - The process in which the original design capacities of a structure or its element are increased or improved.

Synthetic Fibres - Synthetic fibres are manufactured from certain thermoplastic polymers such as polyolefins, polyamide (nylon) and polyester.

Tangent Modulus - The slope of the stress-strain curve in the inelastic region, at any stress level as determined by compression test of a small specimen.

Thermoplastic - Long chains of molecules lying next to each other, held together in the same position relative to each other by electrostatic attraction.

Thermoset - This can be regarded as a large molecule, as each molecular chain is chemically bound, or cross-linked, to its neighbour. Thermosetting binders are cured once only and can never be reformed, recured or reused.

Unidirectional - The fibre alignment is greater and the maximum fibre content can be obtained. The maximum strength is achieved in the fibre direction. Up to 85% by weight of continuous fibre content can be obtained by filament winding, pultrusion and prepregging.

Whisker - Any fibre material that is a single crystal.

Wire - Any metallic materials with diameter in the order of 0.8 – 6.4 mm.

Woven Cloth - A more refined product than woven rovings. It is usually a bi-directional reinforcement.

Woven Rovings - Continuous strands which may be unidirectionally or bidirectionally orientated.

Yarn or Tow - A number of filaments in a bundle which can be handled as a single unit. A tow is usually bigger than a yarn, having thousands of filaments whereas a yarn usually has a few hundred filaments. A yarn may be spun and twined from staple fibre but a tow is formed from constant filaments.

APPENDIX D

FRP AND ADHESIVE STRENGTHENING SYSTEMS AVAILABLE IN THE UK*

* The following information is extracted from Appendix B of the Concrete Society Technical Report No. 55, "Design guidance for strengthening concrete structures using fibre composite materials", ISBN 0 946691 84 3. Contact details:

The Concrete Society
Century House
Telford Avenue
Crowthorne
Berkshire
RG45 6YS

Tel: 01344 466007, **Fax**: 01344 466008,
www.concrete.org.uk

Table D1 Suppliers of Repair/Strengthening Materials

Supplier	Trade Name	Type of Material
DML Composites	DML Composites	Carbon FRP plate; Carbon fibre sheets; Glass fibre sheet; Aramid fibre sheet
Du Pont de Nemours Int. S.A.	Kevlar®	Aramid fibre tape or sheet Aramid FRP sheet
Exchem M & C	Selfix Carbofibe	Carbon FRP plate; Carbon fibre sheet; Aramid fibre sheet, Glass fibre sheet
Feb MBT	MBrace; Kevlar®	Carbon fibre sheet; Carbon fibre plarte; Aramid fibre tape or sheet
Sumitomo Co. Europe	Replark	Carbon fibre prepreg
SBD	Engorce	Carbon FRP plate; Carbon fibre sheet; Glass fibre sheet
Sika	Sika CarboDur Sika Wrap Hex 230C and 100G	Carbon FRP plate; Carbon fibre sheet; Glass fibre sheet
Toray Europe	Torayca UT70	Carbon fibre sheet

Table D2 Properties of Carbon Fibre Composite Plate Materials

Trade Name	Strength (N/mm^2)	Modulus (kN/mm^2)	Thickness (mm)	Width (mm)
DML Composites	2100 1400	140 360	up to 30 up to 30	up to 1400 up to 1400
Enforce	2200-2500 2200-2500	165 210	1.2, 1.4, 2.1 1.2, 1.4, 2.1	10, 50, 80, 90, 100, 120 50, 80, 90, 100, 120, 150
MBrace LM MBrace HM	>2200 >2200	150 200	1.2, 1.4 1.4	50, 80, 100, 120 50, 80, 100, 120, 150, 200
Selfix Carbofibe S Selfix Carbofibe M Selfix Carbofibe H	2800 3200 1600	150 200 280	1.2, 1.4 1.2, 1.4 1.2, 1.4	50, 80, 120 50, 80, 120 50, 80, 120
Sika CarboDur S Sika CarboDur M Sika CarboDur H	3050 2900 1450	165 210 300	1.2, 1.4 1.4 1.4	50, 60, 80, 90, 100, 120,150 60, 90, 100 50

Table D3 Properties of FRP sheet Materials[#]

Trade Name	Fibre	Strength (N/mm^2)	Modulus (kN/mm^2)	Weight (g/mm^2)	Effective thickness (mm)	Width (mm)
DML Composites	Carbon Glass Aramid	4900 3400 2800	230 70 115	150-900 200-1200 200,300		300-1500 350,500 340
Enforce	Carbon Carbob Glass Aramid	3900 2650 1700 2900	240 640 65 120	200 400 350 290, 420	0.117 0.235 0.135 0.2, 0.29	300 300 680 300
Kevlar®	Aramid	2100	120	280, 420	0.19, 0.29	100-500
MBrace	Carbon Carbon Glass	3550 3000 1550	235 380 74	300 300 915	0.11, 0.165 0.165 0.118	500 500 500
Replark	Carbon Carbon Carbon	3400 2900 1900	230 390 640	200 300 300	0.111-0.167 0.165 0.143	250-500 250-500 250-500
Selfix Carbofibe E Selfix Carbofibe C Selfix Carbofibe AR	Glass Carbon Aramid	1099* 1417* 1086*	42* 120* 61*	432 300 240	0.167 0.167 0.167	150, 300 150, 300 150, 300
Sika Wrap Hex 230C Sika Wrap Hex 100G	Carbon Glass	3500 2250	230 70	230 840		610 1270
Torayca UT70-20 Torayca UT70-30	Carbon Carbon	4090 42220	230 235	200 300	0.111 0.167	100-1000 100-1000

Unless stated otherwise, these indicative property values are for dry fibres.
* Results normalised to 55% fibre volume using Selfix Carbofibe laminating resin.

Table D4 Properties of Epoxy Adhesives

Property	Supplier and Trade Name			
	Exchem	MBT	SBD	Sika
	Resifix 31	MBrace lam. adhesive	Epoxy Plus	Sikadur
Tensile Strength (N/mm^2)	24	30	19	30
Flexural strength (N/mm^2)	55	100	35	-
Shear Strength (N/mm^2)	22	-	18	-
Flexural Modulus (kN/mm^2)	6.5	3.5	9.8	12.8
Shear Modulus (kN/mm^2)	3.8	-	-	-
Glass Transition Temperature T_g, (°C)	60	56	60, 80	62

Table D5 Properties of Laminating Resins

Property	Supplier				
	MBT	SBD	DML	Sika	Sumitomo
Tensile Strength (N/mm^2)	50	17	81	30	29
Flexural strength (N/mm^2)	120	28	-	-	-
Flexural Modulus (kN/mm^2)	3	5	-	3.8	2.5
Glass Transition Temperature T_g, (°C)	55	60, 80	59	53	55

Note: All the properties in these table were compiled from manufacturer's technical brochures by the Concrete Society FRP Composite Strengthening Committee. This information is believed to be correct as at the end of 2000. The Concrete Society recommends that for design purposes, actual properties must be obtained from the manufacturer. As test methods vary, the information should detail the bases of information, including testing and property evaluation methods, frequency of testing and standard deviation.

APPENDIX E

OFFICIAL REPORTS ON THE STATUS OF INFRASTRUCTURES IN THE UNITED STATES AND THE UNITED KINGDOM

The American Society of Civil Engineers (ASCE) has published a series of "Report Cards" on the status of America's Infrastructure. The latest report card was published in March 2001, and is available on the Internet at: **http://www.asce.org/reportcard/** as shown in Figure E1. The previous report was published in 1998, as shown in Figure E2. The Institution of Civil Engineers and the New Civil Engineer magazine have also jointly published a report on "The State of the Nation – measuring the quality of UK's infrastructure" as shown in Figure E3.

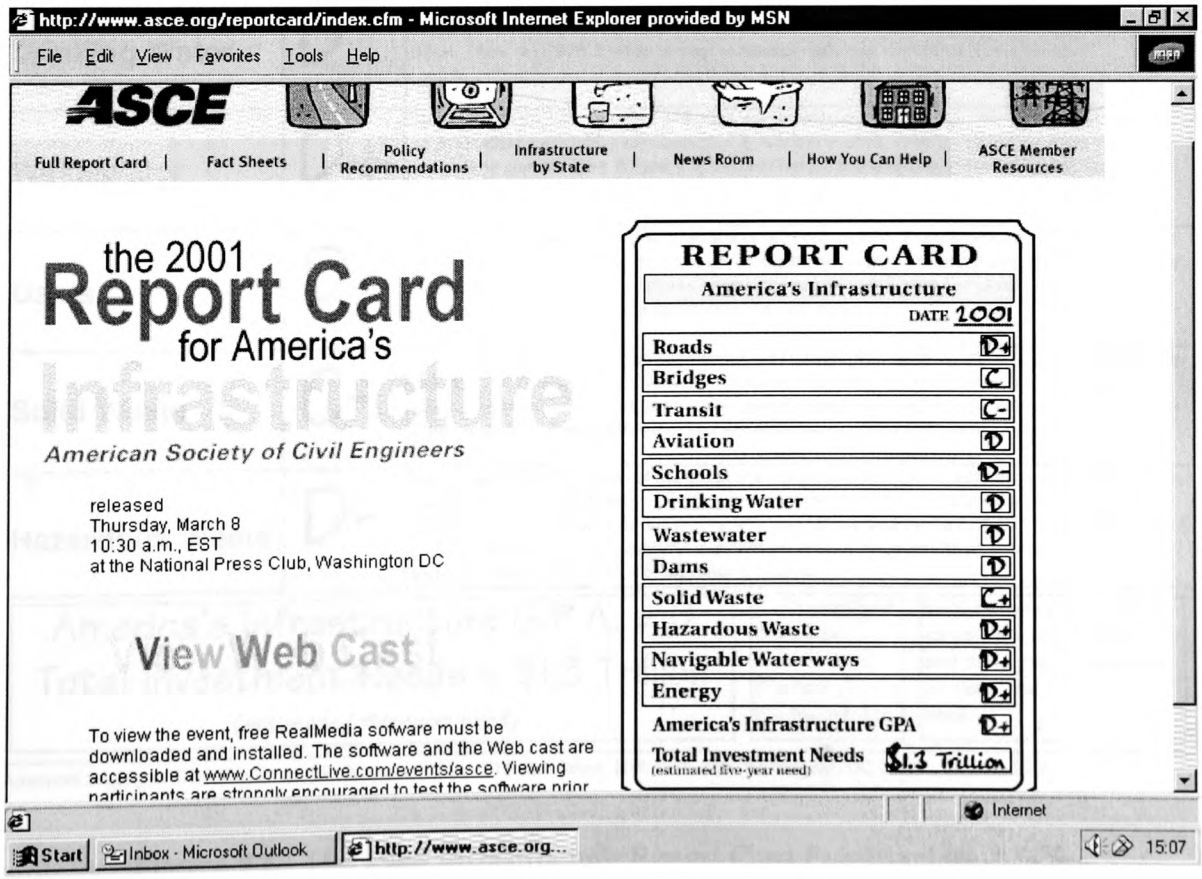

Figure E1 The Latest Report Card Published by ASCE

ASCE
American Society of Civil Engineers

1998 Report Card for America's Infrastructure

Subject	Grade	Comments
Roads	D-	More than half (59 percent) of our roadways are in poor, mediocre or fair condition. More than 70 percent of peak-hour traffic occurs in congested conditions. It will cost $263 billion to eliminate the backlog of needs and maintain repair levels. Another $94 billion is needed for modest improvement -- a $357 billion total.
Bridges	C-	Nearly one of every three bridges (31.4 percent) is rated structurally deficient or functionally obsolete. It will require $80 billion to eliminate the current backlog of bridge deficiencies and maintain repair levels.
Mass Transit	C	Twenty percent of buses, 23 percent of rail vehicles, and 38 percent of rural and specialized vehicles are in deficient condition. Twenty-one percent of rail track requires improvement. Forty-eight percent of rail maintenance buildings, 65 percent of rail yards and 46 percent of signals and communication equipment are in fair or poor condition. The investment needed to maintain conditions is $39 billion. It would take up to $72 billion to improve conditions.
Aviation	C-	There are 22 airports that are seriously congested. Passenger enplanements are expected to climb 3.9 percent annually to 827.1 million in 2008. At current capacity, this growth will lead to gridlock by 2004 or 2005. Estimates for capital investment needs range from $40-60 billion in the next five years to meet design requirements and expand capacity to meet demand.
Schools	F	One-third of all schools need extensive repair or replacement. Nearly 60 percent of schools have at least one major building problem, and more than half have inadequate environmental conditions. Forty-six percent lack basic wiring to support computer systems. It will cost about $112 billion to repair, renovate and modernize our schools. Another $60 billion in new construction is needed to accommodate the 3 million new students expected in the next decade.
Drinking Water	D	More than 16,000 community water systems (29 percent) did not comply with the Safe Drinking Water Act standards in 1993. The total infrastructure need remains large -- $138.4 billion. More than $76.8 billion of that is needed right now to protect public health.
Wastewater	D+	Today, 60 percent of our rivers and lakes are fishable and swimmable. There remain an estimated 300,000 to 400,000 contaminated groundwater sites. America needs to invest roughly $140 billion over the next 20 years in its wastewater treatment systems. An additional 2,000 plants may be necessary by the year 2016.
Dams	D	There are 2,100 regulated dams that are considered unsafe. Every state has at least one high-hazard dam, which upon failure would cause significant loss of life and property. There were more than 200 documented dam failures across the nation in the past few years. It would cost about $1 billion to rehabilitate documented unsafe dams.
Solid Waste	C-	Total non-hazardous municipal solid waste will increase from 208 to 218 million tons annually by the year 2000, even though the per capita waste generation rate will decrease from 1,606 to 1,570 pounds per person per year. Total expenditures for managing non-hazardous municipal solid waste in 1991 were $18 billion and are expected to reach $75 billion by the year 2000.
Hazardous Waste	D-	More than 530 million tons of municipal and industrial hazardous waste is generated in the U.S. each year. Since 1980, only 423 (32 percent) of the 1,200 Superfund sites on the National Priorities List have been cleaned up. The NPL is expected to grow to 2,000 in the next several years. The price tag for Superfund and related clean up programs is an estimated $750 billion and could rise to $1 trillion over the next 30 years.

America's Infrastructure G.P.A. = D
Total Investment Needs = $1.3 Trillion
(estimated five-year need)

A = Exceptional
B = Good
C = Mediocre
D = Poor
F = Inadequate

Each category was evaluated on the basis of condition and performance, capacity vs. need, and funding vs. need.

American Society of Civil Engineers, Washington Office, 1015 15th Street, NW, Suite 600, Washington, DC 20005; 202/789-2200

Figure E2 The 1998 Infrastructure Report Card Published by ASCE

Winter 2000

New Civil Engineer NCE

The State of the Nation

measuring the quality of the UK's infrastructure

Prepared by the Institution of Civil Engineers and New Civil Engineer magazine

THE INSTITUTION OF CIVIL ENGINEERS

Category	Grade	Change	Comment	Action needed	Sustainability Grade
Overall	C	↑	While there are few visible signs of improvement in the UK's infrastructure over the last six months, there has been unprecedented Government commitment towards transport and urban development which promises to drive major improvements in the quality of lives. However, the public is growing tired of talk - it is now time for the government to act. There is an opportunity to deliver long term policies, thanks to the UK's current political and economic stability. But insufficient statutory tools are available to kick-start the neglected waste and energy sectors, which if allowed to decline further, threaten to undo the benefits of transport and regeneration investment. The private sector is ready and willing to play a massive role in developing the UK's infrastructure as will the entire construction profession. Current workload predictions are likely to stretch the industry's resources but improvements in efficiency and productivity will be necessary to meet this challenge. We face an opportunity for both the public and private sectors to work to change the face of the nation - delivery is the next challenge.	Government must deliver on its investment promises so that real benefits are delivered quickly and recognised by the public. The private sector has a huge role to play and industry regulators must strike a balance between protecting the public and encouraging investment. Bureaucracy still needs to be tackled. Planning policy must be simplified to reduce the risks on project delivery. The construction industry also needs to invest more in training to boost available skills and continue to improve value for money. Clear leadership is still required to solve the nation's waste and energy problems.	C
Road	C	↑	Transport spending plans published recently by the UK Government point the way to a much-needed increase in expenditure on the trunk route network over the next ten years. Reducing traffic congestion on trunk roads, which carry about a third of all traffic and two thirds of all road freight, is correctly targeted as it is perceived by users to be "the biggest single problem". But surveys by the County Surveyors' Society and the AA note that, in addition to congestion due to sheer volume of traffic, the extent of road closures following major accidents have also risen by a third in the last three years. Revenue from above inflation fuel duty increases has now been ring-fenced for highway maintenance and indicates that Government, having accepted that the trunk route network is vital to the UK economy, is prepared to use hypothecation. However, there are still concerns about both the condition of the network's bridges, particularly with 44 tonne, six-axle lorries cleared for use from February 2001, and a continuing view that the network lacks consistent standard across the nation. Nonetheless, it is recognised that central Government now at least has the intention to invest.	The Government's intentions to improve the UK's road network, as set out in the ten year transport spending plan, must now be converted into action with real increases in expenditure. Work by the Highways Agency and the National Road Maintenance Condition Survey Executive should now enable the annual road condition survey to include the trunk route network and to deliver real performance targets. The DETR backed "Best Value in Highway Maintenance Project" should be embraced by the Scottish Executive and used to permit proper comparisons and benchmarking across the Nation.	C
Rail	C+	—	The accident at Hatfield has increased the public focus on rail safety and could impact substantially on the direction of short and medium term investment. The total rail spending by government and the private sector is expected to exceed £60bn over the next ten years to cope with a predicted 50% growth in passenger traffic and an 80% rise in freight during this period. The Regulator has partially recognised the increased income that Railtrack requires to enhance the rail system and the shadow Strategic Rail Authority is encouraging investment by awarding longer franchises to train operating companies. Spending priorities have been identified as the West and East Coast Mainlines, the Channel Tunnel Rail Link and the upgrading of London Underground. Safety improvements such as the Train Protection Warning System and Automatic Train Protection will also be a priority but will place some constraints on key skills over the next few years. New products and technologies, particularly computer based signalling systems, are still being constrained by bureaucratic approvals procedures.	The Government and Railtrack must act quickly and decisively to resolve the existing uncertainty as to the condition of the railway infrastructure. This must include the timings of the key Railtrack enhancement contracts and firm investment plans must be hammered out as soon as new longer franchises are awarded to train operating companies. Contractors have been increasing capabilities in the recent past and will need a consistent and planned release of new work to tackle the workload effectively. Short supply of specialist resources, such as signalling, will need to be resolved but a collaborative approach to delivery could be very effective in reducing dependency on these skills.	B+
Local transport	D+	↑	The Government's ten-year plan for transport promises a significant boost to Local Authorities' spending aspirations. Allocations for capital investment are set to rise by over 60% next year and will continue to increase to more than double current levels by 2003. Plans to improve bus infrastructure schemes to increase passenger journeys by 10% and funding for 25 new rapid transit lines mark a major turn around for public transport services that have been in decline for over forty years. Private sector cash is also promised to help transform long neglected local transport systems. Local Authorities have also welcomed the Government's commitment to eliminate the multi-billion pound backlog in highways maintenance within the next ten years and local economies look set to benefit from these essential improvements. The deterioration of local bridges and highways is often not apparent to the public and for many years maintenance resources have been lost to other more visible services. Lobbying by local authorities does now appear to have pushed the issue of maintenance up the political agenda. There has also been an alarming rise in compensation claims made by the public due to unsafe infrastructure.	The Government must demonstrate its commitment to the ten year transport plan through generous settlements in the five year Local Transport Plans to be announced in December. If local transport is to deliver the step change in quality proposed by Government, there will have to be strong financial support for the initiatives being brought forward by local authorities to improve all modes of transport.	C-

20

NEW CIVIL ENGINEER 9 NOVEMBER 2000

Figure E3a Report on UK Infrastructure Published by ICE and NCE (Part 1)

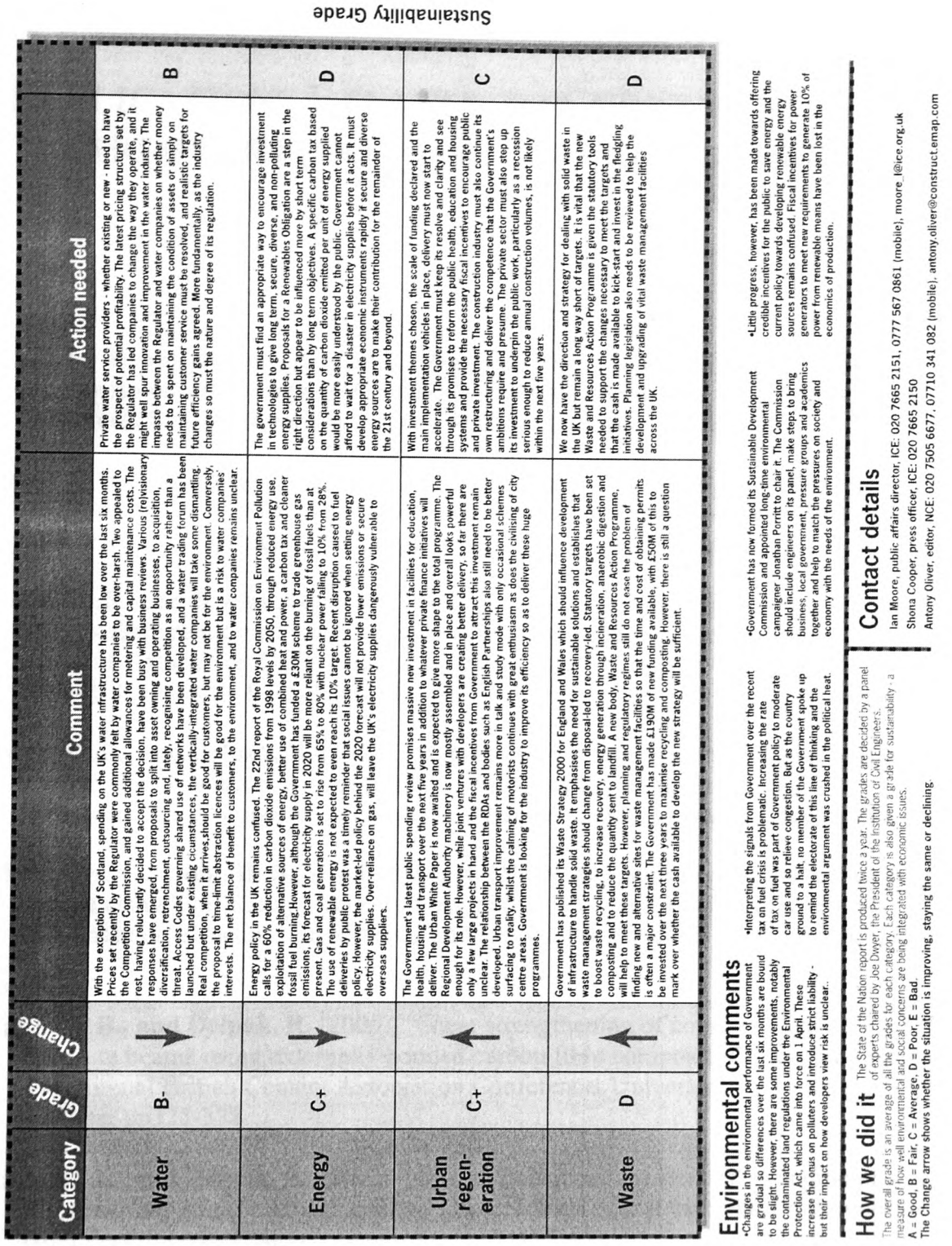

Category	Grade	Change	Comment	Action needed	Sustainability Grade
Water	B-	→	With the exception of Scotland, spending on the UK's water infrastructure has been low over the last six months. Prices set recently by the Regulator were commonly felt by water companies to be over-harsh. Two appealed to the Competition Commission, and gained additional allowances for metering and capital maintenance costs. The rest, having reluctantly decided to accept the decision, have been busy with business reviews. Various (re)visionary responses have emerged, from proposals to split into asset owning and operating businesses, to acquisition, diversification, retrenchment, outsourcing and, lately, recognising competition as an opportunity rather than a threat. Access Codes governing shared use of networks have been developed, and a water trading forum has been launched but under existing circumstances, the vertically-integrated water companies will take some dismantling. Real competition, when it arrives,should be good for customers, but may not be for the environment. Conversely, the proposal to time-limit abstraction licences will be good for the environment but is a risk to water companies' interests. The net balance of benefit to customers, to the environment, and to water companies remains unclear.	Private water service providers - whether existing or new - need to have the prospect of potential profitability. The latest pricing structure set by the Regulator has led companies to change the way they operate, and it might well spur innovation and improvement in the water industry. The impasse between the Regulator and water companies on whether money needs to be spent on maintaining the condition of assets or simply on maintaining customer service must be resolved, and realistic targets for future efficiency gains agreed. Mere fundamentally, as the industry changes so must the nature and degree of its regulation.	B
Energy	C+	→	Energy policy in the UK remains confused. The 22nd report of the Royal Commission on Environment Pollution calls for a 60% reduction in carbon dioxide emissions from 1998 levels by 2050, through reduced energy use, exploitation of alternative sources of energy, better use of combined heat and power, a carbon tax and cleaner fossil fuel burning.However, although the Government has funded a £30M scheme to trade greenhouse gas emissions, its forecast for electricity supply in 2020 will be more reliant on the burning of fossil fuels than at present. Gas and coal generation is set to rise from 65% to 80% with nuclear power falling to 10% from 28%. The use of renewable energy is not expected to even reach its 10% target. Recent disruption caused to fuel deliveries by public protest was a timely reminder that social issues cannot be ignored when setting energy policy. However, the market-led policy behind the 2020 forecast will not provide lower emissions or secure electricity supplies. Over-reliance on gas, will leave the UK's electricity supplies dangerously vulnerable to overseas suppliers.	The government must find an appropriate way to encourage investment in technologies to give long term, secure, diverse, and non-polluting energy supplies. Proposals for a Renewables Obligation are a step in the right direction but appear to be influenced more by short term considerations than by long term objectives. A specific carbon tax based on the quantity of carbon dioxide emitted per unit of energy supplied would be more easily understood by the public. Government cannot afford to wait for a disaster in electricity supplies before it acts. It must develop appropriate economic instruments rapidly if secure and diverse energy sources are to make their contribution for the remainder of the 21st century and beyond.	D
Urban regen-eration	C+	←	The Government's latest public spending review promises massive new investment in facilities for education, health, housing and transport over the next five years in addition to whatever private finance initiatives will deliver. The Urban White Paper is now awaited and is expected to give more shape to the total programme. The Regional Development Authority machinery is now mostly assembled and in place and overall looks powerful enough for its role. However, while joint ventures with developers are creating better delivery, so far there are only a few large projects in hand and the fiscal incentives from Government to attract this investment remain unclear. The relationship between the RDAs and bodies such as English Partnerships also still need to be better developed. Urban transport improvement remains more in talk and study mode with only occasional schemes surfacing to reality, whilst the calming of motorists continues with great enthusiasm as does the civilising of city centre areas. Government is looking for the industry to improve its efficiency so as to deliver these huge programmes.	With investment themes chosen, the scale of funding declared and the main implementation vehicles in place, delivery must now start to accelerate. The Government must keep its resolve and clarity and see through its promises to reform the public health, education and housing systems and provide the necessary fiscal incentives to encourage public and private investment. The construction industry must also continue its own restructuring and deliver the competence that the Government's ambitions require and presume. The private sector must also step up its investment to underpin the public work, particularly as a recession serious enough to reduce annual construction volumes, is not likely within the next five years.	C
Waste	D	←	Government has published its Waste Strategy 2000 for England and Wales which should influence development of infrastructure to handle solid waste. It emphasises the need for sustainable solutions and establishes that waste management strategies should change from disposal-led to recovery-led. Statutory targets have been set to boost waste recycling, to increase recovery, energy generation through incineration, anaerobic digestion and composting and to reduce the quantity sent to landfill. A new body, Waste and Resources Action Programme, will help to meet these targets. However, planning and regulatory regimes still do not ease the problem of finding new and alternative sites for waste management facilities so that the time and cost of obtaining permits is often a major constraint. The Government has made £190M of new funding available, with £50M of this to be invested over the next three years to maximise recycling and composting. However, there is still a question mark over whether the cash available to develop the new strategy will be sufficient.	We now have the direction and strategy for dealing with solid waste in the UK but remain a long way short of targets. It is vital that the new Waste and Resources Action Programme is given the statutory tools needed to support the changes necessary to meet the targets and that the cash is made available to kick-start and invest in the fledgling initiatives. Planning legislation also needs to be reviewed to help the development and upgrading of vital waste management facilities across the UK.	D

Environmental comments

•Changes in the environmental performance of Government are gradual so differences over the last six months are bound to be slight. However, there are some improvements, notably the contaminated land regulations under the Environmental Protection Act, which came into force on 1 April. These increase the onus on polluters and introduce strict liability - but their impact on how developers view risk is unclear.

•Interpreting the signals from Government over the recent tax on fuel crisis is problematic. Increasing the rate of tax on fuel was part of Government policy to moderate car use and so relieve congestion. But as the country ground to a halt, no member of the Government spoke up to remind the electorate of this line of thinking and the environmental argument was crushed in the political heat.

•Government has now formed its Sustainable Development Commission and appointed long-time environmental campaigner Jonathan Porritt to chair it. The Commission should include engineers on its panel, make steps to bring business, local government, pressure groups and academics together and help to match the pressures on society and economy with the needs of the environment.

•Little progress, however, has been made towards offering credible incentives for the public to save energy and the current policy towards developing renewable energy sources remains confused. Fiscal incentives for power generators to meet new requirements to generate 10% of power from renewable means have been lost in the economics of production.

How we did it

The State of the Nation report is produced twice a year. The grades are decided by a panel of experts chaired by Joe Dwyer, the President of the Institution of Civil Engineers.

The overall grade is an average of all the grades for each category. Each category is also given a grade for sustainability - a measure of how well environmental and social concerns are being integrated with economic issues.

A = Good, B = Fair, C = Average, D = Poor, E = Bad.

The Change arrow shows whether the situation is improving, staying the same or declining.

Contact details

Ian Moore, public affairs director, ICE: 020 7665 2151, 0777 567 0861 (mobile), moore_i@ice.org.uk
Shona Cooper, press officer, ICE: 020 7665 2150
Antony Oliver, editor, NCE: 020 7505 6677, 07710 341 082 (mobile), antony.oliver@construct.emap.com

Figure E3b Report on UK Infrastructure Published by ICE and NCE (Part 2)

APPENDIX F

PUBLICATIONS RELATED TO CURRENT STUDY ON STRUCTURAL REPAIR AND STRENGTHENING

Tann, D. B., and Delpak, R. (1997), "Repair and strengthening of mechanically damaged concrete beams", Proceedings 5th International Conference on Building Materials, Structures and Techniques, Vilnius, Lithuania, pp102-110.

Tann, D. B., and Delpak, R. (1999), "Experimental investigation of concrete beams reinforced with narrow carbon fibre strips", Proceedings of the 8th International Conference of Structural Faults and Repair, 13-15 July, London.

Tann, D. B., and Delpak, R. (1999), "Repair and strengthening of RC beams using carbon fibre reinforced plastic composites", Proceedings of the 9th Annual British Cement Association Conference on Higher Education and the Concrete Industry, Cardiff University, 8-9 July, pp191-205

Tann, D. B., and Delpak, R. (1999), "Behaviour of concrete beams strengthened by carbon fibre reinforced plastic (CFRP) composites", The 6th International Conference on Composite Engineering, 27 June - 3 July, Orlando, USA, pp833-834.

Shih, J. K. C., Tann, D. B., and Delpak, R. (1999), "Repair of reinforced concrete beams using high strength cementitious mortars", International Conference on Advances on Structural Engineering and Mechanics, Seoul, 23-25 August, pp1185-1191.

Tann, D. B., and Delpak, R. (2000), "Shear strengthening of continuous reinforced concrete beams using externally bonded carbon fibre composites", Proceedings the 10th Annual British Cement Association Conference, University of Birmingham, 29-30 June, pp325-338.

Tann, D. B., and Delpak, R. (2000), "Design guidelines for flexural strengthening of RC structures using FRP composites", Proceedings of International Conference on High Performance Concrete, Hong Kong, pp447-457.

Tann, D. B., and Delpak, R. (2000), "Ductility of FRP strengthened RC beams", The 7th International Conference on Composite Engineering, 3-8 July, Denver, USA, pp865-866.

Shih, J. K. C., Delpak, R., Hu, B. and Tann, D. B. (2000), "Finite element modelling of behaviour of reinforced concrete beams in fire," International Conference on Computing in Structural Technology, Leuven, Belgium, Civil-Comp Press, pp115-118.

Hu, B, Delpak, R. Andreou, E. and Tann, D. B. (2000), "Finite element analysis of reinforced concrete structures using externally bonded FRP composites," International Conference on Computing in Structural Technology, Leuven, Belgium, Civil-Comp Press, pp125-128.

Other FRP Strengthening Related Public Presentations by the Candidate:

"Carbon Fibre Reinforced Plastic - A Flexible Friend", Presentation to the British Association for the Advancement of Sciences, Wales Branch, University of Wales Cardiff, 4 March 1999.

"Structural Repair and Strengthening, R & D and Design Practice", Presented to the Concrete Society Wales Region's Concrete Day, 15 September 1999, University of Glamorgan Conference Centre.

"Strengthening for ductility and high performance of reinforced concrete structures using externally bonded FRP composites", Conference on Advances in Composites for Strengthening Civil Engineering Structures, Aston University, 16 May 2000.

"An Overview on the Design Issues Relating to FRP Strengthening", Presentation to the Institution of Structural Engineers, Wales Branch, 18 September 2000.